Institut für Molekulare Medizin

Direktor: Univ.-Prof. Dr. rer. nat. Sebastian Wesselborg

Habilitationsschrift

Balancing Cell Life and Death:

Signal Transduction of Apoptosis and Autophagy

zur Erlangung der Venia Legendi

für das Fach Molekulare Medizin

vorgelegt der Medizinischen Fakultät

der Heinrich-Heine-Universität Düsseldorf

von

Dr. rer. nat. Björn Stork

aus Herford

Dekan: Herr Univ.-Prof. Dr. med. Joachim Windolf

Eingereicht am 23.05.2013

Contents

CONTENTS ..... **III**

ZUSAMMENFASSUNG ..... **V**

1. STATE OF THE ART **1**

1.1 APOPTOSIS 1

1.1.1 Morphology of Apoptosis *3*

1.1.2 Molecular Regulation of Apoptosis *3*

1.1.2.1 Extrinsic Apoptosis Pathway 7

1.1.2.2 Intrinsic Apoptosis Pathway 11

1.1.3 Therapies targeting apoptosis *19*

1.2 AUTOPHAGY 21

1.2.1 Types of Autophagy and Morphology *21*

1.2.2 Molecular Regulation of Autophagy *23*

1.2.2.1 The PI3K class III complex 25

1.2.2.2 WIPI/Atg18 proteins & Atg2 27

1.2.2.3 Atg9/Atg9A 28

1.2.2.4 Two ubiquitin-like conjugation systems in autophagy: Atg12-Atg5 and Atg8-PE 29

1.2.2.5 Final stage of autophagy: autophagosome-lysosome fusion 34

1.2.3 The Ulk1-Atg13-FIP200-Atg101 complex *34*

1.2.3.1 The yeast Atg1-Atg13-Atg17 complex 34

1.2.3.2 The Ulk1-Atg13-FIP200-Atg101 complex in higher eukaryotes 37

1.2.3.3 Regulation of the Ulk complex by post-translational modifications 42

1.2.3.4 Structural aspects of the Ulk complex 51

1.2.3.5 Downstream targets of the Ulk1 complex 51

1.2.4 Molecular hierarchy of Atg proteins *54*

1.2.5 Physiological Role of Autophagy *56*

1.2.5.1 Autophagy and cancer 56

1.2.5.2 Autophagy and the immune system 57

1.2.5.3 The Ulk1 complex in disease 58

1.3 CRITICAL NODES REGULATING APOPTOSIS-AUTOPHAGY NETWORK 58
1.3.1 The PI3K/PDK1/Akt/mTOR signaling axis 59
1.3.2 Ca^{2+} signaling 68
1.3.3 Beclin 1-Bcl-2 interaction 71
1.3.4 The tumor suppressor p53 74
1.3.5 Proteolytic crosstalk between apoptosis and autophagy 77

2. SUMMARIES OF SELECTED RESEARCH ARTICLES 79

2.1 SUBCELLULAR LOCALIZATION OF GRB2 BY THE ADAPTOR PROTEIN DOK-3 RESTRICTS THE INTENSITY OF CA^{2+} SIGNALING IN B CELLS 79
2.2 THE AKT INHIBITOR TRICIRIBINE SENSITIZES PROSTATE CARCINOMA CELLS TO TRAIL-INDUCED APOPTOSIS. 82
2.3 THE 3-PHOSPHOINOSITIDE-DEPENDENT PROTEIN KINASE 1 (PDK1) CONTROLS UPSTREAM PI3K EXPRESSION AND PIP_3 GENERATION 83
2.4 TRIGGERING OF A NOVEL INTRINSIC APOPTOSIS PATHWAY BY THE KINASE INHIBITOR STAUROSPORINE: ACTIVATION OF CASPASE-9 IN THE ABSENCE OF APAF-1 86
2.5 AMPK-INDEPENDENT INDUCTION OF AUTOPHAGY BY CYTOSOLIC CA^{2+} INCREASE 88
2.6 ULK1-MEDIATED PHOSPHORYLATION OF AMPK CONSTITUTES A NEGATIVE REGULATORY FEEDBACK LOOP 91
2.7 ATG13 AND FIP200 ACT INDEPENDENTLY OF ULK1 AND ULK2 IN AUTOPHAGY INDUCTION 94

3. CONCLUSION 98

4. BIBLIOGRAPHY 99

5. ABBREVIATIONS 124

6. CURRICULUM VITAE 130

7. PUBLICATION LIST 131

7.1 ORIGINAL WORKS 131
7.2 REVIEWS, BOOK CHAPTERS AND ADDITIONAL PUBLICATIONS 132

8. ADDENDUM 134

Zusammenfassung

Die Kontrolle der zellulären Homöostase ist von zentraler Bedeutung für die korrekte Funktion vielzelliger Organismen. Das Fehlen dieser Kontrolle manifestiert sich in verschiedenen Erkrankungen, einschließlich Krebs und neurodegenerativen Krankheiten. Jede beliebige Zelle ist Signalen aus der extrazellulären Umgebung ausgesetzt, die wiederum unterschiedliche biologische Reaktionen hervorrufen. Dazu gehören Aktivierung, Differenzierung, Proliferation, das Überleben der Zelle oder der Zelltod.

Die Entscheidung zwischen Überleben und Tod der Zelle ist besonders unter Stressbedingungen wichtig. Zu diesen Bedingungen gehören zum Beispiel DNA-schädigende Behandlungen, Nährstoffmangel oder Immunreaktionen. Diese stressinduzierenden Faktoren können zu einem vorübergehenden oder permanenten Zellzyklusarrest (auch als Seneszenz bezeichnet), zur sogenannten mitotischen Katastrophe, zur regulierten Nekrose, zur Apoptose oder zur Autophagie führen. Zusätzlich wurden in der Vergangenheit alternative Zelltodformen identifiziert, zum Beispiel Entose, Netose, Kornifikation, Pyroptose oder Parthanatos (Übersicht in Galluzzi et al., 2012). Häufig existieren Kombinationen oder eine geordnete zeitliche Abfolge dieser Prozesse. Dadurch wird eine dynamische Regulierung des Zellschicksals ermöglicht. In der vorliegenden Habilitationsschrift liegt der Fokus auf Apoptose und Autophagie sowie auf den gemeinsamen Kontrollmechanismen dieser beiden Prozesse.

Bei der Apoptose handelt es sich um die programmierte Form des Zelltods. Generell existieren zwei Hauptwege der Apoptose-Induktion, d.h. der extrinsische Todesrezeptorweg und der intrinsische mitochondriale Weg. Letzterer wird z.B. nach DNA-Schädigung induziert. Wir konnten zeigen, dass der pan-Kinaseinhibitor Staurosporin neben dem mitochondrialen Weg einen neuartigen intrinsischen Apoptose-Signalweg induzieren kann (s. Kapitel 2.4). Einen zentralen Einfluss auf das „apoptotische Potential“ einer Zelle haben anti-apoptotische Überlebenssignalwege. Ein wichtiges Beispiel ist der PI3K/PDK1/Akt-Signalweg. Die einzelnen Komponenten dieser Signaltransduktionskette sind in Tumorzellen häufig übermäßig aktiviert. Dementsprechend basieren gegenwärtige Therapien auf der Inhibierung dieser Komponenten. Wir konnten darlegen, dass die Inhibierung der Serin/Threonin-Proteinkinase Akt humane Prostatakarzinomzellen für die Todesrezeptor-abhängige Apoptose sensibilisiert (s. Kapitel 2.2). Des Weiteren konnten wir einen transkriptionellen Rückkopplungsmechanismus im PI3K/PDK1/Akt-Signalweg identifizieren, welcher unter Umständen bei dem Einsatz von Inhibitoren berücksichtigt werden muss (s. Kapitel 2.3).

Im Gegensatz dazu ist die Autophagie ein zytoprotektiver Mechanismus, der Zellen das Überleben unter Stressbedingungen ermöglicht. Ein zentraler Komplex für die Autophagie-Induktion ist der

Ulk1-Kinasekomplex. In unseren Arbeiten konnten wir zeigen, dass die Serin/Threonin-Kinase Ulk1 die vorgeschaltete Kinase AMPK inhibiert. Diese negative Rückkopplung stellt eventuell eine Möglichkeit dar, Autophagieprozesse zu beenden (s. Kapitel 2.6). Schließlich konnten wir beweisen, dass Autophagie auch unabhängig von Ulk1 induziert werden kann (s. Kapitel 2.7).

Es gibt zahlreiche Überschneidungen zwischen apoptotischen und autophagischen Prozessen, und zwar sowohl bei den vorgeschalteten Regulationsmechanismen als auch bei den eigentlichen Effektorproteinen. Neben dem oben erwähnten PI3K/PDK1/Akt-Signalweg ist die intrazelluläre Ca^{2+}-Konzentration eine wichtige Determinante bei der Regulierung der beiden Prozesse. Zum einen konnten wir einen regulatorischen Mechanismus der Ca^{2+}-Mobilisierung in B-Lymphozyten beschreiben (s. Kapitel 2.1). Zum anderen konnten wir darlegen, dass ein Anstieg der zytosolischen Ca^{2+}-Konzentration Autophagie unabhängig von den Kinasen AMPK und mTOR induzieren kann (s. Kapitel 2.5).

Apoptose und Autophagie sowie deren Dysregulation sind an zahlreichen pathologischen Prozessen beteiligt. Während der Tumorgenese kann ein Übergewicht an anti-apoptotischen Signalen zu einer malignen Transformation der Zelle oder zur Entwicklung von Therapieresistenzen führen. Eine erhöhte Autophagierate dagegen wirkt sich eher präventiv auf die Tumorentwicklung aus. Im Gegensatz dazu scheint die Inhibierung der Autophagie die Regression eines vorhandenen Tumors zu unterstützen (Übersicht in Mizushima et al., 2008). Zusammenfassend konnten wir verschiedene Mechanismen erarbeiten, wie Apoptose und Autophagie im Besonderen und das Zellschicksal im Allgemeinen reguliert werden. Dementsprechend soll die vorliegende Arbeit das Verständnis für diese beiden Prozesse fördern und ergänzen, um in Zukunft die Wirksamkeit bestehender Therapiemöglichkeiten zu verbessern bzw. um neue Therapiewege zu eröffnen.

1. State of the Art

The control of cellular homeostasis is central for the accurate function of multicellular organisms. The absence of this control is manifested in diverse malignancies, including cancer and neurodegenerative diseases. Any given cell receives signals from its extracellular environment, which lead to a diverse set of biological responses. These include activation, differentiation, proliferation, cell survival, or cell death.

The decision between cell survival and cell death is especially important when cells are exposed to stress conditions. These could include DNA damage-inducing treatment, nutrient deprivation, or immune responses. Such conditions can lead to transient or permanent cell cycle arrest (the later referred to as senescence), mitotic catastrophe, regulated necrosis, apoptosis or autophagy. Additionally, different alternative subroutines of cell death have been identified, e.g. entosis, netosis, cornification, pyroptosis and parthanatos (reviewed in Galluzzi et al., 2012). Frequently, there exist combinations or chronological sequences of these processes, leading to a dynamic regulation of cell fate.

In the presented habilitation thesis, the focus is brought into apoptosis and autophagy, and their partially common regulation. Apoptosis is the programmed form of cell death, whereas autophagy is a cytoprotective mechanism for cells to survive stress conditions. There exists significant cross-talk between these two processes, which might either occur at upstream regulating pathways or at the level of the effector core machineries. The processes of apoptosis and autophagy and their dysregulation are involved in different disease settings. For example, during tumorigenesis an imbalance in favor of anti-apoptotic signaling contributes to the malignant transformation of cells or the establishment of therapy resistance. In contrast, it appears that enhanced autophagy is beneficial for the prevention of tumorigenesis or tumor progression, whereas the inhibition of autophagy appears to support tumor regression (Mizushima et al., 2008). Accordingly, the presented work intends to improve the understanding of these two cell fate-regulating processes, in order to ultimately enhance the efficacy of existing therapies or to design novel therapeutic approaches, respectively.

1.1 Apoptosis

In 1972, Kerr and colleagues proposed the term “apoptosis” for a mechanism of controlled cell deletion. They defined the morphological features and suggested that apoptosis is an “active, inherently programmed phenomenon” (Kerr et al., 1972). The term apoptosis was suggested by

Professor James Cormack, who worked at the Department of Greek at the University of Aberdeen at that time. This term originates from the Greek word ἀπόπτωσις, literally describing the "falling off" of petals from flowers or leaves from trees (Kerr et al., 1972). To date, apoptosis is synonymously used for programmed cell death type I. Apoptosis can be viewed as antagonist of mitosis, and it is involved in a wide range of cellular processes, including embryogenesis, control of cell numbers in multicellular organisms, elimination of autoreactive lymphocytes, down-regulation of immune responses, or elimination of tumor cells or virus-infected cells.

Initially the nematode *Caenorhabditis elegans* (*C. elegans*) has been used to study the apoptosis signaling pathways. In this model system, always the same 131 cells out of 1,090 cells die during development, resulting in 959 somatic cells in the adult organism (Danial & Korsmeyer, 2004). In pioneering works with the *C. elegans* model system, Sydney Brenner, John Sulston and H. Robert Horvitz initiated the research field of programmed cell death, and the three researchers received the 2002 Nobel Prize in Medicine “for their discoveries concerning genetic regulation of organ development and programmed cell death”. In 1986, Ellis and Horvitz reported that wild-type functions of the genes *cell death abnormal-3* (*ced-3*) and *ced-4* are required for the initiation of programmed cell death in *C. elegans* (Ellis & Horvitz, 1986). In 1992, Hengartner et al. reported that *ced-9* protects cells from programmed cell death (Hengartner et al., 1992). Today it is known that the proteins CED-3, CED-4 and CED-9 represent the mammalian orthologs of caspase-3, Apaf-1, and Bcl-2, respectively (Fernandes-Alnemri et al., 1994; Hengartner & Horvitz, 1994; Nicholson et al., 1995; Schlegel et al., 1995; Tewari et al., 1995; Xue et al., 1996; Zou et al., 1997). The functions of these proteins will be explained in the following chapters.

In contrast to necrotic cell death, there is no release of intracellular proteins during apoptosis, thus avoiding the generation of an inflammatory response. Accordingly, apoptosis is a quiescent cellular suicide ensuring the survival of the whole organism. Apoptotic effector machineries are conserved across metazoan species. However, in 1997 apoptosis was also described for baker’s yeast *Saccharomyces cerevisiae*, and the existence of a programmed cell death in this unicellular organism has been confirmed since then (Madeo et al., 1997; Carmona-Gutierrez et al., 2010). Given its participation in different cellular processes, the dysregulation of apoptosis contributes to the pathogenesis of several diseases including tumorigenesis, neurodegeneration, and infectious diseases.

1.1.1 Morphology of Apoptosis

In their publication, Kerr et al. already described the morphologic alterations accompanying apoptosis. The authors describe that apoptosis takes place in two separate stages, i.e. the formation of so-called apoptotic bodies and their subsequent phagocytosis and degradation by other cells (Kerr et al., 1972). The second stage is now referred to as clearance and is regulated by "find-me" and "eat-me" signals released by apoptotic cells. The proper clearance of apoptotic cells is important in order to prevent secondary necrosis of dying cells and to avoid undesired immune responses (reviewed in Nagata et al., 2010; Ravichandran, 2011). Early stages of the apoptotic program are accompanied by the condensation of both cytoplasm and chromatin (pyknosis), leading to cellular and nuclear shrinkage (Kerr et al., 1972; Elmore, 2007). Apoptotic bodies are small membrane-surrounded vesicles of varying size. They contain the remnants of an apoptotic cell, i.e. cytoplasm with tightly packed organelles with or without nuclear fragments (Elmore, 2007). The organelle integrity is still maintained within apoptotic bodies. The formation of apoptotic bodies is mediated by plasma membrane blebbing, karyorrhexis (i.e. nuclear fragmentation), and transfer of cellular components into apoptotic bodies (Elmore, 2007). On the molecular level, one hallmark of apoptosis is the externalization of the "eat-me" signal phosphatidylserine, which is normally localized at the inner leaflet of the plasma membrane (Fadok et al., 1992).

1.1.2 Molecular Regulation of Apoptosis

Generally, there exist two major pathways how apoptosis can be induced in cells, i.e. the extrinsic or death receptor-mediated pathway and the intrinsic mitochondrial pathway. The extrinsic pathway is initiated by plasma membrane-resident death receptors, whereas the intrinsic pathway is initiated from within the cell upon cellular damage. These two pathways will be explained in detail in chapters 1.1.2.1 and 1.1.2.2, respectively. To date, the molecular machinery regulating both apoptosis pathways is well defined, and can be subdivided in different functional groups: 1) cysteine proteases specific for aspartic acid (caspases), 2) members of the B-cell CLL/lymphoma 2 (Bcl-2) family, 3) adapter proteins serving as scaffolds for apoptosis-inducing macromolecular complexes, 4) pro-apoptotic proteins released from damaged mitochondria, 5) death receptors and their corresponding ligands, and 6) inhibitors of apoptosis signaling (figure 1). In 1989, two groups identified a protease involved in the processing of interleukin-1β, and termed this enzyme IL-1β converting enzyme (ICE) (Black et al., 1989; Kostura et al., 1989). ICE was the first member of a cysteine protease family specific for motifs containing aspartic acids (caspases). First it was suggested that ICE is the mammalian ortholog of CED-3 (Yuan et al., 1993), and indeed overexpression of ICE induced

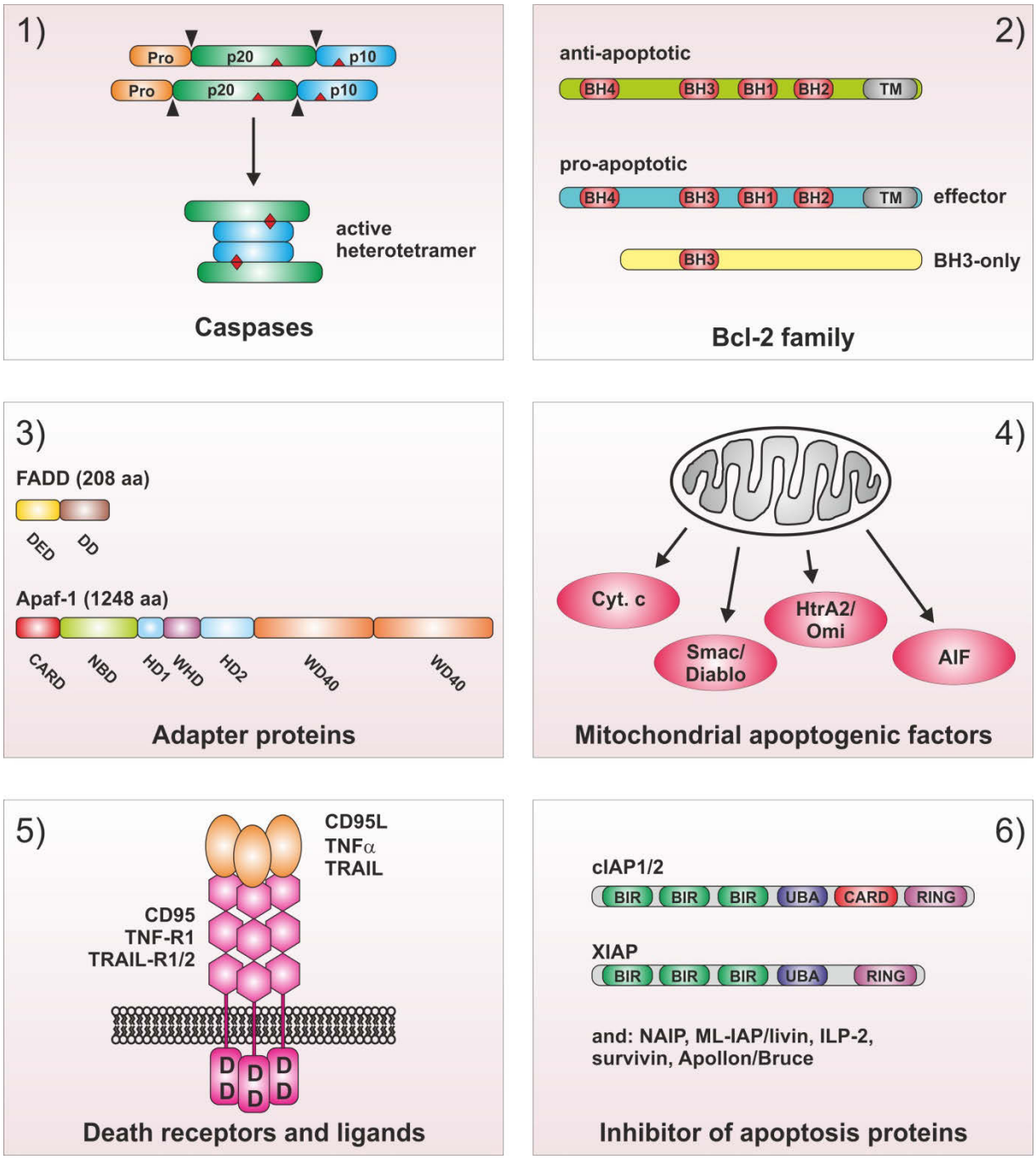

Figure 1: Functional units of apoptosis signaling: 1) cysteine proteases specific for aspartic acid (caspases), 2) anti- and pro-apoptotic members of the B-cell CLL/lymphoma 2 (Bcl-2) family, 3) adapter proteins FADD and Apaf-1 serving as scaffolds for apoptosis-inducing macromolecular complexes, 4) pro-apoptotic proteins released from damaged mitochondria, 5) death receptors and their corresponding ligands, and 6) inhibitors of apoptosis signaling.

apoptosis in fibroblasts (Miura et al., 1993). In 1996, the term “caspase” was proposed for this protease family (Alnemri et al., 1996). Subsequently, it was reported that CED-3 is more similar to caspase-3 (also termed CPP32, Yama, or apopain) than to ICE/caspase-1 (Fernandes-Alnemri et al., 1994; Nicholson et al., 1995; Schlegel et al., 1995; Tewari et al., 1995; Xue et al., 1996; Danial &

Korsmeyer, 2004). Until now, 15 different mammalian caspases have been identified (Chowdhury et al., 2008). Generally, these can be subdivided into caspases regulating inflammatory processes (caspase-1, -4, -5, -11, -12, -13 and -14) and caspases regulating apoptosis (caspase-2, -3, -6, -7, -8, -9, -10 and -15) (Chowdhury et al., 2008; McIlwain et al., 2013). The latter can be further subdivided into caspases controlling the initiation of the apoptotic program, i.e. the initiator caspases-2/-8/-9/-10, and the caspases responsible for the execution of apoptosis, i.e. effector or executioner caspases-3/-6/-7. In human, caspase-11 and caspase-15 are absent, and caspase-12 is a pseudo-caspase (Lamkanfi et al., 2004; Chowdhury et al., 2008). Next to their roles in inflammation and apoptosis, caspases have been implicated in the regulation of cell survival, cell shape, migration, proliferation, and differentiation (reviewed in Lamkanfi et al., 2007; Kuranaga, 2012). Herein, only the apoptosis-relevant caspases will be discussed. Caspases are synthesized as inactive procaspases, and activation requires the proteolytic processing at two specific aspartic acid residues. The presence of aspartic acid within the cleavage motif enables caspases to auto-activate or to trans-activate each other. These cleavages result in the removal of the pro-domain (except for caspase-9) and the generation of a small subunit and a large subunit of approximately 10 and 20 kDa, respectively. Active caspases contain two large and two small subunits forming a heterotetramer [$p20_2$-$p10_2$] (Chowdhury et al., 2008). The large fragment contains the catalytic dyad residues C and H, and the small subunit contributes to the formation of the substrate binding groove (Pop & Salvesen, 2009). Generally, initiator caspases are activated in the context of macromolecular complexes (in detail described in 1.1.2.1 and 1.1.2.2, respectively). To date, several macromolecular protein complexes have been identified in which caspases are essentially involved: the death-inducing signaling complex (DISC), the apoptosome, the piddosome, the necrosome, and the ripoptosome. In order to be recruited to these complexes, the pro-domains of initiator caspases contain interaction domains which homo-dimerize with the corresponding domain of the adaptor protein serving as scaffold for the complex. Accordingly, caspase-8 and -10 contain tandem death domains (DDs) in their pro-domain, and caspase-2 and -9 a caspase-recruitment domain (CARD) (McIlwain et al., 2013). Since effector caspases are cleaved and thus activated by initiator caspases, they only harbor a short pro-domain. The partial proteolysis of caspases is the basis for the detection of apoptosis induction by immunoblotting. Caspases require a tetrapeptide recognition motif for substrate cleavage, and this can be utilized for fluorogenic *in vitro* enzymatic assays. For that, caspase-specific tetrapeptides are fused to aminomethylcoumarin. Active caspases cleave this synthetic substrate, and the fluorescence of free aminomethylcoumarin can be detected. Within the context of apoptosis induction in cells, a plethora of caspase substrates has been identified. One of the first reported caspase substrates was the 116 kDa poly(ADP-ribose) polymerase (PARP), which is cleaved upon apoptosis induction resulting in an 85 kDa fragment (Kaufmann et al., 1993; Lazebnik et al., 1994; Tewari et al., 1995).

This cleavage can also be monitored by immunoblotting. Another central caspase-substrate is the inhibitor of caspase-activated DNase (ICAD; also termed DNA fragmentation factor of 45 kDa, DFF45) (Liu et al., 1997; Enari et al., 1998). ICAD is normally associated with CAD (alternatively called DFF40). Upon apoptosis induction, ICAD is cleaved and CAD can enter the nucleus, where it catalyzes the degradation of chromosomal DNA. Since the chromosomal DNA is cleaved at internucleosomal sites during apoptosis, the typical "DNA laddering" was frequently detected by agarose gel electrophoresis (Compton, 1992). Alternatively, the resulting hypodiploid nuclei can be monitored by flow cytometry (Nicoletti et al., 1991). In 1998, Stroh and Schulze-Osthoff reported 65 caspase substrates, and five years later this number had risen to more than 280 (Stroh & Schulze-Osthoff, 1998; Fischer et al., 2003). In 2011, Crawford and Wells stated that the number of human proteins reportedly cleaved by caspases is approaching 1,000, which represents nearly 5% of the proteome (Crawford & Wells, 2011). To date, different large-scale proteomic approaches have been undertaken to decipher the caspase-dependent apoptotic signature (Dix et al., 2008; Mahrus et al., 2008; Agard et al., 2012; Shimbo et al., 2012). Furthermore, there exist different searchable databases or prediction tools for caspase substrates in the internet, e.g. www.casbase.org, bioinf.gen.tcd.ie/casbah, or wellslab.ucsf.edu/degrabase (Wee et al., 2006; Luthi & Martin, 2007; Crawford et al., 2013).

The catalytic activity of caspases is directly counterbalanced by the inhibitors of apoptosis (IAPs). To date, eight mammalian family members have been identified: NAIP, c-IAP1, c-IAP2, XIAP, survivin, Apollon/Bruce, ML-IAP/livin, and ILP-2 (reviewed in de Almagro & Vucic, 2012). In 1993, the first IAPs were identified in baculoviral genomes (Crook et al., 1993; Birnbaum et al., 1994; de Almagro & Vucic, 2012). The characteristic of IAPs is the presence of 1-3 baculoviral IAP repeats (BIR) domains, which are zinc-binding domains with a length of approximately 80 amino acids (de Almagro & Vucic, 2012). The BIR domains are mainly responsible for the binding of caspases. Additionally, several IAPs contain a ubiquitin-associated (UBA) domain [c-IAP1, c-IAP2, XIAP, and ILP-2] and a really interesting new gene (RING) domain [c-IAP1, c-IAP2, XIAP, ML-IAP, and ILP-2] (de Almagro & Vucic, 2012). The most extensively studied IAP with regard to the regulation of apoptosis is XIAP (Vaux & Silke, 2003; de Almagro & Vucic, 2012). XIAP binds caspases through its BIR2 or BIR3 domain, respectively. The BIR2 domain and the linker between BIR1 and BIR2 of XIAP inhibit caspase-3 and -7 by a two-site interaction mechanism (Huang et al., 2001; Riedl et al., 2001; Suzuki et al., 2001b; Scott et al., 2005). In contrast, caspase-9 is inhibited by the XIAP BIR3 domain (Srinivasula et al., 2001; Shiozaki et al., 2003). The BIR3 domain of XIAP associates with the N-terminal peptide of the linker region between large and small subunit of caspase-9, which becomes exposed after proteolytic processing of procaspase-9 at D315. The BIR3-binding motif is ATPF (Srinivasula et al., 2001). Notably, there exist also inhibitors of the inhibitors, and these apoptogenic factors are released from mitochondria (see chapter 1.1.2.2) (reviewed in Vaux, 2011). One of these factors is the second mitochondria-derived

activator of caspases (Smac; alternatively called direct IAP binding protein with low pI, DIABLO) competitively binds to XIAP via its AVPI motif, thus replacing caspase-9 (Srinivasula et al., 2000; Wu et al., 2000; Ekert et al., 2001; reviewed in Vaux, 2011; de Almagro & Vucic, 2012).

1.1.2.1 Extrinsic Apoptosis Pathway

The extrinsic apoptosis pathway is initiated at the plasma membrane upon binding of death receptor ligands to their cognate receptors. The death receptors (DRs) contain an intracellular death domain (DD) and belong to the tumor necrosis factor receptor (TNF-R) superfamily. The DD is important for the recruitment of downstream adapter proteins which likewise contain a DD. To date, six DD-containing members have been identified: 1) CD95 (also Fas, APO-1, DR2), 2) TRAIL-R1 (also APO-2, DR4), 3) TRAIL-R2 (also DR5, KILLER, TRICK2), 4) TNF-R1 (also DR1, CD120a, p55 and p60), 5) TRAMP (also APO-3, LARD, WSL-1, DR3), and 6) DR6 (Lavrik et al., 2005; Kantari & Walczak, 2011). These receptors are activated by their respective ligands, i.e. CD95L (also FasL, APO-1L), TRAIL (also APO-2L), TNF, and TL1A (Lavrik et al., 2005; Kantari & Walczak, 2011). With regard to DR6, it has been reported that an N-terminal fragment of the β-amyloid precursor protein (APP) binds to it and regulates neuron death via the activation of caspase-6 (Nikolaev et al., 2009). Next to DD-containing death receptors, four decoy death receptors have been identified, which can bind to death receptor ligands but do not possess a functional DD and accordingly cannot transduce the signal. These decoy receptors (DcRs) include TRAIL-R3 (also DcR1), TRAIL-R4 (also DcR2), DcR3 and osteoprotegrin (OPG) (Lavrik et al., 2005). Generally, DD-containing death receptors can be subdivided into two groups. The first group recruits the adapter protein Fas-associated death domain (FADD) upon stimulation and assembles the death-inducing signaling complex (DISC) (Lavrik et al., 2005; Kantari & Walczak, 2011). In turn, TNF-R1 and TRAMP recruit the adapter protein TNF-R1-associated death domain (TRADD). TRADD-recruiting receptors participate in the regulation of diverse processes, including transcription, apoptosis, and a programmed form of necrosis called necroptosis (see below) (reviewed in Declercq et al., 2009; Vandenabeele et al., 2010; Cabal-Hierro & Lazo, 2012; Lee et al., 2012; Vanlangenakker et al., 2012; Kaczmarek et al., 2013).

In 1989, the groups of Nagata and Krammer reported the isolation of monoclonal antibodies, which revealed cytolytic activity (Trauth et al., 1989; Yonehara et al., 1989). These antibodies were designated anti-Fas and anti-APO-1, respectively. Subsequently, the two groups reported the identification and cloning of the corresponding cellular antigens Fas and APO-1 (Itoh et al., 1991; Oehm et al., 1992). Fas/APO-1 is composed of three extracellular cysteine-rich repeats, a transmembrane domain, and an intracellular DD (Itoh et al., 1991; Lavrik et al., 2005). Nagata's group

also demonstrated that mice carrying the lymphoproliferation (lpr) mutation have defects in the Fas antigen (Watanabe-Fukunaga et al., 1992). In 1993, the same group reported the molecular cloning of the Fas ligand (FasL) (Suda et al., 1993), and it was demonstrated that mice suffering from the generalized lymphoproliferative disease (gld) carry a point mutation in the FasL gene (Takahashi et al., 1994). The CD95/TRAIL-R subgroup of death receptors recruits the intracellular adapter protein Fas-associating protein with a novel death domain (FADD; also termed mediator or receptor-induced toxicity 1, MORT1) via homotypic interaction (Boldin et al., 1995; Chinnaiyan et al., 1995). Expression of an N-terminally truncated FADD variant attenuated apoptosis induction, indicating that this region harbors a death effector domain (DED) (Chinnaiyan et al., 1995; Chinnaiyan et al., 1996). In 1995, Krammer's group reported that an intracellular complex is formed upon death receptor crosslinking, and they coined the term death-inducing signaling complex (DISC) (Kischkel et al., 1995). They found that FADD is one component of the DISC. Additionally, a 55 kDa-component was purified. One year later, two groups identified caspase-8 – originally termed FADD-like ICE (FLICE) or MORT1-associated CED-3 homolog (MACH) – as component of the DISC (Boldin et al., 1996; Muzio et al., 1996). Simultaneously, caspase-8 was cloned by Fernandes-Alnemri et al. and termed mammalian CED-3 homolog 5 (Mch5) (Fernandes-Alnemri et al., 1996). The prodomain of caspase-8 also harbors two DEDs, and the following model of caspase-8 recruitment to the DISC was established: upon ligand-binding to the receptor, FADD is recruited to the receptor via homotypic DD interaction. Then, caspase-8 is recruited to FADD via homotypic DED interaction and becomes activated at the DISC (Medema et al., 1997). Two functionally active caspase-8 isoforms have been reported, and both are recruited to the DISC (Scaffidi et al., 1997). Procaspase-10 (also Mch4) likewise contains tandem DDs in its prodomain and is thus recruited to the DISC (Kischkel et al., 2001; Sprick et al., 2002). Caspase-10 is the closest relative of caspase-8. However, its contribution to apoptosis induction is still debated and conflicting results have been reported (reviewed in McIlwain et al., 2013). Kischkel et al. showed that caspase-10 can induce apoptosis when caspase-8 is absent (Kischkel et al., 2001). In contrast, Sprick et al. reported that caspase-10 is recruited to the DISC but cannot functionally substitute caspase-8 (Sprick et al., 2002). Furthermore, caspase-10 has been implicated in atypical CD95-induced and death-receptor-independent apoptosis pathways (reviewed in McIlwain et al., 2013). Finally, caspase-10 is not present in mice (Janicke et al., 2006). Next to procaspase-8 and -10, cellular FLICE-inhibitory proteins (c-FLIPs) are recruited to the DISC and inhibit or promote apoptosis (reviewed in Lavrik & Krammer, 2012). To date five c-FLIP proteins have been described, i.e. three isoforms (short, long, and Raji) and two cleavage products (Lavrik & Krammer, 2012). The short and the long isoform have first been reported by Tschopp's group in 1997 (Irmler et al., 1997). Essentially, the long isoform represents a catalytically inactive caspase-8 molecule, in which the catalytic cysteine residue is replaced by a tyrosine (Irmler et al., 1997). The short and the Raji isoform and the two

cleavage products block caspase-8 activation and apoptosis. The long isoform was shown to block apoptosis at low CD95L concentrations, and to enhance apoptosis at high CD95L concentrations or at high expression levels of the short FLIP isoforms (Fricker et al., 2010).

Several models for the activation of initiator caspases have been proposed, including the induced proximity model, the proximity-induced dimerization model, and the induced conformation model (see also chapter 1.1.2.2 for caspase-9 activation) (reviewed in Kantari & Walczak, 2011). Generally, it appears that the DISC-mediated activation of procaspase-8 itself is a complex process depending on oligomerization and involving the generation of several cleavage products which are catalytically active (reviewed in Lavrik & Krammer, 2012). With regard to caspase-8 activation, Chang et al. proposed an interdimer processing mechanism of caspase-8 (Chang et al., 2003). In this model, two procaspase-8 molecules form a dimer through an interaction between their protease domains. These dimers are proteolytically active and cleave neighboring dimers at the linker between large and small subunit. This in turn leads to a conformational change of the region connecting the prodomain with the large subunit. Subsequently this linker becomes cleaved and caspase-8 is fully active (Chang et al., 2003). Complementing this model, MacFarlane's group reported the reconstitution of a DISC using only purified CD95, FADD and procaspase-8 (Hughes et al., 2009). They discovered a two-step activation mechanism involving both dimerization and proteolytic cleavage. Dimerization of procaspase-8 yields an active complex which accepts only itself or c-FLIP as substrate. For full activation proteolytic cleavage is required. This also broadens the substrate repertoire which might be cleaved by caspase-8, e.g. the apoptotic substrates caspase-3 and the Bcl-2 family protein Bid (see chapter 1.1.2.2) (Hughes et al., 2009). Supporting these results, Oberst et al. showed that full caspase-8 activation requires both inducible dimerization and inducible cleavage, and that one of the two processes alone is insufficient (Oberst et al., 2010).

Historically, it has been proposed that a trimeric death receptor ligand induces the trimerization of death receptors. However, different works indicated that death receptors exist as preformed trimers, and that these trimers are clustered by death receptor ligands, which are equally arranged in clusters (reviewed in Mace & Riedl, 2010). Accordingly, the intracellular DISC forms clusters, and these are presumably bridged by death receptors and/or FADD (Carrington et al., 2006; Sandu et al., 2006; Scott et al., 2009). It has been assumed that the stoichiometry of death receptor to FADD to DED-containing protein (procaspase-8, procaspase-10, c-FLIPs) within the DISC clusters is 1:1:1 (Krammer et al., 2007). Scott et al. reported the crystal structure of human CD95-FADD death domain complex. The complex revealed four FADD death domains bound to four CD95 death domains. The authors showed that an opening of the CD95 death domain exposes the FADD binding site and simultaneously generates a CD95-CD95 bridge (Scott et al., 2009). An alternative structure was

published by Wang et al., and they described an asymmetric oligomeric complex composed of 5-7 CD95 DDs and 5 FADD DDs (Wang et al., 2010). The crystal structure presented by Scott et al. was also challenged by a manuscript from Esposito et al., who also predominantly detected a complex with 5:5 stoichiometry (Esposito et al., 2010). However, all analyses mentioned above were neither based on full length proteins nor on native DISCs. Recently, two groups analyzed the stoichiometry of CD95- or TRAIL-R-assembled native DISCs. They found that the amount of DED-containing proteins (procaspase-8, procaspase-10, c-FLIPs) exceeds the amount of FADD several-fold (Dickens et al., 2012; Schleich et al., 2012; Schleich et al., 2013). Both works suggest a DED chain model, in which DED-containing proteins form homo- and heterodimers. Apparently the DED chain lengths depend on the signal strength mediated by the death receptor ligands, and on the availability of the different DED-containing proteins. Generally, the DED chain model supports caspase-8 activation by interdimer processing described above. Furthermore, the model provides a functional explanation for the presence of tandem DEDs in procaspase-8, procaspase-10, and c-FLIPs (Dickens et al., 2012). Adding even another facet of FADD-dependent death receptor signaling, it appears that a second complex is formed upon CD95 stimulation, which was termed complex II (reviewed in Lavrik & Krammer, 2012). Complex II contributes to caspase-8 activation and contains FADD, procaspase-8 and c-FLIP, but lacks CD95 (Lavrik et al., 2008; Geserick et al., 2009; Lavrik & Krammer, 2012). It has been speculated that the platforms generated by the DED chain model might dissociate into the cytosol when they reached a certain size (Schleich et al., 2012). Generally, the existence of a complex II was first described for TNF/TNF-R signaling (see below) (Micheau & Tschopp, 2003).

Caspase-8 activation and activity are presumably also modulated by post-translational modifications. Matthess et al. reported that Cdk1/cyclin B1 phosphorylates procaspase-8 at S387 in mitotic cells and thus blocks CD95-induced apoptosis (Matthess et al., 2010). Similarly, phosphorylation of procaspase-8 at Y380 by Src kinase has also been shown to inhibit CD95-mediated apoptosis (Cursi et al., 2006). Jin et al. reported that Cullin3-based polyubiquitination of procaspase-8 is rather pro-apoptotic, leading to processing and full activation of caspase-8 (see also chapter 1.3.5) (Jin et al., 2009).

In 1998, Krammer's group reported that there exist two types of CD95 apoptotic pathways (Scaffidi et al., 1998; reviewed in Lavrik & Krammer, 2012). In type I cells, large amounts of caspase-8 are activated by the DISC within seconds, and overexpression of Bcl-2 or Bcl-x_L (see chapter 1.1.2.2) cannot block caspase-8 activation and apoptosis. In contrast, in type II cells DISC-formation is strongly reduced, and apoptosis can be blocked by overexpression of Bcl-2 or Bcl-x_L. Additionally, in type II cells caspase-3 activation occurs following the loss of the mitochondrial transmembrane potential (Scaffidi et al., 1998). It turned out that type II cells depend on a mitochondrial

amplification loop initiated by caspase-8-mediated cleavage of the pro-apoptotic Bcl-2 family protein Bid (see chapter 1.1.2.2) (Li et al., 1998; Luo et al., 1998; Gross et al., 1999; reviewed in Kantari & Walczak, 2011). Notably, Bid is mandatory for CD95-induced apoptosis in hepatocytes (type II cells), but dispensable in thymocytes (type I cells) (Yin et al., 1999; Kaufmann et al., 2007; Lavrik & Krammer, 2012). In 2008, Gonzalvez et al. demonstrated that caspase-8 translocation to the mitochondrial membrane, where it oligomerizes and is further activated, is necessary for an efficient type II response. The authors show that the accumulation and activation of caspase-8 depend on the mitochondrial phospholipid cardiolipin, which thus provides an activating platform on which Bid is cleaved (Gonzalvez et al., 2008; Kantari & Walczak, 2011; Schug et al., 2011). Next to the differences in DISC formation, it has been suggested that the expression levels of XIAP contribute to the type I-type II distinction (Jost et al., 2009).

Unlike CD95 and TRAIL-Rs, the TNF-R does not assemble a DISC. Generally, two different complexes can be assembled following ligand-binding to the TNF-R1 (reviewed in Declercq et al., 2009; Vandenabeele et al., 2010; Cabal-Hierro & Lazo, 2012; Lee et al., 2012; Vanlangenakker et al., 2012; Kaczmarek et al., 2013). Complex I contains TRADD, TRAF2/5, RIPK1, IAPs, and the linear ubiquitin assembly complex (LUBAC). This highly ubiquitinated complex remains associated with the receptor and induces the activation of NF-κB, JNK and p38 signaling pathways. In contrast, internalization of TNF-R1 leads to the release of this complex and to the recruitment of procaspase-8 and FADD. This complex IIa mediates apoptosis. However, if caspase-8 recruitment or activity is blocked, receptor-interacting serine/threonine-protein kinase 1 (RIPK1) and RIPK3 accumulate at the complex and become phosphorylated. This complex IIb (alternatively called necrosome) triggers necroptosis, which is a programmed form of necrosis (reviewed in Declercq et al., 2009; Vandenabeele et al., 2010; Cabal-Hierro & Lazo, 2012; Lee et al., 2012; Vanlangenakker et al., 2012; Kaczmarek et al., 2013). Accordingly, macromolecular complexes downstream of the TNF-R can mediate survival/inflammatory signaling, apoptosis, and necroptosis. Recently, two groups identified a cytosolic complex containing RIPK1, FADD, and caspase-8. This complex – termed ripoptosome – spontaneously assembles upon c-IAP depletion independently of death receptor activation. Like complex II, the ripoptosome can initiate caspase-8-dependent apoptosis or RIPK3-dependent necroptosis (Bertrand & Vandenabeele, 2011; Feoktistova et al., 2011; Tenev et al., 2011).

1.1.2.2 Intrinsic Apoptosis Pathway

The intrinsic or mitochondrial apoptosis pathway is induced under cell-intrinsic stress conditions, e.g. DNA-damage. The central organelle for this cell death pathway is the mitochondrion, which inducibly

releases different pro-apoptotic factors under these stress conditions. Members of the Bcl-2 family are the central regulators of mitochondrial integrity and thus key elements for the regulation of the intrinsic apoptosis pathway. In 1994, Hengartner and Horvitz reported that *ced-9* encodes a functional homolog of mammalian Bcl-2 (Hengartner & Horvitz, 1994). The Bcl-2 gene itself was identified by the analysis of the t(14:18) chromosomal translocation found in B-cell lymphomas and the cloning of the resulting breakpoint region (Pegoraro et al., 1984; Tsujimoto et al., 1984; Bakhshi et al., 1985; Cleary & Sklar, 1985; Tsujimoto et al., 1985). Shortly afterwards the cDNA and the amino acid sequence of Bcl-2 were published (Cleary et al., 1986; Tsujimoto & Croce, 1986). In the early 1990's, different groups reported that Bcl-2 negatively regulates apoptosis (Vaux et al., 1988; McDonnell et al., 1989; Hockenbery et al., 1990; Nunez et al., 1990; Henderson et al., 1991; Sentman et al., 1991; Strasser et al., 1991), and Bcl-2 was one of the first identified oncogenes which blocks programmed cell death and does not positively influence cell proliferation (Danial & Korsmeyer, 2004). Mammals express a whole family of Bcl-2 proteins, which can be subdivided into anti- and pro-apoptotic family members. Next to Bcl-2 itself, the anti-apoptotic members include Bcl-x_L, Bcl-w, Mcl-1, A1/Bfl-1, and Bcl-B (Boise et al., 1993; Kozopas et al., 1993; Lin et al., 1993; Choi et al., 1995; Gibson et al., 1996; Ke et al., 2001). These anti-apoptotic family members are multidomain proteins which share homology within specific conserved regions, i.e. the Bcl-2 homology (BH) 1-4 domains (Danial & Korsmeyer, 2004). The first identified pro-apoptotic family member was Bcl-2-associated X protein (Bax) (Oltvai et al., 1993). The pro-apoptotic family members are further subdivided into multidomain proteins and BH3-only proteins. The multidomain proteins include Bak, Bax and Bok/Mtd, and they share structural features of all four BH domains with their anti-apoptotic relatives (Oltvai et al., 1993; Chittenden et al., 1995; Farrow et al., 1995; Kiefer et al., 1995; Hsu et al., 1997; Inohara et al., 1998; Kvansakul et al., 2008; Strasser et al., 2011). The BH3-only family includes a diverse variety of proteins, and the best characterized pro-apoptotic members are Bad, Bid, Bik/Nbk, Bim/Bod, Bmf, Hrk/DP5, Noxa, and Puma/Bbc3 (reviewed in (Lomonosova & Chinnadurai, 2008; Strasser et al., 2011; Happo et al., 2012)). Of these proteins, Bid is of special interest, since it connects the extrinsic and intrinsic apoptosis pathways. Bid is a substrate of activated caspase-8, and Bid cleavage generates a truncated Bid (tBid). This truncated version translocates to mitochondria and induces the intrinsic apoptosis pathway (Li et al., 1998). In addition, several other proteins have been reported to possess a BH3 domain, e.g. Bcl-G_S, Beclin 1, BNIP1, BNIP3, BNIP3L/NIX, Egl-1, and Mcl-1S, or a BH3-like domain, e.g. ApoL1, ApoL6, BRCC2, ERBB4/HER4, ERBB2/HER2, MAP-1, MULE, p193, SphK2, Spike, and TGM2 (reviewed in (Lomonosova & Chinnadurai, 2008)).

The Bcl-2 family proteins regulate the mitochondria-dependent intrinsic apoptosis pathway by controlling the mitochondria outer membrane permeabilization (MOMP). MOMP is directly regulated by the pro-apoptotic multidomain proteins Bax and Bak, whereas the role of Bok is less well defined.

Upon activation, Bax/Bak change conformation and induce MOMP by insertion into the outer mitochondrial membrane and oligomerization. Accordingly, Bax/Bak-deficient cells are resistant to different pro-apoptotic stimuli (Lindsten et al., 2000; Wei et al., 2001; Zong et al., 2001). Anti- and pro-apoptotic Bcl-2 proteins function in a molecular system of "checks and balances", i.e. they antagonize each other through binding and release. Of note, there exist different preferences of interactions between anti- and pro-apoptotic family members (reviewed in Dewson & Kluck, 2009; Leber et al., 2010b; Shamas-Din et al., 2011; Strasser et al., 2011; Westphal et al., 2011). The BH1-3 domains of anti-apoptotic members are in close proximity to each other and thus form a hydrophobic groove which can accommodate the BH3-domains of either multidomain or BH3-only pro-apoptotic family members (Muchmore et al., 1996; Sattler et al., 1997; Danial & Korsmeyer, 2004). Generally, two different models have been proposed to explain the activation of Bax/Bak and are briefly introduced in the following. In the "indirect activation model", Bax/Bak are bound by anti-apoptotic Bcl-2 proteins. Neutralization of the latter by BH3-only proteins induces Bax/Bak oligomerization and MOMP (Willis et al., 2005; Uren et al., 2007; Willis et al., 2007). In the "direct activation model", certain BH3-only proteins – presumably Bim, tBid, and Puma – can directly activate Bax/Bak, and thus function as activators. BH3-only activators or the effector proteins Bax/Bak are bound by anti-apoptotic Bcl-2 proteins and can be released by the competitive binding of sensitizer BH3-only proteins (Letai et al., 2002; Kuwana et al., 2005; Kim et al., 2009). Direct activators might target the hydrophobic groove on Bax/Bak. However, for Bax it has been suggested that BH3 activators bind to a distal site formed by α-helices 1 and 6 ("rear site") (Gavathiotis et al., 2008; Kim et al., 2009; Gavathiotis et al., 2010; Strasser et al., 2011). Indeed, Leshchiner et al. recently demonstrated that photoreactive BH3 ligands crosslink to the hydrophobic groove of Bak and to the "rear site" of Bax (Leshchiner et al., 2013). The "direct activation model" was refined by differentiating between BH3-only sensitizers and de-repressors (Chipuk et al., 2010). Sensitizers bind to anti-apoptotic Bcl-2 proteins, and this prevents the inhibition of subsequently induced direct activators. In turn, de-repressors release direct activators which are bound by anti-apoptotic Bcl-2 proteins. Since one single model cannot explain all experimentally obtained results, it is very likely that both models contribute to apoptotic death *in realitas*. Indeed, by engineering mice expressing Bim variants with BH3 domains derived from Puma, Noxa or Bad, Merino et al. demonstrated that the full pro-apoptotic function of Bim involves both binding of anti-apoptotic Bcl-2 members and Bax, respectively (Merino et al., 2009). Accordingly, different combinations and additions to these two general models have been suggested. In the "embedded together model", the importance of the mitochondrial membrane is strengthened (Leber et al., 2007; Bogner et al., 2010; Leber et al., 2010b; Shamas-Din et al., 2011). Recruitment to this lipid environment induces conformational changes within Bcl-2 proteins, which are required for protein-protein interaction. In this model, cytoplasmic

anti-apoptotic Bcl-2 proteins are recruited to the membrane and are activated by sensitizers, activators, and Bax/Bak. At the mitochondrial membrane, anti-apoptotic proteins inhibit activators and Bax/Bak to prevent MOMP. In turn, sensitizers displace activators and Bax/Bak from anti-apoptotic proteins to promote apoptosis (Leber et al., 2007; Bogner et al., 2010; Leber et al., 2010b; Shamas-Din et al., 2011). This model is also supported by data obtained from Lovell et al. (Lovell et al., 2008). Using FRET and an *in vitro* liposome approach, they reported that an ordered series of steps is required to induce MOMP, including conformational changes, protein-protein and protein-lipid interactions upon membrane binding of tBid (Lovell et al., 2008). A unified model of Bax/Bak activation has also been proposed by Dewson and Kuck (Dewson & Kluck, 2009), which also involves spontaneous and auto-activation of Bax/Bak. Strasser et al. recently proposed the "priming-capture-displacement" model (Strasser et al., 2011). In this model, Bax/Bak become primed spontaneously or by BH3-only activators, but immediately captured by anti-apoptotic Bcl-2 proteins. Primed Bax/Bak is then displaced by BH3-only proteins for full activation (Strasser et al., 2011). Finally, another attempt to unify these different models was undertaken by Llambi et al. (Llambi et al., 2011). They identified two different "modes" by which anti-apoptotic proteins can block MOMP: by sequestering BH3-only activator proteins ("mode 1"), or by binding active Bax/Bak ("mode 2"). Interestingly, they found that mode 1 sequestration is less efficient and more easily de-repressed than mode 2 (Llambi et al., 2011). Collectively, it appears that a combination of the two general models is effective in cells, and presumably in a cell type- and context-dependent manner. Additionally, alternative regulatory mechanisms of Bax/Bak activation will have to be considered in future refinements of these models, e.g. Bax phosphorylation or heat-induced conformational change (Villunger et al., 2011). Furthermore, next to Bim, tBid and Puma a direct Bax/Bak activation has also been suggested for Noxa, Bmf, or p53 (Chipuk et al., 2004; Leu et al., 2004; Dai et al., 2011; Du et al., 2011).

Monomeric Bax is a cytosolic protein, and its C-terminal hydrophobic α9-helix occupies the hydrophobic groove (Suzuki et al., 2000). During Bax activation (potentially at the "rear site"), this helix is released and localizes Bax to the membrane. In turn, the C-terminal α9-helix of Bak is constitutively inserted in the mitochondrial outer membrane (MOM) (Chipuk et al., 2010; Strasser et al., 2011; Westphal et al., 2011). Two alternative models have also been proposed for Bax/Bak oligomerization ultimately leading to MOMP (reviewed in (Strasser et al., 2011)). In the first model, this oligmerization occurs via the multimerization of symmetric dimers. In 2008, Dewson et al. reported that Bak exposes its BH3 domain and homodimerizes via BH3-hydrophobic groove interactions, resulting in symmetric or face-to-face Bak dimers (Dewson et al., 2008). One year later they showed that these dimers can oligomerize via an α6:α6 interface (Dewson et al., 2009). Similarly, it was demonstrated that the Bax BH3 domain is also exposed during activation (Gavathiotis et al., 2010; Zhang et al., 2010). In the second model, two Bak molecules form an

asymmetric “face-to-back” dimer, which is formed via BH3-“rear site” interactions. Subsequently, additional monomers are recruited (Shamas-Din et al., 2011; Strasser et al., 2011). Recently, the symmetric homodimer-model has been supported by crystal structure analyses of Bax and Bak in complexes with BH3 peptides (Czabotar et al., 2013; Moldoveanu et al., 2013). Furthermore, it appears that a planar lipophilic surface on the Bax homodimer binds the MOM (Czabotar et al., 2013). Finally, two different possibilities exist in regard to the pores formed by Bax and Bak: 1) they represent proteinaceous pores, or 2) they facilitate the formation of lipidic pores (reviewed in Westphal et al., 2011). It has been reported that Bax inserts α-helices 5 and 6 into membranes prior to oligomerization, which might contribute to pore formation (Annis et al., 2005). Recently, Kushnareva et al. suggested that oligomerization of a catalyst protein, which is not Bax, enables MOMP through a membrane remodeling event (Kushnareva et al., 2012). Future studies will have to reveal the exact nature of the molecular structures leading to MOMP. Nevertheless, the main result of MOMP is the release of different apoptogenic factors initiating the apoptotic machinery. So far different factors have been identified, including cytochrome c, Smac/DIABLO, Omi (also known as HtrA2), apoptosis inducing factor (AIF), or endonuclease G (endoG) (reviewed in Vaux, 2011).

Cytochrome c is a 12 kDa protein normally localized in the intermembrane space between outer and inner mitochondrial membrane. Under normal healthy conditions, cytochrome c is an essential factor for mitochondrial respiration, since it shuttles electrons between complex III and complex IV of the respiratory chain located in the inner mitochondrial membrane. However, under apoptosis-inducing conditions, cytochrome c is released into the cytosol and represents an essential factor for the initiation of the intrinsic pathway (reviewed in Kulikov et al., 2012).

In 1996, Wang’s group reported an *in vitro* system that could be used for caspase-3 activation (Liu et al., 1996). They showed that dATP or dADP and two additional factors are important for caspase-3 activation, and they called them apoptotic protease activating factor-1 (Apaf-1) and -2. In the same manuscript they identified Apaf-2 as cytochrome c. One year later the same group reported that the factor Apaf-1 actually represents two factors, Apaf-1 and the additional Apaf-3 (Zou et al., 1997). They identified Apaf-1 as a 130 kDa adapter protein containing an N-terminal region homologous to CED-3, followed by a CED-4 homology domain, and several WD40 repeats in the C-terminal half. Finally, they identified Apaf-3 as caspase-9 (Li et al., 1997). Soon after that, the term “apoptosome” has been coined, essentially describing a complex of Apaf-1/procaspase-9 that is controlled by anti-apoptotic Bcl-2 proteins (Hengartner, 1997; Tsujimoto, 1998). It has been previously suggested that Bcl-x_L controls the Apaf-1/caspase-9 complex through direct interaction with Apaf-1 (Hu et al., 1998a; Pan et al., 1998), which would essentially mimic the situation in *C. elegans*, in which CED-9 directly binds to CED-4 (Chinnaiyan et al., 1997; James et al., 1997; Spector et al., 1997; Wu et al., 1997a; Wu

et al., 1997b). However, soon it was realized that anti-apoptotic Bcl-2 proteins do not directly associate with Apaf-1 and that an alternative mechanism is responsible for their function (Moriishi et al., 1999). Additionally, it was suggested that Apaf-1 oligomerization is a prerequisite for caspase-9 activation, and it appeared that the WD-40 repeat region regulates Apaf-1 self-association (Hu et al., 1998b; Srinivasula et al., 1998). Furthermore, forced dimerization of procaspase-9 resulted in its processing and subsequent apoptosis (Hu et al., 1998b). In 1999, several groups reported that cytochrome c and dATP/ATP are required for Apaf-1 oligomerization and subsequent caspase-9 activation (Cain et al., 1999; Hu et al., 1999; Saleh et al., 1999; Zou et al., 1999). Cain et al. described the formation of a 700 kDa-complex and termed it aposome (Cain et al., 1999). In contrast, Zou et al. described a 1.3 MDa-complex. Notably, they suggested that this complex contains at least eight Apaf-1 molecules, and they proposed a ring-like structure for the caspase-9-activating complex (Zou et al., 1999). In the same year, the crystal structure of the Apaf-1 CARD in association with the caspase-9 CARD was determined (Qin et al., 1999). During the last decade, crystallographic studies substantially contributed to deciphering and understanding the mechanistic details underlying caspase-9 activation. In 2002, the first three-dimensional structure of the apoptosome at a resolution of 27 Å was published (Acehan et al., 2002). This study revealed a wheel-like particle with 7-fold symmetry, i.e. the apoptosome contains seven spokes and a central hub. Notably, the authors suggested that the conformation of the hub alters upon procaspase-9 binding, involving an upward movement. Three years later, ADP-bound and WD-40-deleted Apaf-1 was crystallized (Riedl et al., 2005). Apaf-1 contains four domains, i.e. an N-terminal CARD, a nucleotide-binding and oligomerization domain (NOD), an arm, and a regulatory domain. The NOD is composed of a nucleotide-binding domain (NBD), a helical domain 1 (HD1), and a winged helix domain (WHD). The helical domain 2 (HD2) represents the arm and links the NOD with the regulatory domain. The latter is composed of WD-40 repeats which form 7- and 6-blade β-propellers (reviewed in Reubold & Eschenburg, 2012; Yuan & Akey, 2013). In the same year, the structure of the apoptosome at 12.8 Å was reported (Yu et al., 2005), and Wang's group reported that cytochrome c binding to Apaf-1 induces hydrolysis of the bound dATP to dADP, which is then replaced by dATP again (Kim et al., 2005). The nucleotide exchange has later been confirmed in an alternative model for Apaf-1 transition from its monomeric form to the apoptosome, although the preceding dATP hydrolysis step has been debated (Reubold et al., 2009). Integrating all these data, the following model for apoptosome assembly has been established. Upon binding of cytochrome c to the WD-40 repeats, Apaf-1 undergoes a conformational change and potentially hydrolyzes a bound (d)ATP. Subsequent nucleotide exchange of (d)ADP for (d)ATP generates an assembly-competent Apaf-1 monomer. In this model, seven Apaf-1 CARDs form the central ring of the apoptosome, and the seven NODs are laterally associated to form the hub. The HD2s link the hub to the cytochrome c-bound regulatory domains (Yu et al., 2005).

Ultimately, procaspase-9 is recruited to this complex via CARD-CARD interactions (Acehan et al., 2002). It should be noted that also the crystal structure of full length Apaf-1 has been reported (Reubold et al., 2011). Apparently, Apaf-1 CARD is not capped by the WD40 β-propellers but rather accessible. It has been proposed that Apaf-1 could interact with procaspase-9 already before or during apoptosome formation (Yuan & Akey, 2013). With regard to the nucleotides, either dATP or ATP promotes Apaf-1 assembly if cytochrome c is present. Considering the cellular concentrations of these nucleotides, it has been suggested that ATP/ADP likely represent the major cofactors for Apaf-1 (Reubold et al., 2009; Yuan & Akey, 2013).

Unlike other initiator caspases, the CARD-containing prodomain is not removed during apoptosis. Furthermore, it has been previously reported that caspase-9 only exerts substantial catalytic activity when bound to the apoptosome (Rodriguez & Lazebnik, 1999; Stennicke et al., 1999; Bratton et al., 2001; Bratton & Salvesen, 2010). Since there are seven Apaf-1 CARDs building the central hub of the apoptosome, it has initially been assumed that seven procaspase-9 molecules are necessary to saturate binding sites on the apoptosome (Acehan et al., 2002). However, recently it has been proposed that each apoptosome contains only 1-2 caspase-9 molecules (Malladi et al., 2009). In this study, the authors proposed that the apoptosome functions as a "molecular timer". Procaspase-9 is recruited to the apoptosome with high affinity. Then procaspase-9 either directly activates procaspase-3, or becomes autocatalytically processed. Processing reduces the affinity for the apoptosome and thus activates the timer. As long as processed caspase-9 is not replaced by another procaspase-9, it contributes to the activation of caspase-3 (Malladi et al., 2009; Bratton & Salvesen, 2010). Importantly, processing of caspase-9 enables the binding of the BIR3 domain of XIAP, which prevents caspase-9 dimerization (Srinivasula et al., 2001; Shiozaki et al., 2003; Bratton & Salvesen, 2010). Accordingly, caspase-9 processing reduces the affinity for the apoptosome and makes the protease accessible for XIAP (Bratton & Salvesen, 2010). Generally, there exist two models how caspase-9 is activated on the apoptosome: 1) the proximity-induced dimerization model, or 2) the proximity-induced association/allosteric model (alternatively termed induced conformation model) (reviewed in Thornberry & Lazebnik, 1998; Shi, 2004; Bao & Shi, 2007; Reubold & Eschenburg, 2012; Yuan & Akey, 2013). In the proximity-induced dimerization model, procaspase-9 molecules are able to process and activate each other if brought into close contact (Renatus et al., 2001; Boatright et al., 2003; Pop et al., 2006). In the proximity-induced association/allosteric model, binding of procaspase-9 to the apoptosome induces a conformational change in the monomeric form leading to activation (Rodriguez & Lazebnik, 1999; Shiozaki et al., 2002; Chao et al., 2005). Chao et al. engineered a constitutively dimeric caspase-9. Although this enzyme exhibited higher catalytic activity than wild-type caspase-9, the activity was significantly lower than that of Apaf-1-activated caspase-9 (Chao et al., 2005). Recently, two publications from Akey's group support a proximity-induced association

model (Yuan et al., 2010; Yuan et al., 2011; reviewed in Yuan & Akey, 2013). They published the structure of the apoptosome associated with caspase-9 CARD at 9.5 Å. Apparently, the central hub is mainly constructed by the NOD. Of note, each Apaf-1 CARD interacts with a caspase-9 CARD and the resulting heterodimers form a flexible tethered "disk" located above the central hub. According to their data, 5-7 procaspase-9 molecules are bound to the apoptosome to assemble the CARD-CARD disk (Yuan et al., 2010). Additionally, they calculated a 3D reconstruction of the procaspase-9 apoptosome without symmetry restraints. It was suggested that the p20/p10 catalytic domains of a single procaspase-9 molecule interact with the neighboring Apaf-1 NOD region of the central hub, thus activating a single p20/p10 pair. Most interestingly, the flexible CARD disk is acentric and tilted relative to the hub. This might indicate that the binding of additional catalytic caspase-9 subunits is sterically hindered (Yuan et al., 2011).

Next to procaspase-9, procaspase-2 contains an N-terminal CARD. In 2002, Read et al. reported that procaspase-2 is recruited to a large protein complex independent of cytochrome c and Apaf-1 (Read et al., 2002). Two years later, Tschopp's group discovered that procaspase-2 is activated within a complex containing the p53-induced protein with a death domain (PIDD) and the adapter protein RIP-associated ICH-1/CED-3 homologous protein with a death domain (RAIDD) (Tinel & Tschopp, 2004). The authors proposed that the piddosome regulates apoptosis induced by genotoxic stress. However, already in this first report describing the piddosome, additional functions of this complex were postulated (Tinel & Tschopp, 2004; Janssens & Tinel, 2012). Meanwhile, different alternative PIDD-containing platforms have been identified (reviewed in Janssens & Tinel, 2012). Apparently, the different piddosomes control processes like cell cycle, DNA repair, and NF-κB activation (Janssens & Tinel, 2012).

Downstream of the caspase-9 apoptosome, procaspase-3 is cleaved. This leads to the generation of hemiactive procaspase-3/caspase-3 dimers and completely activated caspase-3 dimers (Yuan et al., 2011). It has been previously demonstrated that active caspase-3 associates with the apoptosome, whereas procaspase-3 does not (Bratton et al., 2001). Yuan et al. also reported that caspase-3 and caspase-9 have overlapping binding sites on the apoptosome. They suggest that the hemiactive procaspase-3/caspase-3 dimers might bind to the apoptosome to increase the probability to become fully activated (Yuan et al., 2011).

The pathways of the extrinsic and the intrinsic apoptosis machinery are schematically depicted in figure 2.

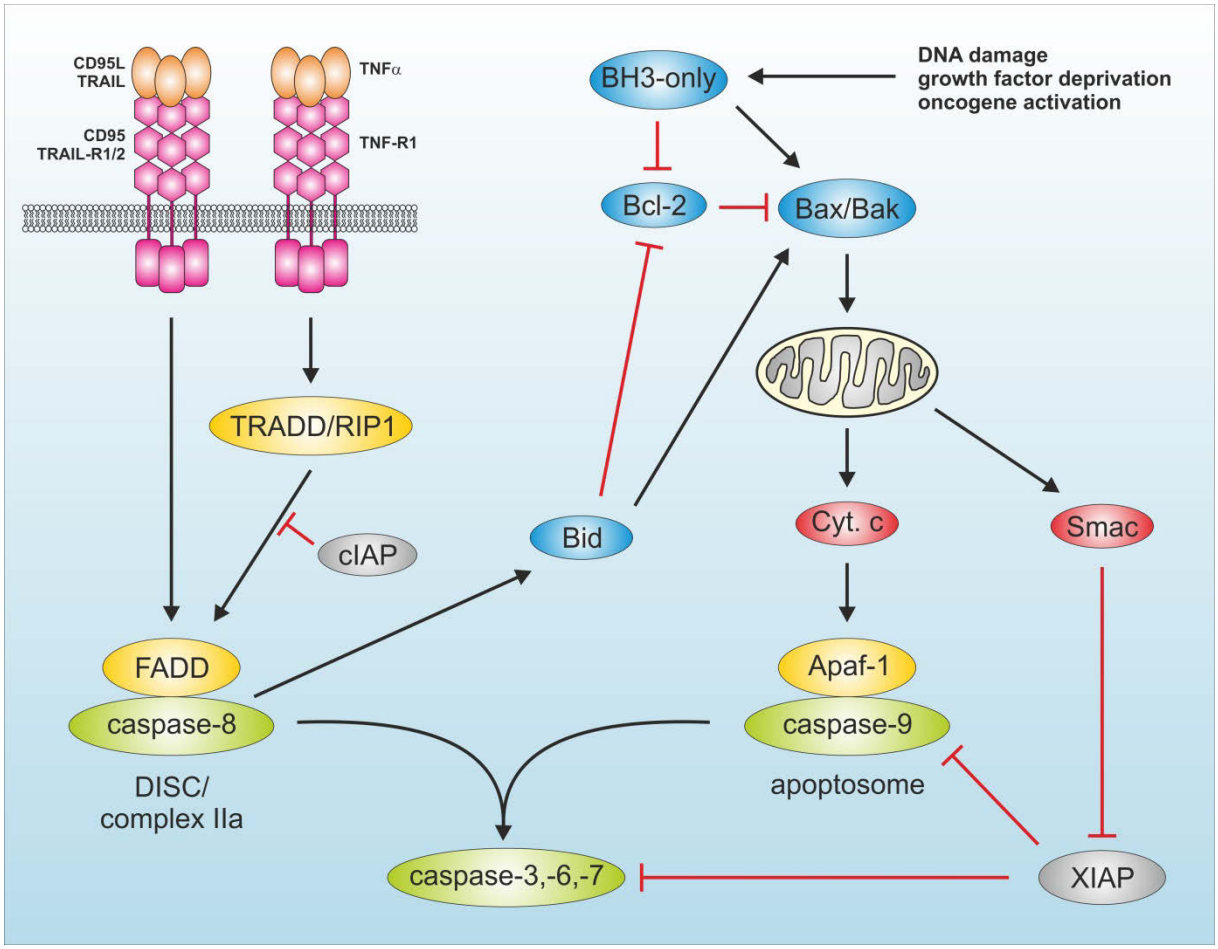

Figure 2: Signaling pathways of the extrinsic or death receptor-mediated pathway and the intrinsic mitochondrial pathway.

1.1.3 Therapies targeting apoptosis

Resisting cell death is one central hallmark of cancer (Hanahan & Weinberg, 2000; Hanahan & Weinberg, 2011). Accordingly, the apoptotic machinery represents an attractive target for therapeutic intervention. Different entry points of the apoptosis signaling pathway have been chosen for therapeutic regimens, and some of them will be briefly introduced in the following.

With regard to the death receptor signaling pathway, TRAIL and agonistic anti-TRAIL-R antibodies have already been evaluated in several clinical trials (reviewed in Dimberg et al., 2013). In contrast to CD95L and TNF, TRAIL specifically induces apoptosis in cancer cells but not in normal cells (Ashkenazi et al., 1999; Bonavida et al., 1999; Walczak et al., 1999; Dimberg et al., 2013). Furthermore, clinical trials using TRAIL-based therapies revealed low toxicity in patients (Dimberg et al., 2013). Unfortunately, TRAIL and TRAIL-R agonists also showed relatively small therapeutic effects when used as monotherapy (Dimberg et al., 2013). Accordingly, current approaches rely on the

combination of therapies, directly targeting the mechanisms contributing to TRAIL resistance (Dimberg et al., 2013). Furthermore, there is ongoing research in order to identify prognostic biomarkers in order to predict responsiveness to TRAIL therapy (Dimberg et al., 2013).

BH3 mimetics are another group of compounds which are currently evaluated in clinical trials. Per definition, BH3 mimetics bind to anti-apoptotic Bcl-2 family members and induce the intrinsic pathway of apoptosis. Accordingly, they function as sensitizers. Several BH3 mimetics have been developed so far (reviewed in Lessene et al., 2008; Leber et al., 2010a; Billard, 2012; Davids & Letai, 2012). Of these, ABT-737 is probably the best characterized one. It was discovered by Olsterdorf et al. in 2005 (Oltersdorf et al., 2005). It inhibits Bcl-2, Bcl-x_L and Bcl-w with high affinity, but does not bind Mcl-1 and A1. Accordingly, Mcl-1 expression confers resistance to tumor cells, and combination therapies with agents that inactivate Mcl-1 have been suggested (van Delft et al., 2006). In contrast to several other putative BH3 mimetics, ABT-737-induced apoptosis depends on Bax/Bak, indicating that it is an authentic BH3-mimetic (van Delft 2006). ABT-263 (navitoclax) is the oral version of ABT-737 which is currently evaluated in clinical trials. The other two BH3-mimetics which are tested in the clinic are GX15-070 (obatoclax) and AT-101 (gossypol isomer) (Billard, 2012). Both compounds bind all anti-apoptotic Bcl-2 family members with rather low affinity, and their modes of action apparently include Noxa activation, caspase-independent apoptosis, and autophagy (Billard, 2012). Recently, Gavathiotis et al. described the direct and selective small-molecule activation of pro-apoptotic Bax. The compound named Bam7 engages the “rear site” of Bax described above and thus induces Bax-dependent apoptosis (Gavathiotis et al., 2012).

In recent years, the antagonism of IAPs has also evolved as valuable therapeutic approach. Experimentally, this can be achieved by antisense nucleotides or Smac mimetics (de Almagro & Vucic, 2012). The latter are therapeutical compounds mimicking the action of Smac/DIABLO. Smac mimetics can be further subdivided into peptides, Smac-encoding polynucleotides, or small molecule compounds (Chen & Huerta, 2009). As described above, Smac interacts with IAPs via its N-terminal tetrapeptide AVPI (Srinivasula et al., 2001). This information has been exploited to design Smac mimetics either containing or mimicking this amino acid sequence. The small compound mimetics can be further subdivided into mono- or bivalent antagonists (de Almagro & Vucic, 2012). The latter can simultaneously bind to the BIR2 and BIR3 of XIAP, thus activating caspases more efficiently (de Almagro & Vucic, 2012).

1.2 Autophagy

The term autophagy originates from the Greek expressions αὐτός (autos = self) and φαγεῖν (phagein = to eat), literally meaning the self-eating of a cell. Next to the ubiquitin-proteasome system (UPS), autophagy is the second major pathway for the degradation of intracellular cargo. Autophagy occurs at basal levels in any cell to carry out the proper degradation of long-lived proteins, protein aggregates or damaged organelles, ultimately ensuring cellular homeostasis. However, different stress conditions can cause the active induction of the autophagic machinery. These stress conditions include nutrient deprivation, growth factor withdrawal, hypoxia, or pathogen infection. Of note, the basic autophagic machinery is conserved among different eukaryotes, including yeast, animals, and plants.

1.2.1 Types of Autophagy and Morphology

In 1962, Ashford and Porter observed cytoplasmic components, i.e. mitochondria or remnants thereof, in lysosomes of hepatic cells which had been perfused with glucagon (Ashford & Porter, 1962). In the same year, Novikoff and Essner observed similar mitochondria-containing vacuoles in hepatic cells from mice intravenously treated with the detergent Triton WR-1339 (Novikoff & Essner, 1962). They termed these structures cytolysomes. In 1963, Christian de Duve suggested the name “autophagic vacuoles” for these cytolysomes and “autophagy” for the process of cellular self-eating (Klionsky, 2008). In 1967, Christian de Duve and colleagues showed that glucagon indeed induces autophagy (Deter et al., 1967; Deter & De Duve, 1967; Yang & Klionsky, 2010).

Today, autophagy has become an intensely investigated field of research. This might partly be attributed to the fact that the process of autophagy or its dysregulation contribute to the onset of diverse human diseases or clinically relevant processes, including cancer, neurodegeneration, immune responses, or aging (Levine & Kroemer, 2008; Mizushima et al., 2008; Ravikumar et al., 2010; Choi et al., 2013a). There exist three types of autophagy, i.e. macroautophagy, microautophagy, and chaperone-mediated autophagy (Mizushima et al., 2011). Within chaperone-mediated autophagy, target proteins are directly recognized by cytosolic chaperones and transported across the lysosomal membrane (Mizushima et al., 2011). Microautophagy describes a process by which the lysosomal membrane directly engulfs small portions of the cytoplasm (Mizushima et al., 2011). Macroautophagy (herein referred to as autophagy) is probably the best studied type of autophagic processes. During the process of autophagy, cytoplasmic cargo is enveloped within a double-membraned vesicle, called autophagosome. Autophagosomes are transported to and fuse

with lysosomes, leading to the generation of auto(phago)lysosomes. Within autolysosomes, the sequestered cargo and the inner membrane of the autophagosome are degraded, and the resulting molecular building blocks such as amino acids or fatty acids are transported back to the cytosol through lysosomal permeases and are available for anabolic processes (Klionsky, 2007; Mizushima, 2007). Autophagy might be non-selective, leading to the bulk degradation of cytoplasm. However, in recent years different selective forms of autophagy have been identified and characterized, leading to the specific degradation of organelles or pathogens. These selective pathways include the autophagic degradation of mitochondria (mitophagy), peroxisomes (pexophagy), endoplasmic reticulum (reticulophagy), ribosomes (ribophagy), protein aggregates (aggrephagy), lipid droplets (lipophagy), spermatozoon-inherited organelles following fertilization (allophagy), secretory granules within pancreatic cells (zymophagy), or intracellular pathogens (xenophagy) (Klionsky et al., 2007; Al Rawi et al., 2012; Reggiori et al., 2012; Sato & Sato, 2012).

The formation of autophagosomes is a central hallmark of autophagy, and includes different discrete steps, i.e. nucleation, elongation and closure of the double-membraned vesicle. The cellular source of the autophagosomal membrane has been controversially discussed in the recent past. In yeast, a specific platform for the biogenesis of autophagosomes has been identified, the pre-autophagosomal structure (PAS) (Suzuki et al., 2001a). The PAS is a single punctate structure adjacent to the yeast vacuole, where most of the Atg proteins (see below) are present (Mizushima et al., 2011). From the PAS the isolation membrane (IM; also referred to as phagophore) is generated, which envelopes cytoplasmic cargo to ultimately form the complete autophagosome (Mizushima et al., 2011). In 2008, Axe et al. reported that the phosphatidylinositol 3-phosphate (PI3P)-binding protein double FYVE domain-containing protein 1 (DFCP1) translocates to a punctate compartment upon nutrient starvation in mammalian cells (Axe et al., 2008). The observed compartment is in dynamic equilibrium with the ER and provides a platform for the generation of the isolation membrane and the release of fully formed autophagosomes (Axe et al., 2008). Since these structures were seen in association with the underlying ER forming an Ω-like shape, the authors termed them “omegasomes” (Axe et al., 2008). Interestingly, so far no DFCP1 homolog has been reported for yeast (Axe et al., 2008). Two further groups confirmed the physical connection between the ER and the IM by 3D electron microscopy (Hayashi-Nishino et al., 2009; Yla-Anttila et al., 2009). One of these groups proposed that the ER forms a cradle encircling the IM (Hayashi-Nishino et al., 2009). Collectively, these results strongly suggest that the IM originates from specialized subdomains of the ER. However, different other sources have been suggested. For example, it has been reported that mitochondria supply membranes for autophagosomes during starvation (Hailey et al., 2010). Apparently, autophagosome formation is dependent on ER/mitochondria connections. It has been

proposed that these connections are necessary to transfer phosphatidylserine (PS) to the mitochondria, where PS is converted to phosphatidylethanolamine (PE). PE in turn is the target of Atg8/LC3-conjugation, which is one of two ubiquitin-like conjugation systems involved in autophagy (described below). Recently, Yoshimori's group demonstrated that autophagosomes themselves form at ER-mitochondria contact sites (Hamasaki et al., 2013). Next to the ER and mitochondria, additional sources for autophagosomal membrane lipids have been reported, including the Golgi complex, recycling endosomes, the nuclear envelope and the plasma membrane (reviewed in Tooze & Yoshimori, 2010; Mizushima et al., 2011; Longatti & Tooze, 2012). Presumably, different sources contribute to the completion of autophagosomes, presumably also depending on the autophagy-inducing stimulus and on the cargo to be degraded.

1.2.2 Molecular Regulation of Autophagy

In the late 1990's, another era of autophagy research has evolved, leading to the molecular characterization of this process (Yang & Klionsky, 2010). In 1993, Tsukada and Ohsumi reported the isolation and characterization of fifteen *S. cerevisiae* mutants that displayed defective autophagy and named them *apg1-15* (autophagy) (Tsukada & Ohsumi, 1993). Similar screens were performed by other research groups, and the identified mutants defective in either autophagy, pexophagy, or the cytoplasm-to-vacuole pathway were called *aut*, *cvt*, *pdd*, *gsa*, *pag*, or *paz*, respectively (Thumm et al., 1994; Harding et al., 1995; Titorenko et al., 1995; Yuan et al., 1997; Sakai et al., 1998; Mukaiyama et al., 2002; Klionsky et al., 2003). In 2003, Klionsky and colleagues proposed a unified nomenclature for the so-called autophagy-related genes, Atgs (Klionsky et al., 2003). Recently, Atg36 has been identified in yeast (Motley et al., 2012). Most of the yeast Atgs have homologs in the mammalian system. However, sometimes homology is only based on function but not on sequence, as will be exemplarily discussed below. Additionally, there exists one mammalian Atg, Atg101, which does not have an obvious counterpart in yeast (Hosokawa et al., 2009b; Mercer et al., 2009). Frequently, in mammals different isoforms of a certain yeast Atg exist. Furthermore, different non-Atg proteins are involved in the regulation and process of autophagy, e.g. the mammalian/mechanistic target of rapamycin (mTOR), Akt, Bcl-2, DFCP1, or vacuolar protein sorting protein 34 (Vps34), which is the catalytic subunit of the class III phosphatidylinositol 3-kinase (PI3K). Finally, different functions of Atgs in non-autophagic processes have been reported (reviewed in Subramani & Malhotra, 2013).

Functionally, mammalian Atgs can be subdivided in six functional clusters (figure 3): 1) the Ulk1-Atg13-FIP200-Atg101 protein kinase complex, 2) the PI3K class III complex containing the core proteins Vps34, p150 and Beclin 1, 3) the PI3P-binding WIPI/Atg18-Atg2 complex, 4) the multi-

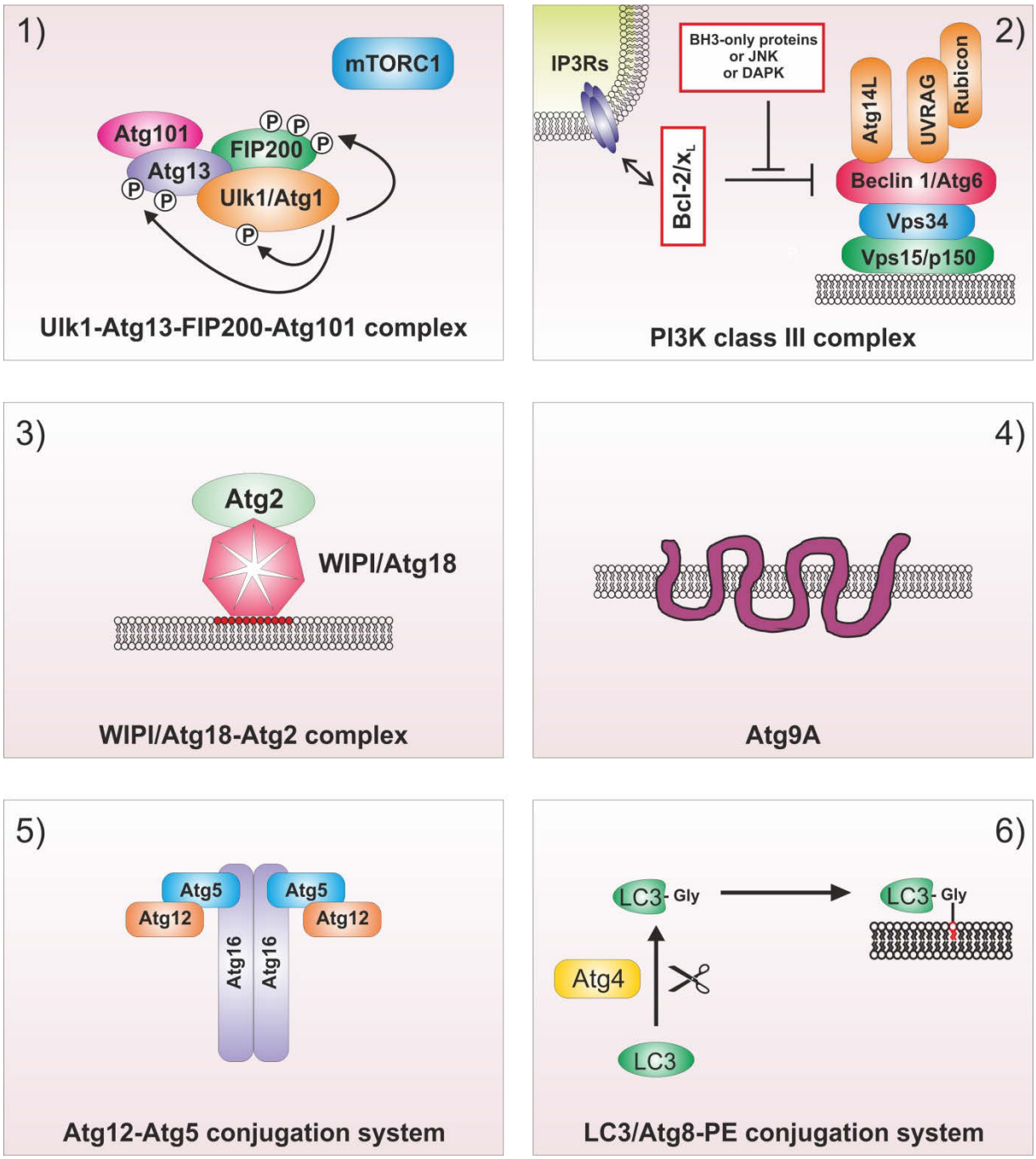

Figure 3: Functional clusters of autophagy signaling: 1) the Ulk1-Atg13-FIP200-Atg101 protein kinase complex, 2) the PI3K class III complex containing the core proteins Vps34, p150 and Beclin 1, 3) the PI3P-binding WIPI/Atg18-Atg2 complex, 4) the multi- spanning transmembrane protein Atg9A, 5) the ubiquitin-like Atg5/Atg12 system and 6) the ubiquitin-like LC3 conjugation system.

spanning transmembrane protein Atg9A, 5) the ubiquitin-like Atg5/Atg12 system and 6) the ubiquitin-like LC3 conjugation system (reviewed in Mizushima et al., 2011). These six modules regulate different steps during autophagosome biogenesis, i.e. vesicle nucleation, elongation of the autophagosomal membrane, and autophagosome completion. The role of the Ulk1-Atg13-FIP200-Atg101 kinase complex is described in section 1.2.3. This complex is centrally involved in the

initiation of autophagic processes. The autophagy-related functions of the other five modules are briefly summarized in the following.

1.2.2.1 The PI3K class III complex

Next to the Ulk1-Atg13-FIP200-Atg101 complex, a second multiprotein-complex is important for the formation of autophagosomes. In yeast, the class III phosphatidylinositol 3-kinase (PI3K class III) Vps34 functions in both autophagy and sorting of vacuolar proteins. Two separate Vps34 subcomplexes have been identified to mediate these functions (Kihara et al., 2001). The autophagy-regulating complex I contains Vps34, Vps15, Vps30, and Atg14. In contrast, the sorting of vacuolar proteins is mediated by complex II, which contains Vps38 instead of Atg14 (Kihara et al., 2001). Accordingly, the unique complex-subunits Atg14 and Vps38 regulate the intracellular localization and the specific functions of these two complexes. Atg14 mediates the localization of complex I to the PAS, whereas Vps38 controls the localization of complex II to endosomes (Obara et al., 2006; Obara & Ohsumi, 2011).

Similar to the situation in yeast, different PI3K class III complexes could be identified in mammals (reviewed in Matsunaga et al., 2009a; Funderburk et al., 2010; He & Levine, 2010; Kang et al., 2011). The mammalian PI3K class III core complex consists of the catalytic subunit Vps34, the adaptor Vps15 (p150), and Beclin 1 (Atg6). Beclin 1 forms the scaffold for the recruitment of additional activators or repressors of the PI3K class III complex. In the recent past, three major subcomplexes have been reported, which contain either Atg14L, UV radiation resistance-associated gene protein (UVRAG), or a dimer of UVRAG and RUN domain protein as Beclin 1 interacting and cysteine-rich containing (Rubicon).

Atg14-like (Atg14L; alternatively called Beclin 1-associated autophagy-related key regulator, Barkor) is the putative mammalian homolog of yeast Atg14 and was identified by four different groups (Itakura et al., 2008; Sun et al., 2008; Matsunaga et al., 2009b; Zhong et al., 2009). Accordingly, the Atg14L containing PI3K class III complex likely represents the functional equivalent to yeast complex I. Atg14L co-localizes with several marker proteins on isolation membranes, indicating that this complex is involved in an early stage of autophagy. Furthermore, Atg14L-silencing suppresses autophagosome formation (Itakura et al., 2008; Sun et al., 2008; Matsunaga et al., 2009b; Zhong et al., 2009). It has additionally been shown that Atg14L increases Vps34 catalytic activity in a Beclin 1-dependent manner (Zhong et al., 2009). Binding of Atg14L to Beclin 1 is mediated via their respective coiled coil domains (Sun et al., 2008; Matsunaga et al., 2009b; Zhong et al., 2009).

In parallel, all four groups reported that the interactions of Atg14L or UVRAG with the PI3K class III core complex are mutually exclusive, which is probably due to their overlapping binding sites in Beclin 1 (Itakura et al., 2008; Sun et al., 2008; Matsunaga et al., 2009b; Zhong et al., 2009), and accordingly it has been suggested that UVRAG represents the mammalian Vps38 (Itakura et al., 2008; Itakura & Mizushima, 2009). Along these lines, UVRAG was shown to primarily associate with Rab9-positive late endosomes and partially with Rab5/Rab7-positive endocytic compartments, and UVRAG knockdown did not influence autophagic flux and GFP-LC3 dot formation (see chapter 1.2.2.4) (Itakura et al., 2008). In contrast, UVRAG has originally been attributed a role in autophagy signaling (Liang et al., 2006). It has been reported that Beclin 1 and UVRAG interdependently induce autophagy (Liang et al., 2006). Furthermore, Takahashi et al. demonstrated that Bif-1 (also termed endophilin B1) interacts with Beclin 1 through UVRAG, and that loss of Bif-1 suppresses autophagosome formation (Takahashi et al., 2007). In parallel, Liang et al. suggest that UVRAG-mediated activation of the Beclin 1/Vps34 complex suppresses the proliferation and tumorigenicity of human colon cancer cells, and Takahashi et al. observed that Bif-1 knockout enhances spontaneous tumor development (Liang et al., 2006; Takahashi et al., 2007). However, the interplay between UVRAG-dependent autophagy and tumor suppression has also been controversially discussed. Knævelsrud et al. demonstrated that UVRAG mutations associated with microsatellite unstable colon cancer do not affect autophagy (Knaevelsrud et al., 2010). Taken together, the role of UVRAG for initial stages of autophagy remains rather elusive. In 2008, Liang et al. reported that UVRAG interacts with the class C Vps complex, which is a key component of the endosomal fusion machinery (Liang et al., 2008b). This interaction promotes the GTPase activity of Rab7 and autophagosome fusion with late endosomes/lysosomes. The authors also showed that UVRAG enhanced endocytic trafficking, directly supporting the above described UVRAG localization studies. Most interestingly, the effect on autophagosome maturation was independent of Beclin 1, indicating that UVRAG might play a dual role in autophagy regulation: 1) in combination with Beclin 1 during autophagosome formation and 2) in combination with C Vps/Rab7 during autophagosome maturation (Liang et al., 2008b).

Finally, two of the four groups additionally identified Rubicon as negative regulator of autophagy (Matsunaga et al., 2009b; Zhong et al., 2009). Rubicon is alternatively called Beclin 1 associated RUN domain containing protein (Baron) (Sun et al., 2009). Rubicon was only found in UVRAG-containing Beclin 1/Vps34-complexes, but not in Atg14L-containing ones. Furthermore, Rubicon knockdown also affected rather autophagosome maturation and endocytic trafficking (Matsunaga et al., 2009b; Zhong et al., 2009). However, Zhong et al. observed that Rubicon inhibits Vps34 kinase activity only in the absence of Beclin 1 overexpression, suggesting that the negative regulatory role exerted by Rubicon is Beclin 1-independent (Zhong et al., 2009). Supporting this notion, it has been speculated

that Rubicon interferes with pro-autophagic Rab GTPases via its RUN domain, and that sequestering of Rubicon by Beclin 1 would vice versa promote autophagy (Funderburk et al., 2010). Currently, the dynamics of the above described complexes are intensively investigated, and especially the Beclin 1-dependency of UVRAG and/or Rubicon complexes has to be clarified.

Next to the stable binding of Atg14L, UVRAG and Rubicon to Beclin 1, multiple Beclin 1-interacting proteins have been identified which bind rather transiently or specifically under certain conditions (reviewed in Funderburk et al., 2010; He & Levine, 2010; Kang et al., 2011). Importantly, these associated proteins include viral and cellular Bcl-2 homologs, thus establishing a direct connection between apoptosis and autophagy signaling pathways (see section 1.3.3) (Liang et al., 1998; Pattingre et al., 2005; Feng et al., 2007a; Maiuri et al., 2007b; Oberstein et al., 2007; Ku et al., 2008; Sinha et al., 2008; Wei et al., 2008; E et al., 2009). Additional Beclin 1-interacting proteins include AMBRA1 (Fimia et al., 2007), estrogen-receptor (John et al., 2008), FYVE-CENT (Sagona et al., 2011), HMGB1 (Kang et al., 2010; Tang et al., 2010), MyD88/TRIF (Shi & Kehrl, 2008), nPIST (Yue et al., 2002), PINK1 (Michiorri et al., 2010), Rab5 (Ravikumar et al., 2008), SLAM (Berger et al., 2010), survivin (Niu et al., 2010), and VMP1 (Ropolo et al., 2007), or the viral proteins HIV NEF (Kyei et al., 2009), HSV-1 ICP34.5 (Orvedahl et al., 2007), and the influenza virus M2 protein (Gannage et al., 2009).

The product of the PI3K class III catalytic activity is phosphatidylinositol 3-phosphate (PI3P). This lipid then recruits further downstream effectors such as DFCP1 (see above) and proteins of the Atg18/WIPI-family (see below). This has been confirmed by work from Mizushima's and Yoshimori's groups, showing that knockdown of Atg14L or Vps34 leads to the disappearance of DFCP1- or WIPI1-positive puncta, respectively (Itakura & Mizushima, 2010; Matsunaga et al., 2010).

1.2.2.2 WIPI/Atg18 proteins & Atg2

The Atg18 proteins constitute the second important family of PI3P effectors. Whereas in yeast three family members have been identified so far, i.e. Atg18, Atg21 and HSV2/Ygr223c, in mammals four Atg18 homologs have been isolated, i.e. WD-repeat protein interacting with phosphoinositides 1-4 (WIPI1-4) (Proikas-Cezanne et al., 2004; Stromhaug et al., 2004; Mizushima et al., 2011). DFCP1 binds to PI3P via its FYVE-domain, which was named after the first four proteins shown to contain it, i.e. Fab1, YOTB/ZK632.12, Vac1, and EEA1 (Stenmark et al., 1996). In contrast, the Atg18/WIPI proteins bind to PI3P (and $PI3,5P_2$) via a seven-bladed β-propeller. Accordingly, the three yeast proteins and the four WIPIs have been called "PROPPINs" (Michell et al., 2006). These proteins are WD40-repeat containing proteins and require an FRRG-motif for PI3P-binding (Dove et al., 2004; Jeffries et al.,

2004; Stromhaug et al., 2004). Recently, two groups reported the crystal structure of yeast HSV2/Ygr223c, and these works indicate that there are two phosphoinositide binding sites in PROPPINS (Baskaran et al., 2012; Krick et al., 2012). Yeast Atg18 is important for autophagy, whereas Atg21 and HSV2/Ygr223c are rather involved in the Cvt pathway and in micronucleophagy, respectively (Barth et al., 2001; Barth et al., 2002; Krick et al., 2008; Mizushima et al., 2011). In 2010, Nair et al. reported that Atg18 and Atg21 facilitate the recruitment of Atg8–PE to the site of autophagosome formation (Nair et al., 2010). During autophagy, Atg18 is in complex with Atg2 (Obara et al., 2008), and recently it was demonstrated that autophagosome formation can be achieved in the absence of Atg18 by expressing engineered PAS-targeted Atg2 (Kobayashi et al., 2012). In mammals, WIPI1 and WIPI2 share highest homology to Atg18 and have thus been reported to be involved in autophagy (Polson et al., 2010). During autophagosome biogenesis, WIPI1/2 colocalize with the Beclin 1/Vps34 complex component Atg14L, but not with the second PI3P effector DFCP1 (Itakura & Mizushima, 2010; Mizushima et al., 2011). It has been suggested that WIPI1/2 localize to the isolation membrane, whereas DFCP1 localizes to the omegasome (Mizushima et al., 2011). Subsequently it was demonstrated that WIPI2 positively regulates LC3-lipidation (see below) and thus obviously contributes to the maturation process of omegasomes to autophagosomes (Polson et al., 2010). Two mammalian Atg2 homologs have been identified, Atg2A and Atg2B, and their simultaneous silencing causes a block in the autophagic flux (Velikkakath et al., 2012). Interestingly, Atg2A/B also regulate lipid droplet morphology (Velikkakath et al., 2012).

1.2.2.3 Atg9/Atg9A

Atg9 is the only multi-spanning transmembrane protein among the Atgs (reviewed in Tooze, 2010; Webber & Tooze, 2010). In yeast, it was demonstrated that Atg9 concentrates in clusters comprised of vesicles and tubules, and that these compartments contribute to the *de novo* formation of the PAS (Mari et al., 2010). Recently, Ohsumi's group reported that single-membrane and Golgi-derived Atg9-vesicles with a diameter of 30-60 nm assemble to the PAS upon starvation (Yamamoto et al., 2012). These vesicles apparently become part of the isolation membrane and the outer autophagosomal membrane. Upon autophagosome completion, Atg9 clusters are recycled back to the cytoplasm (Yamamoto et al., 2012). It has been shown earlier that Atg9 is recruited to the PAS by Atg17 and that Atg9 cycling depends on Atg1-Atg13 and Atg18-Atg2 complexes, respectively (Reggiori et al., 2004; Sekito et al., 2009). However, it has been noted that the Atg9-positive vesicles described above are unlikely a major supplier of lipids for autophagosome biogenesis (Yamamoto et al., 2012). In 2006, it has been reported that the mammalian Atg9 ortholog Atg9A (also referred to as mAtg9 or Atg9L1) is localized in the trans-Golgi network and in early, late and recycling endosomes (Young et al., 2006; Orsi et al., 2012). Upon starvation, Atg9A is redistributed to peripheral, endosomal

membranes positive for the autophagosomal marker GFP-LC3 (see below) (Young et al., 2006). Like in yeast, this redistribution depends on the mammalian Atg1 homolog Ulk1, which will be explained in detail in chapter 1.2.3 (Young et al., 2006). Recently an Atg9A compartment in mammals has been proposed which is similar to the one observed in yeast (Orsi et al., 2012). The authors suggest that Atg9A resides on a distinct tubular-vesicular compartment, and that this "Atg9 reservoir" continuously emanates from vacuolar recycling endosome-like structures by tubulation. They observed that subcellular Atg9A localization is regulated by Ulk1 and WIPI2. However, Ulk1 and WIPI2 are not required for the recruitment of Atg9A to early DFCP1-positive omegasomes (Orsi et al., 2012). Similar observations were previously made by other groups. For example, it has been demonstrated that Atg9A and Ulk1 independently localize to the autophagosome formation site during canonical autophagy and Parkin-mediated mitophagy (see below), and that Atg9A and Ulk1 are independently recruited to *Salmonella*-containing vacuoles during xenophagy (Kageyama et al., 2011; Itakura et al., 2012a). Although Atg9A is essential for the formation of phagophores, it appears that Atg9A only transiently interacts with autophagosomes and does not integrate into the autophagosomal membrane (Orsi et al., 2012).

1.2.2.4 Two ubiquitin-like conjugation systems in autophagy: Atg12-Atg5 and Atg8-PE

Two ubiquitin-like conjugation systems are centrally involved in the expansion of autophagosomes: 1) Atg12-Atg5 system and 2) Atg8-phosphatidylethanolamine (PE) system (reviewed in Geng & Klionsky, 2008). Within these conjugation systems, Atg12 and Atg8 represent the ubiquitin-like proteins, which are conjugated by E1-, E2- and E3-like enzymatic activities to Atg5 and PE, respectively. Within the first system, Atg12 is activated by the E1-like enzyme Atg7. Subsequently Atg12 is transferred to the E2-like Atg10 and irreversibly conjugated to K130 (human sequence) of Atg5 (Mizushima et al., 1998a; Shintani et al., 1999; Tanida et al., 1999; Geng & Klionsky, 2008). So far the existence of an E3-like activity for the Atg12-Atg5 system has not been identified, and it appears that Atg5 is the only target of the ubiquitin-like Atg12 (Geng & Klionsky, 2008). The Atg12–Atg5 conjugate interacts with Atg16, and this complex forms a homo-oligomer (Mizushima et al., 1999; Kuma et al., 2002; Geng & Klionsky, 2008). All yeast Atgs involved in the Atg12-Atg5 conjugation system have mammalian counterparts with identical or similar functions, including an Atg16-like protein (Atg16L) (Mizushima et al., 1998b; Tanida et al., 2001; Mizushima et al., 2002; Mizushima et al., 2003; Geng & Klionsky, 2008). In yeast, this multimeric complex has a molecular weight of approximately 350 kDa, and it has been suggested that the complex consists of an Atg12–Atg5-Atg16 tetramer (Kuma et al., 2002). In mammals, the complex eluted in fractions corresponding

to 400 kDa and 800 kDa, indicating that it might be composed of four or eight sets of Atg12–Atg5-Atg16L (Mizushima et al., 2003). However, a crystallographic study combined with analytical ultracentrifugation experiments revealed that yeast Atg16 forms a parallel coiled-coil dimer (Fujioka et al., 2010). The E1-like Atg7, the E2-like Atg3 and the conjugation acceptor Atg5 are essential for autophagy, and neonates of *Atg7*-/-, *Atg3*-/- and *Atg5*-/- mice die at day 1 after birth due to the neonatal starvation period (Kuma et al., 2004; Komatsu et al., 2005; Sou et al., 2008). Within the second conjugation system, Atg8 is activated by the common E1-like enzyme Atg7 and then transferred to the E2-like Atg3 (Ichimura et al., 2000; Geng & Klionsky, 2008). However, prior to Atg8 activation by Atg7, the C-terminal R117 has to be removed by the proteolytic activity of Atg4 in order to expose G116 (Kirisako et al., 2000; Geng & Klionsky, 2008). Interestingly, it has been demonstrated that the Atg12–Atg5 conjugate possesses an E3-like activity for Atg8 conjugation to PE (Hanada et al., 2007; Fujioka et al., 2008). Although Atg16 is not important for efficient Atg8-PE conjugation *in vitro*, it is required for Atg8-PE formation *in vivo* (Hanada et al., 2007). Atg16 recruits Atg12–Atg5 to the PAS and thus determines the site of Atg8 lipidation (Suzuki et al., 2001a; Suzuki et al., 2007). Two recent structural reports further support this link between the two conjugation systems. First, the crystal structure of Atg12–Atg5 indicates that Atg12 serves as binding module for the E2-like Atg3, essentially facilitating the transfer of Atg8 from Atg3 to the PE in the membrane (Noda et al., 2013). Second, apparently the Atg12–Atg5 conjugate enhances the E2 activity of Atg3 by rearranging its catalytic site (Sakoh-Nakatogawa et al., 2013).

In the mammalian system, so far nine Atg8 orthologs have been reported. These can be subdivided into two families: 1) the LC3 subfamily consisting of microtubule-associated proteins 1A/1B light chain 3A (MAP1LC3A or briefly LC3A; two splice variants), LC3B, LC3B2, and LC3C, and 2) the GABARAP-GATE16 subfamily consisting of the γ-aminobutyric acid receptor associated protein (GABARAP), GABARAPL1 (also termed Atg8L or GEC1), Golgi-associated ATPase enhancer of 16 kDa (GATE16, also termed GABARAPL2) and GABARAPL3 (Paz et al., 2000; Xin et al., 2001; He et al., 2003; Hemelaar et al., 2003; Tanida et al., 2003; Kabeya et al., 2004; Tanida et al., 2006; Weidberg et al., 2010; Shpilka et al., 2011; Bai et al., 2012). Additionally, four different mammalian Atg4 isoforms have been identified, i.e. Atg4A-D (also referred to as autophagin-1-4) (Marino et al., 2003; Scherz-Shouval et al., 2003). LC3B is probably the most extensively studied mammalian Atg8 protein, and it is cleaved C-terminally of G120 within the first six minutes of synthesis (Kabeya et al., 2000; Kabeya et al., 2004). Atg4-mediated cleavage of LC3 generates a cytosolic truncated LC3-I fragment of 18 kDa, which lacks the 22 C-terminal amino acids of the pro-form (Kabeya et al., 2000). Interestingly, the different Atg4 isoforms possess selective preferences regarding their Atg8 family substrates (Kabeya et al., 2004; Li et al., 2011b). Subsequently, LC3-I is converted to the lipidated LC3-II isoform

in an E1/E2/E3-cascade similar to the yeast system (Tanida et al., 2001; Tanida et al., 2002; Kabeya et al., 2004). Accordingly, the mammalian Atg12-Atg5 conjugate interacts with Atg16L, which targets the conjugate to the isolation membrane (Mizushima et al., 2001; Mizushima et al., 2003). There the Atg12–Atg5-Atg16L complex exerts its E3-like function and thus determines the site of LC3 lipidation (Fujita et al., 2008). This has been supported by the observation that forced expression of Atg16L1 at the plasma membrane led to ectopic LC3 lipidation at that site (Fujita et al., 2008). Similarly to LC3 conversion, the other mammalian Atg8 family members are processed by Atg4 isoforms, form E1- and E2-intermediates with Atg7 and Atg3, and are targeted to the autophagosome (Tanida et al., 2001; Tanida et al., 2002; Tanida et al., 2003; Kabeya et al., 2004; Tanida et al., 2004).

The detection of PE-conjugated GFP-LC3 at the autophagosomal double-membrane by confocal laser scanning microscopy is an established method for the analysis of autophagic processes (Klionsky et al., 2012). This method has even been optimized by using the tandem fluorescence mRFP-EGFP-LC3 fusion protein (Kimura et al., 2007). Upon fusion of mature autophagosomes with lysosomes, the resulting low pH quenches the GFP fluorescence and accordingly autolysosomes can be detected as RFP-only structures (Kimura et al., 2007). By this means, the autophagic flux can be monitored. Recently, an improved tandem fluorescence-tagged mTagRFP-mWasabi-LC3 has been described, which is more acid-sensitive (Zhou et al., 2012). Alternatively, the conjugation of LC3 to PE can also be detected by immunoblot analysis, since the lipidated LC3-II exhibits a slightly increased mobility in SDS-PAGE compared to the unlipidated LC3-I. In contrast to the Atg12-Atg5 conjugate, Atg8/LC3 proteins can be deconjugated from PE by the activity of Atg4 isoforms (Kirisako et al., 2000). Recently, the importance of this deconjugation reaction has been characterized. It appears that it is important to maintain an appropriate supply of Atg8/LC3 at early stages of autophagy, and to facilitate the maturation into fusion-capable autophagosomes at later stages (Yu et al., 2012).

Both conjugates, i.e. Atg12-Atg5 and Atg8/LC3-PE, are targeted to membranes during the autophagic process. Whereas Atg12-Atg5-Atg16L is mainly found at the isolation membrane (Mizushima et al., 2001; Mizushima et al., 2003), Atg8/LC3-PE is present on the autophagosomal membrane throughout the whole process of vesicle biogenesis. The exact function of this “decoration” of the autophagosomal membrane is still intensely investigated. In 2007, Ohsumi’s group reported that Atg8 mediates the tethering and hemifusion of liposomes *in vitro*, and the authors suggested that this function contributes to the expansion of the isolation membrane *in vivo* (Nakatogawa et al., 2007). Additionally, it has been reported that the amount of Atg8 determines the size of autophagosomes (Xie et al., 2008). Generally it is tempting to speculate that the different Atg8 family proteins are selectively incorporated into the autophagosomal membrane depending on the autophagic stimulus, the step during the autophagic flux, or the cargo to be degraded. The latter two

aspects are supported by two recent manuscripts. The first manuscript proposes that LC3 proteins are rather involved in the elongation of the autophagosomal membrane whereas GATE-16/GABARAP proteins function during the later stages of autophagosome maturation (Weidberg et al., 2010). The second work reports that LC3C is required for efficient xenophagic clearance of *Salmonella Typhimurium* (von Muhlinen et al., 2012). This observation leads over to the best studied function of Atg8 family proteins, i.e. enabling the cell to differentially handle the cargo during selective autophagy. In recent years, a new class of cargo-recognition receptors has been identified and characterized, and they have been termed autophagy receptors or adapters (Kirkin et al., 2009b; Dikic et al., 2010; Kraft et al., 2010; Sumpter & Levine, 2010; Johansen & Lamark, 2011; Shaid et al., 2013). These autophagy receptors are centrally involved in the recognition of cargo during selective autophagy processes, e.g. mitophagy or xenophagy. In 2005, Bjørkøy et al. discovered that p62 (alternatively called sequestosome 1) forms protein aggregates which are degraded by autophagy (Bjorkoy et al., 2005). In turn, inhibition of autophagy resulted in an increase of p62 protein levels. The authors suggested that p62 links polyubiquitinated proteins to the autophagic machinery via LC3. The same group could demonstrate that p62 directly binds to Atg8/LC3 (Pankiv et al., 2007). They found an evolutionarily conserved 22-residue amino acid sequence within p62 which mediates the binding to LC3. This region was dubbed the LC3-interacting region (LIR), LC3 recognition sequence (LRS), or Atg8-family interacting motif (AIM), respectively (Pankiv et al., 2007; Ichimura et al., 2008; Noda et al., 2010). Johansen et al. compiled a sequence logo from 25 different LIR motifs from 21 different proteins. It appears that LIR motif contains eight amino acids and is $X_{-3}X_{-2}X_{-1}W_0X_1X_2L_3$ (Johansen & Lamark, 2011). In this sequence, W might be replaced by F or Y (aromatic residue), L by I or V (large, hydrophobic residue), and acidic amino acids are frequently found in the $X_{-3}X_{-2}X_{-1}$ positions. This suggestion was later confirmed by a compilation of 26 published LIR sequences (Alemu et al., 2012). Next to the LIR, p62 possess an ubiquitin-associated (UBA) domain and a Phox and Bem1p (PB1) domain, through which p62 can homo-oligomerize or bind to protein kinases. Accordingly, Johansen et al. proposed three required features of autophagy receptors: 1) existence of a LIR motif, 2) specific recognition of cargo, and 3) ability to polymerize (Johansen & Lamark, 2011). Interestingly, Mizushima's group demonstrated that the targeting of p62 to the autophagosome formation site depends on the ability to self-associate, but not on LC3 or any other classical Atg (Itakura & Mizushima, 2011). The authors suggest that subsequently p62 oligomers are incorporated into autophagosomes in an LC3-dependent manner. In addition to p62, several other autophagy receptors have been identified to date, including neighbour of breast cancer 1 (NBR1), optineurin (OPTN), nuclear domain 10 protein 52 (NDP52), or cellular Casitas B-lineage lymphoma (c-Cbl) (Kirkin et al., 2009a; Thurston et al., 2009; Wild et al., 2011; Sandilands et al., 2012; reviewed in Kirkin et al., 2009b; Dikic et al., 2010; Kraft et al., 2010; Sumpter & Levine, 2010; Johansen &

Lamark, 2011; Shaid et al., 2013). C-Cbl was shown to target active Src tyrosine kinase to autophagosomes (Sandilands et al., 2012). Of note, this targeting is mediated by the LIR of c-Cbl, but does apparently not involve the ubiquitin-binding domain of c-Cbl (Sandilands et al., 2012; Shaid et al., 2013). Next to autophagy receptors which interact with both ubiquitin and LC3, other proteins have been identified which contribute to selective autophagy processes. These include proteins which interact with ubiquitin (e.g. HDAC6), which bind to LC3 (e.g. Nix), or which indirectly associate with ubiquitinated proteins or LC3 (e.g. Alfy, BAG3, or Tecpr1) (reviewed in Shaid et al., 2013). Nix is a mitochondrial protein and is involved in the mitochondrial clearance during developmental processes, e.g. the maturation of erythrocytes (Novak et al., 2010). In contrast, mitophagy of damaged mitochondria involves the action of PTEN-induced putative protein kinase 1 (PINK1) and the E3 ubiquitin ligase Parkin (reviewed in Youle & Narendra, 2011; Novak, 2012; Ashrafi & Schwarz, 2013). It has been suggested that Parkin hyper-ubiquitinates targets in the outer mitochondrial membrane, which are then recognized by p62. However, the involvement of p62 in damage-induced mitophagy is controversially discussed (reviewed in Youle & Narendra, 2011; Novak, 2012; Ashrafi & Schwarz, 2013). Recently, the Parkin-dependent ubiquitylome in response to mitochondrial depolarization has been reported (Sarraf et al., 2013). Furthermore, the authors found depolarization-dependent association of Parkin with numerous targets of the mitochondrial outer membrane, autophagy receptors, and the proteasome. Interestingly, the autophagy receptors p62, NDP52, and Tax1BP1 were found to be depolarization-dependently ubiquitinated and associated with Parkin (Sarraf et al., 2013). Future studies will have to delineate how ubiquitin signals regulate the selection of autophagy cargo. It is likely that additional autophagy receptors will be identified in the future, and next to “classical” autophagy receptors other forms of receptors will emerge. For example, cargo recognition by Tecpr1 is ubiquitin-independent. Instead, Tecpr1 binds to Atg5 and WIPI2 (Behrends et al., 2010; Ogawa et al., 2011). Finally, post-translational modifications such as phosphorylation might influence the function of autophagy receptors and presumably the cargo selection process, as shown for p62 and optineurin (Matsumoto et al., 2011; Wild et al., 2011).

Although the lipidation of LC3 is the basis for several standard detection methods of autophagy – including LC3 turnover assay by immunoblotting or puncta detection of fluorescently-labeled LC3 by confocal microscopy – several caveats have to be considered. Apparently, LC3 lipidation can occur in an autophagy-independent manner (reviewed in Mizushima et al., 2010). LC3-II can be detected in cells in which certain Atgs are deleted, e.g. in *Fip200*-/- MEFs (Hara et al., 2008), *Becn1*-/- ES cells (Matsui et al., 2007), *BECN1*-/- DT40 (own unpublished observation), *Ulk1*-/- MEFs (Kundu et al., 2008; Jung et al., 2009), *Ulk1/2*-/- MEFs (Cheong et al., 2011; McAlpine et al., 2013), or in cells in which certain Atgs are severely reduced by RNAi, e.g. Beclin 1 (Zeng et al., 2006; Matsui et al., 2007), Atg13 (Chan et al., 2009; Hosokawa et al., 2009a; Jung et al., 2009), Ulk2 (Jung et al., 2009), Atg14L

(Itakura et al., 2008), or Vps34 (Itakura et al., 2008). A similar observation was made for the yeast system. Atg8-PE was detected in yeast strains deficient for Atg1, Atg2, Atg6, Atg9, Atg13, Atg14, Atg16, or Atg17, and slightly also in strains deficient for Atg 5 or Atg12 (Suzuki et al., 2001a). These observations indicate that LC3 is lipidated under conditions in which the autophagic flux is inhibited. Along these lines, in 2007 Green's group described that particles that engage TLRs on macrophages while they are phagocytosed trigger LC3 recruitment to the phagosome (Sanjuan et al., 2007). This processed was termed LC3-associated phagocytosis (LAP). LAP requires Atg5 and Atg7 and is preceded by Beclin 1 recruitment and PI3K kinase activity (Sanjuan et al., 2007). Importantly, LC3 recruitment to the phagosomes was not associated with observable double-membrane structures. Next to TLR ligand-coated particles, LAP was observed upon phagocytosis of beads with LPS, killed yeast, or *E. coli* bacteria (Sanjuan et al., 2007). This indicates that autophagy proteins contribute to the elimination of pathogens not only through canonical autophagy/xenophagy, but also through LAP. Finally, a similar decoration of single membrane structures with LC3 was also described for phagosomes containing apoptotic cells, macropinosomes, and entotic vacuoles (Florey et al., 2011; Martinez et al., 2011; reviewed in Florey & Overholtzer, 2012).

1.2.2.5 Final stage of autophagy: autophagosome-lysosome fusion

The final step of the autophagic flux has elucidated on the molecular level in the recent past. Upon closure of the mature autophagosome, almost all Atgs detach from the autophagosomal membrane except for LC3. Mizushima's group demonstrated that subsequently the soluble N-ethylmaleimide-sensitive factor attachment protein receptor (SNARE) protein syntaxin 17 (Stx17) translocates to the outer autophagosomal membrane (Itakura et al., 2012b). Fusion with lysosomes is then mediated by the interaction between autophagosome-resident Stx17, synaptosomal-associated protein 29 (SNAP-29), and the lysosome-resident vesicle-associated membrane protein 8 (VAMP8) (Itakura et al., 2012b).

1.2.3 The Ulk1-Atg13-FIP200-Atg101 complex

1.2.3.1 The yeast Atg1-Atg13-Atg17 complex

In 1997, Ohsumi`s group showed that the *apg1/atg1* gene discovered in their first screen for autophagy-defective yeast strains encodes a protein kinase (Apg1p/Atg1), and they reported an overall homology to *C. elegans* UNC-51 protein (Matsuura et al., 1997). Furthermore, they showed

that Atg1 overexpression suppressed the autophagy-defective phenotype in the *Δapg13/atg13* strain, indicating a linkage between Atg1 and Atg13 (Funakoshi et al., 1997). In the following years, it was demonstrated that Atg1 and its associated proteins are centrally involved in the initiation of autophagic processes, and the exact molecular details were deciphered. Of note, yeast Atg1 associates with pathway-specific sets of Atg proteins, regulating either canonical autophagy or the yeast-specific cytoplasm-to-vacuole targeting (Cvt) pathway, respectively (reviewed in Mizushima, 2010; Alers et al., 2012b; Alers et al., 2012a; Wong et al., 2013). During canonical autophagy, Atg1 associates with Atg13, Atg17, Atg29 and Atg31. In contrast, during the Cvt pathway, Atg1 interacts with Atg11, Atg13, Atg20, Atg24 and Vac8 (Mizushima, 2010). Accordingly, Atg17, Atg29 and Atg31 are selectively important for autophagy (Kamada et al., 2000; Kawamata et al., 2005; Kabeya et al., 2007). These three Atgs form a ternary 2:2:2-stoichiometric complex, which is constitutively assembled and represents a scaffold for the recruitment of further Atgs to the PAS (Suzuki et al., 2007; Kawamata et al., 2008; Kabeya et al., 2009). Upon starvation, Atg1 binds to Atg17, and this association is primarily mediated by Atg13 (Cheong et al., 2005; Kabeya et al., 2005). Both the Atg1-Atg13 kinase complex and the autophagy-specific Atg17-Atg29-Atg31 complex cooperatively regulate the subsequent recruitment of downstream Atgs to the PAS, and for this function their physical interaction is mandatory (Cheong et al., 2008; Kawamata et al., 2008). It has been suggested that Atg1 fulfills a structural role during early steps of PAS organization, and that Atg1 kinase activity regulates the dynamics of Atg movement at the PAS (Cheong et al., 2008).

In 1998, Noda and Ohsumi reported that autophagy is negatively regulated by the protein kinase target of rapamycin (TOR), and that rapamycin accordingly induces the autophagic flux (Noda & Ohsumi, 1998). Two years later, Kamada et al. published a pioneering work demonstrating that this TOR-dependent control of autophagy is mediated by the Atg1 kinase complex (Kamada et al., 2000). The authors observed that both starvation and rapamycin enhanced the kinase activity of Atg1. Furthermore, Atg13 is hyperphosphorylated by TOR, resulting in a reduced affinity to Atg1. Accordingly, rapamycin treatment favors the dephosphorylation of Atg13 and its association with Atg1, resulting in increased Atg1 activity. Finally, the authors reported that rapamycin-induced Atg1 activity was decreased in the *Δatg17* strain, indicating that both Atg13 and Atg17 are important for Atg1 activation (Kamada et al., 2000). Subsequently the same group discovered that TOR phosphorylates Atg13 at S437, S438, S646, and S649. The authors mutated these four sites and four additional putative TOR sites (S348, S496, S535, S541) to alanines, and demonstrated that phosphorylation of the Atg13-8SA mutant was largely eliminated. Most importantly, expression of the non-phosphorylatable Atg13-8SA mutant induced autophagy independently of TOR activity or nutrient status, apparently mimicking rapamycin treatment (Kamada et al., 2010).

Notably, a recent work reports that Atg1 and Atg13 constitutively interact *in vivo*, irrespective of nutrient availability (Kraft et al., 2012). Of note, this situation would resemble the Ulk1 complex constitution in higher eukaryotes (see below). Although the authors confirmed that binding of Atg13 to Atg1 indeed promotes its kinase activity and is important for efficient autophagy *in vivo*, the described observation would suggest that Atg1 activation in yeast is not exclusively controlled by regulated Atg13 binding, but rather involves additional levels of control. This could include conformational alterations or recruitment of additional factors regulated by the Atg13 phospho-status. Additionally, Atg1 phosphorylation itself appears to be important for activation. The last aspect has already been confirmed by two independent studies. Kijanska et al. identified 29 phosphorylation sites in Atg1, of which five were up- or down-regulated upon rapamycin treatment (Kijanska et al., 2010). Two sites (T226 and S230) are located in the activation loop of the kinase domain, and mutation of either of these two sites abolished Atg1 kinase activity and its function in autophagy (Kijanska et al., 2010). The authors already speculated that these two sites represent trans-autophosphorylation sites which rely on transient dimerization of Atg1. Autophosphorylation of T226 was confirmed by Yeh et al., and they additionally showed that this modification was increased by stimuli inducing autophagy (Yeh et al., 2010). Furthermore, T226 phosphorylation of Atg1 required the presence of Atg13 and Atg17 (Yeh et al., 2010). One year later the same group demonstrated that Atg13-promoted self-interaction of Atg1 is a prerequisite for the subsequent T226 autophosphorylation within the Atg1 activation loop (Yeh et al., 2011). However, next to TOR-regulation and Atg1 autophosphorylation additional kinases have been implicated in the regulation of the yeast Atg1-Atg13 complex, including PKA, Ksp1, Sch9, which is the yeast ortholog of mammalian Akt or p70S6K, or Snf1p, which is the yeast ortholog of the mammalian AMP-activated protein kinase (AMPK) (Wang et al., 2001; Budovskaya et al., 2005; Yorimitsu et al., 2007; Stephan et al., 2009; Umekawa & Klionsky, 2012). Additionally, the phospho-status of the Atg1-Atg13 complex is likely to be regulated by phosphatases. For example, the Tap42-PP2A signaling pathway has been shown to regulate the initiation of autophagy, and autophagosome formation induced by Tap42-inhibition depends on Atg1 (Yorimitsu et al., 2009). With regard to the downstream Atg1 substrates which regulate the initiation of autophagy in yeast, the current knowledge is less complete. As described above, Atg9 cycling depends on Atg1-Atg13, but apparently the kinase activity of Atg1 is not important (Reggiori et al., 2004). Although different *in vitro* substrates have been identified for Atg1 by a global phosphorylation analysis, including Atg8 and Atg18, their *in vivo* relevance awaits further confirmation (Ptacek et al., 2005).

1.2.3.2 The Ulk1-Atg13-FIP200-Atg101 complex in higher eukaryotes

Atg1 has orthologs in the nematode *C. elegans* and the fruit fly *D. melanogaster*, i.e. UNC-51 and Atg1, respectively. In mammals, so far five orthologs have been identified, i.e. Ulk1, Ulk2, Ulk3, Ulk4, and STK36 (also termed fused) (reviewed in Chan & Tooze, 2009; Mizushima, 2010; Alers et al., 2012b; Alers et al., 2012a; Wong et al., 2013). In 1998, murine Ulk1 was cloned and its similarity to yeast Atg1 and *C. elegans* UNC-51 was reported (Yan et al., 1998). Ulk1 consists of an N-terminal serine/threonine protein kinase domain, followed by a proline/serine (P/S)-rich domain and a conserved C-terminal domain (CTD). Shortly afterwards the same group reported the identification of human Ulk1 and murine Ulk2, respectively (Kuroyanagi et al., 1998; Yan et al., 1999a). In 2007, Tooze's group performed an siRNA screen of the kinome and identified Ulk1 as an autophagy-modulating kinase (Chan et al., 2007). Knockdown of Ulk1 in HEK293 cells blocked the autophagic response upon amino acid starvation or rapamycin treatment, respectively. Additionally, the authors described distinct functional regions of Ulk1. Overexpression of kinase-active or kinase-dead Ulk1 (K46R) inhibited autophagy to a similar extent. Furthermore, truncated versions of kinase-active Ulk1 lacking either the CTD (aa 829-1051 of human Ulk1) or the last three C-terminal amino acids VYA exhibited an increased dominant negative effect. These last three C-terminal amino acids represent a PDZ domain-binding motif (named according to the first three proteins discovered to share this domain, i.e. PSD95, Dlg1, zo-1). The authors were able to map down the minimal region necessary for the dominant negative effect to aa 1-351 of Ulk1, encompassing the kinase domain (aa 1-278) and a region containing autophosphorylation sites (Yan et al., 1998; Chan et al., 2007). Subsequently, Mizushima's group reported that Ulk1 and Ulk2 co-localize with Atg16L1 and are accordingly targeted to the IM (Hara et al., 2008). Interestingly, these Ulk1/2 puncta could not be detected in *Atg5*-/- MEFs. However, this observation was later re-fined by the same group. It appears that Atg5 is not required for the recruitment of Ulk1 to the IM, but possibly important for keeping Ulk1 at the membrane (Itakura & Mizushima, 2010). Mizushima's group also analyzed the importance of Ulk1 kinase activity. They observed that overexpression of kinase-dead Ulk1 (K46N) functions as a dominant-negative mutant (Hara et al., 2008). In contrast, overexpression of wild-type Ulk1 led to morphologic alterations of the cell and was cytotoxic (Hara et al., 2008). These results are similar to observations made upon Atg1 overexpression in *D. melanogaster*, which results in apoptotic cell death (Scott et al., 2007). In 2009, a work by Tooze's group re-assessed the dominant negative effect of the Ulk1 kinase-dead version (Chan et al., 2009). This time the authors generated a K46I mutant and detected a stronger dominant negative effect compared to wt Ulk1 or the K46R mutant described above. Apparently, the kinase activity of Ulk1 has to be significantly lowered to transform Ulk1 into a dominant negative protein (Chan et al., 2009). Accordingly, autophosphorylation was

severely impaired in the K46I version. The dominant-negative potency of the kinase-dead Ulk1 was unaltered when the PDZ-domain-binding motif was deleted, but depended on a 7-residue motif within the CTD (aa sequence: IERRLSA) (Chan et al., 2009). Collectively, these data led the authors to propose a model in which the reduced autophosphorylation of kinase-dead Ulk1 causes a conformational change resulting in the exposure of the dominant-negatively acting CTD. Notably, knockdown of Ulk2 did not reveal any effect on autophagy induction in HEK293 cells, indicating that at least in this cellular system Ulk1 and Ulk2 cannot compensate each other during autophagy induction (Chan et al., 2007). However, compensatory roles of these two kinases can be deduced from the corresponding knockout mouse models. Ulk1-deficient mice are viable and survive neonatal starvation periods (Kundu et al., 2008). Nonetheless, these mice reveal a delayed clearance of mitochondria from reticulocytes, indicating some differential roles of Ulk1 and Ulk2 for selective autophagy in general and for mitophagy in particular. Similarly, *Ulk2*-/- mice are viable and do not show an overt autophagy phenotype (Cheong et al., 2011). In contrast, Ulk1/2-double-deficient mice die shortly after birth, similar to mice deficient for Atg3, Atg5 or Atg7 (see above) (Cheong et al., 2011). Furthermore, autophagy induced by amino acid starvation is completely blocked in MEFs of these double-deficient mice (Cheong et al., 2011). The homology between Ulk1 and Ulk2 comprises the full length of the kinases, i.e. kinase domain, PS-rich domain, and CTD. In contrast, homology towards the other Ulk family members is restricted to the kinase domain (reviewed in Chan & Tooze, 2009; Mizushima, 2010; Alers et al., 2012b; Alers et al., 2012a; Wong et al., 2013). However, Ulk3 overexpression induced autophagy and premature senescence in the human fetal lung fibroblast cell line IMR90 (Young et al., 2009).

In 2007, Meijer et al. analyzed the degree of conservation for different Atgs between different species (Meijer et al., 2007). They predicted that the protein KIAA0652 (GenBank accession AAH02378) represents the human ortholog of yeast Atg13. Notably, they failed to identify Atg17 and Atg29 orthologs in higher eukaryotes (Meijer et al., 2007). Additionally, an Atg31 ortholog has not been reported in higher eukaryotes so far (Mizushima et al., 2011; Alers et al., 2012a). However, in 2008 Mizushima's group reported that the focal adhesion kinase family interacting protein of 200 kDa (FIP200) is an Ulk1-interacting protein (Hara et al., 2008). Originally, FIP200 has been identified as a proline-rich tyrosine kinase 2 (Pyk2)- and focal adhesion kinase (FAK)-interacting protein which inhibits Pyk2 and FAK by direct binding to the kinase domains (Ueda et al., 2000; Abbi et al., 2002). FIP200 is also referred to as retinoblastoma 1-inducible coiled-coil 1 (RB1CC1), since it has been shown to regulate retinoblastoma 1 (RB1) expression (Chano et al., 2002). FIP200 is ubiquitously expressed and is involved in multiple cellular processes, including cell survival, protein synthesis and cell growth, cell proliferation, cell spreading and migration, cell differentiation, embryonic development, and tumorigenesis (reviewed in Gan & Guan, 2008). According to these multiple roles

performed by FIP200, several FIP200-interacting proteins next to Pyk2 and FAK have been identified so far, including Atg16L1, TSC1, p53, PP1, ASK1, TRAF2, Arkadia E3-ligase, COP1 E3-ligase, hSNF5, PIASy, β-catenin, ActA, and stathmin (Maucuer et al., 1995; Pfeuffer et al., 2000; Gan et al., 2005; Melkoumian et al., 2005; Chano et al., 2006; Gan et al., 2006; Meiselbach et al., 2006; Chano et al., 2010; Koinuma et al., 2011; Morselli et al., 2011; Ochi et al., 2011; Choi et al., 2013b; Gammoh et al., 2013; Kobayashi et al., 2013; Nishimura et al., 2013). The interactions with TSC1 and p53 influence autophagic signaling pathways and are discussed below. Due to the function of FIP200 as central cellular signaling node, it has been reported that *Fip200*-/- mice die between embryonic day (E) 13.5 and E16.5 due to heart failure and liver degeneration (Gan et al., 2006). FIP200 comprises of a putative nuclear localization signal (NLS) within the N-terminal half of the protein, a large coiled-coil domain and a leucine zipper motif at the C-terminus (Gan & Guan, 2008). With regard to the subcellular localization, FIP200 has been reported to localize in the cytoplasm, the nucleus and at focal adhesions (Gan & Guan, 2008). The interaction between Ulk1 and FIP200 requires the CTD of Ulk1, and subsequently it has been speculated that FIP200 might be the factor that is titrated out by the 7aa-motif during the overexpression of kinase-dead Ulk1 (Hara et al., 2008; Chan et al., 2009). Similar to Ulk1/2, FIP200 localizes to the IM upon amino acid or serum starvation (Hara et al., 2008). Furthermore, in FIP200-deficient MEFs autophagy induction is blocked, and the defect in autophagosome formation occurs downstream of mTOR (Hara et al., 2008). Finally, both Ulk1 stability and phosphorylation are reduced in *Fip200*-/- MEFs, indicating that FIP200 is important for Ulk1 kinase activity (Hara et al., 2008). Within the discussion section of this first report demonstrating the importance of FIP200 for autophagy, the authors already speculate that FIP200 might represent the functional counterpart of yeast Atg17. Several observations lead the authors to this conclusion: 1) both Atg17 and FIP200 possess several coiled-coil domains, 2) Atg17/FIP200 are required for Atg1/Ulk1 kinase activity, 3) Atg17/FIP200 are necessary for Atg1/Ulk1 targeting to the PAS/IM, 4) Atg17/FIP200 serve as scaffolds for multiple interacting proteins, and 5) Atg17 and FIP200 are mutually exclusively expressed in different species (Hara et al., 2008; Hara & Mizushima, 2009). As described below, this assumption was subsequently confirmed by several reports.

Following the prediction by Meijer et al., several groups demonstrated that KIAA0652 indeed represents the human Atg13 ortholog (Chan et al., 2009; Ganley et al., 2009; Hosokawa et al., 2009a; Jung et al., 2009). Furthermore, three of these reports deciphered the mechanistic details how mTOR regulates autophagy through the mammalian Ulk1-Atg13-FIP200 complex. Human Atg13 is a 517 aa protein (isoform 1) and exhibits a 16% identity to its yeast ortholog (Hosokawa et al., 2009a). Chan et al. showed that knockdown of Atg13 blocks starvation-induced LC3 lipidation and Atg9 re-distribution. They found that Atg13 binds to the CTD of Ulk1/2, but not to the 7-aa-motif mediating the dominant-negative effect of kinase-dead Ulk1 (Chan et al., 2009). Additionally, it was

demonstrated that Atg13 serves as substrate for Ulk1/2 and that the association between Ulk proteins and Atg13 is not affected by the nutritional status or Atg13 phosphorylation (Chan et al., 2009). In three almost simultaneously published studies by the groups of Mizushima, Kim and Jiang, the mechanistic details how the mammalian Ulk1-Atg13-FIP200 complex regulates autophagy and how mTOR transduces signals to this complex were elucidated. Atg13 interacts with both Ulk1/2 and FIP200 (Ganley et al., 2009; Hosokawa et al., 2009a; Jung et al., 2009). It appears that the association between Ulk1 and FIP200 significantly depends on Atg13, but one group also demonstrated that Ulk1 can independently interact with Atg13 and FIP200 (Ganley et al., 2009). Kim's group reported that the last 75 aa of Atg13 are mandatory for Ulk1/2 binding, and the last 134 aa for binding of both FIP200 and Ulk1/2 (Jung et al., 2009). Gel filtration analyses by Mizushima's group revealed that Ulk1, Atg13 and FIP200 can be detected within a 3-MDa-complex (Hosokawa et al., 2009a). FIP200 is exclusively found in this mega-complex, and this complex cannot be detected in FIP200-/- cells, indicating that FIP200 significantly contributes to the elution volume of this complex. Additionally, Ulk1 and Atg13 were recovered in 300-500 kDa- and 200-400 kDa-fractions, respectively (Hosokawa et al., 2009a). The Jiang group performed gel filtration experiments with recombinant proteins and observed the three components within a complex with a molecular weight > 1 MDa (Ganley et al., 2009). All three components of the complex localize to the isolation membrane upon induction of autophagy, and the assembly of the complex is not sensitive to starvation. Furthermore, Atg13 and FIP200 are required for maximal Ulk1 kinase activity, Ulk1 stability, and Ulk1 recruitment to the isolation membrane. In turn, both Atg13 and FIP200 are substrates for Ulk proteins. All three groups observed that either starvation or rapamycin treatment result in a faster migration of Ulk1 and Atg13 in SDS-PAGE, and all three groups clearly demonstrated that mTOR phosphorylates both Ulk1 and Atg13 (Ganley et al., 2009; Hosokawa et al., 2009a; Jung et al., 2009). Furthermore, Mizushima's group showed that the mTOR complex 1 (mTORC1) associates with the 3-MDa-complex under nutrient-rich conditions and dissociates under starvation (Hosokawa et al., 2009a). This interaction is mediated by the mTORC1 component raptor and the PS-domain of Ulk1. Accordingly, the Atg13-interacting CTD of Ulk1 is not necessary for mTORC1 recruitment (Hosokawa et al., 2009a). Additionally, the mTOR complex 2 (mTORC2) component does not interact with Ulk1 (Hosokawa et al., 2009a). Of note, the mTORC1 binding site has alternatively been mapped to the kinase domain of Ulk1 (Lee et al., 2010).

Finally, a fourth component of the Ulk kinase complex has been identified and characterized independently by two groups. This component does not have any obvious ortholog in *S. cerevisiae* and was thus termed Atg101 (Hosokawa et al., 2009b; Mercer et al., 2009). Of note, the closely related fission yeast *S. pombe* apparently harbours an Atg101 ortholog named Mug66 (Martin-Castellanos et al., 2005; Hosokawa et al., 2009b). Atg101 directly interacts with the Ulk1 kinase

complex through Atg13, and this association is independent of nutrient supply (Hosokawa et al., 2009b). Mercer et al. mapped the Atg101-binding site in Atg13 to amino acids 112 to 220 (Mercer et al., 2009). In contrast to the results described above, the binding site of Atg13-Atg101 within Ulk1 was mapped to the N-terminal half of the PS-rich domain, proximal to the kinase domain (Mercer et al., 2009). Notably, siRNA-mediated depletion of Atg101 suppresses GFP-LC3 puncta formation or GST-BHMT fragmentation, indicating that Atg101 is essential for autophagy (Hosokawa et al., 2009b; Mercer et al., 2009). Finally, Atg101 positively influences the stability and the basal phosphorylation of both Atg13 and Ulk1 (Hosokawa et al., 2009b; Mercer et al., 2009). Although yeast and higher eukaryotes share some overlapping components of the Atg1/Ulk1 complexes, e.g. Atg1/Ulk1 itself and Atg13, there exist significant differences in complex constitution. As described above, yeast Atg11 and Atg17 serve as scaffolds during Cvt pathway or autophagy, respectively. It appears that FIP200 and Atg101 have overtaken some corresponding functions, since primary sequence orthologs of Atg11 and Atg17 do not exist in higher eukaryotes. Although FIP200 presumably represents a functional Atg17 ortholog (Hara & Mizushima, 2009), it should be noted that FIP200 is listed as Atg11 family member in the NCBI Pfam database and is structurally similar to *S. pombe* and *C. elegans* Atg11s (Steffan, 2010). Additionally, Atg101 has been reported to show similarity to yeast Atg17 (Steffan, 2010).

Taking all the experimental observations summarized above into consideration, the following model has been established: under nutrient-rich conditions, mTORC1 associates with the Ulk1-Atg13-FIP200-Atg101 complex and phosphorylates Ulk1 and Atg13. Under starvation conditions, mTORC1 dissociates from this mega-complex, and the inhibitory mTOR-dependent phospho-sites within Ulk1 and Atg13 become dephosphorylated. Active Ulk1 then autophosphorylates and phosphorylates Atg13 and FIP200, ultimately leading to the initiation of autophagosome formation. However, this proposed model leaves central remaining questions open, which will be partially addressed below or are currently investigated: 1) how does mTOR-dependent phosphorylation of Ulk1 and Atg13 keep the constitutively assembled complex in an inactive state, 2) which phosphatases dephosphorylate these inhibitory mTOR-sites and how does this contribute to the activation of the complex, 3) how is the phospho-status of Ulk1 and Atg13 regulated in mTOR-independent pathways, 4) what is the role of the Ulk-dependent phospho-sites in Atg13 and FIP200, 5) are additional interacting proteins and/or further post-translational modifications of this complex necessary for its autophagy-inducing function, and most importantly 6) how does the Ulk1-Atg13-FIP200-Atg101 complex initiate the autophagy signaling machinery?

1.2.3.3 Regulation of the Ulk complex by post-translational modifications

According to the above described model, the phospho-status of the Ulk1-Atg13-FIP200-Atg101 complex is central for the regulation of autophagic processes. In general, global phosphorylation of Ulk1 and Atg13 is decreased under starvation conditions and FIP200 phosphorylation is decreased under fed conditions (Ganley et al., 2009; Hosokawa et al., 2009a; Jung et al., 2009; Mizushima, 2010; Wong et al., 2013). In other words, it appears that the phospo-status of Ulk1 and Atg13 primarily depends on mTOR, whereas the phospho-status of FIP200 mainly depends on Ulk1, respectively. Using high-resolution tandem mass spectrometry, Dorsey et al. identified 16 phosphorylation sites within Ulk1 purified from cells grown under nutrient-rich conditions. These phospho-acceptor sites are distributed over the full length protein, i.e. within the kinase domain (3 sites), the PS-rich domain (9 sites) and the CTD (4 sites) (Dorsey et al., 2009). The authors suggested that S341 within the PS-rich domain and T1046 within the CTD represent Ulk1 autophosphorylation sites and that S1042 represents a PKA-site (human amino acid positions are given). Using a SILAC-based approach, Shang et al. compared the Ulk1 phospho-states under fed and starvation conditions, respectively (Shang et al., 2011). They identified 13 phospho-sites within Ulk1, and two of these sites revealed a more than 10-fold decrease in phosphorylation level upon starvation, i.e. S638 and S758. Both sites became dephosphorylated by rapamycin treatment or mTOR knockdown, and accordingly the authors suggested that mTOR mediates the phosphorylation of these sites (Shang et al., 2011). Phospho-S758 was also identified by Dorsey et al., and its mTOR-dependent phosphorylation was confirmed by Kim et al. (Kim et al., 2011). Finally, Mack et al. recently reported the identification of 30 phospho-acceptor sites within Ulk1. Of these sites, six were constitutively phosphorylated, and 24 sites revealed a phospho-status dependent on the nutritional conditions (Mack et al., 2012). Notably, 16 of these sites had not been reported before. Interestingly, the SILAC-based approach by Shang et al. revealed that total phosphorylation levels of Atg13 were low under nutrient-rich conditions and stayed largely unaltered upon starvation (Shang et al., 2011). The authors could only identify phosphorylation of Atg13 S361 (isoform 1), and phosphorylation of this site did not significantly change during starvation (Shang et al., 2011). This would indicate that rather the Ulk1 phospho-status than the Atg13 phospho-status governs autophagy initiation. Additional mTOR-dependent sites of mammalian Atg13 have not been reported so far (Alers et al., 2012b; Wong et al., 2013). Upon nutrient depletion, mTORC1 dissociates from the Ulk1-Atg13-FIP200-Atg101 complex, and Ulk1 becomes activated. This leads to Ulk1 autophosphorylation and transphosphorylation of Atg13 and FIP200, respectively. Bach et al. found that phosphorylation of T180 within the kinase-activation loop of Ulk1 is required for Ulk1 autophosphorylation activity (Bach et al., 2011). This site is homologous to the site described for yeast Atg1 (Kijanska et al., 2010; Yeh et al., 2010). With regard to Ulk1-

dependent sites in Atg13, only one phospho-acceptor site has been published, directly confirming the above described results using the SILAC-approach. Joo et al. showed that the Hsp90-Cdc37 chaperone complex regulates mitophagy by modulating Ulk1 stability and function. They reported that Ulk1-mediated phosphorylation of Atg13 at S318 is required for the release of Atg13 from an Ulk1-Hsp90-Cdc37 complex and for the recruitment of Atg13 to damaged mitochondria, where it contributes to Parkin-mediated mitophagy (Joo et al., 2011). These results might account for the selective role of Ulk1 for the mitochondrial clearance during reticulocyte development described above. Notably, overexpression of a non-phosphorylatable Atg13 S318A mutant showed a dominant-negative effect on mitophagy, whereas basal or starvation-induced autophagy were unaffected (Joo et al., 2011). We were able to identify five Ulk1-dependent phospho-sites of Atg13 by an *in vitro* kinase assay, and this is discussed in detail in chapter 2.6. To date, the Ulk1-dependent phospho-sites of FIP200 have not been reported.

On the basis of its central role for the regulation of the Ulk1-Atg13-FIP200-Atg101 complex, mTOR has been dubbed the "gatekeeper" of autophagy. As is described in chapter 1.3.1, mTOR integrates 1) nutrient signals, e.g. generated by growth factors or amino acids, 2) energy signals, e.g. controlled by the cellular AMP/ATP ratio, and 3) stress signals such as hypoxia or DNA damage (reviewed in Zoncu et al., 2011b; Laplante & Sabatini, 2012; Jewell et al., 2013). The growth factor and energy inputs are essentially controlled by the serine/threonine protein kinases Akt and AMP-activated protein kinase (AMPK), which both function as upstream regulators of mTOR. Both kinases have also been implicated in the direct regulation of the Ulk1 kinase complex. As described in detail in chapter 1.3.1, the serine/threonine kinase Akt (also termed protein kinase B, PKB) translates signals received by receptor tyrosine kinases or receptor-associated tyrosine kinases into a diverse array of intracellular responses, including cell cycle control, metabolism, apoptosis, or autophagy. Bach et al. showed that Ulk1 serves as direct substrate for Akt. The authors observed that insulin induces the Akt-dependent phosphorylation of Ulk1 at S775 (human sequence) (Bach et al., 2011). This site is also conserved in Ulk2. Additionally, they demonstrated that insulin-dependent repression of autophagy is independent of mTOR, since insulin completely blocked rapamycin-induced LC3 lipidation (Bach et al., 2011). AMPK is the main sensor for cellular energy levels. AMPK consists of three subunits, i.e. the catalytic α-subunit and the regulatory β- and γ-subunits, respectively. Additionally, there exist several isoforms of the different subunits, i.e. α1-2, β1-2, and γ1-3 (reviewed in Hardie, 2011; Hardie et al., 2012b; Hardie et al., 2012a). In order to exert its full catalytic activity, the α-subunit has to be phosphorylated within its activation loop at T172. This phosphorylation might be carried out by different upstream regulatory kinases. These include the ubiquitously expressed and constitutively active liver kinase B1 (LKB1), the Ca^{2+}-activated Ca^{2+}/calmodulin-dependent kinase kinase β

(CaMKK β), or the transforming growth factor β-activated kinase-1 (TAK1) (Hawley et al., 2003; Woods et al., 2003; Hawley et al., 2005; Hurley et al., 2005; Woods et al., 2005; Momcilovic et al., 2006; Herrero-Martin et al., 2009). Notably, it has been shown that TRAIL induces TAK1-dependent AMPK activation and subsequent autophagy, and it has been speculated that this signaling cascade contributes to the resistance of non-transformed cells against TRAIL-induced apoposis (see chapter 1.1.3) (Herrero-Martin et al., 2009). Besides T172 phosphorylation of the α-subunit, the heterotrimeric AMPK complex is controlled by the regulatory β- and γ-subunits. The γ-subunits contain four repeats of a sequence motif termed cystathionine β-synthase (CBS) repeat. In the AMPK γ-subunit, these four repeats form a disk with four ligand-binding sites. In the mammalian γ1-subunit, site 2 is apparently always unoccupied and site 4 contains a permanently bound AMP, whereas sites 1 and 3 competitively bind AMP, ADP or ATP and thus function as sensors for the energy status of the cell. Specifically, AMP binding to site 1 contributes to allosteric AMPK activation, whereas binding of AMP or ADP to site 3 protects against dephosphorylation of T172 (Xiao et al., 2007; Xiao et al., 2011; Hardie et al., 2012b). The β-subunits bridge α- and γ-subunits and additionally contain a carbohydrate-binding module (CBM). This CBM binds to glycogen particles, and thus target AMPK to downstream substrates located in these cellular glycogen stores, such as glycogen synthase (Carling & Hardie, 1989; Hudson et al., 2003; Polekhina et al., 2003; Jorgensen et al., 2004; Hardie et al., 2012b). Furthermore, it has been suggested that AMPK senses both the short-term availability of energy in form of adenosine nucleotides and the medium-term availability in form of glycogen (McBride et al., 2009). In 2001, Wang and colleagues reported that the yeast AMPK-ortholog Snf1p is a positive regulator of autophagy and probably functions via Atg1 and/or Atg13, respectively (Wang et al., 2001). Subsequently, several reports analyzed the role of AMPK for mammalian autophagy. Although an initial study reported that the AMPK-activating substances adenosine, AICA riboside and N6-mercaptopurine riboside inhibit autophagy (Samari & Seglen, 1998), subsequently several works supported a positive regulatory role of AMPK for mammalian autophagy (Meley et al., 2006; Liang et al., 2007; Matsui et al., 2007; Viana et al., 2008). Generally, this positive effect of AMPK on autophagy has been attributed to its capability to inhibit mTOR. The inhibition of mTORC1 can be achieved by two different pathways, either by AMPK-mediated phosphorylation of the upstream regulator tuberous sclerosis complex 2 (TSC2) or by AMPK-mediated phosphorylation of the mTORC1-subunit raptor (see also chapter 1.3.1) (Inoki et al., 2003; Gwinn et al., 2008). However, in recent years a direct regulation of the Ulk1-Atg13-FIP200-Atg101 complex by AMPK has been established, which is accordingly mTOR-independent. Furthermore, due to the results obtained with the yeast ortholog Snf1p described above, it has been suggested that this direct AMPK-mediated regulation of autophagy arose at an earlier stage during eukaryotic evolution (Hardie, 2011). How does this direct regulation work? We and others demonstrated that AMPK directly interacts with

Ulk1 (see chapter 2.6 and Behrends et al., 2010; Lee et al., 2010; Egan et al., 2011; Kim et al., 2011; Shang et al., 2011; Mack et al., 2012; Sanchez et al., 2012). We discovered that Ulk1 phosphorylates all three subunits of AMPK, and our results and their implications are further discussed in chapter 2.6. Interestingly, several groups reported that AMPK phosphorylates Ulk1 (Egan et al., 2011; Kim et al., 2011; Shang et al., 2011; Mack et al., 2012). However, different groups mapped different phospho-acceptor sites in the Ulk1 amino acid sequence. Together with the proteomic screens analyzing the global nutrient-dependent Ulk1 phosphorylation described above, a rather complex picture of the "Ulk1 phospho-barcode" evolves. The different identified phospho-sites are summarized in table 1 and reviewed in Alers et al. and Wong et al. (Alers et al., 2012b; Wong et al., 2013). However, three Ulk1 phospho-sites appear to be of particular interest, since they were reported by three or more independent groups, i.e. S556, S638, and S758 of human Ulk1 sequence (Wong et al., 2013). Nutrient status-dependent phosphorylation of Ulk1 at S638 and S758 was already mentioned above, since these are the two sites with the strongest decrease in phosphorylation level upon starvation as detected by Shang et al. (Shang et al., 2011). AMPK-dependent S556 phosphorylation was reported by Egan et al.. They screened for proteins that bound to recombinant 14-3-3 proteins in wild-type but not in AMPK-deficient cells and identified Ulk1 (Egan et al., 2011). S556 became phosphorylated upon treatment with the AMPK activator phenformin, and this result was confirmed by performing an *in vitro* kinase assay (Egan et al., 2011). S556 phosphorylation was also confirmed by the SILAC-approach of Shang et al. (Shang et al., 2011). Interestingly, this site revealed an approximately 7-fold decrease in phosphorylation level upon starvation, which is the third strongest change behind that of S638 and S758 (Shang et al., 2011). Two additional studies demonstrated that phospho-S556 represents a major site for AMPK-dependent 14-3-3 binding (Bach et al., 2011; Mack et al., 2012). AMPK-catalyzed S638 phosphorylation of Ulk1 was reported by Egan et al. and by Mack et al. (Egan et al., 2011; Mack et al., 2012). The latter group reported that S638 is the predominant AMPK-dependent phospho-site in Ulk1 both *in vitro* and *in vivo* (Mack et al., 2012). Notably, Shang et al. showed that S638 can be phosphorylated by both mTOR and AMPK, respectively (Shang et al., 2011). Finally, S758 has been characterized as authentic mTOR-dependent Ulk1 phospho-site by Kim et al. and Shang et al. (Kim et al., 2011; Shang et al., 2011), and this site was also reported to be phosphorylated by Dorsey et al. (Dorsey et al., 2009). However, the first two groups differ significantly in the physiological outcome of S758 phosphorylation. Kim et al. reported that phospho-S758 prevents association of AMPK and Ulk1, and thus the AMPK-mediated activation of Ulk1. Accordingly, mTOR inhibition would result in the association of AMPK and Ulk1 (Kim et al., 2011). In contrast, Shang et al. suggest that phospho-S758 promotes the interaction between Ulk1 and AMPK. Accordingly, mTOR inhibition would result in the dissociation of AMPK from Ulk1 (Shang et al., 2011). Notably, the Ulk1 mutant S758A initiates

Table 1: Published Ulk1 phospho-sites (human amino acid sequence)

	Site	Dorsey	Egan	Kim	Shang	Bach	Mack
Kinase	S87	X					
	T180					X	
	S195	X					
	S224	X					
P/S-rich domain	S317			X			X
	S341	X			X		
	S403						X
	S405				X		
	S411						X
	S450	X			X		X
	S467	X	X				
	T468				X		
	S469	X			X		
	S477						X
	S479	X			X		X
	*S482	X					
	S495						X
	S505				X		
	S522	X					X
	S533				X		X
	S544						X
	S556		X		X	X	X
	T575		X				
	*S614						X
	S623	X			X		X
	T625						X
	T636						X
	S638		X		X	X	X
	T660						X
	S694						X
	T695						X
	S696						X
	S716						X
	S719						X
	S748						X
	T755						X
	S758	X		X	X		X
	T764						X
	S775					X	X
	*S777			X			X
	S781						X
CTD	S866	X					
	S912	X					
	S1042	X					X
	T1046	X					

Color code: AMPK | mTOR | Ulk1 | Akt | PKA

(Residues indicated with * refer to the position in murine sequence, since the position is not conserved in human. P/S-rich domain, proline/serine-rich domain; CTD, C-terminal domain)

starvation-induced autophagy faster at an early time point, although it does not change the maximum autophagic capacity. This observation lead the authors speculate that the AMPK-Ulk1 interaction serves as "sequestering reservoir" which retains Ulk1 under nutrient-rich conditions (Shang et al., 2011). Collectively, this discrepancy already emphasizes that the AMPK-dependent regulation of the Ulk1 complex is far from being completely characterized. However, it has been stated that the function of AMPK in autophagy is rather a "fine-tuning" than an "on-off switch" (Wong et al., 2013). Supporting this note, Kim et al. report that only glucose starvation-induced autophagy is blocked in *Ampkα1/α2*-/- MEFs, but not amino acid starvation-induced autophagy (Kim et al., 2011). Similarly, Mack et al. observed that AMPK is not absolutely essential for autophagy at early and intermediate stages of EBSS-starvation, but increases the efficiency of the process (Mack et al., 2012).

Apparently, mTOR, Akt, AMPK and presumably additional kinases (see prediction in Mack et al., 2012) contribute to the regulation of the Ulk1-Atg13-FIP200-Atg101 complex. It is conceivable that these phosphorylation processes depend on different factors, i.e. cell type or autophagic stimulus. Additionally, there appear to exist significant differences between metazoan lineages in the regulation of the Ulk kinase complex. Chang and Neufeld reported the regulation of this complex in *D. melanogaster* in parallel to the works on the mammalian complex. Interestingly, they reported common and divergent aspects. Like for the mammalian system, Atg13 is essential for starvation-induced autophagy, the Atg1-Atg13 interaction is independent of the nutrient status, and Atg13 is required for the autophagy-promoting function of Atg1 (Chang & Neufeld, 2009). In contrast to the mammalian system, Atg13 is hyperphosphorylated under starvation conditions, indicating that the Atg13 phospho-status might be more dependent on Atg1 than on TOR in *D. melanogaster*. Furthermore, the authors demonstrated that Atg13 overexpression blocks autophagy and that TOR associates with Atg1/Atg13 independently of nutrient supply.

Next to the diversity among different species, different cell types and different autophagy-inducing stimuli, the complexity of this regulatory system is even increased by two additional aspects: 1) the action of phosphatases and 2) Ulk1-dependent feedback signaling targeting the upstream kinases. It can be assumed that phosphatases contribute to the dephosphorylation of the mTOR-sites in Ulk1 and Atg13, respectively (Wong et al., 2013). Notably, the direct interaction between Ulk1 complex components and protein phosphatases has been documented. For example, UNC-51 interacts with the protein phosphatase 2A (PP2A) in *C. elegans*, and FIP200 harbors a docking motif for protein phosphatase 1 (PP1) (Meiselbach et al., 2006; Ogura et al., 2010). However, the dephosphorylation of specific sites by specific phosphatases has not been reported yet. Generally, the phosphatase inhibitor okadaic acid is viewed as inhibitor of autophagy (Blankson et al., 1995; Samari et al., 2005;

Banreti et al., 2012; Magnaudeix et al., 2013; Wong et al., 2013). Furthermore, PP2A has already been implicated in the regulation of autophagic processes (Yorimitsu et al., 2009; Banreti et al., 2012; Magnaudeix et al., 2013; Yin et al., 2013). Frequently, PP2A is viewed as positive regulator of autophagic processes. Banreti et al. found that two different PP2A complexes regulate starvation-induced autophagy in *D. melanogaster*. One complex functions upstream of TOR, the other serves as target for TOR and was suggested to regulate the elongation of autophagosomes (Banreti et al., 2012). Notably, Atg17 and Atg101 have been proposed as potential substrates of the second PP2A complex (Banreti et al., 2012). Magnaudeix et al. recently demonstrated that PP2A blockade by okadaic acid or the shRNA-mediated knockdown of the catalytic subunit results in the inhibition of both basal autophagy and autophagy induced by different stimuli, such as starvation, ER stress, rapamycin, or proteasome inhibition (Magnaudeix et al., 2013). In contrast, the negative regulation of autophagy by PP2A enzymes has also been described. As described above, for the yeast system a model has been proposed in which autophagy is negatively regulated by the Tap42-PP2A pathway (Yorimitsu et al., 2009). The authors state that Atg1 activity is needed for autophagy induction upon inactivation of Tap42 or PP2A, but that Atg1 is not necessarily the direct target of this inhibition (Yorimitsu et al., 2009). Additionally, Yin et al. reported that PP2A is reduced in cisplatin-resistant ovarian cancer cells and patients' tissues. In turn, overexpression of PP2A decreased protective autophagy and sensitized ovarian cancer cells to cisplatin-induced cell death (Yin et al., 2013). However, it should be noted that PP2A enzymes fulfill multiple cellular functions with several different interacting proteins, and the involvement of additional or more selective phosphatases in the regulation of autophagy is currently intensely investigated. Next to phosphatase-mediated dephosphorylation processes, it has been postulated that feedback signaling pathways originating from the Ulk kinase complex contribute to the shaping of an autophagic response. Apparently, Ulk1 can directly influence its upstream regulators mTOR and AMPK, respectively. We were able to identify Ulk1-dependent regulation of AMPK, and our experimental evidence is discussed in chapter 2.6. With regard to mTOR, it has been well documented that Atg1/Ulk1 activity affects this kinase and its downstream signaling. In 2007, two groups independently reported that Atg1 overexpression in *D. melanogaster* negatively regulates S6K activity. S6K is a downstream target of (m)TOR and S6K phosphorylation at T389 catalyzed by TOR was inhibited by Atg1 overexpression, resulting in a reduced cell growth (Lee et al., 2007; Scott et al., 2007). Similarly, Jung et al. observed an increased S6K phosphorylation at T389 upon knockdown of Atg13 or Ulk1, respectively (Jung et al., 2009). Congruent to these observations, Chang and Neufeld reported that Atg1-Atg13 complexes regulate TOR by modulating its intracellular distribution and trafficking (Chang & Neufeld, 2009). However, these reports only indirectly show the effect of Atg1/Ulk1 on mTOR activity. Two recent reports proved that activated Ulk1 directly phosphorylates raptor and thus inhibits mTORC1 signaling

(Dunlop et al., 2011; Jung et al., 2011). Dunlop et al. suggest that raptor phosphorylation impairs substrate docking to mTORC1. Collectively, these reports indicate that there is a close connection between mTOR-dependent cell growth control and autophagy signaling. Again another level of complexity is added by the fact that the Ulk1 kinase complex component FIP200 interacts with TSC1, which is an upstream regulator of mTOR (Gan et al., 2005; Chano et al., 2006). Interaction of FIP200 with the TSC1-TSC2 complex results in the inhibition of this complex, ultimately leading to increased mTOR activity, S6K phosphorylation, and cell growth. One group reported that FIP200 induces ubiquitination and subsequent degradation of TSC1 (Chano et al., 2006). Taken together, it appears that Ulk1 and FIP200 have opposite effects on the regulation of mTOR activity, and future studies have to reveal the respective relative contributions, which might be again influenced by cell type or nutrient status.

In general, kinase-catalyzed phosphorylations and phosphatase-mediated dephosphorylations are the major molecular switches regulating the autophagy-initiating Ulk1 complex. However, in the recent past alternative post-translational modifications have been implicated in this regulation, i.e. ubiquitination and acetylation. As described above, ubiquitination plays an essential role for cargo recognition during selective autophagy processes. Furthermore, this post-translational modification links the two major cellular degradation pathways, i.e. the ubiquitin-proteasome system (UPS) and selective autophagy. Meanwhile it is well established that interference with one pathway influences the flux through the other (Korolchuk et al., 2010). It appears that blockade of the UPS induces up-regulation of autophagy, and different possible explanations mediating this crosstalk have been suggested, e.g. the unfolded protein response, p53, and HDAC6 (Korolchuk et al., 2010). In turn, blockade of autophagy has been suggested to decrease the UPS flux. This might be caused by accumulated p62, which binds ubiquitinated proteins and prevents their delivery to the proteasome (Korolchuk et al., 2010). The crosstalk between the two degradative machineries is also dependent on the type of the ubiquitin chain. The ubiquitin monomer harbors seven lysine residues, and dependent on which lysine is utilized for linkage, the resulting chains are called K6, K11, K27, K29, K33, K48, or K63 (Shaid et al., 2013). Additionally, linear chains are generated by the conjugation to the N-terminal methionine (M1). As a rough rule, K48 chains represent the canonical signal to target proteins to the proteasome, whereas K63 chains target proteins to autophagosomal degradation (Shaid et al., 2013). There are several lines of evidence that the Ulk1 complex is modified by ubiquitin chains as well. Zhou et al. reported that nerve growth factor (NGF) can induce the interaction of Ulk1 with the NGF receptor TrkA (Zhou et al., 2007). This apparently occurs through K63-polyubiquitination of Ulk1 and binding of Ulk1 to p62, which then recruits Ulk1 to TrKA receptor complexes. By this means, Ulk proteins apparently participate in the regulation of filopodia extension and neurite branching during sensory axon outgrowth (Zhou et al., 2007). The study by Joo et al.

described above reporting Ulk1-catalyzed phosphorylation of Atg13 at S318 indirectly confirms Ulk1 ubiquitination. The authors demonstrate the interaction between the Hsp90-Cdc37 chaperone complex and Ulk1. Disruption of this association by the Hsp90 antagonist 17-allylamino-17-demethoxygeldanamycin (17AAG) leads to Ulk1 destabilization, which can be inhibited with the proteasome inhibitor MG132 (Joo et al., 2011). Finally, Nazio et al. recently reported that mTOR does not only regulate the Ulk complex by phosphorylation, but also indirectly by regulating Ulk1 ubiquitination (Nazio et al., 2013). In this study the authors show that under basal conditions mTOR phosphorylates AMBRA1 and thus keeps it inactive. Upon autophagy induction, AMBRA1 enhances Ulk1 kinase activity and stability and promotes Ulk1 self-association by enhancing K63 ubiquitination of Ulk1 through the AMBRA1-associated E3-ligase tumor necrosis receptor-associated factor 6 (TRAF6) (Nazio et al., 2013). In turn, Ulk1 phosphorylates AMBRA1 and thus promotes it detachment from the dynein complex (in detail described below) (Di Bartolomeo et al., 2010). Interestingly, Nazio and colleagues only found K63-linked ubiquitin chains attached to Ulk1 (Nazio et al., 2013). Notably, Chang and Neufeld already observed that Atg1 and Atg13 levels were affected by TOR function in *D. melanogaster*, i.e. reduced levels in cells with high TOR activity and increased in cells with low TOR activity (Chang & Neufeld, 2009). Generally, it appears that the components of the Ulk1 complex are important for their mutual stabilization. Ulk1 is destabilized in cells deficient for Atg13, FIP200 or Atg101 (Ganley et al., 2009; Hosokawa et al., 2009a; Hosokawa et al., 2009b; Jung et al., 2009). Similarly, FIP200 is destabilized in cells deficient for Atg13 (Hosokawa et al., 2009a), and Atg13 is reduced in Atg101-depleted cells (Hosokawa et al., 2009b; Mercer et al., 2009). Future analyses will have to reveal the contribution of the UPS to this (de-)stabilizing effects.

Next to ubiquitination, acetylation has been reported to regulate autophagy. Gammoh et al. report that the histone deacetylase (HDAC) inhibitor suberoylanilide hydroxamic acid (SAHA) activates autophagy via the inhibition of mTOR and transcriptional up-regulation of LC3 expression (Gammoh et al., 2012). The authors confirmed that the SAHA-mediated induction of autophagy depends on Ulk1/2. Recently, the direct acetylation of Ulk1 was reported. Lin et al. found that glycogen synthase kinase 3 (GSK3), which is activated by growth factor deprivation and resulting Akt inactivation, phosphorylates and thus activates acyltransferase TIP60 (Lin et al., 2012). Activated TIP60 in turn acetylates and stimulates Ulk1. Ulk1 acetylation presumably occurs at K162 and/or K606, and a non-acetylatable Ulk1 mutant failed to rescue autophagy in *Ulk1*−/− MEFs. Furthermore, inhibition of GSK3 blocked autophagy induced by growth factor deprivation, but not by glucose starvation (Lin et al., 2012). Next to the direct Akt-mediated Ulk1 phosphorylation described above, the GSK3-TIP60-Ulk1 axis is another example how Akt-dependent signals are transduced to the Ulk1 complex independently of mTOR.

1.2.3.4 Structural aspects of the Ulk complex

Recently, the first articles have been published dealing with the structures of the yeast Atg1 complex. Ragusa et al. reported the crystal structure of a 2:2:2 complex of Atg17, Atg29 and Atg31 (Ragusa et al., 2012). Atg17 is crescent-shaped with a 10 nm radius of curvature. During PAS organization and autophagy, the Atg17-Atg29-Atg31 complex dimerizes, and each dimer contains two complete crescents. The authors termed the C-terminal region of Atg1 the "early autophagy targeting/tethering" (EAT) domain, since the EAT domain was shown to sense membrane curvature, dimerize, and tether lipid vesicles (Ragusa et al., 2012). The same group recently published the crystal structure of the N-terminal domain of yeast Atg13 (Jao et al., 2013). Atg13 contains a HORMA (Hop1p, Rev7p, Mad2) domain at its N-terminus. The HORMA domain is dispensable for the interaction with Atg1 or Atg13 recruitment to the PAS, but is required for autophagy and the recruitment of the PI3K subunit Atg14. Additionally, they discovered a pair of conserved arginine residues which possible constitute a phosphate sensor. The authors propose that the HORMA domain accordingly might function as a phospho-regulatable conformational switch (Jao et al., 2013). To date, crystal structures for the mammalian Ulk1 complex have not been published yet, but this is likely a question of time.

1.2.3.5 Downstream targets of the Ulk1 complex

With regard to the downstream signaling events initiated by the Ulk1 complex and ultimately leading to the induction of autophagy, several observations have been made but the exact molecular details remain somewhat obscure. Different Ulk1 substrates have been reported, but their exact contribution to the induction of autophagy has to be examined.

Di Bartolomeo et al. showed that Ulk1 phosphorylates AMBRA1, which interacts with the Beclin 1/Vps34-complex (Di Bartolomeo et al., 2010). This phosphorylation triggers the dissociation of AMBRA1 and the associated PI3K class III complex from dynein light chains 1/2. The resulting relocalization of this complex to the ER allows for the nucleation of autophagosomes (Di Bartolomeo et al., 2010). Considering the results by Nazio et al. described above, there apparently exists a mutual regulatory circuit involving Ulk1 and AMBRA1, i.e. AMBRA1 regulates the stability and kinase activity of Ulk1 by controlling its ubiquitination, and in turn Ulk1 regulates the association of AMBRA1 with the cytoskeleton via phosphorylation.

Another connection of Ulk1-dependent signaling to the cytoskeleton was proposed by Tang et al.. They could show that overexpression of *Drosophila* Atg1 induces the phosphorylation-dependent

activation of the actin-associated motor protein myosin II (Tang et al., 2011). Atg1 phosphorylates Spaghetti-squash activator (Sqa), which is a myosin light chain kinase (MLCK)-like protein. Atg1-mediated phosphorylation of Sqa at T279 leads to its activation. This in turn results in the Sqa-dependent phosphorylation of Spaghetti-squash (Sqh), which is the *Drosophila* myosin II regulatory light chain (MLC), and the activation of myosin. Furthermore, depletion of Sqa or inhibition of myosin II activation hampered the formation of autophagosomes upon starvation. With regard to the mammalian system, the authors demonstrated that Ulk1 interacts with the Sqa-ortholog zipper-interacting protein kinase (ZIPK; alternatively termed death-associated protein kinase 3, DAPK3). Co-expression of kinase-inactive ZIPK with wild-type Ulk1 resulted in a mobility shift, which was not observed upon co-expression with kinase-inactive Ulk1 and which was abolished by CIP phosphatase treatment. These data suggest that Ulk1 might phosphorylate ZIPK. Notably, ZIPK phosphorylation at T180, T225 and T265 is required for full enzymatic activity (Graves et al., 2005), and ZIPK T265 corresponds to Sqa T279 (Tang et al., 2011). Similar to the observations made in *Drosophila*, ZIPK depletion or inhibition of myosin II function suppressed starvation-induced autophagic flux in mammalian cells. Finally, the authors found that the Ulk1-ZIPK-myosin II axis is important for Atg9 trafficking upon starvation, and they propose that myosin II might represent the motor protein regulating subcellular Atg9 movement (Tang et al., 2011).

Apparently there is also crosstalk between the Ulk1 complex and components of the ubiquitin-like conjugation systems. Three recently published articles focused on the interaction between Atg1/Ulk1 and Atg8 family proteins. Notably, the association of Ulk1 with Gate16 and GABARAP was already described in the year 2000 by Okazaki et al., and they mapped the interaction sites to Ulk1 amino acids 287-416 (Okazaki et al., 2000). In the first of the three recent publications, Kraft et al. showed that Atg8 binds to a LIR within Atg1 (Kraft et al., 2012). They suggest that Atg8 targets Atg1 to autophagosomes where it might contribute to autophagosome maturation and/or their fusion to lysosomes. Additionally, the Atg8-Atg1 interaction targets the Atg1 complex for vacuolar degradation. The authors also demonstrated that mammalian Ulk1 harbors a LIR and that Ulk1 interacts with GABARAP, Gate16 and LC3B, thus directly confirming the results previously obtained by Okazaki et al.. Similar to their observations in yeast, Ulk1 was LIR-dependently targeted to autophagosomes (Kraft et al., 2012). In the second manuscript, Nakatogawa et al. independently confirmed the association between yeast Atg8 and Atg1 (Nakatogawa et al., 2012). Mutation of the Atg8 family interacting motif (AIM) of Atg1 abolishes Atg1 transport to and degradation in vacuoles. Interestingly, AIM mutation caused a significant defect in autophagy, but did not affect PAS organization or the initiation of IM formation (Nakatogawa et al., 2012). This result suggests that there are indeed two functions of Atg1/Ulk1: 1) initiation of IM formation and 2) autophagosome expansion/maturation and/or fusion to vacuoles/lysosomes. Finally, the Ulk1 LIR domain (D^{356}FVMV)

was also described by Alemu et al. (Alemu et al., 2012). Notably, they additionally found LIR sequences within Atg13 (D^{443}FVMI) and FIP200 (D^{701}FETI). Apparently, all three components of the Ulk1 complex have preferences towards the GABARAP-subfamily of mammalian Atg8 proteins. As described in chapter 1.2.2.4, the GATE-16/GABARAP family was reported to play a role in later stages of autophagy, indirectly suggesting that the Ulk1 complex components have a function at a later stage, too. Alemu et al. verified that the LIR motif in Ulk1 is required for the association of Ulk1 with phagophores and/or autophagosomes. However, in contrast to the two reports by Kraft et al. and Nakatogawa et al., they state that Ulk1 is mainly degraded by the proteasome with only marginal contribution from autophagy, which is in accordance to observations made by Joo et al. (Joo et al., 2011). Interestingly, Suttangkakul et al. identified four Atg1 and two Atg13 isoforms in *Arabidopsis thaliana* (Suttangkakul et al., 2011). The authors showed that Atg1/Atg13 complexes are delivered to the plant vacuole with Atg8-decorated autophagic bodies. Another level of crosstalk between the Ulk1 kinase complex and the ubiquitin-like conjugation systems was deciphered recently by two works. Jiang's and Mizushima's group reported that FIP200 can directly interact with Atg16L1 (Gammoh et al., 2013; Nishimura et al., 2013). Gammoh et al. mapped the binding site within Atg16L1 to amino acids 229-242 and named this region FIP200-binding domain (FBD). Importantly, deletion of the FBD does neither abolish Atg16L1-binding to Atg5 nor self-dimerization. Expression of the FBD-deleted Atg16L1 in the Atg16L1-negative background could not fully reconstitute autophagy induced by amino acid starvation or the mTOR-inhibitor Torin1 (Gammoh et al., 2013). Similar results were reported by Nishimura et al. (Nishimura et al., 2013). They showed that the FIP200-Atg16L1 interaction is independent of Atg14L or PI3P, and that the interaction is important for Atg16L1 targeting to the IM. The authors narrowed down the interaction domain to two regions of Atg16L1, i.e. amino acids 230-250 (roughly overlapping with the FBD reported by Gammoh et al.) and 288-300. They additionally suggest that the Atg12-Atg5-Atg16L1 complex and the Ulk1-Atg13-FIP200-Atg101 complex form one large unit in the cytoplasm, which then targets the IM. Accordingly, the authors describe their unpublished observation that Ulk1 and Atg5 are recruited to the same compartment with similar kinetics. Most surprisingly, they observed a blockade of the autophagic flux when they express an Atg16L1Δ(230-300) mutant in *Atg16l1*-/- MEFs, but not when expressing the Atg16L1(1-230) version, which also lacks the FIP200-interacting domain. They proposed a model involving a self-inhibitory role for the C-terminal WD-repeat domain of Atg16L1. If this domain is deleted, the N-terminal half of Atg16L1 uncoordinatedly targets membranes, including the autophagosome formation site (Nishimura et al., 2013). Collectively, the observations described above support a role of the Ulk1 complex not only for autophagy initiation but also for later steps of the autophagic cascade. The signaling machinery upstream and downstream of the Ulk1 complex is summarized in figure 4.

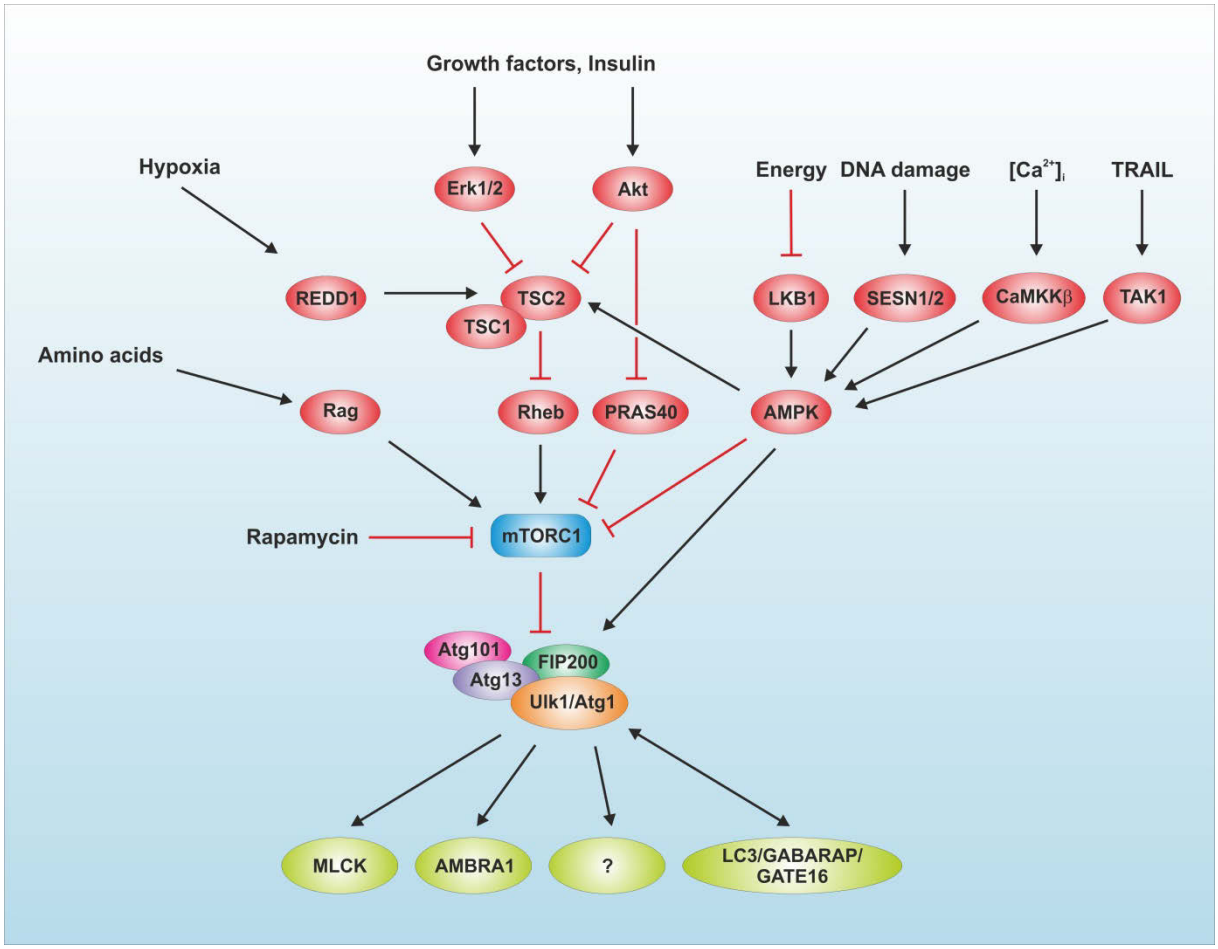

Figure 4: Signaling machinery upstream and downstream of the Ulk1 complex.

However, there likely exist additional Ulk1 substrates which contribute to the regulation of the autophagic flux in a phosphorylation-dependent manner. The identification and characterization of these Ulk1 substrates will greatly enhance our understanding of autophagy signaling pathways. Finally, it has to be noted that there apparently exist kinase-independent autophagic Ulk1 functions, and non-autophagic functions of Ulk1 complex components (reviewed in Wong et al., 2013).

1.2.4 Molecular hierarchy of Atg proteins

The functional units established by the Atgs are recruited to the PAS or the IM in a defined order, and the analysis of the hierarchical appearance of Atgs has been subject of several investigations. In 2007, Ohsumi's group reported the hierarchy of Atg proteins in PAS organization of yeast (Suzuki et al., 2007; Mizushima et al., 2011). Apparently, Atg17 functions as scaffold for the recruitment of the other Atgs to the PAS. Atg1-Atg13, Atg9 and the PI3K complex I (analogous to mammalian PI3K class

III complex) act in initial stages, whereas Atg18-Atg2, Atg16-Atg5-Atg12 and Atg8-PE units are recruited to the PAS subsequently. In 2013, Suzuki et al. fine-mapped the localization of Atgs during autophagosome formation in yeast (Suzuki et al., 2013). The authors defined specific localization sites: 1) the vacuole-IM contact site (VICS), 2) the IM, and 3) the edge of the IM close to the ER (IM edge). They showed that Atg13, Atg17 and the yeast PI3K complex I localize to the VICS, whereas Atg1, Atg8 and the Atg16-Atg5-Atg12 complex label the VICS and the IM. Finally, Atg2-Atg18 and Atg9 localized at the IM edge (Suzuki et al., 2013).

Mizushima's group performed a hierarchical analysis of mammalian Atgs (Itakura & Mizushima, 2010). Upon starvation, Ulk1, Atg14, WIPI1, LC3 and Atg16L1 are recruited to the identical compartment, whereas DFCP1 localizes adjacently to these Atgs. Apparently, the Ulk1 complex is the most upstream unit, and this unit is required for the recruitment of the Atg14L-containing PI3K class III complex. Puncta formation of DFCP1 and WIPI1 requires the presence of FIP200 and Atg14L. Finally, LC3 and the Atg16L1-Atg5-Atg12 complex are the most downstream units (Itakura & Mizushima, 2010). Later it could be shown that Atg9A and FIP200 independently localize to the autophagosome formation site, but that both are necessary for the recruitment of the downstream factors Atg14L and WIPI1 (Itakura et al., 2012a).

Notably, the Atg recruitment hierarchy appears to depend on the autophagic stimulus. For example, Ulk1 and Atg9 localize independently to the autophagosome formation site during starvation-induced autophagy, mitophagy, and *Salmonella* xenophagy (Kageyama et al., 2011; Itakura et al., 2012a). In contrast, LC3 recruitment depends on FIP200 and PI3K class III complex during starvation-induced autophagy, whereas LC3 recruitment to CCCP-depolarized mitochondria or *Salmonella*-containing vacuoles (SCVs) is independent of FIP200 or Atg9A, respectively (Kageyama et al., 2011; Itakura et al., 2012a). These data indicate that there exist differences between canonical autophagy and selective autophagy processes such as mitophagy or xenophagy. With regard to *Salmonella*-xenophagy, Noda et al. recently proposed a "Three-axis model" for Atg recruitment (Noda et al., 2012). In this model, Ulk1 and Atg9A are recruited independently to SCVs. Within the third axis, LC3 is recruited to SCVs by the Atg16L1 complex, but this recruitment does not depend on the other factors. The authors propose that the SCVs might represent an alternative membrane target for Atg16L1 recruitment, which is not present during starvation-induced autophagy (Noda et al., 2012). It is tempting to speculate that a similar mechanism holds true for LC3 recruitment during mitophagy. However, this awaits further clarification, since neither Atg5 nor Atg16L1 were detected on depolarized mitochondria (Itakura et al., 2012a).

Recently, the exocyst complex has been implicated as protein scaffold for the autophagy machinery. The exocyst is a hetero-octameric complex involved in post-Golgi trafficking and vesicle tethering to

the plasma membrane (Farre & Subramani, 2011). Bodemann et al. discovered that two exocyst subcomplexes containing either Sec5 or Exo84 regulate starvation-induced autophagy (Bodemann et al., 2011). In this model, the Sec5 exocyst subcomplex exhibits a perinuclear localization and harbors the Ulk1 kinase and PI3K class III complexes. However, this subcomplex is autophagy-inactive. Along these lines, mTORC1 associated with the Sec5-subcomplex. Upon nutrient-deprivation, the Ras-like small GTPase RalB is activated, interacts with the exocyst, and promotes the replacement of Sec5 by Exo84. The Exo84-subcomplex is autophagy-active, and serves as platform for catalytically active Ulk1 and Beclin 1/Vps34 complexes. Furthermore, the autophagy-active Exo84-subcomplex is localized to cytosolic puncta, presumably representing sites of autophagosome formation (Bodemann et al., 2011; Farre & Subramani, 2011).

1.2.5 Physiological Role of Autophagy

Autophagy and its dysregulation have been implicated in different human diseases or processes. Since our major research foci are oncology and immunology, the role of autophagy during tumorigenesis and immune responses is briefly summarized in the following.

1.2.5.1 Autophagy and cancer

Generally, autophagic signaling pathways appear to be closely connected to oncogenic signaling pathways. Various activated oncogenes generally inhibit, e.g. PI3K, Akt, mTOR, or Bcl-2, respectively. In turn, autophagy is stimulated by mutated or epigenetically silenced tumor suppressor genes, e.g. p53, PTEN, DAPK, or TSC1/TSC2, respectively (Botti et al., 2006; Mizushima et al., 2008). In recent years, the ambivalent role of autophagy for cancer development has been characterized. On the one hand autophagy functions as cyto-protective mechanism, and thus contributes to the survival of cancer cells under nutrient-deprived conditions frequently found in tumors or metastasizing cancer cells (Brech et al., 2009). Additionally, it could be shown that these cyto-protective effects support the resistance of cancer cells to metabolic or genotoxic stress induced by hormonal deprivation, chemotherapy or radiation (Abedin et al., 2007; Carew et al., 2007; Mizushima et al., 2008; Chen & Karantza, 2011). Accordingly, the disruption of autophagic signaling pathways has evolved as a therapeutic strategy and is applied in many preclinical studies and ongoing clinical trials (reviewed in Chen & Karantza, 2011)). On the other hand, it was demonstrated that various Atgs suppress tumor growth and that accordingly different autophagy-compromised mice are tumor-prone, e.g. *Becn1*+/-, *Atg4c*-/- and *Bif-1*-/- mice, mice with liver-specific *Atg7*-deletion or mosaic deletion of *Atg5* (Qu et al., 2003; Yue et al., 2003; Marino et al., 2007; Takahashi et al., 2007; Takamura et al., 2011; Long &

Ryan, 2012). Furthermore, *Atg6/Beclin 1* is mono-allelically deleted in 40-75% of all human breast, ovarian or prostate carcinomas (Mizushima et al., 2008). In addition to its tumor suppressing effects, it has been postulated that autophagy might function as an alternative cell death mechanism. In *Drosophila*, autophagy is required for the cell death observed during salivary gland development (Berry & Baehrecke, 2007). *In vitro* studies indicated that the abrogation of autophagy prevented cell death (Schwarze & Seglen, 1985; Shimizu et al., 2004; Yu et al., 2004; Azad et al., 2008; Long & Ryan, 2012), and autophagy appears to be responsible for cell death in cancer cells which lack essential apoptotic regulators such as Bax/Bak or caspases (Shimizu et al., 2004; Fazi et al., 2008; Galluzzi et al., 2012). Collectively, these data form the basis for various preclinical studies supporting autophagy induction for cancer treatment (reviewed in Chen & Karantza, 2011). However, although autophagosomes are frequently observed in dying cells exposed to anti-cancer drugs, in most cases the induction of autophagy probably represents an adaptive survival response to counteract death (Long & Ryan, 2012). Thus, it has been recommended that the functional role of autophagy in cell death execution has to be validated by the pharmacological and/or genetic inhibition of the autophagic machinery and not by the mere detection of autophagic markers (Galluzzi et al., 2012). Of note, Kroemer and colleagues recently performed a screen involving 1377 cytotoxic compounds and found that none of them induce cell death by autophagy (Shen et al., 2011; Long & Ryan, 2012). In summary, it has been proposed that the pro- and anti-tumorigenic potential of autophagy is tumor stage-dependent (Rosenfeldt & Ryan, 2009). Taking this into consideration, therapies based on autophagy induction might be beneficial for the prevention of tumorigenesis or tumor progression, whereas treatments employing the inhibition of autophagy likely support tumor regression (Mizushima et al., 2008). The ambivalent role of autophagy for cancer development is also supported by observations on the molecular level. Recently, Gong et al. reported that the putative tumor suppressor Beclin 1 is required for the tumorigenicity of breast cancer stem-like cells (Gong et al., 2013).

1.2.5.2 Autophagy and the immune system

It is very well established that autophagic signaling pathways influence diverse immunological processes, and this has been reviewed in several articles (Deretic, 2011; Levine et al., 2011; Deretic, 2012). Briefly, autophagy influences both innate and adaptive immune responses. Furthermore, autophagy directly exerts effector functions during infections. The xenophagic clearance of intracellular pathogens and the involvement of autophagy receptors are mentioned above. With regard to innate immunity, autophagy regulates the production of inflammatory cytokines and the

signaling of pattern recognition receptors (PRRs). With regard to adaptive immunity, autophagy is centrally involved in the homeostasis of T- and B-lymphocytes and in antigen presentation.

1.2.5.3 The Ulk1 complex in disease

So far, the components of the Ulk1 complex have mainly served as prognostic markers for certain tumors. However, again the observations are sometimes controversial. Jiang et al. showed that high Ulk1 expression is a novel biomarker for patients with esophageal squamous cell carcinoma (Jiang et al., 2011). Similarly, Pike et al. demonstrated that the ATF4-dependent transcriptional up-regulation of Ulk1 supports cancer cell survival. Furthermore, the authors state that Ulk1 expression is associated with a poor prognosis in breast cancer (Pike et al., 2013). Along these lines, Wei et al. reported that FIP200 deletion inhibited mammary tumor initiation, supporting a tumorigenic role for the Ulk1 complex in breast cancer (Wei et al., 2011). In contrast, Tang et al. described that low expression of Ulk1 is associated with breast cancer progression (Tang et al., 2012). Collectively, these first reports indicate that the expression levels of Ulk1 complex components might represent useful biomarkers for certain cancers. However, additional investigations are necessary to unravel the exact function of this complex for tumorigenesis and tumor progression. The link between the Ulk1 complex/autophagy and the tumor suppressor p53 is summarized in chapter 1.3.4.

Besides a potential role in tumor development, a tagging single nucleotide polymorphism (SNP) in the *ULK1* gene was associated with susceptibility to Crohn's disease (Henckaerts et al., 2011). In another study, Crohn's disease was associated with two different *ULK1* SNPs. Phenotypic analysis revealed an association with a young adult age at first diagnosis (17-40 years) and an inflammatory behavior (Morgan et al., 2012). Notably, polymorphisms in the gene encoding the FIP200-interacting Atg16L have previously been identified as risk factors for Crohn's disease (reviewed in Nguyen et al., 2013).

1.3 Critical Nodes regulating apoptosis-autophagy network

Different signaling molecules and pathways have been implicated in the regulation of both apoptosis and autophagy. This common control ensures a dynamic crosstalk between both cell fate-determining processes. In the following chapters five signaling nodes will be briefly introduced: 1) PI3K/PDK1/Akt/mTOR signaling pathway, 2) Ca^{2+}-dependent signaling, 3) Beclin 1-Bcl-2 interaction, 4)

p53-mediated regulation, and 5) proteolytic crosstalk between apoptosis and autophagy. The five nodes and their interrelations are depicted in figure 5.

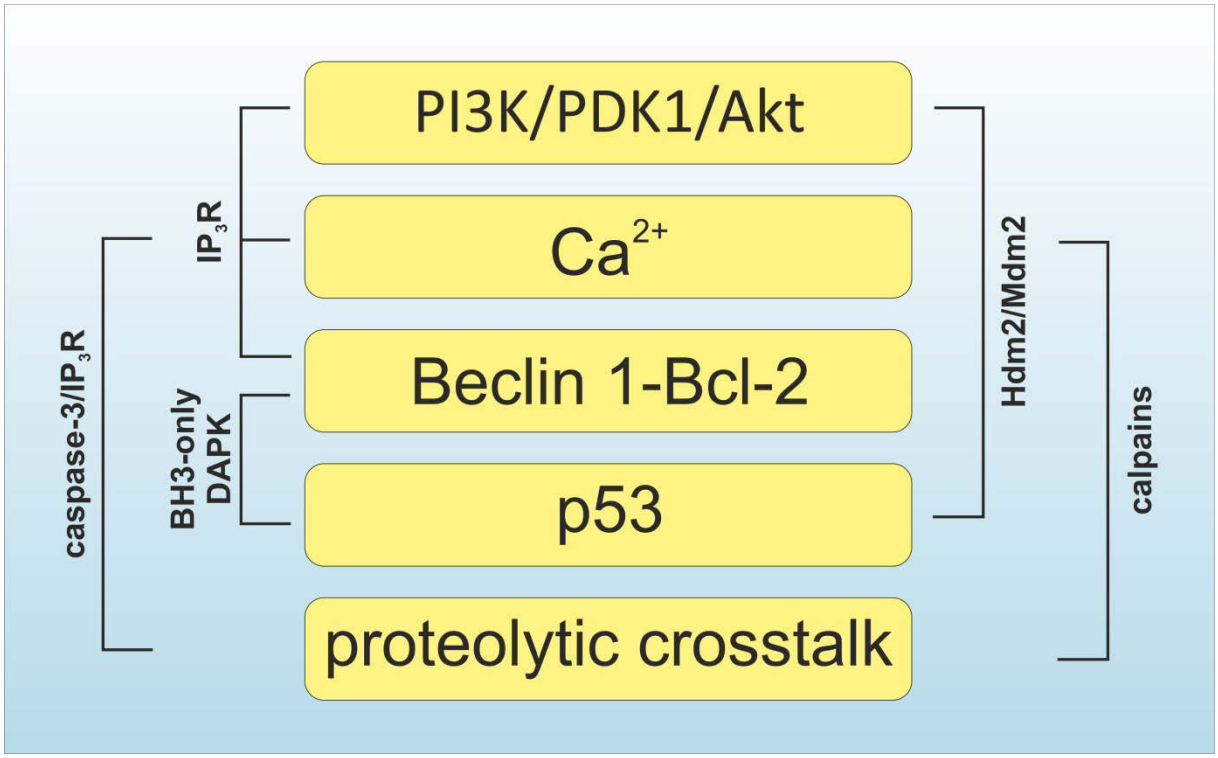

Figure 5: Critical Nodes regulating the apoptosis-autophagy network.

1.3.1 The PI3K/PDK1/Akt/mTOR signaling axis

The PI3K/PDK1/Akt/mTOR signaling axis is centrally involved in many different cellular processes, including cell growth, proliferation, metabolism, survival, and autophagy. Phosphatidylinositol 3-kinases (PI3Ks) are lipid kinases, which phosphorylate the D3 position of the inositol ring. Thus, different 3-phosphoinositide "ZIP codes" are generated at different cellular membranes, i.e. PI3P, phosphatidylinositol 3,4-bisphosphate [$PI(3,4)P_2$], and phosphatidylinositol 3,4,5-trisphosphate [$PI(3,4,5)P_3$] (reviewed in Vanhaesebroeck et al., 2010; Vanhaesebroeck et al., 2012). The fourth cellular 3-phosphoinositide phosphatidylinositol 3,5-bisphosphate [$PI(3,5)P_2$] is generated from PI3P by PIKfyve-catalyzed D5-phosphorylation (Vanhaesebroeck et al., 2010). There exist three classes of PI3Ks, which are grouped according to their substrate specificity and their sequence homology. Probably the most well studied group are class I PI3Ks, which generate $PI(3,4,5)P_3$ from $PI(4,5)P_2$. Class I PI3Ks consist of a catalytic p110 subunit (p110α, p110β, p110γ, and p110δ) and a regulatory subunit. Class I PI3Ks are further subdivided into class IA and class IB. The class IA isoforms p110α,

p110β and p110δ associate with the p85 subfamily of regulatory subunits (p85α, p85β, p55α, p50α, and p55γ). The class IB p110γ isoform associates with p101 or p84/p87 subunits. There exist three different class II isoforms, i.e. PI3K-C2α, PI3K-C2β and PI3K-C2γ. So far only one class III PI3K has been identified, i.e. Vps34. Vps34 plays an essential role for the induction of autophagy (s. chapters 1.2.2.1 and 1.3.3). In this chapter, the focus will be on class I PI3Ks. The molecular antagonists of PI3Ks are lipid phosphatases, which remove phosphate groups from the inositol ring (Blero et al., 2007; Liu & Bankaitis, 2010). The reaction catalyzed by class I PI3Ks is directly reversed by phosphatase and tensin homolog deleted on chromosome 10 (PTEN) (Liu & Bankaitis, 2010).

Historically, it has been postulated that PI3K class IA subfamily is activated downstream of receptor (-associated) tyrosine kinases (RTKs) and that class IB kinase activation is controlled by G protein-coupled receptors (GPCRs) (Engelman et al., 2006). However, recent findings indicate that class IA isoforms receive input from GPCRs and that p110γ signals downstream of RTKs following Ras activation (Vanhaesebroeck et al., 2010). Tyrosine kinases that activate the class I PI3Ks include RTKs such as insulin or growth factor receptors, or members of the Src and Syk/ZAP70 family of tyrosine kinases, which transmit signals downstream of antigen receptors (Bradshaw, 2010; Lemmon & Schlessinger, 2010). Upon generation of $PI(3,4,5)P_3$, different effector proteins are recruited to this phosphoinositide, including kinases, adapter proteins, and regulators of small GTPases (Vanhaesebroeck et al., 2010). With regard to kinases, the phosphoinositide-dependent kinase 1 (PDK1) and Akt (also termed protein kinase B, PKB) are the most well studied mediators of PI3K signaling. Both kinases belong to the AGC kinase family, and PDK1 has been dubbed the master regulator of AGC kinases, since it contributes to the activation of at least 23 AGC kinases including isoforms of Akt, p70S6K, SGK, PKC, PKN and RSK (Mora et al., 2004; Pearce et al., 2010). For the majority of AGC kinases, complete activation involves the phosphorylation of two conserved motifs. One motif lies within the activation segment (also termed T-loop) of the catalytic domain, and the second hydrophobic motif resides within a region C-terminal of the kinase domain (Pearce et al., 2010). PDK1 catalyzes the phosphorylation of the activation segment of the kinases listed above (Alessi et al., 1997a; Alessi et al., 1997b; Stokoe et al., 1997; Alessi et al., 1998; Chou et al., 1998; Dutil et al., 1998; Le Good et al., 1998; Pullen et al., 1998; Stephens et al., 1998; Dong et al., 1999; Jensen et al., 1999; Kobayashi & Cohen, 1999; Kobayashi et al., 1999; Park et al., 1999; Richards et al., 1999; Balendran et al., 2000; Dong et al., 2000; Flynn et al., 2000; Frodin et al., 2000), and mechanistic details have been nicely summarized in different review articles (Mora et al., 2004; Pearce et al., 2010). PDK1 contains a kinase domain and a C-terminal pleckstrin homology (PH) domain, which mediates recruitment to $PI(3,4,5)P_3$ or $PI(3,4)P_2$ (Alessi et al., 1997a; Alessi et al., 1997b; Currie et al., 1999; Bayascas, 2010). Notably, PDK1 is constitutively active (Alessi et al.,

1997a), and essentially two different mechanisms have been established to explain how constitutively active PDK1 regulates the inducible activation of downstream kinases. In the case of Akt isoforms, the simultaneous recruitment of PDK1 and Akt to PI(3,4,5)P_3 at the plasma membrane is a key step. Like PDK1, Akt isoforms possess a PH domain (see below). Upon PI3K-dependent generation of PI(3,4,5)P_3, PDK1 and Akt co-localize at the plasma membrane, and additionally PI(3,4,5)P_3-binding induces a conformational change of Akt. This in turn results in the subsequent PDK1-catalyzed phosphorylation of Akt at T308 in the activation segment (Currie et al., 1999). The phosphorylation of S473 in the hydrophobic motif is catalyzed by mTORC2 (see below), leading to full Akt activation (Sarbassov et al., 2005). All other AGC kinases activated by PDK1 lack a PH domain, which precludes the activation by PH-dependent co-localization at the plasma membrane (Bayascas, 2008). In these cases, the phospho-acceptor site within the hydrophobic motif is phosphorylated first by upstream kinases, e.g. mTORC1 or mTORC2 (Bayascas, 2008; Pearce et al., 2010). The phosphorylated hydrophobic motif then binds to a small phosphate binding groove within the PDK1 kinase domain, which is termed the PDK1-interacting fragment (PIF) pocket (Balendran et al., 2000; Biondi et al., 2000; Biondi et al., 2001; Mora et al., 2004; Bayascas, 2008; Pearce et al., 2010). Notably, atypical PKC or PKN isoforms possess an acidic phospho-mimetic D or E residue in the hydrophobic motif, which appears to mediate the interaction with the PIF pocket (Mora et al., 2004; Pearce et al., 2010). Following this association, PDK1 phosphorylates the activation segment and activates the kinase (Mora et al., 2004; Pearce et al., 2010). Interestingly, Alessi's group recently reported that Akt may also be activated by a PIF pocket-dependent mechanism (Najafov et al., 2012). It appears that mTORC2-mediated phosphorylation of Akt at S437 enables PDK1 to bind via its PIF pocket. Although in this scenario PDK1 does not need to bind PI(3,4,5)P_3, apparently Akt must still bind to PI(3,4,5)P_3 in order to be activated by PDK1 (Najafov et al., 2012). Collectively, this data would nicely explain why Akt is still partially activated in knockin mice expressing a PDK1 mutant with an inactivated PH domain (Bayascas et al., 2008).

In mammalian cells three Akt isoforms exist, i.e. Akt1, Akt2, and Akt 3 (alternatively called PKBα, PKBβ, and PKBγ) (Gonzalez & McGraw, 2009; Hers et al., 2011). The isoforms are ubiquitously expressed, but expression levels vary depending on the cell and tissue type (Carnero, 2010). In 1977, Staal and colleagues reported the isolation of the murine retrovirus AKT8 from a spontaneous thymoma of an AKR mouse (Staal et al., 1977). Ten years later Staal reported the cloning of the presumed viral oncogene and termed it v-akt (Staal, 1987). Within the same publication, the cloning of the two human homologs Akt1 and Akt2 were reported. Additionally, an Akt1 allele amplification was identified in a primary gastric adenocarcinoma, prompting the author to speculate that Akt "may be involved in the pathogenesis of some human malignancies" (Staal, 1987). This assumption has

been proven true as will be described below. All three Akt isoforms contain three structurally distinct regions, i.e. an N-terminal PH domain, a catalytic domain, and a C-terminal extension containing the regulatory hydrophobic motif (Kumar & Madison, 2005). The PH domain is connected to the catalytic domain via a linker region, which is the least conserved region of the Akt isoforms (Kumar & Madison, 2005). In 1996, Alessi et al. reported the Akt consensus sequence with R-x-R-y-z-S/T-hyd (with x = any amino acid, y,z = small residues other than G, S/T = phosphorylation site, and hyd = bulky hydrophobic residue) (Alessi et al., 1996). This consensus sequence was later complemented and predicted as R-K-R-x-R-T-Y-S-F-G (with x = any amino acid and S = phosphorylation site) (Obata et al., 2000). To date, more than 100 substrates of Akt isoforms have been reported, and an actual list can be found in the internet at www.phosphosite.org. Akt isoforms regulate a large variety of cellular processes, e.g. cell survival, cell growth, differentiation, cell cycle, translation, transcription, metabolism, and autophagy. In this thesis, the focus will be on the substrates related to cell survival and autophagy signaling.

Generally Akt has been designated as pro-survival kinase, since activated Akt phosphorylates a range of substrates leading to a rather anti-apoptotic state of the cell (reviewed in (Duronio, 2008; Parcellier et al., 2008)). Both intrinsic and extrinsic apoptosis pathway are targeted by Akt. In table 2 (adapted and modified from Duronio, 2008) different apoptosis-related substrates of Akt are listed.

In 1997, several groups reported the Akt-mediated phosphorylation of the pro-apoptotic Bad at S136 (Datta et al., 1997; del Peso et al., 1997; Blume-Jensen et al., 1998). This leads to the binding of 14-3-3 proteins (Masters et al., 2001), which in turn enables Bad phosphorylation at S155 within the BH3 domain by PKA and RSK1. This latter phosphorylation leads to the disruption of the Bad-Bcl-2 interaction and thus promotes cell survival (Datta et al., 2000; Tan et al., 2000). However, other reports question the importance of Akt-mediated Bad phosphorylation for cell survival (reviewed in Duronio, 2008). Other members of the Bcl-2 family have also been reported to be phosphorylated and thus regulated by Akt, such as Bax, Bim-EL, and Bcl-x_S (Gardai et al., 2004; Xin & Deng, 2005; Qi et al., 2006; Wei et al., 2009). Next to the direct phosphorylation by Akt, the phosphorylation status of different Bcl-2 family proteins is also indirectly regulated via the Akt substrate glycogen synthase kinase 3 (GSK3). For example, both Bax and Mcl-1 are phosphorylated by GSK3 and thus activated and destabilized, respectively (Linseman et al., 2004; Maurer et al., 2006; Ding et al., 2007a; Ding et al., 2007b). Since GSK3 is inhibited by Akt-catalyzed phosphorylation (reviewed in Cohen & Frame, 2001), Akt activation leads to the inactivation of Bax or the stabilization of Mcl-1, respectively. The key effector proteins of apoptosis, i.e. caspases, have also been demonstrated to represent Akt substrates. Cardone et al. reported an Akt-mediated inhibitory phosphorylation of caspase-9 at S196 (Cardone et al., 1998). However, the relevance of this observation is still debated since an

Table 2: Published Akt substrates with a role in apoptosis

Substrate	Phospho-site (human position)	Outcome	Reference
Acinus-S	S422, S537	Inhibition of cleavage	Hu 2005
ASK1	S83	Decreased kinase activity	Kim 2001
Bad	S136	Binding of 14-3-3 proteins	Del Peso 1997, Datta 1997, Blume-Jensen 1998
Bax	S184	Retention of Bax in cytoplasm; association with antiapoptotic Bcl2 family members	Gardai 2004, Xin 2005
Bcl-x_S	S106	Dissociation from VDAC	Wei 2009
Bim-EL	S87	Attenuation of pro-apoptotic function	Qi 2006
Caspase-8	T263	Putative inhibition of processing	Kang 2006, Shim 2004
Caspase-9	S196	Inhibition of protease activity	Cardone 1998
CREB	S133	Activation; recruitment of co-activator CBP	Du 1998
FoxO1 FoxO3A FoxO4	T24, S256, S319 T32, S253, S315 T32, S197, S262	Binding of 14-3-3 proteins; nuclear exclusion	Rena 1999, Biggs 1999, Tang 1999, del Peso 1999 Brunet 1999 Kops 1999, Takaishi 1999
GSK3α GSK3β	S21 S9	Inhibition	Cross 1995 Cross 1995
Omi/HtrA2	S212	Attenuation of protease activity	Yang 2007
IKK-α	T23	Induction of IKK activity	Ozes 1999, Kane 1999, Romashkova 1999
IP_3R	S2690	Suppression of downstream caspase activation; potentially reduced Ca^{2+} release activity	Khan 2006, Szado 2008
Mdm2	S166/S186	Nuclear import; increased p53 ubiquitination	Mayo 2001, Gottlieb 2002
MLK3	S674	Inhibition	Barthwal 2003
SEK1/MAPKK4	S80	Inhibition	Park 2002
XIAP	S87	Stabilization	Dan 2004
YAP1	S127	Binding of 14-3-3 proteins; localization to cytoplasm; reduced p73 activity	Basu 2003

(adapted and modified from Duronio, 2008)

orthologous site is absent in monkey, mouse, rat, dog and zebrafish isoforms (Fujita et al., 1999; Allan & Clarke, 2009). Interestingly, Shultz et al. demonstrated that Akt regulates the ratio between caspase-9 splice variants a (catalytically active) and b (catalytically inactive) by phosphorylating the RNA splicing factor SRp30a (Shultz et al., 2010). Caspase-8 has also been suggested as an Akt target protein. However, so far the evidence is rather indirect since cell lysates were employed for the *in vitro* kinase assays using caspase-8-derived peptides containing an Akt consensus sequence surrounding T263 (Shim et al., 2004; Kang et al., 2006). IAPs and their inhibitors are additional targets of Akt. Dan et al. reported that Akt phosphorylates and thus stabilizes XIAP (Dan et al., 2004). In turn, mitochondria-released Omi/HtrA2 is phosphorylated on S212, leading to an attenuation of its protease activity (Yang et al., 2007). Acinus is a nuclear factor which is cleaved by caspase-3 and is required for apoptotic chromatin condensation (Sahara et al., 1999; Parcellier et al., 2008). In 2005, Hu et al. demonstrated that Akt phosphorylates Acinus and inhibits its proteolytic cleavage, thus preventing chromatin condensation (Hu et al., 2005). IP_3Rs are central regulators of cytosolic Ca^{2+} concentrations (see chapter 1.3.2), and are centrally involved in the crosstalk between PI3K/Akt signaling, Ca^{2+} signaling, and Beclin 1-Bcl-2 signaling. Khan et al. showed that IP_3Rs represent Akt substrates (Khan et al., 2006). Interestingly, expression of a non-phosphorylatable mutant did not influence IP_3R channel activity, but staurosporine-induced caspase-3 activation was enhanced, indicating that Akt-mediated IP_3R phosphorylation may limit the apoptotic effects of Ca^{2+} (Khan et al., 2006). The Akt-dependent phospho-site in IP_3R1 was confirmed by Szado et al. (Szado et al., 2008). However, in contrast to Khan et al. the found a reduced Ca^{2+} release activity upon phosphorylation. Akt also influences the apoptotic program by crosstalk with the JNK/p38 stress signaling pathways (reviewed in Parcellier et al., 2008). It has been reported that different upstream kinases of JNK/p38 become phosphorylated by Akt, e.g. ASK1, MLK3, and SEK1/MAPKK4 (Kim et al., 2001; Park et al., 2002; Barthwal et al., 2003). Finally, Akt controls apoptosis on transcriptional level by regulating major classes of transcription factors, including the forkhead box O family of transcription factors (FoxOs), NF-κB, p53/p73 family, and cAMP-response element binding protein (CREB). The Akt-mediated control of these transcription factors and their control of apoptosis related genes are summarized in various review articles (Brunet et al., 2001; Duronio, 2008; Parcellier et al., 2008; Hers et al., 2011; Zhang et al., 2011a). Again, this regulation can occur in either direct or indirect fashion. Whereas FoxOs and CREB are direct substrates of Akt, NF-κB and p53/p73 pathways are indirectly affected by Akt activity. Additionally, Akt can either positively (CREB, NF-κB) or negatively (FoxOs, p53/p73) regulate the induction of transcription. There exist multiple interconnections between Akt and p53, e.g. Akt phosphorylates the ubiquitin ligase Mdm2, leading to its nuclear import and increased p53 ubiquitination (Mayo & Donner, 2001; Gottlieb et al., 2002). This leads to reduced expression of several pro-apoptotic genes (see chapter 1.3.4). In turn, activated p53 induces the

expression of PTEN (Stambolic et al., 2001), which negatively regulates Akt activity. With regard to p73, it was shown that Akt phosphorylates the Yes-associated protein 1 (YAP1) at S127 and thus inhibits its function as co-activator or p73 (Basu et al., 2003). In addition, Akt has an important role in the positive regulation of NF-κB-mediated transcription. This regulation is mainly mediated by the Akt-catalyzed phosphorylation and activation of I-κB kinase-α (IKK-α), which results in the phosphorylation of I-κB and its subsequent degradation (Kane et al., 1999; Ozes et al., 1999; Romashkova & Makarov, 1999). NF-κB target genes include the anti-apoptotic proteins Bcl-2, Bcl-x_L, FLIP, and c-IAP1/2, respectively. Akt-catalyzed phosphorylation of FoxO1, FoxO3A and FoxO4 transcription factors leads to their binding to 14-3-3 proteins and their retention in the cytoplasm (Biggs et al., 1999; Brunet et al., 1999; del Peso et al., 1999; Kops et al., 1999; Rena et al., 1999; Takaishi et al., 1999; Tang et al., 1999). This in turn prevents the transcription of pro-apoptotic target genes such as the BH3-only family proteins Bim and Puma or the death receptor ligands FasL and TRAIL. In contrast, Akt-mediated phosphorylation of CREB at S133 enables the binding of the co-activator CREB-binding protein (CBP) and the transcription of pro-survival genes such as Bcl-2 and Mcl-1 (Du & Montminy, 1998). Naturally, table 2 is likely to be incomplete, and ongoing research aims at the identification of additional anti-apoptotic Akt substrates. However, it has to be noted that Akt has also be connected to pro-apoptotic signal transduction under certain circumstances (reviewed in Los et al., 2009). Van Gorp et al. reported that chronic Akt activation leads to oxidative stress, which results in FoxO3a up-regulation and subsequent cell death (van Gorp et al., 2006). Furthermore, Akt was shown to sensitize cells to ROS-mediated apoptosis (Nogueira et al., 2008).

Next to the direct phosphorylation of Ulk1 by Akt described in chapter 1.2.3.3, the most important entry point for Akt to regulate autophagy is mTOR. In chapter 1.2.3 it is described how mTOR controls the induction of the autophagic program. In this chapter the inputs for mTOR are described, with focus on the PI3K/PDK1/Akt axis as one central regulatory pathway. Rapamycin (alternatively termed sirolimus) is a macrolide produced by *Streptomyces hygroscopicus* bacteria, which were isolated from an Easter Island (Rapa Nui) soil sample (Vezina et al., 1975). In 1993, TOR1 and TOR2 were identified in yeast, and shortly after that the mammalian ortholog (Cafferkey et al., 1993; Kunz et al., 1993; Brown et al., 1994; Sabatini et al., 1994; Sabers et al., 1995). The serine/threonine kinase mTOR is the catalytic subunit of two distinct complexes, i.e. mTORC1 and mTORC2, respectively (reviewed in Zoncu et al., 2011b; Laplante & Sabatini, 2012). The two complexes contain unique associated proteins serving as scaffolds and determining the substrate specificity of the complexes, i.e. regulatory-associated protein of mTOR (raptor) and rapamycin-insensitive companion of mTOR (rictor), respectively (Hara et al., 2002; Kim et al., 2002; Sarbassov et al., 2004). Next to these two proteins, the two complexes harbor additional specific interacting proteins: mTORC1 contains the

proline-rich Akt substrate of 40 kDa (PRAS40), while mTORC2 contains the mammalian stress-activated map kinase-interacting protein 1 (mSin1) and the protein observed with rictor 1 and 2 (protor1/2) (Frias et al., 2006; Jacinto et al., 2006; Yang et al., 2006; Pearce et al., 2007; Sancak et al., 2007; Thedieck et al., 2007; Vander Haar et al., 2007; Wang et al., 2007). However, the two complexes also share some components: mammalian lethal with sec-13 protein 8 (mLST8, also termed G protein β subunit-like, GβL), DEP domain containing mTOR-interacting protein (DEPTOR), and the Tti1/Tel2 complex (Loewith et al., 2002; Kim et al., 2003; Jacinto et al., 2004; Peterson et al., 2009; Kaizuka et al., 2010). mTOR contains a cluster of HEAT (huntingtin, elongation factor 3, a subunit of protein phosphatase 2A, TOR1) repeats at the N-terminus. These are followed by FAT (FRAP, ATM, TRRAP) domain, the FKBP12-rapamycin binding (FRB) domain, the catalytic kinase domain, and a FAT domain at the C-terminus (FATC) (reviewed in Zoncu et al., 2011b; Laplante & Sabatini, 2012). Rapamycin binds to the FK506 binding protein of 12 kDa (FKBP12), and this complex inhibits mTOR when it is part of mTORC1, but not when it is part of mTORC2 (Loewith et al., 2002; Jacinto et al., 2004; Sarbassov et al., 2004). However, this is a simplistic view, since Sarbassov et al. demonstrated that prolonged rapamycin treatment inhibits mTORC2 assembly. They observed that in many cell types this results in mTORC2 levels below those needed to maintain Akt signaling (Sarbassov et al., 2006). Next to the control of autophagic processes, mTOR controls a plethora of cellular processes. In detail, mTORC1 regulates protein synthesis, lipid synthesis, lysosome biogenesis, and energy metabolism, whereas mTORC2 is mainly involved in survival signaling and cytoskeletal organization (reviewed in Laplante & Sabatini, 2012). With regard to protein synthesis, mTORC1 directly phosphorylates p70S6 kinase (p70S6K) and eukaryotic translation initiation factor 4E (eIF4E)-binding protein 1 (4E-BP1) (reviewed in Ma & Blenis, 2009).

As mentioned in chapter 1.2.3.3, mTORC1 integrates nutrient signals (e.g. growth factors or amino acids), energy signals (e.g. AMP/ATP ratio), and stress signals (e.g. hypoxia or DNA damage). Akt is the central mediator to transmit growth factor signals to mTOR. Akt phosphorylates tuberous sclerosis 2 protein (TSC2; also termed tuberin), which together with TSC1 (also termed hamartin) forms the TSC1-TSC2 complex. Four to five different Akt-dependent phospho-sites have been reported, and TSC2 phosphorylation inhibits the GTPase activating protein (GAP) activity for the small GTPase Ras homolog enriched in brain (Rheb) (Inoki et al., 2002; Manning et al., 2002a; Potter et al., 2002). In turn, GTP-loaded Rheb stimulates the kinase activity of mTORC1 (Saucedo et al., 2003; Stocker et al., 2003). Accordingly, activated Akt inhibits the Rheb-inhibiting TSC2-TSC1 complex, leading to mTORC1 activation. In an alternative pathway, Akt phosphorylates the proline-rich Akt substrate of 40 kDa (PRAS40), which then is bound by 14-3-3 proteins and hence cannot inhibit mTORC1 anymore (Kovacina et al., 2003; Sancak et al., 2007; Thedieck et al., 2007; Vander Haar et al., 2007; Wang et al., 2007). Finally, it has also been reported that Akt directly phosphorylates mTOR

at S2448 (Nave et al., 1999; Sekulic et al., 2000). However, later it was discovered that S2448 phosphorylation is likely catalyzed by the downstream p70S6K (Chiang & Abraham, 2005). Collectively, mTORCs function upstream, i.e. S473 phosphorylation by mTORC2, and downstream of Akt, i.e. Akt-dependent activation of mTORC1. Next to the PI3K/Akt axis, growth factors might control mTOR activity via the Ras-Raf-MEK-ERK pathway or via the Wnt pathway (reviewed in Zoncu et al., 2011b). The amino acid signaling upstream of mTOR has also been elucidated recently (reviewed in Zoncu et al., 2011b; Laplante & Sabatini, 2012; Jewell et al., 2013). Amino acid induced activation of mTORC1 depends on Rag family of small GTPases (Kim et al., 2008; Sancak et al., 2008). There exist four family members in mammals, i.e. RagA-D. They form heterodimers of either RagA or RagB with RagC or RagD. In the presence of amino acids, Rag GTPases acquire an active conformation, in which RagA/B are GTP-loaded and RagC/D are GDP-loaded. Active Rag heterodimers associate with raptor and translocate mTORC1 to the lysosomal surface. There, the Rag GTPases dock to trimeric complex termed Ragulator, consisting of MP1, p14, and p18 (Sabatini et al., 1994; Sancak et al., 2010). On the surface of lysosomes, mTORC1 becomes activated by Rheb, which is generally found on endomembranes (Laplante & Sabatini, 2012). Completing this interplay between Rag-Ragulator and Rheb on the lysosomal surface, Zoncu et al. reported an inside-out model of amino acid sensing which requires the vacuolar H^+-ATPase (v-ATPase). Apparently, amino acids accumulating within the lysosomal lumen regulate the physical interaction between v-ATPase and Ragulator (Zoncu et al., 2011a).

Energy signals are mainly transduced to mTOR via AMPK (see also chapter 1.2.3.3). Under energy-depleted conditions, AMPK phosphorylates TSC2 and thus stimulates the GAP activity of TSC1-TSC2 for Rheb, which leads to mTOR inhibition (Corradetti et al., 2004; Inoki et al., 2006). Alternatively, AMPK directly phosphorylates raptor, thus promoting 14-3-3 binding and mTORC1 inhibition (Gwinn et al., 2008). Finally, stress signals like hypoxia or DNA damage also inhibit mTORC1 via the TSC1-TSC2 complex (reviewed in Zoncu et al., 2011b; Laplante & Sabatini, 2012). Hypoxia activates TSC1-TSC2 via AMPK or the protein regulated in development and DNA damage response 1 (REDD1) (Brugarolas et al., 2004; Reiling & Hafen, 2004; DeYoung et al., 2008). DNA damage induces the p53-dependent expression of sestrin 1 and 2, which in turn activate AMPK (see chapter 1.3.4) (Budanov & Karin, 2008). Additionally, TSC2 and the AMPK β-subunits are transcriptional targets of p53 (see chapter 1.3.4) (Feng et al., 2007b).

Frequently, components of the PI3K/PDK1/Akt/mTOR signaling axis are aberrantly activated in tumors, and negative regulators of this pathway such as PTEN or TSC1-TSC2 are inactivated or deleted (Chiang & Abraham, 2007; Engelman, 2009). Accordingly, the components of this central signaling pathway are attractive targets for therapeutic intervention. Different inhibitors of PI3K,

PDK1, Akt and mTOR were or currently are clinically evaluated. They are all kinases and accordingly "druggable" targets (Carnero, 2010). With regard to mTOR inhibition, not only rapamycin and rapalogs have been developed or tested, but also ATP-competitive inhibitors, which accordingly inhibit both mTORC1 and mTORC2 (reviewed in Zoncu et al., 2011b; Laplante & Sabatini, 2012). These compounds include Torin1, PP242, PP30, AZD8055, Ku-0063794, WAY-600, WYE-687, and WYE-354 (Feldman et al., 2009; Garcia-Martinez et al., 2009; Thoreen et al., 2009; Yu et al., 2009; Chresta et al., 2010). Interestingly, these inhibitors are more efficient than rapamycin even in mTORC2-deficient cells, supporting the existence of rapamycin-resistant functions of mTORC1 (Feldman et al., 2009; Thoreen et al., 2009; Laplante & Sabatini, 2012). Furthermore, there exist dual inhibitors of PI3K and mTOR due to the similarity of their catalytic domains (Zoncu et al., 2011b; Laplante & Sabatini, 2012).

1.3.2 Ca^{2+} signaling

Bivalent Ca^{2+} ions likely represent the most universal mediators of signal transduction. The intracellular Ca^{2+} concentration $[Ca^{2+}]_i$ is tightly controlled. A 20,000fold gradient is maintained across the plasma membrane, with a $[Ca^{2+}]_i$ of approximately 100 nM in resting cells (Clapham, 2007). Upon reception of a Ca^{2+}-mobilizing stimulus, $[Ca^{2+}]_i$ might increase >10fold within milliseconds (Clapham, 2007). Elevation of $[Ca^{2+}]_i$ might be executed by two basic mechanisms, i.e. influx across the plasma membrane or release from intracellular stores like the ER or the sarcoplasmic reticulum (SR). Ca^{2+} ions mediate signal transduction essentially via two mechanisms: 1) by direct binding to a target protein containing a Ca^{2+}-binding domain, e.g. the EF hand domain or the C2 domain, or 2) via Ca^{2+} adaptor proteins. The best studied Ca^{2+} adapter protein is calmodulin, which amplifies the size of the Ca^{2+} ion to the scale of a protein (Clapham, 2007). Hundreds of Ca^{2+}/calmodulin-regulated enzymes have been identified to date, with calcineurin and Ca^{2+}/calmodulin-dependent kinase (CaMK) as two prominent examples. There exist a huge variety of Ca^{2+} channels mediating the influx across the plasma membrane, and they are defined by their mode of activation, e.g. voltage-gated, ligand-gated, or receptor-activated Ca^{2+} channels (Barritt, 1999). Release of Ca^{2+} from intracellular stores is mainly mediated by IP_3 receptors (IP_3Rs) or the closely related ryanodine receptors (RyRs) (Taylor & Tovey, 2010). There exist three mammalian isoforms of IP_3Rs, and the Ca^{2+}-conducting pore is formed by homotetramers (Taylor & Tovey, 2010). IP_3Rs are activated by Ca^{2+}, and sensitivity is regulated by IP_3. Activation of G protein-coupled receptors, receptor tyrosine kinases, or receptor-associated tyrosine kinases leads to the activation of phospholipase C (PLC)-β or γ, respectively. The activated

PLCs catalyze the cleavage of phosphatidylinositol-4,5-bisphosphate into diacylglycerol (DAG) and the freely diffusible IP_3.

Ca^{2+} ions play an important role for the control of cell fate decisions, and they are involved in the regulation of apoptosis, proliferation, and differentiation. Recently, the function of Ca^{2+} ions for the control of autophagic processes has been revealed (see chapter 2.5). Apparently, the connection between ER-localized IP_3Rs and mitochondria-resident channels is of central importance for the decision between survival and apoptosis (reviewed in Decuypere et al., 2011b; Giorgi et al., 2012). Ca^{2+} transfer across the outer mitochondrial membrane is mainly mediated by the voltage-dependent anion channel (VDAC) (Gincel et al., 2001; Decuypere et al., 2011b; Giorgi et al., 2012). The understanding of Ca^{2+} transport across the inner mitochondrial membrane has also been increased recently (reviewed in Drago et al., 2011). Palty et al. characterized the mitochondrial Ca^{2+}/Na^{+} antiporter (Palty et al., 2010). Additionally, the mitochondrial Ca^{2+} uniporter MCU and its regulator mitochondrial Ca^{2+} uptake 1 (MICU1) were described (Perocchi et al., 2010; Baughman et al., 2011; De Stefani et al., 2011). Three different scenarios can be anticipated (reviewed in Decuypere et al., 2011b). Firstly, under normal physiological conditions Ca^{2+} ions released by the ER-resident IP_3Rs are taken up by the mitochondria. This process ensures normal mitochondrial functions such as ATP production. Secondly, if the Ca^{2+} transfer to the mitochondrion exerts a certain threshold, the induction of apoptosis is promoted. Thirdly, a decreased Ca^{2+} uptake by the mitochondria supports the induction of autophagy. This could be explained by a reduced mitochondrial ATP production and subsequent AMPK activation due to an elevated AMP/ATP ratio (Cardenas et al., 2010; Decuypere et al., 2011a; Decuypere et al., 2011b; Cardenas & Foskett, 2012).

Next to the transfer of Ca^{2+} between ER and mitochondria, the IP_3Rs themselves apparently are mediators of the crosstalk between apoptosis and autophagy. Different anti- and pro-apoptotic members of the Bcl-2 family regulate Ca^{2+} release, and several groups reported that IP_3Rs are targets of anti-apoptotic Bcl-2 proteins, including Bcl-2, Bcl-x_L, and Mcl-1 (reviewed in Decuypere et al., 2011a; Decuypere et al., 2011b; Cardenas & Foskett, 2012; Giorgi et al., 2012; Monaco et al., 2013). Interestingly, different modes of action have been proposed to explain the Ca^{2+}-regulating function of Bcl-2 proteins and will be briefly summarized in the following (reviewed in Decuypere et al., 2011b). First, it was reported that Bcl-2 forms a macromolecular complex with IP_3Rs. Apparently, the amount of bound Bcl-2 increases if the ratio between anti- and pro-apoptotic Bcl-2 proteins increases, e.g. by deletion of Bax and Bak (Oakes et al., 2005). It was suggested that Bcl-2 regulates the phosphorylation status of IP_3R and sensitizes them for IP_3, resulting in an enhanced Ca^{2+} leak from the ER and a reduced steady state level of Ca^{2+} in the ER. Second, different groups reported the binding of Bcl-2, Bcl-x_L or Mcl-1 to the C-terminus of IP_3Rs, thereby allosterically activating them

and/or sensitizing them to subsaturating IP_3 concentrations (White et al., 2005; Li et al., 2007; Eckenrode et al., 2010). Thirdly, Bcl-2 was reported to inhibit IP_3-induced Ca^{2+}-release without altering the luminal ER Ca^{2+}-content (Chen et al., 2004; Zhong et al., 2006; Rong et al., 2008; Rong et al., 2009). Furthermore, in T lymphocytes Bcl-2 differentially regulated Ca^{2+} signals according to the strength of the incoming T cell antigen receptor (TCR) signal (Zhong et al., 2006). Notably, the interaction site on IP_3Rs was mapped to the central regulatory domain, and not to the C-terminus (Rong et al., 2008). Furthermore, the association was mediated by the Bcl-2 BH4 domain, which is not involved in its binding to the C-terminus (Rong et al., 2009). In 2010, Monaco et al. suggested the different anti-apoptotic Bcl-proteins differently interact with IP_3Rs. Two years later the same group demonstrated that a difference in one single residue in the BH4 domains of Bcl-2 and Bcl-x_L determines IP_3R binding (Monaco et al., 2012). Recently, they presented a convincing hypothesis how these differences might be integrated. Apparently, Bcl-2 binds via is BH4 domain to the central regulatory domain of IP_3Rs. This association reduces large global Ca^{2+} transients, which are pro-apoptotic. In contrast, Bcl-x_L engages its hydrophobic groove (see chapter 1.1.2.2) to interact with the C-terminal region of IP_3Rs, thus promoting IP_3R sensitivity towards low IP_3 concentrations and mediating pro-survival Ca^{2+} oscillations (Monaco et al., 2013). Finally and fourthly, Bcl-x_L regulates the expression of IP_3Rs via regulation of NFATc2 (Li et al., 2002). As briefly mentioned above, pro-apoptotic Bcl-2 family members participate in the regulation of ER Ca^{2+} homeostasis (Scorrano et al., 2003; Oakes et al., 2005; Jones et al., 2007). Additionally, other factors were shown to affect IP_3R function during apoptosis (reviewed in Decuypere et al., 2011b). IP_3R1 was reported to interact with cytochrome c (Boehning et al., 2003). This interaction represents a feed-forward mechanism amplifying apoptosis, since cytochrome c blocks Ca^{2+}-dependent inhibition of IP_3R function and supports a dysregulated Ca^{2+}-release. Later the same group reported that a cell permeant peptide derived from the IP_3R1 binding site inhibits staurosporine- and CD95L-induced apoptosis (Boehning et al., 2005). Finally, IP_3R1 is a substrate for caspase-3 (Hirota et al., 1999; Assefa et al., 2004). Caspase-3 cleaves IP_3R1 at $D^{1888}EVD*R^{1892}$ (murine sequence) and this removes the N-terminal regulatory domain (Hirota et al., 1999; Decuypere et al., 2011b). Apparently, this truncation generates a “channel only” variant which permits IP_3-independent Ca^{2+}-release during apoptosis (Assefa et al., 2004).

With regard to the regulation of autophagy, different effector mechanisms depending on IP_3Rs have been suggested. One is the above described signaling pathway, mediated by a reduced Ca^{2+} transfer to mitochondria, the thus resulting reduced ATP production and subsequent AMPK activation (Cardenas et al., 2010; Cardenas & Foskett, 2012). It has also been proposed that this mechanism mediates the anti-apoptotic effects of Bcl-2 proteins. In this hypothesis, Bcl-2/Bcl-x_L sensitize IP_3Rs and thus allow for low level Ca^{2+} transfer to mitochondria, which is required for sufficient ATP

production (Cardenas & Foskett, 2012). An alternative model depends on the association between anti-apoptotic Bcl-2 proteins and Beclin 1. This is further explained in chapter 1.3.3. Finally, there appears to be crosstalk between IP_3Rs and mTOR (reviewed in Decuypere et al., 2011a). It was demonstrated that mTOR phosphorylates IP_3R subtypes 2 and 3 and thus positively influences their Ca^{2+}-release activity (Fregeau et al., 2011; Regimbald-Dumas et al., 2011). Notably, there exist also contrary findings about mTOR activity in DT40 cells deficient for all three IP_3R isoforms (reviewed in Decuypere et al., 2011a). Khan et al. report that mTOR activity is decreased in these cells (Khan & Joseph, 2010). In contrast, Cardenas et al. observed an unaltered mTOR activation status, suggesting that their mitochondria-dependent AMPK activation described above functions via an mTOR-independent pathway (Cardenas et al., 2010). The impact of cytosolic Ca^{2+} is discussed in chapter 2.5.

1.3.3 Beclin 1-Bcl-2 interaction

An alternative regulatory connection between autophagy and apoptosis is mediated by the direct interaction of the pro-autophagic Beclin 1 with members of the anti-apoptotic Bcl-2 family, including Bcl-2, Bcl-x_L, Bcl-w, Mcl-1, and viral Bcl-2 proteins (Liang et al., 1998; Pattingre et al., 2005; Erlich et al., 2007; Feng et al., 2007a; Maiuri et al., 2007a; Maiuri et al., 2007b; Oberstein et al., 2007; Ku et al., 2008; Sinha et al., 2008; E et al., 2009). Beclin 1 was originally identified as Bcl-2-interacting protein by a yeast-two-hybrid screen (Liang et al., 1998). The functional relevance of this interaction has been described by Pattingre et al. in 2005 (Pattingre et al., 2005). They showed that Bcl-2 can inhibit starvation-induced and Beclin 1-dependent autophagy. This has been confirmed for viral Bcl-2 proteins derived from human Kaposi's sarcoma-associated herpesvirus or murine γ-herpesvirus 68 (Pattingre et al., 2005; Ku et al., 2008; Sinha et al., 2008; E et al., 2009). Beclin 1 contains a Bcl-2 homology 3 (BH3) domain and binds to the hydrophobic BH3-binding cleft of Bcl-2 (Erlich et al., 2007; Feng et al., 2007a; Maiuri et al., 2007b; Oberstein et al., 2007). Although the interaction between Beclin 1 and Bcl-2 inhibits autophagy induction by nutrient deprivation, Beclin 1 does not suppress the anti-apoptotic function of Bcl-2, as would be expected from "classical" BH3-only proteins (Ciechomska et al., 2009b).

The interaction between Beclin 1 and Bcl-2 is regulated by several stimuli, including competitive binding, self-association, phosphorylation, or ubiquitination (reviewed in Kang et al., 2011). The Beclin 1 BH3 domain might be competitively displaced by other BH3-only proteins or by BH3 mimetics, e.g. ABT737 (Erlich et al., 2007; Maiuri et al., 2007a; Maiuri et al., 2007b). Alternatively, membrane-anchored receptors or adaptors, e.g. IP_3Rs or toll-like receptor associated Myd88/TRIF, might induce the disruption of the Beclin 1-Bcl-2 interaction (reviewed in He & Levine, 2010). Finally,

it has also been reported that reactive oxygen species promote cytosolic translocation of high mobility group box 1 (HMGB1), where it interacts with Beclin 1 and thus displaces Bcl-2 (Tang et al., 2010). It has also been discussed that Beclin 1-homo-oligomerization might provide a scaffold for further protein-protein interactions and displacement of Bcl-2 proteins (Kang et al., 2011). Additionally, post-translational modifications of both interacting proteins might modulate the Beclin 1-Bcl-2 interaction. Interestingly, both components serve as phospho-acceptor proteins. Zalckvar et al. reported that the death-associated protein kinase (DAPK) phosphorylates Beclin 1 at T119, which is located within the BH3 domain (Zalckvar et al., 2009). In turn, Bcl-2 might be phosphorylated by the mitogen-activated protein kinases ERK and JNK, respectively. Wei et al. reported that JNK phosphorylates T69, S70 and S87 within the non-structured loop between BH3 and BH4 of Bcl-2 (Wei et al., 2008). Next to the direct displacement of Bcl-2 by HMGB1 described above, it has been suggested that HMGB1 promotes the activation of ERK1/2, resulting in the ERK1/2-mediated phosphorylation of Bcl-2 and its dissociation from Beclin 1 (Tang et al., 2010). Interestingly, it has been reported that viral Bcl-2 proteins inhibit autophagy more effectively than cellular Bcl-2 proteins. This has been explained by either a stronger affinity of viral Bcl-2 proteins to Beclin 1 or the fact that viral Bcl-2 orthologs lack the JNK-dependent phosphorylation sites described above (Ku et al., 2008; Liang et al., 2008a; Sinha et al., 2008; Wei et al., 2008). It appears that the Bcl-2-dependent blockade of autophagy might be a viral strategy to ensure latency. Finally, it was demonstrated that K117 within the BH3 domain of Beclin 1 is a major ubiquitination site (Shi & Kehrl, 2010). Accordingly, the authors speculate that TRAF6-mediated K63-linked ubiquitination at this site influences the association between Beclin 1 and Bcl-2.

The interaction between Bcl-2 and Beclin 1 occurs both at the mitochondrion and at the ER, and both mitochondrion- and ER-targeted Bcl-2 reduce LC3-II accumulation induced by overexpression of Beclin 1 (Ciechomska et al., 2009a). However, starvation-induced autophagy is most efficiently inhibited by ER-localized Bcl-2 (Pattingre et al., 2005; Ciechomska et al., 2009a). In 2009, Vicencio et al. reported the identification of a trimeric complex consisting of IP_3Rs, Beclin 1 and Bcl-2 (Vicencio et al., 2009). Apparently IP_3Rs facilitate the interaction between Beclin 1 and Bcl-2, thus indirectly impairing autophagy. Upon IP_3R inhibition, this trimeric complex dissociates and autophagy is induced. The authors further suggest that the Ca^{2+} channel function of the IP_3Rs is not contributing to the autophagy-inhibitory effect, since siRNA-mediated knockdown of Beclin 1 had no effect on cytosolic or luminal ER Ca^{2+} levels (Vicencio et al., 2009). However, this IP_3R scaffolding model needs further validation, since it has been challenged by other groups (reviewed in Decuypere et al., 2011a; Cardenas & Foskett, 2012). For example, in DT40 cells deficient for all three IP_3Rs, association between Beclin 1 and Bcl-2 is not affected (Khan & Joseph, 2010). Notably, Khan et al. state that the absence of IP_3Rs in the triple-knockout DT40 cells results in higher levels of basal autophagy, which

would confirm the results by Vicenco et al.. However, reconstitution with a functionally inactive D2550A IP_3R mutant did not result in a suppression of the autophagic flux, indicating that the Ca^{2+} channel function of IP_3Rs is important for the regulation of autophagy (Khan & Joseph, 2010). Along these lines, Decuypere et al. suggest that IP_3R-mediated Ca^{2+} signaling and autophagy induction are indeed two interrelated processes (Decuypere et al., 2011c). They showed that IP_3Rs are sensitized upon starvation, and that this sensitization depends on Beclin 1. In their model, Beclin 1 shuttles from Bcl-2 to the ligand binding domain of the IP_3Rs upon starvation, indirectly confirming the importance of ER-localized Bcl-2 to modulate autophagy (see above). Next to IP_3Rs, another ER-localized transmembrane protein has been implicated in the regulation of the Beclin 1-Bcl-2 association. Chang et al. reported the identification of the nutrient-deprivation autophagy factor-1 (NAF-1), and its requirement for Bcl-2 at the ER to functionally antagonize Beclin 1-dependent autophagy (Chang et al., 2010). Additionally, NAF-1 also interacts with IP_3Rs. Interaction with IP_3Rs was also shown for different Bcl-2 family members (see chapter 1.3.2; reviewed in Decuypere et al., 2011a; Decuypere et al., 2011b; Cardenas & Foskett, 2012; Giorgi et al., 2012; Monaco et al., 2013). Future studies will have to further elucidate the interplay between IP_3Rs, other ER-localized proteins, Bcl-2 family members, and Beclin 1. However, a central role for the regulation of autophagy has also been attributed to mitochondria-localized Bcl-2. Strappazzon et al. showed that the positive autophagy regulator AMBRA1 preferentially binds to the mitochondrial pool of Bcl-2. Upon starvation, AMBRA1 is released and competes with Bcl-2 for binding to mitochondria- or ER-localized Beclin 1 (Strappazzon et al., 2011). Taken together, it appears that Bcl-2 proteins interfere with Beclin 1 function by at least two different ways, i.e. directly by binding of Beclin 1 or indirectly by binding to the positive regulator AMBRA1 (Strappazzon et al., 2011; Tooze & Codogno, 2011).

To date, two different models have been brought up to explain the Bcl-2-dependent inhibition of Beclin 1 (reviewed in Zhou et al., 2011). First, Pattingre et al. detected that Bcl-2 overexpression interferes with the formation of the Beclin 1-Vps34 complex (Pattingre et al., 2005). Furthermore, they confirmed that the functional activity of the PI3K class III complex is reduced. Second, Noble et al. demonstrated that Beclin 1 forms a dimer in solution, which is bound by Bcl-2 proteins. UVRAG disrupts this Beclin 1 dimer interface and thus UVRAG-Beclin 1 heterodimers are assembled, which presumably cause the activation of autophagy. In turn, Bcl-2 proteins reduce the affinity of UVRAG for Beclin 1 and thus stabilize Beclin 1 homodimers (Noble et al., 2008). Generally, only Atg14L, UVRAG and Rubicon are stably associated with the PI3K class III core complex (Funderburk et al., 2010). Accordingly, the unstable or transient interaction of Beclin 1 with Bcl-2 proteins allows the dynamic regulation of autophagic processes.

1.3.4 The tumor suppressor p53

In 1979, six different groups reported the identification of a protein with a molecular weight of approximately 53 kDa. This protein associates with the simian virus 40 (SV40) large T antigen, and was present in chemically induced sarcomas, leukemias, spontaneously transformed fibroblasts, and cells transformed by SV40 and murine sarcoma virus (DeLeo et al., 1979; Kress et al., 1979; Lane & Crawford, 1979; Linzer & Levine, 1979; Melero et al., 1979; Smith et al., 1979). Since then, p53 became one of the most extensively studied molecules in life sciences. p53 is a transcription factor which controls a diverse set of cellular processes, including cell cycle, apoptosis, senescence, autophagy and metabolism, and several review articles have highlighted the importance of this transcription factor (Vousden & Lane, 2007; Vousden & Ryan, 2009; Zuckerman et al., 2009; Farnebo et al., 2010; Muller & Vousden, 2013). The p53 family consists of three members in human, i.e. p53, p63 and p73, and their origins and evolution have been summarized recently (Belyi et al., 2010). Another level of complexity is added to the p53-dependent signal transduction by post-translational modifications, which include phosphorylation, acetylation, methylation, mono- and poly-ubiquitination, sumoylation, O-GlcNAcylation, neddylation, dimethylation, and ADP-ribosylation (Gu & Zhu, 2012). Due to its predominant expression in transformed cell lines, it was initially believed that p53 functions as an oncogene contributing to cellular transformation. However, wild-type p53 is a tumor suppressor protein. The *TP53* gene is mutated in approximately 50% of all human tumors, and mutated p53 either exerts a dominant negative role or even acquires oncogenic functions (Muller & Vousden, 2013). Mutant p53 protein is frequently overexpressed in tumors, and the detection of abnormally high p53 levels is indicative for p53 mutations in tumor samples (Morselli et al., 2008). Wild-type p53 is normally expressed at low levels in healthy cells, and these levels are controlled by the ubiquitin ligase human double minute 2 (Hdm2, Mdm2 in mice), which is itself a p53 target gene (Haupt et al., 1997; Honda et al., 1997; Kubbutat et al., 1997). p53 expression increases upon exposure to various forms of stress, including genotoxic stress induced by radiation or chemotherapeutics, oncogene activation, telomere erosion, ribosomal stress, or hypoxia. Generally, a cell can respond to these stressors by different means. Usually, the cell will initiate a transient cell cycle arrest and try to repair the produced damage. This process is centrally regulated by p53 and its target p21 (also termed cyclin-dependent kinase inhibitor 1). However, if repair is not possible, the cell will ultimately undergo senescence or apoptosis (Ryan, 2011).

Apoptotic cell death is also centrally regulated by p53, which on the one hand induces the expression of numerous pro-apoptotic genes and on the other hand represses the expression of anti-apoptotic genes. Additionally, p53 can induce apoptosis by transcription-independent mechanisms. Pro-apoptotic genes controlled by p53 include members of the Bcl-2 family (Bax, Bid, Puma, Noxa),

effectors of apoptosis (Apaf-1, caspase-6, caspase-8), death receptors and their ligands (CD95, TRAIL-R2, CD95L, TRAIL), and additional factors (AEN/ISG20L1, p53AIP1, PERP, PIG3) (reviewed in Zuckerman et al., 2009). Besides the trans-activation of pro-apoptotic factors, p53 contributes to the trans-repression of anti-apoptotic molecules, e.g. Bcl-2, survivin, ARC, or gelactin-3 (Zuckerman et al., 2009). The transcription-independent effects of p53 are exerted at mitochondria, where p53 apparently fulfills both enabling and activating BH3-only functions (reviewed in Vaseva & Moll, 2009). p53 interacts with Bcl-2 and Bcl-x_L and neutralizes their inhibitory effect on pro-apoptotic Bax, Bak, and Bid. Furthermore, p53 directly interacts with Bak and liberates it from an inhibitory complex with Mcl-1. Finally, p53 interacts with Bax in a “hit and run” manner and thus promotes it oligomerization (Vaseva & Moll, 2009). Nevertheless, it has also been shown that forced expression of p53 at mitochondria was per se insufficient to induce apoptosis (Essmann et al., 2005).

In recent years it became evident that p53 also contributes to the regulation of autophagy (reviewed in Tasdemir et al., 2008a; Maiuri et al., 2009b; Vousden & Ryan, 2009; Galluzzi et al., 2010; Maiuri et al., 2010; Ryan, 2011). Again this control can be subdivided into transcription-dependent and -independent branches. Furthermore, p53 has been involved in both the positive and negative regulation of autophagy, and similar to the p53-dependent induction of cell cycle arrest or apoptosis it appears that the exact outcome of p53 signaling on autophagy depends on the cellular context. As a general rule, nuclear localized p53 promotes autophagy on the transcriptional level, whereas cytoplasmic p53 inhibits autophagy independently of transcription (Tasdemir et al., 2008a; Maiuri et al., 2009b). p53 positively regulates the expression of target genes which exert a negative effect on mTOR activity, e.g. AMPKβ1/2 subunits, TSC2, or sestrins 1 and 2 (Feng et al., 2007b; Budanov & Karin, 2008; Maiuri et al., 2009a; Galluzzi et al., 2010). Sestrin 1 and 2 are negative regulators of mTOR signaling through the activation of AMPK and AMPK-mediated phosphorylation of TSC2 (Budanov & Karin, 2008). For sestrin2 it was demonstrated that it functions as positive regulator of autophagy in p53-proficient cells (Maiuri et al., 2009a). Furthermore, both Ulk1 and Ulk2 are transcriptional targets of p53 (Gao et al., 2011). Additionally, different p53 target genes which contribute to apoptotic responses have also been implicated in the positive regulation of autophagy, such as DRAM, DAPK-1, Bax, Bad, BNIP, Puma, and AEN/ISG20L1 (Crighton et al., 2006; Crighton et al., 2007; Maiuri et al., 2007a; Harrison et al., 2008; Yee et al., 2009; Zalckvar et al., 2009; Zhang & Ney, 2009; Eby et al., 2010; reviewed in Galluzzi et al., 2010; Ryan, 2011). The damage-regulated autophagy modulator (DRAM) is a lysosomal protein that induces autophagy in a p53-dependent manner (Crighton et al., 2006; Crighton et al., 2007). Notably, overexpression of DRAM alone does not cause significant cell death, but DRAM appears to be mandatory for p53-dependent apoptosis induced by doxorubicin (Crighton et al., 2006; Crighton et al., 2007). The death-associated protein kinase-1 (DAPK-1) promotes autophagy by phosphorylating Beclin 1 (see chapter 1.3.3) and by

binding to the microtubule-associated protein 1B (MAP1B), which is an anti-autophagic LC3-interacting protein (Harrison et al., 2008; Zalckvar et al., 2009; Galluzzi et al., 2010). Bax and the BH3-only proteins Bad, BNIP3 and Puma presumably also positively regulate autophagy by disrupting the association of Beclin 1 with anti-apoptotic Bcl-2 family members (Maiuri et al., 2007a; Yee et al., 2009; Zhang & Ney, 2009; Galluzzi et al., 2010).

In 2008, Kroemer's group reported that inhibition of p53 induces autophagy in enucleated cells, and that cytoplasmic p53 was able to repress enhanced autophagy observed in p53-deficient cells (Tasdemir et al., 2008a; Tasdemir et al., 2008b). Additionally, the authors demonstrated that different pro-autophagic stimuli such as starvation, rapamycin, tunicamycin or lithium induced the Hdm2/Mdm2-dependent degradation of p53. Work from the same group showed that also mutant p53 protein localized in the cytoplasm inhibits autophagy (Morselli et al., 2008). These data clearly suggest that the non-nuclear pool of p53 negatively regulates autophagic processes (Tasdemir et al., 2008a; Maiuri et al., 2009b; Galluzzi et al., 2010; Maiuri et al., 2010). Three years later, Kroemer's group reported that p53 physically interacts with the Ulk1 complex component FIP200 (Morselli et al., 2011). Furthermore, p53 harboring a single mutation (K382R) failed to interact with FIP200 and to inhibit autophagy in reconstituted p53-/- HCT116 cells (Morselli et al., 2011). Livesey et al. suggested that the interaction between p53 and the high mobility group box 1 (HMGB1) regulates the balance between autophagy and apoptosis (Livesey et al., 2012). In their model, loss of p53 increases cytosolic HMGB1 and thus autophagy, whereas loss of HMGB1 increases cytosolic p53 and decreases autophagy. Naidu et al. report that the SUMO E3 ligase PIASy activates the acetyltransferase TIP60 (Naidu et al., 2012). Then, PIASy-catalyzed K386 sumoylation and TIP60-catalyzed K120 acetylation of p53 promote cytoplasmic p53 accumulation and autophagy. Importantly, these results support a role of TIP60-dependent acetylation for the regulation of autophagy (see chapter 1.2.3.3).

In turn, it has also been demonstrated that Atgs and autophagy regulate p53. Recently it was shown that Beclin 1 stabilizes p53 through the regulation of the ubiquitin-specific proteases (USPs) 10 and 13 (Liu et al., 2011). The authors identified a small molecule inhibitor called specific and potent autophagy inhibitor-1 (spautin-1), that promotes Beclin 1 degradation by inhibiting USP10 and USP13. In turn, Beclin 1 associates with USP13 and controls the stability of USP10 and USP13. Since USP10 catalyzes the deubiquitination of p53, Beclin 1 apparently controls p53 levels (Liu et al., 2011). In line with this, two works from the Avantaggiati group revealed that mutant p53 levels are regulated by autophagy. Glucose restriction induces p53 mutant deacetylation and subsequent degradation by autophagy (Rodriguez et al., 2012). Under basal growth conditions, pharmacological or RNAi-mediated inhibition of autophagy results in p53 mutant stabilization, whereas overexpression of Beclin 1 or Ulk1 results in p53 mutant depletion (Chalhoub & Baker, 2009;

Choudhury et al., 2013). Collectively, there appears to exist significant crosstalk between p53 signaling and the autophagic machinery, and future studies will likely reveal additional interactions.

1.3.5 Proteolytic crosstalk between apoptosis and autophagy

Central effector proteins of apoptotic processes are proteases such as caspases or calpains. In recent years it has been described that autophagy-relevant proteins are cleaved by these proteases, resulting in an altered or abolished function. It could be shown that Atg5 plays a dual role in autophagy and apoptosis. Lethal stress leads to calpain-mediated cleavage of the 33 kDa-large Atg5 (Yousefi et al., 2006). The C-terminus is removed and a 24 kDa-large fragment is generated. This fragment is devoid of its autophagy-inducing properties. Instead, it has a pro-apoptotic effect. The Atg5-fragment translocates to mitochondria and enhances the permeabilization of the outer mitochondrial membrane (Yousefi et al., 2006). Recently, Oral et al. described that Atg3 is cleaved by caspase-8 during death receptor-induced apoptosis (Oral et al., 2012). Furthermore, several reports describe that Beclin 1 is directly cleaved by caspases and that this cleavage links autophagic and apoptotic signaling pathways (Cho et al., 2009; Luo & Rubinsztein, 2010; Wirawan et al., 2010; Zhu et al., 2010; Li et al., 2011a; Rohn et al., 2011). It has been suggested that Beclin 1 cleavage destroys its pro-autophagic activity and that simultaneously the resulting C-terminal Beclin 1 fragment sensitizes cells to apoptosis. Additionally, a recombinant C-terminal Beclin 1 fragment induced the release of pro-apoptotic factors from isolated mitochondria (Wirawan et al., 2010). Like Atg5, it has also been reported that Beclin1 can be cleaved by calpains (Russo et al., 2011). Whereas the caspase-mediated cleavage of Atg5, Atg3 and Beclin 1 leads to a blockade of autophagy, it has been reported that the cleavage of Atg4D by caspase-3 generates a truncated version with increased autophagic activity (Betin & Lane, 2009). Nevertheless, this fragment is cytotoxic and putatively enhances the mitochondrial apoptosis pathway. The “proteolytic cross-talk” between autophagy and apoptosis is complemented by several additional observations. By the usage of a global *in vitro* cleavage approach, Norman et al. demonstrated that caspases and calpain 1 can cleave several Atgs, amongst others confirming the cleavages of Atg5 and Beclin 1 described above (Norman et al., 2010).

In turn, autophagy influences caspase signaling. On the one hand, it has recently been proposed that autophagy contributes to caspase activation. Laussmann et al. observed that proteasome inhibition leads to the autophagy-dependent apical activation of caspase-8 (Laussmann et al., 2011). Supporting this observation, it has been suggested that the autophagosomal membrane serves as platform for an intracellular DISC-mediated activation of caspase-8 and apoptosis (Young et al., 2012). Finally, the pro-apoptotic function of procaspase-8 polyubiquitination (see chapter 1.1.2.1) is

presumably mediated by p62-dependent aggregation of caspase-8, thus ensuring processing and full activation (Jin et al., 2009). On the other hand, it has been suggested that autophagy inhibits apoptosis through the degradation of pro-apoptotic factors including caspases (reviewed in Gordy & He, 2012). Apparently, this *a priori* cytoprotective function of autophagy supports tumor resistance to anticancer drugs. As described above, TRAIL is currently assessed as antitumor therapeutic, since its pro-apoptotic effects are mainly restricted to tumor cells (Ashkenazi et al., 1999; Walczak et al., 1999; Dimberg et al., 2013). Studies by Rabinowich's group indicated that TRAIL induces cytoprotective autophagy in apoptosis-resistant tumor cells, and that this resistance can be overcome by the inhibition of autophagy (Han et al., 2008; Hou et al., 2008). Subsequently this group could decipher the molecular details underlying this observation: TRAIL-activated caspase-8 is continuously sequestered by autophagosomes, where it becomes degraded upon fusion with lysosomes (Hou et al., 2010). Collectively, it appears that there exists a mutual proteolytic control of apoptosis and autophagy signaling: active caspases cleave Atgs, and autophagy mediates the degradation of caspases (reviewed in Gordy & He, 2012).

2. Summaries of Selected Research Articles

2.1 Subcellular localization of Grb2 by the adaptor protein Dok-3 restricts the intensity of Ca^{2+} signaling in B cells

Stork B, Neumann K, Goldbeck I, Alers S, Kähne T, Naumann M, Engelke M, Wienands J.
EMBO J 2007;26:1140-1149.

(The published and herein discussed data are part of the dissertation by Dr. Björn Stork. The data were published following to his conferral of a doctorate.)

B lymphocytes are central components of adaptive immunity. The main effector function of B lymphocytes that have been differentiated to plasma cells is the production of soluble immunoglobulins. Membrane-bound immunoglobulins on the B cell surface serve as antigen receptors. During B cell development, signals transduced by this B cell antigen receptor (BCR) lead to different physiological responses. Stimulation of the BCRs on immature B cells induces apoptosis, anergy, or receptor editing, whereas identical BCRs on the surface of mature B cells mediate activation and/or proliferation (reviewed in Wang & Clark, 2003; LeBien & Tedder, 2008; von Boehmer & Melchers, 2010). Notably, BCR ligation triggers distinct Ca^{2+} mobilization profiles in developing and mature B lymphocytes (Koncz et al., 2002; Engelke et al., 2007). The cytosolic concentration of Ca^{2+} in turn critically influences apoptotic and autophagic signaling pathways (see 2.4).

Elevation of the cytosolic Ca^{2+} concentration downstream of the BCR is regulated by the Ca^{2+} initiation complex, consisting of the adapter protein SLP-65 and the Ca^{2+}-mobilizing enzymes Btk and PLC-γ2, respectively (Engelke et al., 2007). We previously showed that the growth factor receptor-bound protein 2 (Grb2) exerts an inhibitory effect on BCR-induced Ca^{2+} mobilization (Stork et al., 2004). Furthermore, we demonstrated that the tyrosine-phosphorylated linker for activation of T cells family member 2 (LAT2) abolishes this inhibition by sequestering Grb2 (Stork et al., 2004).

Next we investigated how Grb2 negatively regulates BCR-induced Ca^{2+} mobilization. During our search for the downstream effectors, we observed that the main tyrosine kinase substrate with an apparent molecular weight of approximately 50 kDa remains unphosphorylated in *GRB2*-/- DT40 cells, as detected by anti-phospho-tyrosine immunoblotting. We were able to identify this protein by mass spectrometry as the adapter protein downstream of kinase-3 (Dok-3). We generated Dok-3-deficient DT40 cells and analyzed their capacity to mobilize Ca^{2+}. Interestingly, we found that Dok-3 - similar to Grb2- is a negative regulator of BCR-induced Ca^{2+}-mobilization. We furthermore postulate that Dok-3 and Grb2 represent a functional unit regarding this inhibitory effect, since the adapter

proteins inducibly interact and the expression of a dominant negative Grb2 variant does not reveal any effect on Ca^{2+}-mobilization in the Dok-3-deficient background. Further analyses revealed that PH domain-mediated plasma membrane association of Dok-3 and its phosphorylation at Y331 (chicken amino acid sequence), which allows the inducible interaction with the SH2 domain of Grb2, are prerequisites for the Ca^{2+} regulatory function. We confirmed by confocal microscopy that Dok-3 is constitutively localized at the plasma membrane, and that Dok-3 recruits cytosolic Grb2 to the plasma membrane upon BCR stimulation via the phospho-Y331/SH2 interaction. In contrast, the previously reported association of Dok-3 with the lipid phosphatase SHIP and the tyrosine kinase Csk appear to be dispensable for this effect. We next searched for the enzymatic activity that is controlled by the Dok-3/Grb2 module, and we were able to identify PLC-γ2 as the downstream effector protein. Activity-regulating PLC-γ2 phosphorylation at Y759 was significantly increased in *DOK-3*-/- DT40, and accordingly IP_3 generation was higher in Dok-3- or Grb2-deficient DT40 cells, respectively.

In summary, we could show that the phosphorylated forms of Dok-3 and LAT2 constitute two functionally different 'membrane zip codes' for Grb2 in order to balance Ca^{2+} mobilization profiles during B cell development. The adapter protein Dok-3 exerts its inhibitory regulation of Ca^{2+} mobilization by inducible plasma membrane recruitment of the ubiquitously expressed Grb2. When bound to Dok-3, Grb2 suppresses Btk-mediated PLC-γ2 phosphorylation at Y759. We propose that the negative feedback regulation by the Dok-3/Grb2 module may play a prominent role in limiting the Ca^{2+} response in immature B cells like DT40. However, mature B lymphocytes usually reveal a robust Ca^{2+} mobilization and accordingly need to sequester Grb2 away from its inhibitory binding partner Dok-3. It appears that LAT2 provides such a function. LAT2 expression is upregulated during B cell maturation (Stork et al., 2004; Wang et al., 2005), and DT40 B cells show an increased Ca^{2+} mobilization upon expression of wild-type LAT2 (Stork et al., 2004).

In a subsequent work by the group of my doctoral thesis supervisor, it could be shown that the Dok-3-Grb2 complex is translocated to BCR microsignalosomes (Losing et al., 2013). It appears that Dok-3 recruits Grb2 to the plasma membrane, and Grb2 in turn controls the targeting to these microsignalosomes. Within these BCR microclusters, the Dok-3-Grb2 complex attenuates Lyn-dependent activation of the tyrosine kinase Syk (Losing et al., 2013). Since Syk is upstream of Btk, the described regulation of Lyn activity might explain the observed effect on PLC-γ2 phosphorylation.

The Ca^{2+}-regulatory function of the adapter proteins Dok-3 and Grb2 described above was also confirmed *in vivo*. B cells derived from Dok-3-deficient mice hyperproliferated, exhibited increased Ca^{2+} mobilization, and enhanced activation of NF-κB, JNK and p38 upon BCR stimulation (Ng et al., 2007). Furthermore, Dok-3-deficient mice possess higher IgM levels in their sera and mount

increased humoral immune responses towards T cell-independent antigens (Ng et al., 2007). Similar to Dok-3-deficient cells, Grb2-deficient primary B cells exhibited an enhanced BCR-induced Ca^{2+} mobilization (Ackermann et al., 2011). Additionally, the B cell-specific deletion of Grb2 resulted in a decreased number of mature follicular B cells in the periphery caused by a differentiation block and decreased B cell survival (Ackermann et al., 2011). Collectively, these data confirm the importance of the adapter proteins Dok-3 and Grb2 for B cell homeostasis in general and for the regulation of Ca^{2+} signaling in particular. The sequestration of Grb2 from this inhibitory complex by LAT2 or other B cell-resident Grb2-binding transmembrane proteins such as surface IgG or IgE, CD19, CD22, CD72 or FcγRIIb (reviewed in Neumann et al., 2009) might represent the basis for dynamic and differential BCR signal transduction which ultimately determines B cell fate.

The fine-tuning of Ca^{2+} mobilization is central for cell fate determination during B cell development. Koncz et al. described that the late phase of Ca^{2+} mobilization corresponding to the Ca^{2+} influx across the plasma membrane was “somewhat lower in immature B cells” (Koncz et al., 2002). Furthermore, my previous group demonstrated by multicolor flow cytometry that the extracellular Ca^{2+} influx is increased in immature T2 and mature B lymphocytes compared to immature T1 cells (Engelke et al., 2007). Different groups showed that cytosolic Ca^{2+} concentrations differently affect key transcription factor pathways in B lymphocytes, such as NFAT or NF-κB pathways, respectively (Dolmetsch et al., 1997; Healy et al., 1997; Scharenberg et al., 2007). It appears that amplitude and duration of the Ca^{2+} signal govern the activation of these transcription factors. A model has been established which combines Ca^{2+} signals with tolerance induction in the B cell compartment. This model postulates that non-tolerizing antigens induce a robust and sustained Ca^{2+} mobilization leading to the activation of both NFAT and NF-κB. In turn, tolerizing antigens only provoke a weak sustained Ca^{2+} influx, by which only NFAT but not NF-κB is activated (Dolmetsch et al., 1997; Healy et al., 1997; Scharenberg et al., 2007). Accordingly, cytosolic Ca^{2+} concentrations directly affect B cell development and tolerance induction.

2.2 The Akt inhibitor triciribine sensitizes prostate carcinoma cells to TRAIL-induced apoptosis

Dieterle A, Orth R, Daubrawa M, Grotemeier A, Alers S, Ullrich S, Lammers R, Wesselborg S, Stork B.
Int J Cancer 2009;125:932-941.

(The published and herein discussed data are part of the dissertation by Dr. Alexandra Dieterle)

Following my doctoral thesis and the work on B cell-specific cell fate decisions, my research focus shifted to the general signal transduction pathways of the cell fate-determining processes of apoptosis and autophagy, respectively. Both pathways are directly regulated by the PI3K-PDK1-Akt survival pathway, which plays a central role in diverse physiological processes. Additionally, its aberrant activation is frequently associated with the malignant transformation of tumor cells. Generally, activated Akt phosphorylates a variety of substrates, leading to an anti-apoptotic status of the cell (reviewed in Duronio, 2008). Accordingly, the targeting of this pathway has been implicated in the development of novel therapeutic approaches. Currently, different inhibitors of components of this pathway are evaluated in clinical trials, including PI3K inhibitors (Kurtz & Ray-Coquard, 2012), and Akt inhibitors (Lindsley, 2010; Pal et al., 2010; Mattmann et al., 2011). The nucleoside analog triciribine (TCN) has also been shown to function as an Akt inhibitor (Yang et al., 2004). So far, two clinical phase I trials, which evaluate the efficacy of TCN in patients with advanced hematologic malignancies or metastatic cancer, have been completed (ClincalTrials.gov Identifier: NCT00642031 and NCT00363454).

In our study, we investigated the efficiency of TCN in combination with conventional anticancer drugs or death receptor ligands to induce apoptosis in prostate cancer cell lines. At present, treatments of prostate cancer include prostatectomy or radiation therapy (Majumder & Sellers, 2005). Additionally, patients suffering from relapsing cancer or metastasis are treated by androgenic hormone deprivation (Majumder & Sellers, 2005). However, a major clinical complication is the development of hormone-refractory/castrate-resistant cancer, which usually displays a high resistance to chemotherapy (Seruga et al., 2011). We demonstrated that TCN is effective in the prostate carcinoma cell line PC-3, which is highly resistant to chemotherapy or irradiation (He et al., 2012, and references therein). Treatment of PC-3 cells with TCN leads to a reduced phosphorylation of Akt T308 and S473, respectively. In parallel, Akt-mediated phosphorylation of GSK3β is significantly reduced upon TCN treatment. Next we analyzed whether TCN sensitizes PC-3 cells for stimuli engaging the mitochondrial apoptosis pathway. However, the chemotherapeutics etoposide and mitomycin c do not efficiently induce apoptosis in PC-3 cells, and the apoptosis-inducing capacity was not increased upon co-incubation with TCN. We also investigated whether TCN influences the death receptor-

induced apoptosis pathway. Notably, TCN amplifies TRAIL- and anti-CD95-induced apoptosis in this prostate carcinoma cell line, as indicated by the detection of hypodiploid nuclei or caspase cleavage. In the following experiments, we especially focused on the combination of TRAIL with TCN, since both agents are currently under evaluation in clinical trials. We also demonstrated that the apoptosis-amplifying effect of TCN depends on the activation status of Akt. The prostate carcinoma cell line LNCaP was sensitized to TRAIL-induced apoptosis by TCN to a similar extent as PC-3 cells. In contrast, Du145 prostate cancer cells were largely resistant to this combinatory treatment. Interestingly, in PC-3 and LNCaP cells Akt is present and phosphorylated at T308 and S473, whereas both Akt expression and phosphorylation are not detectable in Du145 cells. Finally, we demonstrated that Akt inhibition in PC-3 cells leads to an increased Bid cleavage upon TRAIL treatment. It appears that the inhibition of Akt facilitates caspase-8-mediated processing of Bid, although caspase-8 activity itself is not affected by TCN.

Our data directly confirm that constitutive Akt signaling is a prerequisite for TCN-mediated sensitization of prostate carcinoma cells (and presumably other tumor entities) to TRAIL-induced apoptosis. Generally, the inhibition of pro-survival pathways and the concomitant activation of apoptosis pathways represent a valuable tool to improve the efficiency of cancer therapies. Akt is over-expressed and/or activated in all major cancers, thereby elevating the threshold for the induction of apoptosis (Lindsley, 2010). Accordingly, different small molecules inhibiting Akt are currently evaluated in (pre-)clinical development and clinical trials (Lindsley, 2010; Pal et al., 2010; Mattmann et al., 2011). Additionally, other components of this survival signaling axis are therapeutically targeted, including PI3Ks and mTOR, respectively (Chiang & Abraham, 2007; Engelman, 2009; Kurtz & Ray-Coquard, 2012).

2.3 The 3-phosphoinositide-dependent protein kinase 1 (PDK1) controls upstream PI3K expression and PIP_3 generation

Dieterle AM, Böhler P, Keppeler H, Alers S, Berleth N, Drießen S, Hieke N, Pietkiewicz S, Löffler AS, Peter C, Gray A, Leslie NR, Shinohara H, Kurosaki T, Engelke M, Wienands J, Bonin M, Wesselborg S, Stork B.
Oncogene 2013;accepted.

(The published and herein discussed data are part of the dissertations by Dr. Alexandra Dieterle and Philip Böhler [in progress])

The DT40 model system is a useful tool to analyze the anti-apoptotic signaling by PDK1 and Akt. Apparently, the constitutive deletion of either protein kinase is lethal, indicating that both kinases

contribute to a tonic survival signaling (Pogue et al., 2000; Shinohara et al., 2007). In order to analyze the anti-apoptotic effect on a global scale, we made use of a DT40 cell line in which PDK1 can be inducibly deleted (Shinohara et al., 2007). In this cell line, the loxP-marked PDK1 locus can be disrupted by 4-hydroxytamoxifen-induced activation of the Cre recombinase. First, we confirmed that PDK1 depletion leads to the induction of apoptosis in this cell line. Additionally, we observed that the ablation of PDK1 expression results in a sensitization of DT40 cells to BCR-induced apoptosis. Next we aimed at the analysis of overall transcriptional alterations upon PDK1 knockout. Accordingly, we performed a microarray analysis of PDK1-proficient and -deficient DT40 cells. Interestingly, we found that the transcripts of the PI3K subunits p85α, p110β, and p110δ, which are usually upstream of PDK1, are increased upon PDK1 deletion. Furthermore, other phosphoinositide-modifying enzymes regulating the levels of the PI3K product PI(3,4,5)P3 were also affected by the loss of PDK1, e.g. PIP5K1-β was up-regulated and INPP5B was down-regulated. The Src-family tyrosine kinase Lyn which contributes to the activation of PI3K downstream of the BCR was also up-regulated. We verified the results obtained by the microarray analysis on the transcript level by RT-PCR and on the protein level by immunoblotting. The results obtained by the genetic deletion of PDK1 were phenocopied by the application of the PDK1 inhibitor BX-795 (Feldman et al., 2005). Both PDK1 deletion and inhibition resulted in a blockade of Akt-dependent phosphorylation processes, as detected by the analysis of the phospho-status of GSK3β, TSC2, and FoxO1. The PDK1-dependent transcriptional regulation of PI3K subunits was not only restricted to the DT40 cell line, but was also demonstrated in the human B cell lines DG75 and Ramos and in the human prostate carcinoma cell line PC-3 by applying the PDK1 inhibitor BX-795. These results indicate that the observed regulation also occurs in the human system and in non-lymphoid cells. Exogenous expression of PDK1 blocked both apoptosis and transcriptional up-regulation of PI3K subunits upon PDK1 deletion, directly confirming that these effects were caused by the loss of PDK1. Next we wanted to know which transcription factors might contribute to this transcriptional control. Therefore, we performed an *in silico* analysis of transcription factor binding sites in the promoter regions of the regulated genes. We primarily identified binding sites for ETS factors, sex/testis determining and related HMG box factors, forkhead domain factors, heat shock factors, and cAMP-responsive element binding (CREB) proteins. Since FoxOs and CREB were previously reported to be regulated by the PI3K/PDK1/Akt axis, we focused on these transcription factors. In contrast, other Akt-regulated transcription factors such as p53 or NF-κB were not enriched in the corresponding promoter regions. We found that pharmacological activation or inhibition of CREB lead to the up- or down-regulation of Lyn. Furthermore, pharmacological inhibition of FoxO1 partially blocked the up-regulation of PI3K subunits p85α, p110β and p110δ upon PDK1 depletion or inhibition. Collectively, these data suggest that CREB and FoxO transcription factors at least contribute to the transcriptional control. Next we

asked whether the product of the PI3K-catalyzed reaction, $PI(3,4,5)P_3$, also increases upon PDK1 deletion. This was indeed the case as detected by FRET-based quantification of cellular $PI(3,4,5)P_3$ levels or by confocal microscopy of a GFP-tagged PH domain derived from PDK1. The latter was recruited to the plasma membrane upon PDK1 deletion, and this translocation could be blocked by treatment with the pan-specific PI3K inhibitor GDC-0941. As described in chapter 1.3.1, PDK1 regulates different downstream AGC kinases via PH domain- or PIF-pocket-dependent mechanisms. These two branches of regulation can be distinguished by expressing PH domain-mutated (K465E, human aa sequence) or PIF pocket-mutated (L155E, human aa sequence) PDK1 in the PDK1-knockout background. Interestingly, exogenous expression of single-mutated PDK1 variants partially inhibited up-regulation of PI3K subunits upon PDK1 knockout. However, the doubly-mutated PDK1 mimicked the knockout phenotype, indicating that both PDK1-dependent signaling branches contribute to the transcriptional control. Finally, we observed that the PDK1 downstream effector proteins Akt and mTOR are apparently also involved in this regulation, since treatment of different lymphoid cell lines with the Akt inhibitor MK2206 or the mTOR inhibitor rapamycin resulted in similar transcriptional alterations.

Our data reveal yet another level of feedback control of the PI3K/PDK1/Akt/mTOR signaling axis. In recent years, several feedback loops have been discovered (reviewed in Carracedo & Pandolfi, 2008). The most prominent feedback mechanism is dependent on mTORC1 activity and targets the insulin receptor substrate-1 (IRS-1), which is an adapter that mediates PI3K activation downstream of receptor tyrosine kinases. Following activation of mTORC1 and its substrate p70S6K, IRS-1 is both transcriptionally down-regulated and post-translationally inhibited. Additionally, several other feedback mechanisms have been proposed which target the PI3K/PDK1/Akt pathway, e.g. involving the up-regulation of insulin-like growth factor 1 (IGF1) or activation of IGF1-R, respectively (Wan et al., 2007; Tamburini et al., 2008). Recently, Chandarlapaty et al. reported Akt-dependent suppression of receptor tyrosine kinase expression and activity (Chandarlapaty et al., 2011). These feedback regulatory mechanisms also have an impact on therapeutic approaches, e.g. current strategies employing mTOR inhibitors might be subverted by the undesired activation of PI3K signaling (Carracedo et al., 2008; Carracedo & Pandolfi, 2008). Accordingly, we propose that the efficiency of current therapeutic approaches based on mTOR inhibition might be further improved by the parallel inhibition of PI3K, PDK1, or Akt. Furthermore, even the PI3K product $PI(3,4,5)P_3$ might represent an attractive therapeutic target. Recently, Miao et al. described non-phosphoinositide small molecule antagonists called PITenins/PITs, which block $PI(3,4,5)P_3$-PH domain interactions (Miao et al., 2010).

2.4 Triggering of a novel intrinsic apoptosis pathway by the kinase inhibitor staurosporine: activation of caspase-9 in the absence of Apaf-1

Manns J, Daubrawa M, Driessen S, Paasch F, Hoffmann N, Löffler A, Lauber K, Dieterle A, Alers S, Iftner T, Schulze-Osthoff K, Stork B*, Wesselborg S*.
FASEB J 2011;25:3250-3261.
*equal contribution

(The published and herein discussed data are part of the dissertations by Dr. Joachim Manns and Dr. Merle Mayer, née Daubrawa)

Generally, radio- and chemotherapy work as DNA-damaging treatments which engage the intrinsic mitochondrial pathway to induce apoptosis (Belka et al., 2000; Engels et al., 2000). Therefore, many cancer cells become resistant to these treatments by the blockade of the intrinsic pathway. This might be achieved by either up-regulation of anti-apoptotic members of the Bcl-2 family, down-regulation of pro-apoptotic Bcl-2 proteins, epigenetic down-regulation of Apaf-1, increased expression of IAPs, or mutations in effector caspases (reviewed in Johnstone et al., 2002). Accordingly, current research strategies aim at the identification of novel intrinsic apoptosis pathways, which cannot be blocked by the mechanisms described above and which are effective in cells that are otherwise resistant to conventional radio- or chemotherapy.

In this study, we employed the pan-specific kinase inhibitor staurosporine (STS) as pro-apoptotic agent. STS is frequently used as positive control in apoptosis assays, and it induces caspase activation within 3-4 hours (Stepczynska et al., 2001). Using caspase-8- or FADD-deficient Jurkat T lymphocytes, we demonstrated that STS induces apoptosis independently of the death receptor signaling pathway. Additionally, STS is effective in Jurkat T cells expressing Bcl-2 variants constitutively targeted to the ER or to mitochondria, directly confirming that STS can function independently of the ER stress or the mitochondrial apoptosis pathway. The partial independency of the canonical intrinsic apoptosis pathway was further supported by the observation that STS induces apoptosis in various cell lines overexpressing either Bcl-2 or Bcl-x_L. However, STS-induced apoptosis is completely blocked in caspase-9-deficient Jurkat T cells, DT40 B cells, or mouse embryonic fibroblasts. The next step was to analyze the contribution of Apaf-1 to STS-induced apoptosis. Notably, STS activates caspase-9 in the absence of Apaf-1 or apoptosome formation. Collectively, we conclude that STS can induce apoptosis in target cells by a dual mode of action. First, STS induces the classical intrinsic apoptosis pathway similar to conventional anticancer drugs, including cytochrome c-release from mitochondria and apoptosome-dependent activation of caspase-9. Second, STS might induce apoptosis independently of the apoptosome and its scaffolding protein Apaf-1. Interestingly, STS-induced apoptosis is completely blocked in caspase-9-deficient Jurkat T cells reconstituted with cDNA encoding a CARD-

deficient caspase-9 variant. This indicates that the CARD domain of caspase-9 is not only important for the recruitment of caspase-9 to the apoptosome during the classical mitochondrial pathway, but also for the apoptosome-independent activation of caspase-9. Since the CARD usually mediates homotypic domain interactions, we are currently investigating the involvement of alternative CARD-containing proteins in STS-induced apoptosis. In parallel, we are focusing on alterations of the phosphorylation status of caspase-9 during activation. So far, different kinases have been reported to phosphorylate caspase-9, including PKA, Akt, ERK1/2, CDK1, DYRK1A, c-Abl, CK2, and PKCζ (reviewed in Allan & Clarke, 2009). Surprisingly, the usage of specific inhibitors for the listed kinases did not mimic the effect of STS, i.e. apoptosis was not induced. The phospho-acceptor sites of caspase-9 are mainly located in the large subunit or in the linker regions connecting the CARD with the large subunit and the large subunit with the small subunit. A major inhibitory phosphorylation-site within the first linker region appears to be T125, which is phosphorylated by ERK1/2, CDK1, or DYRK1A and thus integrates multiple signaling pathways (Allan et al., 2003; Allan & Clarke, 2007; Martin et al., 2008; Seifert et al., 2008). T125 phosphorylation inhibits caspase-9 activation, but the exact mechanistic details remain rather elusive (Allan & Clarke, 2009). However, there is evidence that the linker between CARD and large subunit is involved in the binding of the catalytic domain to the hub of the apoptosome, suggesting that a phospho-acceptor in this region might indeed fulfill a regulatory function (Yuan et al., 2011; Reubold & Eschenburg, 2012; Yuan & Akey, 2013). However, several additional phospho-sites have been reported (reviewed in Allan & Clarke, 2009). Next to the ineffectiveness of specific kinase inhibitors to induce apoptosis, neither did the expression of non-phosphorylatable S/T-to-A or phospho-mimicking S/T-to-E caspase-9 mutants of the putative phospho-acceptor sites in caspase-9-deficient Jurkat cells sensitize cells to apoptosis or inhibit apoptosis, respectively (unpublished own observation). Accordingly, in our view the exact *in vivo* phosphorylation status of caspase-9 before and during apoptosis awaits further clarification.

In summary, we believe that the in-depth characterization of this novel intrinsic apoptosis pathway leading to the activation of caspase-9 will be a valuable approach for the development of therapies targeting cancer cells which are resistant to conventional chemotherapeutics or irradiation. Especially the up-regulation of anti-apoptotic Bcl-2 family proteins or the down-regulation of Apaf-1 might be overcome by an alternative caspase-9 activation mechanism.

Several non-canonical activation mechanisms have been reported for caspase-9. Different groups reported the cleavage of caspase-9 by activated caspase-8 (McDonnell et al., 2003; Gyrd-Hansen et al., 2006). However, we can exclude this possibility, since STS readily induced apoptosis in caspase-8-deficient Jurkat. Another group reported an Apaf-1-independent apoptosis induction (Belmokhtar et al., 2003). However, this pathway was equally independent of caspase-3 or caspase-9 cleavage. Bitzer et al. showed that Sendai virus infection triggers apoptosis independently of cytochrome c or Apaf-1,

respectively (Bitzer et al., 2002). The authors speculate that viral infection leads to the up-regulation of alternative CARD-containing proteins or that one of the viral proteins itself could mediate a similar function. Apaf-1-independent caspase-9 activation was described for the CARD-proteins Bcl-10 (also termed mE10) and Nod1 (Inohara et al., 1999; Yan et al., 1999b). Currently we are analyzing the potential contribution of CARD-containing proteins to STS-induced apoptosis. Alternatively, Bitzer et al. discuss the processing of caspase-9 by alternative cellular proteases like cathepsins or calpains. However, we observed that inhibitors for these proteases did not hamper STS-induced apoptosis (unpublished own observation). It has also been reported that caspase-12 or Smac might induce cytochrome c/Apaf-1-independent activation of caspase-9 and apoptosis (Chauhan et al., 2001; Morishima et al., 2002), and we are currently investigating this possibility. In 2010, Nagata's group reported that STS, but not etoposide, induces caspase-3 and caspase-9 processing in E14.5 fetal thymocytes of *Apaf-1*-/- mice (Nagasaka et al., 2010). Recently, this group confirmed the existence of a staurosporine-inducible apoptosis pathway which is independent of the apoptosome-scaffolding protein Apaf-1 (Imao & Nagata, 2013). However, they also claim that this pathway works independently of caspase-9. Future studies will have to reveal the exact mechanistic details of these potentially multiple non-canonical apoptosis pathways. This is especially important since staurosporine and its derivatives are currently evaluated in clinical trials (Fuse et al., 2005; Lapenna & Giordano, 2009; Imao & Nagata, 2013).

2.5 AMPK-independent induction of autophagy by cytosolic Ca^{2+} increase

Grotemeier A, Alers S, Pfisterer S, Paasch F, Daubrawa M, Dieterle A, Viollet B, Wesselborg S, Proikas-Cezanne T, Stork B.
Cell Signal 2010;22:914-925.

(The published and herein discussed data are part of the dissertations by Dr. Antje Löffler, née Grotemeier, and Dr. Sebastian Alers)

A low nutrient supply is the classical inducer of autophagic responses. Under starvation conditions the autophagic machinery provides otherwise unavailable building blocks for protein synthesis and ATP production. The presence of growth factors and insulin inhibits the autophagic pathway mainly via the Akt-mTOR axis. In contrast, low energy levels of the cell as indicated by a high AMP-to-ATP ratio are sensed by the AMP-activated protein kinase (AMPK). As described in 1.2.3.3, AMPK is a trimeric complex containing a catalytic α-subunit and regulatory β- and γ-subunits, respectively (Hardie, 2011; Hardie et al., 2012b). In order to be active, AMPK has to be phosphorylated at T172 of

the α-subunit. Different kinases have been reported to phosphorylate T172 and thus to activate AMPK, including LKB1, CaMKK β, and TAK1 (Hawley et al., 2003; Woods et al., 2003; Hawley et al., 2005; Hurley et al., 2005; Woods et al., 2005; Momcilovic et al., 2006; Herrero-Martin et al., 2009). It has been postulated that a rise in the cytosolic Ca^{2+} concentration leads to the inactivation of mTOR and the subsequent activation of autophagy via the CaMKK β-AMPK signaling axis (Hoyer-Hansen et al., 2007). Recently it could be shown that amino acid withdrawal results in an increase of cytosolic Ca^{2+} and an activation of CaMKK β, directly linking starvation conditions to this Ca^{2+}-dependent activation of autophagy (Ghislat et al., 2012).

In this study, we aimed at the in-depth characterization of this Ca^{2+}-CaMKK β-AMPK signaling pathway. In our study we used the SERCA-inhibitor thapsigargin (TG) to increase the cytosolic Ca^{2+} concentration. TG induced the autophagic flux in Jurkat T lymphocytes, DT40 B lymphocytes, and U2-OS osteosarcoma cells as detected by LC3 turnover assay, mCitrine-LC3 puncta formation assay, and an automated GFP-WIPI puncta formation assay. The effects were mainly mediated by the TG-induced elevation of the cytosolic Ca^{2+} concentration, since the induction of the autophagic flux could be entirely blocked by cell-permeable Ca^{2+}-chelator BAPTA-AM. Since it has been previously reported that TG-induced autophagy involves AMPK-mediated inhibition of mTOR, we next analyzed mTOR activity. Interestingly, phosphorylation of the mTOR substrate p70S6K was not reduced in Jurkat T cells and DT40 B cells upon TG treatment. Additionally, Ulk1 phosphorylation remained unaffected following TG treatment as indicated by an unaltered migrational behavior in SDS-PAGE. In contrast, rapamycin and the mTORC1/2-specific inhibitor Ku-0063794 induced both p70S6K dephosphorylation and Ulk1 dephosphorylation. These data suggest that TG-induced autophagy does not involve mTOR inhibition. Following the upstream signaling cascade, we next investigated the contribution of AMPK to TG-induced autophagy. To achieve this, we employed MEFs deficient for both isoforms of the catalytic α-subunit (*Ampkα1α2*-/- MEFs). Interestingly, TG induced LC3 lipidation in these cells, which again could be blocked by BAPTA-AM. Furthermore, p70S6K phosphorylation remained unaltered, confirming the induction of autophagy independently of mTOR inhibition. Following the signaling cascade further upstream, we next analyzed the contribution of CaMKK to TG-induced autophagy by utilizing the CaMKK α/β-inhibitor STO-609. STO-609 partially inhibited TG-induced GFP-WIPI puncta formation in U2-OS cells and LC3 lipidation in Jurkat T cells and wild-type MEFs. In the latter two, AMPKα phosphorylation at T172 was significantly reduced. In contrast, in *Ampkα1α2*-/- MEFs STO-609 did not exhibit any inhibitory potential on TG-induced LC3-lipidation, indicating that CaMKK participates in the AMPK-dependent branch of autophagy induction but not in the AMPK-independent one.

Collectively, we demonstrated that a rise in intracellular Ca^{2+} concentration might induce autophagy independently of mTOR inhibition or AMPK activation, respectively. The importance of Ca^{2+} for autophagic responses has been controversially discussed in the past. Different research groups demonstrated that elevated intracellular Ca^{2+} concentrations promote autophagy, and our experimental results using the Ca^{2+}-chelating BAPTA-AM directly confirm this view. We and others made use of the SERCA inhibitor thapsigargin to increase cytosolic Ca^{2+} concentrations (this manuscript and Hoyer-Hansen et al., 2007; Sakaki et al., 2008). Admittantly, prolonged treatment with this compound will induce ER stress, which itself might lead to the induction of autophagy. However, we did not observe a similar induction of autophagy with the known ER stressor tunicamycin, and autophagy induction was blockable by Ca^{2+}-buffering with BAPTA-AM. Supporting these results, Gao et al. showed that exogenously introduced Ca^{2+} in the form of Ca^{2+} phosphate precipitates induced autophagy (Gao et al., 2008). In contrast, different other groups reported that Ca^{2+} inhibits autophagy. The first publication dealing with Ca^{2+} and the regulation of autophagy by the Seglen group suggested that thapsigargin inhibits autophagy and that autophagy depends on the presence of Ca^{2+} in intracellular storage compartments (Gordon et al., 1993). The autophagy-inhibiting function of thapsigargin was also reported by other groups (Williams et al., 2008; Ganley et al., 2011). Notably, different groups showed the IP_3R-mediated inhibition of autophagy (Criollo et al., 2007; Vicencio et al., 2009; Cardenas et al., 2010; Khan & Joseph, 2010). Two mechanisms have been proposed to explain the involvement of IP_3Rs in autophagy regulation (for details see chapter 1.3.2; reviewed in Decuypere et al., 2011a; Decuypere et al., 2011b; Cardenas & Foskett, 2012). First, IP_3Rs function as scaffolds for the Beclin 1-Bcl-2 interaction. Second, the basal activity of IP_3Rs ensures the supply of mitochondria with Ca^{2+}, which results in ATP production and subsequent AMPK-mediated inhibition of autophagy. The opposing views of the role of Ca^{2+} for autophagy have been nicely summarized by Decuypere et al. (Decuypere et al., 2011a). Furthermore, the authors present a model integrating both hypotheses. They suggest that basal IP_3R-mediated Ca^{2+} signals suppress autophagy through mitochondrial pathways, whereas Ca^{2+} signals induced under stress conditions result in an elevated cytosolic Ca^{2+} concentration and the induction of autophagy (Decuypere et al., 2011a). Collectively, the existence of both activating and inhibitory functions of Ca^{2+} during autophagy in combination with the impact of mitochondrial Ca^{2+}-uptake on the regulation of apoptosis confirms the importance of Ca^{2+} as central regulator of these two cell fate processes.

Although the previously reported Ca^{2+}-CaMKK-AMPK signaling axis is confirmed by our data, there appear to exist alternative pathways to connect cytosolic Ca^{2+} with the induction of autophagy. Furthermore, mTOR inhibition is apparently not a prerequisite for this induction. In the meantime, different autophagy-inducing stimuli have been identified which act mTOR-independently. These include lithium and L-690,330, which both inhibit inositol monophosphatase and thus lower IP_3

levels, small molecule enhancers of rapamycin, and trehalose (reviewed in Sarkar et al., 2009). Additionally, two independent screens with small molecule libraries revealed several FDA-approved drugs which were able to induce mTOR-independent autophagy pathways (Zhang et al., 2007; Williams et al., 2008). One of these screens resulted in the identification of an IP_3/Ca^{2+}-regulated cyclical mTOR-independent autophagy pathway, with multiple entry points for FDA-approved drugs (Williams et al., 2008). Finally, an siRNA screen by Yuan's group showed that under normal growth conditions upregulation of autophagy solely depends on PI3K class III activation and not on mTOR inhibition (Lipinski et al., 2010). Different growth factors and cytokines inhibit PI3K class III activity through multiple pathways, including MAPK-ERK1/2, Stat3, Akt/FoxO3, and CXCR4/GPCR pathways (Lipinski et al., 2010). Taken together, all these data support our observation that mTOR inhibition is not mandatory for the activation of the autophagic flux. Recent studies indicate that especially the activities of the kinases AMPK and Akt contribute to the mTOR-independent regulation of autophagy. As discussed above, AMPK directly regulates the Ulk1-Atg13-FIP200-Atg101 complex and can induce autophagy independently of mTOR inhibition. In turn, suppression of autophagy can be mediated independently of mTOR. Active Akt, which normally inhibits autophagy via the activation of mTOR, has been shown to inhibit autophagy induced with Torin1, which is an ATP-competitive inhibitor of mTOR (Thoreen et al., 2009). Akt directly phosphorylates Beclin 1 and inhibits autophagy by the formation of a phospho-Beclin 1/14-3-3/vimentin intermediate filament complex (Wang et al., 2012). In summary, future therapeutic regimens targeting the autophagy machinery will have to take these mTOR-independent pathways into consideration.

2.6 Ulk1-mediated phosphorylation of AMPK constitutes a negative regulatory feedback loop

Löffler AS, Alers S, Dieterle AM, Keppeler H, Franz-Wachtel M, Kundu M, Campbell DG, Wesselborg S, Alessi DR, Stork B.
Autophagy 2011;7:696-706.

(The published and herein discussed data are part of the dissertation by Dr. Antje Löffler)

Since it has been reported that FIP200 contributes to both mTOR-dependent and -independent autophagy pathways (Hara et al., 2008), we next focused on the autophagy inititiator complex composed of Ulk1, Atg13, FIP200, and Atg101, respectively. At first, we aimed at the identification of both Ulk1 substrates and interacting proteins. For that, we generated Flp-In™ T-Rex™ 293 cells stably expressing GFP-Ulk1 wild-type or GFP-Ulk1 ΔCTD, which lacks the C-terminal domain. The Ulk1

proteins were purified from these cells, and co-immunopurified proteins were identified by mass spectrometry. Next to known interacting proteins, including Raptor (component of mTORC1), Atg13, FIP200 and Atg101, we were able to identify all three AMPK subunits as novel Ulk1-interacting proteins. The heterotrimeric AMPK also interacts with the C-terminally truncated version of Ulk1, indicating that this region is dispensable for the interaction. The interaction between these two kinases could be confirmed by immunopurification and subsequent immunoblot analyses. Furthermore, the association was demonstrated for endogenous proteins. We next asked whether AMPK functions as a substrate for Ulk1. We performed *in vitro* kinase assays and observed that all three subunits of AMPK serve as phospho-acceptors for Ulk1 kinase activity. Additionally, we were able to map the Ulk1-dependent phosphorylation sites by mass spectrometry. Within the α-subunit, Ulk1 phosphorylates residues which are C-terminally located to the kinase domain. Within the β-subunit, the phospho-acceptor sites are located at the N-terminus of the glycogen-binding domain and in the region connecting the glycogen-binding domain and the C-terminal domain, which mediates the association with the α- and γ-subunit, respectively. Within the γ-subunit, Ulk1 catalyzes the phosphorylation of residues located in the linker region between the cystathionine β-synthase motifs 3 and 4, which form one of two AMP/ATP-binding Bateman domains (see chapter 1.2.3.3). Next we wanted to elucidate the physiological function of Ulk1-mediated phosphorylation of AMPK. As mentioned above, T172 in the activation loop of the catalytic α-subunit has to be phosphorylated for AMPK activation. Interestingly, we observed that the ectopic expression of catalytically active GFP-Ulk1 decreased the starvation-induced AMPK activation compared to cells expressing the catalytic-dead version of GFP-Ulk1, as detected by T172 phosphorylation. Furthermore, reduced AMPK activity was detectable in cells expressing GFP-Ulk1 wild-type by analyzing phosphorylation of the AMPK substrate acetyl-CoA carboxylase (ACC). These observations were confirmed in two cellular model systems expressing Ulk1 at endogenous levels. First, starvation-induced AMPK activation was higher in Ulk1-deficient MEFs compared to wild-type MEFs. A further increase in AMPK activation could be achieved by the additional knockdown of Ulk2 in *Ulk1*-/- MEFs. Second, Ulk1 knockdown in HEK293 cells resulted in a similar elevation of AMPK activation and activity, as detected by the analysis of AMPKα T172 and Raptor/ACC phosphorylation, respectively.

Taken together, in this work we were able to demonstrate that the energy-sensing kinase AMPK serves as substrate for the autophagy-inducing kinase Ulk1. Ulk1-mediated phosphorylation of AMPK results in a reduced activation and activity of AMPK. Generally, AMPK has been shown to modulate autophagy via the regulation of mTOR. AMPK can inhibit mTOR and thus activate autophagy by phosphorylating TSC2 or Raptor, respectively (see chapter 1.3.1). Simultaneously to or following our publication, several other groups reported the interaction between Ulk1 and AMPK (Behrends et al., 2010; Lee et al., 2010; Egan et al., 2011; Kim et al., 2011; Shang et al., 2011; Mack et al., 2012;

Sanchez et al., 2012). Notably, four of these groups reported the AMPK-mediated phosphorylation and activation of Ulk1 (Egan et al., 2011; Kim et al., 2011; Shang et al., 2011; Mack et al., 2012). Although there exist some controversial views about the exact phospho-sites in Ulk1 and the outcome of phosphorylation (see chapter 1.2.3.3), these reports directly confirm the existence of mTOR-independent regulation of autophagy. However, our data indicate that the *vice versa*-phosphorylation of AMPK by Ulk1 establishes a negative regulatory feedback loop, which potentially contributes to the termination of an autophagic response. This is especially remarkable since in the past years the main focus was drawn on the signaling pathways leading to the induction of autophagy. Regarding the termination of autophagy, an mTOR-dependent "gas and brake" model has been proposed (Koren et al., 2010). The autophagy-suppressing death-associated protein 1 (DAP1) is phosphorylated by mTOR at S3 and S51, and thus kept in an inactive state. Upon starvation, inactivation of mTOR not only induces autophagy ("gas"), but also leads to the dephosphorylation and activation of DAP1 ("brake") (Koren et al., 2010). Alternatively, it has been reported that mTOR becomes re-activated upon prolonged starvation (Yu et al., 2010). This re-activation is autophagy-dependent. Interestingly, the authors report that increased mTOR activity attenuates autophagy and leads to the generation of lysosomal tubules, which ultimately mature into functional lysosomes (Yu et al., 2010). Next to mTOR re-activation, further mechanisms have been identified to negatively regulate autophagy, including negative regulation of PI3P synthesis, inhibition of the two ubiquitin-like conjugations systems involved in the elongation of the autophagosomal membrane, and inhibition of the autophagosome-lysosome fusion (reviewed in Liang, 2010). The negative regulatory feedback loop identified by our group adds further complexity to the mutual regulation of the kinases AMPK, mTOR and Ulk1, respectively. Future studies will have to reveal the chronology of these phosphorylation processes, which presumably contribute to the dynamics of autophagic responses. The kinase-triangle AMPK-mTOR-Ulk1 is also a promising target for the therapeutic intervention in cancer. So far, no specific inhibitors for Ulk1 have been reported. However, mTOR inhibitors (rapalogs and ATP-competitive inhibitors) are currently evaluated in clinical trials (reviewed in Wander et al., 2011; Zhang et al., 2011b; Willems et al., 2012). Interestingly, the role of AMPK during cancerogenesis appears to be ambivalent. Generally, activated AMPK blocks cell growth through the inhibition of mTOR and a reduced *de novo* synthesis of lipids (Carling et al., 2012). These tumor-suppressing properties form the basis for the application of AMPK-activating compounds such as AICA riboside, A-769662, and metformin (Carling et al., 2012; Hardie et al., 2012a). In contrast, it has been reported that AMPK positively influences cell migration, mitosis, and glycolysis, which would point towards a tumor-promoting function of this kinase and hence beneficial effects of AMPK inhibitors in cancer therapy (Carling et al., 2012). The understanding of the interplay between the autophagy-inducing kinase Ulk1 and the energy-sensing kinase AMPK will be of interest for future

therapeutic interventions. We are currently trying to contribute to this understanding by characterizing the physiological relevance of the Ulk1-dependent phospho-acceptor sites within the different AMPK subunits.

2.7 Atg13 and FIP200 act independently of Ulk1 and Ulk2 in autophagy induction

Alers S, Löffler AS, Paasch F, Dieterle AM, Keppeler H, Lauber K, Campbell DG, Fehrenbacher B, Schaller M, Wesselborg S, Stork B.
Autophagy 2011;7:1424-1433.

(The published and herein discussed data are part of the dissertation by Dr. Sebastian Alers)

As described in the previous chapters, the Ulk1-Atg13-FIP200-Atg101 complex is centrally involved in the regulation of autophagic responses. To characterize the importance of the individual components for the function of the complex, we made use of the chicken DT40 knockout system. At first, we generated *ATG13*-/- DT40 cells. Atg13-deficiency entirely blocks basal and starvation-induced autophagy, as analyzed by LC3 immunoblotting, detection of autophagosomes by electron microscopy, and detection of mCitrine-LC3- or mRFP-EGFP-LC3-positive puncta by confocal microscopy. In the established model, starvation leads to the dissociation of mTORC1 from the Ulk1-Atg13-FIP200-Atg101 complex and to the subsequent autophosphorylation of Ulk1 and Ulk1-mediated trans-phosphorylation of Atg13 and FIP200, respectively. Accordingly, we next focused on Ulk1 and its nearest relative Ulk2. Both isoforms have been implicated in the regulation of autophagic processes (reviewed in Alers et al., 2012b; Alers et al., 2012a). We generated DT40 cells deficient for both Ulk1 and Ulk2. Surprisingly, double-deficient cell lines did not reveal any signs of impaired autophagy. In parallel, we determined the Ulk1-dependent phospho-acceptor sites in Atg13 by an *in vitro*-kinase assay. Reconstitution of Atg13-deficient DT40 cells with a cDNA encoding a non-phosphorylatable Atg13 variant (S/T-to-A mutations) did not block the induction of autophagy, underlining our results with the *ULK1*-/- *ULK2*-/- DT40 cells. Collectively, it appears that these two Ulk isoforms are dispensable for the induction of autophagy in this cell line. Additionally, inhibition of the upstream kinase mTOR is similarly dispensable for the induction of autophagy, since usage of the mTOR inhibitors Torin1 or rapamycin did not result in either LC3 lipidation or altered Atg13 migration in SDS-PAGE. Next we investigated whether the interaction between Atg13 and FIP200 is important for the function as autophagy initiation complex. We found that Atg13 mRNA is alternatively spliced in DT40 cells. Notably, only those Atg13 variants containing the amino acids encoded by exon 12 of

the chicken Atg13 locus were capable to interact with FIP200, as detected by co-immunopurification. Additionally, only these Atg13 variants reconstituted the autophagy flux in *ATG13*-/- DT40 cells.

Collectively, our data indicate that Atg13 is essential for both basal and starvation-induced autophagy. Apparently, this function in autophagy initiation strictly requires the interaction between Atg13 and FIP200. In contrast, both the presence of Ulk1 or Ulk2 and their upstream regulation by mTOR are dispensable for the induction of autophagy. Currently we are analyzing whether alternative kinases or post-translational modifications contribute to this Ulk1/2-independent regulation. We cannot entirely exclude that the other Ulk isoforms, i.e. Ulk3, Ulk4 and STK36, participate in the regulation of this initiation complex. However, these isoforms differ significantly in their C-terminus, which is centrally involved in the interaction with Atg13 and FIP200 in Ulk1 and Ulk2. Furthermore, the siRNA-mediated knockdown of Ulk3 did not reveal any effect on autophagy in DT40 cells (this manuscript), and Ulk4 has been classified as pseudokinase lacking catalytic activity (Manning et al., 2002b; Boudeau et al., 2006; Gautel, 2011). Future studies will have to reveal the potential influence of Ulk3 and STK36 on autophagy signaling pathways. So far, there is only one report stating that the overexpression of Ulk3 in a human fibroblast cell line induces autophagy and senescence (Young et al., 2009).

Recently, two groups reported the generation of Ulk1/2 doubly deficient MEFs. Cheong et al. observed that Ulk1/2 are required for autophagy induced by amino acid deprivation, but not by glucose deprivation (Cheong et al., 2011). The authors report that glucose deprivation results in enhanced amino acid catabolism and thus to elevated levels of cellular ammonia. Apparently, ammonia-induced autophagy occurs independently of Ulk1 and Ulk2. This concept has been extended recently by Gammoh et al. (Gammoh et al., 2013). They claim that the interaction between FIP200 and Atg16L1 distinguishes between Ulk1 complex-dependent and -independent autophagy, since an Atg16L1 mutant incapable of binding to FIP200 supported glucose starvation-induced autophagy, but not amino acid starvation-induced autophagy. However, this model has been challenged by McAlpine et al. recently. Although they observed differential pathways that respond to amino acid and glucose starvation, they state that increased autophagy upon these two stimuli is disrupted by the combined loss of Ulk1 and Ulk2 in MEFs (McAlpine et al., 2013). However, the authors admit that “some residual autophagy occurs even under ULK1/2-deficiency” (McAlpine et al., 2013). Nevertheless, further experiments will have to reveal the exact functions of Ulk1 and Ulk2 under different starvation conditions. The differences between Ulk1/2 doubly deficient DT40 cells and MEFs might be caused by the evolutionary divergence of aves and mammalia (Alers et al., 2012a). Alternatively, the fact that these two model systems represent two different cell types, i.e. B lymphocytes versus fibroblasts, might contribute to this discrepancy. Additionally, it has to be

determined if the several reported mTOR-independent autophagy pathways rely on Ulk1 activation, which has not been done systematically until now. Notably, LC3-associated phagocytosis apparently does not require components of the Ulk1 complex (Martinez et al., 2011; Florey & Overholtzer, 2012).

Interestingly there exist additional hints indicating an autonomous function of Atg13 for autophagy. Joo et al. reported that Atg13 is released from Ulk1 in order to be recruited to damaged mitochondria and to mediate mitophagy (Joo et al., 2011). With regard to the yeast system, Kraft et al. state that "The autophagy defects of Atg13 mutants unable to interact with Atg1 are however less pronounced when compared to cells deleted for Atg13, indicating that Atg13 may have functions outside of the Atg1 complex" (Kraft et al., 2012). Currently we are trying to elucidate the autonomous role of Atg13 during autophagic processes.

Next to Ulk1/2-independent autophagy, different other non-canonical autophagy pathways have been reported, which are executed independently of different Atgs (reviewed in Codogno et al., 2012). Nishida et al. reported an Atg5/Atg7-independent autophagy pathway (Nishida et al., 2009). This pathway does not involve LC3 lipidation but still requires the Ulk1-Atg13-FIP200 complex and the Beclin 1-Vps34 complex, respectively. Additionally, Beclin 1- and Vps34-independent autophagy induced by the polyphenol resveratrol or the neurotoxin 1-methyl-4-phenylpyridinium has been demonstrated (Zhu et al., 2007; Scarlatti et al., 2008). Interestingly, different groups reported that Beclin 1-independent autophagy does not necessarily include independency of the Vps34-WIPI-Atg5-LC3 signaling axis (Codogno et al., 2012). For example, two independent reports describe that autophagy induced by arsenic trioxide or the BH3 mimetic gossypol is independent of Beclin 1 but depends on Vps34 (Gao et al., 2010; Smith et al., 2010). The Vps34-independency of resveratrol-induced autophagy has been challenged recently. Mauthe et al. observed that resveratrol induces WIPI1-dependent LC3 lipidation without formation of WIPI1-positive structures (Mauthe et al., 2011). In turn, Tooze's group reported that resveratrol induces the formation of WIPI2-positive puncta (Polson et al., 2010). In the manuscript mentioned above, the same group reported that glucose starvation-induced autophagy does not involve PI3P generation or WIPI2 puncta formation, although this pathway required Ulk1 and Ulk2 (McAlpine et al., 2013). Notably, selective forms of autophagy apparently also utilize different combinations of the functional Atg units. It was demonstrated that carbonyl cyanide m-chlorophenylhydrazone (CCCP), which causes mitochondrial damage and subsequent mitophagy, induces LC3 lipidation which solely depended on Atg9 vesicles, but not on the Ulk1-Atg13-FIP200 complex or the Beclin 1-Vps34 complex, respectively (Chen et al., 2013). In contrast, Mizushima and colleagues previously reported that Atg9 and the Ulk1 complex are independently recruited to depolarized mitochondria, and that both are required for the recruitment

of downstream Atgs except LC3, which could be recruited to CCCP-induced depolarized mitochondria in *Fip200*-/- MEFs and *Atg9a*-/- MEFs (Itakura et al., 2012a). Collectively, the potential existence of multiple non-canonical autophagy pathways increases the overall complexity of autophagy signaling pathways. It is tempting to speculate that different pro-autophagic stimuli and the various types of selectively degraded cargo employ different sets of Atgs from the autophagic toolbox in order to adequately induce autophagy. Furthermore, these non-canonical pathways will have to be considered for the design of therapeutic compounds that aim to modulate autophagy.

Our data suggest a central role of the Atg13-FIP200 interaction for autophagic processes. We could confirm this by the generation of FIP200-deficient DT40 cells, which essentially phenocopy *ATG13*-/- DT40 cells regarding autophagy signaling (unpublished results). We assume that the inhibition of the Atg13-FIP200 interaction might represent an attractive therapeutic target under disease conditions which rely on autophagy, since interference with this interaction probably disrupts both Ulk1/2-dependent and -independent autophagy signaling pathways.

3. Conclusion

In summary, our works contributed to a better understanding of the signal transduction pathways of apoptosis and autophagy. The central focus was put on the dynamic regulation of these two pathways, which is mainly achieved by protein phosphorylation processes. Kinases are per se attractive targets for the design of therapeutics, and accordingly the understanding of this modification for the execution of apoptosis and/or autophagy is of central importance. However, there are additional post-translational modification processes, and their involvement in the modulation of these two cell fate-deciding processes will be investigated in the future.

Most of the pathways described in this thesis are dysregulated in tumors, leading either to resistance to cell death or to increased cell survival. As described, the apoptosis machinery is already targeted by different therapeutics, including TRAIL-R agonists, BH3- or Smac-mimetics. Similarly, the pro-survival PI3K/PDK1/Akt/mTOR pathway is exploited by different therapies. With regard to the autophagy machinery, current clinical trials are mainly aiming at the inhibition of autophagy (Chen & Karantza, 2011). Since there are currently no therapeutics available which specifically target autophagy regulators, these trials mainly rely on the usage of chloroquine or hydroxychloroquine, which block the fusion of autophagosomes with lysosomes. This notion underscores the urgent need for specific compounds directly aiming at autophagy-regulating proteins. Ulk1 is the sole protein kinase among the Atgs, and it can be assumed that specific inhibitors for this kinase (or its related isoforms) will be reported soon. Additionally, other components of the Ulk1 complex might be “druggable”, e.g. by the inhibition of protein-protein interactions. Furthermore, it has to be determined at which stage of a disease the inhibition or activation of autophagy is desirable. Interestingly, recently a candidate therapeutic autophagy-inducing peptide has been reported, which is based on a Beclin 1 amino acid sequence (Shoji-Kawata et al., 2013).

In the future, the malignancy-dependent alterations of these two cell fate decision pathways will have to be analyzed for the individual patient. Furthermore, this personalized medicine will be based on the combination of different therapeutic approaches, distinctly activating or inhibiting the pathways described in this thesis.

4. Bibliography

Abbi S, Ueda H, Zheng C et al. (2002). Regulation of focal adhesion kinase by a novel protein inhibitor FIP200. *Molecular biology of the cell* **13**: 3178-3191

Abedin MJ, Wang D, McDonnell MA et al. (2007). Autophagy delays apoptotic death in breast cancer cells following DNA damage. *Cell Death Differ* **14**: 500-510

Acehan D, Jiang X, Morgan DG et al. (2002). Three-dimensional structure of the apoptosome: implications for assembly, procaspase-9 binding, and activation. *Mol Cell* **9**: 423-432

Ackermann JA, Radtke D, Maurberger A et al. (2011). Grb2 regulates B-cell maturation, B-cell memory responses and inhibits B-cell Ca2+ signalling. *EMBO J* **30**: 1621-1633

Agard NJ, Mahrus S, Trinidad JC et al. (2012). Global kinetic analysis of proteolysis via quantitative targeted proteomics. *Proc Natl Acad Sci U S A* **109**: 1913-1918

Al Rawi S, Louvet-Vallee S, Djeddi A et al. (2012). Allophagy: a macroautophagic process degrading spermatozoid-inherited organelles. *Autophagy* **8**: 421-423

Alemu EA, Lamark T, Torgersen KM et al. (2012). ATG8 family proteins act as scaffolds for assembly of the ULK complex: sequence requirements for LC3-interacting region (LIR) motifs. *J Biol Chem* **287**: 39275-39290

Alers S, Löffler AS, Wesselborg S et al. (2012a). The incredible ULKs. *Cell Commun Signal* **10**: 7

Alers S, Löffler AS, Wesselborg S et al. (2012b). Role of AMPK-mTOR-Ulk1/2 in the regulation of autophagy: cross talk, shortcuts, and feedbacks. *Mol Cell Biol* **32**: 2-11

Alessi DR, Caudwell FB, Andjelkovic M et al. (1996). Molecular basis for the substrate specificity of protein kinase B; comparison with MAPKAP kinase-1 and p70 S6 kinase. *FEBS Lett* **399**: 333-338

Alessi DR, Deak M, Casamayor A et al. (1997a). 3-Phosphoinositide-dependent protein kinase-1 (PDK1): structural and functional homology with the Drosophila DSTPK61 kinase. *Curr Biol* **7**: 776-789

Alessi DR, James SR, Downes CP et al. (1997b). Characterization of a 3-phosphoinositide-dependent protein kinase which phosphorylates and activates protein kinase Balpha. *Curr Biol* **7**: 261-269

Alessi DR, Kozlowski MT, Weng QP et al. (1998). 3-Phosphoinositide-dependent protein kinase 1 (PDK1) phosphorylates and activates the p70 S6 kinase in vivo and in vitro. *Curr Biol* **8**: 69-81

Allan LA, Clarke PR (2007). Phosphorylation of caspase-9 by CDK1/cyclin B1 protects mitotic cells against apoptosis. *Mol Cell* **26**: 301-310

Allan LA, Clarke PR (2009). Apoptosis and autophagy: Regulation of caspase-9 by phosphorylation. *FEBS J* **276**: 6063-6073

Allan LA, Morrice N, Brady S et al. (2003). Inhibition of caspase-9 through phosphorylation at Thr 125 by ERK MAPK. *Nat Cell Biol* **5**: 647-654

Alnemri ES, Livingston DJ, Nicholson DW et al. (1996). Human ICE/CED-3 protease nomenclature. *Cell* **87**: 171

Annis MG, Soucie EL, Dlugosz PJ et al. (2005). Bax forms multispanning monomers that oligomerize to permeabilize membranes during apoptosis. *EMBO J* **24**: 2096-2103

Ashford TP, Porter KR (1962). Cytoplasmic components in hepatic cell lysosomes. *J Cell Biol* **12**: 198-202

Ashkenazi A, Pai RC, Fong S et al. (1999). Safety and antitumor activity of recombinant soluble Apo2 ligand. *The Journal of clinical investigation* **104**: 155-162

Ashrafi G, Schwarz TL (2013). The pathways of mitophagy for quality control and clearance of mitochondria. *Cell Death Differ* **20**: 31-42

Assefa Z, Bultynck G, Szlufcik K et al. (2004). Caspase-3-induced truncation of type 1 inositol trisphosphate receptor accelerates apoptotic cell death and induces inositol trisphosphate-independent calcium release during apoptosis. *J Biol Chem* **279**: 43227-43236

Axe EL, Walker SA, Manifava M et al. (2008). Autophagosome formation from membrane compartments enriched in phosphatidylinositol 3-phosphate and dynamically connected to the endoplasmic reticulum. *J Cell Biol* **182**: 685-701

Azad MB, Chen Y, Henson ES et al. (2008). Hypoxia induces autophagic cell death in apoptosis-competent cells through a mechanism involving BNIP3. *Autophagy* **4**: 195-204

Bach M, Larance M, James DE et al. (2011). The serine/threonine kinase ULK1 is a target of multiple phosphorylation events. *Biochem J* **440**: 283-291

Bai H, Inoue J, Kawano T et al. (2012). A transcriptional variant of the LC3A gene is involved in autophagy and frequently inactivated in human cancers. *Oncogene* **31**: 4397-4408

Bakhshi A, Jensen JP, Goldman P et al. (1985). Cloning the chromosomal breakpoint of t(14;18) human lymphomas: clustering around JH on chromosome 14 and near a transcriptional unit on 18. *Cell* **41**: 899-906

Balendran A, Biondi RM, Cheung PC et al. (2000). A 3-phosphoinositide-dependent protein kinase-1 (PDK1) docking site is required for the phosphorylation of protein kinase Czeta (PKCzeta) and PKC-related kinase 2 by PDK1. *J Biol Chem* **275**: 20806-20813

Banreti A, Lukacsovich T, Csikos G et al. (2012). PP2A regulates autophagy in two alternative ways in Drosophila. *Autophagy* **8**: 623-636

Bao Q, Shi Y (2007). Apoptosome: a platform for the activation of initiator caspases. *Cell Death Differ* **14**: 56-65

Barritt GJ (1999). Receptor-activated Ca2+ inflow in animal cells: a variety of pathways tailored to meet different intracellular Ca2+ signalling requirements. *Biochem J* **337 (Pt 2)**: 153-169

Barth H, Meiling-Wesse K, Epple UD et al. (2001). Autophagy and the cytoplasm to vacuole targeting pathway both require Aut10p. *FEBS Lett* **508**: 23-28

Barth H, Meiling-Wesse K, Epple UD et al. (2002). Mai1p is essential for maturation of proaminopeptidase I but not for autophagy. *FEBS Lett* **512**: 173-179

Barthwal MK, Sathyanarayana P, Kundu CN et al. (2003). Negative regulation of mixed lineage kinase 3 by protein kinase B/AKT leads to cell survival. *J Biol Chem* **278**: 3897-3902

Baskaran S, Ragusa MJ, Boura E et al. (2012). Two-site recognition of phosphatidylinositol 3-phosphate by PROPPINs in autophagy. *Mol Cell* **47**: 339-348

Basu S, Totty NF, Irwin MS et al. (2003). Akt phosphorylates the Yes-associated protein, YAP, to induce interaction with 14-3-3 and attenuation of p73-mediated apoptosis. *Mol Cell* **11**: 11-23

Baughman JM, Perocchi F, Girgis HS et al. (2011). Integrative genomics identifies MCU as an essential component of the mitochondrial calcium uniporter. *Nature* **476**: 341-345

Bayascas JR (2008). Dissecting the role of the 3-phosphoinositide-dependent protein kinase-1 (PDK1) signalling pathways. *Cell Cycle* **7**: 2978-2982

Bayascas JR (2010). PDK1: the major transducer of PI 3-kinase actions. *Curr Top Microbiol Immunol* **346**: 9-29

Bayascas JR, Wullschleger S, Sakamoto K et al. (2008). Mutation of the PDK1 PH domain inhibits protein kinase B/Akt, leading to small size and insulin resistance. *Mol Cell Biol* **28**: 3258-3272

Behrends C, Sowa ME, Gygi SP et al. (2010). Network organization of the human autophagy system. *Nature* **466**: 68-76

Belka C, Rudner J, Wesselborg S et al. (2000). Differential role of caspase-8 and BID activation during radiation- and CD95-induced apoptosis. *Oncogene* **19**: 1181-1190

Belmokhtar CA, Hillion J, Dudognon C et al. (2003). Apoptosome-independent pathway for apoptosis. Biochemical analysis of APAF-1 defects and biological outcomes. *J Biol Chem* **278**: 29571-29580

Belyi VA, Ak P, Markert E et al. (2010). The origins and evolution of the p53 family of genes. *Cold Spring Harb Perspect Biol* **2**: a001198

Berger SB, Romero X, Ma C et al. (2010). SLAM is a microbial sensor that regulates bacterial phagosome functions in macrophages. *Nat Immunol* **11**: 920-927

Berry DL, Baehrecke EH (2007). Growth arrest and autophagy are required for salivary gland cell degradation in Drosophila. *Cell* **131**: 1137-1148

Bertrand MJ, Vandenabeele P (2011). The Ripoptosome: death decision in the cytosol. *Mol Cell* **43**: 323-325

Betin VM, Lane JD (2009). Caspase cleavage of Atg4D stimulates GABARAP-L1 processing and triggers mitochondrial targeting and apoptosis. *J Cell Sci* **122**: 2554-2566

Biggs WH, 3rd, Meisenhelder J, Hunter T et al. (1999). Protein kinase B/Akt-mediated phosphorylation promotes nuclear exclusion of the winged helix transcription factor FKHR1. *Proc Natl Acad Sci U S A* **96**: 7421-7426

Billard C (2012). Design of novel BH3 mimetics for the treatment of chronic lymphocytic leukemia. *Leukemia* **26**: 2032-2038

Biondi RM, Cheung PC, Casamayor A et al. (2000). Identification of a pocket in the PDK1 kinase domain that interacts with PIF and the C-terminal residues of PKA. *EMBO J* **19**: 979-988

Biondi RM, Kieloch A, Currie RA et al. (2001). The PIF-binding pocket in PDK1 is essential for activation of S6K and SGK, but not PKB. *EMBO J* **20**: 4380-4390

Birnbaum MJ, Clem RJ, Miller LK (1994). An apoptosis-inhibiting gene from a nuclear polyhedrosis virus encoding a polypeptide with Cys/His sequence motifs. *J Virol* **68**: 2521-2528

Bitzer M, Armeanu S, Prinz F et al. (2002). Caspase-8 and Apaf-1-independent caspase-9 activation in Sendai virus-infected cells. *J Biol Chem* **277**: 29817-29824

Bjorkoy G, Lamark T, Brech A et al. (2005). p62/SQSTM1 forms protein aggregates degraded by autophagy and has a protective effect on huntingtin-induced cell death. *J Cell Biol* **171**: 603-614

Black RA, Kronheim SR, Merriam JE et al. (1989). A pre-aspartate-specific protease from human leukocytes that cleaves pro-interleukin-1 beta. *J Biol Chem* **264**: 5323-5326

Blankson H, Holen I, Seglen PO (1995). Disruption of the cytokeratin cytoskeleton and inhibition of hepatocytic autophagy by okadaic acid. *Exp Cell Res* **218**: 522-530

Blero D, Payrastre B, Schurmans S et al. (2007). Phosphoinositide phosphatases in a network of signalling reactions. *Pflugers Arch* **455**: 31-44

Blume-Jensen P, Janknecht R, Hunter T (1998). The kit receptor promotes cell survival via activation of PI 3-kinase and subsequent Akt-mediated phosphorylation of Bad on Ser136. *Curr Biol* **8**: 779-782

Boatright KM, Renatus M, Scott FL et al. (2003). A unified model for apical caspase activation. *Mol Cell* **11**: 529-541

Bodemann BO, Orvedahl A, Cheng T et al. (2011). RalB and the exocyst mediate the cellular starvation response by direct activation of autophagosome assembly. *Cell* **144**: 253-267

Boehning D, Patterson RL, Sedaghat L et al. (2003). Cytochrome c binds to inositol (1,4,5) trisphosphate receptors, amplifying calcium-dependent apoptosis. *Nat Cell Biol* **5**: 1051-1061

Boehning D, van Rossum DB, Patterson RL et al. (2005). A peptide inhibitor of cytochrome c/inositol 1,4,5-trisphosphate receptor binding blocks intrinsic and extrinsic cell death pathways. *Proc Natl Acad Sci U S A* **102**: 1466-1471

Bogner C, Leber B, Andrews DW (2010). Apoptosis: embedded in membranes. *Curr Opin Cell Biol* **22**: 845-851

Boise LH, Gonzalez-Garcia M, Postema CE et al. (1993). bcl-x, a bcl-2-related gene that functions as a dominant regulator of apoptotic cell death. *Cell* **74**: 597-608

Boldin MP, Goncharov TM, Goltsev YV et al. (1996). Involvement of MACH, a novel MORT1/FADD-interacting protease, in Fas/APO-1- and TNF receptor-induced cell death. *Cell* **85**: 803-815

Boldin MP, Varfolomeev EE, Pancer Z et al. (1995). A novel protein that interacts with the death domain of Fas/APO1 contains a sequence motif related to the death domain. *J Biol Chem* **270**: 7795-7798

Bonavida B, Ng CP, Jazirehi A et al. (1999). Selectivity of TRAIL-mediated apoptosis of cancer cells and synergy with drugs: the trail to non-toxic cancer therapeutics (review). *International journal of oncology* **15**: 793-802

Botti J, Djavaheri-Mergny M, Pilatte Y et al. (2006). Autophagy signaling and the cogwheels of cancer. *Autophagy* **2**: 67-73

Boudeau J, Miranda-Saavedra D, Barton GJ et al. (2006). Emerging roles of pseudokinases. *Trends Cell Biol* **16**: 443-452

Bradshaw JM (2010). The Src, Syk, and Tec family kinases: distinct types of molecular switches. *Cell Signal* **22**: 1175-1184

Bratton SB, Salvesen GS (2010). Regulation of the Apaf-1-caspase-9 apoptosome. *J Cell Sci* **123**: 3209-3214

Bratton SB, Walker G, Srinivasula SM et al. (2001). Recruitment, activation and retention of caspases-9 and -3 by Apaf-1 apoptosome and associated XIAP complexes. *EMBO J* **20**: 998-1009

Brech A, Ahlquist T, Lothe RA et al. (2009). Autophagy in tumour suppression and promotion. *Mol Oncol* **3**: 366-375

Brown EJ, Albers MW, Shin TB et al. (1994). A mammalian protein targeted by G1-arresting rapamycin-receptor complex. *Nature* **369**: 756-758

Brugarolas J, Lei K, Hurley RL et al. (2004). Regulation of mTOR function in response to hypoxia by REDD1 and the TSC1/TSC2 tumor suppressor complex. *Genes Dev* **18**: 2893-2904

Brunet A, Bonni A, Zigmond MJ et al. (1999). Akt promotes cell survival by phosphorylating and inhibiting a Forkhead transcription factor. *Cell* **96**: 857-868

Brunet A, Datta SR, Greenberg ME (2001). Transcription-dependent and -independent control of neuronal survival by the PI3K-Akt signaling pathway. *Curr Opin Neurobiol* **11**: 297-305

Budanov AV, Karin M (2008). p53 target genes sestrin1 and sestrin2 connect genotoxic stress and mTOR signaling. *Cell* **134**: 451-460

Budovskaya YV, Stephan JS, Deminoff SJ et al. (2005). An evolutionary proteomics approach identifies substrates of the cAMP-dependent protein kinase. *Proc Natl Acad Sci U S A* **102**: 13933-13938

Cabal-Hierro L, Lazo PS (2012). Signal transduction by tumor necrosis factor receptors. *Cell Signal* **24**: 1297-1305

Cafferkey R, Young PR, McLaughlin MM et al. (1993). Dominant missense mutations in a novel yeast protein related to mammalian phosphatidylinositol 3-kinase and VPS34 abrogate rapamycin cytotoxicity. *Mol Cell Biol* **13**: 6012-6023

Cain K, Brown DG, Langlais C et al. (1999). Caspase activation involves the formation of the aposome, a large (approximately 700 kDa) caspase-activating complex. *J Biol Chem* **274**: 22686-22692

Cardenas C, Foskett JK (2012). Mitochondrial Ca(2+) signals in autophagy. *Cell Calcium* **52**: 44-51

Cardenas C, Miller RA, Smith I et al. (2010). Essential regulation of cell bioenergetics by constitutive InsP3 receptor Ca2+ transfer to mitochondria. *Cell* **142**: 270-283

Cardone MH, Roy N, Stennicke HR et al. (1998). Regulation of cell death protease caspase-9 by phosphorylation. *Science* **282**: 1318-1321

Carew JS, Nawrocki ST, Cleveland JL (2007). Modulating autophagy for therapeutic benefit. *Autophagy* **3**: 464-467

Carling D, Hardie DG (1989). The substrate and sequence specificity of the AMP-activated protein kinase. Phosphorylation of glycogen synthase and phosphorylase kinase. *Biochimica et biophysica acta* **1012**: 81-86

Carling D, Thornton C, Woods A et al. (2012). AMP-activated protein kinase: new regulation, new roles? *Biochem J* **445**: 11-27

Carmona-Gutierrez D, Eisenberg T, Buttner S et al. (2010). Apoptosis in yeast: triggers, pathways, subroutines. *Cell Death Differ* **17**: 763-773

Carnero A (2010). The PKB/AKT pathway in cancer. *Curr Pharm Des* **16**: 34-44

Carracedo A, Baselga J, Pandolfi PP (2008). Deconstructing feedback-signaling networks to improve anticancer therapy with mTORC1 inhibitors. *Cell Cycle* **7**: 3805-3809

Carracedo A, Pandolfi PP (2008). The PTEN-PI3K pathway: of feedbacks and cross-talks. *Oncogene* **27**: 5527-5541

Carrington PE, Sandu C, Wei Y et al. (2006). The structure of FADD and its mode of interaction with procaspase-8. *Mol Cell* **22**: 599-610

Chalhoub N, Baker SJ (2009). PTEN and the PI3-kinase pathway in cancer. *Annu Rev Pathol* **4**: 127-150

Chan EY, Kir S, Tooze SA (2007). siRNA screening of the kinome identifies ULK1 as a multidomain modulator of autophagy. *J Biol Chem* **282**: 25464-25474

Chan EY, Longatti A, McKnight NC et al. (2009). Kinase-inactivated ULK proteins inhibit autophagy via their conserved C-terminal domains using an Atg13-independent mechanism. *Mol Cell Biol* **29**: 157-171

Chan EY, Tooze SA (2009). Evolution of Atg1 function and regulation. *Autophagy* **5**: 758-765

Chandarlapaty S, Sawai A, Scaltriti M et al. (2011). AKT inhibition relieves feedback suppression of receptor tyrosine kinase expression and activity. *Cancer Cell* **19**: 58-71

Chang DW, Xing Z, Capacio VL et al. (2003). Interdimer processing mechanism of procaspase-8 activation. *EMBO J* **22**: 4132-4142

Chang NC, Nguyen M, Germain M et al. (2010). Antagonism of Beclin 1-dependent autophagy by BCL-2 at the endoplasmic reticulum requires NAF-1. *EMBO J* **29**: 606-618

Chang YY, Neufeld TP (2009). An Atg1/Atg13 complex with multiple roles in TOR-mediated autophagy regulation. *Mol Biol Cell* **20**: 2004-2014

Chano T, Ikebuchi K, Ochi Y et al. (2010). RB1CC1 activates RB1 pathway and inhibits proliferation and cologenic survival in human cancer. *PLoS One* **5**: e11404

Chano T, Ikegawa S, Kontani K et al. (2002). Identification of RB1CC1, a novel human gene that can induce RB1 in various human cells. *Oncogene* **21**: 1295-1298

Chano T, Saji M, Inoue H et al. (2006). Neuromuscular abundance of RB1CC1 contributes to the non-proliferating enlarged cell phenotype through both RB1 maintenance and TSC1 degradation. *Int J Mol Med* **18**: 425-432

Chao Y, Shiozaki EN, Srinivasula SM et al. (2005). Engineering a dimeric caspase-9: a re-evaluation of the induced proximity model for caspase activation. *PLoS Biol* **3**: e183

Chauhan D, Hideshima T, Rosen S et al. (2001). Apaf-1/cytochrome c-independent and Smac-dependent induction of apoptosis in multiple myeloma (MM) cells. *J Biol Chem* **276**: 24453-24456

Chen D, Chen X, Li M et al. (2013). CCCP-Induced LC3 lipidation depends on Atg9 whereas FIP200/Atg13 and Beclin 1/Atg14 are dispensable. *Biochem Biophys Res Commun* **432**: 226-230

Chen DJ, Huerta S (2009). Smac mimetics as new cancer therapeutics. *Anticancer Drugs* **20**: 646-658

Chen N, Karantza V (2011). Autophagy as a therapeutic target in cancer. *Cancer Biol Ther* **11**: 157-168

Chen R, Valencia I, Zhong F et al. (2004). Bcl-2 functionally interacts with inositol 1,4,5-trisphosphate receptors to regulate calcium release from the ER in response to inositol 1,4,5-trisphosphate. *J Cell Biol* **166**: 193-203

Cheong H, Lindsten T, Wu J et al. (2011). Ammonia-induced autophagy is independent of ULK1/ULK2 kinases. *Proc Natl Acad Sci U S A* **108**: 11121-11126

Cheong H, Nair U, Geng J et al. (2008). The Atg1 kinase complex is involved in the regulation of protein recruitment to initiate sequestering vesicle formation for nonspecific autophagy in Saccharomyces cerevisiae. *Mol Biol Cell* **19**: 668-681

Cheong H, Yorimitsu T, Reggiori F et al. (2005). Atg17 regulates the magnitude of the autophagic response. *Mol Biol Cell* **16**: 3438-3453

Chiang GG, Abraham RT (2005). Phosphorylation of mammalian target of rapamycin (mTOR) at Ser-2448 is mediated by p70S6 kinase. *J Biol Chem* **280**: 25485-25490

Chiang GG, Abraham RT (2007). Targeting the mTOR signaling network in cancer. *Trends Mol Med* **13**: 433-442

Chinnaiyan AM, O'Rourke K, Lane BR et al. (1997). Interaction of CED-4 with CED-3 and CED-9: a molecular framework for cell death. *Science* **275**: 1122-1126

Chinnaiyan AM, O'Rourke K, Tewari M et al. (1995). FADD, a novel death domain-containing protein, interacts with the death domain of Fas and initiates apoptosis. *Cell* **81**: 505-512

Chinnaiyan AM, Tepper CG, Seldin MF et al. (1996). FADD/MORT1 is a common mediator of CD95 (Fas/APO-1) and tumor necrosis factor receptor-induced apoptosis. *J Biol Chem* **271**: 4961-4965

Chipuk JE, Kuwana T, Bouchier-Hayes L et al. (2004). Direct activation of Bax by p53 mediates mitochondrial membrane permeabilization and apoptosis. *Science* **303**: 1010-1014

Chipuk JE, Moldoveanu T, Llambi F et al. (2010). The BCL-2 family reunion. *Mol Cell* **37**: 299-310

Chittenden T, Harrington EA, O'Connor R et al. (1995). Induction of apoptosis by the Bcl-2 homologue Bak. *Nature* **374**: 733-736

Cho DH, Jo YK, Hwang JJ et al. (2009). Caspase-mediated cleavage of ATG6/Beclin-1 links apoptosis to autophagy in HeLa cells. *Cancer Lett* **274**: 95-100

Choi AM, Ryter SW, Levine B (2013a). Autophagy in human health and disease. *N Engl J Med* **368**: 651-662

Choi JD, Ryu M, Ae Park M et al. (2013b). FIP200 inhibits beta-catenin-mediated transcription by promoting APC-independent beta-catenin ubiquitination. *Oncogene* **32**: 2421-2432

Choi SS, Park IC, Yun JW et al. (1995). A novel Bcl-2 related gene, Bfl-1, is overexpressed in stomach cancer and preferentially expressed in bone marrow. *Oncogene* **11**: 1693-1698

Chou MM, Hou W, Johnson J et al. (1998). Regulation of protein kinase C zeta by PI 3-kinase and PDK-1. *Curr Biol* **8**: 1069-1077

Choudhury S, Kolukula VK, Preet A et al. (2013). Dissecting the pathways that destabilize mutant p53: The proteasome or autophagy? *Cell Cycle* **12**: 1022-1029

Chowdhury I, Tharakan B, Bhat GK (2008). Caspases - an update. *Comp Biochem Physiol B Biochem Mol Biol* **151**: 10-27

Chresta CM, Davies BR, Hickson I et al. (2010). AZD8055 is a potent, selective, and orally bioavailable ATP-competitive mammalian target of rapamycin kinase inhibitor with in vitro and in vivo antitumor activity. *Cancer Res* **70**: 288-298

Ciechomska IA, Goemans CG, Tolkovsky AM (2009a). Why doesn't Beclin 1, a BH3-only protein, suppress the anti-apoptotic function of Bcl-2? *Autophagy* **5**: 880-881

Ciechomska IA, Goemans GC, Skepper JN et al. (2009b). Bcl-2 complexed with Beclin-1 maintains full anti-apoptotic function. *Oncogene* **28**: 2128-2141

Clapham DE (2007). Calcium signaling. *Cell* **131**: 1047-1058

Cleary ML, Sklar J (1985). Nucleotide sequence of a t(14;18) chromosomal breakpoint in follicular lymphoma and demonstration of a breakpoint-cluster region near a transcriptionally active locus on chromosome 18. *Proc Natl Acad Sci U S A* **82**: 7439-7443

Cleary ML, Smith SD, Sklar J (1986). Cloning and structural analysis of cDNAs for bcl-2 and a hybrid bcl-2/immunoglobulin transcript resulting from the t(14;18) translocation. *Cell* **47**: 19-28

Codogno P, Mehrpour M, Proikas-Cezanne T (2012). Canonical and non-canonical autophagy: variations on a common theme of self-eating? *Nat Rev Mol Cell Biol* **13**: 7-12

Cohen P, Frame S (2001). The renaissance of GSK3. *Nat Rev Mol Cell Biol* **2**: 769-776

Compton MM (1992). A biochemical hallmark of apoptosis: internucleosomal degradation of the genome. *Cancer Metastasis Rev* **11**: 105-119

Corradetti MN, Inoki K, Bardeesy N et al. (2004). Regulation of the TSC pathway by LKB1: evidence of a molecular link between tuberous sclerosis complex and Peutz-Jeghers syndrome. *Genes Dev* **18**: 1533-1538

Crawford ED, Seaman JE, Agard N et al. (2013). The DegraBase: a database of proteolysis in healthy and apoptotic human cells. *Mol Cell Proteomics* **12**: 813-824

Crawford ED, Wells JA (2011). Caspase substrates and cellular remodeling. *Annu Rev Biochem* **80**: 1055-1087

Crighton D, Wilkinson S, O'Prey J et al. (2006). DRAM, a p53-induced modulator of autophagy, is critical for apoptosis. *Cell* **126**: 121-134

Crighton D, Wilkinson S, Ryan KM (2007). DRAM links autophagy to p53 and programmed cell death. *Autophagy* **3**: 72-74

Criollo A, Maiuri MC, Tasdemir E et al. (2007). Regulation of autophagy by the inositol trisphosphate receptor. *Cell Death Differ* **14**: 1029-1039

Crook NE, Clem RJ, Miller LK (1993). An apoptosis-inhibiting baculovirus gene with a zinc finger-like motif. *J Virol* **67**: 2168-2174

Currie RA, Walker KS, Gray A et al. (1999). Role of phosphatidylinositol 3,4,5-trisphosphate in regulating the activity and localization of 3-phosphoinositide-dependent protein kinase-1. *Biochem J* **337 (Pt 3)**: 575-583

Cursi S, Rufini A, Stagni V et al. (2006). Src kinase phosphorylates Caspase-8 on Tyr380: a novel mechanism of apoptosis suppression. *EMBO J* **25**: 1895-1905

Czabotar PE, Westphal D, Dewson G et al. (2013). Bax crystal structures reveal how BH3 domains activate Bax and nucleate its oligomerization to induce apoptosis. *Cell* **152**: 519-531

Dai H, Smith A, Meng XW et al. (2011). Transient binding of an activator BH3 domain to the Bak BH3-binding groove initiates Bak oligomerization. *J Cell Biol* **194**: 39-48

Dan HC, Sun M, Kaneko S et al. (2004). Akt phosphorylation and stabilization of X-linked inhibitor of apoptosis protein (XIAP). *J Biol Chem* **279**: 5405-5412

Danial NN, Korsmeyer SJ (2004). Cell death: critical control points. *Cell* **116**: 205-219

Datta SR, Dudek H, Tao X et al. (1997). Akt phosphorylation of BAD couples survival signals to the cell-intrinsic death machinery. *Cell* **91**: 231-241

Datta SR, Katsov A, Hu L et al. (2000). 14-3-3 proteins and survival kinases cooperate to inactivate BAD by BH3 domain phosphorylation. *Mol Cell* **6**: 41-51

Davids MS, Letai A (2012). Targeting the B-cell lymphoma/leukemia 2 family in cancer. *J Clin Oncol* **30**: 3127-3135

de Almagro MC, Vucic D (2012). The inhibitor of apoptosis (IAP) proteins are critical regulators of signaling pathways and targets for anti-cancer therapy. *Exp Oncol* **34**: 200-211

De Stefani D, Raffaello A, Teardo E et al. (2011). A forty-kilodalton protein of the inner membrane is the mitochondrial calcium uniporter. *Nature* **476**: 336-340

Declercq W, Vanden Berghe T, Vandenabeele P (2009). RIP kinases at the crossroads of cell death and survival. *Cell* **138**: 229-232

Decuypere JP, Bultynck G, Parys JB (2011a). A dual role for Ca(2+) in autophagy regulation. *Cell Calcium* **50**: 242-250

Decuypere JP, Monaco G, Bultynck G et al. (2011b). The IP(3) receptor-mitochondria connection in apoptosis and autophagy. *Biochim Biophys Acta* **1813**: 1003-1013

Decuypere JP, Welkenhuyzen K, Luyten T et al. (2011c). Ins(1,4,5)P3 receptor-mediated Ca2+ signaling and autophagy induction are interrelated. *Autophagy* **7**: 1472-1489

del Peso L, Gonzalez-Garcia M, Page C et al. (1997). Interleukin-3-induced phosphorylation of BAD through the protein kinase Akt. *Science* **278**: 687-689

del Peso L, Gonzalez VM, Hernandez R et al. (1999). Regulation of the forkhead transcription factor FKHR, but not the PAX3-FKHR fusion protein, by the serine/threonine kinase Akt. *Oncogene* **18**: 7328-7333

DeLeo AB, Jay G, Appella E et al. (1979). Detection of a transformation-related antigen in chemically induced sarcomas and other transformed cells of the mouse. *Proc Natl Acad Sci U S A* **76**: 2420-2424

Deretic V (2011). Autophagy in immunity and cell-autonomous defense against intracellular microbes. *Immunol Rev* **240**: 92-104

Deretic V (2012). Autophagy: an emerging immunological paradigm. *J Immunol* **189**: 15-20

Deter RL, Baudhuin P, De Duve C (1967). Participation of lysosomes in cellular autophagy induced in rat liver by glucagon. *The Journal of cell biology* **35**: C11-16

Deter RL, De Duve C (1967). Influence of glucagon, an inducer of cellular autophagy, on some physical properties of rat liver lysosomes. *The Journal of cell biology* **33**: 437-449

Dewson G, Kluck RM (2009). Mechanisms by which Bak and Bax permeabilise mitochondria during apoptosis. *J Cell Sci* **122**: 2801-2808

Dewson G, Kratina T, Czabotar P et al. (2009). Bak activation for apoptosis involves oligomerization of dimers via their alpha6 helices. *Mol Cell* **36**: 696-703

Dewson G, Kratina T, Sim HW et al. (2008). To trigger apoptosis, Bak exposes its BH3 domain and homodimerizes via BH3:groove interactions. *Mol Cell* **30**: 369-380

DeYoung MP, Horak P, Sofer A et al. (2008). Hypoxia regulates TSC1/2-mTOR signaling and tumor suppression through REDD1-mediated 14-3-3 shuttling. *Genes Dev* **22**: 239-251

Di Bartolomeo S, Corazzari M, Nazio F et al. (2010). The dynamic interaction of AMBRA1 with the dynein motor complex regulates mammalian autophagy. *J Cell Biol* **191**: 155-168

Dickens LS, Boyd RS, Jukes-Jones R et al. (2012). A death effector domain chain DISC model reveals a crucial role for caspase-8 chain assembly in mediating apoptotic cell death. *Mol Cell* **47**: 291-305

Dikic I, Johansen T, Kirkin V (2010). Selective autophagy in cancer development and therapy. *Cancer Res* **70**: 3431-3434

Dimberg LY, Anderson CK, Camidge R et al. (2013). On the TRAIL to successful cancer therapy? Predicting and counteracting resistance against TRAIL-based therapeutics. *Oncogene* **32**: 1341-1350

Ding Q, He X, Hsu JM et al. (2007a). Degradation of Mcl-1 by beta-TrCP mediates glycogen synthase kinase 3-induced tumor suppression and chemosensitization. *Mol Cell Biol* **27**: 4006-4017

Ding Q, He X, Xia W et al. (2007b). Myeloid cell leukemia-1 inversely correlates with glycogen synthase kinase-3beta activity and associates with poor prognosis in human breast cancer. *Cancer Res* **67**: 4564-4571

Dix MM, Simon GM, Cravatt BF (2008). Global mapping of the topography and magnitude of proteolytic events in apoptosis. *Cell* **134**: 679-691

Dolmetsch RE, Lewis RS, Goodnow CC et al. (1997). Differential activation of transcription factors induced by Ca2+ response amplitude and duration. *Nature* **386**: 855-858

Dong LQ, Landa LR, Wick MJ et al. (2000). Phosphorylation of protein kinase N by phosphoinositide-dependent protein kinase-1 mediates insulin signals to the actin cytoskeleton. *Proc Natl Acad Sci U S A* **97**: 5089-5094

Dong LQ, Zhang RB, Langlais P et al. (1999). Primary structure, tissue distribution, and expression of mouse phosphoinositide-dependent protein kinase-1, a protein kinase that phosphorylates and activates protein kinase Czeta. *J Biol Chem* **274**: 8117-8122

Dorsey FC, Rose KL, Coenen S et al. (2009). Mapping the phosphorylation sites of Ulk1. *J Proteome Res* **8**: 5253-5263

Dove SK, Piper RC, McEwen RK et al. (2004). Svp1p defines a family of phosphatidylinositol 3,5-bisphosphate effectors. *EMBO J* **23**: 1922-1933

Drago I, Pizzo P, Pozzan T (2011). After half a century mitochondrial calcium in- and efflux machineries reveal themselves. *EMBO J* **30**: 4119-4125

Du H, Wolf J, Schafer B et al. (2011). BH3 domains other than Bim and Bid can directly activate Bax/Bak. *J Biol Chem* **286**: 491-501

Du K, Montminy M (1998). CREB is a regulatory target for the protein kinase Akt/PKB. *J Biol Chem* **273**: 32377-32379

Dunlop EA, Hunt DK, Acosta-Jaquez HA et al. (2011). ULK1 inhibits mTORC1 signaling, promotes multisite Raptor phosphorylation and hinders substrate binding. *Autophagy* **7**: 737-747

Duronio V (2008). The life of a cell: apoptosis regulation by the PI3K/PKB pathway. *Biochem J* **415**: 333-344

Dutil EM, Toker A, Newton AC (1998). Regulation of conventional protein kinase C isozymes by phosphoinositide-dependent kinase 1 (PDK-1). *Curr Biol* **8**: 1366-1375

E X, Hwang S, Oh S et al. (2009). Viral Bcl-2-mediated evasion of autophagy aids chronic infection of gammaherpesvirus 68. *PLoS Pathog* **5**: e1000609

Eby KG, Rosenbluth JM, Mays DJ et al. (2010). ISG20L1 is a p53 family target gene that modulates genotoxic stress-induced autophagy. *Mol Cancer* **9**: 95

Eckenrode EF, Yang J, Velmurugan GV et al. (2010). Apoptosis protection by Mcl-1 and Bcl-2 modulation of inositol 1,4,5-trisphosphate receptor-dependent Ca2+ signaling. *J Biol Chem* **285**: 13678-13684

Egan DF, Shackelford DB, Mihaylova MM et al. (2011). Phosphorylation of ULK1 (hATG1) by AMP-activated protein kinase connects energy sensing to mitophagy. *Science* **331**: 456-461

Ekert PG, Silke J, Hawkins CJ et al. (2001). DIABLO promotes apoptosis by removing MIHA/XIAP from processed caspase 9. *J Cell Biol* **152**: 483-490

Ellis HM, Horvitz HR (1986). Genetic control of programmed cell death in the nematode C. elegans. *Cell* **44**: 817-829

Elmore S (2007). Apoptosis: a review of programmed cell death. *Toxicol Pathol* **35**: 495-516

Enari M, Sakahira H, Yokoyama H et al. (1998). A caspase-activated DNase that degrades DNA during apoptosis, and its inhibitor ICAD. *Nature* **391**: 43-50

Engelke M, Engels N, Dittmann K et al. (2007). Ca(2+) signaling in antigen receptor-activated B lymphocytes. *Immunol Rev* **218**: 235-246

Engelman JA (2009). Targeting PI3K signalling in cancer: opportunities, challenges and limitations. *Nat Rev Cancer* **9**: 550-562

Engelman JA, Luo J, Cantley LC (2006). The evolution of phosphatidylinositol 3-kinases as regulators of growth and metabolism. *Nat Rev Genet* **7**: 606-619

Engels IH, Stepczynska A, Stroh C et al. (2000). Caspase-8/FLICE functions as an executioner caspase in anticancer drug-induced apoptosis. *Oncogene* **19**: 4563-4573

Erlich S, Mizrachy L, Segev O et al. (2007). Differential interactions between Beclin 1 and Bcl-2 family members. *Autophagy* **3**: 561-568

Esposito D, Sankar A, Morgner N et al. (2010). Solution NMR investigation of the CD95/FADD homotypic death domain complex suggests lack of engagement of the CD95 C terminus. *Structure* **18**: 1378-1390

Essmann F, Pohlmann S, Gillissen B et al. (2005). Irradiation-induced translocation of p53 to mitochondria in the absence of apoptosis. *J Biol Chem* **280**: 37169-37177

Fadok VA, Voelker DR, Campbell PA et al. (1992). Exposure of phosphatidylserine on the surface of apoptotic lymphocytes triggers specific recognition and removal by macrophages. *J Immunol* **148**: 2207-2216

Farnebo M, Bykov VJ, Wiman KG (2010). The p53 tumor suppressor: a master regulator of diverse cellular processes and therapeutic target in cancer. *Biochem Biophys Res Commun* **396**: 85-89

Farre JC, Subramani S (2011). Rallying the exocyst as an autophagy scaffold. *Cell* **144**: 172-174

Farrow SN, White JH, Martinou I et al. (1995). Cloning of a bcl-2 homologue by interaction with adenovirus E1B 19K. *Nature* **374**: 731-733

Fazi B, Bursch W, Fimia GM et al. (2008). Fenretinide induces autophagic cell death in caspase-defective breast cancer cells. *Autophagy* **4**: 435-441

Feldman ME, Apsel B, Uotila A et al. (2009). Active-site inhibitors of mTOR target rapamycin-resistant outputs of mTORC1 and mTORC2. *PLoS Biol* **7**: e38

Feldman RI, Wu JM, Polokoff MA et al. (2005). Novel small molecule inhibitors of 3-phosphoinositide-dependent kinase-1. *J Biol Chem* **280**: 19867-19874

Feng W, Huang S, Wu H et al. (2007a). Molecular basis of Bcl-xL's target recognition versatility revealed by the structure of Bcl-xL in complex with the BH3 domain of Beclin-1. *J Mol Biol* **372**: 223-235

Feng Z, Hu W, de Stanchina E et al. (2007b). The regulation of AMPK beta1, TSC2, and PTEN expression by p53: stress, cell and tissue specificity, and the role of these gene products in modulating the IGF-1-AKT-mTOR pathways. *Cancer Res* **67**: 3043-3053

Feoktistova M, Geserick P, Kellert B et al. (2011). cIAPs block Ripoptosome formation, a RIP1/caspase-8 containing intracellular cell death complex differentially regulated by cFLIP isoforms. *Mol Cell* **43**: 449-463

Fernandes-Alnemri T, Armstrong RC, Krebs J et al. (1996). In vitro activation of CPP32 and Mch3 by Mch4, a novel human apoptotic cysteine protease containing two FADD-like domains. *Proc Natl Acad Sci U S A* **93**: 7464-7469

Fernandes-Alnemri T, Litwack G, Alnemri ES (1994). CPP32, a novel human apoptotic protein with homology to Caenorhabditis elegans cell death protein Ced-3 and mammalian interleukin-1 beta-converting enzyme. *J Biol Chem* **269**: 30761-30764

Fimia GM, Stoykova A, Romagnoli A et al. (2007). Ambra1 regulates autophagy and development of the nervous system. *Nature* **447**: 1121-1125

Fischer U, Janicke RU, Schulze-Osthoff K (2003). Many cuts to ruin: a comprehensive update of caspase substrates. *Cell Death Differ* **10**: 76-100

Florey O, Kim SE, Sandoval CP et al. (2011). Autophagy machinery mediates macroendocytic processing and entotic cell death by targeting single membranes. *Nat Cell Biol* **13**: 1335-1343

Florey O, Overholtzer M (2012). Autophagy proteins in macroendocytic engulfment. *Trends Cell Biol* **22**: 374-380

Flynn P, Mellor H, Casamassima A et al. (2000). Rho GTPase control of protein kinase C-related protein kinase activation by 3-phosphoinositide-dependent protein kinase. *J Biol Chem* **275**: 11064-11070

Fregeau MO, Regimbald-Dumas Y, Guillemette G (2011). Positive regulation of inositol 1,4,5-trisphosphate-induced Ca2+ release by mammalian target of rapamycin (mTOR) in RINm5F cells. *J Cell Biochem* **112**: 723-733

Frias MA, Thoreen CC, Jaffe JD et al. (2006). mSin1 is necessary for Akt/PKB phosphorylation, and its isoforms define three distinct mTORC2s. *Curr Biol* **16**: 1865-1870

Fricker N, Beaudouin J, Richter P et al. (2010). Model-based dissection of CD95 signaling dynamics reveals both a pro- and antiapoptotic role of c-FLIPL. *J Cell Biol* **190**: 377-389

Frodin M, Jensen CJ, Merienne K et al. (2000). A phosphoserine-regulated docking site in the protein kinase RSK2 that recruits and activates PDK1. *EMBO J* **19**: 2924-2934

Fujioka Y, Noda NN, Fujii K et al. (2008). In vitro reconstitution of plant Atg8 and Atg12 conjugation systems essential for autophagy. *J Biol Chem* **283**: 1921-1928

Fujioka Y, Noda NN, Nakatogawa H et al. (2010). Dimeric coiled-coil structure of Saccharomyces cerevisiae Atg16 and its functional significance in autophagy. *J Biol Chem* **285**: 1508-1515

Fujita E, Jinbo A, Matuzaki H et al. (1999). Akt phosphorylation site found in human caspase-9 is absent in mouse caspase-9. *Biochem Biophys Res Commun* **264**: 550-555

Fujita N, Itoh T, Omori H et al. (2008). The Atg16L complex specifies the site of LC3 lipidation for membrane biogenesis in autophagy. *Mol Biol Cell* **19**: 2092-2100

Funakoshi T, Matsuura A, Noda T et al. (1997). Analyses of APG13 gene involved in autophagy in yeast, Saccharomyces cerevisiae. *Gene* **192**: 207-213

Funderburk SF, Wang QJ, Yue Z (2010). The Beclin 1-VPS34 complex--at the crossroads of autophagy and beyond. *Trends Cell Biol* **20**: 355-362

Fuse E, Kuwabara T, Sparreboom A et al. (2005). Review of UCN-01 development: a lesson in the importance of clinical pharmacology. *J Clin Pharmacol* **45**: 394-403

Galluzzi L, Morselli E, Kepp O et al. (2010). Defective autophagy control by the p53 rheostat in cancer. *Cell Cycle* **9**: 250-255

Galluzzi L, Vitale I, Abrams JM et al. (2012). Molecular definitions of cell death subroutines: recommendations of the Nomenclature Committee on Cell Death 2012. *Cell Death Differ* **19**: 107-120

Gammoh N, Florey O, Overholtzer M et al. (2013). Interaction between FIP200 and ATG16L1 distinguishes ULK1 complex-dependent and -independent autophagy. *Nat Struct Mol Biol* **20**: 144-149

Gammoh N, Lam D, Puente C et al. (2012). Role of autophagy in histone deacetylase inhibitor-induced apoptotic and nonapoptotic cell death. *Proc Natl Acad Sci U S A* **109**: 6561-6565

Gan B, Guan JL (2008). FIP200, a key signaling node to coordinately regulate various cellular processes. *Cellular signalling* **20**: 787-794

Gan B, Melkoumian ZK, Wu X et al. (2005). Identification of FIP200 interaction with the TSC1-TSC2 complex and its role in regulation of cell size control. *The Journal of cell biology* **170**: 379-389

Gan B, Peng X, Nagy T et al. (2006). Role of FIP200 in cardiac and liver development and its regulation of TNFalpha and TSC-mTOR signaling pathways. *The Journal of cell biology* **175**: 121-133

Ganley IG, Lam du H, Wang J et al. (2009). ULK1.ATG13.FIP200 complex mediates mTOR signaling and is essential for autophagy. *J Biol Chem* **284**: 12297-12305

Ganley IG, Wong PM, Gammoh N et al. (2011). Distinct autophagosomal-lysosomal fusion mechanism revealed by thapsigargin-induced autophagy arrest. *Mol Cell* **42**: 731-743

Gannage M, Dormann D, Albrecht R et al. (2009). Matrix protein 2 of influenza A virus blocks autophagosome fusion with lysosomes. *Cell Host Microbe* **6**: 367-380

Gao P, Bauvy C, Souquere S et al. (2010). The Bcl-2 homology domain 3 mimetic gossypol induces both Beclin 1-dependent and Beclin 1-independent cytoprotective autophagy in cancer cells. *J Biol Chem* **285**: 25570-25581

Gao W, Ding WX, Stolz DB et al. (2008). Induction of macroautophagy by exogenously introduced calcium. *Autophagy* **4**: 754-761

Gao W, Shen Z, Shang L et al. (2011). Upregulation of human autophagy-initiation kinase ULK1 by tumor suppressor p53 contributes to DNA-damage-induced cell death. *Cell Death Differ* **18**: 1598-1607

Garcia-Martinez JM, Moran J, Clarke RG et al. (2009). Ku-0063794 is a specific inhibitor of the mammalian target of rapamycin (mTOR). *Biochem J* **421**: 29-42

Gardai SJ, Hildeman DA, Frankel SK et al. (2004). Phosphorylation of Bax Ser184 by Akt regulates its activity and apoptosis in neutrophils. *J Biol Chem* **279**: 21085-21095

Gautel M (2011). Cytoskeletal protein kinases: titin and its relations in mechanosensing. *Pflugers Arch* **462**: 119-134

Gavathiotis E, Reyna DE, Bellairs JA et al. (2012). Direct and selective small-molecule activation of proapoptotic BAX. *Nat Chem Biol* **8**: 639-645

Gavathiotis E, Reyna DE, Davis ML et al. (2010). BH3-triggered structural reorganization drives the activation of proapoptotic BAX. *Mol Cell* **40**: 481-492

Gavathiotis E, Suzuki M, Davis ML et al. (2008). BAX activation is initiated at a novel interaction site. *Nature* **455**: 1076-1081

Geng J, Klionsky DJ (2008). The Atg8 and Atg12 ubiquitin-like conjugation systems in macroautophagy. 'Protein modifications: beyond the usual suspects' review series. *EMBO Rep* **9**: 859-864

Geserick P, Hupe M, Moulin M et al. (2009). Cellular IAPs inhibit a cryptic CD95-induced cell death by limiting RIP1 kinase recruitment. *The Journal of cell biology* **187**: 1037-1054

Ghislat G, Patron M, Rizzuto R et al. (2012). Withdrawal of essential amino acids increases autophagy by a pathway involving Ca2+/calmodulin-dependent kinase kinase-beta (CaMKK-beta). *J Biol Chem* **287**: 38625-38636

Gibson L, Holmgreen SP, Huang DC et al. (1996). bcl-w, a novel member of the bcl-2 family, promotes cell survival. *Oncogene* **13**: 665-675

Gincel D, Zaid H, Shoshan-Barmatz V (2001). Calcium binding and translocation by the voltage-dependent anion channel: a possible regulatory mechanism in mitochondrial function. *Biochem J* **358**: 147-155

Giorgi C, Baldassari F, Bononi A et al. (2012). Mitochondrial Ca(2+) and apoptosis. *Cell Calcium* **52**: 36-43

Gong C, Bauvy C, Tonelli G et al. (2013). Beclin 1 and autophagy are required for the tumorigenicity of breast cancer stem-like/progenitor cells. *Oncogene* **32**: 2261-2272

Gonzalez E, McGraw TE (2009). The Akt kinases: isoform specificity in metabolism and cancer. *Cell Cycle* **8**: 2502-2508

Gonzalvez F, Schug ZT, Houtkooper RH et al. (2008). Cardiolipin provides an essential activating platform for caspase-8 on mitochondria. *J Cell Biol* **183**: 681-696

Gordon PB, Holen I, Fosse M et al. (1993). Dependence of hepatocytic autophagy on intracellularly sequestered calcium. *J Biol Chem* **268**: 26107-26112

Gordy C, He YW (2012). The crosstalk between autophagy and apoptosis: where does this lead? *Protein Cell* **3**: 17-27

Gottlieb TM, Leal JF, Seger R et al. (2002). Cross-talk between Akt, p53 and Mdm2: possible implications for the regulation of apoptosis. *Oncogene* **21**: 1299-1303

Graves PR, Winkfield KM, Haystead TA (2005). Regulation of zipper-interacting protein kinase activity in vitro and in vivo by multisite phosphorylation. *J Biol Chem* **280**: 9363-9374

Gross A, Yin XM, Wang K et al. (1999). Caspase cleaved BID targets mitochondria and is required for cytochrome c release, while BCL-XL prevents this release but not tumor necrosis factor-R1/Fas death. *J Biol Chem* **274**: 1156-1163

Gu B, Zhu WG (2012). Surf the post-translational modification network of p53 regulation. *Int J Biol Sci* **8**: 672-684

Gwinn DM, Shackelford DB, Egan DF et al. (2008). AMPK phosphorylation of raptor mediates a metabolic checkpoint. *Mol Cell* **30**: 214-226

Gyrd-Hansen M, Farkas T, Fehrenbacher N et al. (2006). Apoptosome-independent activation of the lysosomal cell death pathway by caspase-9. *Mol Cell Biol* **26**: 7880-7891

Hailey DW, Rambold AS, Satpute-Krishnan P et al. (2010). Mitochondria supply membranes for autophagosome biogenesis during starvation. *Cell* **141**: 656-667

Hamasaki M, Furuta N, Matsuda A et al. (2013). Autophagosomes form at ER-mitochondria contact sites. *Nature* **495**: 389-393

Han J, Hou W, Goldstein LA et al. (2008). Involvement of protective autophagy in TRAIL resistance of apoptosis-defective tumor cells. *J Biol Chem* **283**: 19665-19677

Hanada T, Noda NN, Satomi Y et al. (2007). The Atg12-Atg5 conjugate has a novel E3-like activity for protein lipidation in autophagy. *J Biol Chem* **282**: 37298-37302

Hanahan D, Weinberg RA (2000). The hallmarks of cancer. *Cell* **100**: 57-70

Hanahan D, Weinberg RA (2011). Hallmarks of cancer: the next generation. *Cell* **144**: 646-674

Happo L, Strasser A, Cory S (2012). BH3-only proteins in apoptosis at a glance. *J Cell Sci* **125**: 1081-1087

Hara K, Maruki Y, Long X et al. (2002). Raptor, a binding partner of target of rapamycin (TOR), mediates TOR action. *Cell* **110**: 177-189

Hara T, Mizushima N (2009). Role of ULK-FIP200 complex in mammalian autophagy: FIP200, a counterpart of yeast Atg17? *Autophagy* **5**: 85-87

Hara T, Takamura A, Kishi C et al. (2008). FIP200, a ULK-interacting protein, is required for autophagosome formation in mammalian cells. *J Cell Biol* **181**: 497-510

Hardie DG (2011). AMP-activated protein kinase: an energy sensor that regulates all aspects of cell function. *Genes Dev* **25**: 1895-1908

Hardie DG, Ross FA, Hawley SA (2012a). AMP-activated protein kinase: a target for drugs both ancient and modern. *Chem Biol* **19**: 1222-1236

Hardie DG, Ross FA, Hawley SA (2012b). AMPK: a nutrient and energy sensor that maintains energy homeostasis. *Nature reviews Molecular cell biology* **13**: 251-262

Harding TM, Morano KA, Scott SV et al. (1995). Isolation and characterization of yeast mutants in the cytoplasm to vacuole protein targeting pathway. *J Cell Biol* **131**: 591-602

Harrison B, Kraus M, Burch L et al. (2008). DAPK-1 binding to a linear peptide motif in MAP1B stimulates autophagy and membrane blebbing. *J Biol Chem* **283**: 9999-10014

Haupt Y, Maya R, Kazaz A et al. (1997). Mdm2 promotes the rapid degradation of p53. *Nature* **387**: 296-299

Hawley SA, Boudeau J, Reid JL et al. (2003). Complexes between the LKB1 tumor suppressor, STRAD alpha/beta and MO25 alpha/beta are upstream kinases in the AMP-activated protein kinase cascade. *J Biol* **2**: 28

Hawley SA, Pan DA, Mustard KJ et al. (2005). Calmodulin-dependent protein kinase kinase-beta is an alternative upstream kinase for AMP-activated protein kinase. *Cell Metab* **2**: 9-19

Hayashi-Nishino M, Fujita N, Noda T et al. (2009). A subdomain of the endoplasmic reticulum forms a cradle for autophagosome formation. *Nat Cell Biol* **11**: 1433-1437

He C, Levine B (2010). The Beclin 1 interactome. *Curr Opin Cell Biol* **22**: 140-149

He H, Dang Y, Dai F et al. (2003). Post-translational modifications of three members of the human MAP1LC3 family and detection of a novel type of modification for MAP1LC3B. *J Biol Chem* **278**: 29278-29287

He Z, Mangala LS, Theriot CA et al. (2012). Cell killing and radiosensitizing effects of atorvastatin in PC3 prostate cancer cells. *J Radiat Res* **53**: 225-233

Healy JI, Dolmetsch RE, Timmerman LA et al. (1997). Different nuclear signals are activated by the B cell receptor during positive versus negative signaling. *Immunity* **6**: 419-428

Hemelaar J, Lelyveld VS, Kessler BM et al. (2003). A single protease, Apg4B, is specific for the autophagy-related ubiquitin-like proteins GATE-16, MAP1-LC3, GABARAP, and Apg8L. *J Biol Chem* **278**: 51841-51850

Henckaerts L, Cleynen I, Brinar M et al. (2011). Genetic variation in the autophagy gene ULK1 and risk of Crohn's disease. *Inflamm Bowel Dis* **17**: 1392-1397

Henderson S, Rowe M, Gregory C et al. (1991). Induction of bcl-2 expression by Epstein-Barr virus latent membrane protein 1 protects infected B cells from programmed cell death. *Cell* **65**: 1107-1115

Hengartner MO (1997). Apoptosis. CED-4 is a stranger no more. *Nature* **388**: 714-715

Hengartner MO, Ellis RE, Horvitz HR (1992). Caenorhabditis elegans gene ced-9 protects cells from programmed cell death. *Nature* **356**: 494-499

Hengartner MO, Horvitz HR (1994). C. elegans cell survival gene ced-9 encodes a functional homolog of the mammalian proto-oncogene bcl-2. *Cell* **76**: 665-676

Herrero-Martin G, Hoyer-Hansen M, Garcia-Garcia C et al. (2009). TAK1 activates AMPK-dependent cytoprotective autophagy in TRAIL-treated epithelial cells. *EMBO J* **28**: 677-685

Hers I, Vincent EE, Tavare JM (2011). Akt signalling in health and disease. *Cell Signal* **23**: 1515-1527

Hirota J, Furuichi T, Mikoshiba K (1999). Inositol 1,4,5-trisphosphate receptor type 1 is a substrate for caspase-3 and is cleaved during apoptosis in a caspase-3-dependent manner. *J Biol Chem* **274**: 34433-34437

Hockenbery D, Nunez G, Milliman C et al. (1990). Bcl-2 is an inner mitochondrial membrane protein that blocks programmed cell death. *Nature* **348**: 334-336

Honda R, Tanaka H, Yasuda H (1997). Oncoprotein MDM2 is a ubiquitin ligase E3 for tumor suppressor p53. *FEBS Lett* **420**: 25-27

Hosokawa N, Hara T, Kaizuka T et al. (2009a). Nutrient-dependent mTORC1 association with the ULK1-Atg13-FIP200 complex required for autophagy. *Mol Biol Cell* **20**: 1981-1991

Hosokawa N, Sasaki T, Iemura S et al. (2009b). Atg101, a novel mammalian autophagy protein interacting with Atg13. *Autophagy* **5**: 973-979

Hou W, Han J, Lu C et al. (2008). Enhancement of tumor-TRAIL susceptibility by modulation of autophagy. *Autophagy* **4**: 940-943

Hou W, Han J, Lu C et al. (2010). Autophagic degradation of active caspase-8: a crosstalk mechanism between autophagy and apoptosis. *Autophagy* **6**: 891-900

Hoyer-Hansen M, Bastholm L, Szyniarowski P et al. (2007). Control of macroautophagy by calcium, calmodulin-dependent kinase kinase-beta, and Bcl-2. *Mol Cell* **25**: 193-205

Hsu SY, Kaipia A, McGee E et al. (1997). Bok is a pro-apoptotic Bcl-2 protein with restricted expression in reproductive tissues and heterodimerizes with selective anti-apoptotic Bcl-2 family members. *Proc Natl Acad Sci U S A* **94**: 12401-12406

Hu Y, Benedict MA, Ding L et al. (1999). Role of cytochrome c and dATP/ATP hydrolysis in Apaf-1-mediated caspase-9 activation and apoptosis. *EMBO J* **18**: 3586-3595

Hu Y, Benedict MA, Wu D et al. (1998a). Bcl-XL interacts with Apaf-1 and inhibits Apaf-1-dependent caspase-9 activation. *Proc Natl Acad Sci U S A* **95**: 4386-4391

Hu Y, Ding L, Spencer DM et al. (1998b). WD-40 repeat region regulates Apaf-1 self-association and procaspase-9 activation. *J Biol Chem* **273**: 33489-33494

Hu Y, Yao J, Liu Z et al. (2005). Akt phosphorylates acinus and inhibits its proteolytic cleavage, preventing chromatin condensation. *EMBO J* **24**: 3543-3554

Huang Y, Park YC, Rich RL et al. (2001). Structural basis of caspase inhibition by XIAP: differential roles of the linker versus the BIR domain. *Cell* **104**: 781-790

Hudson ER, Pan DA, James J et al. (2003). A novel domain in AMP-activated protein kinase causes glycogen storage bodies similar to those seen in hereditary cardiac arrhythmias. *Current biology : CB* **13**: 861-866

Hughes MA, Harper N, Butterworth M et al. (2009). Reconstitution of the death-inducing signaling complex reveals a substrate switch that determines CD95-mediated death or survival. *Mol Cell* **35**: 265-279

Hurley RL, Anderson KA, Franzone JM et al. (2005). The Ca2+/calmodulin-dependent protein kinase kinases are AMP-activated protein kinase kinases. *J Biol Chem* **280**: 29060-29066

Ichimura Y, Kirisako T, Takao T et al. (2000). A ubiquitin-like system mediates protein lipidation. *Nature* **408**: 488-492

Ichimura Y, Kumanomidou T, Sou YS et al. (2008). Structural basis for sorting mechanism of p62 in selective autophagy. *J Biol Chem* **283**: 22847-22857

Imao T, Nagata S (2013). Apaf-1- and Caspase-8-independent apoptosis. *Cell Death Differ* **20**: 343-352

Inohara N, Ekhterae D, Garcia I et al. (1998). Mtd, a novel Bcl-2 family member activates apoptosis in the absence of heterodimerization with Bcl-2 and Bcl-XL. *J Biol Chem* **273**: 8705-8710

Inohara N, Koseki T, del Peso L et al. (1999). Nod1, an Apaf-1-like activator of caspase-9 and nuclear factor-kappaB. *J Biol Chem* **274**: 14560-14567

Inoki K, Li Y, Zhu T et al. (2002). TSC2 is phosphorylated and inhibited by Akt and suppresses mTOR signalling. *Nat Cell Biol* **4**: 648-657

Inoki K, Ouyang H, Zhu T et al. (2006). TSC2 integrates Wnt and energy signals via a coordinated phosphorylation by AMPK and GSK3 to regulate cell growth. *Cell* **126**: 955-968

Inoki K, Zhu T, Guan KL (2003). TSC2 mediates cellular energy response to control cell growth and survival. *Cell* **115**: 577-590

Irmler M, Thome M, Hahne M et al. (1997). Inhibition of death receptor signals by cellular FLIP. *Nature* **388**: 190-195

Itakura E, Kishi-Itakura C, Koyama-Honda I et al. (2012a). Structures containing Atg9A and the ULK1 complex independently target depolarized mitochondria at initial stages of Parkin-mediated mitophagy. *J Cell Sci* **125**: 1488-1499

Itakura E, Kishi-Itakura C, Mizushima N (2012b). The hairpin-type tail-anchored SNARE syntaxin 17 targets to autophagosomes for fusion with endosomes/lysosomes. *Cell* **151**: 1256-1269

Itakura E, Kishi C, Inoue K et al. (2008). Beclin 1 forms two distinct phosphatidylinositol 3-kinase complexes with mammalian Atg14 and UVRAG. *Mol Biol Cell* **19**: 5360-5372

Itakura E, Mizushima N (2009). Atg14 and UVRAG: mutually exclusive subunits of mammalian Beclin 1-PI3K complexes. *Autophagy* **5**: 534-536

Itakura E, Mizushima N (2010). Characterization of autophagosome formation site by a hierarchical analysis of mammalian Atg proteins. *Autophagy* **6**: 764-776

Itakura E, Mizushima N (2011). p62 Targeting to the autophagosome formation site requires self-oligomerization but not LC3 binding. *J Cell Biol* **192**: 17-27

Itoh N, Yonehara S, Ishii A et al. (1991). The polypeptide encoded by the cDNA for human cell surface antigen Fas can mediate apoptosis. *Cell* **66**: 233-243

Jacinto E, Facchinetti V, Liu D et al. (2006). SIN1/MIP1 maintains rictor-mTOR complex integrity and regulates Akt phosphorylation and substrate specificity. *Cell* **127**: 125-137

Jacinto E, Loewith R, Schmidt A et al. (2004). Mammalian TOR complex 2 controls the actin cytoskeleton and is rapamycin insensitive. *Nat Cell Biol* **6**: 1122-1128

James C, Gschmeissner S, Fraser A et al. (1997). CED-4 induces chromatin condensation in Schizosaccharomyces pombe and is inhibited by direct physical association with CED-9. *Curr Biol* **7**: 246-252

Janicke RU, Sohn D, Totzke G et al. (2006). Caspase-10 in mouse or not? *Science* **312**: 1874

Janssens S, Tinel A (2012). The PIDDosome, DNA-damage-induced apoptosis and beyond. *Cell Death Differ* **19**: 13-20

Jao CC, Ragusa MJ, Stanley RE et al. (2013). A HORMA domain in Atg13 mediates PI 3-kinase recruitment in autophagy. *Proc Natl Acad Sci U S A* **110**: 5486-5491

Jeffries TR, Dove SK, Michell RH et al. (2004). PtdIns-specific MPR pathway association of a novel WD40 repeat protein, WIPI49. *Mol Biol Cell* **15**: 2652-2663

Jensen CJ, Buch MB, Krag TO et al. (1999). 90-kDa ribosomal S6 kinase is phosphorylated and activated by 3-phosphoinositide-dependent protein kinase-1. *J Biol Chem* **274**: 27168-27176

Jewell JL, Russell RC, Guan KL (2013). Amino acid signalling upstream of mTOR. *Nature reviews Molecular cell biology* **14**: 133-139

Jiang S, Li Y, Zhu YH et al. (2011). Intensive expression of UNC-51-like kinase 1 is a novel biomarker of poor prognosis in patients with esophageal squamous cell carcinoma. *Cancer Sci* **102**: 1568-1575

Jin Z, Li Y, Pitti R et al. (2009). Cullin3-based polyubiquitination and p62-dependent aggregation of caspase-8 mediate extrinsic apoptosis signaling. *Cell* **137**: 721-735

Johansen T, Lamark T (2011). Selective autophagy mediated by autophagic adapter proteins. *Autophagy* **7**: 279-296

John S, Nayvelt I, Hsu HC et al. (2008). Regulation of estrogenic effects by beclin 1 in breast cancer cells. *Cancer Res* **68**: 7855-7863

Johnstone RW, Ruefli AA, Lowe SW (2002). Apoptosis: a link between cancer genetics and chemotherapy. *Cell* **108**: 153-164

Jones RG, Bui T, White C et al. (2007). The proapoptotic factors Bax and Bak regulate T Cell proliferation through control of endoplasmic reticulum Ca(2+) homeostasis. *Immunity* **27**: 268-280

Joo JH, Dorsey FC, Joshi A et al. (2011). Hsp90-Cdc37 chaperone complex regulates Ulk1- and Atg13-mediated mitophagy. *Mol Cell* **43**: 572-585

Jorgensen SB, Nielsen JN, Birk JB et al. (2004). The alpha2-5'AMP-activated protein kinase is a site 2 glycogen synthase kinase in skeletal muscle and is responsive to glucose loading. *Diabetes* **53**: 3074-3081

Jost PJ, Grabow S, Gray D et al. (2009). XIAP discriminates between type I and type II FAS-induced apoptosis. *Nature* **460**: 1035-1039

Jung CH, Jun CB, Ro SH et al. (2009). ULK-Atg13-FIP200 complexes mediate mTOR signaling to the autophagy machinery. *Mol Biol Cell* **20**: 1992-2003

Jung CH, Seo M, Otto NM et al. (2011). ULK1 inhibits the kinase activity of mTORC1 and cell proliferation. *Autophagy* **7**: 1212-1221

Kabeya Y, Kamada Y, Baba M et al. (2005). Atg17 functions in cooperation with Atg1 and Atg13 in yeast autophagy. *Mol Biol Cell* **16**: 2544-2553

Kabeya Y, Kawamata T, Suzuki K et al. (2007). Cis1/Atg31 is required for autophagosome formation in Saccharomyces cerevisiae. *Biochem Biophys Res Commun* **356**: 405-410

Kabeya Y, Mizushima N, Ueno T et al. (2000). LC3, a mammalian homologue of yeast Apg8p, is localized in autophagosome membranes after processing. *EMBO J* **19**: 5720-5728

Kabeya Y, Mizushima N, Yamamoto A et al. (2004). LC3, GABARAP and GATE16 localize to autophagosomal membrane depending on form-II formation. *J Cell Sci* **117**: 2805-2812

Kabeya Y, Noda NN, Fujioka Y et al. (2009). Characterization of the Atg17-Atg29-Atg31 complex specifically required for starvation-induced autophagy in Saccharomyces cerevisiae. *Biochem Biophys Res Commun* **389**: 612-615

Kaczmarek A, Vandenabeele P, Krysko DV (2013). Necroptosis: the release of damage-associated molecular patterns and its physiological relevance. *Immunity* **38**: 209-223

Kageyama S, Omori H, Saitoh T et al. (2011). The LC3 recruitment mechanism is separate from Atg9L1-dependent membrane formation in the autophagic response against Salmonella. *Mol Biol Cell* **22**: 2290-2300

Kaizuka T, Hara T, Oshiro N et al. (2010). Tti1 and Tel2 are critical factors in mammalian target of rapamycin complex assembly. *J Biol Chem* **285**: 20109-20116

Kamada Y, Funakoshi T, Shintani T et al. (2000). Tor-mediated induction of autophagy via an Apg1 protein kinase complex. *J Cell Biol* **150**: 1507-1513

Kamada Y, Yoshino K, Kondo C et al. (2010). Tor directly controls the Atg1 kinase complex to regulate autophagy. *Mol Cell Biol* **30**: 1049-1058

Kane LP, Shapiro VS, Stokoe D et al. (1999). Induction of NF-kappaB by the Akt/PKB kinase. *Curr Biol* **9**: 601-604

Kang HY, Shim D, Kang SS et al. (2006). Protein kinase B inhibits endostatin-induced apoptosis in HUVECs. *J Biochem Mol Biol* **39**: 97-104

Kang R, Livesey KM, Zeh HJ et al. (2010). HMGB1: a novel Beclin 1-binding protein active in autophagy. *Autophagy* **6**: 1209-1211

Kang R, Zeh HJ, Lotze MT et al. (2011). The Beclin 1 network regulates autophagy and apoptosis. *Cell Death Differ* **18**: 571-580

Kantari C, Walczak H (2011). Caspase-8 and bid: caught in the act between death receptors and mitochondria. *Biochim Biophys Acta* **1813**: 558-563

Kaufmann SH, Desnoyers S, Ottaviano Y et al. (1993). Specific proteolytic cleavage of poly(ADP-ribose) polymerase: an early marker of chemotherapy-induced apoptosis. *Cancer Res* **53**: 3976-3985

Kaufmann T, Tai L, Ekert PG et al. (2007). The BH3-only protein bid is dispensable for DNA damage- and replicative stress-induced apoptosis or cell-cycle arrest. *Cell* **129**: 423-433

Kawamata T, Kamada Y, Kabeya Y et al. (2008). Organization of the pre-autophagosomal structure responsible for autophagosome formation. *Mol Biol Cell* **19**: 2039-2050

Kawamata T, Kamada Y, Suzuki K et al. (2005). Characterization of a novel autophagy-specific gene, ATG29. *Biochem Biophys Res Commun* **338**: 1884-1889

Ke N, Godzik A, Reed JC (2001). Bcl-B, a novel Bcl-2 family member that differentially binds and regulates Bax and Bak. *J Biol Chem* **276**: 12481-12484

Kerr JF, Wyllie AH, Currie AR (1972). Apoptosis: a basic biological phenomenon with wide-ranging implications in tissue kinetics. *Br J Cancer* **26**: 239-257

Khan MT, Joseph SK (2010). Role of inositol trisphosphate receptors in autophagy in DT40 cells. *J Biol Chem* **285**: 16912-16920

Khan MT, Wagner L, 2nd, Yule DI et al. (2006). Akt kinase phosphorylation of inositol 1,4,5-trisphosphate receptors. *J Biol Chem* **281**: 3731-3737

Kiefer MC, Brauer MJ, Powers VC et al. (1995). Modulation of apoptosis by the widely distributed Bcl-2 homologue Bak. *Nature* **374**: 736-739

Kihara A, Noda T, Ishihara N et al. (2001). Two distinct Vps34 phosphatidylinositol 3-kinase complexes function in autophagy and carboxypeptidase Y sorting in Saccharomyces cerevisiae. *J Cell Biol* **152**: 519-530

Kijanska M, Dohnal I, Reiter W et al. (2010). Activation of Atg1 kinase in autophagy by regulated phosphorylation. *Autophagy* **6**: 1168-1178

Kim AH, Khursigara G, Sun X et al. (2001). Akt phosphorylates and negatively regulates apoptosis signal-regulating kinase 1. *Mol Cell Biol* **21**: 893-901

Kim DH, Sarbassov DD, Ali SM et al. (2002). mTOR interacts with raptor to form a nutrient-sensitive complex that signals to the cell growth machinery. *Cell* **110**: 163-175

Kim DH, Sarbassov DD, Ali SM et al. (2003). GbetaL, a positive regulator of the rapamycin-sensitive pathway required for the nutrient-sensitive interaction between raptor and mTOR. *Mol Cell* **11**: 895-904

Kim E, Goraksha-Hicks P, Li L et al. (2008). Regulation of TORC1 by Rag GTPases in nutrient response. *Nat Cell Biol* **10**: 935-945

Kim H, Tu HC, Ren D et al. (2009). Stepwise activation of BAX and BAK by tBID, BIM, and PUMA initiates mitochondrial apoptosis. *Mol Cell* **36**: 487-499

Kim HE, Du F, Fang M et al. (2005). Formation of apoptosome is initiated by cytochrome c-induced dATP hydrolysis and subsequent nucleotide exchange on Apaf-1. *Proc Natl Acad Sci U S A* **102**: 17545-17550

Kim J, Kundu M, Viollet B et al. (2011). AMPK and mTOR regulate autophagy through direct phosphorylation of Ulk1. *Nat Cell Biol* **13**: 132-141

Kimura S, Noda T, Yoshimori T (2007). Dissection of the autophagosome maturation process by a novel reporter protein, tandem fluorescent-tagged LC3. *Autophagy* **3**: 452-460

Kirisako T, Ichimura Y, Okada H et al. (2000). The reversible modification regulates the membrane-binding state of Apg8/Aut7 essential for autophagy and the cytoplasm to vacuole targeting pathway. *J Cell Biol* **151**: 263-276

Kirkin V, Lamark T, Sou YS et al. (2009a). A role for NBR1 in autophagosomal degradation of ubiquitinated substrates. *Mol Cell* **33**: 505-516

Kirkin V, McEwan DG, Novak I et al. (2009b). A role for ubiquitin in selective autophagy. *Mol Cell* **34**: 259-269

Kischkel FC, Hellbardt S, Behrmann I et al. (1995). Cytotoxicity-dependent APO-1 (Fas/CD95)-associated proteins form a death-inducing signaling complex (DISC) with the receptor. *EMBO J* **14**: 5579-5588

Kischkel FC, Lawrence DA, Tinel A et al. (2001). Death receptor recruitment of endogenous caspase-10 and apoptosis initiation in the absence of caspase-8. *J Biol Chem* **276**: 46639-46646

Klionsky DJ (2007). Autophagy: from phenomenology to molecular understanding in less than a decade. *Nat Rev Mol Cell Biol* **8**: 931-937

Klionsky DJ (2008). Autophagy revisited: a conversation with Christian de Duve. *Autophagy* **4**: 740-743

Klionsky DJ, Abdalla FC, Abeliovich H et al. (2012). Guidelines for the use and interpretation of assays for monitoring autophagy. *Autophagy* **8**: 445-544

Klionsky DJ, Cregg JM, Dunn WA, Jr. et al. (2003). A unified nomenclature for yeast autophagy-related genes. *Dev Cell* **5**: 539-545

Klionsky DJ, Cuervo AM, Dunn WA, Jr. et al. (2007). How shall I eat thee? *Autophagy* **3**: 413-416

Knaevelsrud H, Ahlquist T, Merok MA et al. (2010). UVRAG mutations associated with microsatellite unstable colon cancer do not affect autophagy. *Autophagy* **6**: 863-870

Kobayashi S, Yoneda-Kato N, Itahara N et al. (2013). The COP1 E3-ligase interacts with FIP200, a key regulator of mammalian autophagy. *BMC Biochem* **14**: 1

Kobayashi T, Cohen P (1999). Activation of serum- and glucocorticoid-regulated protein kinase by agonists that activate phosphatidylinositide 3-kinase is mediated by 3-phosphoinositide-dependent protein kinase-1 (PDK1) and PDK2. *Biochem J* **339 (Pt 2)**: 319-328

Kobayashi T, Deak M, Morrice N et al. (1999). Characterization of the structure and regulation of two novel isoforms of serum- and glucocorticoid-induced protein kinase. *Biochem J* **344 Pt 1**: 189-197

Kobayashi T, Suzuki K, Ohsumi Y (2012). Autophagosome formation can be achieved in the absence of Atg18 by expressing engineered PAS-targeted Atg2. *FEBS Lett* **586**: 2473-2478

Koinuma D, Shinozaki M, Nagano Y et al. (2011). RB1CC1 protein positively regulates transforming growth factor-beta signaling through the modulation of Arkadia E3 ubiquitin ligase activity. *The Journal of biological chemistry* **286**: 32502-32512

Komatsu M, Waguri S, Ueno T et al. (2005). Impairment of starvation-induced and constitutive autophagy in Atg7-deficient mice. *J Cell Biol* **169**: 425-434

Koncz G, Bodor C, Kovesdi D et al. (2002). BCR mediated signal transduction in immature and mature B cells. *Immunol Lett* **82**: 41-49

Kops GJ, de Ruiter ND, De Vries-Smits AM et al. (1999). Direct control of the Forkhead transcription factor AFX by protein kinase B. *Nature* **398**: 630-634

Koren I, Reem E, Kimchi A (2010). DAP1, a novel substrate of mTOR, negatively regulates autophagy. *Curr Biol* **20**: 1093-1098

Korolchuk VI, Menzies FM, Rubinsztein DC (2010). Mechanisms of cross-talk between the ubiquitin-proteasome and autophagy-lysosome systems. *FEBS Lett* **584**: 1393-1398

Kostura MJ, Tocci MJ, Limjuco G et al. (1989). Identification of a monocyte specific pre-interleukin 1 beta convertase activity. *Proc Natl Acad Sci U S A* **86**: 5227-5231

Kovacina KS, Park GY, Bae SS et al. (2003). Identification of a proline-rich Akt substrate as a 14-3-3 binding partner. *J Biol Chem* **278**: 10189-10194

Kozopas KM, Yang T, Buchan HL et al. (1993). MCL1, a gene expressed in programmed myeloid cell differentiation, has sequence similarity to BCL2. *Proc Natl Acad Sci U S A* **90**: 3516-3520

Kraft C, Kijanska M, Kalie E et al. (2012). Binding of the Atg1/ULK1 kinase to the ubiquitin-like protein Atg8 regulates autophagy. *EMBO J* **31**: 3691-3703

Kraft C, Peter M, Hofmann K (2010). Selective autophagy: ubiquitin-mediated recognition and beyond. *Nat Cell Biol* **12**: 836-841

Krammer PH, Arnold R, Lavrik IN (2007). Life and death in peripheral T cells. *Nat Rev Immunol* **7**: 532-542

Kress M, May E, Cassingena R et al. (1979). Simian virus 40-transformed cells express new species of proteins precipitable by anti-simian virus 40 tumor serum. *J Virol* **31**: 472-483

Krick R, Busse RA, Scacioc A et al. (2012). Structural and functional characterization of the two phosphoinositide binding sites of PROPPINs, a beta-propeller protein family. *Proc Natl Acad Sci U S A* **109**: E2042-2049

Krick R, Henke S, Tolstrup J et al. (2008). Dissecting the localization and function of Atg18, Atg21 and Ygr223c. *Autophagy* **4**: 896-910

Ku B, Woo JS, Liang C et al. (2008). Structural and biochemical bases for the inhibition of autophagy and apoptosis by viral BCL-2 of murine gamma-herpesvirus 68. *PLoS Pathog* **4**: e25

Kubbutat MH, Jones SN, Vousden KH (1997). Regulation of p53 stability by Mdm2. *Nature* **387**: 299-303

Kulikov AV, Shilov ES, Mufazalov IA et al. (2012). Cytochrome c: the Achilles' heel in apoptosis. *Cell Mol Life Sci* **69**: 1787-1797

Kuma A, Hatano M, Matsui M et al. (2004). The role of autophagy during the early neonatal starvation period. *Nature* **432**: 1032-1036

Kuma A, Mizushima N, Ishihara N et al. (2002). Formation of the approximately 350-kDa Apg12-Apg5.Apg16 multimeric complex, mediated by Apg16 oligomerization, is essential for autophagy in yeast. *J Biol Chem* **277**: 18619-18625

Kumar CC, Madison V (2005). AKT crystal structure and AKT-specific inhibitors. *Oncogene* **24**: 7493-7501

Kundu M, Lindsten T, Yang CY et al. (2008). Ulk1 plays a critical role in the autophagic clearance of mitochondria and ribosomes during reticulocyte maturation. *Blood* **112**: 1493-1502

Kunz J, Henriquez R, Schneider U et al. (1993). Target of rapamycin in yeast, TOR2, is an essential phosphatidylinositol kinase homolog required for G1 progression. *Cell* **73**: 585-596

Kuranaga E (2012). Beyond apoptosis: caspase regulatory mechanisms and functions in vivo. *Genes Cells* **17**: 83-97

Kuroyanagi H, Yan J, Seki N et al. (1998). Human ULK1, a novel serine/threonine kinase related to UNC-51 kinase of Caenorhabditis elegans: cDNA cloning, expression, and chromosomal assignment. *Genomics* **51**: 76-85

Kurtz JE, Ray-Coquard I (2012). PI3 kinase inhibitors in the clinic: an update. *Anticancer Res* **32**: 2463-2470

Kushnareva Y, Andreyev AY, Kuwana T et al. (2012). Bax activation initiates the assembly of a multimeric catalyst that facilitates Bax pore formation in mitochondrial outer membranes. *PLoS Biol* **10**: e1001394

Kuwana T, Bouchier-Hayes L, Chipuk JE et al. (2005). BH3 domains of BH3-only proteins differentially regulate Bax-mediated mitochondrial membrane permeabilization both directly and indirectly. *Mol Cell* **17**: 525-535

Kvansakul M, Yang H, Fairlie WD et al. (2008). Vaccinia virus anti-apoptotic F1L is a novel Bcl-2-like domain-swapped dimer that binds a highly selective subset of BH3-containing death ligands. *Cell Death Differ* **15**: 1564-1571

Kyei GB, Dinkins C, Davis AS et al. (2009). Autophagy pathway intersects with HIV-1 biosynthesis and regulates viral yields in macrophages. *J Cell Biol* **186**: 255-268

Lamkanfi M, Festjens N, Declercq W et al. (2007). Caspases in cell survival, proliferation and differentiation. *Cell Death Differ* **14**: 44-55

Lamkanfi M, Kalai M, Vandenabeele P (2004). Caspase-12: an overview. *Cell Death Differ* **11**: 365-368

Lane DP, Crawford LV (1979). T antigen is bound to a host protein in SV40-transformed cells. *Nature* **278**: 261-263

Lapenna S, Giordano A (2009). Cell cycle kinases as therapeutic targets for cancer. *Nat Rev Drug Discov* **8**: 547-566

Laplante M, Sabatini DM (2012). mTOR signaling in growth control and disease. *Cell* **149**: 274-293

Laussmann MA, Passante E, Dussmann H et al. (2011). Proteasome inhibition can induce an autophagy-dependent apical activation of caspase-8. *Cell Death Differ* **18**: 1584-1597

Lavrik I, Golks A, Krammer PH (2005). Death receptor signaling. *J Cell Sci* **118**: 265-267

Lavrik IN, Krammer PH (2012). Regulation of CD95/Fas signaling at the DISC. *Cell Death Differ* **19**: 36-41

Lavrik IN, Mock T, Golks A et al. (2008). CD95 stimulation results in the formation of a novel death effector domain protein-containing complex. *The Journal of biological chemistry* **283**: 26401-26408

Lazebnik YA, Kaufmann SH, Desnoyers S et al. (1994). Cleavage of poly(ADP-ribose) polymerase by a proteinase with properties like ICE. *Nature* **371**: 346-347

Le Good JA, Ziegler WH, Parekh DB et al. (1998). Protein kinase C isotypes controlled by phosphoinositide 3-kinase through the protein kinase PDK1. *Science* **281**: 2042-2045

Leber B, Geng F, Kale J et al. (2010a). Drugs targeting Bcl-2 family members as an emerging strategy in cancer. *Expert Rev Mol Med* **12**: e28

Leber B, Lin J, Andrews DW (2007). Embedded together: the life and death consequences of interaction of the Bcl-2 family with membranes. *Apoptosis* **12**: 897-911

Leber B, Lin J, Andrews DW (2010b). Still embedded together binding to membranes regulates Bcl-2 protein interactions. *Oncogene* **29**: 5221-5230

LeBien TW, Tedder TF (2008). B lymphocytes: how they develop and function. *Blood* **112**: 1570-1580

Lee EW, Seo J, Jeong M et al. (2012). The roles of FADD in extrinsic apoptosis and necroptosis. *BMB Rep* **45**: 496-508

Lee JW, Park S, Takahashi Y et al. (2010). The association of AMPK with ULK1 regulates autophagy. *PLoS One* **5**: e15394

Lee SB, Kim S, Lee J et al. (2007). ATG1, an autophagy regulator, inhibits cell growth by negatively regulating S6 kinase. *EMBO Rep* **8**: 360-365

Lemmon MA, Schlessinger J (2010). Cell signaling by receptor tyrosine kinases. *Cell* **141**: 1117-1134

Leshchiner ES, Braun CR, Bird GH et al. (2013). Direct activation of full-length proapoptotic BAK. *Proc Natl Acad Sci U S A* **110**: E986-995

Lessene G, Czabotar PE, Colman PM (2008). BCL-2 family antagonists for cancer therapy. *Nat Rev Drug Discov* **7**: 989-1000

Letai A, Bassik MC, Walensky LD et al. (2002). Distinct BH3 domains either sensitize or activate mitochondrial apoptosis, serving as prototype cancer therapeutics. *Cancer Cell* **2**: 183-192

Leu JI, Dumont P, Hafey M et al. (2004). Mitochondrial p53 activates Bak and causes disruption of a Bak-Mcl1 complex. *Nat Cell Biol* **6**: 443-450

Levine B, Kroemer G (2008). Autophagy in the pathogenesis of disease. *Cell* **132**: 27-42

Levine B, Mizushima N, Virgin HW (2011). Autophagy in immunity and inflammation. *Nature* **469**: 323-335

Li C, Fox CJ, Master SR et al. (2002). Bcl-X(L) affects Ca(2+) homeostasis by altering expression of inositol 1,4,5-trisphosphate receptors. *Proc Natl Acad Sci U S A* **99**: 9830-9835

Li C, Wang X, Vais H et al. (2007). Apoptosis regulation by Bcl-x(L) modulation of mammalian inositol 1,4,5-trisphosphate receptor channel isoform gating. *Proc Natl Acad Sci U S A* **104**: 12565-12570

Li H, Wang P, Sun Q et al. (2011a). Following cytochrome c release, autophagy is inhibited during chemotherapy-induced apoptosis by caspase 8-mediated cleavage of Beclin 1. *Cancer Res* **71**: 3625-3634

Li H, Zhu H, Xu CJ et al. (1998). Cleavage of BID by caspase 8 mediates the mitochondrial damage in the Fas pathway of apoptosis. *Cell* **94**: 491-501

Li M, Hou Y, Wang J et al. (2011b). Kinetics comparisons of mammalian Atg4 homologues indicate selective preferences toward diverse Atg8 substrates. *J Biol Chem* **286**: 7327-7338

Li P, Nijhawan D, Budihardjo I et al. (1997). Cytochrome c and dATP-dependent formation of Apaf-1/caspase-9 complex initiates an apoptotic protease cascade. *Cell* **91**: 479-489

Liang C (2010). Negative regulation of autophagy. *Cell Death Differ* **17**: 1807-1815

Liang C, E X, Jung JU (2008a). Downregulation of autophagy by herpesvirus Bcl-2 homologs. *Autophagy* **4**: 268-272

Liang C, Feng P, Ku B et al. (2006). Autophagic and tumour suppressor activity of a novel Beclin1-binding protein UVRAG. *Nat Cell Biol* **8**: 688-699

Liang C, Lee JS, Inn KS et al. (2008b). Beclin1-binding UVRAG targets the class C Vps complex to coordinate autophagosome maturation and endocytic trafficking. *Nat Cell Biol* **10**: 776-787

Liang J, Shao SH, Xu ZX et al. (2007). The energy sensing LKB1-AMPK pathway regulates p27(kip1) phosphorylation mediating the decision to enter autophagy or apoptosis. *Nat Cell Biol* **9**: 218-224

Liang XH, Kleeman LK, Jiang HH et al. (1998). Protection against fatal Sindbis virus encephalitis by beclin, a novel Bcl-2-interacting protein. *J Virol* **72**: 8586-8596

Lin EY, Orlofsky A, Berger MS et al. (1993). Characterization of A1, a novel hemopoietic-specific early-response gene with sequence similarity to bcl-2. *J Immunol* **151**: 1979-1988

Lin SY, Li TY, Liu Q et al. (2012). GSK3-TIP60-ULK1 signaling pathway links growth factor deprivation to autophagy. *Science* **336**: 477-481

Lindsley CW (2010). The Akt/PKB family of protein kinases: a review of small molecule inhibitors and progress towards target validation: a 2009 update. *Curr Top Med Chem* **10**: 458-477

Lindsten T, Ross AJ, King A et al. (2000). The combined functions of proapoptotic Bcl-2 family members bak and bax are essential for normal development of multiple tissues. *Mol Cell* **6**: 1389-1399

Linseman DA, Butts BD, Precht TA et al. (2004). Glycogen synthase kinase-3beta phosphorylates Bax and promotes its mitochondrial localization during neuronal apoptosis. *J Neurosci* **24**: 9993-10002

Linzer DI, Levine AJ (1979). Characterization of a 54K dalton cellular SV40 tumor antigen present in SV40-transformed cells and uninfected embryonal carcinoma cells. *Cell* **17**: 43-52

Lipinski MM, Hoffman G, Ng A et al. (2010). A genome-wide siRNA screen reveals multiple mTORC1 independent signaling pathways regulating autophagy under normal nutritional conditions. *Dev Cell* **18**: 1041-1052

Liu J, Xia H, Kim M et al. (2011). Beclin1 controls the levels of p53 by regulating the deubiquitination activity of USP10 and USP13. *Cell* **147**: 223-234

Liu X, Kim CN, Yang J et al. (1996). Induction of apoptotic program in cell-free extracts: requirement for dATP and cytochrome c. *Cell* **86**: 147-157

Liu X, Zou H, Slaughter C et al. (1997). DFF, a heterodimeric protein that functions downstream of caspase-3 to trigger DNA fragmentation during apoptosis. *Cell* **89**: 175-184

Liu Y, Bankaitis VA (2010). Phosphoinositide phosphatases in cell biology and disease. *Prog Lipid Res* **49**: 201-217

Livesey KM, Kang R, Vernon P et al. (2012). p53/HMGB1 complexes regulate autophagy and apoptosis. *Cancer Res* **72**: 1996-2005

Llambi F, Moldoveanu T, Tait SW et al. (2011). A unified model of mammalian BCL-2 protein family interactions at the mitochondria. *Mol Cell* **44**: 517-531

Loewith R, Jacinto E, Wullschleger S et al. (2002). Two TOR complexes, only one of which is rapamycin sensitive, have distinct roles in cell growth control. *Mol Cell* **10**: 457-468

Lomonosova E, Chinnadurai G (2008). BH3-only proteins in apoptosis and beyond: an overview. *Oncogene* **27 Suppl 1**: S2-19

Long JS, Ryan KM (2012). New frontiers in promoting tumour cell death: targeting apoptosis, necroptosis and autophagy. *Oncogene*

Longatti A, Tooze SA (2012). Recycling endosomes contribute to autophagosome formation. *Autophagy* **8**: 1682-1683

Los M, Maddika S, Erb B et al. (2009). Switching Akt: from survival signaling to deadly response. *Bioessays* **31**: 492-495

Losing M, Goldbeck I, Manno B et al. (2013). The Dok-3/Grb2 protein signal module attenuates Lyn kinase-dependent activation of Syk kinase in B cell antigen receptor microclusters. *J Biol Chem* **288**: 2303-2313

Lovell JF, Billen LP, Bindner S et al. (2008). Membrane binding by tBid initiates an ordered series of events culminating in membrane permeabilization by Bax. *Cell* **135**: 1074-1084

Luo S, Rubinsztein DC (2010). Apoptosis blocks Beclin 1-dependent autophagosome synthesis: an effect rescued by Bcl-xL. *Cell Death Differ* **17**: 268-277

Luo X, Budihardjo I, Zou H et al. (1998). Bid, a Bcl2 interacting protein, mediates cytochrome c release from mitochondria in response to activation of cell surface death receptors. *Cell* **94**: 481-490

Luthi AU, Martin SJ (2007). The CASBAH: a searchable database of caspase substrates. *Cell Death Differ* **14**: 641-650

Ma XM, Blenis J (2009). Molecular mechanisms of mTOR-mediated translational control. *Nat Rev Mol Cell Biol* **10**: 307-318

Mace PD, Riedl SJ (2010). Molecular cell death platforms and assemblies. *Curr Opin Cell Biol* **22**: 828-836

Mack HI, Zheng B, Asara JM et al. (2012). AMPK-dependent phosphorylation of ULK1 regulates ATG9 localization. *Autophagy* **8**: 1197-1214

Madeo F, Frohlich E, Frohlich KU (1997). A yeast mutant showing diagnostic markers of early and late apoptosis. *J Cell Biol* **139**: 729-734

Magnaudeix A, Wilson CM, Page G et al. (2013). PP2A blockade inhibits autophagy and causes intraneuronal accumulation of ubiquitinated proteins. *Neurobiol Aging* **34**: 770-790

Mahrus S, Trinidad JC, Barkan DT et al. (2008). Global sequencing of proteolytic cleavage sites in apoptosis by specific labeling of protein N termini. *Cell* **134**: 866-876

Maiuri MC, Criollo A, Tasdemir E et al. (2007a). BH3-only proteins and BH3 mimetics induce autophagy by competitively disrupting the interaction between Beclin 1 and Bcl-2/Bcl-X(L). *Autophagy* **3**: 374-376

Maiuri MC, Galluzzi L, Morselli E et al. (2010). Autophagy regulation by p53. *Curr Opin Cell Biol* **22**: 181-185

Maiuri MC, Le Toumelin G, Criollo A et al. (2007b). Functional and physical interaction between Bcl-X(L) and a BH3-like domain in Beclin-1. *EMBO J* **26**: 2527-2539

Maiuri MC, Malik SA, Morselli E et al. (2009a). Stimulation of autophagy by the p53 target gene Sestrin2. *Cell Cycle* **8**: 1571-1576

Maiuri MC, Tasdemir E, Criollo A et al. (2009b). Control of autophagy by oncogenes and tumor suppressor genes. *Cell Death Differ* **16**: 87-93

Majumder PK, Sellers WR (2005). Akt-regulated pathways in prostate cancer. *Oncogene* **24**: 7465-7474

Malladi S, Challa-Malladi M, Fearnhead HO et al. (2009). The Apaf-1*procaspase-9 apoptosome complex functions as a proteolytic-based molecular timer. *EMBO J* **28**: 1916-1925

Manning BD, Tee AR, Logsdon MN et al. (2002a). Identification of the tuberous sclerosis complex-2 tumor suppressor gene product tuberin as a target of the phosphoinositide 3-kinase/akt pathway. *Mol Cell* **10**: 151-162

Manning G, Whyte DB, Martinez R et al. (2002b). The protein kinase complement of the human genome. *Science* **298**: 1912-1934

Mari M, Griffith J, Rieter E et al. (2010). An Atg9-containing compartment that functions in the early steps of autophagosome biogenesis. *J Cell Biol* **190**: 1005-1022

Marino G, Salvador-Montoliu N, Fueyo A et al. (2007). Tissue-specific autophagy alterations and increased tumorigenesis in mice deficient in Atg4C/autophagin-3. *J Biol Chem* **282**: 18573-18583

Marino G, Uria JA, Puente XS et al. (2003). Human autophagins, a family of cysteine proteinases potentially implicated in cell degradation by autophagy. *J Biol Chem* **278**: 3671-3678

Martin-Castellanos C, Blanco M, Rozalen AE et al. (2005). A large-scale screen in S. pombe identifies seven novel genes required for critical meiotic events. *Curr Biol* **15**: 2056-2062

Martin MC, Allan LA, Mancini EJ et al. (2008). The docking interaction of caspase-9 with ERK2 provides a mechanism for the selective inhibitory phosphorylation of caspase-9 at threonine 125. *J Biol Chem* **283**: 3854-3865

Martinez J, Almendinger J, Oberst A et al. (2011). Microtubule-associated protein 1 light chain 3 alpha (LC3)-associated phagocytosis is required for the efficient clearance of dead cells. *Proc Natl Acad Sci U S A* **108**: 17396-17401

Masters SC, Yang H, Datta SR et al. (2001). 14-3-3 inhibits Bad-induced cell death through interaction with serine-136. *Mol Pharmacol* **60**: 1325-1331

Matsui Y, Takagi H, Qu X et al. (2007). Distinct roles of autophagy in the heart during ischemia and reperfusion: roles of AMP-activated protein kinase and Beclin 1 in mediating autophagy. *Circ Res* **100**: 914-922

Matsumoto G, Wada K, Okuno M et al. (2011). Serine 403 phosphorylation of p62/SQSTM1 regulates selective autophagic clearance of ubiquitinated proteins. *Mol Cell* **44**: 279-289

Matsunaga K, Morita E, Saitoh T et al. (2010). Autophagy requires endoplasmic reticulum targeting of the PI3-kinase complex via Atg14L. *J Cell Biol* **190**: 511-521

Matsunaga K, Noda T, Yoshimori T (2009a). Binding Rubicon to cross the Rubicon. *Autophagy* **5**: 876-877

Matsunaga K, Saitoh T, Tabata K et al. (2009b). Two Beclin 1-binding proteins, Atg14L and Rubicon, reciprocally regulate autophagy at different stages. *Nat Cell Biol* **11**: 385-396

Matsuura A, Tsukada M, Wada Y et al. (1997). Apg1p, a novel protein kinase required for the autophagic process in Saccharomyces cerevisiae. *Gene* **192**: 245-250

Matthess Y, Raab M, Sanhaji M et al. (2010). Cdk1/cyclin B1 controls Fas-mediated apoptosis by regulating caspase-8 activity. *Mol Cell Biol* **30**: 5726-5740

Mattmann ME, Stoops SL, Lindsley CW (2011). Inhibition of Akt with small molecules and biologics: historical perspective and current status of the patent landscape. *Expert Opin Ther Pat* **21**: 1309-1338

Maucuer A, Camonis JH, Sobel A (1995). Stathmin interaction with a putative kinase and coiled-coil-forming protein domains. *Proceedings of the National Academy of Sciences of the United States of America* **92**: 3100-3104

Maurer U, Charvet C, Wagman AS et al. (2006). Glycogen synthase kinase-3 regulates mitochondrial outer membrane permeabilization and apoptosis by destabilization of MCL-1. *Mol Cell* **21**: 749-760

Mauthe M, Jacob A, Freiberger S et al. (2011). Resveratrol-mediated autophagy requires WIPI-1-regulated LC3 lipidation in the absence of induced phagophore formation. *Autophagy* **7**: 1448-1461

Mayo LD, Donner DB (2001). A phosphatidylinositol 3-kinase/Akt pathway promotes translocation of Mdm2 from the cytoplasm to the nucleus. *Proc Natl Acad Sci U S A* **98**: 11598-11603

McAlpine F, Williamson LE, Tooze SA et al. (2013). Regulation of nutrient-sensitive autophagy by uncoordinated 51-like kinases 1 and 2. *Autophagy* **9**: 361-373

McBride A, Ghilagaber S, Nikolaev A et al. (2009). The glycogen-binding domain on the AMPK beta subunit allows the kinase to act as a glycogen sensor. *Cell Metab* **9**: 23-34

McDonnell MA, Wang D, Khan SM et al. (2003). Caspase-9 is activated in a cytochrome c-independent manner early during TNFalpha-induced apoptosis in murine cells. *Cell Death Differ* **10**: 1005-1015

McDonnell TJ, Deane N, Platt FM et al. (1989). bcl-2-immunoglobulin transgenic mice demonstrate extended B cell survival and follicular lymphoproliferation. *Cell* **57**: 79-88

McIlwain DR, Berger T, Mak TW (2013). Caspase functions in cell death and disease. *Cold Spring Harb Perspect Med* **3**: a008656

Medema JP, Scaffidi C, Kischkel FC et al. (1997). FLICE is activated by association with the CD95 death-inducing signaling complex (DISC). *EMBO J* **16**: 2794-2804

Meijer WH, van der Klei IJ, Veenhuis M et al. (2007). ATG genes involved in non-selective autophagy are conserved from yeast to man, but the selective Cvt and pexophagy pathways also require organism-specific genes. *Autophagy* **3**: 106-116

Meiselbach H, Sticht H, Enz R (2006). Structural analysis of the protein phosphatase 1 docking motif: molecular description of binding specificities identifies interacting proteins. *Chemistry & biology* **13**: 49-59

Melero JA, Stitt DT, Mangel WF et al. (1979). Identification of new polypeptide species (48-55K) immunoprecipitable by antiserum to purified large T antigen and present in SV40-infected and -transformed cells. *Virology* **93**: 466-480

Meley D, Bauvy C, Houben-Weerts JH et al. (2006). AMP-activated protein kinase and the regulation of autophagic proteolysis. *J Biol Chem* **281**: 34870-34879

Melkoumian ZK, Peng X, Gan B et al. (2005). Mechanism of cell cycle regulation by FIP200 in human breast cancer cells. *Cancer research* **65**: 6676-6684

Mercer CA, Kaliappan A, Dennis PB (2009). A novel, human Atg13 binding protein, Atg101, interacts with ULK1 and is essential for macroautophagy. *Autophagy* **5**: 649-662

Merino D, Giam M, Hughes PD et al. (2009). The role of BH3-only protein Bim extends beyond inhibiting Bcl-2-like prosurvival proteins. *J Cell Biol* **186**: 355-362

Miao B, Skidan I, Yang J et al. (2010). Small molecule inhibition of phosphatidylinositol-3,4,5-triphosphate (PIP3) binding to pleckstrin homology domains. *Proc Natl Acad Sci U S A* **107**: 20126-20131

Micheau O, Tschopp J (2003). Induction of TNF receptor I-mediated apoptosis via two sequential signaling complexes. *Cell* **114**: 181-190

Michell RH, Heath VL, Lemmon MA et al. (2006). Phosphatidylinositol 3,5-bisphosphate: metabolism and cellular functions. *Trends Biochem Sci* **31**: 52-63

Michiorri S, Gelmetti V, Giarda E et al. (2010). The Parkinson-associated protein PINK1 interacts with Beclin1 and promotes autophagy. *Cell Death Differ* **17**: 962-974

Miura M, Zhu H, Rotello R et al. (1993). Induction of apoptosis in fibroblasts by IL-1 beta-converting enzyme, a mammalian homolog of the C. elegans cell death gene ced-3. *Cell* **75**: 653-660

Mizushima N (2007). Autophagy: process and function. *Genes Dev* **21**: 2861-2873

Mizushima N (2010). The role of the Atg1/ULK1 complex in autophagy regulation. *Curr Opin Cell Biol* **22**: 132-139

Mizushima N, Kuma A, Kobayashi Y et al. (2003). Mouse Apg16L, a novel WD-repeat protein, targets to the autophagic isolation membrane with the Apg12-Apg5 conjugate. *J Cell Sci* **116**: 1679-1688

Mizushima N, Levine B, Cuervo AM et al. (2008). Autophagy fights disease through cellular self-digestion. *Nature* **451**: 1069-1075

Mizushima N, Noda T, Ohsumi Y (1999). Apg16p is required for the function of the Apg12p-Apg5p conjugate in the yeast autophagy pathway. *EMBO J* **18**: 3888-3896

Mizushima N, Noda T, Yoshimori T et al. (1998a). A protein conjugation system essential for autophagy. *Nature* **395**: 395-398

Mizushima N, Sugita H, Yoshimori T et al. (1998b). A new protein conjugation system in human. The counterpart of the yeast Apg12p conjugation system essential for autophagy. *J Biol Chem* **273**: 33889-33892

Mizushima N, Yamamoto A, Hatano M et al. (2001). Dissection of autophagosome formation using Apg5-deficient mouse embryonic stem cells. *J Cell Biol* **152**: 657-668

Mizushima N, Yoshimori T, Levine B (2010). Methods in mammalian autophagy research. *Cell* **140**: 313-326

Mizushima N, Yoshimori T, Ohsumi Y (2002). Mouse Apg10 as an Apg12-conjugating enzyme: analysis by the conjugation-mediated yeast two-hybrid method. *FEBS Lett* **532**: 450-454

Mizushima N, Yoshimori T, Ohsumi Y (2011). The role of Atg proteins in autophagosome formation. *Annu Rev Cell Dev Biol* **27**: 107-132

Moldoveanu T, Grace CR, Llambi F et al. (2013). BID-induced structural changes in BAK promote apoptosis. *Nat Struct Mol Biol* **20**: 589-597

Momcilovic M, Hong SP, Carlson M (2006). Mammalian TAK1 activates Snf1 protein kinase in yeast and phosphorylates AMP-activated protein kinase in vitro. *J Biol Chem* **281**: 25336-25343

Monaco G, Decrock E, Akl H et al. (2012). Selective regulation of IP3-receptor-mediated Ca2+ signaling and apoptosis by the BH4 domain of Bcl-2 versus Bcl-Xl. *Cell Death Differ* **19**: 295-309

Monaco G, Vervliet T, Akl H et al. (2013). The selective BH4-domain biology of Bcl-2-family members: IP3Rs and beyond. *Cell Mol Life Sci* **70**: 1171-1183

Mora A, Komander D, van Aalten DM et al. (2004). PDK1, the master regulator of AGC kinase signal transduction. *Semin Cell Dev Biol* **15**: 161-170

Morgan AR, Lam WJ, Han DY et al. (2012). Association Analysis of ULK1 with Crohn's Disease in a New Zealand Population. *Gastroenterol Res Pract* **2012**: 715309

Moriishi K, Huang DC, Cory S et al. (1999). Bcl-2 family members do not inhibit apoptosis by binding the caspase activator Apaf-1. *Proc Natl Acad Sci U S A* **96**: 9683-9688

Morishima N, Nakanishi K, Takenouchi H et al. (2002). An endoplasmic reticulum stress-specific caspase cascade in apoptosis. Cytochrome c-independent activation of caspase-9 by caspase-12. *J Biol Chem* **277**: 34287-34294

Morselli E, Shen S, Ruckenstuhl C et al. (2011). p53 inhibits autophagy by interacting with the human ortholog of yeast Atg17, RB1CC1/FIP200. *Cell Cycle* **10**: 2763-2769

Morselli E, Tasdemir E, Maiuri MC et al. (2008). Mutant p53 protein localized in the cytoplasm inhibits autophagy. *Cell Cycle* **7**: 3056-3061

Motley AM, Nuttall JM, Hettema EH (2012). Pex3-anchored Atg36 tags peroxisomes for degradation in Saccharomyces cerevisiae. *EMBO J* **31**: 2852-2868

Muchmore SW, Sattler M, Liang H et al. (1996). X-ray and NMR structure of human Bcl-xL, an inhibitor of programmed cell death. *Nature* **381**: 335-341

Mukaiyama H, Oku M, Baba M et al. (2002). Paz2 and 13 other PAZ gene products regulate vacuolar engulfment of peroxisomes during micropexophagy. *Genes Cells* **7**: 75-90

Muller PA, Vousden KH (2013). p53 mutations in cancer. *Nat Cell Biol* **15**: 2-8

Muzio M, Chinnaiyan AM, Kischkel FC et al. (1996). FLICE, a novel FADD-homologous ICE/CED-3-like protease, is recruited to the CD95 (Fas/APO-1) death--inducing signaling complex. *Cell* **85**: 817-827

Nagasaka A, Kawane K, Yoshida H et al. (2010). Apaf-1-independent programmed cell death in mouse development. *Cell Death Differ* **17**: 931-941

Nagata S, Hanayama R, Kawane K (2010). Autoimmunity and the clearance of dead cells. *Cell* **140**: 619-630

Naidu SR, Lakhter AJ, Androphy EJ (2012). PIASy-mediated Tip60 sumoylation regulates p53-induced autophagy. *Cell Cycle* **11**: 2717-2728

Nair U, Cao Y, Xie Z et al. (2010). Roles of the lipid-binding motifs of Atg18 and Atg21 in the cytoplasm to vacuole targeting pathway and autophagy. *J Biol Chem* **285**: 11476-11488

Najafov A, Shpiro N, Alessi DR (2012). Akt is efficiently activated by PIF-pocket- and PtdIns(3,4,5)P3-dependent mechanisms leading to resistance to PDK1 inhibitors. *Biochem J* **448**: 285-295

Nakatogawa H, Ichimura Y, Ohsumi Y (2007). Atg8, a ubiquitin-like protein required for autophagosome formation, mediates membrane tethering and hemifusion. *Cell* **130**: 165-178

Nakatogawa H, Ohbayashi S, Sakoh-Nakatogawa M et al. (2012). The autophagy-related protein kinase Atg1 interacts with the ubiquitin-like protein Atg8 via the Atg8 family interacting motif to facilitate autophagosome formation. *J Biol Chem* **287**: 28503-28507

Nave BT, Ouwens M, Withers DJ et al. (1999). Mammalian target of rapamycin is a direct target for protein kinase B: identification of a convergence point for opposing effects of insulin and amino-acid deficiency on protein translation. *Biochem J* **344 Pt 2**: 427-431

Nazio F, Strappazzon F, Antonioli M et al. (2013). mTOR inhibits autophagy by controlling ULK1 ubiquitylation, self-association and function through AMBRA1 and TRAF6. *Nat Cell Biol* **15**: 406-416

Neumann K, Oellerich T, Urlaub H et al. (2009). The B-lymphoid Grb2 interaction code. *Immunol Rev* **232**: 135-149

Ng CH, Xu S, Lam KP (2007). Dok-3 plays a nonredundant role in negative regulation of B-cell activation. *Blood* **110**: 259-266

Nguyen HT, Lapaquette P, Bringer MA et al. (2013). Autophagy and Crohn's Disease. *J Innate Immun*

Nicholson DW, Ali A, Thornberry NA et al. (1995). Identification and inhibition of the ICE/CED-3 protease necessary for mammalian apoptosis. *Nature* **376**: 37-43

Nicoletti I, Migliorati G, Pagliacci MC et al. (1991). A rapid and simple method for measuring thymocyte apoptosis by propidium iodide staining and flow cytometry. *J Immunol Methods* **139**: 271-279

Nikolaev A, McLaughlin T, O'Leary DD et al. (2009). APP binds DR6 to trigger axon pruning and neuron death via distinct caspases. *Nature* **457**: 981-989

Nishida Y, Arakawa S, Fujitani K et al. (2009). Discovery of Atg5/Atg7-independent alternative macroautophagy. *Nature* **461**: 654-658

Nishimura T, Kaizuka T, Cadwell K et al. (2013). FIP200 regulates targeting of Atg16L1 to the isolation membrane. *EMBO Rep* **14**: 284-291

Niu TK, Cheng Y, Ren X et al. (2010). Interaction of Beclin 1 with survivin regulates sensitivity of human glioma cells to TRAIL-induced apoptosis. *FEBS Lett* **584**: 3519-3524

Noble CG, Dong JM, Manser E et al. (2008). Bcl-xL and UVRAG cause a monomer-dimer switch in Beclin1. *J Biol Chem* **283**: 26274-26282

Noda NN, Fujioka Y, Hanada T et al. (2013). Structure of the Atg12-Atg5 conjugate reveals a platform for stimulating Atg8-PE conjugation. *EMBO Rep* **14**: 206-211

Noda NN, Ohsumi Y, Inagaki F (2010). Atg8-family interacting motif crucial for selective autophagy. *FEBS Lett* **584**: 1379-1385

Noda T, Kageyama S, Fujita N et al. (2012). Three-Axis Model for Atg Recruitment in Autophagy against Salmonella. *Int J Cell Biol* **2012**: 389562

Noda T, Ohsumi Y (1998). Tor, a phosphatidylinositol kinase homologue, controls autophagy in yeast. *J Biol Chem* **273**: 3963-3966

Nogueira V, Park Y, Chen CC et al. (2008). Akt determines replicative senescence and oxidative or oncogenic premature senescence and sensitizes cells to oxidative apoptosis. *Cancer Cell* **14**: 458-470

Norman JM, Cohen GM, Bampton ET (2010). The in vitro cleavage of the hAtg proteins by cell death proteases. *Autophagy* **6**: 1042-1056

Novak I (2012). Mitophagy: a complex mechanism of mitochondrial removal. *Antioxid Redox Signal* **17**: 794-802

Novak I, Kirkin V, McEwan DG et al. (2010). Nix is a selective autophagy receptor for mitochondrial clearance. *EMBO Rep* **11**: 45-51

Novikoff AB, Essner E (1962). Cytolysomes and mitochondrial degeneration. *J Cell Biol* **15**: 140-146

Nunez G, London L, Hockenbery D et al. (1990). Deregulated Bcl-2 gene expression selectively prolongs survival of growth factor-deprived hemopoietic cell lines. *J Immunol* **144**: 3602-3610

Oakes SA, Scorrano L, Opferman JT et al. (2005). Proapoptotic BAX and BAK regulate the type 1 inositol trisphosphate receptor and calcium leak from the endoplasmic reticulum. *Proc Natl Acad Sci U S A* **102**: 105-110

Obara K, Ohsumi Y (2011). PtdIns 3-Kinase Orchestrates Autophagosome Formation in Yeast. *J Lipids* **2011**: 498768

Obara K, Sekito T, Niimi K et al. (2008). The Atg18-Atg2 complex is recruited to autophagic membranes via phosphatidylinositol 3-phosphate and exerts an essential function. *J Biol Chem* **283**: 23972-23980

Obara K, Sekito T, Ohsumi Y (2006). Assortment of phosphatidylinositol 3-kinase complexes--Atg14p directs association of complex I to the pre-autophagosomal structure in Saccharomyces cerevisiae. *Mol Biol Cell* **17**: 1527-1539

Obata T, Yaffe MB, Leparc GG et al. (2000). Peptide and protein library screening defines optimal substrate motifs for AKT/PKB. *J Biol Chem* **275**: 36108-36115

Oberst A, Pop C, Tremblay AG et al. (2010). Inducible dimerization and inducible cleavage reveal a requirement for both processes in caspase-8 activation. *J Biol Chem* **285**: 16632-16642

Oberstein A, Jeffrey PD, Shi Y (2007). Crystal structure of the Bcl-XL-Beclin 1 peptide complex: Beclin 1 is a novel BH3-only protein. *J Biol Chem* **282**: 13123-13132

Ochi Y, Chano T, Ikebuchi K et al. (2011). RB1CC1 activates the p16 promoter through the interaction with hSNF5. *Oncol Rep* **26**: 805-812

Oehm A, Behrmann I, Falk W et al. (1992). Purification and molecular cloning of the APO-1 cell surface antigen, a member of the tumor necrosis factor/nerve growth factor receptor superfamily. Sequence identity with the Fas antigen. *J Biol Chem* **267**: 10709-10715

Ogawa M, Yoshikawa Y, Kobayashi T et al. (2011). A Tecpr1-dependent selective autophagy pathway targets bacterial pathogens. *Cell Host Microbe* **9**: 376-389

Ogura K, Okada T, Mitani S et al. (2010). Protein phosphatase 2A cooperates with the autophagy-related kinase UNC-51 to regulate axon guidance in Caenorhabditis elegans. *Development* **137**: 1657-1667

Okazaki N, Yan J, Yuasa S et al. (2000). Interaction of the Unc-51-like kinase and microtubule-associated protein light chain 3 related proteins in the brain: possible role of vesicular transport in axonal elongation. *Brain Res Mol Brain Res* **85**: 1-12

Oltersdorf T, Elmore SW, Shoemaker AR et al. (2005). An inhibitor of Bcl-2 family proteins induces regression of solid tumours. *Nature* **435**: 677-681

Oltvai ZN, Milliman CL, Korsmeyer SJ (1993). Bcl-2 heterodimerizes in vivo with a conserved homolog, Bax, that accelerates programmed cell death. *Cell* **74**: 609-619

Oral O, Oz-Arslan D, Itah Z et al. (2012). Cleavage of Atg3 protein by caspase-8 regulates autophagy during receptor-activated cell death. *Apoptosis* **17**: 810-820

Orsi A, Razi M, Dooley HC et al. (2012). Dynamic and transient interactions of Atg9 with autophagosomes, but not membrane integration, are required for autophagy. *Mol Biol Cell* **23**: 1860-1873

Orvedahl A, Alexander D, Talloczy Z et al. (2007). HSV-1 ICP34.5 confers neurovirulence by targeting the Beclin 1 autophagy protein. *Cell Host Microbe* **1**: 23-35

Ozes ON, Mayo LD, Gustin JA et al. (1999). NF-kappaB activation by tumour necrosis factor requires the Akt serine-threonine kinase. *Nature* **401**: 82-85

Pal SK, Reckamp K, Yu H et al. (2010). Akt inhibitors in clinical development for the treatment of cancer. *Expert Opin Investig Drugs* **19**: 1355-1366

Palty R, Silverman WF, Hershfinkel M et al. (2010). NCLX is an essential component of mitochondrial Na+/Ca2+ exchange. *Proc Natl Acad Sci U S A* **107**: 436-441

Pan G, O'Rourke K, Dixit VM (1998). Caspase-9, Bcl-XL, and Apaf-1 form a ternary complex. *J Biol Chem* **273**: 5841-5845

Pankiv S, Clausen TH, Lamark T et al. (2007). p62/SQSTM1 binds directly to Atg8/LC3 to facilitate degradation of ubiquitinated protein aggregates by autophagy. *J Biol Chem* **282**: 24131-24145

Parcellier A, Tintignac LA, Zhuravleva E et al. (2008). PKB and the mitochondria: AKTing on apoptosis. *Cell Signal* **20**: 21-30

Park HS, Kim MS, Huh SH et al. (2002). Akt (protein kinase B) negatively regulates SEK1 by means of protein phosphorylation. *J Biol Chem* **277**: 2573-2578

Park J, Leong ML, Buse P et al. (1999). Serum and glucocorticoid-inducible kinase (SGK) is a target of the PI 3-kinase-stimulated signaling pathway. *EMBO J* **18**: 3024-3033

Pattingre S, Tassa A, Qu X et al. (2005). Bcl-2 antiapoptotic proteins inhibit Beclin 1-dependent autophagy. *Cell* **122**: 927-939

Paz Y, Elazar Z, Fass D (2000). Structure of GATE-16, membrane transport modulator and mammalian ortholog of autophagocytosis factor Aut7p. *J Biol Chem* **275**: 25445-25450

Pearce LR, Huang X, Boudeau J et al. (2007). Identification of Protor as a novel Rictor-binding component of mTOR complex-2. *Biochem J* **405**: 513-522

Pearce LR, Komander D, Alessi DR (2010). The nuts and bolts of AGC protein kinases. *Nat Rev Mol Cell Biol* **11**: 9-22

Pegoraro L, Palumbo A, Erikson J et al. (1984). A 14;18 and an 8;14 chromosome translocation in a cell line derived from an acute B-cell leukemia. *Proc Natl Acad Sci U S A* **81**: 7166-7170

Perocchi F, Gohil VM, Girgis HS et al. (2010). MICU1 encodes a mitochondrial EF hand protein required for Ca(2+) uptake. *Nature* **467**: 291-296

Peterson TR, Laplante M, Thoreen CC et al. (2009). DEPTOR is an mTOR inhibitor frequently overexpressed in multiple myeloma cells and required for their survival. *Cell* **137**: 873-886

Pfeuffer T, Goebel W, Laubinger J et al. (2000). LaXp180, a mammalian ActA-binding protein, identified with the yeast two-hybrid system, co-localizes with intracellular Listeria monocytogenes. *Cell Microbiol* **2**: 101-114

Pike LR, Singleton DC, Buffa F et al. (2013). Transcriptional up-regulation of ULK1 by ATF4 contributes to cancer cell survival. *Biochem J* **449**: 389-400

Pogue SL, Kurosaki T, Bolen J et al. (2000). B cell antigen receptor-induced activation of Akt promotes B cell survival and is dependent on Syk kinase. *J Immunol* **165**: 1300-1306

Polekhina G, Gupta A, Michell BJ et al. (2003). AMPK beta subunit targets metabolic stress sensing to glycogen. *Current biology : CB* **13**: 867-871

Polson HE, de Lartigue J, Rigden DJ et al. (2010). Mammalian Atg18 (WIPI2) localizes to omegasome-anchored phagophores and positively regulates LC3 lipidation. *Autophagy* **6**

Pop C, Salvesen GS (2009). Human caspases: activation, specificity, and regulation. *J Biol Chem* **284**: 21777-21781

Pop C, Timmer J, Sperandio S et al. (2006). The apoptosome activates caspase-9 by dimerization. *Mol Cell* **22**: 269-275

Potter CJ, Pedraza LG, Xu T (2002). Akt regulates growth by directly phosphorylating Tsc2. *Nat Cell Biol* **4**: 658-665

Proikas-Cezanne T, Waddell S, Gaugel A et al. (2004). WIPI-1alpha (WIPI49), a member of the novel 7-bladed WIPI protein family, is aberrantly expressed in human cancer and is linked to starvation-induced autophagy. *Oncogene* **23**: 9314-9325

Ptacek J, Devgan G, Michaud G et al. (2005). Global analysis of protein phosphorylation in yeast. *Nature* **438**: 679-684

Pullen N, Dennis PB, Andjelkovic M et al. (1998). Phosphorylation and activation of p70s6k by PDK1. *Science* **279**: 707-710

Qi XJ, Wildey GM, Howe PH (2006). Evidence that Ser87 of BimEL is phosphorylated by Akt and regulates BimEL apoptotic function. *J Biol Chem* **281**: 813-823

Qin H, Srinivasula SM, Wu G et al. (1999). Structural basis of procaspase-9 recruitment by the apoptotic protease-activating factor 1. *Nature* **399**: 549-557

Qu X, Yu J, Bhagat G et al. (2003). Promotion of tumorigenesis by heterozygous disruption of the beclin 1 autophagy gene. *J Clin Invest* **112**: 1809-1820

Ragusa MJ, Stanley RE, Hurley JH (2012). Architecture of the Atg17 complex as a scaffold for autophagosome biogenesis. *Cell* **151**: 1501-1512

Ravichandran KS (2011). Beginnings of a good apoptotic meal: the find-me and eat-me signaling pathways. *Immunity* **35**: 445-455

Ravikumar B, Imarisio S, Sarkar S et al. (2008). Rab5 modulates aggregation and toxicity of mutant huntingtin through macroautophagy in cell and fly models of Huntington disease. *J Cell Sci* **121**: 1649-1660

Ravikumar B, Sarkar S, Davies JE et al. (2010). Regulation of mammalian autophagy in physiology and pathophysiology. *Physiological reviews* **90**: 1383-1435

Read SH, Baliga BC, Ekert PG et al. (2002). A novel Apaf-1-independent putative caspase-2 activation complex. *J Cell Biol* **159**: 739-745

Reggiori F, Komatsu M, Finley K et al. (2012). Selective types of autophagy. *International journal of cell biology* **2012**: 156272

Reggiori F, Tucker KA, Stromhaug PE et al. (2004). The Atg1-Atg13 complex regulates Atg9 and Atg23 retrieval transport from the pre-autophagosomal structure. *Dev Cell* **6**: 79-90

Regimbald-Dumas Y, Fregeau MO, Guillemette G (2011). Mammalian target of rapamycin (mTOR) phosphorylates inositol 1,4,5-trisphosphate receptor type 2 and increases its Ca(2+) release activity. *Cell Signal* **23**: 71-79

Reiling JH, Hafen E (2004). The hypoxia-induced paralogs Scylla and Charybdis inhibit growth by down-regulating S6K activity upstream of TSC in Drosophila. *Genes Dev* **18**: 2879-2892

Rena G, Guo S, Cichy SC et al. (1999). Phosphorylation of the transcription factor forkhead family member FKHR by protein kinase B. *J Biol Chem* **274**: 17179-17183

Renatus M, Stennicke HR, Scott FL et al. (2001). Dimer formation drives the activation of the cell death protease caspase 9. *Proc Natl Acad Sci U S A* **98**: 14250-14255

Reubold TF, Eschenburg S (2012). A molecular view on signal transduction by the apoptosome. *Cell Signal* **24**: 1420-1425

Reubold TF, Wohlgemuth S, Eschenburg S (2009). A new model for the transition of APAF-1 from inactive monomer to caspase-activating apoptosome. *J Biol Chem* **284**: 32717-32724

Reubold TF, Wohlgemuth S, Eschenburg S (2011). Crystal structure of full-length Apaf-1: how the death signal is relayed in the mitochondrial pathway of apoptosis. *Structure* **19**: 1074-1083

Richards SA, Fu J, Romanelli A et al. (1999). Ribosomal S6 kinase 1 (RSK1) activation requires signals dependent on and independent of the MAP kinase ERK. *Curr Biol* **9**: 810-820

Riedl SJ, Li W, Chao Y et al. (2005). Structure of the apoptotic protease-activating factor 1 bound to ADP. *Nature* **434**: 926-933

Riedl SJ, Renatus M, Schwarzenbacher R et al. (2001). Structural basis for the inhibition of caspase-3 by XIAP. *Cell* **104**: 791-800

Rodriguez J, Lazebnik Y (1999). Caspase-9 and APAF-1 form an active holoenzyme. *Genes Dev* **13**: 3179-3184

Rodriguez OC, Choudhury S, Kolukula V et al. (2012). Dietary downregulation of mutant p53 levels via glucose restriction: mechanisms and implications for tumor therapy. *Cell Cycle* **11**: 4436-4446

Rohn TT, Wirawan E, Brown RJ et al. (2011). Depletion of Beclin-1 due to proteolytic cleavage by caspases in the Alzheimer's disease brain. *Neurobiol Dis* **43**: 68-78

Romashkova JA, Makarov SS (1999). NF-kappaB is a target of AKT in anti-apoptotic PDGF signalling. *Nature* **401**: 86-90

Rong YP, Aromolaran AS, Bultynck G et al. (2008). Targeting Bcl-2-IP3 receptor interaction to reverse Bcl-2's inhibition of apoptotic calcium signals. *Mol Cell* **31**: 255-265

Rong YP, Bultynck G, Aromolaran AS et al. (2009). The BH4 domain of Bcl-2 inhibits ER calcium release and apoptosis by binding the regulatory and coupling domain of the IP3 receptor. *Proc Natl Acad Sci U S A* **106**: 14397-14402

Ropolo A, Grasso D, Pardo R et al. (2007). The pancreatitis-induced vacuole membrane protein 1 triggers autophagy in mammalian cells. *J Biol Chem* **282**: 37124-37133

Rosenfeldt MT, Ryan KM (2009). The role of autophagy in tumour development and cancer therapy. *Expert Rev Mol Med* **11**: e36

Russo R, Berliocchi L, Adornetto A et al. (2011). Calpain-mediated cleavage of Beclin-1 and autophagy deregulation following retinal ischemic injury in vivo. *Cell Death Dis* **2**: e144

Ryan KM (2011). p53 and autophagy in cancer: guardian of the genome meets guardian of the proteome. *Eur J Cancer* **47**: 44-50

Sabatini DM, Erdjument-Bromage H, Lui M et al. (1994). RAFT1: a mammalian protein that binds to FKBP12 in a rapamycin-dependent fashion and is homologous to yeast TORs. *Cell* **78**: 35-43

Sabers CJ, Martin MM, Brunn GJ et al. (1995). Isolation of a protein target of the FKBP12-rapamycin complex in mammalian cells. *J Biol Chem* **270**: 815-822

Sagona AP, Nezis IP, Bache KG et al. (2011). A tumor-associated mutation of FYVE-CENT prevents its interaction with Beclin 1 and interferes with cytokinesis. *PLoS One* **6**: e17086

Sahara S, Aoto M, Eguchi Y et al. (1999). Acinus is a caspase-3-activated protein required for apoptotic chromatin condensation. *Nature* **401**: 168-173

Sakai Y, Koller A, Rangell LK et al. (1998). Peroxisome degradation by microautophagy in Pichia pastoris: identification of specific steps and morphological intermediates. *J Cell Biol* **141**: 625-636

Sakaki K, Wu J, Kaufman RJ (2008). Protein kinase Ctheta is required for autophagy in response to stress in the endoplasmic reticulum. *J Biol Chem* **283**: 15370-15380

Sakoh-Nakatogawa M, Matoba K, Asai E et al. (2013). Atg12-Atg5 conjugate enhances E2 activity of Atg3 by rearranging its catalytic site. *Nat Struct Mol Biol* **20**: 433-439

Saleh A, Srinivasula SM, Acharya S et al. (1999). Cytochrome c and dATP-mediated oligomerization of Apaf-1 is a prerequisite for procaspase-9 activation. *J Biol Chem* **274**: 17941-17945

Samari HR, Moller MT, Holden L et al. (2005). Stimulation of hepatocytic AMP-activated protein kinase by okadaic acid and other autophagy-suppressive toxins. *Biochem J* **386**: 237-244

Samari HR, Seglen PO (1998). Inhibition of hepatocytic autophagy by adenosine, aminoimidazole-4-carboxamide riboside, and N6-mercaptopurine riboside. Evidence for involvement of amp-activated protein kinase. *J Biol Chem* **273**: 23758-23763

Sancak Y, Bar-Peled L, Zoncu R et al. (2010). Ragulator-Rag complex targets mTORC1 to the lysosomal surface and is necessary for its activation by amino acids. *Cell* **141**: 290-303

Sancak Y, Peterson TR, Shaul YD et al. (2008). The Rag GTPases bind raptor and mediate amino acid signaling to mTORC1. *Science* **320**: 1496-1501

Sancak Y, Thoreen CC, Peterson TR et al. (2007). PRAS40 is an insulin-regulated inhibitor of the mTORC1 protein kinase. *Mol Cell* **25**: 903-915

Sanchez AM, Csibi A, Raibon A et al. (2012). AMPK promotes skeletal muscle autophagy through activation of forkhead FoxO3a and interaction with Ulk1. *J Cell Biochem* **113**: 695-710

Sandilands E, Serrels B, McEwan DG et al. (2012). Autophagic targeting of Src promotes cancer cell survival following reduced FAK signalling. *Nat Cell Biol* **14**: 51-60

Sandu C, Morisawa G, Wegorzewska I et al. (2006). FADD self-association is required for stable interaction with an activated death receptor. *Cell Death Differ* **13**: 2052-2061

Sanjuan MA, Dillon CP, Tait SW et al. (2007). Toll-like receptor signalling in macrophages links the autophagy pathway to phagocytosis. *Nature* **450**: 1253-1257

Sarbassov DD, Ali SM, Kim DH et al. (2004). Rictor, a novel binding partner of mTOR, defines a rapamycin-insensitive and raptor-independent pathway that regulates the cytoskeleton. *Curr Biol* **14**: 1296-1302

Sarbassov DD, Ali SM, Sengupta S et al. (2006). Prolonged rapamycin treatment inhibits mTORC2 assembly and Akt/PKB. *Mol Cell* **22**: 159-168

Sarbassov DD, Guertin DA, Ali SM et al. (2005). Phosphorylation and regulation of Akt/PKB by the rictor-mTOR complex. *Science* **307**: 1098-1101

Sarkar S, Ravikumar B, Floto RA et al. (2009). Rapamycin and mTOR-independent autophagy inducers ameliorate toxicity of polyglutamine-expanded huntingtin and related proteinopathies. *Cell Death Differ* **16**: 46-56

Sarraf SA, Raman M, Guarani-Pereira V et al. (2013). Landscape of the PARKIN-dependent ubiquitylome in response to mitochondrial depolarization. *Nature* **496**: 372-376

Sato M, Sato K (2012). Maternal inheritance of mitochondrial DNA: degradation of paternal mitochondria by allogeneic organelle autophagy, allophagy. *Autophagy* **8**: 424-425

Sattler M, Liang H, Nettesheim D et al. (1997). Structure of Bcl-xL-Bak peptide complex: recognition between regulators of apoptosis. *Science* **275**: 983-986

Saucedo LJ, Gao X, Chiarelli DA et al. (2003). Rheb promotes cell growth as a component of the insulin/TOR signalling network. *Nat Cell Biol* **5**: 566-571

Scaffidi C, Fulda S, Srinivasan A et al. (1998). Two CD95 (APO-1/Fas) signaling pathways. *EMBO J* **17**: 1675-1687

Scaffidi C, Medema JP, Krammer PH et al. (1997). FLICE is predominantly expressed as two functionally active isoforms, caspase-8/a and caspase-8/b. *J Biol Chem* **272**: 26953-26958

Scarlatti F, Maffei R, Beau I et al. (2008). Role of non-canonical Beclin 1-independent autophagy in cell death induced by resveratrol in human breast cancer cells. *Cell Death Differ* **15**: 1318-1329

Scharenberg AM, Humphries LA, Rawlings DJ (2007). Calcium signalling and cell-fate choice in B cells. *Nat Rev Immunol* **7**: 778-789

Scherz-Shouval R, Sagiv Y, Shorer H et al. (2003). The COOH terminus of GATE-16, an intra-Golgi transport modulator, is cleaved by the human cysteine protease HsApg4A. *J Biol Chem* **278**: 14053-14058

Schlegel J, Peters I, Orrenius S (1995). Isolation and partial characterization of a protease involved in Fas-induced apoptosis. *FEBS Lett* **364**: 139-142

Schleich K, Krammer PH, Lavrik IN (2013). The chains of death: a new view on caspase-8 activation at the DISC. *Cell Cycle* **12**: 193-194

Schleich K, Warnken U, Fricker N et al. (2012). Stoichiometry of the CD95 death-inducing signaling complex: experimental and modeling evidence for a death effector domain chain model. *Mol Cell* **47**: 306-319

Schug ZT, Gonzalvez F, Houtkooper RH et al. (2011). BID is cleaved by caspase-8 within a native complex on the mitochondrial membrane. *Cell Death Differ* **18**: 538-548

Schwarze PE, Seglen PO (1985). Reduced autophagic activity, improved protein balance and enhanced in vitro survival of hepatocytes isolated from carcinogen-treated rats. *Exp Cell Res* **157**: 15-28

Scorrano L, Oakes SA, Opferman JT et al. (2003). BAX and BAK regulation of endoplasmic reticulum Ca2+: a control point for apoptosis. *Science* **300**: 135-139

Scott FL, Denault JB, Riedl SJ et al. (2005). XIAP inhibits caspase-3 and -7 using two binding sites: evolutionarily conserved mechanism of IAPs. *EMBO J* **24**: 645-655

Scott FL, Stec B, Pop C et al. (2009). The Fas-FADD death domain complex structure unravels signalling by receptor clustering. *Nature* **457**: 1019-1022

Scott RC, Juhasz G, Neufeld TP (2007). Direct induction of autophagy by Atg1 inhibits cell growth and induces apoptotic cell death. *Current biology : CB* **17**: 1-11

Seifert A, Allan LA, Clarke PR (2008). DYRK1A phosphorylates caspase 9 at an inhibitory site and is potently inhibited in human cells by harmine. *FEBS J* **275**: 6268-6280

Sekito T, Kawamata T, Ichikawa R et al. (2009). Atg17 recruits Atg9 to organize the pre-autophagosomal structure. *Genes Cells* **14**: 525-538

Sekulic A, Hudson CC, Homme JL et al. (2000). A direct linkage between the phosphoinositide 3-kinase-AKT signaling pathway and the mammalian target of rapamycin in mitogen-stimulated and transformed cells. *Cancer Res* **60**: 3504-3513

Sentman CL, Shutter JR, Hockenbery D et al. (1991). bcl-2 inhibits multiple forms of apoptosis but not negative selection in thymocytes. *Cell* **67**: 879-888

Seruga B, Ocana A, Tannock IF (2011). Drug resistance in metastatic castration-resistant prostate cancer. *Nat Rev Clin Oncol* **8**: 12-23

Shaid S, Brandts CH, Serve H et al. (2013). Ubiquitination and selective autophagy. *Cell Death Differ* **20**: 21-30

Shamas-Din A, Brahmbhatt H, Leber B et al. (2011). BH3-only proteins: Orchestrators of apoptosis. *Biochim Biophys Acta* **1813**: 508-520

Shang L, Chen S, Du F et al. (2011). Nutrient starvation elicits an acute autophagic response mediated by Ulk1 dephosphorylation and its subsequent dissociation from AMPK. *Proc Natl Acad Sci U S A* **108**: 4788-4793

Shen S, Kepp O, Michaud M et al. (2011). Association and dissociation of autophagy, apoptosis and necrosis by systematic chemical study. *Oncogene* **30**: 4544-4556

Shi CS, Kehrl JH (2008). MyD88 and Trif target Beclin 1 to trigger autophagy in macrophages. *J Biol Chem* **283**: 33175-33182

Shi CS, Kehrl JH (2010). TRAF6 and A20 regulate lysine 63-linked ubiquitination of Beclin-1 to control TLR4-induced autophagy. *Sci Signal* **3**: ra42

Shi Y (2004). Caspase activation: revisiting the induced proximity model. *Cell* **117**: 855-858

Shim D, Kang HY, Jeon BW et al. (2004). Protein kinase B inhibits apoptosis induced by actinomycin D in ECV304 cells through phosphorylation of caspase 8. *Arch Biochem Biophys* **425**: 214-220

Shimbo K, Hsu GW, Nguyen H et al. (2012). Quantitative profiling of caspase-cleaved substrates reveals different drug-induced and cell-type patterns in apoptosis. *Proc Natl Acad Sci U S A* **109**: 12432-12437

Shimizu S, Kanaseki T, Mizushima N et al. (2004). Role of Bcl-2 family proteins in a non-apoptotic programmed cell death dependent on autophagy genes. *Nat Cell Biol* **6**: 1221-1228

Shinohara H, Maeda S, Watarai H et al. (2007). IkappaB kinase beta-induced phosphorylation of CARMA1 contributes to CARMA1 Bcl10 MALT1 complex formation in B cells. *J Exp Med* **204**: 3285-3293

Shintani T, Mizushima N, Ogawa Y et al. (1999). Apg10p, a novel protein-conjugating enzyme essential for autophagy in yeast. *EMBO J* **18**: 5234-5241

Shiozaki EN, Chai J, Rigotti DJ et al. (2003). Mechanism of XIAP-mediated inhibition of caspase-9. *Mol Cell* **11**: 519-527

Shiozaki EN, Chai J, Shi Y (2002). Oligomerization and activation of caspase-9, induced by Apaf-1 CARD. *Proc Natl Acad Sci U S A* **99**: 4197-4202

Shoji-Kawata S, Sumpter R, Leveno M et al. (2013). Identification of a candidate therapeutic autophagy-inducing peptide. *Nature* **494**: 201-206

Shpilka T, Weidberg H, Pietrokovski S et al. (2011). Atg8: an autophagy-related ubiquitin-like protein family. *Genome Biol* **12**: 226

Shultz JC, Goehe RW, Wijesinghe DS et al. (2010). Alternative splicing of caspase 9 is modulated by the phosphoinositide 3-kinase/Akt pathway via phosphorylation of SRp30a. *Cancer Res* **70**: 9185-9196

Sinha S, Colbert CL, Becker N et al. (2008). Molecular basis of the regulation of Beclin 1-dependent autophagy by the gamma-herpesvirus 68 Bcl-2 homolog M11. *Autophagy* **4**: 989-997

Smith AE, Smith R, Paucha E (1979). Characterization of different tumor antigens present in cells transformed by simian virus 40. *Cell* **18**: 335-346

Smith DM, Patel S, Raffoul F et al. (2010). Arsenic trioxide induces a beclin-1-independent autophagic pathway via modulation of SnoN/SkiL expression in ovarian carcinoma cells. *Cell Death Differ* **17**: 1867-1881

Sou YS, Waguri S, Iwata J et al. (2008). The Atg8 conjugation system is indispensable for proper development of autophagic isolation membranes in mice. *Mol Biol Cell* **19**: 4762-4775

Spector MS, Desnoyers S, Hoeppner DJ et al. (1997). Interaction between the C. elegans cell-death regulators CED-9 and CED-4. *Nature* **385**: 653-656

Sprick MR, Rieser E, Stahl H et al. (2002). Caspase-10 is recruited to and activated at the native TRAIL and CD95 death-inducing signalling complexes in a FADD-dependent manner but can not functionally substitute caspase-8. *EMBO J* **21**: 4520-4530

Srinivasula SM, Ahmad M, Fernandes-Alnemri T et al. (1998). Autoactivation of procaspase-9 by Apaf-1-mediated oligomerization. *Mol Cell* **1**: 949-957

Srinivasula SM, Datta P, Fan XJ et al. (2000). Molecular determinants of the caspase-promoting activity of Smac/DIABLO and its role in the death receptor pathway. *J Biol Chem* **275**: 36152-36157

Srinivasula SM, Hegde R, Saleh A et al. (2001). A conserved XIAP-interaction motif in caspase-9 and Smac/DIABLO regulates caspase activity and apoptosis. *Nature* **410**: 112-116

Staal SP (1987). Molecular cloning of the akt oncogene and its human homologues AKT1 and AKT2: amplification of AKT1 in a primary human gastric adenocarcinoma. *Proc Natl Acad Sci U S A* **84**: 5034-5037

Staal SP, Hartley JW, Rowe WP (1977). Isolation of transforming murine leukemia viruses from mice with a high incidence of spontaneous lymphoma. *Proc Natl Acad Sci U S A* **74**: 3065-3067

Stambolic V, MacPherson D, Sas D et al. (2001). Regulation of PTEN transcription by p53. *Mol Cell* **8**: 317-325

Steffan JS (2010). Does Huntingtin play a role in selective macroautophagy? *Cell Cycle* **9**: 3401-3413

Stenmark H, Aasland R, Toh BH et al. (1996). Endosomal localization of the autoantigen EEA1 is mediated by a zinc-binding FYVE finger. *J Biol Chem* **271**: 24048-24054

Stennicke HR, Deveraux QL, Humke EW et al. (1999). Caspase-9 can be activated without proteolytic processing. *J Biol Chem* **274**: 8359-8362

Stepczynska A, Lauber K, Engels IH et al. (2001). Staurosporine and conventional anticancer drugs induce overlapping, yet distinct pathways of apoptosis and caspase activation. *Oncogene* **20**: 1193-1202

Stephan JS, Yeh YY, Ramachandran V et al. (2009). The Tor and PKA signaling pathways independently target the Atg1/Atg13 protein kinase complex to control autophagy. *Proc Natl Acad Sci U S A* **106**: 17049-17054

Stephens L, Anderson K, Stokoe D et al. (1998). Protein kinase B kinases that mediate phosphatidylinositol 3,4,5-trisphosphate-dependent activation of protein kinase B. *Science* **279**: 710-714

Stocker H, Radimerski T, Schindelholz B et al. (2003). Rheb is an essential regulator of S6K in controlling cell growth in Drosophila. *Nat Cell Biol* **5**: 559-565

Stokoe D, Stephens LR, Copeland T et al. (1997). Dual role of phosphatidylinositol-3,4,5-trisphosphate in the activation of protein kinase B. *Science* **277**: 567-570

Stork B, Engelke M, Frey J et al. (2004). Grb2 and the non-T cell activation linker NTAL constitute a Ca(2+)-regulating signal circuit in B lymphocytes. *Immunity* **21**: 681-691

Strappazzon F, Vietri-Rudan M, Campello S et al. (2011). Mitochondrial BCL-2 inhibits AMBRA1-induced autophagy. *EMBO J* **30**: 1195-1208

Strasser A, Cory S, Adams JM (2011). Deciphering the rules of programmed cell death to improve therapy of cancer and other diseases. *EMBO J* **30**: 3667-3683

Strasser A, Harris AW, Cory S (1991). bcl-2 transgene inhibits T cell death and perturbs thymic self-censorship. *Cell* **67**: 889-899

Stroh C, Schulze-Osthoff K (1998). Death by a thousand cuts: an ever increasing list of caspase substrates. *Cell Death Differ* **5**: 997-1000

Stromhaug PE, Reggiori F, Guan J et al. (2004). Atg21 is a phosphoinositide binding protein required for efficient lipidation and localization of Atg8 during uptake of aminopeptidase I by selective autophagy. *Mol Biol Cell* **15**: 3553-3566

Subramani S, Malhotra V (2013). Non-autophagic roles of autophagy-related proteins. *EMBO Rep* **14**: 143-151

Suda T, Takahashi T, Golstein P et al. (1993). Molecular cloning and expression of the Fas ligand, a novel member of the tumor necrosis factor family. *Cell* **75**: 1169-1178

Sumpter R, Jr., Levine B (2010). Autophagy and innate immunity: triggering, targeting and tuning. *Semin Cell Dev Biol* **21**: 699-711

Sun Q, Fan W, Chen K et al. (2008). Identification of Barkor as a mammalian autophagy-specific factor for Beclin 1 and class III phosphatidylinositol 3-kinase. *Proc Natl Acad Sci U S A* **105**: 19211-19216

Sun Q, Fan W, Zhong Q (2009). Regulation of Beclin 1 in autophagy. *Autophagy* **5**: 713-716

Suttangkakul A, Li F, Chung T et al. (2011). The ATG1/ATG13 protein kinase complex is both a regulator and a target of autophagic recycling in Arabidopsis. *Plant Cell* **23**: 3761-3779

Suzuki K, Akioka M, Kondo-Kakuta C et al. (2013). Fine mapping of autophagy-related proteins during autophagosome formation in Saccharomyces cerevisiae. *J Cell Sci*

Suzuki K, Kirisako T, Kamada Y et al. (2001a). The pre-autophagosomal structure organized by concerted functions of APG genes is essential for autophagosome formation. *EMBO J* **20**: 5971-5981

Suzuki K, Kubota Y, Sekito T et al. (2007). Hierarchy of Atg proteins in pre-autophagosomal structure organization. *Genes Cells* **12**: 209-218

Suzuki M, Youle RJ, Tjandra N (2000). Structure of Bax: coregulation of dimer formation and intracellular localization. *Cell* **103**: 645-654

Suzuki Y, Nakabayashi Y, Nakata K et al. (2001b). X-linked inhibitor of apoptosis protein (XIAP) inhibits caspase-3 and -7 in distinct modes. *J Biol Chem* **276**: 27058-27063

Szado T, Vanderheyden V, Parys JB et al. (2008). Phosphorylation of inositol 1,4,5-trisphosphate receptors by protein kinase B/Akt inhibits Ca2+ release and apoptosis. *Proc Natl Acad Sci U S A* **105**: 2427-2432

Takahashi T, Tanaka M, Brannan CI et al. (1994). Generalized lymphoproliferative disease in mice, caused by a point mutation in the Fas ligand. *Cell* **76**: 969-976

Takahashi Y, Coppola D, Matsushita N et al. (2007). Bif-1 interacts with Beclin 1 through UVRAG and regulates autophagy and tumorigenesis. *Nat Cell Biol* **9**: 1142-1151

Takaishi H, Konishi H, Matsuzaki H et al. (1999). Regulation of nuclear translocation of forkhead transcription factor AFX by protein kinase B. *Proc Natl Acad Sci U S A* **96**: 11836-11841

Takamura A, Komatsu M, Hara T et al. (2011). Autophagy-deficient mice develop multiple liver tumors. *Genes Dev* **25**: 795-800

Tamburini J, Chapuis N, Bardet V et al. (2008). Mammalian target of rapamycin (mTOR) inhibition activates phosphatidylinositol 3-kinase/Akt by up-regulating insulin-like growth factor-1 receptor signaling in acute myeloid leukemia: rationale for therapeutic inhibition of both pathways. *Blood* **111**: 379-382

Tan Y, Demeter MR, Ruan H et al. (2000). BAD Ser-155 phosphorylation regulates BAD/Bcl-XL interaction and cell survival. *J Biol Chem* **275**: 25865-25869

Tang D, Kang R, Livesey KM et al. (2010). Endogenous HMGB1 regulates autophagy. *J Cell Biol* **190**: 881-892

Tang ED, Nunez G, Barr FG et al. (1999). Negative regulation of the forkhead transcription factor FKHR by Akt. *J Biol Chem* **274**: 16741-16746

Tang HW, Wang YB, Wang SL et al. (2011). Atg1-mediated myosin II activation regulates autophagosome formation during starvation-induced autophagy. *EMBO J* **30**: 636-651

Tang J, Deng R, Luo RZ et al. (2012). Low expression of ULK1 is associated with operable breast cancer progression and is an adverse prognostic marker of survival for patients. *Breast Cancer Res Treat* **134**: 549-560

Tanida I, Komatsu M, Ueno T et al. (2003). GATE-16 and GABARAP are authentic modifiers mediated by Apg7 and Apg3. *Biochem Biophys Res Commun* **300**: 637-644

Tanida I, Mizushima N, Kiyooka M et al. (1999). Apg7p/Cvt2p: A novel protein-activating enzyme essential for autophagy. *Mol Biol Cell* **10**: 1367-1379

Tanida I, Sou YS, Ezaki J et al. (2004). HsAtg4B/HsApg4B/autophagin-1 cleaves the carboxyl termini of three human Atg8 homologues and delipidates microtubule-associated protein light chain 3- and GABAA receptor-associated protein-phospholipid conjugates. *J Biol Chem* **279**: 36268-36276

Tanida I, Sou YS, Minematsu-Ikeguchi N et al. (2006). Atg8L/Apg8L is the fourth mammalian modifier of mammalian Atg8 conjugation mediated by human Atg4B, Atg7 and Atg3. *FEBS J* **273**: 2553-2562

Tanida I, Tanida-Miyake E, Komatsu M et al. (2002). Human Apg3p/Aut1p homologue is an authentic E2 enzyme for multiple substrates, GATE-16, GABARAP, and MAP-LC3, and facilitates the conjugation of hApg12p to hApg5p. *J Biol Chem* **277**: 13739-13744

Tanida I, Tanida-Miyake E, Ueno T et al. (2001). The human homolog of Saccharomyces cerevisiae Apg7p is a Protein-activating enzyme for multiple substrates including human Apg12p, GATE-16, GABARAP, and MAP-LC3. *J Biol Chem* **276**: 1701-1706

Tasdemir E, Chiara Maiuri M, Morselli E et al. (2008a). A dual role of p53 in the control of autophagy. *Autophagy* **4**: 810-814

Tasdemir E, Maiuri MC, Galluzzi L et al. (2008b). Regulation of autophagy by cytoplasmic p53. *Nat Cell Biol* **10**: 676-687

Taylor CW, Tovey SC (2010). IP(3) receptors: toward understanding their activation. *Cold Spring Harb Perspect Biol* **2**: a004010

Tenev T, Bianchi K, Darding M et al. (2011). The Ripoptosome, a signaling platform that assembles in response to genotoxic stress and loss of IAPs. *Mol Cell* **43**: 432-448

Tewari M, Quan LT, O'Rourke K et al. (1995). Yama/CPP32 beta, a mammalian homolog of CED-3, is a CrmA-inhibitable protease that cleaves the death substrate poly(ADP-ribose) polymerase. *Cell* **81**: 801-809

Thedieck K, Polak P, Kim ML et al. (2007). PRAS40 and PRR5-like protein are new mTOR interactors that regulate apoptosis. *PLoS One* **2**: e1217

Thoreen CC, Kang SA, Chang JW et al. (2009). An ATP-competitive mammalian target of rapamycin inhibitor reveals rapamycin-resistant functions of mTORC1. *J Biol Chem* **284**: 8023-8032

Thornberry NA, Lazebnik Y (1998). Caspases: enemies within. *Science* **281**: 1312-1316

Thumm M, Egner R, Koch B et al. (1994). Isolation of autophagocytosis mutants of Saccharomyces cerevisiae. *FEBS Lett* **349**: 275-280

Thurston TL, Ryzhakov G, Bloor S et al. (2009). The TBK1 adaptor and autophagy receptor NDP52 restricts the proliferation of ubiquitin-coated bacteria. *Nat Immunol* **10**: 1215-1221

Tinel A, Tschopp J (2004). The PIDDosome, a protein complex implicated in activation of caspase-2 in response to genotoxic stress. *Science* **304**: 843-846

Titorenko VI, Keizer I, Harder W et al. (1995). Isolation and characterization of mutants impaired in the selective degradation of peroxisomes in the yeast Hansenula polymorpha. *J Bacteriol* **177**: 357-363

Tooze SA (2010). The role of membrane proteins in mammalian autophagy. *Semin Cell Dev Biol* **21**: 677-682

Tooze SA, Codogno P (2011). Compartmentalized regulation of autophagy regulators: fine-tuning AMBRA1 by Bcl-2. *EMBO J* **30**: 1185-1186

Tooze SA, Yoshimori T (2010). The origin of the autophagosomal membrane. *Nat Cell Biol* **12**: 831-835

Trauth BC, Klas C, Peters AM et al. (1989). Monoclonal antibody-mediated tumor regression by induction of apoptosis. *Science* **245**: 301-305

Tsujimoto Y (1998). Role of Bcl-2 family proteins in apoptosis: apoptosomes or mitochondria? *Genes Cells* **3**: 697-707

Tsujimoto Y, Cossman J, Jaffe E et al. (1985). Involvement of the bcl-2 gene in human follicular lymphoma. *Science* **228**: 1440-1443

Tsujimoto Y, Croce CM (1986). Analysis of the structure, transcripts, and protein products of bcl-2, the gene involved in human follicular lymphoma. *Proc Natl Acad Sci U S A* **83**: 5214-5218

Tsujimoto Y, Finger LR, Yunis J et al. (1984). Cloning of the chromosome breakpoint of neoplastic B cells with the t(14;18) chromosome translocation. *Science* **226**: 1097-1099

Tsukada M, Ohsumi Y (1993). Isolation and characterization of autophagy-defective mutants of Saccharomyces cerevisiae. *FEBS Lett* **333**: 169-174

Ueda H, Abbi S, Zheng C et al. (2000). Suppression of Pyk2 kinase and cellular activities by FIP200. *The Journal of cell biology* **149**: 423-430

Umekawa M, Klionsky DJ (2012). The Ksp1 kinase regulates autophagy via the target of rapamycin complex 1 (TORC1) pathway. *J Biol Chem*

Uren RT, Dewson G, Chen L et al. (2007). Mitochondrial permeabilization relies on BH3 ligands engaging multiple prosurvival Bcl-2 relatives, not Bak. *J Cell Biol* **177**: 277-287

van Delft MF, Wei AH, Mason KD et al. (2006). The BH3 mimetic ABT-737 targets selective Bcl-2 proteins and efficiently induces apoptosis via Bak/Bax if Mcl-1 is neutralized. *Cancer Cell* **10**: 389-399

van Gorp AG, Pomeranz KM, Birkenkamp KU et al. (2006). Chronic protein kinase B (PKB/c-akt) activation leads to apoptosis induced by oxidative stress-mediated Foxo3a transcriptional up-regulation. *Cancer Res* **66**: 10760-10769

Vandenabeele P, Galluzzi L, Vanden Berghe T et al. (2010). Molecular mechanisms of necroptosis: an ordered cellular explosion. *Nat Rev Mol Cell Biol* **11**: 700-714

Vander Haar E, Lee SI, Bandhakavi S et al. (2007). Insulin signalling to mTOR mediated by the Akt/PKB substrate PRAS40. *Nat Cell Biol* **9**: 316-323

Vanhaesebroeck B, Guillermet-Guibert J, Graupera M et al. (2010). The emerging mechanisms of isoform-specific PI3K signalling. *Nat Rev Mol Cell Biol* **11**: 329-341

Vanhaesebroeck B, Stephens L, Hawkins P (2012). PI3K signalling: the path to discovery and understanding. *Nat Rev Mol Cell Biol* **13**: 195-203

Vanlangenakker N, Vanden Berghe T, Vandenabeele P (2012). Many stimuli pull the necrotic trigger, an overview. *Cell Death Differ* **19**: 75-86

Vaseva AV, Moll UM (2009). The mitochondrial p53 pathway. *Biochim Biophys Acta* **1787**: 414-420

Vaux DL (2011). Apoptogenic factors released from mitochondria. *Biochim Biophys Acta* **1813**: 546-550

Vaux DL, Cory S, Adams JM (1988). Bcl-2 gene promotes haemopoietic cell survival and cooperates with c-myc to immortalize pre-B cells. *Nature* **335**: 440-442

Vaux DL, Silke J (2003). Mammalian mitochondrial IAP binding proteins. *Biochem Biophys Res Commun* **304**: 499-504

Velikkakath AK, Nishimura T, Oita E et al. (2012). Mammalian Atg2 proteins are essential for autophagosome formation and important for regulation of size and distribution of lipid droplets. *Mol Biol Cell* **23**: 896-909

Vezina C, Kudelski A, Sehgal SN (1975). Rapamycin (AY-22,989), a new antifungal antibiotic. I. Taxonomy of the producing streptomycete and isolation of the active principle. *J Antibiot (Tokyo)* **28**: 721-726

Viana R, Aguado C, Esteban I et al. (2008). Role of AMP-activated protein kinase in autophagy and proteasome function. *Biochem Biophys Res Commun* **369**: 964-968

Vicencio JM, Ortiz C, Criollo A et al. (2009). The inositol 1,4,5-trisphosphate receptor regulates autophagy through its interaction with Beclin 1. *Cell Death Differ* **16**: 1006-1017

Villunger A, Labi V, Bouillet P et al. (2011). Can the analysis of BH3-only protein knockout mice clarify the issue of 'direct versus indirect' activation of Bax and Bak? *Cell Death Differ* **18**: 1545-1546

von Boehmer H, Melchers F (2010). Checkpoints in lymphocyte development and autoimmune disease. *Nat Immunol* **11**: 14-20

von Muhlinen N, Akutsu M, Ravenhill BJ et al. (2012). LC3C, bound selectively by a noncanonical LIR motif in NDP52, is required for antibacterial autophagy. *Mol Cell* **48**: 329-342

Vousden KH, Lane DP (2007). p53 in health and disease. *Nat Rev Mol Cell Biol* **8**: 275-283

Vousden KH, Ryan KM (2009). p53 and metabolism. *Nat Rev Cancer* **9**: 691-700

Walczak H, Miller RE, Ariail K et al. (1999). Tumoricidal activity of tumor necrosis factor-related apoptosis-inducing ligand in vivo. *Nature medicine* **5**: 157-163

Wan X, Harkavy B, Shen N et al. (2007). Rapamycin induces feedback activation of Akt signaling through an IGF-1R-dependent mechanism. *Oncogene* **26**: 1932-1940

Wander SA, Hennessy BT, Slingerland JM (2011). Next-generation mTOR inhibitors in clinical oncology: how pathway complexity informs therapeutic strategy. *J Clin Invest* **121**: 1231-1241

Wang L, Harris TE, Roth RA et al. (2007). PRAS40 regulates mTORC1 kinase activity by functioning as a direct inhibitor of substrate binding. *J Biol Chem* **282**: 20036-20044

Wang L, Yang JK, Kabaleeswaran V et al. (2010). The Fas-FADD death domain complex structure reveals the basis of DISC assembly and disease mutations. *Nat Struct Mol Biol* **17**: 1324-1329

Wang LD, Clark MR (2003). B-cell antigen-receptor signalling in lymphocyte development. *Immunology* **110**: 411-420

Wang RC, Wei Y, An Z et al. (2012). Akt-mediated regulation of autophagy and tumorigenesis through Beclin 1 phosphorylation. *Science* **338**: 956-959

Wang Y, Horvath O, Hamm-Baarke A et al. (2005). Single and combined deletions of the NTAL/LAB and LAT adaptors minimally affect B-cell development and function. *Mol Cell Biol* **25**: 4455-4465

Wang Z, Wilson WA, Fujino MA et al. (2001). Antagonistic controls of autophagy and glycogen accumulation by Snf1p, the yeast homolog of AMP-activated protein kinase, and the cyclin-dependent kinase Pho85p. *Mol Cell Biol* **21**: 5742-5752

Watanabe-Fukunaga R, Brannan CI, Copeland NG et al. (1992). Lymphoproliferation disorder in mice explained by defects in Fas antigen that mediates apoptosis. *Nature* **356**: 314-317

Webber JL, Tooze SA (2010). New insights into the function of Atg9. *FEBS Lett* **584**: 1319-1326

Wee LJ, Tan TW, Ranganathan S (2006). SVM-based prediction of caspase substrate cleavage sites. *BMC Bioinformatics* **7 Suppl 5**: S14

Wei H, Wei S, Gan B et al. (2011). Suppression of autophagy by FIP200 deletion inhibits mammary tumorigenesis. *Genes Dev* **25**: 1510-1527

Wei MC, Zong WX, Cheng EH et al. (2001). Proapoptotic BAX and BAK: a requisite gateway to mitochondrial dysfunction and death. *Science* **292**: 727-730

Wei Y, Pattingre S, Sinha S et al. (2008). JNK1-mediated phosphorylation of Bcl-2 regulates starvation-induced autophagy. *Mol Cell* **30**: 678-688

Wei Z, Qi J, Dai Y et al. (2009). Haloperidol disrupts Akt signalling to reveal a phosphorylation-dependent regulation of pro-apoptotic Bcl-XS function. *Cell Signal* **21**: 161-168

Weidberg H, Shvets E, Shpilka T et al. (2010). LC3 and GATE-16/GABARAP subfamilies are both essential yet act differently in autophagosome biogenesis. *EMBO J* **29**: 1792-1802

Westphal D, Dewson G, Czabotar PE et al. (2011). Molecular biology of Bax and Bak activation and action. *Biochim Biophys Acta* **1813**: 521-531

White C, Li C, Yang J et al. (2005). The endoplasmic reticulum gateway to apoptosis by Bcl-X(L) modulation of the InsP3R. *Nat Cell Biol* **7**: 1021-1028

Wild P, Farhan H, McEwan DG et al. (2011). Phosphorylation of the autophagy receptor optineurin restricts Salmonella growth. *Science* **333**: 228-233

Willems L, Tamburini J, Chapuis N et al. (2012). PI3K and mTOR signaling pathways in cancer: new data on targeted therapies. *Curr Oncol Rep* **14**: 129-138

Williams A, Sarkar S, Cuddon P et al. (2008). Novel targets for Huntington's disease in an mTOR-independent autophagy pathway. *Nat Chem Biol* **4**: 295-305

Willis SN, Chen L, Dewson G et al. (2005). Proapoptotic Bak is sequestered by Mcl-1 and Bcl-xL, but not Bcl-2, until displaced by BH3-only proteins. *Genes Dev* **19**: 1294-1305

Willis SN, Fletcher JI, Kaufmann T et al. (2007). Apoptosis initiated when BH3 ligands engage multiple Bcl-2 homologs, not Bax or Bak. *Science* **315**: 856-859

Wirawan E, Vande Walle L, Kersse K et al. (2010). Caspase-mediated cleavage of Beclin-1 inactivates Beclin-1-induced autophagy and enhances apoptosis by promoting the release of proapoptotic factors from mitochondria. *Cell Death Dis* **1**: e18

Wong PM, Puente C, Ganley IG et al. (2013). The ULK1 complex: sensing nutrient signals for autophagy activation. *Autophagy* **9**: 124-137

Woods A, Dickerson K, Heath R et al. (2005). Ca2+/calmodulin-dependent protein kinase kinase-beta acts upstream of AMP-activated protein kinase in mammalian cells. *Cell Metab* **2**: 21-33

Woods A, Johnstone SR, Dickerson K et al. (2003). LKB1 is the upstream kinase in the AMP-activated protein kinase cascade. *Curr Biol* **13**: 2004-2008

Wu D, Wallen HD, Inohara N et al. (1997a). Interaction and regulation of the Caenorhabditis elegans death protease CED-3 by CED-4 and CED-9. *J Biol Chem* **272**: 21449-21454

Wu D, Wallen HD, Nunez G (1997b). Interaction and regulation of subcellular localization of CED-4 by CED-9. *Science* **275**: 1126-1129

Wu G, Chai J, Suber TL et al. (2000). Structural basis of IAP recognition by Smac/DIABLO. *Nature* **408**: 1008-1012

Xiao B, Heath R, Saiu P et al. (2007). Structural basis for AMP binding to mammalian AMP-activated protein kinase. *Nature* **449**: 496-500

Xiao B, Sanders MJ, Underwood E et al. (2011). Structure of mammalian AMPK and its regulation by ADP. *Nature* **472**: 230-233

Xie Z, Nair U, Klionsky DJ (2008). Atg8 controls phagophore expansion during autophagosome formation. *Mol Biol Cell* **19**: 3290-3298

Xin M, Deng X (2005). Nicotine inactivation of the proapoptotic function of Bax through phosphorylation. *J Biol Chem* **280**: 10781-10789

Xin Y, Yu L, Chen Z et al. (2001). Cloning, expression patterns, and chromosome localization of three human and two mouse homologues of GABA(A) receptor-associated protein. *Genomics* **74**: 408-413

Xue D, Shaham S, Horvitz HR (1996). The Caenorhabditis elegans cell-death protein CED-3 is a cysteine protease with substrate specificities similar to those of the human CPP32 protease. *Genes Dev* **10**: 1073-1083

Yamamoto H, Kakuta S, Watanabe TM et al. (2012). Atg9 vesicles are an important membrane source during early steps of autophagosome formation. *J Cell Biol* **198**: 219-233

Yan J, Kuroyanagi H, Kuroiwa A et al. (1998). Identification of mouse ULK1, a novel protein kinase structurally related to C. elegans UNC-51. *Biochem Biophys Res Commun* **246**: 222-227

Yan J, Kuroyanagi H, Tomemori T et al. (1999a). Mouse ULK2, a novel member of the UNC-51-like protein kinases: unique features of functional domains. *Oncogene* **18**: 5850-5859

Yan M, Lee J, Schilbach S et al. (1999b). mE10, a novel caspase recruitment domain-containing proapoptotic molecule. *J Biol Chem* **274**: 10287-10292

Yang L, Dan HC, Sun M et al. (2004). Akt/protein kinase B signaling inhibitor-2, a selective small molecule inhibitor of Akt signaling with antitumor activity in cancer cells overexpressing Akt. *Cancer Res* **64**: 4394-4399

Yang L, Sun M, Sun XM et al. (2007). Akt attenuation of the serine protease activity of HtrA2/Omi through phosphorylation of serine 212. *J Biol Chem* **282**: 10981-10987

Yang Q, Inoki K, Ikenoue T et al. (2006). Identification of Sin1 as an essential TORC2 component required for complex formation and kinase activity. *Genes Dev* **20**: 2820-2832

Yang Z, Klionsky DJ (2010). Eaten alive: a history of macroautophagy. *Nat Cell Biol* **12**: 814-822

Yee KS, Wilkinson S, James J et al. (2009). PUMA- and Bax-induced autophagy contributes to apoptosis. *Cell Death Differ* **16**: 1135-1145

Yeh YY, Shah KH, Herman PK (2011). An Atg13 protein-mediated self-association of the Atg1 protein kinase is important for the induction of autophagy. *J Biol Chem* **286**: 28931-28939

Yeh YY, Wrasman K, Herman PK (2010). Autophosphorylation within the Atg1 activation loop is required for both kinase activity and the induction of autophagy in Saccharomyces cerevisiae. *Genetics* **185**: 871-882

Yin X, Zhang N, Di W (2013). Regulation of LC3-Dependent Protective Autophagy in Ovarian Cancer Cells by Protein Phosphatase 2A. *Int J Gynecol Cancer* **23**: 630-641

Yin XM, Wang K, Gross A et al. (1999). Bid-deficient mice are resistant to Fas-induced hepatocellular apoptosis. *Nature* **400**: 886-891

Yla-Anttila P, Vihinen H, Jokitalo E et al. (2009). 3D tomography reveals connections between the phagophore and endoplasmic reticulum. *Autophagy* **5**: 1180-1185

Yonehara S, Ishii A, Yonehara M (1989). A cell-killing monoclonal antibody (anti-Fas) to a cell surface antigen co-downregulated with the receptor of tumor necrosis factor. *J Exp Med* **169**: 1747-1756

Yorimitsu T, He C, Wang K et al. (2009). Tap42-associated protein phosphatase type 2A negatively regulates induction of autophagy. *Autophagy* **5**: 616-624

Yorimitsu T, Zaman S, Broach JR et al. (2007). Protein kinase A and Sch9 cooperatively regulate induction of autophagy in Saccharomyces cerevisiae. *Mol Biol Cell* **18**: 4180-4189

Youle RJ, Narendra DP (2011). Mechanisms of mitophagy. *Nat Rev Mol Cell Biol* **12**: 9-14

Young AR, Chan EY, Hu XW et al. (2006). Starvation and ULK1-dependent cycling of mammalian Atg9 between the TGN and endosomes. *J Cell Sci* **119**: 3888-3900

Young AR, Narita M, Ferreira M et al. (2009). Autophagy mediates the mitotic senescence transition. *Genes Dev* **23**: 798-803

Young MM, Takahashi Y, Khan O et al. (2012). Autophagosomal membrane serves as platform for intracellular death-inducing signaling complex (iDISC)-mediated caspase-8 activation and apoptosis. *J Biol Chem* **287**: 12455-12468

Yousefi S, Perozzo R, Schmid I et al. (2006). Calpain-mediated cleavage of Atg5 switches autophagy to apoptosis. *Nat Cell Biol* **8**: 1124-1132

Yu K, Toral-Barza L, Shi C et al. (2009). Biochemical, cellular, and in vivo activity of novel ATP-competitive and selective inhibitors of the mammalian target of rapamycin. *Cancer Res* **69**: 6232-6240

Yu L, Alva A, Su H et al. (2004). Regulation of an ATG7-beclin 1 program of autophagic cell death by caspase-8. *Science* **304**: 1500-1502

Yu L, McPhee CK, Zheng L et al. (2010). Termination of autophagy and reformation of lysosomes regulated by mTOR. *Nature* **465**: 942-946

Yu X, Acehan D, Menetret JF et al. (2005). A structure of the human apoptosome at 12.8 A resolution provides insights into this cell death platform. *Structure* **13**: 1725-1735

Yu ZQ, Ni T, Hong B et al. (2012). Dual roles of Atg8-PE deconjugation by Atg4 in autophagy. *Autophagy* **8**: 883-892

Yuan J, Shaham S, Ledoux S et al. (1993). The C. elegans cell death gene ced-3 encodes a protein similar to mammalian interleukin-1 beta-converting enzyme. *Cell* **75**: 641-652

Yuan S, Akey CW (2013). Apoptosome structure, assembly, and procaspase activation. *Structure* **21**: 501-515

Yuan S, Yu X, Asara JM et al. (2011). The holo-apoptosome: activation of procaspase-9 and interactions with caspase-3. *Structure* **19**: 1084-1096

Yuan S, Yu X, Topf M et al. (2010). Structure of an apoptosome-procaspase-9 CARD complex. *Structure* **18**: 571-583

Yuan W, Tuttle DL, Shi YJ et al. (1997). Glucose-induced microautophagy in Pichia pastoris requires the alpha-subunit of phosphofructokinase. *J Cell Sci* **110 (Pt 16)**: 1935-1945

Yue Z, Horton A, Bravin M et al. (2002). A novel protein complex linking the delta 2 glutamate receptor and autophagy: implications for neurodegeneration in lurcher mice. *Neuron* **35**: 921-933

Yue Z, Jin S, Yang C et al. (2003). Beclin 1, an autophagy gene essential for early embryonic development, is a haploinsufficient tumor suppressor. *Proc Natl Acad Sci U S A* **100**: 15077-15082

Zalckvar E, Berissi H, Mizrachy L et al. (2009). DAP-kinase-mediated phosphorylation on the BH3 domain of beclin 1 promotes dissociation of beclin 1 from Bcl-XL and induction of autophagy. *EMBO Rep* **10**: 285-292

Zeng X, Overmeyer JH, Maltese WA (2006). Functional specificity of the mammalian Beclin-Vps34 PI 3-kinase complex in macroautophagy versus endocytosis and lysosomal enzyme trafficking. *J Cell Sci* **119**: 259-270

Zhang J, Ney PA (2009). Role of BNIP3 and NIX in cell death, autophagy, and mitophagy. *Cell Death Differ* **16**: 939-946

Zhang L, Yu J, Pan H et al. (2007). Small molecule regulators of autophagy identified by an image-based high-throughput screen. *Proc Natl Acad Sci U S A* **104**: 19023-19028

Zhang X, Tang N, Hadden TJ et al. (2011a). Akt, FoxO and regulation of apoptosis. *Biochim Biophys Acta* **1813**: 1978-1986

Zhang YJ, Duan Y, Zheng XF (2011b). Targeting the mTOR kinase domain: the second generation of mTOR inhibitors. *Drug Discov Today* **16**: 325-331

Zhang Z, Zhu W, Lapolla SM et al. (2010). Bax forms an oligomer via separate, yet interdependent, surfaces. *J Biol Chem* **285**: 17614-17627

Zhong F, Davis MC, McColl KS et al. (2006). Bcl-2 differentially regulates Ca2+ signals according to the strength of T cell receptor activation. *J Cell Biol* **172**: 127-137

Zhong Y, Wang QJ, Li X et al. (2009). Distinct regulation of autophagic activity by Atg14L and Rubicon associated with Beclin 1-phosphatidylinositol-3-kinase complex. *Nat Cell Biol* **11**: 468-476

Zhou C, Zhong W, Zhou J et al. (2012). Monitoring autophagic flux by an improved tandem fluorescent-tagged LC3 (mTagRFP-mWasabi-LC3) reveals that high-dose rapamycin impairs autophagic flux in cancer cells. *Autophagy* **8**: 1215-1226

Zhou F, Yang Y, Xing D (2011). Bcl-2 and Bcl-xL play important roles in the crosstalk between autophagy and apoptosis. *FEBS J* **278**: 403-413

Zhou X, Babu JR, da Silva S et al. (2007). Unc-51-like kinase 1/2-mediated endocytic processes regulate filopodia extension and branching of sensory axons. *Proc Natl Acad Sci U S A* **104**: 5842-5847

Zhu JH, Horbinski C, Guo F et al. (2007). Regulation of autophagy by extracellular signal-regulated protein kinases during 1-methyl-4-phenylpyridinium-induced cell death. *Am J Pathol* **170**: 75-86

Zhu Y, Zhao L, Liu L et al. (2010). Beclin 1 cleavage by caspase-3 inactivates autophagy and promotes apoptosis. *Protein Cell* **1**: 468-477

Zoncu R, Bar-Peled L, Efeyan A et al. (2011a). mTORC1 senses lysosomal amino acids through an inside-out mechanism that requires the vacuolar H(+)-ATPase. *Science* **334**: 678-683

Zoncu R, Efeyan A, Sabatini DM (2011b). mTOR: from growth signal integration to cancer, diabetes and ageing. *Nature reviews Molecular cell biology* **12**: 21-35

Zong WX, Lindsten T, Ross AJ et al. (2001). BH3-only proteins that bind pro-survival Bcl-2 family members fail to induce apoptosis in the absence of Bax and Bak. *Genes Dev* **15**: 1481-1486

Zou H, Henzel WJ, Liu X et al. (1997). Apaf-1, a human protein homologous to C. elegans CED-4, participates in cytochrome c-dependent activation of caspase-3. *Cell* **90**: 405-413

Zou H, Li Y, Liu X et al. (1999). An APAF-1.cytochrome c multimeric complex is a functional apoptosome that activates procaspase-9. *J Biol Chem* **274**: 11549-11556

Zuckerman V, Wolyniec K, Sionov RV et al. (2009). Tumour suppression by p53: the importance of apoptosis and cellular senescence. *J Pathol* **219**: 3-15

5. Abbreviations

17AAG	17-allylamino-17-demethoxygeldanamycin
4E-BP1	eukaryotic translation initiation factor 4E (eIF4E)-binding protein 1
aa	amino acid
ACC	acetyl-CoA carboxylase
AEN	apoptosis-enhancing nuclease
AICAR	5-Aminoimidazole-4-carboxamide 1-β-D-ribofuranoside
AIF	apoptosis-inducing factor
AIM	Atg8-family interacting motif
Alfy	Autophagy-linked FYVE protein
AMBRA1	Activating molecule in Beclin 1-regulated autophagy protein 1
AMPK	AMP-activated protein kinase
Apaf	apoptotic protease activating factor
apg	autophagy
ASK1	apoptosis signal-regulating kinase 1
ATF4	Activating transcription factor 4
Atg	autophagy-related gene
aut	autophagy
Bad	Bcl-2 antagonist of cell death
BAG3	Bcl-2-associated athanogene 3
Bak	Bcl-2 homologous antagonist/killer
β-APP	β-amyloid precursor protein
BAPTA-AM	1,2-Bis(2-aminophenoxy)ethane-N,N,N',N'-tetraacetic acid tetrakis(acetoxymethyl ester)
Barkor	Beclin 1-associated autophagy-related key regulator
Baron	Beclin-1 associated RUN domain containing protein
Bax	Bcl-2-associated X protein
Bbc3	Bcl-2-binding component 3
Bcl	B-cell CLL/lymphoma
BCR	B cell antigen receptor
BH	Bcl-2 homology
Bif-1	Bax-interacting factor 1
Bik	Bcl-2-interacting killer
Bim-S/-L/-EL	Bcl2-interacting mediator of cell death (short, long, extra long)
BIR	baculoviral IAP repeats
Bmf	Bcl-2-modifying factor
BNIP	BCL2/adenovirus E1B 19 kDa protein-interacting protein
BNIP3L	BNIP3-like
Bod	Bcl-2-related ovarian death protein
Bok	Bcl-2-related ovarian killer protein
BRCC2	breast cancer cell protein 2
Btk	Bruton tyrosine kinase
c-Abl	cellular Abelson tyrosine protein kinase
CaMKK	Ca^{2+}/calmodulin-dependent kinase kinase
cAMP	cyclic AMP
CARD	caspase-recruitment domain
CBM	carbohydrate-binding module
CBP	CREB-binding protein
CBS	cystathionine β-synthase
c-Cbl	cellular Casitas B-lineage lymphoma
CCCP	carbonyl cyanide m-chlorophenylhydrazone
CD	cluster of differentiation
Cdk	cyclin-dependent kinase
ced	cell death abnormal
c-FLIP	cellular FLICE-inhibitory proteins
c-IAP	cellular inhibitor of apoptosis

CK2	casein kinase 2
CLL	chronic lymphocytic leukemia
COP1	constitutive photomorphogenesis protein 1
CPP32	cysteine protease p32
CREB	cAMP-response element binding protein
CTD	C-terminal domain
Cvt	cytoplasm-to-vacuole targeting
(d)ADP	(2'-deoxy)adenosine diphosphate
DAG	diacylglycerol
(d)AMP	(2'-deoxy)adenosine monophosphate
DAP1	death-associated protein 1
DAPK	death-associated protein kinase
(d)ATP	(2'-deoxy)adenosine triphosphate
DcR	decoy receptor
DD	death domain
DED	death effector domain
DEPTOR	DEP domain containing mTOR-interacting protein
DFCP1	double FYVE domain-containing protein 1
DFF	DNA fragmentation factor
DIABLO	direct IAP-binding protein with low pI
DISC	death-inducing signaling complex
DNA	deoxyribonucleic acid
Dok-3	downstream of kinase-3
DR	death receptor
DRAM	damage-regulated autophagy modulator
DYRK	Dual specificity tyrosine-phosphorylation-regulated kinase
EAT	early autophagy targeting/tethering
(E)GFP	(enhanced) green fluorescent protein
endoG	endonuclease G
ER	endoplasmic reticulum
ERK	extracellular signal-regulated kinase
Exo84	exocyst complex protein of 84 kDa
FADD	Fas-associating protein with a novel death domain
FAK	focal adhesion kinase
Fas	Fas antigen
FasL	Fas ligand
FAT	FRAP, ATM, TRRAP
FBD	FIP200-binding domain
FcγRIIb	Fcγ receptor IIb
FIP200	FAK family interacting protein of 200 kDa
FKBP12	FK506 binding protein of 12 kDa
FLICE	FADD-like ICE
FoxO	forkhead box protein O
FRB	FKBP12-rapamycin binding
FRET	Förster resonance energy transfer
FYVE	Fab1, YOTB/ZK632.12, Vac1, EEA1 (first four proteins discovered to share this domain)
GABARAP	γ-aminobutyric acid receptor associated protein
GABARAPL	GABARAP-like
GAP	GTPase activating protein
GATE16	Golgi-associated ATPase enhancer of 16 kDa
gld	generalized lymphoproliferative disease
GPCR	G protein-coupled receptor
Grb2	growth factor receptor-bound 2
gsa	glucose-induced selective autophagy
GSK3	glycogen synthase kinase 3
GβL	G protein β subunit-like

HD	helical domain
HDAC	histone deacetylase
Hdm2	human double minute 2
HEAT	huntingtin, elongation factor 3, a subunit of protein phosphatase 2A, TOR1
HEK293	human embryonic kidney 293 cell line
HIV	human immunodeficiency virus
HMGB1	high mobility group box 1
HORMA	Hop1p, Rev7p, Mad2
Hrk	protein harakiri
Hsp90	heat shock protein of 90 kDa
HtrA2	high temperature requirement protein A2
I-κB	inhibitor of κB
IAP	inhibitor of apoptosis
(I)CAD	(inhibitor of) caspase-activated DNase
ICE	IL-1β converting enzyme
Ig	immunoglobulin
IGF1	insulin-like growth factor 1
IGF1(-R)	insulin-like growth factor 1 (receptor)
IKK-α	I-κB kinase-α
ILP-2	Inhibitor of apoptosis-like protein 2
IM	isolation membrane
INPP5B	inositol polyphosphate 5-phosphatase
IP_3(R)	inositol 1,4,5-trisphosphate (receptor)
IRS-1	insulin receptor substrate-1
ISG20L1	interferon-stimulated 20 kDa exonuclease-like 1
JNK	c-Jun N-terminal kinase
kDa	kilodalton
LAP	LC3-associated phagocytosis
LARD	lymphocyte-associated receptor of death
LAT2	linker for activation of T cells family member 2
LIR	LC3-interacting region
LKB1	liver kinase 1
lpr	lymphoproliferation
LPS	lipopolysaccharide
LRS	LC3 recognition sequence
LUBAC	linear ubiquitin assembly complex
MACH	MORT1-associated CED-3 homolog
MAP1B	microtubule-associated protein 1B
(MAP1)LC3	(microtubule-associated proteins 1A/1B) light chain 3
MAPK	mitogen-activated protein kinase
MAPKK4	mitogen-activated protein kinase kinase 4
Mch	mammlian ced-3 homolog
Mcl-1	myeloid cell leukemia 1
MCU	mitochondrial Ca^{2+} uniporter
Mdm2	mouse double minute 2
mE10	mammalian CARD-containing adapter molecule E10
MEF	mouse embryonic fibroblast
MEK	MAPK/ERK kinase
MICU1	mitochondrial Ca^{2+} uptake 1
MLC(K)	myosin light chain (kinase)
ML-IAP	Melanoma inhibitor of apoptosis protein
MLK3	mixed lineage kinase 3
mLST8	mammalian lethal with sec-13 protein 8
MOM(P)	mitochondria outer membrane (permeabilization)
MORT1	mediator or receptor-induced toxicity 1
mSin1	mammalian stress-activated map kinase-interacting protein 1
Mtd	protein matador

(m)TOR	(mechanistic or mammalian) target of rapamycin
mTORC	mTOR complex
MULE	Mcl-1 ubiquitin ligase E3
MyD88	myeloid differentiation factor 88
NAF-1	nutrient-deprivation autophagy factor-1
NAIP	Neuronal apoptosis inhibitory protein
NBD	nucleotide-binding domain
Nbk	natural born killer
NBR1	neighbour of breast cancer 1
NDP52	nuclear domain 10 protein 52
NEF	negative factor
NF-κB	nuclear factor for κ gene in B lymphocytes
NFAT	nuclear factor of activated T cells
NGF	nerve growth factor
Nix	NIP3-like protein X
NLS	nuclear localization sequence
NOD	nucleotide-binding and oligomerization domain
Nod1	nucleotide-binding and oligomerization domain-containing protein 1
nPIST	neuronal PDZ protein interacting specifically with TC10
NTAL	non-T cell activation linker
OPG	osteoprotegrin
OPTN	optineurin
p53AIP1	p53-regulated apoptosis-inducing protein 1
p70S6K	p70 S6 kinase
pag	peroxisome degradation via autophagy
Parkin	Parkinson juvenile disease protein
PARP	poly(ADP-ribose) polymerase
PAS	pre-autophagosomal structure
paz	pexophagy zeocin-resistant
PB1	Phox and Bem1p
pdd	peroxisome degradation-deficient
PDK1	3-phosphoinositide-dependent protein kinase 1
PDZ	PSD95, Dlg1, zo-1 (first three proteins discovered to share this domain)
PE	phosphatidylethanolamine
PERP	p53 apoptosis effector related to PMP-22
PH	pleckstrin homology
$PI(3,4)P_2$	phosphatidylinositol 3,4-bisphosphate
$PI(3,4,5)P_3$ or PIP_3	phosphatidylinositol 3,4,5-trisphosphate
$PI(3,5)P_2$	phosphatidylinositol 3,5-bisphosphate
PI3K	phosphatidylinositol 3-kinase
PI3P	phosphatidylinositol 3-phosphate
PIASy	protein inhibitor of activated STAT protein y
PIDD	p53-induced protein with a death domain
PIF	PDK1-interacting fragment
PIG3	p53-induced gene 3 protein
PIKfyve	FYVE finger-containing phosphoinositide kinase
PINK1	PTEN-induced putative protein kinase 1
PIP5K1-β	phosphatidylinositol 4-phosphate 5-kinase type I β
PKA	protein kinase A
PKB	protein kinase B
PKC	protein kinase C
PKN	protein kinase N
PLC	phospholipase C
PP1	protein phosphatase 1
PP2A	protein phosphatase 2A
PRAS40	proline-rich Akt substrate of 40 kDa
protor	protein observed with rictor
PRR	pattern recognition receptor

PS	phosphatidylserine
PTEN	phosphatase and tensin homolog deleted on chromosome 10
Puma	p53 up-regulated modulator of apoptosis
Pyk2	proline-rich tyrosine kinase 2
RAIDD	RIP-associated ICH-1/CED-3 homologous protein with a death domain
raptor	regulatory-associated protein of mTOR
Ras	abbreviation originated from rat sarcoma
RB1	retinoblastoma 1
RB1CC1	RB1-inducible coiled-coil 1
REDD1	regulated in development and DNA damage response 1
RFP	red fluorescent protein
Rheb	Ras homolog enriched in brain
rictor	rapamycin-insensitive companion of mTOR
RING	really interesting new gene
RIPK	receptor-interacting serine/threonine-protein kinase
RNA	ribonucleic acid
RNAi	RNA interference
ROS	reactive oxygen species
RSK	ribosomal protein S6 kinase
RTK	receptor (-associated) tyrosine kinase
Rubicon	RUN domain protein as Beclin 1 interacting and cysteine-rich containing
RyR	ryanodine receptor
SAHA	suberoylanilide hydroxamic acid
SAPK	stress-activated protein kinase
SCV	*Salmonella*-containing vacuole
SDS-PAGE	sodium dodecylsulfate
Sec5	exocyst complex component Sec5
SEK1	SAPK/ERK kinase 1
SERCA	sarcoplasmic/endoplasmic reticulum Ca^{2+}-ATPase
SGK	serum/glucocorticoid-regulated kinase
SH	Src homology
SHIP	SH2 domain-containing inositol 5-phosphatase
SILAC	stable isotopes labeling by amino acids in cell culture
siRNA	small/short/silencing RNA
SLP-56	SH2 domain-containing leukocyte protein of 65 kDa
SMAC	second mitochondria-derived activator of caspase
SNAP-29	synaptosomal-associated protein 29
SNARE	soluble N-ethylmaleimide-sensitive factor attachment protein receptor
SNP	single nucleotide polymorphism
spautin-1	specific and potent autophagy inhibitor-1
SphK2	sphingosine kinase 2
Sqa	Spaghetti-squash activator
Sqh	Spaghetti-squash
Stat3	signal transducer and activator of transcription 3
STK36	Serine/threonine-protein kinase 36
STS	staurosporine
Stx17	syntaxin 17
SV40	simian virus 40
Syk	spleen tyrosine kinase
TAK1	transforming growth factor β-activated kinase-1
(t)Bid	(truncated) BH3-interacting domain death agonist
TCN	triciribine
TCR	T cell antigen receptor
Tecpr1	tectonin β-propeller repeat-containing protein 1
TG	thapsigargin
TGM2	transglutaminase-2
TIP60	Tat-interactive protein of 60 kDa
TLR	toll-like receptor

TNF(-R)	tumor necrosis factor (receptor)
TRADD	TNFR1-associated death domain
TRAF	tumor necrosis receptor-associated factor
TRAIL(-R)	TNF-related apoptosis-inducing ligand (receptor)
TRAMP	TNF receptor-related apoptosis-mediating protein
TRICK2	TRAIL receptor inducer of cell killing 2
TRIF	Toll-interleukin-1 receptor domain-containing adapter protein inducing IFNβ
TSC	tuberous sclerosis complex
Tti1/Tel2	Tel two interacting protein 1/telomere maintenance 2
UBA	ubiquitin-associated
Ulk	UNC-51-like kinase
UNC-51	uncoordinated 51
UPS	ubiquitin proteasome system
USP	ubiquitin-specific protease
UVRAG	UV radiation resistance-associated gene protein
VAMP8	vesicle-associated membrane protein 8
VAMP8	vesicle-associated membrane protein 8
v-ATPase	vacuolar H^+-ATPase
VDAC	voltage-dependent anion channel
VICS	vacuole-IM contact site
VMP1	vacuole membrane protein 1
Vps	vacuolar protein sorting protein
WHD	winged helix domain
WIPI	WD-repeat protein interacting with phosphoinositides
XIAP	X-linked IAP
YAP1	Yes-associated protein 1
ZAP70	zeta-chain associated protein of 70 kDa
ZIPK	zipper-interacting protein kinase

For L-amino acids, the single-letter code was used.

6. Curriculum Vitae

DR. RER. NAT. BJÖRN STORK

Date of birth: August 25th 1975

Place of birth: Herford (Germany)

Scientific Career History

since 09/2011	Group leader at the Institute of Molecular Medicine, University of Düsseldorf, Director: Prof. Dr. S. Wesselborg
07/2009-12/2009	Research stay in the Department of Biochemistry, Institute of Cancer Research, Norwegian Radium Hospital (Oslo, Norway), Director: Prof. Dr. H. Stenmark
10/2006-08/2011	Junior group leader in the research section 'Molecular Gastroenterology and Hepatology' at the Department of Internal Medicine I, University of Tübingen, Director: Prof. Dr. S. Wesselborg
07/2002-09/2006	Dissertation in the Department of Biochemistry and Molecular Immunology (University of Bielefeld), in the Department of Cellular and Molecular Immunology (University of Göttingen), and at Kansai Medical University (Osaka, Japan),
	Supervisors: Prof. Dr. J. Wienands, Prof. Dr. T. Kurosaki
	Title: '*A molecular basis for differential Ca^{2+} signalling in B lymphocytes*' (mit Auszeichnung)
08/2001-04/2002	Diploma thesis in the Department of Biochemistry and Molecular Immunology, University of Bielefeld, Supervisor: Prof. Dr. J. Wienands
	Title: '*How does the antigen receptor on B lymphocytes organize the Ca^{2+} initiation complex?*' (mit Auszeichnung)
01/2000-08/2000	Semester at McGill University, Montréal, Canada
1996-2001	Studies of Biochemistry, University of Bielefeld

7. Publication list

7.1 Original works

	Publication
1.	Dieterle AM, Böhler P, Keppeler H, Alers S, Berleth N, Drießen S, Hieke N, Pietkiewicz S, Löffler AS, Peter C, Gray A, Leslie NR, Shinohara H, Kurosaki T, Engelke M, Wienands J, Bonin M, Wesselborg S, Stork B. The 3-phosphoinositide-dependent protein kinase 1 (PDK1) controls upstream PI3K expression and PIP_3 generation. **Oncogene** 2013;accepted
2.	Beck D, Niessner H, Smalley KS, Flaherty K, Paraiso KH, Busch C, Sinnberg T, Vasseur S, Iovanna JL, Drießen S, Stork B, Wesselborg S, Schaller M, Biedermann T, Bauer J, Lasithiotakis K, Weide B, Eberle J, Schittek B, Schadendorf D, Garbe C, Kulms D, Meier F. Vemurafenib potently induces endoplasmic reticulum stress-mediated apoptosis in BRAFV600E melanoma cells. **Sci Signal** 2013; 6(260):ra7
3.	Lösing M, Goldbeck I, Manno B, Oellerich T, Schnyder T, Bohnenberger H, Stork B, Urlaub H, Batista FD, Wienands J, Engelke M. The Dok-3/Grb2 signal module attenuates Lyn-dependent activation of Syk in B cell antigen receptor microclusters. **J Biol Chem** 2013;288:2303-2313.
4.	Alers S, Löffler AS, Paasch F, Dieterle AM, Keppeler H, Lauber K, Campbell DG, Fehrenbacher B, Schaller M, Wesselborg S, Stork B. Atg13 and FIP200 act independently of Ulk1 and Ulk2 in autophagy induction. **Autophagy** 2011;7:1424-1433.
5.	Manns J, Daubrawa M, Driessen S, Paasch F, Hoffmann N, Löffler A, Lauber K, Dieterle A, Alers S, Iftner T, Schulze-Osthoff K, Stork B*, Wesselborg S*. Triggering of a novel intrinsic apoptosis pathway by the kinase inhibitor staurosporine: activation of caspase-9 in the absence of Apaf-1. **FASEB J** 2011;25:3250-3261.
6.	Löffler AS, Alers S, Dieterle AM, Keppeler H, Franz-Wachtel M, Kundu M, Campbell DG, Wesselborg S, Alessi DR, Stork B. Ulk1-mediated phosphorylation of AMPK constitutes a negative regulatory feedback loop. **Autophagy** 2011;7:696-706.
7.	Grotemeier A, Alers S, Pfisterer S, Paasch F, Daubrawa M, Dieterle A, Viollet B, Wesselborg S, Proikas-Cezanne T, Stork B. AMPK-independent induction of autophagy by cytosolic Ca^{2+} increase. **Cell Signal** 2010;22:914-925.
8.	Jacobi CA, Schiffner F, Henkel M, Waibel M, Stork B, Daubrawa M, Eberl L, Gregor M, Wesselborg S. Effects of bacterial N-acyl homoserine lactones on human Jurkat T lymphocytes-OdDHL induces apoptosis via the mitochondrial pathway. **Int J Med Microbiol** 2009;299:509-519.

9.	Dieterle A, Orth R, Daubrawa M, Grotemeier A, Alers S, Ullrich S, Lammers R, Wesselborg S, Stork B. The Akt inhibitor triciribine sensitizes prostate carcinoma cells to TRAIL-induced apoptosis. **Int J Cancer** 2009;125:932-941.
10.	Ranta F, Düfer M, Stork B, Wesselborg S, Drews G, Häring HU, Lang F, Ullrich S. Regulation of calcineurin activity in insulin-secreting cells: stimulation by Hsp90 during glucocorticoid-induced apoptosis. **Cell Signal** 2008;20:1780-1786.
11.	Fluhr H, Krenzer S, Stein GM, Stork B, Deperschmidt M, Wallwiener D, Wesselborg S, Zygmunt M, Licht P. Interferon-gamma and tumor necrosis factor-alpha sensitize primarily resistant human endometrial stromal cells to Fas-mediated apoptosis. **J Cell Sci** 2007;120:4126-4133.
12.	Stork B, Neumann K, Goldbeck I, Alers S, Kähne T, Naumann M, Engelke M, Wienands J. Subcellular localization of Grb2 by the adaptor protein Dok-3 restricts the intensity of Ca^{2+} signaling in B cells. **EMBO J** 2007;26:1140-1149.
13.	Stork B, Engelke M, Frey J, Horejsi V, Hamm-Baarke A, Schraven B, Kurosaki T, Wienands J. Grb2 and the non-T cell activation linker NTAL constitute a Ca^{2+}-regulating signal circuit in B lymphocytes. **Immunity** 2004;21:681-691.

*** equal contribution**

7.2 Reviews, Book Chapters and Additional Publications

	Reviews
14.	Klionsky D, …, Stork B, … (1296 authors). Guidelines for the use and interpretation of assays for monitoring autophagy. **Autophagy** 2012;8:445-544.
15.	Alers S, Löffler AS, Wesselborg S, Stork B. The incredible ULKs. **Cell Commun Signal** 2012;10:7.
16.	Alers S, Löffler AS, Wesselborg S, Stork B. Role of AMPK-mTOR-Ulk1/2 in the Regulation of Autophagy: Cross Talk, Shortcuts, and Feedbacks. **Mol Cell Biol** 2012;32:2-11.
17.	Engelke M, Engels N, Dittmann K, Stork B, Wienands J. Ca^{2+} signaling in antigen receptor-activated B lymphocytes. **Immunol Rev** 2007;218:235-246.

	Book Chapters
18.	Stork B, Alers S, Löffler AS, Wesselborg S. Regulation of Autophagy by Protein Phosphorylation. **Protein Phosphorylation in Human Health** 2012: 97-128. InTech Open
19.	Wesselborg S, Stork B. Apoptosis. **Encyclopedia of Molecular Mechanisms of Disease** 2009: 133-135. Springer-Verlag
	Additional Publications
20.	Stork B, Dieterle A, Wesselborg S. Überwindung der Therapieresistenz durch Akt/PKB-Inhibition. **Laborwelt** 2009;10(5):4-6

8. Addendum

Selected Research Articles summarized in chapter 2

The EMBO Journal (2007) 26, 1140–1149 | © 2007 European Molecular Biology Organization | All Rights Reserved 0261-4189/07
www.embojournal.org

THE EMBO JOURNAL

Subcellular localization of Grb2 by the adaptor protein Dok-3 restricts the intensity of Ca^{2+} signaling in B cells

Björn Stork[1,3], Konstantin Neumann[1,3], Ingo Goldbeck[1,3], Sebastian Alers[1], Thilo Kähne[2], Michael Naumann[2], Michael Engelke[1] and Jürgen Wienands[1,*]

[1]Institute of Cellular and Molecular Immunology, Georg August University of Göttingen, Göttingen, Germany and [2]Institute of Experimental Internal Medicine, Otto von Guericke University, Magdeburg, Germany

Spatial and temporal modulation of intracellular Ca^{2+} fluxes controls the cellular response of B lymphocytes to antigen stimulation. Herein, we identify the hematopoietic adaptor protein Dok-3 (downstream of kinase-3) as a key component of negative feedback regulation in Ca^{2+} signaling from the B-cell antigen receptor. Dok-3 localizes at the inner leaflet of the plasma membrane and is a major substrate for activated Src family kinase Lyn. Phosphorylated Dok-3 inhibits antigen receptor-induced Ca^{2+} elevation by recruiting cytosolic Grb2, which acts at this location as a negative regulator of Bruton's tyrosine kinase. This leads to diminished activation of phospholipase C-γ2 and reduced production of soluble inositol trisphosphate. Hence, the Dok-3/Grb2 module is a membrane-associated signaling organizer, which orchestrates the interaction efficiency of Ca^{2+}-mobilizing enzymes.

The EMBO Journal (2007) **26,** 1140–1149. doi:10.1038/sj.emboj.7601557; Published online 8 February 2007
Subject Categories: signal transduction; immunology
Keywords: adaptor proteins; B-cell activation; Ca^{2+} mobilization; plasma membrane recruitment; tyrosine phosphorylation

Introduction

Development, survival and activation of B lymphocytes are tightly controlled by intracellular Ca^{2+} ions, which act as second messengers in a wide range of signaling pathways (Gallo *et al*, 2006). The regulation of Ca^{2+} concentrations is a key function of the B-cell antigen receptor (BCR). BCR ligation triggers elevation of intracellular Ca^{2+} concentrations through activation of spleen tyrosine kinase Syk and subsequent phosphorylation of the adaptor protein SLP-65 (Wienands *et al*, 1998) (alternatively called BLNK, (Fu *et al*, 1998) or BASH, (Goitsuka *et al*, 1998)). Phosphorylated SLP-65 recruits Bruton's tyrosine kinase (Btk) and phospholipase C-γ2 (PLC-γ2) into a trimolecular Ca^{2+} initiation complex (Hashimoto *et al*, 1999; Ishiai *et al*, 1999a, b; Su *et al*, 1999; Chiu *et al*, 2002). This allows phosphorylation-mediated activation of PLC-γ2, which in turn hydrolyzes membrane phospholipids to yield soluble inositol trisphosphate (IP3) (Kurosaki and Tsukada, 2000). IP3 receptors are ligand-gated Ca^{2+} channels located in the membrane of the endoplasmic reticulum (ER), which stores intracellular Ca^{2+}. Hence, IP3 production causes the release of Ca^{2+} from the ER into the cytosol. The IP3-driven intracellular Ca^{2+} flux is followed by entry of Ca^{2+} from the extracellular space through weakly characterized membrane channels (Parekh and Putney, 2005; Putney, 2005). This biphasic character of the Ca^{2+} response allows shaping of the Ca^{2+} signal in the dimensions space and time, which is thought to contribute to cell fate determination during B-cell differentiation (Dolmetsch *et al*, 1997, 1998). Indeed, Koncz *et al* (2002) and Hoek *et al* (2006) reported differential Ca^{2+} signaling in BCR-activated splenic B-cell populations, which represent distinct developmental stages and are known to respond to antigen stimulation with induction of either anergy, clonal deletion or proliferation (Niiro and Clark, 2002).

Several negative regulators of the Ca^{2+} activation cascade have been described. Most prominently, the SH2 domain-containing 5′-inositol phosphatase (SHIP) interferes with membrane recruitment and concomitant activation of Btk or PLC-γ2 by disrupting the lipid binding motifs for the enzyme's pleckstrin homology (PH) domains at the inner leaflet of the plasma membrane (Ono *et al*, 1997; Bolland *et al*, 1998; Okada *et al*, 1998; Kim *et al*, 1999; Brauweiler *et al*, 2000). Also the protein tyrosine phosphatase SHP-1 and the inhibitory C-Src kinase (Csk) are implicated in the attenuation of BCR-regulated Ca^{2+} elevation and inhibition of cellular activation (Ono *et al*, 1997; Adachi *et al*, 2001). Our group has recently described the downmodulation of intra- and extracellular Ca^{2+} fluxes by the adaptor protein Grb2 (growth factor receptor-bound protein 2) (Stork *et al*, 2004). Grb2 is expressed in all cell types and throughout the B-cell lineage. It is composed of a central Src homology (SH) 2 domain flanked on either side by one SH3 domain (Lowenstein *et al*, 1992). DT40 B-cell mutants, which were rendered deficient for Grb2 expression by gene targeting (Hashimoto *et al*, 1998), but not their wild-type counterparts, showed a sustained biphasic Ca^{2+} response following BCR engagement (Stork *et al*, 2004). This raised the question how Grb2-positive B cells of the peripheral lymph organs mount a full Ca^{2+} response, which is mandatory for their antigen-mediated activation and differentiation. It turned out that stimulation-induced recruitment of cytosolic Grb2 into the lipid raft fraction of the plasma membrane prevents Ca^{2+} inhibition (Stork *et al*, 2004). Relocalization can be achieved

*Correspondence: Institute of Cellular and Molecular Immunology, Georg August University of Göttingen, Humboldtallee 34, 37073 Göttingen, Germany. Tel.: +49 (0)551 39 5812; Fax: +49 (0)551 39 5843, E-mail: jwienan@uni-goettingen.de
[3]These authors contributed equally to this work

Received: 17 October 2006; accepted: 19 December 2006; published online: 8 February 2007

by transmembrane adaptor proteins such as NTAL (non-T-cell activation linker), which upon tyrosine phosphorylation bind the SH2 domain of Grb2. NTAL expression is low in developing B cells showing a weak Ca^{2+} response, but high in mature B cells with robust Ca^{2+} elevation (Stork *et al*, 2004; Hoek *et al*, 2006). A number of additional transmembrane adaptor proteins with consensus binding sites for the Grb2 SH2 domain exist (Horejsi *et al*, 2004) and may subrogate NTAL function, for example, in NTAL-deficient mouse mutants, which possess immunocompetent B cells (Wang *et al*, 2005). The effector proteins that execute Grb2-mediated Ca^{2+} inhibition are unknown. Here we report the identification of the critical Grb2 partner for Ca^{2+} inhibition as the hematopoietic adaptor protein Dok-3 (Cong *et al*, 1999; Lemay *et al*, 2000). SH2-mediated recruitment of Grb2 to tyrosine-phosphorylated Dok-3 at the plasma membrane attenuates Btk-mediated PLC-γ2 phosphorylation independently of SHIP and Csk. Unlike positive Grb2 regulators with transmembraneous and palmitoylated polypeptide anchors, Dok-3 is tethered at the inner side of the plasma membrane through its PH domain. Hence, Dok-3 appears to direct Grb2 into a distinct membrane compartment. In this location Grb2 acts as a negative regulator of Btk, resulting in diminished PLC-γ2 activity. These findings exert a molecular basis for differential Ca^{2+} signals in B cells and moreover, directly enforce the concept that precise membrane compartmentalization of signaling elements determines positive versus negative cellular responses.

Results

Grb2 controls inducible phosphorylation of Dok-3, the main tyrosine kinase substrate protein in DT40 B cells

To assess the signaling role of Grb2 in B cells, we analyzed BCR-induced tyrosine phosphorylation in wild-type and

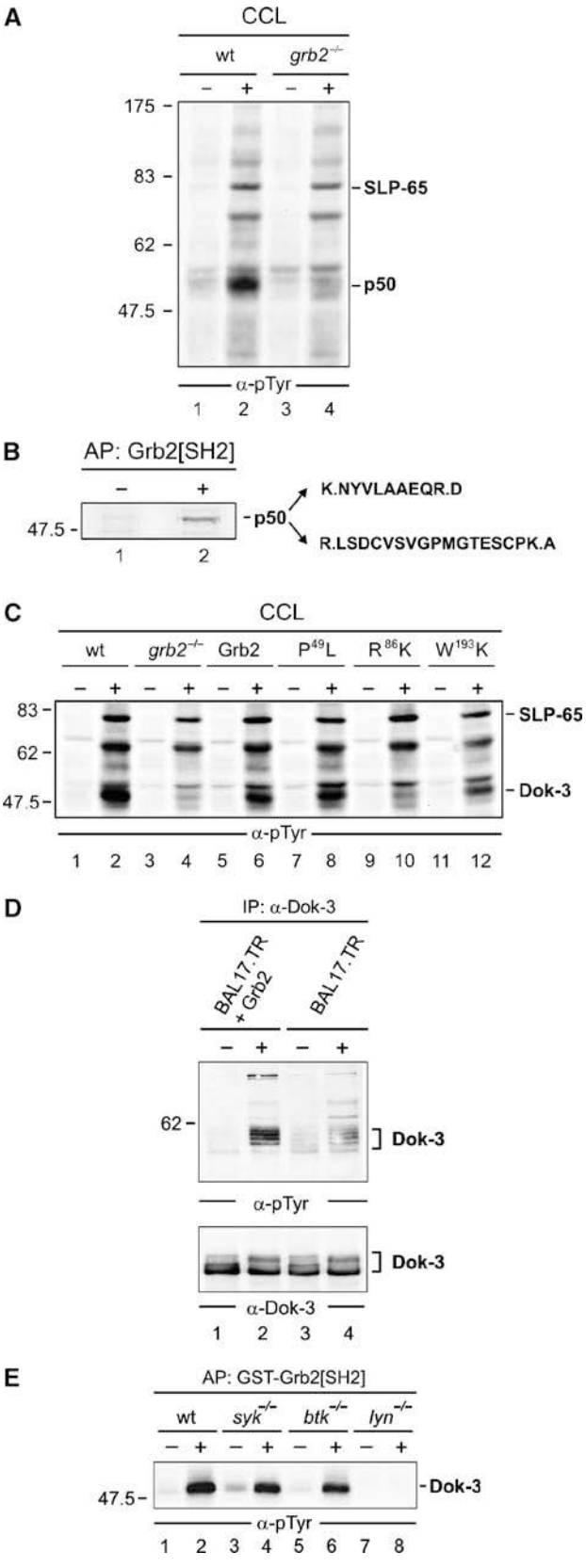

Figure 1 Grb2 controls Lyn-mediated phosphorylation of the adaptor protein Dok-3. (**A**) Wild-type (wt) and Grb2-deficient (*grb2*$^{-/-}$) DT40 cells (lanes 1, 2 and 3, 4) were left untreated (−) or stimulated through their BCRs for 3 min (+). Equal amounts of proteins from cleared cellular lysates (CCL) were analyzed by anti-phosphotyrosine (α-pTyr) immunoblotting. (**B**) The major phosphotyrosine-containing protein, p50, was affinity-purified (AP) by GST-Grb2[SH2] from stimulated DT40 cells (lane 2), silver-stained, excised, digested by trypsine and peptide products were analyzed by ESI-Trap mass spectrometry. Purified proteins from unstimulated cells served as negative control (lane 1). The obtained amino-acid sequences are shown (single-letter code) with lysine (K) and arginine (R) being inferred from trypsine cleavage specificity (indicated by dots). These sequences matched a partial chicken EST (GenBank accession number XP_427516). Full-length chicken cDNA was isolated and submitted to GenBank with the accession number EF051736 (see also Supplementary Figure S1). (**C**) Wild-type (lanes 1 and 2) and *grb2*$^{-/-}$ DT40 cells (lanes 3 and 4) reconstituted with either wild-type Grb2 (lanes 5 and 6) or Grb2 variants, in which one of the three SH domains has been inactivated by single amino-acid substitution (N-terminal SH3 domain, $P^{49}L$; SH2 domain, $R^{86}K$; C-terminal SH3 domain, $W^{193}K$; lanes 7–12), were left untreated (−) or stimulated through their BCRs (+). Equal amounts of proteins from CCL were subjected to anti-pTyr immunoblotting. To confirm equal loading, phospho-SLP-65 was detected separately by anti-SLP-65 immunoblotting (data not shown). (**D**) Murine Bal17.TR B cells, deficient for Grb2 expression, were transfected with an expression vector for Grb2 (lanes 1 and 2) or the empty vector as control (lanes 3 and 4) and left untreated (−) or stimulated through their BCRs (+). CCL were subjected to anti-Dok-3 immunoprecipitation and purified proteins were analyzed by immunoblotting with antibodies to pTyr and Dok-3 (upper and lower panels, respectively). (**E**) Resting (−) or BCR-activated (+) wild-type DT40 cells (lanes 1 and 2) or variants deficient for the protein tyrosine kinase Syk (lanes 3 and 4), Btk (lanes 5 and 6) or Lyn (lanes 7 and 8) were lysed and subjected to affinity purification with GST-Grb2[SH2]. Phosphorylated Dok-3 was detected by anti-pTyr immunoblotting. Relative molecular masses of marker proteins are indicated on the left in kDa.

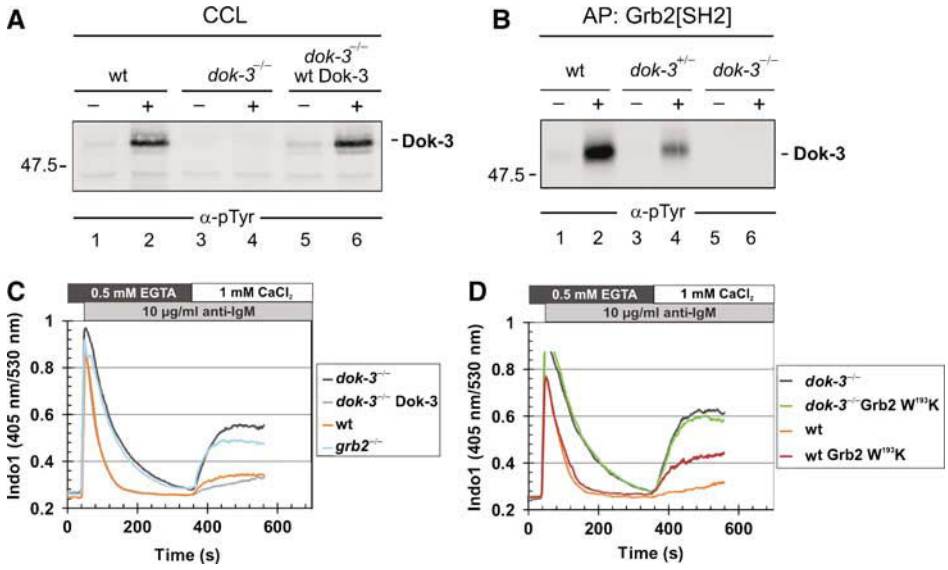

Figure 2 Gene targeting reveals a negative regulatory role of Dok-3. (**A**) Dok-3-deficient DT40 B cells were generated by targeted disruption of both *dok-3* alleles (*dok-3*$^{-/-}$, see Materials and methods for details), and absence of tyrosine-phosphorylated p50/Dok-3 in cleared cellular lysates (CCL) of resting (−) and BCR-activated (+) cells was tested by anti-pTyr immunoblotting (lanes 3 and 4). As control, wild-type DT40 and Dok-3-reconstituted *dok-3*$^{-/-}$ cells were analyzed in parallel (lanes 1 and 2 and 5 and 6, respectively). (**B**) Wild-type DT40 cells (lanes 1 and 2), heterozygous *dok-3*$^{+/-}$ (lanes 3 and 4) and homozygous *dok-3*$^{-/-}$ mutants (lanes 5 and 6) were left untreated (−) or stimulated through their BCRs (+). Cell lysates were subjected to affinity purification with the GST-Grb2[SH2] fusion protein and proteins so obtained were analyzed by anti-pTyr immunoblotting. Relative molecular mass of marker protein is indicated in (A) and (B) on the left in kDa. (**C, D**) BCR-induced intra- and extracellular Ca^{2+} mobilization of the indicated DT40 cells was recorded by flow cytometry as described in detail in Materials and methods. Briefly, cells were loaded with Indo-1 and release of intracellular Ca^{2+} was measured for 6 min in the presence of EGTA. Subsequently, extracellular Ca^{2+} was restored to 1 mM in order to monitor Ca^{2+} entry across the plasma membrane. Lines represent wild-type DT40 (orange), *dok-3*$^{-/-}$ mutants (black), Dok-3-reconstituted *dok-3*$^{-/-}$ cells (gray), *grb2*$^{-/-}$ mutants (blue) and wild-type and *dok-3*$^{-/-}$ transfectants expressing the dominant-negative $W^{193}K$ version of Grb2 (brown and green, respectively). Data are representative of at least three independent measurements.

Grb2-deficient DT40 cells. Anti-phosphotyrosine (pTyr) immunoblotting of cleared cellular lysates revealed that the main tyrosine kinase substrate protein, migrating with an apparent molecular mass of approximately 50 kDa (p50), remains almost unphosphorylated in the absence of Grb2 (Figure 1A). The association of phosphorylated p50 with the Grb2 SH2 domain (data not shown) was employed to affinity-purify large amounts of p50 from stimulated DT40 cells in order to determine the peptide profile of tryptic digestion products by mass spectrometry (Figure 1B). The obtained peptide amino-acid sequences matched to a partial chicken EST (GenBank accession number XP_427516), which shows highest homology to the murine adaptor protein downstream of kinase-3 (Dok-3). Murine Dok-3 encompasses one PH and one PTB domain at its N-terminal end, followed by consensus tyrosine phosphorylation motifs in the C-terminal half (Lemay *et al*, 2000). Our cloning of the full-length avian *dok-3* cDNA revealed that this overall structure is evolutionary conserved and that avian Dok-3 shares 68% and 62% amino-acid sequence homology to its murine and human orthologs, respectively (Supplementary Figure S1). The identity of p50 and Dok-3 was confirmed by anti-Dok-3 immunopurification (data not shown). Further reconstitution experiments with Grb2-deficient cells showed that efficient Dok-3 phosphorylation is independent of the N-terminal SH3 domain of Grb2, but requires the SH2 and C-terminal SH3 domains (Figure 1C, lanes 7–12). Similar to avian Dok-3, efficient tyrosine phosphorylation of murine Dok-3 is also dependent on Grb2 expression, as revealed by our analysis of Grb2-deficient mouse B-cell line Bal-17.TR and its Grb2-reconstituted transfectants (Figure 1D). As shown in Figure 1E, inducible tyrosine phosphorylation of Dok-3 is detectable in the absence of Syk (lanes 3 and 4) and Btk (lanes 5 and 6), but requires expression of the Src family kinase Lyn (lanes 7 and 8). Collectively, these data identify the intracellular adaptor protein Dok-3 as a major substrate of Src family kinases in activated B cells. The efficiency of Dok-3 tyrosine phosphorylation is, however, critically dependent on the additional presence of Grb2, which we have previously described as a negative regulator of BCR-induced Ca^{2+} mobilization.

Dok-3 is a negative regulator of BCR-induced Ca^{2+} mobilization

To functionally characterize Dok-3, we generated a Dok-3-deficient DT40 variant by gene targeting (see Materials and methods and Supplementary Figure S2A for details). Successful inactivation of *dok-3* alleles and ablation of protein expression was confirmed by genomic PCR analysis (Supplementary Figure S2B) and anti-pTyr immunoblotting of cleared cellular lysates, Grb2[SH2]-purified proteins and anti-Dok-3-immunoprecipitates (Figure 2A and B; Supplementary Figure S2C). Note that Dok-3 tyrosine phosphorylation is considerably reduced in heterozygous *dok-3*$^{+/-}$ cells (Figure 2B, lanes 1–4).

Given the reported role of Grb2 for BCR-induced Ca^{2+} signaling (Stork *et al*, 2004), we next tested this response in various DT40 cell lines, which are positive or negative for Dok-3 or Grb2 (Figure 2C). In marked contrast to wild-type DT40 cells, Dok-3-deficient cells show a biphasic Ca^{2+} profile, which is almost identical to that of Grb2-deficient cells (Figure 2C, orange, black and blue lines). The monophasic Ca^{2+} response of wild-type DT40 cells, which is characteristic for B cells with an immature phenotype (Koncz *et al*, 2002; Stork *et al*, 2004; Hoek *et al*, 2006), was

restored in the Dok-3 mutant cells upon reconstitution with wild-type Dok-3 (gray line). These results show that similar to Grb2, Dok-3 is a negative regulatory element of BCR-induced Ca^{2+} mobilization. Moreover, both adaptor proteins appear to function in a common signaling pathway. To further confirm the latter notion, we employed a dominant-negative Grb2 mutant protein, which harbors an inactivated C-terminal SH3 domain ($W^{193}K$). Expression of Grb2 $W^{193}K$ in DT40 cells overwrote the inhibitory function of endogenous wild-type Grb2 and allowed extracellular Ca^{2+} influx (Figure 2D, brown and orange lines). In marked contrast, expression of the Grb2 $W^{193}K$ protein in Dok-3-deficient DT40 cells had no effect on the Ca^{2+} profile (black and green lines), which strongly suggests that Dok-3 and Grb2 build a functional unit to attenuate BCR-induced Ca^{2+} mobilization.

Plasma membrane tethering and association to Grb2 are sufficient for Dok-3 to inhibit Ca^{2+} signaling

To elucidate the structural requirements of Dok-3 for Ca^{2+} inhibition, we expressed a series of HA-tagged Dok-3 mutants (see Figure 3A) in *dok-3*$^{-/-}$ cells. Inactivation of the PTB domain ($R^{197}A$) had no effect on the ability of Dok-3 to

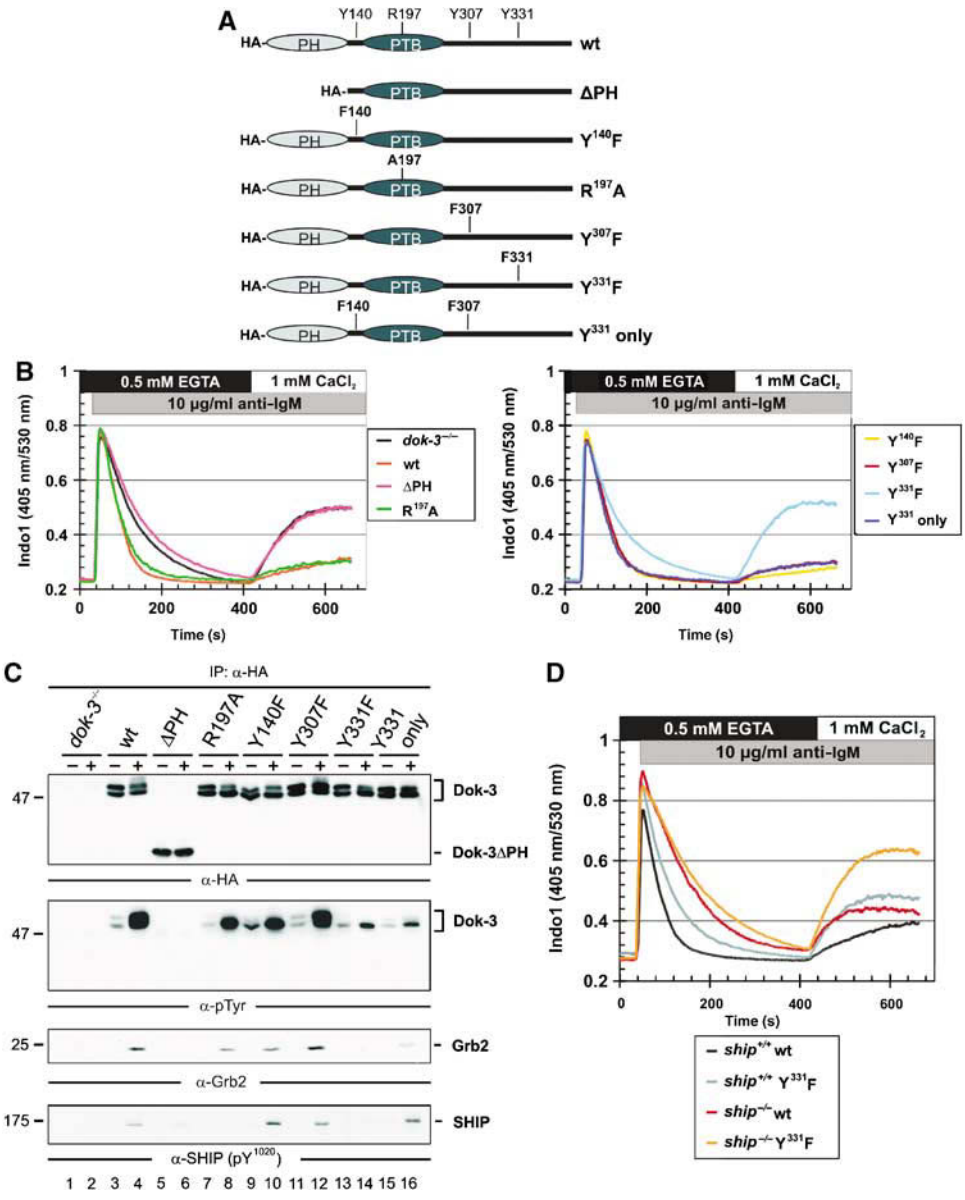

Figure 3 Dok-3 and Grb2 build a functional unit, that inhibits Ca^{2+} flux independent of SHIP. (**A**) Schematic representation of expression constructs encoding HA-tagged versions of wild-type Dok-3, a PH domain deletion mutant (ΔPH) or mutants encompassing amino-acid exchanges depicted in single-letter code. (**B**) Expression vectors were introduced by retroviral transduction in *dok-3*$^{-/-}$ mutants and BCR-induced Ca^{2+} mobilization of the transfectants was measured by flow cytometry, as described in the legend to Figure 2. Wild-type DT40 cells and empty vector transfectants of *dok-3*$^{-/-}$ mutants served as control (see inlay for color code). (**C**) Wild-type and DT40 variants described in (B) were left untreated (−) or BCR-activated (+) and lysates were subjected to anti-HA immunoprecipitation. Expression and tyrosine phosphorylation of Dok-3 proteins, as well as their association to Grb2 and SHIP, were detected by sequential immunoblotting with antibodies to HA, pTyr, Grb2 and SHIP (upper to lower panels, respectively). (**D**) BCR-induced Ca^{2+} fluxes were analyzed as described in the legend to Figure 2 in SHIP-deficient DT40 cells (*ship*$^{-/-}$, brown) and *ship*$^{-/-}$ transfectants expressing a Dok-3 $Y^{331}F$ variant that counteracts Ca^{2+} inhibition by endogenous wild-type Dok-3 (orange). As control, parental DT40 cells, which are positive for endogenous SHIP and Dok-3 (black), and the Dok-3 $Y^{331}F$ transfectants (gray) were analyzed in parallel, demonstrating the dominant-negative function of Dok-3 $Y^{331}F$.

prevent extracellular Ca^{2+} entry (Figure 3B, left panel, green and orange lines). Deletion of the PH domain (ΔPH) abolished Dok-3-mediated Ca^{2+} inhibition, which resulted in a biphasic response that was indistinguishable from that observed in cells with no Dok-3 expression (left panel, red and black lines). Single and dual Y-to-F amino-acid substitutions revealed that among the consensus tyrosine phosphorylation motifs of Dok-3, only that at Y^{331} is essential and sufficient for Ca^{2+} inhibition, whereas those at Y^{140} and Y^{307} are dispensable (right panel). Immunoprecipitation with anti-HA antibodies and subsequent immunoblot analysis showed that wild-type and mutant Dok-3 proteins are expressed by the transfectants at similar levels (Figure 3C, upper panel). This setting was also used to investigate the tyrosine phosphorylation status of the various Dok-3 proteins by anti-pTyr immunoblotting (Figure 3C, second panel). Inducible phosphorylation was easily and at almost identical levels detectable for wild-type Dok-3 (lanes 3 and 4) and Dok-3 mutants $R^{197}A$ and $Y^{140}F$ and $Y^{307}F$ (lanes 7–12), which all promoted the same biphasic Ca^{2+} profile (see above). In marked contrast, the Dok-3ΔPH protein did not become phosphorylated (lanes 5 and 6), and that of the $Y^{331}F$ mutant was strongly diminished (lanes 13 and 14). Both of these Dok-3 mutants were unable to support Ca^{2+} inhibition (see above). A strongly reduced tyrosine phosphorylation was also observed for the Y^{331} only protein (lanes 15 and 16) that, however, was fully capable of attenuating BCR-induced Ca^{2+} flux (see above). Collectively, we conclude that PH domain-mediated plasma membrane localization of Dok-3 is a requisite for Ca^{2+} inhibition, which itself is tightly associated with Dok-3 tyrosine phosphorylation. The latter event *per se* appears to be necessary but not sufficient for Ca^{2+} regulation. Rather, specific phosphorylation at Y^{331} is the second key element of Dok-3-mediated Ca^{2+} regulation.

Phosphorylation of Y^{331} creates a consensus binding site for the Grb2 SH2 domain. Indeed, the inducible association of Dok-3 with Grb2 was lost in cells expressing the $Y^{331}F$ mutant of Dok-3 (Figure 3C, third panel, lanes 13 and 14). Also the signaling-inactive ΔPH domain mutant did not co-immunoprecipitate with Grb2 (Figure 3C, third panel, lanes 5 and 6). For all other Dok-3 mutants, which retained their inhibitory capacity, BCR-induced complex formation with Grb2 was preserved (lanes 7–12). Hence, the biochemical property of inducible Grb2 association directly correlates with the functional ability of Dok-3 to downmodulate Ca^{2+} signals. This further demonstrates that Dok-3 and Grb2 together constitute a Ca^{2+}-regulating signaling module.

Dok-3 has been previously reported to associate with SHIP and Csk via the PTB domain and phospho-Y^{307}, respectively (Lemay *et al*, 2000; Robson *et al*, 2004). Indeed, the $R^{197}A$ amino-acid exchange in the PTB domain of Dok-3 abolished SHIP binding, which moreover appeared to require specific phosphorylation at Y^{331} (Figure 3C, lower panel). SHIP, however, is a well-known inhibitor of BCR-induced Ca^{2+} elevation, and it was therefore unexpected that disruption of the Dok-3/SHIP complex had no effect on the Ca^{2+} response. Hence, we wanted to confirm the missing role of SHIP with a second experimental setting. For this purpose, we employed the $Y^{331}F$ mutant of Dok-3, which counteracted Ca^{2+} inhibition by wild-type Dok-3, and when expressed in DT40 cells allowed for entry of extracellular Ca^{2+} (Figure 3D, black and gray lines). We reasoned that if Dok-3 controls Ca^{2+} through SHIP, expression of the $Y^{331}F$ dominant-negative version in SHIP-deficient cells should have no effect on the extracellular Ca^{2+} influx observed in these cells (Figure 3D, brown line). However, and consistent with our mutational analysis described above, expression of the $Y^{331}F$ mutant in *ship*$^{-/-}$ cells strongly augmented intra- and extracellular Ca^{2+} mobilization (orange line). This result demonstrates that inhibition of Ca^{2+} signals by endogenous wild-type Dok-3 is independent of SHIP expression. Final proof that SHIP is not a major downstream effector of Dok-3 came from the biochemical analysis of SHIP itself and its downstream target, the kinase Akt (alternatively called PKB). Neither phosphorylation of SHIP nor of Akt/PKB was drastically altered in the absence of Dok-3 expression (Supplementary Figure S3A). Similar to SHIP, also the catalytic activity of the Dok-3 binding partner Csk appeared unaltered in *dok-3*$^{-/-}$ cells (Supplementary Figure S3B), which further supports our mutational analysis. In summary, SHIP and Csk are both dispensable for Dok-3-mediated regulation of Ca^{2+}, demonstrating that these proteins do not function together in a common Ca^{2+} signaling pathway.

PLC-γ2 is a target of Dok-3

In search for an enzymatic activity that is under the control of Dok-3, we focused on PLC-γ2. First, we tested the overall tyrosine phosphorylation status of PLC-γ2, which appeared to be very similar in the presence and absence of Dok-3 (Figure 4A). Using a site-specific antibody that detects phosphorylation of Y^{759} (in human PLC-γ2), we observed drastic differences between Dok-3-positive and Dok-3-negative cells (Figure 4B). The kinetic and extent of PLC-γ2 phosphorylation at this specific residue was substantially upregulated in *dok-3*$^{-/-}$ cells (lanes 5–8) compared with wild-type parental cells (lanes 1–4) or Dok-3-reconstituted transfectants (lanes 9–12). Phosphorylation of Y^{759} is known to be dependent on Btk and directly correlates with the enzymatic activity of PLC-γ2 (Humphries *et al*, 2004; Kim *et al*, 2004). Indeed, the hydrolysis of membrane phospholipids was more rapid and efficient in *dok-3*$^{-/-}$ cells than in reconstituted transfectants, as shown by monitoring the intracellular levels of the PLC-γ2 product IP3 (Figure 4C, left panel). The same was also true for *grb2*$^{-/-}$ cells (Figure 4C, right panel). These data identify PLC-γ2 as an effector protein of the Dok-3/Grb2 signaling module.

Membrane-bound Dok-3 controls BCR-induced relocalization of Grb2

Stimulation-dependent plasma membrane anchoring is a critical event for PLC-γ2 function (Nishida *et al*, 2003). This led us to investigate the *in vivo* subcellular localization of Dok-3 and Grb2 in resting and BCR-activated cells by confocal laser scanning microscopy (Figure 5). Dok-3-deficient DT40 cells were reconstituted with GFP-tagged versions of either wild-type or mutant Dok-3. Wild-type Dok-3 was constitutively and almost exclusively localized at the plasma membrane (Figure 5A, upper row). Nonetheless, BCR activation appeared to induce intra-membraneous relocalization of Dok-3, as indicated by the shift from uniform plasma membrane staining in resting cells to dotted fluorescence signals in stimulated cells. Membrane tethering was completely lost for the ΔPH mutant of Dok-3, which was homogeneously distributed in the cytoplasm of the cells (Figure 5A, middle

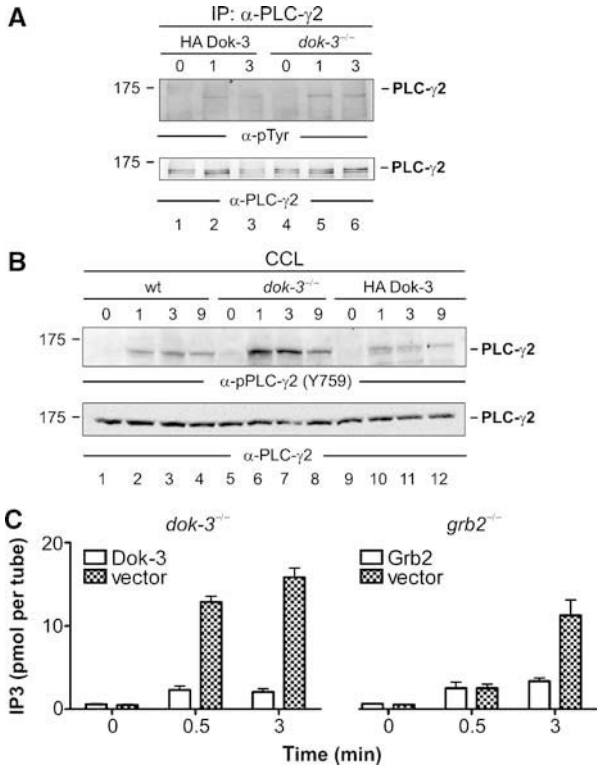

Figure 4 The Dok-3/Grb2 module attenuates PLC-γ2 activity. (**A**) Dok-3-deficient DT40 mutants (lanes 4–6) and reconstituted cells expressing HA-tagged wild-type Dok-3 (lanes 1–3) were left untreated (0) or stimulated through their BCRs for the indicated times (min). Lysates were subjected to anti-PLC-γ2 immunopurification and proteins obtained were analyzed by anti-pTyr and anti-PLC-γ2 immunoblotting (upper and lower panels, respectively). (**B**) Parental DT40 cells (lanes 1–4), *dok-3*$^{-/-}$ mutants (lanes 5–8) and HA-Dok-3-reconstituted transfectants (lanes 9–12) were left untreated (0) or stimulated through their BCRs for the indicated times (min). Cleared cellular lysates (CCL) were subjected to immunoblot analysis with antibodies that specifically detect PLC-γ2 phosphorylation at the Btk-dependent phospho-acceptor site corresponding to Y^{759} in human PLC-γ2 (upper panel). Equal protein loading was confirmed by reprobing the membrane with anti-PLC-γ2 antibodies (lower panel). Relative molecular mass of marker protein is indicated in (A) and (B) on the left in kDa. (**C**) DT40 mutant cells deficient for either Dok-3 (left panel) or Grb2 (right panel) and the empty vector control transfectants (open and filled bars, respectively) were left untreated (0) or BCR-activated for 0.5 or 3 min. IP3 levels in these cells were measured using a competitive binding assay with radiolabelled IP3-binding proteins. Error bars represent s.e.m. of three independent experiments with double preparation.

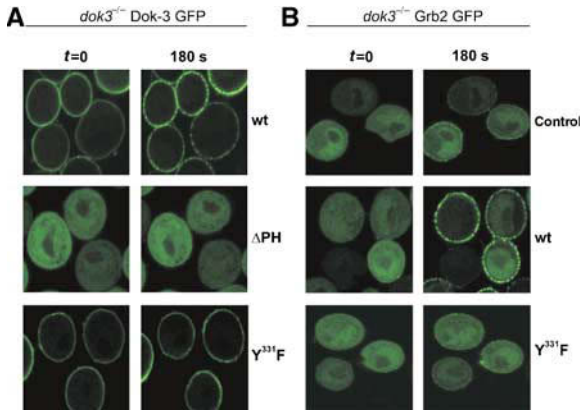

Figure 5 Dok-3 is permanently localized at the plasma membrane and is essential for stimulation-dependent recruitment of Grb2. (**A**) Dok-3-deficient DT40 mutants were transfected with expression constructs encoding fusion proteins between the green fluorescence protein (GFP) at the C terminus and either wild-type Dok-3 (upper row), Dok-3ΔPH (middle row) or Dok-3 $Y^{331}F$ (lower row) at the N terminus. Subcellular localization of Dok-3/GFP fusion proteins in resting ($t = 0$) or BCR-activated (180 s) cells (left and right images) was visualized by confocal laser scanning microscopy. (**B**) *Dok-3*$^{-/-}$ DT40 cells expressing a Grb2/GFP fusion protein were transfected with either empty control vector (upper row) or expression vectors encoding wild-type or $Y^{331}F$ Dok-3 mutants (middle and lower rows). Subcellular Grb2 localization was analyzed as in (A). The Ca^{2+} signaling function of GFP fusion proteins was tested separately (data not shown).

row). The $Y^{331}F$ mutant of Dok-3 behaved like the wild-type protein (Figure 5A, lower row).

Next, we assessed the role of Dok-3 for subcellular localization of Grb2. Expression of GFP-tagged Grb2 in unstimulated *dok-3*$^{-/-}$ cells resulted in fluorescence staining of the cytoplasm but not the plasma membrane (Figure 5B, upper left). Following BCR activation, minute amounts of Grb2 could be detected at the plasma membrane, but the overall staining pattern remained unchanged (Figure 5B, upper right). In marked contrast, in the presence of wild-type Dok-3, the vast majority of Grb2 translocated to the plasma membrane in a stimulation-dependent manner (Figure 5B, middle row). Expression of the $Y^{331}F$ mutant of Dok-3 did not support this relocalization of Grb2 (Figure 5B, lower row). Altogether, our *in vivo* imaging reveals that plasma membrane-bound Dok-3 recruits majority of cytosolic Grb2 in BCR-activated DT40 cells most likely by phospho-Y^{331}/SH2-interaction. Notably, the PH domain-anchored Dok-3 itself undergoes a BCR-triggered clustering within the plasma membrane.

Dok-3 homo-oligomerizes upon BCR activation

To further dissect possible clustering processes of membrane-bound Dok-3, we coexpressed GFP-tagged Dok-3 with HA-tagged versions of wild-type or mutant Dok-3 proteins. Subsequently, their ability to form higher aggregates in resting and BCR-activated cells was biochemically investigated by co-immunoprecipitation experiments in which anti-HA-purified proteins were analyzed by Western blotting with antibodies to GFP and HA (Figure 6, upper and lower panels, respectively). In the analysis of *dok-3*$^{-/-}$ cells, parental cells served as specificity control (lanes 1 and 2). Dok-3-GFP coprecipitated with wild-type Dok-3 from both unstimulated and stimulated cells, but the efficiency strongly increased upon BCR activation (lanes 3 and 4). The stimulation-dependent, but not the constitutive association between Dok-3 proteins, was strongly diminished for those mutants that either lack the PH domain (ΔPH, lanes 5 and 6), possess an inactivated PTB domain ($R^{197}A$, lanes 7 and 8) or cannot be phosphorylated at Y^{140} ($Y^{140}F$, lanes 9 and 10). Phosphorylation of the Grb2-binding site Y^{331} appeared to be dispensable ($Y^{331}F$, lanes 11 and 12). These data demonstrate a homotypic and inducible aggregation of Dok-3 proteins. For BCR-triggered upregulation of this interaction, Dok-3 must be localized at the plasma membrane, which allows for phosphorylation at Y^{140} (see also Figure 3C, lanes 5 and 6). Most likely, phospho-Y^{140} is then intermolecularly bound by the PTB domain of a neighboring Dok-3 molecule. The

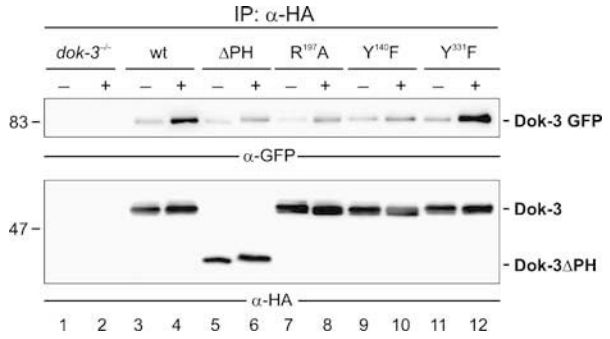

Figure 6 Dok-3 undergoes stimulation-dependent homo-oligomerization. *Dok-3*$^{-/-}$ mutant cells were reconstituted with Dok-3/GFP and subsequently transfected with empty control vector (lanes 1 and 2) or expression constructs for either HA-tagged wild-type Dok-3 (lanes 3 and 4) or the indicated HA-tagged Dok-3 variants (lanes 5–12; for details, see Figure 3A). Lysates were subjected to anti-HA immunoprecipitation. Proteins obtained were analyzed by immunoblotting with antibodies to GFP (upper panel) and HA peptide tag (lower panel). Relative molecular masses of marker proteins are indicated on the left in kDa.

subsequently induced multimerization cascade is independent of Grb2 recruitment and vice versa, Grb2 binding and concomitant Ca^{2+} inhibition is independent of the Dok-3 oligomers (see also Figure 3B and C). Hence, oligomerization of and Ca^{2+} inhibition by Dok-3 proteins are two separate and functionally independent processes.

Discussion

Intracellular elevation of Ca^{2+} in B cells is a tightly regulated process, which involves positive and negative control elements. Interfering with proper regulation of Ca^{2+} signaling is known to perturb humoral immune responses in mouse and man (Wienands, 2000). Herein, we have elucidated mechanistic details of Ca^{2+} inhibition through the adaptor proteins Grb2 and Dok-3. Several lines of evidence obtained by biochemical, genetic and imaging techniques show that following BCR activation, Grb2 and Dok-3 constitute a functional unit in a negative feedback control loop at the plasma membrane. First, following Lyn-mediated phosphorylation, Dok-3 associates with Grb2 by virtue of the Grb2 SH2 domain, which we have previously identified to be mandatory for Grb2-mediated Ca^{2+} inhibition. Interestingly, inducible tyrosine phosphorylation of Dok-3 requires the presence of the binding partner Grb2. This demonstrates the existence of a regulatory circuit, in which Grb2 'instructs' the kinase Lyn to create a specific docking site for the adaptor's SH2 domain. Second, *grb2*$^{-/-}$ and *dok-3*$^{-/-}$ cells exhibit almost identical Ca^{2+} profiles, which are characterized by robust intra- and extracellular Ca^{2+} fluxes. Hence, gene targeting of either *grb2* or *dok-3* is sufficient to convert the weak and monophasic Ca^{2+} response of an immature B cell such as DT40 to that of more mature B cells. Third, the dominant-negative $W^{193}K$ mutant of Grb2 cannot augment the Ca^{2+} response in *dok-3*$^{-/-}$ cells, demonstrating that Grb2 needs Dok-3 for Ca^{2+} signaling. Fourth and vice versa, the $Y^{331}F$ mutant of Dok-3, which cannot associate with Grb2 becomes hardly phosphorylated and is incapable of inhibiting BCR-induced Ca^{2+} mobilization. Moreover, all other tyrosine phosphorylation motifs of Dok-3, which bind other signaling proteins, are dispensable for Ca^{2+} inhibition. Fifth, membrane-associated Dok-3 is able to recruit and relocalize the majority of cytosolic Grb2 to the plasma membrane upon BCR activation. Loss of membrane association abrogates Dok-3 phosphorylation, association to Grb2 and concomitant Ca^{2+} inhibition. In summary, our data show that SH2 domain-mediated recruitment of Grb2 to Dok-3, which is tethered at the plasma membrane via its PH domain and becomes phosphorylated by Lyn, limits the quantity and quality of the BCR-induced Ca^{2+} signal.

Further studies presented in this paper excluded possible effector proteins of the Dok-3/Grb2 module. Importantly, we found no evidence for a role of SHIP, which was a likely candidate, because it is a reported Dok-3-binding protein (Lemay *et al*, 2000; Robson *et al*, 2004), and its lipid phosphatase activity reduces the number of membrane anchor motifs for PH domain-containing signaling proteins of the Ca^{2+}-activating pathway (Damen *et al*, 1996). We confirmed the *in vivo* association between SHIP and the PTB domain of Dok-3, but the Dok-3/Grb2 module neither requires this interaction nor the expression of SHIP at all to inhibit Ca^{2+} fluxes. Also the phosphorylation-dependent association of Dok-3 with Csk is dispensable for Ca^{2+} signaling and inhibitory phosphorylation of Lyn. Finally, we demonstrated homo-oligomerization of Dok-3 proteins mediated by the PTB domain and phospho-Y^{140}, but our mutational analysis of these intramolecular interaction sites excluded that this process participates in Ca^{2+} inhibition. Hetero-oligomerization between Dok-1 and Dok-2 had been previously reported to play a role in CD2 signaling in T cells (Boulay *et al*, 2005).

Two key observations provide mechanistic insight into the pathway downstream of the Dok-3/Grb2 module; that is, the substantially enhanced phosphorylation of PLC-γ2 at Y^{759} in *dok-3*$^{-/-}$ cells, which was accompanied by increased IP3 production and, the critical importance of the C-terminal SH3 domain of Grb2 for Ca^{2+} inhibition (see also Stork *et al*, 2004). The first results unmask Btk as the target of the Dok-3/Grb2 module because phosphorylation of Y^{759} in PLC-γ2 is strictly Btk-dependent and required for sustained Ca^{2+} elevation (Humphries *et al*, 2004; Kim *et al*, 2004). Our latter finding suggests how Dok-3-associated Grb2 can inhibit Btk function. Two conserved SH3 domain recognition motifs in the Tec homology (TH) domain of Btk are implicated in the regulation of kinase activity (Vihinen *et al*, 1996; Yamadori *et al*, 1999; Hansson *et al*, 2001; Okoh and Vihinen, 2002). Recruitment of Grb2 to phospho-Dok-3 may bring Grb2 into the vicinity of membrane-anchored Btk. Note that both Dok-3 and Btk are tethered at the plasma membrane through their PH domains and hence may reside in the same membrane sub-compartment. Colocalization of Dok-3/Grb2 with Btk could permit the C-terminal SH3 domain of Grb2 to bind the proline-rich regions in Btk and directly suppress its enzymatic activity. Alternatively, association between Grb2 and Btk occurs already in the cytosol, and phosphorylated Dok-3 targets the Grb2/Btk complex to a membrane compartment, where Btk cannot interact with PLC-γ2 for activation. For this purpose, PLC-γ2 needs to be located in lipid rafts, which explains why Grb2 recruitment to phosphorylated lipid raft residents, such as NTAL, facilitates sustained Ca^{2+} elevation (Stork *et al*, 2004). A sequestering function of the Dok-3/Grb2 module for Btk is supported by the ability of Dok-3 to inhibit Ras activation (Honma *et al*, 2006). In any

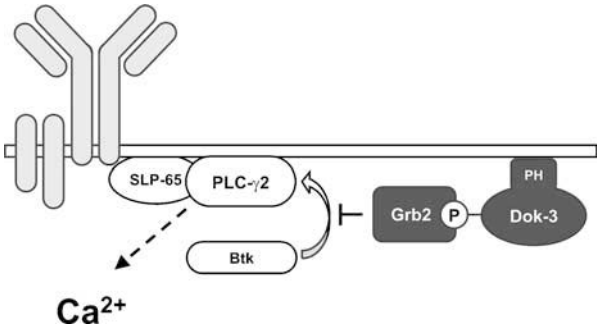

Figure 7 Inhibition of BCR-induced Ca^{2+} signaling by the Dok-3/Grb2 module. The Dok-3 adaptor protein is tethered at the inner side of the plasma membrane by virtue of its PH domain. Following tyrosine phosphorylation in activated B cells, Dok-3 recruits Grb2, which at this specific subcellular location attenuates Btk-dependent activation of PLC-γ2 by interfering with the proper formation of the SLP-65-assembled Ca^{2+} initiation complex and/or inhibiting the enzymatic activity of Btk. Positive and negative regulators of Ca^{2+} elevation are illustrated by open and filled boxes, respectively. The BCR complex is depicted in gray.

case phosphorylated Dok-3 appears to provide a 'membrane zip code' for Grb2 and the two models are not necessarily mutually exclusive (see Figure 7). A combination of biochemical and imaging methods will be required to finally elucidate the mode of action of the Dok-3/Grb2/Btk signaling module. It is tempting to speculate that the negative regulatory signal circuit described in this manuscript is involved in anergizing immature B cells upon auto-antigen encounter.

Materials and methods

Cells, Abs and reagents

Chicken DT40 cells were cultured in RPMI 1640 supplemented with 10% FCS, 1% chicken serum, 3 mM L-glutamine, 50 μM β-ME and antibiotics. Grb2- and SHIP-deficient DT40 cells are described by Ono *et al* (1997) and Hashimoto *et al* (1998). Mouse Bal17.TR B cells were kindly provided by Anthony de Franco (University of California, San Francisco, USA) and cultured in RPMI 1640 containing 10% FCS, 2 mM L-glutamine, 2 mM pyruvate, 50 μM β-ME and antibiotics (Harmer and DeFranco, 1999). Cell stimulation and lysis were performed as described by Stork *et al* (2004). Rabbit anti-mouse Dok-3 antibodies were kindly provided by André Veillette (IRCM, Montreal, Canada) (Lemay *et al*, 2000). Monoclonal antibodies to pTyr (4G10) and Grb2 (3F2) were purchased from Upstate Biotechnology (USA). Anti-Akt and phospho-specific antibodies to SHIP (Y^{1020}), Src (Y^{416}), Lyn (Y^{507}) and Akt (S^{473}) were purchased from Cell Signaling Technology (USA). Rabbit anti-PLC-γ2 (Q-20) and mAb rat anti-HA (3F10) were purchased from Santa Cruz Biotechnology (USA) and Roche (Switzerland), respectively. GST fusion proteins of Grb2[SH2] and Grb2[SH3] were prepared and used as described previously (Grabbe and Wienands, 2006).

Mass spectrometric analysis

DT40 (5×10^8) cells were stimulated with M4 and lysates were subjected to Grb2[SH2] affinity purification. After SDS–PAGE, proteins were visualized by silver staining. Proteins of interest were excised and in-gel-digested in an adapted manner according to Shevchenko *et al* (1996). Peptides generated were subjected to a 75-μm ID, 5-cm PepMap C18-column (Dionex, Germany). Peptide separation was performed by an acetonitrile gradient at 300 nl/min using an Ultimate/Swichos Nano-HPLC (Dionex, Germany) online coupled via a nano-spray source (Bruker, Germany) to a Esquire HCT Iontrap mass spectrometer (Bruker, Germany). Mass spectra were acquired in negative MS/MS mode, tuned for tryptic peptides. Processing of the MS/MS-spectra was performed by the use of Data Analysis and BioTools softwares from Bruker, Germany. Database search was done on the current NCBI protein database using an in-house MASCOT server.

Expression constructs and generation of Dok-3-deficient DT40 cells

The targeting vectors pDok-3-neo and pDok-3-hisD (see Supplementary Figure S2A) were constructed to insert neomycin and histidinol resistance cassettes into intron 1 of avian *dok-3* alleles. The resistance cassettes were flanked by 1.8 and 2.9 kb at the 5′- and 3′-sites, respectively. For this purpose, genomic *dok-3* fragments were amplified from DT40 genomic DNA using the primers 5′-TAGCACAGCTGTAGAGATGGCAGTG-3′ and 5′-AGCACATGAAGT CATCGCTTCTCC-3′ (left arm), and 5′-GCACGTTATGGGTGACAT CATGGCAG-3′ and 5′-GAAGATGTTCTCATAGAGATGCTCGG-3′ (right arm). Targeting vectors were introduced by electroporation at 550 V and 25 μF. For selection, G418 was used at 2 mg/ml and histidinol at 1 mg/ml. Dok-3-deficient clones were screened by PCR and immunoblot analysis. Further details of the targeting strategy and selection of Dok-3-deficient clones are described in Supplementary Figure S2. Full-length avian *dok-3* cDNA was obtained by RT–PCR with RNA from DT40 cells by using 5′-CAGTTGCTTTGGCTGAAT CAGTCAC-3′ and 5′-TTTTGTTACGGCGCCCCCTGGCGG-3′ as forward and reverse primers, respectively. The GenBank accession number of avian *dok-3* cDNA is EF051736. Wild-type chicken *dok-3* cDNA was cloned into pCRII-TOPO vector. Coding sequences for HA tag were introduced at the 5′- and eGFP at the 3′-sites of the Dok-3 cDNA by PCR. The different Dok-3 variants were obtained using site-directed mutagenesis. All *dok-3* cDNAs were directly ligated into the expression vectors pMSCV (BD Biosciences, USA) and pApuroII (Kurosaki *et al*, 1994). The generation of Grb2 constructs (GenBank accession number EF062570) and retroviral transduction or electroporation of expression vectors are described in Stork *et al*, (2004).

Calcium and IP3 measurements

For Ca^{2+} monitoring, 1×10^6 cells were loaded in 700 μl RPMI containing 5% FCS, 1 μM Indo1-AM (Molecular Probes) and 0.015% Pluronic F127 (Molecular Probes, USA) at 30°C for 25 min. Subsequently, the cell suspension was diluted two-fold with RPMI 10% FCS and incubated for 10 min at 37°C. Cells were washed and prepared for measurements as described earlier (Stork *et al*, 2004). Briefly, to discriminate between mobilization of Ca^{2+} from intra- and extracellular sources, BCR stimulation was performed for 6 min in the presence of 0.5 mM EGTA to remove extracellular Ca^{2+} and to allow for monitoring Ca^{2+} release from ER stores only. After restoring the extracellular Ca^{2+} concentration to 1 mM, entry of Ca^{2+} through ion channels in the plasma membrane was recorded. Changes in the ratio of fluorescence intensities at 405 and 510 nm were monitored on an LSRII cytometer (Becton Dickinson) and analyzed with FlowJo (TriStar). IP3 concentrations were determined using the IP3 Biotrak Assay (GE Healthcare) according to the manufacturer's protocol.

Confocal laser scanning microscopy

A total of 1×10^6 DT40 cells were resuspended in Krebs Ringer solution composed of 10 mM HEPES (pH 7.0), 140 mM NaCl, 4 mM KCl, 1 mM $MgCl_2$, 1 mM $CaCl_2$ and 10 mM glucose. After 30 min of seeding onto chambered coverglasses (Nunc, USA), cells were examined on a Leica TCS SP2 confocal laser scanning microscope. EGFP was excited at a wavelength of 488 nm and emission was recorded at 510 nm.

Supplementary data

Supplementary data are available at *The EMBO Journal* Online (http://www.embojournal.org).

Acknowledgements

We thank Drs André Veillette, Anthony de Franco and Annika Grabbe for providing Dok-3 reagents, Bal17.TR cells and recombinant Grb2 proteins, respectively. Expert technical assistance was provided by Ines Heine. This work was supported by the *Deutsche Forschungsgemeinschaft* through FOR 521.

References

Adachi T, Wienands J, Wakabayashi C, Yakura H, Reth M, Tsubata T (2001) SHP-1 requires inhibitory co-receptors to down-modulate B cell antigen receptor-mediated phosphorylation of cellular substrates. *J Biol Chem* **276:** 26648–26655

Bolland S, Pearse RN, Kurosaki T, Ravetch JV (1998) SHIP modulates immune receptor responses by regulating membrane association of Btk. *Immunity* **8:** 509–516

Boulay I, Nemorin JG, Duplay P (2005) Phosphotyrosine binding-mediated oligomerization of downstream of tyrosine kinase (Dok)-1 and Dok-2 is involved in CD2-induced Dok phosphorylation. *J Immunol* **175:** 4483–4489

Brauweiler A, Tamir I, Dal Porto J, Benschop RJ, Helgason CD, Humphries RK, Freed JH, Cambier JC (2000) Differential regulation of B cell development, activation, and death by the Src homology 2 domain-containing 5′ inositol phosphatase (SHIP). *J Exp Med* **191:** 1545–1554

Chiu CW, Dalton M, Ishiai M, Kurosaki T, Chan AC (2002) BLNK: molecular scaffolding through cis-mediated organization of signaling proteins. *EMBO J* **21:** 6461–6472

Cong F, Yuan B, Goff SP (1999) Characterization of a novel member of the DOK family that binds and modulates Abl signaling. *Mol Cell Biol* **19:** 8314–8325

Damen JE, Liu L, Rosten P, Humphries RK, Jefferson AB, Majerus PW, Krystal G (1996) The 145-kDa protein induced to associate with Shc by multiple cytokines is an inositol tetraphosphate and phosphatidylinositol 3,4,5-trisphosphate 5-phosphatase. *Proc Natl Acad Sci USA* **93:** 1689–1693

Dolmetsch RE, Lewis RS, Goodnow CC, Healy JI (1997) Differential activation of transcription factors induced by Ca^{2+} response amplitude and duration. *Nature* **386:** 855–858

Dolmetsch RE, Xu K, Lewis RS (1998) Calcium oscillations increase the efficiency and specificity of gene expression. *Nature* **392:** 933–936

Fu C, Turck CW, Kurosaki T, Chan AC (1998) BLNK: a central linker protein in B cell activation. *Immunity* **9:** 93–103

Gallo EM, Cante-Barrett K, Crabtree GR (2006) Lymphocyte calcium signaling from membrane to nucleus. *Nat Immunol* **7:** 25–32

Goitsuka R, Fujimura Y, Mamada H, Umeda A, Morimura T, Uetsuka K, Doi K, Tsuji S, Kitamura D (1998) BASH, a novel signaling molecule preferentially expressed in B cells of the bursa of Fabricius. *J Immunol* **161:** 5804–5808

Grabbe A, Wienands J (2006) Human SLP-65 isoforms contribute differently to activation and apoptosis of B lymphocytes. *Blood* **108:** 3761–3768

Hansson H, Smith CI, Hard T (2001) Both proline-rich sequences in the TH region of Bruton's tyrosine kinase stabilize intermolecular interactions with the SH3 domain. *FEBS Lett* **508:** 11–15

Harmer SL, DeFranco AL (1999) The src homology domain 2-containing inositol phosphatase SHIP forms a ternary complex with Shc and Grb2 in antigen receptor-stimulated B lymphocytes. *J Biol Chem* **274:** 12183–12191

Hashimoto A, Okada H, Jiang A, Kurosaki M, Greenberg S, Clark EA, Kurosaki T (1998) Involvement of guanosine triphosphatases and phospholipase C-gamma 2 in extracellular signal-regulated kinase, c-Jun NH2-terminal kinase, and p38 mitogen-activated protein kinase activation by the B cell antigen receptor. *J Exp Med* **188:** 1287–1295

Hashimoto S, Iwamatsu A, Ishiai M, Okawa K, Yamadori T, Matsushita M, Baba Y, Kishimoto T, Kurosaki T, Tsukada S (1999) Identification of the SH2 domain binding protein of Bruton's tyrosine kinase as BLNK—functional significance of Btk-SH2 domain in B-cell antigen receptor-coupled calcium signaling. *Blood* **94:** 2357–2364

Hoek KL, Antony P, Lowe J, Shinners N, Sarmah B, Wente SR, Wang D, Gerstein RM, Khan WN (2006) Transitional B cell fate is associated with developmental stage-specific regulation of diacylglycerol and calcium signaling upon B cell receptor engagement. *J Immunol* **177:** 5405–5413

Honma M, Higuchi O, Shirakata M, Yasuda T, Shibuya H, Iemura S, Natsume T, Yamanashi Y (2006) Dok-3 sequesters Grb2 and inhibits the Ras–Erk pathway downstream of protein-tyrosine kinases. *Genes Cells* **11:** 143–151

Horejsi V, Zhang W, Schraven B (2004) Transmembrane adaptor proteins: organizers of immunoreceptor signalling. *Nat Rev Immunol* **4:** 603–616

Humphries LA, Dangelmaier C, Sommer K, Kipp K, Kato RM, Griffith N, Bakman I, Turk CW, Daniel JL, Rawlings DJ (2004) Tec kinases mediate sustained calcium influx via site-specific tyrosine phosphorylation of the phospholipase Cgamma Src homology 2-Src homology 3 linker. *J Biol Chem* **279:** 37651–37661

Ishiai M, Kurosaki M, Pappu R, Okawa K, Ronko I, Fu C, Shibata M, Iwamatsu A, Chan AC, Kurosaki T (1999a) BLNK required for coupling Syk to PLC gamma 2 and Rac1-JNK in B cells. *Immunity* **10:** 117–125

Ishiai M, Sugawara H, Kurosaki M, Kurosaki T (1999b) Cutting edge: association of phospholipase C-gamma 2 Src homology 2 domains with BLNK is critical for B cell antigen receptor signaling. *J Immunol* **163:** 1746–1749

Kim CH, Hangoc G, Cooper S, Helgason CD, Yew S, Humphries RK, Krystal G, Broxmeyer HE (1999) Altered responsiveness to chemokines due to targeted disruption of SHIP. *J Clin Invest* **104:** 1751–1759

Kim YJ, Sekiya F, Poulin B, Bae YS, Rhee SG (2004) Mechanism of B-cell receptor-induced phosphorylation and activation of phospholipase C-gamma2. *Mol Cell Biol* **24:** 9986–9999

Koncz G, Bodor C, Kovesdi D, Gati R, Sarmay G (2002) BCR mediated signal transduction in immature and mature B cells. *Immunol Lett* **82:** 41–49

Kurosaki T, Takata M, Yamanashi Y, Inazu T, Taniguchi T, Yamamoto T, Yamamura H (1994) Syk activation by the Src-family tyrosine kinase in the B cell receptor signaling. *J Exp Med* **179:** 1725–1729

Kurosaki T, Tsukada S (2000) BLNK: connecting Syk and Btk to calcium signals. *Immunity* **12:** 1–5

Lemay S, Davidson D, Latour S, Veillette A (2000) Dok-3, a novel adapter molecule involved in the negative regulation of immunoreceptor signaling. *Mol Cell Biol* **20:** 2743–2754

Lowenstein EJ, Daly RJ, Batzer AG, Li W, Margolis B, Lammers R, Ullrich A, Skolnik EY, Bar-Sagi D, Schlessinger J (1992) The SH2 and SH3 domain-containing protein GRB2 links receptor tyrosine kinases to ras signaling. *Cell* **70:** 431–442

Niiro H, Clark EA (2002) Regulation of B-cell fate by antigen-receptor signals. *Nat Rev Immunol* **2:** 945–956

Nishida M, Sugimoto K, Hara Y, Mori E, Morii T, Kurosaki T, Mori Y (2003) Amplification of receptor signalling by Ca^{2+} entry-mediated translocation and activation of PLCgamma2 in B lymphocytes. *EMBO J* **22:** 4677–4688

Okada H, Bolland S, Hashimoto A, Kurosaki M, Kabuyama Y, Iino M, Ravetch JV, Kurosaki T (1998) Role of the inositol phosphatase SHIP in B cell receptor-induced Ca^{2+} oscillatory response. *J Immunol* **161:** 5129–5132

Okoh MP, Vihinen M (2002) Interaction between Btk TH and SH3 domain. *Biopolymers* **63:** 325–334

Ono M, Okada H, Bolland S, Yanagi S, Kurosaki T, Ravetch JV (1997) Deletion of SHIP or SHP-1 reveals two distinct pathways for inhibitory signaling. *Cell* **90:** 293–301

Parekh AB, Putney Jr JW (2005) Store-operated calcium channels. *Physiol Rev* **85:** 757–810

Putney Jr JW (2005) Capacitative calcium entry: sensing the calcium stores. *J Cell Biol* **169:** 381–382

Robson JD, Davidson D, Veillette A (2004) Inhibition of the Jun N-terminal protein kinase pathway by SHIP-1, a lipid phosphatase that interacts with the adaptor molecule Dok-3. *Mol Cell Biol* **24:** 2332–2343

Shevchenko A, Wilm M, Vorm O, Mann M (1996) Mass spectrometric sequencing of proteins silver-stained polyacrylamide gels. *Anal Chem* **68:** 850–858

Stork B, Engelke M, Frey J, Horejsi V, Hamm-Baarke A, Schraven B, Kurosaki T, Wienands J (2004) Grb2 and the non-T cell activation linker NTAL constitute a Ca(2+)-regulating signal circuit in B lymphocytes. *Immunity* **21:** 681–691

Su YW, Zhang Y, Schweikert J, Koretzky GA, Reth M, Wienands J (1999) Interaction of SLP adaptors with the SH2 domain of Tec family kinases. *Eur J Immunol* **29:** 3702–3711

Vihinen M, Iwata T, Kinnon C, Kwan SP, Ochs HD, Vorechovsky I, Smith CI (1996) BTKbase, mutation database for X-linked agammaglobulinemia (XLA). *Nucleic Acids Res* **24:** 160–165

Wang Y, Horvath O, Hamm-Baarke A, Richelme M, Gregoire C, Guinamard R, Horejsi V, Angelisova P, Spicka J, Schraven B, Malissen B, Malissen M (2005) Single and combined deletions of

the NTAL/LAB and LAT adaptors minimally affect B-cell development and function. *Mol Cell Biol* **25:** 4455–4465

Wienands J (2000) Signal transduction elements of the B cell antigen receptor and their role in immunodeficiencies. *Immunobiology* **202:** 120–133

Wienands J, Schweikert J, Wollscheid B, Jumaa H, Nielsen PJ, Reth M (1998) SLP-65: a new signaling component in B lymphocytes which requires expression of the antigen receptor for phosphorylation. *J Exp Med* **188:** 791–795

Yamadori T, Baba Y, Matsushita M, Hashimoto S, Kurosaki M, Kurosaki T, Kishimoto T, Tsukada S (1999) Bruton's tyrosine kinase activity is negatively regulated by Sab, the Btk-SH3 domain-binding protein. *Proc Natl Acad Sci USA* **96:** 6341–6346

Int. J. Cancer: **125,** 932–941 (2009)

The Akt inhibitor triciribine sensitizes prostate carcinoma cells to TRAIL-induced apoptosis

Alexandra Dieterle[1], Ronald Orth[1], Merle Daubrawa[1], Antje Grotemeier[1], Sebastian Alers[1], Susanne Ullrich[2], Reiner Lammers[2], Sebastian Wesselborg[1]* and Björn Stork[1]

[1]*Department of Internal Medicine I, University of Tübingen, Tübingen, Germany*
[2]*Department of Internal Medicine IV, University of Tübingen, Tübingen, Germany*

Aberrant PI3K/Akt signaling has been implicated in many human cancers, including prostate carcinomas. Currently different therapeutic strategies target the inhibition of this survival pathway. The nucleoside analog triciribine (TCN), which was initially described as a DNA synthesis inhibitor, has recently been shown to function as an inhibitor of Akt. Here, we demonstrate that TCN inhibits Akt phosphorylation at Thr308 and Ser473 and Akt activity in the human prostate cancer cell line PC-3. In addition, TCN sensitized PC-3 cells to TRAIL- and anti-CD95-induced apoptosis, whereas the cells remained resistant to DNA damaging chemotherapeutics. The observed sensitization essentially depended on the phosphorylation status of Akt. Thus, prostate cancer cell lines displaying constitutively active Akt, *e.g.* PC-3 or LNCaP, were sensitized to death receptor-induced apoptosis. Most importantly with respect to therapeutic application, derivatives of both TCN and TRAIL are already tested in current clinical trials. Therefore, this combinatorial treatment might open a promising therapeutic approach for the elimination of hormone-refractory prostate cancers, which are largely resistant to conventional DNA damaging anticancer drugs or irradiation.

Key words: prostate cancer; TRAIL; Akt; triciribine; apoptosis

Current treatments of prostate cancer include prostatectomy or radiotherapy.[1] Patients with relapsing cancer and revealing metastatic disease are treated by withdrawal of androgenic hormones.[1] However, responses may give way to hormone-refractory prostate cancer that usually comprises high resistance to chemotherapy. Generally, radio- and chemotherapy work as DNA-damaging treatments engaging the intrinsic mitochondrial pathway to induce apoptosis.[2,3] In this pathway, cytochrome c released from the mitochondrion binds to the adaptor protein Apaf-1 and assembles together with the initiator caspase-9 to the so-called apoptosome. Generally, many tumors acquire resistance to radiotherapy or anticancer drugs by inactivation of the intrinsic suicide program.[4]

Recently, it has been shown that the extrinsic death receptor pathway represents a suitable target for cancer treatment. The extrinsic pathway is initiated upon receptor ligation (via CD95 ligand, TNFα or TRAIL), resulting in the assembly of the death-inducing signaling complex (DISC), in which procaspase-8 undergoes autoproteolytic activation.[5] Extrinsic and intrinsic apoptosis pathways are connected by the caspase-8-mediated cleavage of the pro-apoptotic Bcl-2 family member Bid. Truncated Bid (tBid) translocates to mitochondria where it induces the release of cytochrome c.[6] Cells that undergo apoptosis upon death receptor stimulation without support from mitochondria are termed type I cells, whereas cells in which death receptor-mediated apoptosis depends mostly on the intrinsic pathway are designated as type II.[7] While the administration of the death receptor ligands CD95 ligand (FasL, Apo1L) or TNFα leads to severe systemic toxicity,[8,9] the TNF-related apoptosis inducing ligand (TRAIL) has been shown to induce apoptosis in various tumor cells whereas nontransformed cells are unaffected.[10–14] Therefore, TRAIL is currently assessed in clinical trials.[15–18] However, many cancer cells are resistant to TRAIL or develop resistance during therapy.[19–21] Different molecular factors have been proposed to confer TRAIL resistance, including decoy receptors, cFLIP, nuclear factor (NF)-κB, and activation of anti-apoptotic kinases.[21–23] Thus, a combinatorial treatment using TRAIL or TRAIL receptor agonists and agents sensitizing to TRAIL-induced apoptosis might represent the molecular basis for a successful treatment of tumor cells.

Next to inactivation of apoptotic signaling elements tumors also develop therapy resistance by activation of survival signaling such as the phosphatidylinositide 3-kinase (PI3K)/Akt pathway. Activation of PI3K by receptor tyrosine kinases leads to the recruitment of the protein kinase B (PKB/Akt) to the plasma membrane where it is subsequently activated upon phosphorylation at residues Thr308 and Ser473 via phosphoinositide-dependent protein kinase 1 (PDK1) and mammalian target of rapamycin complex 2 (mTORC2), respectively.[24,25] Activated Akt enhances the survival of cells by both the inhibition of pro-apoptotic proteins (*e.g.* Bad or caspase-9) and the activation of anti-apoptotic proteins (*e.g.* Mcl-1).[26–28] Generally, the PI3K/Akt signaling cascade is aberrantly activated in numerous solid tumors. However, pharmacological targeting of the PI3K/Akt survival pathway in tumors has been impeded by the lack of available Akt-specific inhibitors for clinical trials. The tricyclic nucleoside triciribine (TCN) is a purine analog which was initially shown to inhibit DNA synthesis.[29] Recent studies revealed that TCN selectively inhibits the phosphorylation and activation of all three Akt isoforms.[30] In a current phase I dose escalation study with TCN phosphate monohydrate patients with metastatic cancers are treated whose tumors must be positively tested for phospho-Akt (H. Lee Moffitt Cancer Center, Tampa, FL).

Recent reports demonstrate that inactivation of PI3K/Akt signaling sensitizes prostate tumor cells to TRAIL-induced apoptosis. Consequently, we wanted to investigate whether the Akt inhibitor TCN displays a similar effect on TRAIL-induced apoptosis. In the present study, we show that TCN sensitizes to TRAIL-induced apoptosis in prostate carcinoma cells that express constitutively phosphorylated Akt. In contrast, activation of the mitochondrial apoptosis pathway by anticancer drugs was not affected upon TCN administration. Further investigation of the molecular mechanism of the TCN-mediated increase of apoptosis revealed that TCN obviously enhances the TRAIL-induced cleavage of the pro-apoptotic Bcl-2 member Bid. Since TCN and TRAIL are used in first clinical trials our findings might open new combination

Abbreviations: mTOR, mammalian target of rapamycin; PARP, poly (ADP-ribose)polymerase; PEA-15, phosphoprotein enriched in astrocytes of 15 kDa; PI3K, phosphatidylinositol 3-kinase; TCN, triciribine; TRAIL, TNF-related apoptosis inducing ligand.

Grant sponsor: Deutsche Forschungsgemeinschaft; Grant numbers: We 1801/2-4, GK 1302, SFB 773, SFB 685; Grant sponsor: Interdisciplinary Center of Clinical Research, Faculty of Medicine, Tübingen; Grant numbers: *f*ortüne project 1805-0-0, Fö. 01KS9602; Grant sponsor: Wilhelm Sander-Stiftung; Grant number: 2004.099.1; Grant sponsor: Landesforschungsschwerpunktprogramm of the Ministry of Science, Research and Arts (Land Baden-Württemberg); Grant number: 1423-98101.

S.W. and B.S. share equal senior authorship.

***Correspondence to:** Department of Internal Medicine I, Eberhard-Karls-University, Otfried-Müller-Str. 10, D-72076 Tübingen, Germany. Fax: +49-(0)7071-29-4680.
E-mail: sebastian.wesselborg@uni-tuebingen.de

Received 24 September 2008; Accepted after revision 10 February 2009
DOI 10.1002/ijc.24374
Published online 18 February 2009 in Wiley InterScience (www.interscience.wiley.com).

therapies with established drugs that enable the elimination of anticancer drug resistant prostate tumors.

Material and methods

Cells and reagents

PC-3, LNCaP and Du145 human prostate cancer cell lines were obtained from ATCC. All cell lines were maintained in an atmosphere containing 5% CO_2 at 37°C in RPMI 1640 medium (Bio-Whittaker, Lonza, Switzerland) supplemented with 10% (v/v) heat-inactivated fetal calf serum (PAA Laboratories, Cölbe, Germany), 45 units penicillin/ml, 45 μg streptomycin/ml (Bio-Whittaker, Lonza, Switzerland) and 10 mM HEPES (Gibco BRL, Eggenstein, Germany). Anti-phospho-Akt (Thr 308), anti-phospho-Akt (Ser473), anti-Akt, anti-Akt1, anti-FLIP, anti-phospho-GSK-3α/β (Ser21/9), anti-GSK-3β, anti-PEA-15/PED and anti-phospho-p70S6K (Thr389) were purchased from Cell Signaling Technology (New England Biolabs, Frankfurt am Main, Germany), anti-PARP clone C-2-10 from Alexis Biochemicals (Axxora, Lörrach, Germany), anti-caspase-8 clone 12F5 from Bio-CHECK (Münster, Germany), anti-caspase-3 and anti-phospho-PEA-15/PED (Ser116) from Biosource (Solingen, Germany), anti-vinculin hVIN-1 from Sigma (Deisenhofen, Germany) and the agonistic anti-CD95 antibody IgM clone CH11 was obtained from Biomol (Hamburg, Germany). The Akt inhibitors triciribine (TCN), Akti-1/2 and the caspase inhibitor N-(2-Quinolyl)-valyl-aspartyl-(2,6-difluorophenoxy)-methylketon (QVD) were purchased from Calbiochem (Merck, Darmstadt, Germany). rhTRAIL was from R&D Systems (Wiesbaden, Germany), the PI3K inhibitor LY294002 and the mTOR inhibitor rapamycin were purchased from Cell Signaling Technology (New England Biolabs, Frankfurt am Main, Germany) and the Akt inhibitor SH-5 was acquired from Alexis Biochemicals (Axxora, Lörrach, Germany). The anticancer drugs etoposide and mitomycin C were obtained from Sigma (Deisenhofen, Germany) and the clinical pharmacy (Medical Clinics, Tübingen, Germany), respectively. Lipofectamine™ 2000 reagent was purchased from Invitrogen Life Technologies (Karlsruhe, Germany). Small interfering RNA (siRNA) against Akt1 (siGENOME SMARTpool) and nontargeting siRNA (siGENOME control pool) were prepared by Dharmacon (Chicago, IL)

RNA interference

Transfection of PC-3 cells with control or Akt1 siRNA (20 nM; Dharmacon, Chicago, IL) was done using Lipofectamine™ 2000 reagent (Invitrogen Life Technologies, Karlsruhe, Germany) according to manufacturer's protocol. For transfection, 2.9×10^4 cells or 1.6×10^4 cells were seeded in 24- or 48-well-plates, respectively. 72 hr after transfection, cells were treated with TCN, TRAIL or the combination of TRAIL and TCN for the measurement of apoptosis. 72 and 96 hr after transfection, cell extracts were prepared for immunoblotting.

Measurement of apoptosis

For determination of apoptosis, 5×10^4 cells per well were seeded in 48-well-plates and treated for the indicated times with different concentrations of TCN, TRAIL, anti-CD95, rapamycin or chemotherapeutic agents, respectively. The leakage of fragmented DNA from apoptotic nuclei was measured by flow cytometry. Briefly, hypodiploid apoptotic nuclei were prepared by lysing cells in a hypotonic lysis buffer containing 1% sodium citrate, 0.1% Triton X-100 and 50 μg/ml propidium iodide and subsequently analyzed by flow cytometry. Nuclei to the left of 2 N peak containing hypodiploid DNA were considered as apoptotic. Flow cytometric analyses were performed on FACSCalibur (Beckton Dickinson, Heidelberg, Germany) using CellQuest analysis software.

Measurement of caspase activity

Cytosolic extracts of 1×10^5 PC-3 cells were prepared in a lysis buffer containing 0.5% Nonidet P-40, 20 mM Hepes pH 7.4, 84 mM KCl, 10 mM $MgCl_2$, 0.2 mM EDTA, 0.2 mM EGTA, 1 mM dithiothreitol (DTT), 5 μg/ml aprotinin, 1 μg/ml leupeptin, 1 μg/ml pepstatin and 1 mM phenylmethylsulfonyl fluoride (PMSF). Caspase activities were determined by incubation of cell lysates with a 50 μM concentration of the fluorogenic substrate N-acetyl-Asp-Glu-Val-Asp-aminomethylcoumarin (Ac-DEVD-AMC) (Biomol, Hamburg, Germany) in 200 μl of buffer containing 50 mM HEPES pH 7.3, 100 mM NaCl, 10% sucrose, 0.1% CHAPS and 10 mM dithiothreitol. The release of aminomethylcoumarin was measured in a kinetic by spectrofluorimetry using an excitation wavelength of 360 nm and an emission wavelength of 475 nm. Caspase activity was determined as the slope of the resulting linear regressions and expressed in arbitrary fluorescence units per minute. For determination of active caspases *in situ*, 5×10^4 cells per well were seeded in 24-well-plates and treated for the indicated time with TCN and TRAIL. The cells were trypsinized, then centrifuged and resuspended in 5 μM CaspACE FITC-VADfmk (Promega, Mannheim, Germany). Cells were stained for 30 min at 37°C in the dark. Then the cells were washed once with cold PBS, centrifuged and resuspended in cold PBS. CaspACE positive cells were determined by flow cytometry (FL1).

Cell extracts and immunoblotting

Expression and phosphorylation of Akt, phosphorylation of GSK-3α/β and PEA-15/PED, expression of FLIP, phosphorylation of p70S6K and cleavage of caspases and caspase substrates were detected by immunoblotting. 3×10^5 cells per well were seeded into 6-well plates and were treated with the respective inhibitors and apoptotic stimuli. After the indicated time, cells were lysed in a buffer containing 20 mM Tris/HCl (pH 7.5), 150 mM NaCl, 0.5 mM EDTA, 10 μM Na_2MoO_4, 1 mM Na_3VO_4, 10 mM NaF, 2.5 mM NaPP, 1% Triton X-100 and a mixture of protease inhibitors (Sigma, Deisenhofen, Germany). Lysates were clarified by centrifugation at 13,000 rpm for 10 min at 4°C. Subsequently, proteins were separated under reducing conditions on an SDS-polyacrylamide gel and electroblotted to a polyvinylidene difluoride membrane (Amersham Pharmacia, Freiburg, Germany). Membranes were blocked for 1 hr with 5% nonfat dry milk powder in TBS/0.1% Tween-20 and then incubated for 1 hr with respective primary antibodies. Subsequently, the membranes were incubated with the respective peroxidase-conjugated affinity-purified secondary antibodies for 1 hr. Following extensive washing, the reaction was developed by enhanced chemiluminescent staining using ECL reagents (Amersham Pharmacia, Freiburg, Germany).

Results

Triciribine (TCN) inhibits Akt phosphorylation and activity in PC-3 cells

In order to prove the therapeutic drug potential of TCN for the treatment of prostate carcinomas, we first confirmed the inhibitory effect of TCN on the survival kinase Akt by analysis of its phosphorylation status and activity in the prostate carcinoma cell line PC-3 (Fig. 1*a*, lanes 6–9). PC-3 cells are largely resistant to anticancer drugs and irradiation,[14] and express constitutively active Akt.[31] As control PC-3 cells were treated with the upstream PI3K inhibitor LY294002 (lanes 2–5) and the Akt inhibitors Akti-1/2 or SH-5 (lanes 10–17), respectively. At a concentration of 10 μM TCN Akt phosphorylation was inhibited at both Thr308 and Ser473 (lane 8). Accordingly, Akt kinase activity was equally reduced as shown by a decreased detection of phospho-GSK3α/β. TCN mediated reduction in Akt phosphorylation at Ser473 could be detected as early as 10 min after administration and was almost completely abrogated after 60 min (Fig. 1*b*). In contrast to Akti-1/2 and TCN, the Akt-inhibitor SH-5 displayed almost no inhibitory potential. Taken together, TCN effectively inhibited the phosphorylation and consequently the catalytic activity of Akt in PC-3 cells. Therefore, TCN fulfills the prerequisite of interfering with the Akt-dependent survival pathway.

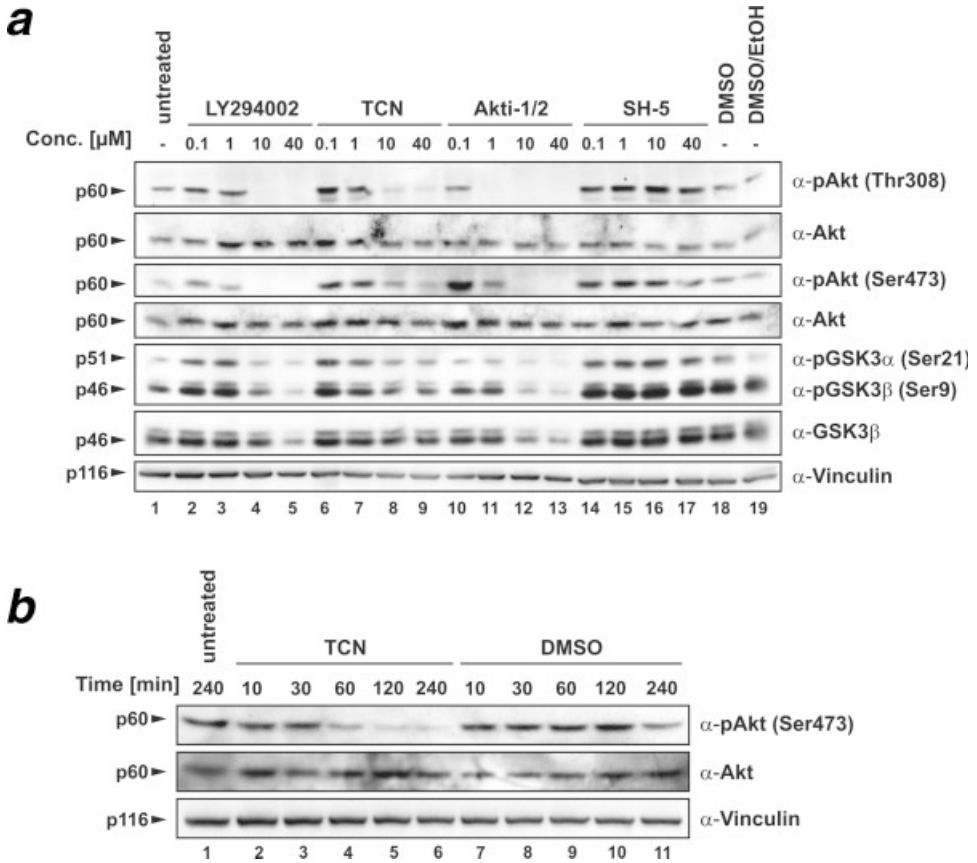

Figure 1 – Effect of the Akt inhibitor TCN on Akt phosphorylation in PC-3 cells. (*a*) Akt phosphorylation and activity is inhibited at a concentration of 10 μM triciribine (TCN). PC-3 cells were treated with indicated doses of different inhibitors (PI3K inhibitor LY294002 and the Akt inhibitors TCN, Akti-1/2 or SH-5), 0.4% DMSO or 0.4% DMSO/EtOH (1:1) for 1 hr. Immunoblots were performed with anti-phospho-Akt (Thr308 or Ser473), anti-Akt, anti-phospho-GSK3α/β (Ser21/Ser9), anti-GSK3β or anti-vinculin antibodies, respectively. (*b*) The optimal incubation time of TCN to inhibit Akt in PC-3 cells is 60 min. PC-3 cells were treated with TCN (10 μM) for various time points. Immunoblot analyses were performed with anti-phospho-Akt (Ser473) or anti-Akt antibodies.

TCN has no effect on the mitochondrial apoptotic pathway

To establish TCN as therapeutic component for the combinatorial treatment of prostate carcinomas, we next analyzed the effect of TCN-treatment on the mitochondrial apoptotic pathway. As apoptotic stimuli we used the anticancer drugs mitomycin C and etoposide that have been shown to directly activate the mitochondrial death pathway.[3] PC-3 cells were treated with the Akt inhibitors TCN or Akti-1/2 alone or in combination with mitomycin C or etoposide, respectively. Both TCN and Akti-1/2 did not induce apoptosis in PC-3 cells on their own (Fig. 2*a*). As previously described,[14] PC-3 cells were resistant to anticancer drugs like mitomycin C or etoposide. However, inhibition of Akt by TCN or Akti-1/2 did not enhance apoptosis induction by mitomycin C or etoposide, respectively (Fig. 2*a*). This observation was further confirmed by *in vitro* caspase activity assays (Fig. 2*b*) and immunoblotting for the caspase substrate poly(ADP-ribose)polymerase (PARP) (Fig. 2*c*). Thus it seems that chemotherapeutic resistance of prostate carcinomas cannot be overcome by the simultaneous inhibition of the Akt-mediated survival pathway.

TCN amplifies death receptor-induced apoptosis

Currently, one of the most promising biotherapeutic agents for cancer treatment is the TNF-related apoptosis-inducing ligand (TRAIL), which has previously been shown to induce apoptosis preferentially in tumor cells.[10–14] However, as in case of most anticancer drugs, TRAIL-responsive tumors develop resistance to TRAIL-treatment during therapy.[19,20] Interestingly in this context, recent studies could demonstrate that inhibition of Akt leads to increased sensitivity of various cancers to TRAIL-mediated apoptosis.[10,21,32-34] Consequently, we wanted to investigate whether TCN comprises a similar potential to increase TRAIL-induced apoptosis in prostate cancer cells. As shown in Figure 3*a*, PC-3 cells were almost resistant to death receptor-induced apoptosis using TRAIL and agonistic anti-CD95 antibodies, respectively. However, the inhibition of the Akt pathway by TCN or Akti-1/2 significantly increased the responsiveness of PC-3 cells to TRAIL and anti-CD95 (Fig. 3*a*). The observation that TCN amplified TRAIL-induced apoptosis in PC-3 cells was further confirmed by two different caspase activity assays. Active caspases were labeled *in situ* with the cell-permeable, FITC-conjugated caspase-inhibitor VAD-fmk. Flow cytometric analysis revealed that there was a clear increase in the amount of cells with active caspases upon combinatorial treatment of PC-3 cells with TCN and TRAIL (Fig. 3*b*, left panel). This result was confirmed by an *in vitro* caspase activity assay using the caspase-3 substrate DEVD-AMC (Fig. 3*b*, middle panel). In both assays the sole inhibition of Akt had no effect, as shown by mono-treatment with TCN. Interestingly, the TCN-mediated amplification of caspase-activity showed different kinetics for TRAIL- and anti-CD95-treatment. In case of TRAIL stimulation, TCN led to an increased caspase activity already after 2–3 hr (Fig. 3*b*, middle panel). In contrast, TCN induced the afore absent caspase activity in anti-CD95-treated PC-3 cells after 6–8 hr (Fig. 3*b*, right panel). Finally, TCN-mediated enhancement of TRAIL-induced apoptosis could also be demonstrated by an increased PARP cleavage upon TRAIL/TCN co-treatment compared

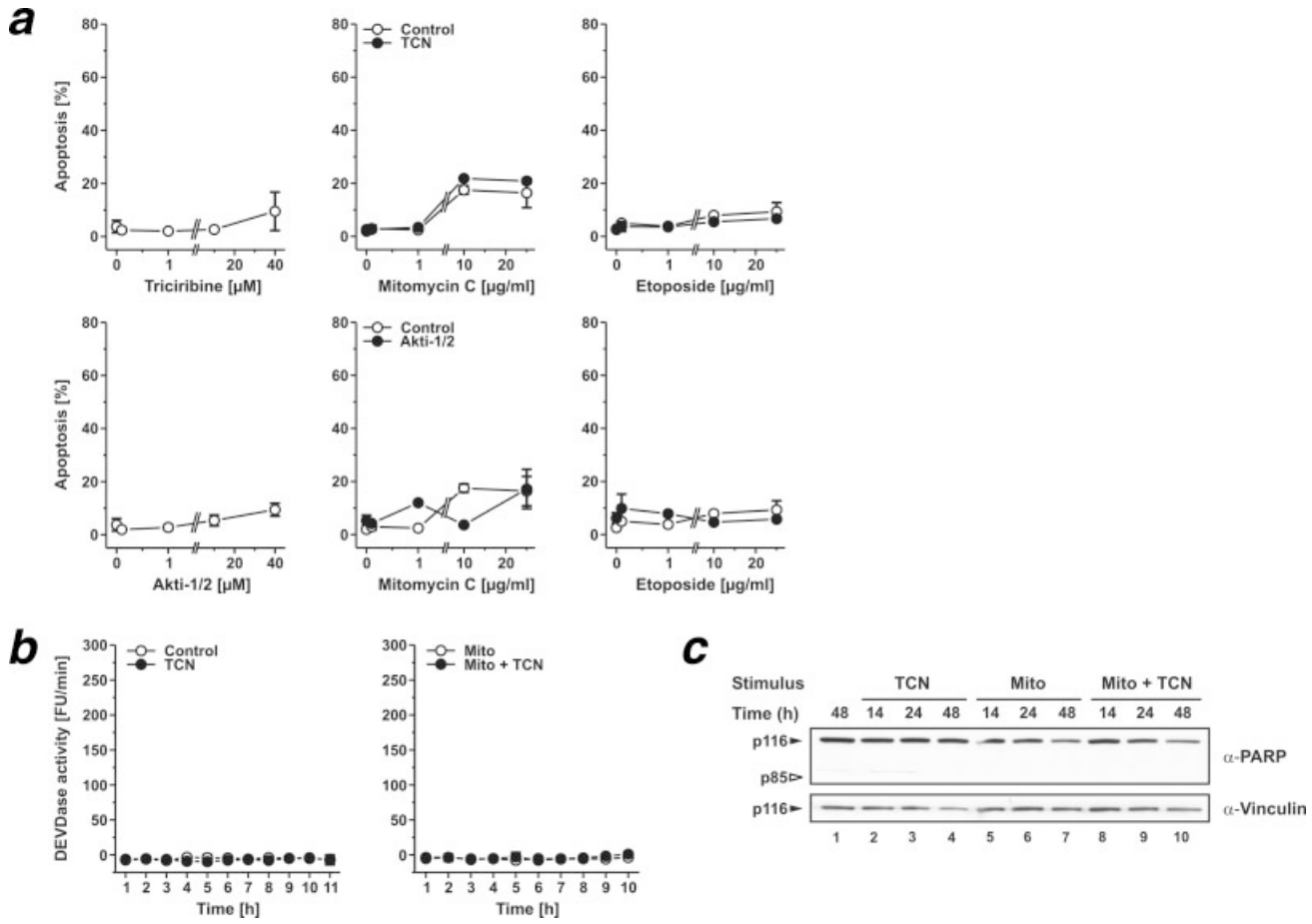

Figure 2 – TCN does not amplify the intrinsic mitochondrial apoptosis signaling pathway. (*a*) TCN does not enhance the apoptosis rate of the chemotherapeutic agents mitomycin C or etoposide in PC-3 cells. PC-3 cells were treated with mitomycin C (0.1, 1, 10, or 25 μg/ml) or etoposide (0.1, 1, 10, or 25 μg/ml) in the presence or absence of either TCN (10 μM) or Akti-1/2 (10 μM) for 48 hr. As a control PC-3 cells were treated with TCN (0.1, 1, 10, or 40 μM) or Akti-1/2 (0.1, 1, 10, or 40 μM). Apoptosis was assessed by propidium iodide staining of hypodiploid apoptotic nuclei and flow cytometry. Data shown are mean of duplicates ± SD and are representative of three independent experiments. (*b*) No caspase activity is detected after incubation of PC-3 cells with mitomycin C in the presence or absence of TCN. PC-3 cells were treated with TCN (10 μM), mitomycin C (Mito; 25 μg/ml) or mitomycin C in combination with TCN for various time points (TCN was preincubated for 1 hr). After stimuli treatment, cell lysates were prepared, incubated with the fluorogenic caspase substrate DEVD-AMC, and measured in a spectrofluorimeter. Caspase activity is given in arbitrary fluorescent units/min. Data shown are mean of duplicates ± SD and are representative of three independent experiments. (*c*) No PARP cleavage is detected after incubation of PC-3 cells with mitomycin C (Mito) in the presence or absence of TCN. PC-3 cells were treated with mitomycin C (Mito; 25 μg/ml) in the presence or absence of TCN (10 μM) for the indicated times. Eighty microgram protein of cell lysates were applied per lane on SDS-polyacrylamide gel. Immunoblots were performed with anti-PARP, and anti-vinculin antibodies.

to TRAIL-treatment alone (Fig. 3*c*, upper panels, lanes 4–11). However, no difference could be detected in the processing of caspase-8 under these two conditions. Again, differences became evident between the combinations TRAIL/TCN and anti-CD95/TCN. PARP cleavage was only detectable after the combined incubation of PC-3 cells with anti-CD95 and TCN after 6 hr (Fig. 3*c*, lower panels, lane 11), which is in accordance with the above described caspase activity assays. In summary, the Akt inhibitor TCN amplifies apoptosis induced by the extrinsic pathway. These results are especially intriguing in regard to the fact that both TCN and TRAIL are currently in clinical trials, thereby opening the perspective of a combinatorial therapeutic approach with these two agents.

Successful treatment of prostate carcinomas with TCN and TRAIL depends on the Akt phosphorylation status

In order to corroborate the combined treatment with TCN and TRAIL as a potential approach for the treatment of prostate carcinomas, we analyzed other prostate cancer cell lines for their responsiveness to TCN and TRAIL co-treatment. The results obtained for the prostate carcinoma cell line LNCaP were similar to those obtained for PC-3 cells, *i.e.* significant amplification of TRAIL-induced apoptosis by TCN (Fig. 4*a*). However, the prostate carcinoma cell line Du145 did not respond to either TRAIL alone or in combination with TCN (Fig. 4*b*). To address this obvious discrepancy, we analyzed the activation status of Akt in these cell lines. Therefore, we investigated the phosphorylation status of Akt at Thr308 and Ser473 by immunoblot analysis. PC-3 cells, which show the most prominent effect upon combined treatment with TCN and TRAIL, revealed a strong constitutive phosphorylation at both residues (Fig. 4*c*, lane 1). LNCaP cells comprised Akt which is similarly phosphorylated at Thr308. However, there was almost no phosphorylation detectable at Ser473 (Fig. 4*c*, lane 2). In contrast, Du145 cells did not reveal any Akt phosphorylation and total expression level of Akt was strongly reduced in this cell line (Fig. 4*c*, lane 3). Thus, the reduced expression level of Akt and the lack of Akt phosphorylation might account for the inaptitude of TCN to augment TRAIL-induced apoptosis in

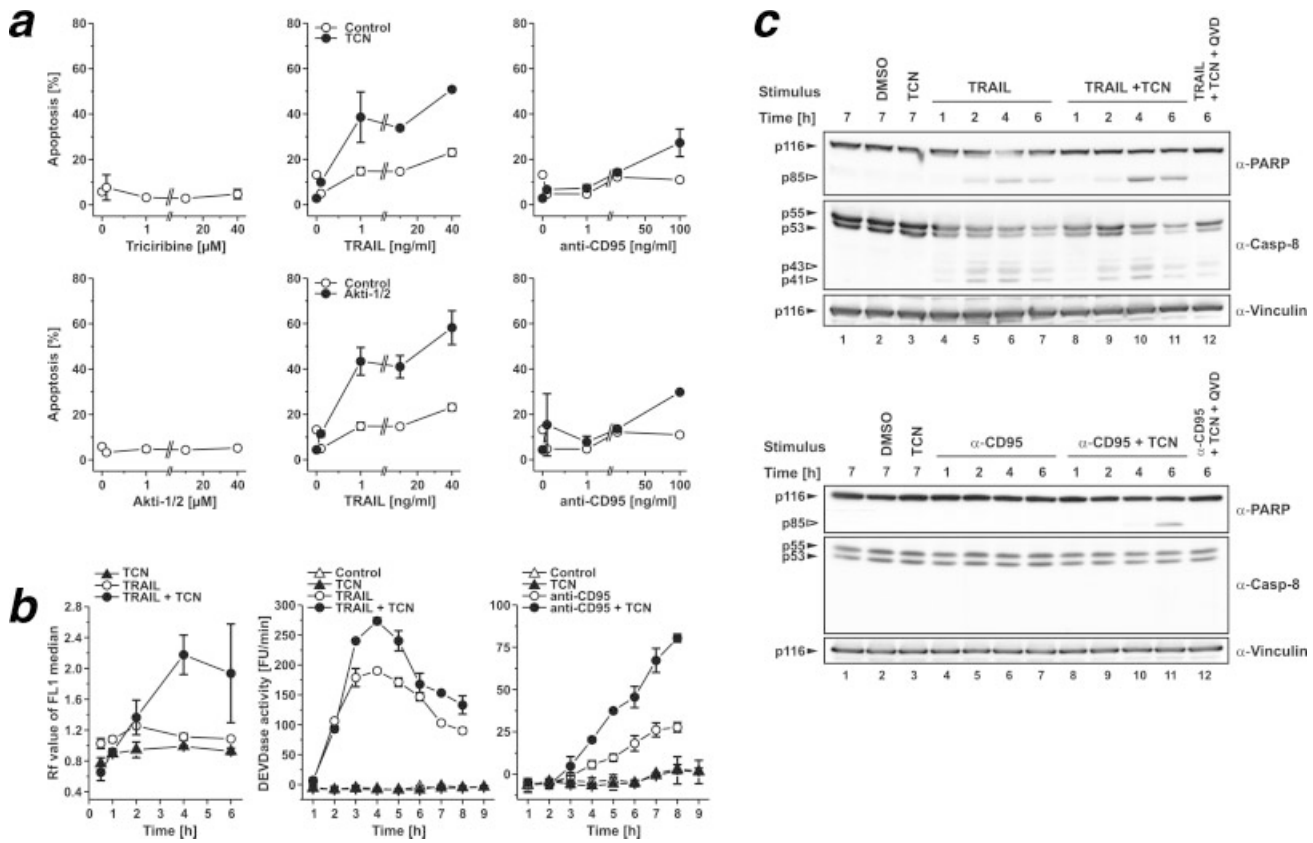

FIGURE 3 – TCN amplifies TRAIL-induced and anti-CD95-induced apoptosis in PC-3 cells. (*a*) TCN enhances TRAIL- and anti-CD95-induced apoptosis in PC-3 cells. PC-3 cells were treated with TRAIL (0.1, 1, 10, or 40 ng/ml) or anti-CD95 (0.1, 1, 10, or 100 ng/ml) in the presence or absence of either TCN (10 μM) or Akti-1/2 (10 μM) for 24 hr. As control PC-3 cells were treated with TCN (0.1, 1, 10 or 40 μM) or Akti-1/2 (0.1, 1, 10 or 40 μM). Apoptosis was assessed by propidium iodide staining of hypodiploid apoptotic nuclei and flow cytometry. Data shown are mean of duplicates ± SD and are representative of three independent experiments. (*b*) TCN increases the TRAIL- and anti-CD95-induced caspase activity in PC-3 cells. PC-3 cells were treated with TRAIL (40 ng/ml) or anti-CD95 (100 ng/ml) in the presence or absence of TCN for various time points (10 μM, TCN was preincubated for 1 hr). After stimuli treatment, the cells were either incubated with FITC-VADfmk and fluorescence was measured via flow cytometry (left panel), or cell lysates were prepared, incubated with the fluorogenic caspase substrate DEVD-AMC, and measured in a spectrofluorimeter (middle and right panel). Caspase activity is given in either Rf values of FL1 median (left panel) or arbitrary fluorescent units/min (middle and right panel). Data shown are mean of duplicates ± SD and are representative of three independent experiments. (*c*) TCN enhances TRAIL-induced PARP cleavage and induces PARP cleavage in anti-CD95 treated PC-3 cells. PC-3 cells were treated with either TRAIL (40 ng/ml) or anti-CD95 (100 ng/ml) in the presence or absence of TCN (10 μM, TCN was preincubated for 1 hr) and the caspase inhibitor QVD (10 μM), and with 0.1% DMSO (diluent control) for the indicated times. Immunoblots were performed with anti-PARP, anti-caspase-8, anti-caspase-3 and anti-vinculin antibodies.

Du145 cells. In order to validate these results in an isogenic background, we down-regulated Akt expression in PC-3 cells by RNA interference (Fig. 5*a*). PC-3 cells expressing reduced levels of Akt were significantly more sensitive to TRAIL-induced apoptosis (Fig. 5*b*). In addition, simultaneous incubation with TCN could not further increase TRAIL-induced apoptosis, clearly showing that TCN-mediated sensitization of TRAIL signaling targets Akt (Fig. 5*b*). Taken together, these data confirm that treatment with TCN/TRAIL might be a successful strategy to overcome anticancer drug-resistance in prostate carcinomas that display an aberrant activation of the Akt-mediated survival pathway.

TCN increases TRAIL-induced cleavage of Bid

Various different mechanisms have been proposed to explain the amplification of TRAIL-induced apoptosis by Akt inhibition, including transcriptional, translational and post-translational processes.[21–23,31] It has been previously shown that Akt-mediated phosphorylation of the phosphoprotein enriched in astrocytes of 15 kDa (PEA-15; also termed phosphoprotein enriched in diabetes, PED) leads to its recruitment to the DISC, ultimately resulting in the inhibition of apoptosis. However, in our cellular model system, we could not detect an altered PEA-15/PED phosphorylation status upon incubation with TCN (Fig. 6*a*). Alternatively, it has been reported that Akt alters expression levels of apoptosis-related proteins such as FLICE-like inhibitory proteins (FLIPs), via the activation of the mammalian target of rapamycin (mTOR).[22] Therefore, we incubated PC-3 cells with rapamaycin and analyzed whether this treatment also amplified TRAIL-induced apoptosis. However, no significant difference could be detected between the incubation with TRAIL alone or in combination with rapamycin (Fig. 6*b*). We also performed immunoblot analyses to test whether TCN or rapamycin affect FLIP expression levels in our cellular model system. Although both TCN and rapamycin inhibited mTOR complex 1 (mTORC1) activity as detected by p70S6 kinase phosphorylation (Fig. 6*c*, lower panels), there were no significant differences in the expression levels of the two splice variants $FLIP_L$ and $FLIP_S$, respectively (Fig. 6*c*, upper and lower panels). It has also been demonstrated that the Akt-mediated survival pathway inhibits apoptotic signals by inhibiting the processing of the pro-apoptotic Bcl-2 member Bid.[21,31,32] Usually, Bid is cleaved by activated caspase-8 and tBid translocates to mitochondria

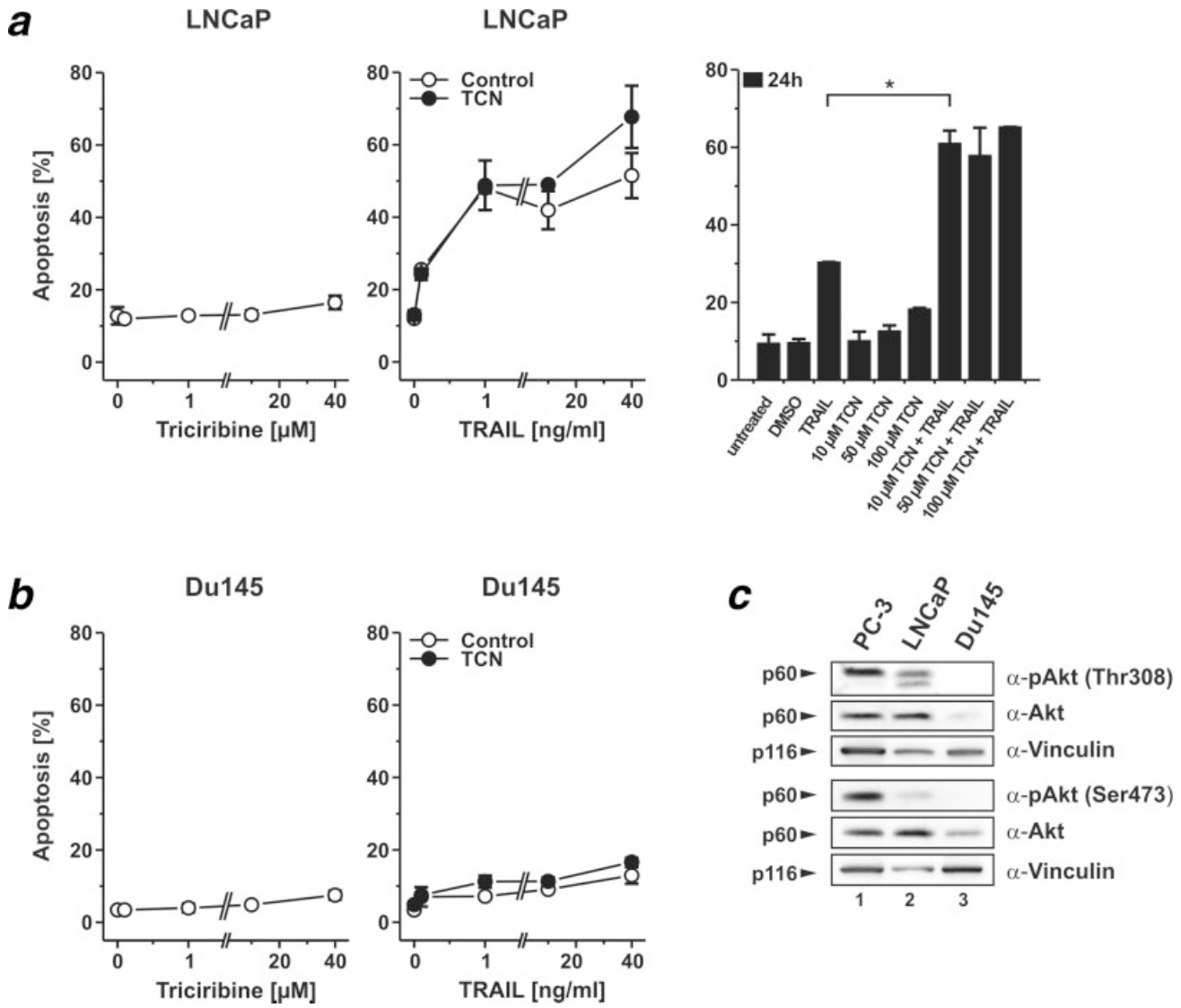

Figure 4 – Effect of TCN on TRAIL-induced apoptosis and phosphorylation of Akt in other prostate cancer cell lines. (*a*) TCN increases TRAIL-induced apoptosis in LNCaP cells. LNCaP cells were treated with either TRAIL (0.1, 1, 10 or 40 ng/ml) in the presence or absence of TCN (10 μM) for 24 hr, or 0.1% DMSO, TRAIL (40 ng/ml), TCN (10, 50 or 100 μM) or the combination of TRAIL (40 ng/ml) and TCN (10, 50 or 100 ng/ml) for 24 hr. Apoptosis was assessed by propidium iodide staining of hypodiploid apoptotic nuclei and flow cytometry. Data shown are mean of duplicates ± SD and are representative of three independent experiments. Asterisk indicates $p < 0.01$ (independent t test). (*b*) TCN does not enhance TRAIL-induced apoptosis in Du145 cells. Du145 cells were treated with TRAIL (0.1, 1, 10 or 40 ng/ml) in the presence or absence of TCN (10 μM) for 24 h. Apoptosis was assessed by propidium iodide staining of hypodiploid apoptotic nuclei and flow cytometry. Data shown are mean of duplicates ± SD and are representative of three independent experiments. (*c*) PC-3 and LNCaP cells show basal phosphorylation of Akt. Lysates of untreated PC-3, LNCaP and Du145 cells were prepared. Immunoblot analyses were performed with anti-phospho-Akt (Thr308 or Ser473), anti-Akt and anti-vinculin antibodies.

where it causes the potent release of cytochrome c, thereby connecting extrinsic and intrinsic apoptotic pathways.[6] Actually, when PC-3 cells were treated with both TCN and TRAIL we observed an increased processing of Bid compared to cells treated with TRAIL alone (Fig. 6*d*). Since Bid cleavage is a pre-mitochondrial event dependent on death receptor ligation, this observation might explain why TCN-mediated amplification does not occur with anticancer drugs that directly activate the mitochondrial death pathway independent of Bid cleavage.

Discussion

The PI3K/Akt signaling pathway represents one of the major survival pathways that is deregulated in many human cancers and contributes to both cancer pathogenesis and therapy resistance. Aberrant activation of this pathway might be caused by various components, including increased growth factor signaling, constitutive activation of PI3K, loss of function of the PI3K antagonist PTEN, or constitutive activation of Akt, respectively.[35] Therefore, current therapeutic approaches target this survival pathway. In this report we demonstrate that the Akt inhibitor TCN sensitizes prostate cancer cells for TRAIL-induced apoptosis, whereas the cells remained resistant to conventional anticancer drugs. The TCN-mediated amplification of death receptor-induced apoptosis essentially depended on the basal Akt activation status, *i.e.* prostate cancer cells revealing high phospho-Akt levels were responsive to this combined treatment. Vice versa, using RNA interference we could confirm that TCN has no sensitizing effect in cells expressing reduced levels of Akt. As a potential mechanism we could

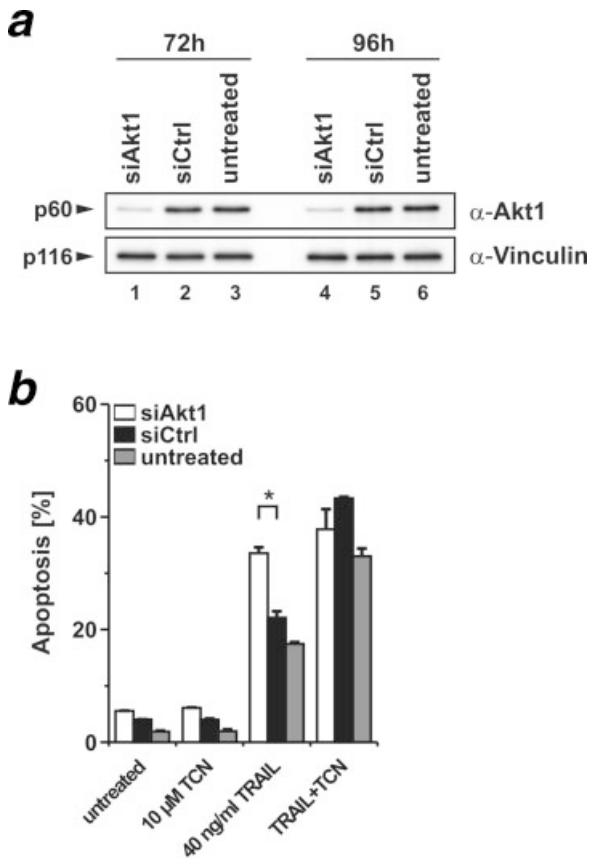

FIGURE 5 – siRNA-mediated down-regulation of Akt expression abolishes sensitizing effect of TCN. (*a*) Down-regulation of Akt in PC-3 cells. PC-3 cells were transfected with an siRNA pool targeting Akt1 (siAkt, 20 nM), a non-targeting siRNA control pool (siCtrl, 20 nM), or left untreated for 72 and 96 hr (time points represent set-up and analysis of apoptosis measurement). Immunoblot analyses were performed using anti-Akt1 and anti-vinculin antibodies, respectively (*b*) Down-regulation of Akt sensitizes PC-3 cells to TRAIL-induced apoptosis. After 72 hr untreated PC-3 cells or cells transfected with either Akt1-targeting siRNA or non-targeting siRNA were treated with TCN (10 μM), TRAIL (40 ng/ml), the combination of TCN and TRAIL or left untreated for additional 24 hr. Apoptosis was assessed by propidium iodide staining of hypodiploid apoptotic nuclei and flow cytometry. Data shown are mean of duplicates ± SD and are representative of three independent experiments. Asterisk indicates $p < 0.01$ (independent t test).

show that TCN amplified TRAIL-induced Bid cleavage, which might result in an enhanced activation of the mitochondrial amplification loop. The fact that derivatives of both TCN and TRAIL are currently assessed in clinical trials opens the intriguing opportunity of a novel combination therapy for prostate cancers and other tumor entities. Furthermore, this combination might also lead to novel therapeutic approaches for diseases like HIV-infection; since it could be shown that TRAIL-mediated apoptosis in HIV-1-infected macrophages is dependent on the inhibition of Akt phosphorylation.[36]

The tricyclic nucleoside analog TCN has been recently discovered to inhibit Akt activity. Accordingly, we can show that Akt phosphorylation and activity is reduced upon TCN-treatment in PC-3 cells. In our experiments TCN shows an inhibitory potential similar to the reported pleckstrin-homology-domain-dependent Akt inhibitor Akti-1/2.[37] PC-3 cells are resistant to DNA-damaging anticancer drugs like mitomycin C and etoposide and this resistance could not be overcome by the parallel inhibition of Akt. However, TCN sensitized PC-3 cells to death receptor-induced apoptosis. Interestingly, we observed a distinct susceptibility between different death receptor pathways. TRAIL by itself already induced caspase-8 cleavage and activation of caspase-3 and cotreatment with TCN increased this effect substantially. In contrast, anti-CD95-treatment alone did not show any caspase activation in PC-3 cells. However, caspases became activated after the combined incubation with anti-CD95 and TCN. Furthermore, caspase activation occurred at earlier time points for TRAIL/TCN-treatment than for anti-CD95/TCN. However, the molecular relevance of this observation remains so far elusive.

Several reports have recently described the observation that constitutively active Akt contributes to TRAIL resistance in prostate cancer. Accordingly, Akt inhibition led to TRAIL-mediated apoptosis.[21,23,31,38,39] Similar results were also obtained for alternative tumor models, *e.g.* leukaemia, multiple myeloma, lung cancer, renal cancer, colon cancer, bladder cancer and thyroid cancer.[10,21,32-34] Various different molecular mechanisms have been suggested to contribute to Akt-regulated TRAIL sensitivity, including transcriptional, translational and post-translational processes.[21-23,31] In initial experiments we focussed on Akt substrates which directly influence death receptor-mediated signaling. The phosphoprotein PEA-15/PED contains death effector domains (DEDs) capable of interacting with DEDs of FADD or caspase-8, respectively. PEA-15/PED is recruited to the DISC of death receptors and can inhibit caspase activation.[40] The inhibitory potential of PEA-15/PED is regulated by Akt-mediated phosphorylation.[41] However, in our experimental setting there was neither a decreased PEA-15/PED phosphorylation nor protein level detectable upon TCN-treatment, indicating that PEA-15/PED does not contribute to the observed sensitization. Yet, we cannot exclude that other Akt substrates directly influence TRAIL-mediated signaling.

It has also been proposed that FLIP is a key controller of TRAIL sensitivity. Studies by Panner *et al*. revealed that active Akt selectively increases FLIP levels and thereby contributes to TRAIL resistance.[22] The proposed mechanism included activation of the mammalian target of rapamycin (mTOR) and its downstream targets S6 kinase (S6K) and elongation/translation initiation factor 4E (eIF4e), which in turn drive flip mRNA translation.[22] Therefore, it was proposed that the combination of TRAIL and rapamycin could increase the apoptosis-inducing potential of TRAIL.[15,22] However, this translational regulation of TRAIL sensitivity does not play a role in our prostate cancer model, since cotreatment with TRAIL and rapamycin did not result in increased apoptosis. It has also been reported that constitutive Akt signaling increases FLIP levels in the androgen-independent prostate cancer cell lines PC-3 and Du145.[42] Yet, we cannot detect any differences in FLIP protein expression. Additionally, flip mRNA levels are unaltered, as confirmed by RT-PCR (data not shown). Nevertheless, we cannot exclude that other Akt-mediated translational regulation also contributes to the observed sensitization, though the kinetics of caspase activation imply a rather direct role of Akt.

Like CD95L, TRAIL can trigger apoptosis in both type I and type II cells.[11] Therefore, we included the detection of Bid cleavage in our analysis. It has been previously suggested that the PI3K/Akt pathway may inhibit apoptotic signals by inhibiting Bid cleavage.[21,31,32] Actually, Bid processing was significantly enhanced upon co-treatment of PC-3 cells with TRAIL and TCN, indicating that Akt might inhibit TRAIL-induced apoptosis at the point of Bid cleavage. It is currently unknown how Akt regulates this processing, since Bid is no direct substrate of Akt. However, it was reported that Bid phosphorylation regulates its cleavage by caspases.[43] Therefore it is conceivable that Akt plays a role in this process, either by increasing caspase-8 activity or by rendering Bid more accessible to proteolytic cleavage. However, the latter possibility seems to be more likely, since there is no detectable alteration in caspase-8 processing upon TRAIL-treatment alone or in combination with TCN.

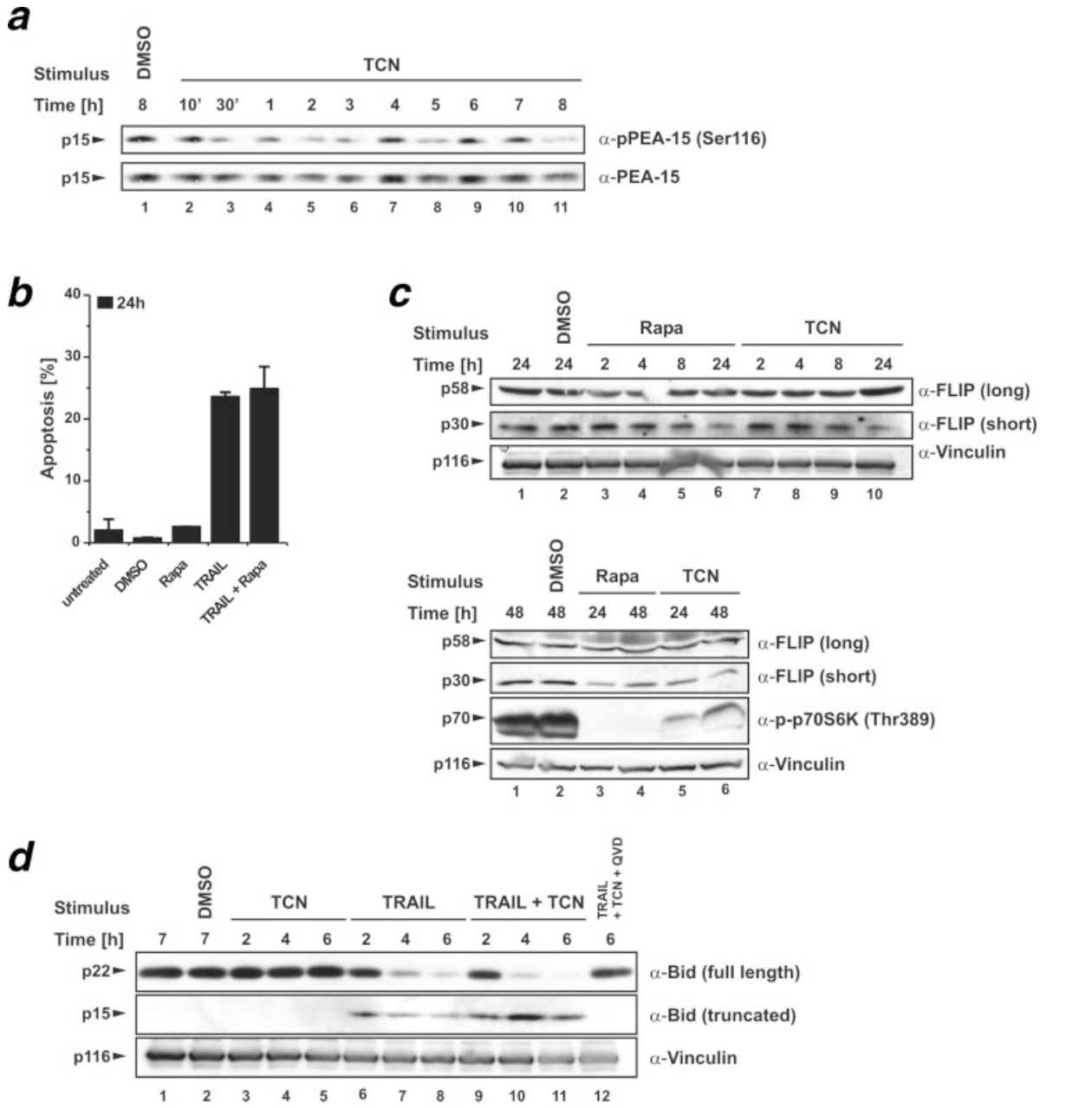

Figure 6 – TCN increases TRAIL-mediated Bid cleavage. (*a*) TCN does not alter phosphorylation of PEA-15/PED. PC-3 cells were treated with TCN (10 μM) for various time points or 0.1% DMSO. Immunoblots were performed with anti-phospho-/PED-15 (Ser116) and anti-PEA-15/PED antibodies. (*b*) Rapamycin does not enhance TRAIL-induced apoptosis in PC-3 cells. PC-3 cells were treated with TRAIL (40 ng/ml), rapamycin (Rapa, 100 nM) or TRAIL in combination with rapamycin for 24 hr. Apoptosis was assessed by propidium iodide staining of hypodiploid apoptotic nuclei and flow cytometry. Data shown are mean of duplicates ± SD and are representative of three independent experiments. (*c*) Rapamycin and TCN do not alter FLIP expression levels in PC-3 cells. PC-3 cells were treated with TCN (10 μM), rapamycin (Rapa, 100 nM), 0.1% DMSO for various times, or left untreated. Immunoblots were performed with anti-FLIP, anti-vinculin, or anti-phospho-p70S6K antibodies, respectively. (*d*) TCN enhances TRAIL-induced Bid cleavage in PC-3 cells. PC-3 cells were treated with TCN (10 μM), TRAIL (40 ng/ml) or TRAIL in combination with TCN for the indicated times (TCN was preincubated for 1 hr). Immunoblots were performed with anti-Bid and anti-vinculin antibodies.

In our study we deliberately focussed on the Akt inhibitor TCN, since this compound is currently evaluated in clinical trials. Alternative Akt-specific inhibitors have also entered clinical trials. However, so far most Akt inhibitors display a rather limited clinical activity as single agents which clearly emphasizes the importance of combinatorial treatments.[44] To date, lipid-based Akt inhibitors are the most developed agents, including the alkylphospholipids perifosine, miltefosine and edelfosine. Perifosine is currently the best characterized Akt inhibitor and is assessed in different phase II studies.[44] However, one study of oral perifosine in refractory androgen-independent prostate cancer did not demonstrate any clinical activity.[45] The recent identification of TCN as an Akt inhibitor has raised new interest in studying this compound and it has been observed that TCN stimulates apoptosis of xenografts of human breast, prostate, ovarian and pancreatic cancer cells exhibiting high Akt activity.[30,44]

In summary, our results provide evidence that the combined application of TRAIL and TCN might be an effective treatment for prostate cancers. Our data indicate that this treatment critically depends on a high constitutive Akt phosphorylation level. This is especially intriguing in regard to recent findings that aberrant activation of the PI3K/Akt pathway may contribute to increased prostate cancer cell invasiveness and to potentially metastatic disease.[46]

Acknowledgements

This work was supported by grants from the Deutsche Forschungsgemeinschaft (RL, SU, SW, BS), the Interdisciplinary Center of Clinical Research, Faculty of Medicine, Tübingen (BS, SW), the Wilhelm Sander-Stiftung (SW) and the Landesforschungsschwerpunktprogramm of the Ministry of Science, Research and Arts of the Land Baden-Württemberg (SW).

References

1. Majumder PK, Sellers WR. Akt-regulated pathways in prostate cancer. Oncogene 2005;24:7465–74.
2. Belka C, Rudner J, Wesselborg S, Stepczynska A, Marini P, Lepple-Wienhues A, Faltin H, Bamberg M, Budach W, Schulze-Osthoff K. Differential role of caspase-8 and BID activation during radiation- and CD95-induced apoptosis. Oncogene 2000;19:1181–90.
3. Engels IH, Stepczynska A, Stroh C, Lauber K, Berg C, Schwenzer R, Wajant H, Janicke RU, Porter AG, Belka C, Gregor M, Schulze Osthoff K, et al. Caspase-8/FLICE functions as an executioner caspase in anticancer drug-induced apoptosis. Oncogene 2000;19:4563–73.
4. Tan TT, White E. Therapeutic targeting of death pathways in cancer: mechanisms for activating cell death in cancer cells. Adv Exp Med Biol 2008;615:81–104.
5. Muzio M, Stockwell BR, Stennicke HR, Salvesen GS, Dixit VM. An induced proximity model for caspase-8 activation. J Biol Chem 1998;273:2926–30.
6. Luo X, Budihardjo I, Zou H, Slaughter C, Wang X. Bid, a Bcl2 interacting protein, mediates cytochrome c release from mitochondria in response to activation of cell surface death receptors. Cell 1998;94:481–90.
7. Barnhart BC, Alappat EC, Peter ME. The CD95 type I/type II model. Semin Immunol 2003;15:185–93.
8. Nagata S. Apoptosis by death factor. Cell 1997;88:355–65.
9. Orlinick JR, Vaishnaw AK, Elkon KB. Structure and function of Fas/Fas ligand. Int Rev Immunol 1999;18:293–308.
10. Oka N, Tanimoto S, Taue R, Nakatsuji H, Kishimoto T, Izaki H, Fukumori T, Takahashi M, Nishitani M, Kanayama HO. Role of phosphatidylinositol-3 kinase/Akt pathway in bladder cancer cell apoptosis induced by tumor necrosis factor-related apoptosis-inducing ligand. Cancer Sci 2006;97:1093–8.
11. Suliman A, Lam A, Datta R, Srivastava RK. Intracellular mechanisms of TRAIL: apoptosis through mitochondrial-dependent and -independent pathways. Oncogene 2001;20:2122–33.
12. Walczak H, Miller RE, Ariail K, Gliniak B, Griffith TS, Kubin M, Chin W, Jones J, Woodward A, Le T, Smith C, Smolak P, et al. Tumoricidal activity of tumor necrosis factor-related apoptosis-inducing ligand in vivo. Nat Med 1999;5:157–63.
13. Ashkenazi A, Pai RC, Fong S, Leung S, Lawrence DA, Marsters SA, Blackie C, Chang L, McMurtrey AE, Hebert A, DeForge L, Koumenis IL, et al. Safety and antitumor activity of recombinant soluble Apo2 ligand. J Clin Invest 1999;104:155–62.
14. Bonavida B, Ng CP, Jazirehi A, Schiller G, Mizutani Y. Selectivity of TRAIL-mediated apoptosis of cancer cells and synergy with drugs: the trail to non-toxic cancer therapeutics (review). Int J Oncol 1999;15:793–802.
15. Falschlehner C, Emmerich CH, Gerlach B, Walczak H. TRAIL signalling: decisions between life and death. Int J Biochem Cell Biol 2007;39:1462–75.
16. Finnberg N, El-Deiry WS. TRAIL death receptors as tumor suppressors and drug targets. Cell Cycle 2008;7.
17. Huang Y, Sheikh MS. TRAIL death receptors and cancer therapeutics. Toxicol Appl Pharmacol 2007;224:284–9.
18. Carlo-Stella C, Lavazza C, Locatelli A, Vigano L, Gianni AM, Gianni L. Targeting TRAIL agonistic receptors for cancer therapy. Clin Cancer Res 2007;13:2313–7.
19. Ozoren N, El-Deiry WS. Cell surface death receptor signaling in normal and cancer cells. Semin Cancer Biol 2003;13:135–47.
20. Poulaki V, Mitsiades CS, McMullan C, Fanourakis G, Negri J, Goudopoulou A, Halikias IX, Voutsinas G, Tseleni-Balafouta S, Miller JW, Mitsiades N. Human retinoblastoma cells are resistant to apoptosis induced by death receptors: role of caspase-8 gene silencing. Invest Ophthalmol Vis Sci 2005;46:358–66.
21. Whang YE, Yuan XJ, Liu Y, Majumder S, Lewis TD. Regulation of sensitivity to TRAIL by the PTEN tumor suppressor. Vitam Horm 2004;67:409–26.
22. Panner A, Parsa AT, Pieper RO. Translational regulation of TRAIL sensitivity. Cell Cycle 2006;5:147–50.
23. Deeb D, Jiang H, Gao X, Al-Holou S, Danyluk AL, Dulchavsky SA, Gautam SC. Curcumin [1,7-bis(4-hydroxy-3-methoxyphenyl)-1-6-heptadine-3,5-dione; C21H20O6] sensitizes human prostate cancer cells to tumor necrosis factor-related apoptosis-inducing ligand/Apo2L-induced apoptosis by suppressing nuclear factor-kappaB via inhibition of the prosurvival Akt signaling pathway. J Pharmacol Exp Ther 2007;321:616–25.
24. Kandel ES, Hay N. The regulation and activities of the multifunctional serine/threonine kinase Akt/PKB. Exp Cell Res 1999;253:210–29.
25. Sarbassov DD, Guertin DA, Ali SM, Sabatini DM. Phosphorylation and regulation of Akt/PKB by the rictor-mTOR complex. Science 2005;307:1098–101.
26. Datta SR, Dudek H, Tao X, Masters S, Fu H, Gotoh Y, Greenberg ME. Akt phosphorylation of BAD couples survival signals to the cell-intrinsic death machinery. Cell 1997;91:231–41.
27. Maurer U, Charvet C, Wagman AS, Dejardin E, Green DR. Glycogen synthase kinase-3 regulates mitochondrial outer membrane permeabilization and apoptosis by destabilization of MCL-1. Mol Cell 2006;21:749–60.
28. Cardone MH, Roy N, Stennicke HR, Salvesen GS, Franke TF, Stanbridge E, Frisch S, Reed JC. Regulation of cell death protease caspase-9 by phosphorylation. Science 1998;282:1318–21.
29. Wotring LL, Townsend LB, Jones LM, Borysko KZ, Gildersleeve DL, Parker WB. Dual mechanisms of inhibition of DNA synthesis by triciribine. Cancer Res 1990;50:4891–9.
30. Yang L, Dan HC, Sun M, Liu Q, Sun XM, Feldman RI, Hamilton AD, Polokoff M, Nicosia SV, Herlyn M, Sebti SM, Cheng JQ. Akt/protein kinase B signaling inhibitor-2, a selective small molecule inhibitor of Akt signaling with antitumor activity in cancer cells overexpressing Akt Cancer Res 2004;64:4394–9.
31. Chen X, Thakkar H, Tyan F, Gim S, Robinson H, Lee C, Pandey SK, Nwokorie C, Onwudiwe N, Srivastava RK. Constitutively active Akt is an important regulator of TRAIL sensitivity in prostate cancer. Oncogene 2001;20:6073–83.
32. Kandasamy K, Srivastava RK. Role of the phosphatidylinositol 3′-kinase/PTEN/Akt kinase pathway in tumor necrosis factor-related apoptosis-inducing ligand-induced apoptosis in non-small cell lung cancer cells. Cancer Res 2002;62:4929–37.
33. Asakuma J, Sumitomo M, Asano T, Hayakawa M. Selective Akt inactivation and tumor necrosis actor-related apoptosis-inducing ligand sensitization of renal cancer cells by low concentrations of paclitaxel. Cancer Res 2003;63:1365–70.
34. Vaculova A, Hofmanova J, Soucek K, Kozubik A. Different modulation of TRAIL-induced apoptosis by inhibition of pro-survival pathways in TRAIL-sensitive and TRAIL-resistant colon cancer cells. FEBS Lett 2006;580:6565–9.
35. Engelman JA, Luo J, Cantley LC. The evolution of phosphatidylinositol 3-kinases as regulators of growth and metabolism. Nat Rev Genet 2006;7:606–19.
36. Huang Y, Erdmann N, Peng H, Herek S, Davis JS, Luo X, Ikezu T, Zheng J. TRAIL-mediated apoptosis in HIV-1-infected macrophages is dependent on the inhibition of Akt-1 phosphorylation. J Immunol 2006;177:2304–13.
37. Barnett SF, Defeo-Jones D, Fu S, Hancock PJ, Haskell KM, Jones RE, Kahana JA, Kral AM, Leander K, Lee LL, Malinowski J, McAvoy EM, et al. Identification and characterization of pleckstrin-homology-domain-dependent and isoenzyme-specific Akt inhibitors. Biochem J 2005;385:399–408.
38. DeFeo-Jones D, Barnett SF, Fu S, Hancock PJ, Haskell KM, Leander KR, McAvoy E, Robinson RG, Duggan ME, Lindsley CW, Zhao Z, Huber HE, et al. Tumor cell sensitization to apoptotic stimuli by selective inhibition of specific Akt/PKB family members. Mol Cancer Ther 2005;4:271–9.
39. Kim YH, Lee YJ. TRAIL apoptosis is enhanced by quercetin through Akt dephosphorylation. J Cell Biochem 2007;100:998–1009.
40. Condorelli G, Vigliotta G, Cafieri A, Trencia A, Andalo P, Oriente F, Miele C, Caruso M, Formisano P, Beguinot F. PED/PEA-15: an

anti-apoptotic molecule that regulates FAS/TNFR1-induced apoptosis. Oncogene 1999;18:4409–15.
41. Trencia A, Perfetti A, Cassese A, Vigliotta G, Miele C, Oriente F, Santopietro S, Giacco F, Condorelli G, Formisano P, Beguinot F. Protein kinase B/Akt binds and phosphorylates PED/PEA-15, stabilizing its antiapoptotic action. Mol Cell Biol 2003;23:4511–21.
42. Panka DJ, Mano T, Suhara T, Walsh K, Mier JW. Phosphatidylinositol 3-kinase/Akt activity regulates c-FLIP expression in tumor cells. J Biol Chem 2001;276:6893–6.
43. Degli Esposti M, Ferry G, Masdehors P, Boutin JA, Hickman JA, Dive C. Post-translational modification of Bid has differential effects on its susceptibility to cleavage by caspase 8 or caspase 3. J Biol Chem 2003;278:15749–57.
44. LoPiccolo J, Granville CA, Gills JJ, Dennis PA. Targeting Akt in cancer therapy. Anticancer Drugs 2007;18:861–74.
45. Posadas EM, Gulley J, Arlen PM, Trout A, Parnes HL, Wright J, Lee MJ, Chung EJ, Trepel JB, Sparreboom A, Chen C, Jones E, et al. A phase II study of perifosine in androgen independent prostate cancer. Cancer Biol Ther 2005;4:1133–7.
46. Shukla S, Maclennan GT, Hartman DJ, Fu P, Resnick MI, Gupta S. Activation of PI3K-Akt signaling pathway promotes prostate cancer cell invasion. Int J Cancer 2007;121:1424–32.

The 3-phosphoinositide-dependent protein kinase 1 (PDK1) controls upstream PI3K expression and PIP_3 generation

Alexandra M. Dieterle[1,‡], Philip Böhler[2,‡], Hildegard Keppeler[1], Sebastian Alers[1], Niklas Berleth[2], Stefan Drießen[2], Nora Hieke[2], Sabine Pietkiewicz[2], Antje S. Löffler[2], Christoph Peter[2], Alex Gray[3], Nick R. Leslie[3], Hisaaki Shinohara[4], Tomohiro Kurosaki[4], Michael Engelke[5], Jürgen Wienands[5], Michael Bonin[6], Sebastian Wesselborg[2], Björn Stork[2,*]

[1]*Department of Internal Medicine I, University Hospital Tübingen, 72076 Tübingen, Germany*

[2]*Institute of Molecular Medicine, University Hospital Düsseldorf, 40225 Düsseldorf, Germany*

[3]*Division of Cell Signaling and Immunology, College of Life Sciences, University of Dundee, Dundee DD1 5EH, Scotland, UK*

[4]*Laboratory for Lymphocyte Differentiation, RIKEN Research Center for Allergy and Immunology, Tsurumi-ku, Yokohama, Kanagawa 230-0045, Japan*

[5]*Cellular and Molecular Immunology, University Hospital Göttingen, 37073 Göttingen, Germany*

[6]*MFT Services, Medical Genetics, University Hospital Tübingen, 72076 Tübingen, Germany*

‡ these authors contributed equally

*Corresponding author: Björn Stork, PhD, Institute of Molecular Medicine, University Hospital Düsseldorf, Building 23.12, Universitätsstr. 1, 40225 Düsseldorf, Germany,
Tel.: +49 (0)211 81 11954, Fax: +49 (0)211 81 12889,
E-mail: bjoern.stork@uni-duesseldorf.de

Running title: PDK1-mediated transcriptional control of PI3K
Keywords: Akt / PDK1 / PI3K / survival / B lymphocytes
Word count: 5734 (Introduction, Results, Discussion, Materials and Methods)

Abstract

The PI3K/PDK1/Akt signaling axis is centrally involved in cellular homeostasis and controls cell growth and proliferation. Due to its key function as regulator of cell survival and metabolism, the dysregulation of this pathway is manifested in several human pathologies including cancers and immunological diseases. Thus, current therapeutic strategies target the components of this signaling cascade. In recent years numerous feedback loops have been identified, which attenuate PI3K/PDK1/Akt-dependent signaling. Here we report the identification of an additional level of feedback regulation, which depends on the negative transcriptional control of PI3K class IA subunits. Genetic deletion of PDK1 or the pharmacological inhibition of its downstream effectors, i.e. Akt and mTOR, relieve this suppression and lead to the up-regulation of PI3K subunits, resulting in enhanced generation of PIP_3. Apparently this transcriptional induction is mediated by the concerted action of different transcription factor families, including CREB and forkhead box O transcription factors. Collectively, we propose that PDK1 functions as a cellular sensor which balances basal PIP_3 generation at levels sufficient for survival but below a threshold being harmful to the cell. Our study suggests that the efficiency of therapies targeting the aberrantly activated PI3K/PDK1/Akt pathway might be increased by the parallel blockade of feedback circuits.

Introduction

The PI3K/PDK1/Akt pathway regulates various cellular processes, including cell growth, survival and proliferation. Accordingly, the dysregulation of this pathway has been implicated in several human cancers and in immunological diseases, and the components of this pathway are attractive targets of current therapeutic strategies (reviewed in [1-8]).

PI3Ks are intracellular lipid kinases, which are grouped into three classes (I - III). Class I PI3Ks generate phosphatidylinositol-3,4,5-trisphosphate (PIP_3) by phosphorylating phosphatidylinositol-4,5-bisphosphate (PIP_2) at the D3 position of the inositol ring.[9] Class I PI3Ks are heterodimers consisting of a p110 catalytic subunit (p110α, p110β, p110δ, and p110γ) and a regulatory subunit. The class IA isoforms p110α, p110β and p110δ pair with the p85 subfamily of regulatory subunits (p85α, p85β, p55α, p50α, and p55γ). The class IB p110γ isoform associates with p101 or p84/p87 subunits.[9,10] In turn, PIP_3 levels are negatively regulated by the action of lipid phosphatases, which remove the different phosphate groups from the inositol ring.[11]

Most of the cellular responses to PI3K activation and PIP_3 generation are mediated by the activation of AGC kinases such as Akt (also termed protein kinase B, PKB), p70S6K, and serum- and glucocorticoid-induced protein kinase (SGK) (reviewed in [12,13]). For full activation, these kinases have to be phosphorylated both in an activation segment (T-loop) and within a hydrophobic motif.[13] The common upstream activator of these kinases is the AGC kinase PDK1, which catalyzes the T-loop phosphorylation.[13-23] PDK1 possesses an N-terminal serine/threonine kinase domain and a C-terminal pleckstrin homology (PH) domain, which binds to PIP_3 and its degradation product phosphatidylinositol-3,4-bisphosphate.[14,15,24,25] The constitutively active PDK1 itself is not stimulated by PI3K.[14] However, the mechanism by which PDK1 activates its substrates is controlled by PIP_3. In case of Akt, PIP_3 induces a conformational change of Akt by binding its N-terminal PH domain, which leads to PDK1-mediated phosphorylation of T308 in the activation segment of

Akt.[25] Full Akt activation is achieved by phosphorylation of S473 within the hydrophobic motif via the mammalian target of rapamycin complex 2 (mTORC2).[26,27] In contrast to Akt, the kinases p70S6K and SGK lack a PH domain. They get phosphorylated in the hydrophobic motif by mTORC1 or mTORC2 following PI3K activation.[13,28,29] The hydrophobic motif phosphorylation does not directly activate p70S6K and SGK, but regulates their interaction with PDK1.[30,31] PDK1 binds to the phosphorylated hydrophobic motif via its PDK1-interacting fragment (PIF) pocket, and consequently phosphorylates the activation segment and thereby activates these kinases.[13] Upon activation of PI3Ks by insulin, growth factors or antigens, AGC kinases get activated and in turn phosphorylate various downstream targets, e.g. glycogen synthase kinase 3β (GSK3β), tuberous sclerosis complex 2 (TSC2), or forkhead box O (FOXO) transcription factors.[6,13] Additionally, in recent years it became evident that PI3K is tightly controlled by its downstream targets, thus providing feedback regulation in response to extracellular signals.[32]

To further characterize the involvement of PDK1 in pro-survival signaling pathways and its contribution to feedback regulation of PI3K, we analyzed the transcriptome in an inducible PDK1 knockout system. We show that upon PDK1 knockout induction in DT40 B lymphocytes class IA PI3K subunits p85α, p110β and p110δ are up-regulated both on mRNA and protein level. Furthermore, we demonstrate that PDK1 depletion increases the amount of the PI3K product PIP_3 in the plasma membrane. It appears that this PDK1-dependent transcriptional repression of PI3K class IA subunits is mainly mediated via the Akt/mTORC1 signaling axis and members of different transcription factor families, including CREB and FOXOs. Collectively, we propose a transcriptional level of feedback regulation targeting the PI3K/PDK1/Akt/mTOR signaling pathway. This novel feedback mechanism might further emphasize the need for dual inhibitors of PI3K and mTOR in cancer therapy.

Results

Tonic PDK1 signaling is essential for survival of DT40 B lymphocytes

To gain further insight into the function of PDK1 in survival signaling, we made use of the conditional *PDK1*-/cond chicken DT40 B cell line (*PDK1*-/cond).[33] In these cells 4-hydroxytamoxifen (OH-TAM)-activated Cre recombinase induces the deletion of the floxed *PDK1* gene. We treated DT40 *PDK1*-/cond cells with OH-TAM and verified the absence of PDK1 expression by immunoblotting. In DT40 wild-type cells OH-TAM alone had no effect on PDK1 expression (Figure 1A).

PDK1 plays an important role in survival signaling and embryos of *Pdk1*-/- mice die at day 9.5.[34] Thus, we analyzed apoptosis in OH-TAM-treated DT40 *PDK1*-/cond and wt cells by measuring hypodiploid nuclei. OH-TAM-treated *PDK1*-/cond cells underwent apoptosis from day six of treatment, but not the wt or EtOH-treated cells (Figure 1B). Since DT40 cells are immature B lymphocytes and therefore respond with apoptosis induction upon crosslinking of the B cell antigen receptor (BCR),[35] we investigated if the loss of PDK1 has any effect on BCR-induced apoptosis. We stimulated DT40 *PDK1*-/cond cells on day four of OH-TAM treatment, on which the cells were PDK1 negative but still viable (Figures 1A and B), with anti-chicken-IgM antibodies and analyzed apoptosis by measuring hypodiploid nuclei. As control, we used EtOH-treated *PDK1*-/cond and wt cells. While loss of PDK1 strongly increased BCR-induced apoptosis, wt cells did not display any differences in BCR-induced apoptosis following OH-TAM treatment (Figure 1C).

Taken together, PDK1 is mandatory for the constitutive survival signaling in DT40 cells and its loss sensitizes these cells to BCR-induced apoptosis.

Microarray analysis of PDK1-*/cond cells*

Next we addressed the question whether PDK1 also regulates long term transcription dynamics. To investigate this, we performed microarray analyses using the Affymetrix

GeneChip® Chicken Genome Array. We treated DT40 *PDK1*-/cond cells with OH-TAM or EtOH to identify PDK1-dependent target genes. Additionally, we treated DT40 wt cells with OH-TAM or EtOH to exclude OH-TAM-dependent effects. Successful depletion of PDK1 in *PDK1*-/cond cells used for microarray analyses was confirmed by immunoblotting and real-time RT-PCR (Supplementary Figure S1A and S1B). Only transcripts which were regulated with ≥ 2 fold changes were considered as relevant. When comparing the transcripts of *PDK1*-/cond and wt cells both treated with OH-TAM, we identified 1696 relevant transcripts. In turn, the comparison of *PDK1*-/cond cells treated with OH-TAM or EtOH revealed 764 relevant transcripts. Altogether 503 transcripts were regulated in both entity lists (Supplementary Figure S1C). Next, we performed global function and pathway analyses of the gene products of the 503 transcripts using Ingenuity Pathway Analysis Software (Supplementary Figure S1D). We could observe that the 503 gene products play key roles in cellular homeostasis and immune responses. Due to the fact that PDK1 deletion is lethal, we were mostly interested in regulated genes of survival signaling pathways. It has been previously reported that transcription factors of the forkhead box O (FOXO) family are regulated via the PI3K/PDK1/Akt signaling pathway.[36,37] In our microarray analysis, several apoptosis-relevant FOXO target genes such as TRAIL, p27Kip1 or Bcl-6 were PDK1-dependently regulated (Figure 2A). Strikingly, our microarray results revealed PDK1-dependent regulation of gene products which regulate the signaling pathway upstream of PDK1. Among these gene products were the phosphatidylinositol 3-kinase (PI3K) class IA subunits p110β and p110δ (catalytic subunits), p85α (regulatory subunit), additional phosphoinositide-modifying enzymes (INPP5B, PIP5K1-β), the PI3K interacting protein 1 (PIK3IP1) and the B cell-specific Src-family tyrosine kinase Lyn (Figure 2A and B). Lyn links the BCR to the activation of PI3K/PDK1/Akt signaling in B lymphocytes, since it directly phosphorylates CD19 and contributes to the activation of the tyrosine kinases Syk and

Btk, which both phosphorylate the B cell adapter for PI3K (BCAP).[38] Tyrosine-phosphorylated CD19 and/or BCAP then recruit the regulatory PI3K subunit p85α.[38]

Next, we performed quantitative real-time RT-PCRs of the *PIK3CB* (PI3K p110β subunit), *PIK3CD* (PI3K p110δ subunit), *PIK3R1* (PI3K p85α subunit), *LYN* (Lyn) and *INPP5B* (phosphoinositide 5-phosphatase) genes in order to confirm the microarray results. We treated DT40 *PDK1*-/cond and wt cells with OH-TAM or EtOH and determined the mRNA level at the indicated time points (Figure 2C). In accordance with the microarray results, *PIK3CB*, *PIK3CD, PIK3R1* and *LYN* were up-regulated, and *INPP5B* was down-regulated.

Taken together, we could show that knockout of PDK1 indirectly alters the PI3K-PDK1 signaling axis by regulating gene transcription of Lyn, PI3K subunits and phosphoinositide-modifying enzymes.

PDK1 negatively regulates expression of PI3K subunits

In order to confirm the results obtained by microarray analysis and RT-PCR on the protein level, we analyzed the expression of the PI3K subunits p110β, p110δ and p85α, Lyn and INPP5B in DT40 *PDK1*-/cond cells treated with OH-TAM or EtOH by immunoblotting. We observed an increase of protein expression of all three PI3K subunits (Figure 3A). Similarly, protein levels of the Src-family kinase Lyn were elevated upon PDK1 depletion (Figure 3A). In contrast and confirming the microarray and RT-PCR results, deletion of PDK1 resulted in a down-regulation of INPP5B (Figure 3B).

To analyze whether known downstream signaling pathways are affected by the loss of PDK1, we analyzed the phosphorylation status of different PDK1 effector proteins following OH-TAM treatment, such as Akt (T308), GSK3β (S9), FOXO1 (S256), and TSC2 (S939). With loss of PDK1, T308 phosphorylation of Akt is strongly reduced in PDK1-deleted cells (Figure 3C). Additionally, phosphorylation of the Akt substrates GSK3β, FOXO1 and TSC2 was significantly decreased, while total expression levels of these proteins remained largely

unaffected (Figure 3C). All results obtained by the OH-TAM-induced PDK1 deletion were compared to the effect of the PDK1 inhibitor BX-795 (ref. [39]). BX-795 essentially pheno-copied the effect of the induced PDK1 deletion, i.e. reduced phosphorylation of Akt and its substrates, up-regulation of the PI3K subunits p110β and p110δ, and down-regulation of INPP5B (Figure 3C).

To prove the PDK1-mediated regulation of PI3K subunit expression in alternative cell models, we treated human DG75 and Ramos B cells with the PDK1 inhibitor BX-795 and analyzed p110β, p110δ and p85α expression. A significant up-regulation of the PI3K subunits was detectable in both cell lines (Supplementary Figure S2A and S2B). Furthermore, we were interested whether the observed transcriptional control is valid for cells derived from solid tumors. Accordingly, we treated prostate carcinoma PC-3 cells with BX-795 for two days. The efficacy of BX-795 in this cell line was confirmed by analyzing the phosphorylation of Akt, GSK3β, TSC2, and FOXO1, respectively. Similar to the B cell lines described above, the expression of the PI3K subunits p110β and p110δ increased upon BX-795 treatment (Supplementary Figure S2C). Collectively, these findings indicate that the PDK1-dependent control of PI3K subunit expression also exists in mammals and in non-lymphoid cells.

To ultimately confirm that the above described effects can be attributed to the loss of PDK1, we reconstituted DT40 *PDK1*-/cond cells with chicken PDK1 cDNA. Expression of chicken PDK1 in knockout cells was able to restore the wild-type phenotype and prevented the decrease of GSK3β phosphorylation and the up-regulation of the PI3K subunits following OH-TAM treatment (Supplementary Figure 3A). Furthermore, exogenous PDK1 expression completely inhibited apoptosis induced by PDK1 knockout (Supplementary Figure 3B).

In summary, the conditional knockout of PDK1 leads to up-regulation of the upstream PI3K subunits p110β, p110δ and p85α in different cellular model systems. This effect can be prevented by the exogenous expression of PDK1.

Promoter analysis of PDK1-*/cond cells*

Since FOXOs are known downstream targets of the PI3K/PDK1/Akt signaling pathway and we observed reduced FOXO1 phosphorylation upon induced PDK1 depletion or BX-795 treatment, we were next interested in the common transcriptional regulation of these genes. Thus, we analyzed the promoter regions of the genes encoding the PI3K subunits p110β, p110δ and p85α, the phosphoinositide-modifying enzymes (INPP5B, PIP5K1-β), the PI3K interacting protein, and Lyn by performing transcription factor mapping using Genomatix Software. Within the promoter regions of these regulated genes we mainly identified binding sites for ETS factors, sex/testis determining and related HMG box factors (SORY), forkhead domain factors (FKHD), heat shock factors, and cAMP-responsive element binding (CREB) proteins (Figure 4A). Next to FOXOs, which belong to the FKHD family, and CREB, the transcription factor families NF-κB and p53 have previously been shown to be regulated by the PDK1-Akt axis.[6,52,53] However, binding sites for both transcription factor families were not significantly enriched in the promoter regions of the analyzed transcripts (Figure 4A), and functional p53 is absent in DT40 cells.[40] Accordingly, we concentrated on the known Akt-regulated transcription factors FOXO and CREB. First we employed the FOXO1 inhibitor AS1842856 (ref. [41]) and analyzed its effect on the transcriptional up-regulation of PI3K subunits upon OH-TAM-induced PDK1-depletion or BX-795-mediated PDK1 inhibition, respectively. Notably, the up-regulation of the PI3K subunits p110β, p110δ and p85α was strongly blocked by the simultaneous inhibition of FOXO1, albeit not completely (Figure 4B). In turn, induction of CREB with forskolin or CREB inhibition with the CBP-CREB interaction inhibitor resulted in the up- or down-regulation of Lyn in DT40 cells (Figure 4C). Additionally, BX-795 treatment led to the induction of CREB-dependent transcription in Jurkat T lymphocytes as detected by a reporter gene assay (Figure 4D). Collectively, these experiments indicate that also the CREB transcription factor (family) might contribute to the transcriptional regulation of the PI3K/PDK1/Akt signaling axis. To further validate these

results, we performed an upstream regulator analysis using Ingenuity Pathway Analysis Software with the two complete entity lists obtained by the microarray analysis. Indeed, both transcription factor families were identified as significant upstream regulators (Supplementary Figure S4).

It appears that the transcriptional regulation of Lyn, PI3K subunits and phosphoinositide-modifying enzymes in response to lack of active PDK1 is mainly mediated by transcription factors of the FOXO and CREB family, although the contribution of additional transcription factor families such as ETS has to be investigated in future studies.

PDK1-deficiency leads to increased PIP_3 levels in the plasma membrane

Since PI3K class I enzymes produce phosphatidylinositol-3,4,5-trisphosphate (PIP_3) and INPP5B can degrade PIP_3, we asked if the abundance of this lipid is affected upon up-regulation of the PI3K subunits and down-regulation of INPP5B following induction of PDK1 knockout. To address this question we treated DT40 *PDK1*-/cond and wt cells with OH-TAM or EtOH and analyzed the amount of PIP_3 in these cells by time-resolved FRET.[42] As controls we treated DT40 *PDK1*-/cond cells with H_2O_2, which activates PI3K, or with the broad-band PI3K inhibitor LY294002. Strikingly, the amount of PIP_3 was significantly increased in the *PDK1*-/cond cells, but not in the control cells (Figure 5A). Furthermore, it appears that an incubation with LY294002 for 30 min is not potent enough to completely block the increase of PIP_3 upon PI3K subunit up-regulation, whereas it is sufficient for control cells.

Subsequently, we asked if increased PIP_3 levels at the plasma membrane can be detected *in vivo* by exogenous expression of the PDK1 PH domain fused to EGFP. For that, we generated DT40 *PDK1*-/cond cells stably expressing fluorescently labeled chicken PDK1-PH domain (EGFP-PH_{chPDK1}) or a mutant version (EGFP-$PH_{chPDK1\text{-}K468E}$), which cannot bind to PIP_3.[43] We induced the deletion of PDK1 in these cells and analyzed the recruitment of the EGFP-tagged PH domain by confocal microscopy. Indeed, the PDK1 knockout led to increased

binding of EGFP-PH_{chPDK1} to the plasma membrane, compared to EtOH treated cells (Figure 5B). Next we wanted to investigate whether the recruitment could be inhibited by the addition of different PI3K inhibitors. Since we observed that incubation with LY294002 for 30 min could not completely block PIP_3 generation (Figure 5A), we made use of a more selective PI3K class I inhibitor (GDC-0941) and treated the cells for 12 hrs. The translocation of EGFP-PH_{chPDK1} to the plasma membrane was entirely blocked by the simultaneous treatment with this pan-specific PI3K class I inhibitor. In contrast, application of the p110β- and p110δ-specific inhibitors TGX-221 and IC87114 (for 24 hrs) only resulted in a partially blocked recruitment, suggesting that the two catalytic PI3K subunits fulfil partially redundant functions. In cells expressing the mutant PH domain no recruitment was detectable, confirming that PH domain translocation depends on PIP_3 in the plasma membrane (Figure 5B).

Collectively, these results indicate that PDK1 negatively regulates the amount of PIP_3 in the plasma membrane via the negative transcriptional regulation of PI3K subunits. This feedback suppression is apparently relieved upon depletion of PDK1.

Akt and mTOR are important for the regulation of PI3K expression

PDK1 is an upstream activator of at least 23 different AGC family protein kinases including Akt, SGK, p70S6K, RSK, PKC and PKN.[12,13] The recruitment and activation of Akt can be blocked by mutating K465 in the PH domain of human PDK1 to glutamate.[43] In contrast, mutation of L155 to glutamate in the PIF-pocket of human PDK1 reduces phosphorylation of SGK and p70S6K.[30,31] To address the relative contribution of the two different branches of PDK1 signaling to the negative transcriptional regulation of PI3K subunits, we mutated the corresponding amino acids in chicken PDK1 (L158 and K468) to glutamate, expressed these mutants in DT40 *PDK1*-/cond cells, and analyzed the ability of both mutations to retain the knockout phenotype. Upon deletion of endogenous PDK1, PI3K subunit expression was

increased in both cell lines expressing the single-mutated PDK1 variants, but not to the extent as in completely PDK1-depleted cells (Figure 6A). In contrast, cells expressing the doubly-mutated PDK1 version retained the knockout phenotype, indicating that both branches of PDK1 signaling are involved in the regulation of PI3K expression (Figure 6A). Next, we directly inhibited Akt using the inhibitor Akti-1/2/3 (MK-2206).[44,45] This led to a strong increase of the expression of the PI3K subunits p110δ and p85α, and to a lesser extent p110β (Figure 6B). Similarly, treatment of human Jurkat T lymphocytes, DG75 B lymphocytes or Nalm-6 B lymphocytes with Akti-1/2/3 resulted in increased p110δ levels (Supplementary Figure 4A).

Several feedback signaling loops targeting the PI3K/PDK1/Akt pathway are controlled by mTOR. Thus, we analyzed the contribution of mTOR to the negative transcriptional regulation of the PI3K subunits. Inhibition of mTORC1 with rapamycin resulted in a similar effect as observed for Akt inhibition, i.e. distinctly increased expression of p85α and p110δ, and slightly increased expression of p110β (Figure 6C). Additionally, we could observe that PDK1-depletion results in a complete inhibition of mTORC1 activity, as detected by phospho-p70S6K immunoblotting (Figure 6D). The rapamycin-mediated increase of PI3K subunit expression could also be demonstrated in Jurkat T lymphocytes (Supplementary Figure 4B). Collectively, we conclude that the Akt-mTORC1 axis is mainly responsible for the negative regulation of PI3K subunit expression downstream of PDK1. Additionally, the above described feedback suppression appears to exist in different species and cell types.

Discussion

The PI3K/PDK1/Akt signaling pathway plays a central role in cellular homeostasis by producing specific "zip codes" at the inner leaflet of the plasma membrane. The PI3K product PIP_3 serves as anchor for the recruitment of downstream effectors, including PDK1 and Akt. It has been confirmed that PIP_3 is the essential component of PI3K-mediated oncogenesis,[46] and accordingly increased levels of PIP_3 caused by either activation of PI3K or inactivation of PTEN are frequently found in tumor cells.[1-7] Concomitantly, aberrantly activated downstream effectors are frequently detectable in these cells. Generally, PI3K and PTEN activity is tightly controlled by a complex network of feedback regulations to maintain basal PIP_3 levels below a threshold for signaling activation. In this report we identified an additional level of feedback control, i.e. the PDK1-dependent transcriptional regulation of PI3K subunits and additional phosphoinositide-modifying enzymes. We could show that depletion of PDK1 or inactivation of its downstream effectors Akt or mTOR lead to the transcriptional up-regulation of enzymes able to elevate PIP_3-levels in the plasma membrane and to the concomitant down-regulation of a PIP_3-degrading phosphatase. This transcriptional control is at least in part mediated by transcription factors of the FOXO and/or CREB family, although we cannot exclude the contribution of additional transcription factors (families) at this stage. Our observations strongly support a model of PDK1-dependent negative feedback regulation and indicate that the PIP_3-binding PDK1 is a central negative regulator of PI3K expression. In this scenario, PDK1 functions as a sensor for PIP_3 levels and orchestrates pro-survival signals via the direct regulation of the activation threshold and signaling strength of Akt and mTOR.

It appears that the sole up-regulation of PI3K subunits is sufficient to increase PIP_3 levels in DT40 B cells and that no additional activating stimulus is necessary. Along these lines, it has been previously reported that the overexpression of wild-type subunits p110β and p110δ is sufficient to induce an oncogenic phenotype in cultured chicken embryonic fibroblasts,[47] and

that p110β and p110δ subunits can lead to basal PI3K activity in PTEN-deficient human prostate cancer cells independently of receptor tyrosine kinase activation.[48]

Multiple branches of PI3K-dependent signal transduction converge on the level of PDK1.[12,13] The model of PDK1 as gatekeeper of PI3K expression levels is attractive, since 1) PDK1 itself is constitutively active and 2) it regulates the activation of several downstream kinases which depend on the PI3K-product PIP_3. This PIP_3-dependency might be either direct, e.g. by PH domain-mediated recruitment in the case of Akt, or indirect, e.g. by PIP_3-induced signaling cascades leading to the phosphorylation of the hydrophobic motif in the case of p70S6K or SGK, respectively.[13] According to our mutational analyses, both branches of PDK1 signaling participate in the negative regulation of PI3K subunit expression. It is tempting to speculate that the different branches of PDK1 signaling differently affect the expression of PI3K subunits. Indeed, the usage of Akti-1/2/3 and rapamycin leads to an up-regulation of p110δ and p85α, whereas the p110β increase is rather moderate. This would suggest that the indirect PIP_3 signaling axis regulates p110β expression. Interestingly, the PH domain mutant in turn does not preferentially regulate the levels of p110δ and p85α, which might be explained by the fact that this mutation does not completely abolish Akt T308 phosphorylation.[43] Furthermore, it has recently been published that Akt might also be activated by a PIF-pocket-dependent mechanism.[49] Accordingly, our data obtained with the pharmacological inhibition of Akt or mTORC1 in different cell lines indicate that this axis is centrally involved in the transcriptional regulation of PI3K expression.

Next to the PI3K catalytic subunits, PIP_3 levels are regulated by additional enzymatic activities. Interestingly, our microarray results revealed that non-PI3K PIP_3-regulating proteins are also regulated on a transcriptional level. These targets include the lipid phosphatase INPP5B, the phosphatidylinositol kinase PIP5K1-β and the PI3K interacting protein 1 (PIK3IP1). Of note, the transcriptional regulation of INPP5B and PIP5K1-β follows

the ultimate goal to increase cellular PIP_3 levels: INPP5B, which accepts PIP_3 as substrate and has been implicated in the systemic dephosphorylation of PIP_3 to PI-3-P,[50] is down-regulated upon PDK1 depletion, while PIP5K1-β, which participates in the synthesis of the PI3K substrate phosphatidylinositol-4,5-bisphosphate,[51] is up-regulated.

At first glance it seems paradoxical that Akt should contribute to the negative regulation of PIP_3-levels, since PIP_3 itself is mandatory for Akt activation and many tumorigenic effects of increased PIP_3 concentrations are mediated by Akt. However, it appears comprehensive that PIP_3 levels are tightly kept at a certain level sufficient for Akt-dependent pro-survival signaling. In this regard one might speculate that "basally active" PDK1/Akt adjust PIP_3 levels to a value which is sufficient for their own activation and the generation of survival signals, but does not exceed a harmful threshold leading to the demise of the cell. Indeed it has been reported that chronic Akt activation leads to apoptosis and that Akt sensitizes cells to reactive oxygen species (ROS)-induced apoptosis.[52-54] Given the existence of this "dark side" of Akt together with the observation that Akt is the only critical target activated by increased PIP_3 concentrations due to loss of PTEN (at least in *Drosophila*),[55] it readily makes sense that PI3K expression levels are adjusted to a certain level. As soon as one interferes with these PI3K/PIP_3 levels necessary for the mere pro-survival machinery, e.g. by PDK1 depletion or Akt inhibition, this repression is relieved and PIP_3 generation is increased.

Major classes of transcription factors are controlled by Akt, such as forkhead box O family of transcription factors (FOXOs), cAMP-response element binding protein (CREB), NF-κB, or p53.[6,56,57] Akt-mediated phosphorylation of CREB enables the binding of accessory proteins which are necessary for the transcription of pro-survival genes such as Bcl-2 and Mcl-1.[6,58,59] According to our data, it appears that either the deletion of PDK1 or the inhibition of Akt might positively affect CREB-dependent transcription. The second major component which participates in the transcriptional control of PI3K subunits and PIP_3-modifying enzymes are members of the FOXO family of transcription factors. Akt-catalyzed phosphorylation of

FOXO1, FOXO3a and FOXO4 transcription factors leads to their binding to 14-3-3 proteins and their retention in the cytoplasm. This in turn prevents the transcription of pro-apoptotic target genes such as the BH3-only family proteins and the Fas-ligand.[6,36] Accordingly, so far CREB and FOXOs have been essentially placed downstream of the PI3K/PDK1/Akt signaling cascade. Although our data suggest that the CREB and FOXO transcription factors mediate the observed up-regulation of Lyn, PI3K subunits and phosphoinositide subunits, we cannot exclude the involvement of additional transcription factor families. Our *in silico* analysis revealed that binding sites for family members of the ETS transcription factor exist in most promoter regions of the relevant genes, and different reports describe the Akt-mediated control of ETS family members or even the cooperativity between CREB and c-Ets1.[60-62] Additionally, a highly conserved transcription factor binding cluster containing an ETS binding sequence has been identified for the murine and human p110δ gene.[63] Nevertheless, further experiments are required to elucidate the exact mechanistic details. This is also underlined by the observation that the Akt effector protein mTOR participates in the described regulation. The kinase mTOR has been shown to be involved the regulation of gene transcription.[64] Gene expression profiling experiments have shown that ~5% of the transcriptome are differentially expressed in response to rapamycin-mediated mTOR inhibition.[65] Accordingly, we cannot exclude that mTOR also directly regulates expression of PI3K subunits and PIP_3-modifying enzymes. The antidromic regulation of PIP_3-generating kinases and the PIP_3-degrading phosphatase INPP5B already indicate that additional factors are necessary for this transcriptional regulation. It is tempting to speculate that different Akt effectors (CREB, FOXOs, mTOR) control the overall signaling strength of the upstream tyrosine kinase-PI3K-PDK1-Akt signaling pathway, e.g. CREB-mediated control of Lyn or FOXO-mediated control PI3K subunits.

In summary, we identified a novel negative feedback regulation of the PI3K/PDK1/Akt pathway. This feedback depends on the PDK1-mediated suppression of regulatory and

catalytic PI3K subunits. Upon PDK1 deletion or Akt inhibition, this suppression is relieved and the corresponding mRNAs are transcribed under the control of CREB/FOXO transcription factors (Figure 6E). This transcriptional feedback regulation adds to the existing "catalogue" of feedback mechanisms which attenuate PI3K/PDK1/Akt signaling. These feedback loops include the mTORC1-dependent transcriptional down-regulation or post-translational inhibition of IRS1/2, IGF-1 or IGF-1R, or the recently reported Akt-dependent suppression of receptor tyrosine kinase expression and activity.[32,66] Collectively, all these regulatory feedback loops underscore the necessity of novel therapeutic strategies based upon combinatorial approaches. In recent years, mTOR inhibitors have been developed as potential therapeutics. However, one might hypothesize that the efficiency of therapies which are mainly aiming at mTOR inhibition could be further improved by the parallel inhibition of PI3K, PIP_3, PDK1 or Akt, depending on the malignancy-dependent existence or emergence of feedback signaling cascades.

Materials and Methods

Cell culture

Chicken DT40 wild-type B cells, human DG75 B cells, human Nalm-6 B cells, human Ramos B cells, human Jurkat T cells, and human prostate carcinoma PC-3 cells were obtained from DSMZ (Braunschweig, Germany). Chicken DT40 conditional *PDK1*-/cond cells (DT40 *PDK1*-/cond) have been previously described [33] and were kindly provided by Tomohiro Kurosaki (RIKEN Research Center for Allergy and Immunology, Yokohama, Japan). All cell lines were maintained in 5% CO_2 at 37°C. All chicken DT40 cell lines were cultivated in RPMI 1640 (Lonza, Cologne, Germany) supplemented with 10% FCS, 1% chicken serum, 3 mM L-glutamine, 50 µM β-mercaptoethanol, 50 U/ml penicillin and 50 µg/ml streptomycin. Human DG75 and Nalm-6 B cells and human PC-3 prostate carcinoma cells were grown in RPMI 1640 supplemented with 10% FCS, 50 U/ml penicillin and 50 µg/ml streptomycin. Human Jurkat T cells and human Ramos B cells were cultivated in RPMI 1640 supplemented with 10% FCS, 10 mM HEPES, 50 U/ml penicillin and 50 µg/ml streptomycin.

Antibodies and reagents

Anti-Akt, anti-phospho-Akt (T308 and S473), anti-FOXO1, anti-phospho-FOXO1 (S256) anti-phospho-GSK3β (S9), and anti-GSK3β antibodies were purchased from Cell Signaling Technology (New England Biolabs, Frankfurt, Germany), anti-Akt1, anti-PI3K p110δ, anti-Lyn and anti-GAPDH antibodies from Abcam (Cambridge, UK), anti-PDK1 and anti-PI3K p85α antibodies from Epitomics (Abcam, Cambridge, UK), anti-PI3K p110β from Santa Cruz (Heidelberg, Germany), anti-Hsp90 from BD Biosciences (Heidelberg, Germany), anti-INPP5B from GeneTex (Irvine, CA, USA), anti-DUSP1 from Novus Biologicals (Acris Antibodies, Herford, Germany), and anti-actin and anti-vinculin from Sigma-Aldrich (Schnelldorf, Germany). 4-Hydroxytamoxifen (OH-TAM) was purchased from Sigma-

Aldrich and the broad-band PI3K inhibitor LY294002 from Cell Signaling Technology. The pan-PI3K inhibitor GDC-0941, the PI3K p110β inhibitor TGX-221, and the PI3K 110δ inhibitor IC-87114 were purchased from Selleckchem (ICS International Clinical Service GmbH, Munich, Germany). Forskolin (FSK), the CBP-CREB interaction inhibitor, and the FOXO1 inhibitor AS1842856 were purchased from Calbiochem (Merck KGaA, Darmstadt, Germany). Anti-chicken-IgM (M4) was obtained from Southern Biotech (Biozol, Eching, Germany). Puromycin was from InvivoGen (Toulouse, France). BX-795 was purchased from Axon Medchem (Groningen, The Netherlands). Akti-1/2/3 (MK-2206) was kindly provided by Dario R. Alessi.

Expression constructs and retroviral infection

Wild-type chicken *PDK1* cDNA was cloned into pMSCVpuro (Clontech, Takara, Saint-Germain-en-Laye, France). cDNA encoding the chicken PDK1 PH domain (codons 409 - 557) was cloned into pEGFP-C1 (Clontech). pMSCVpuro-EGFP-PH_{chPDK1} was generated by cloning of *EGFP-PH_{chPDK1}* cDNA into pMSCVpuro. Substitutions of leucine 158 and lysine 468 to glutamate were generated by site-directed mutagenesis to create a PIF-binding pocket mutant, PH domain mutant, or double mutant chicken PDK1. For retroviral gene transfer, Plat-E cells were transfected with pMSCV-based vectors using FuGENE® 6 transfection reagent (Roche). The MMLV was pseudotyped with VSV-G. DT40 *PDK1*-/cond cells were incubated with retroviral supernatant containing 3 µg/ml Polybrene (Sigma-Aldrich) and selected in medium containing 0.5 µg/ml puromycin.

Reporter gene assay

A number of 4×10^6 Jurkat cells was harvested by centrifugation at 600 rcf for 5 min at 4°C, washed with PBS and transfected with 300 ng of either CREB reporter plasmid or control plasmid (CRE/CREB Reporter Assay Kit, BPS Bioscience, San Diego, CA, USA) using an

Amaxa Nucleofector I device with program K-25 and Solution T (Lonza, Cologne, Germany) according to manufacturer's instructions. After transfection, the cells were incubated at RT for 10 min and were then transfered to pre-warmed medium and incubated overnight. BX-795 was added to a final concentration of 1 or 10 µM, and 0.1% DMSO was used as a negative control. After 24 h of incubation, forskolin (FSK) was added to previously untreated cells to a final concentration of 5 µM. The cells were transferred to a white opaque 96 well plate and incubated for another 6 h. The plate was then centrifuged at 600 rcf for 5 min at 4°C, the cells were washed with PBS, and firefly luciferase activity was measured using a Dual-Luciferase® Reporter Assay System (Promega, Mannheim, Germany) according to the manufacturers instructions using a Synergy MX multiwell reader with dispenser (BioTek, Bad Friedrichshall, Germany).

Measurement of apoptosis

DT40 cells were cultivated in medium containing 0.5 µM OH-TAM or 0.05% EtOH as control. After 48 hrs OH-TAM-treated cells were transferred to normal medium. The leakage of fragmented DNA was measured either four to eight days after beginning of OH-TAM treatment or on day four cells were stimulated with 10 µg/ml anti-chicken-IgM (M4) for 24 hrs and apoptosis was measured. Nuclei were prepared by lysing cells in hypotonic lysis buffer [1% sodium citrate, 0.1% Triton X-100, 50 µg/ml propidium iodide] and subsequently analyzed by flow cytometry. Nuclei to the left of the 2 N peak were considered as apoptotic. Flow cytometric analyses were performed on FACSCalibur (BD Biosciences) using CellQuest software or on LSRFortessa (BD Biosciences) using FACSDiva software.

Cell extracts and immunoblotting

DT40 cells were incubated in medium containing 0.5 µM OH-TAM or 0.05% EtOH as control. After 48 hrs OH-TAM-treated cells were transferred to normal medium and were

harvested at the indicated time points. Following treatment of DT40, DG75, Nalm-6 or Jurkat cells with the different compounds at the indicated concentrations for the indicated times, cells were lysed in lysis buffer [20 mM Tris-HCl pH 7.5, 150 mM NaCl, 0.5 mM EDTA, 1% Triton X-100, 10 mM NaF, 2.5 mM NaPP, 10 µM Na_2MoO_4, 1 mM Na_3VO_4, protease inhibitors (P2714, Sigma)] and lysates were clarified by centrifugation at 16,000 g for 10 min. Equal total protein amounts, as determined by Bradford, were separated on 8% or 10% SDS-polyacrylamide gels and transferred to PVDF membrane (Millipore). Immunoblot analysis was performed using the indicated primary antibodies and appropriate IRDye®800- or IRDye®680-conjugated secondary antibodies (LI-COR Biosciences, Bad Homburg, Germany). Signals were detected with an Odyssey® Infrared Imaging system (LI-COR Biosciences).

Analysis of PIP_3 levels

DT40 cells were incubated in medium containing 0.5 µM 4-hydroxytamoxifen (OH-TAM) or 0.05% EtOH as control. After 48 hrs OH-TAM treated cells were transferred to normal medium. On day four control cells were treated with 10 µM LY294002 (LY) for 30 min (cells treated with OH-TAM or left untreated), 5 mM H_2O_2 for 2 min, or left untreated. Subsequently cells were harvested and the mass of PIP_3 was determined. Cells were precipitated by the addition of 0.5 ml ice cold 0.5 M trichloroacetic acid (TCA) and kept on ice for 5 min. The precipitated cells were collected by centrifugation, TCA was aspirated and the pellet was immediately frozen on dry ice until lipids were extracted. The mass of PIP_3 was estimated using a time-resolved FRET displacement assay as described previously.[42]

Quantitative real-time RT-PCR

Quantitative real-time RT-PCR analysis was performed using the ABI Prism 7000 Sequence Detection System (Applied Biosystems, Darmstadt, Germany) and Maxima™ qPCR Master

Mix (Fermentas, St. Leon-Rot, Germany). Total RNA from 1 x 10^6 cells was isolated using the NucleoSpin™ RNA II-Kit (Macherey & Nagel, Düren, Germany). cDNA was generated from 1 µg of total RNA with 200 U RevertAid H Minus™ reverse transcriptase, 50 µM random hexamers, 400 µM dNTPs, and 1.6 U/µl RiboLock™ RNase inhibitor (all from Fermentas) according to manufacturer's recommendations. 50 ng of the resulting cDNA were applied to qRT-PCR analyses (20 µl final volume) and amplified in the presence of 200 nM primers and 100 nM probe or 300 nM primers in the case of SYBR Green detection with the standard temperature profile (2 min 50°C, 10 min 95°C, 40 cycles 15 s 95°C, 1 min 60°C). Relative quantification was performed employing the standard curve method. The results were normalized on the reference gene 18S rRNA. The cell populations on day zero of OH-TAM treatment were used as calibrator.

Confocal laser scanning microscopy

Cells were resuspended in Krebs Ringer solution [10 mM HEPES pH 7.0, 140 mM NaCl, 4 mM KCl, 1 mM $MgCl_2$, 1 mM $CaCl_2$, 10 mM glucose] and seeded onto chambered coverglasses (Nunc). After 20 min, cells were analyzed on a Leica TCS SP II confocal laser scanning microscope. EGFP was excited at 488 nm.

Conflict of interest

The authors declare no conflict of interest.

Acknowledgments

We thank Dario Alessi for providing MK-2206 and for helpful discussions. This work was supported by grants from the Deutsche Forschungsgemeinschaft SFB 773 (to SW and BS) and GRK 1302 (to SW and BS), and from the Interdisciplinary Center of Clinical Research, Faculty of Medicine, Tübingen (Nachwuchsgruppe 1866-0-0, to BS).

Supplementary information accompanies the paper on the *ONCOGENE* website (http://www.nature.com/onc)

References

1. Bunney TD, Katan M. Phosphoinositide signalling in cancer: beyond PI3K and PTEN. *Nat Rev Cancer* 2010; **10**(5): 342-52.
2. Carnero A. The PKB/AKT pathway in cancer. *Curr Pharm Des* 2010; **16**(1): 34-44.
3. Chalhoub N, Baker SJ. PTEN and the PI3-kinase pathway in cancer. *Annu Rev Pathol* 2009; **4**: 127-50.
4. Cully M, You H, Levine AJ, Mak TW. Beyond PTEN mutations: the PI3K pathway as an integrator of multiple inputs during tumorigenesis. *Nat Rev Cancer* 2006; **6**(3): 184-92.
5. Engelman JA. Targeting PI3K signalling in cancer: opportunities, challenges and limitations. *Nat Rev Cancer* 2009; **9**(8): 550-62.
6. Hers I, Vincent EE, Tavare JM. Akt signalling in health and disease. *Cell Signal* 2011; **23**(10): 1515-27.
7. Vivanco I, Sawyers CL. The phosphatidylinositol 3-Kinase AKT pathway in human cancer. *Nat Rev Cancer* 2002; **2**(7): 489-501.
8. So L, Fruman DA. PI3K signalling in B- and T-lymphocytes: new developments and therapeutic advances. *Biochem J* 2012; **442**(3): 465-81.
9. Engelman JA, Luo J, Cantley LC. The evolution of phosphatidylinositol 3-kinases as regulators of growth and metabolism. *Nat Rev Genet* 2006; **7**(8): 606-19.
10. Vanhaesebroeck B, Guillermet-Guibert J, Graupera M, Bilanges B. The emerging mechanisms of isoform-specific PI3K signalling. *Nat Rev Mol Cell Biol* 2010; **11**(5): 329-41.
11. Liu Y, Bankaitis VA. Phosphoinositide phosphatases in cell biology and disease. *Prog Lipid Res* 2010; **49**(3): 201-17.
12. Mora A, Komander D, van Aalten DM, Alessi DR. PDK1, the master regulator of AGC kinase signal transduction. *Semin Cell Dev Biol* 2004; **15**(2): 161-70.

13. Pearce LR, Komander D, Alessi DR. The nuts and bolts of AGC protein kinases. *Nat Rev Mol Cell Biol* 2010; **11**(1): 9-22.

14. Alessi DR, Deak M, Casamayor A, Caudwell FB, Morrice N, Norman DG *et al.* 3-Phosphoinositide-dependent protein kinase-1 (PDK1): structural and functional homology with the Drosophila DSTPK61 kinase. *Curr Biol* 1997; **7**(10): 776-89.

15. Alessi DR, James SR, Downes CP, Holmes AB, Gaffney PR, Reese CB *et al.* Characterization of a 3-phosphoinositide-dependent protein kinase which phosphorylates and activates protein kinase Balpha. *Curr Biol* 1997; **7**(4): 261-9.

16. Alessi DR, Kozlowski MT, Weng QP, Morrice N, Avruch J. 3-Phosphoinositide-dependent protein kinase 1 (PDK1) phosphorylates and activates the p70 S6 kinase in vivo and in vitro. *Curr Biol* 1998; **8**(2): 69-81.

17. Kobayashi T, Cohen P. Activation of serum- and glucocorticoid-regulated protein kinase by agonists that activate phosphatidylinositide 3-kinase is mediated by 3-phosphoinositide-dependent protein kinase-1 (PDK1) and PDK2. *Biochem J* 1999; **339 (Pt 2)**: 319-28.

18. Kobayashi T, Deak M, Morrice N, Cohen P. Characterization of the structure and regulation of two novel isoforms of serum- and glucocorticoid-induced protein kinase. *Biochem J* 1999; **344 Pt 1**: 189-97.

19. Dong LQ, Zhang RB, Langlais P, He H, Clark M, Zhu L *et al.* Primary structure, tissue distribution, and expression of mouse phosphoinositide-dependent protein kinase-1, a protein kinase that phosphorylates and activates protein kinase Czeta. *J Biol Chem* 1999; **274**(12): 8117-22.

20. Jensen CJ, Buch MB, Krag TO, Hemmings BA, Gammeltoft S, Frodin M. 90-kDa ribosomal S6 kinase is phosphorylated and activated by 3-phosphoinositide-dependent protein kinase-1. *J Biol Chem* 1999; **274**(38): 27168-76.

21. Le Good JA, Ziegler WH, Parekh DB, Alessi DR, Cohen P, Parker PJ. Protein kinase C isotypes controlled by phosphoinositide 3-kinase through the protein kinase PDK1. *Science* 1998; **281**(5385): 2042-5.

22. Park J, Leong ML, Buse P, Maiyar AC, Firestone GL, Hemmings BA. Serum and glucocorticoid-inducible kinase (SGK) is a target of the PI 3-kinase-stimulated signaling pathway. *EMBO J* 1999; **18**(11): 3024-33.

23. Pullen N, Dennis PB, Andjelkovic M, Dufner A, Kozma SC, Hemmings BA *et al.* Phosphorylation and activation of p70s6k by PDK1. *Science* 1998; **279**(5351): 707-10.

24. Bayascas JR. PDK1: the major transducer of PI 3-kinase actions. *Curr Top Microbiol Immunol* 2010; **346**: 9-29.

25. Currie RA, Walker KS, Gray A, Deak M, Casamayor A, Downes CP *et al.* Role of phosphatidylinositol 3,4,5-trisphosphate in regulating the activity and localization of 3-phosphoinositide-dependent protein kinase-1. *Biochem J* 1999; **337 (Pt 3)**: 575-83.

26. Fayard E, Xue G, Parcellier A, Bozulic L, Hemmings BA. Protein kinase B (PKB/Akt), a key mediator of the PI3K signaling pathway. *Curr Top Microbiol Immunol* 2010; **346**: 31-56.

27. Sarbassov DD, Guertin DA, Ali SM, Sabatini DM. Phosphorylation and regulation of Akt/PKB by the rictor-mTOR complex. *Science* 2005; **307**(5712): 1098-101.

28. Burnett PE, Barrow RK, Cohen NA, Snyder SH, Sabatini DM. RAFT1 phosphorylation of the translational regulators p70 S6 kinase and 4E-BP1. *Proc Natl Acad Sci U S A* 1998; **95**(4): 1432-7.

29. Garcia-Martinez JM, Alessi DR. mTOR complex 2 (mTORC2) controls hydrophobic motif phosphorylation and activation of serum- and glucocorticoid-induced protein kinase 1 (SGK1). *Biochem J* 2008; **416**(3): 375-85.

30. Balendran A, Biondi RM, Cheung PC, Casamayor A, Deak M, Alessi DR. A 3-phosphoinositide-dependent protein kinase-1 (PDK1) docking site is required for the

phosphorylation of protein kinase Czeta (PKCzeta) and PKC-related kinase 2 by PDK1. *J Biol Chem* 2000; **275**(27): 20806-13.

31. Biondi RM, Kieloch A, Currie RA, Deak M, Alessi DR. The PIF-binding pocket in PDK1 is essential for activation of S6K and SGK, but not PKB. *EMBO J* 2001; **20**(16): 4380-90.
32. Carracedo A, Pandolfi PP. The PTEN-PI3K pathway: of feedbacks and cross-talks. *Oncogene* 2008; **27**(41): 5527-41.
33. Shinohara H, Maeda S, Watarai H, Kurosaki T. IkappaB kinase beta-induced phosphorylation of CARMA1 contributes to CARMA1 Bcl10 MALT1 complex formation in B cells. *J Exp Med* 2007; **204**(13): 3285-93.
34. Lawlor MA, Mora A, Ashby PR, Williams MR, Murray-Tait V, Malone L *et al.* Essential role of PDK1 in regulating cell size and development in mice. *EMBO J* 2002; **21**(14): 3728-38.
35. Takata M, Homma Y, Kurosaki T. Requirement of phospholipase C-gamma 2 activation in surface immunoglobulin M-induced B cell apoptosis. *J Exp Med* 1995; **182**(4): 907-14.
36. Brunet A, Bonni A, Zigmond MJ, Lin MZ, Juo P, Hu LS *et al.* Akt promotes cell survival by phosphorylating and inhibiting a Forkhead transcription factor. *Cell* 1999; **96**(6): 857-68.
37. Kops GJ, Medema RH, Glassford J, Essers MA, Dijkers PF, Coffer PJ *et al.* Control of cell cycle exit and entry by protein kinase B-regulated forkhead transcription factors. *Mol Cell Biol* 2002; **22**(7): 2025-36.
38. Kurosaki T. Regulation of BCR signaling. *Mol Immunol* 2011; **48**(11): 1287-91.

39. Feldman RI, Wu JM, Polokoff MA, Kochanny MJ, Dinter H, Zhu D *et al.* Novel small molecule inhibitors of 3-phosphoinositide-dependent kinase-1. *J Biol Chem* 2005; **280**(20): 19867-74.
40. Yamazoe M, Sonoda E, Hochegger H, Takeda S. Reverse genetic studies of the DNA damage response in the chicken B lymphocyte line DT40. *DNA Repair (Amst)* 2004; **3**(8-9): 1175-85.
41. Nagashima T, Shigematsu N, Maruki R, Urano Y, Tanaka H, Shimaya A *et al.* Discovery of novel forkhead box O1 inhibitors for treating type 2 diabetes: improvement of fasting glycemia in diabetic db/db mice. *Mol Pharmacol* 2010; **78**(5): 961-70.
42. Gray A, Olsson H, Batty IH, Priganica L, Peter Downes C. Nonradioactive methods for the assay of phosphoinositide 3-kinases and phosphoinositide phosphatases and selective detection of signaling lipids in cell and tissue extracts. *Anal Biochem* 2003; **313**(2): 234-45.
43. Bayascas JR, Wullschleger S, Sakamoto K, Garcia-Martinez JM, Clacher C, Komander D *et al.* Mutation of the PDK1 PH domain inhibits protein kinase B/Akt, leading to small size and insulin resistance. *Mol Cell Biol* 2008; **28**(10): 3258-72.
44. Hirai H, Sootome H, Nakatsuru Y, Miyama K, Taguchi S, Tsujioka K *et al.* MK-2206, an allosteric Akt inhibitor, enhances antitumor efficacy by standard chemotherapeutic agents or molecular targeted drugs in vitro and in vivo. *Mol Cancer Ther* 2010; **9**(7): 1956-67.
45. Lindsley CW. The Akt/PKB family of protein kinases: a review of small molecule inhibitors and progress towards target validation: a 2009 update. *Curr Top Med Chem* 2010; **10**(4): 458-77.

46. Denley A, Gymnopoulos M, Kang S, Mitchell C, Vogt PK. Requirement of phosphatidylinositol(3,4,5)trisphosphate in phosphatidylinositol 3-kinase-induced oncogenic transformation. *Mol Cancer Res* 2009; **7**(7): 1132-8.

47. Kang S, Denley A, Vanhaesebroeck B, Vogt PK. Oncogenic transformation induced by the p110beta, -gamma, and -delta isoforms of class I phosphoinositide 3-kinase. *Proc Natl Acad Sci U S A* 2006; **103**(5): 1289-94.

48. Jiang X, Chen S, Asara JM, Balk SP. Phosphoinositide 3-kinase pathway activation in phosphate and tensin homolog (PTEN)-deficient prostate cancer cells is independent of receptor tyrosine kinases and mediated by the p110beta and p110delta catalytic subunits. *J Biol Chem* 2010; **285**(20): 14980-9.

49. Najafov A, Shpiro N, Alessi DR. Akt is efficiently activated by PIF-pocket- and PtdIns(3,4,5)P3-dependent mechanisms leading to resistance to PDK1 inhibitors. *Biochem J* 2012; **448**(2): 285-95.

50. Shin HW, Hayashi M, Christoforidis S, Lacas-Gervais S, Hoepfner S, Wenk MR *et al.* An enzymatic cascade of Rab5 effectors regulates phosphoinositide turnover in the endocytic pathway. *J Cell Biol* 2005; **170**(4): 607-18.

51. van den Bout I, Divecha N. PIP5K-driven PtdIns(4,5)P2 synthesis: regulation and cellular functions. *J Cell Sci* 2009; **122**(Pt 21): 3837-50.

52. Los M, Maddika S, Erb B, Schulze-Osthoff K. Switching Akt: from survival signaling to deadly response. *Bioessays* 2009; **31**(5): 492-5.

53. Nogueira V, Park Y, Chen CC, Xu PZ, Chen ML, Tonic I *et al.* Akt determines replicative senescence and oxidative or oncogenic premature senescence and sensitizes cells to oxidative apoptosis. *Cancer Cell* 2008; **14**(6): 458-70.

54. van Gorp AG, Pomeranz KM, Birkenkamp KU, Hui RC, Lam EW, Coffer PJ. Chronic protein kinase B (PKB/c-akt) activation leads to apoptosis induced by oxidative stress-mediated Foxo3a transcriptional up-regulation. *Cancer Res* 2006; **66**(22): 10760-9.

55. Stocker H, Andjelkovic M, Oldham S, Laffargue M, Wymann MP, Hemmings BA *et al.* Living with lethal PIP3 levels: viability of flies lacking PTEN restored by a PH domain mutation in Akt/PKB. *Science* 2002; **295**(5562): 2088-91.

56. Brunet A, Datta SR, Greenberg ME. Transcription-dependent and -independent control of neuronal survival by the PI3K-Akt signaling pathway. *Curr Opin Neurobiol* 2001; **11**(3): 297-305.

57. Parcellier A, Tintignac LA, Zhuravleva E, Hemmings BA. PKB and the mitochondria: AKTing on apoptosis. *Cell Signal* 2008; **20**(1): 21-30.

58. Nicholson KM, Anderson NG. The protein kinase B/Akt signalling pathway in human malignancy. *Cell Signal* 2002; **14**(5): 381-95.

59. Wang JM, Chao JR, Chen W, Kuo ML, Yen JJ, Yang-Yen HF. The antiapoptotic gene mcl-1 is up-regulated by the phosphatidylinositol 3-kinase/Akt signaling pathway through a transcription factor complex containing CREB. *Mol Cell Biol* 1999; **19**(9): 6195-206.

60. Bujor AM, Nakerakanti S, Morris E, Hant FN, Trojanowska M. Akt inhibition up-regulates MMP1 through a CCN2-dependent pathway in human dermal fibroblasts. *Exp Dermatol* 2010; **19**(4): 347-54.

61. Figueroa C, Vojtek AB. Akt negatively regulates translation of the ternary complex factor Elk-1. *Oncogene* 2003; **22**(36): 5554-61.

62. Song KS, Lee TJ, Kim K, Chung KC, Yoon JH. cAMP-responding element-binding protein and c-Ets1 interact in the regulation of ATP-dependent MUC5AC gene expression. *J Biol Chem* 2008; **283**(40): 26869-78.

63. Kok K, Nock GE, Verrall EA, Mitchell MP, Hommes DW, Peppelenbosch MP *et al.* Regulation of p110delta PI 3-kinase gene expression. *PLoS One* 2009; **4**(4): e5145.

64. Caron E, Ghosh S, Matsuoka Y, Ashton-Beaucage D, Therrien M, Lemieux S *et al.* A comprehensive map of the mTOR signaling network. *Mol Syst Biol* 2010; **6**: 453.

65. Guertin DA, Guntur KV, Bell GW, Thoreen CC, Sabatini DM. Functional genomics identifies TOR-regulated genes that control growth and division. *Curr Biol* 2006; **16**(10): 958-70.

66. Chandarlapaty S, Sawai A, Scaltriti M, Rodrik-Outmezguine V, Grbovic-Huezo O, Serra V *et al.* AKT inhibition relieves feedback suppression of receptor tyrosine kinase expression and activity. *Cancer Cell* 2011; **19**(1): 58-71.

Figure legends

Figure 1

PDK1 is essential for survival of DT40 cells. (A) Conditional *PDK1-/cond* chicken DT40 B cells (*PDK1*-/cond) and DT40 wt cells were treated with 0.5 μM 4-hydroxytamoxifen (OH-TAM) or 0.05% EtOH for 48 hrs or left untreated (control). Then cells were transferred to normal DT40 medium. On days two to four after beginning of OH-TAM/EtOH treatment cleared cellular lysates were prepared and analyzed for PDK1 and Hsp90 by immunoblotting. Data shown are representative of three independent experiments. (B) DT40 *PDK1*-/cond and wt cells were treated with 0.5 μM OH-TAM or 0.05% EtOH for 48 hrs. Then cells were transferred to normal DT40 medium. On days four to eight after beginning of OH-TAM/EtOH treatment apoptosis was assessed by propidium iodide staining of hypodiploid apoptotic nuclei and flow cytometry. Data shown are mean of triplicates ±SD and are representative of three independent experiments. (C) DT40 *PDK1*-/cond and wt cells were treated with 0.5 μM OH-TAM or 0.05% EtOH for 48 hrs. Then cells were transferred to normal DT40 medium. On day four after beginning of OH-TAM/EtOH treatment cells were stimulated with 10 μg/ml anti-chicken IgM antibody (M4) for 24 hrs. Apoptosis was assessed by propidium iodide staining of hypodiploid apoptotic nuclei and flow cytometry. Data shown are mean of triplicates ±SD and are representative of three independent experiments.

Figure 2

PDK1 negatively regulates transcription of PI3K subunits. (A) The table lists known and newly identified target genes of PDK1 and their regulation in *PDK1*-/cond cells compared to control cells. (B) Cluster analysis for selected probe sets was performed in R 2.15.1. Signal intensities were scaled and centered and the distance between two expression profiles was calculated using manhattan distance measure. Hierarchical cluster analysis was performed

with average linkage. Heatmaps were generated with Bioconductor package *geneplotter*.(C) DT40 *PDK1*-/cond and wt cells were treated with 0.5 µM OH-TAM or 0.05% EtOH for 48 hrs. Then cells were transferred to normal DT40 medium. At the indicated time points the relative mRNA expression of *PIK3CB* (PI3K p110β), *PIK3CD* (PI3K p110δ), *PIK3R1* (PI3K p85α), *LYN* (Lyn) and *INPP5B* was analyzed by quantitative real-time RT-PCR.

Figure 3

PDK1 negatively regulates expression of PI3K subunits. (A) DT40 *PDK1*-/cond and DT40 wt cells were treated with 0.5 µM OH-TAM or 0.05% EtOH for 48 hrs or left untreated. Then cells were transferred to normal DT40 medium. On days two to four after beginning of OH-TAM/EtOH treatment cleared cellular lysates were prepared and analyzed for PI3K p110β, PI3K p110δ, PI3K p85α, Lyn, Hsp90 and vinculin by immunoblotting. Data shown are representative of three independent experiments. Asterisks indicate unspecific background bands. (B) DT40 *PDK1*-/cond cells were treated with 0.05% EtOH or 0.5 µM OH-TAM for 48 hrs. Then cells were transferred to normal DT40 medium and incubated for additional 48 hrs. Cleared cellular lysates were prepared and analyzed for INPP5B and actin by immunoblotting. Data shown are representative of three independent experiments. (C) DT40 *PDK1*-/cond cells were treated with 0.05% EtOH or 0.5 µM OH-TAM for 48 hrs. Then cells were transferred to normal DT40 medium and incubated for additional 48 hrs. Alternatively, DT40 *PDK1*-/cond cells were treated with 10 µM BX-795 for 48 hrs. Cleared cellular lysates were prepared and analyzed for Akt1, phospho-Akt (T308), TSC2, phospho-TSC2 (S939), FOXO1, phospho-FOXO1 (S256), GSK3β, phospho-GSK3β (S9), PI3K p110β, PI3K p110δ, PI3K p85α, INPP5B, GAPDH and actin by immunoblotting. Protein/loading control ratios were calculated and normalized to EtOH-treated controls. Data shown are representative of three independent experiments.

Figure 4

Promoter analysis of PDK1-regulated genes. (A) The promoter regions of the genes encoding the PI3K subunits p110β, p110δ and p85α, the phosphoinositide-modifying enzymes (INPP5B, PIP5K1-β), the PI3K interacting protein, and Lyn were analysed by performing transcription factor mapping using Genomatix Software. The total number of identified promotor regions for these genes is 18 (black bar). The number of promoter regions containing binding sites for the following transcription factors are depicted(grey bars): ETS factors (ETSF), sex/testis determining and related HMG box factors (SORY), forkhead domain factors (FKHD), heat shock factors (HEAT), cAMP-responsive element binding proteins (CREB), NF-κB (NFKB), and p53 family (p53F). (B) DT40 *PDK1*-/cond cells were treated with 0.05% EtOH or 0.5 µM OH-TAM for 48 hrs. Then cells were transferred to normal DT40 medium and incubated for 24 hrs. Either the PDK1 inhibitor BX-795, the FOXO1 inhibitor AS1842856, or both were added to a final concentration of 10 µM, and 0.1% v/v DMSO was used as control. After another 24 hrs, cleared cellular lysates were prepared and analyzed for PDK1, TSC2, phospho-TSC2 (S939), PI3K p110β, PI3K p110δ, PI3K p85α and actin by immunoblotting. Data shown are representative of three independent experiments. (C) DT40 *PDK1*-/cond cells were incubated with 5 µM forskolin (FSK) for the indicated times or with the CREB-CBP interaction inhibitor for 24 hrs with the indicated concentrations. Cleared cellular lysates were prepared and analyzed for Lyn, DUSP1 and vinculin by immunoblotting. Data shown are representative of three independent experiments. (D) Jurkat T lymphocytes were transfected with a CREB reporter plasmid or a control plasmid (CRE/CREB Reporter Assay Kit, BPS Bioscience) as described in material and methods. A plasmid containing a constitutively expressed Renilla luciferase gene served as a control of transfection efficiency. BX-795 was added to a final concentration of 1 or 10 µM,

and 0.1% DMSO was used as a negative control. The cells were incubated for 24 hrs, and forskolin (FSK) was added to previously untreated cells to a final concentration of 5 µM. Firefly luciferase activity was measured using a Dual-Luciferase® Reporter Assay System (Promega) according to the manufacturer's instructions. The firefly luminescence value of each well was divided by the respective renilla luminescence value. Each column was individually compared to the negative control by unpaired two-tailed Student's t test. n = 3, error bars = SD, ** = $p < 0.01$, *** = $p < 0.001$.

Figure 5

PDK1 deficiency increases PIP_3 levels in the plasma m embrane. (A) DT40 *PDK1*-/cond and wt cells were treated with 0.5 µM OH-TAM or 0.05% EtOH for 48 hrs or left untreated. Then cells were transferred to normal DT40 medium. On day four control cells were treated with 10 µM LY294002 (LY) for 30 min (cells treated with OH-TAM or left untreated), 5 mM H_2O_2 for 2 min, or left untreated. PIP_3 levels were measured using a time-resolved FRET displacement assay as described in detail in material and methods. Data shown are mean of triplicates ±SD and are representative of three independent experiments. Asterisk indicates $p < 0.014$ (two-tailed paired t test). (B) DT40 *PDK1*-/cond cells, retrovirally transfected with EGFP-PH(chPDK1 wt) or EGFP-PH(chPDK1 K468E) cDNAs, were treated with 0.5 µM OH-TAM or 0.05% EtOH for 48 hrs. Then cells were transferred to normal DT40 medium and incubated for additional 48 hrs. Alternatively, OH-TAM-treated DT40 *PDK1*-/cond cells expressing EGFP-PH(chPDK1 wt) were incubated with 5 µM GDC-0941 (for 12 hrs prior to analysis), 10 µM TGX-221 (for 24 hrs prior to analysis) or 10 µM IC87114 (for 24 hrs prior to analysis). Cells were analyzed by confocal laser scanning microscopy. Data shown are representative of three independent experiments.

Figure 6

The PDK1 effector proteins Akt and mTOR are involved in the suppression of PI3K subunits. (A) DT40 *PDK1*-/cond cells, retrovirally transfected with chicken PDK1-L158E cDNA (L158E), chicken PDK1-K468E cDNA (K468E), chicken PDK1-L158E/K468E cDNA (L158E/K468E), or empty vector (vec) were treated with 0.5 µM OH-TAM or 0.05% EtOH for 48 hrs. Then cells were transferred to normal DT40 medium. On day four after beginning of OH-TAM/EtOH treatment cleared cellular lysates were prepared and analyzed for PDK1, PI3K p110β, PI3K p110δ, PI3K p85α, phospho-GSK3β (S9), and vinculin by immunoblotting. Data shown are representative of three independent experiments. Asterisks indicate unspecific background bands. (B) DT40 *PDK1*-/cond cells were treated with 1 µM Akti-1/2/3 for 48 hrs. Cleared cellular lysates were prepared and analyzed for PI3K p110β, PI3K p110δ, PI3K p85α, phospho-Akt (T308 and S473), Akt1, phospho-GSK3β (S9), and vinculin by immunoblotting. Data shown are representative of three independent experiments. Asterisk indicates unspecific background band. (C) DT40 *PDK1*-/cond cells were treated with 100 nM rapamycin (Rapa) for 48 hrs. Cleared cellular lysates were prepared and analyzed for PI3K p110β, PI3K p110δ, PI3K p85α, phospho-Akt (T308 and S473), Akt1, phospho-GSK3β (S9), p70S6K, phospho-p70S6K (T389), vinculin, and GAPDH by immunoblotting. Data shown are representative of three independent experiments. (D) DT40 *PDK1*-/cond cells were treated with 0.5 µM OH-TAM or 0.05% EtOH for 48 hrs or left untreated. Then cells were transferred to normal DT40 medium. On day four after beginning of OH-TAM/EtOH treatment cleared cellular lysates were prepared and analyzed for p70S6K, phospho-p70S6K (T389), and GAPDH by immunoblotting. Data shown are representative of three independent experiments. (E) Schematic diagram of the negative feedback regulation of the PI3K/PDK1/Akt signaling pathway. PDK1 activates Akt and other AGC kinases such as

SGK, p70S6K or PKC. These kinases together with their downstream effectors (e.g. mTOR) in turn inhibit the transcription of PI3K subunits via the regulation of transcription factors of the CREB, FOXO, ETS and/or other families. By this means, cellular PIP_3 amounts are fine-tuned to levels which are sufficient for cell survival.

Figure 1

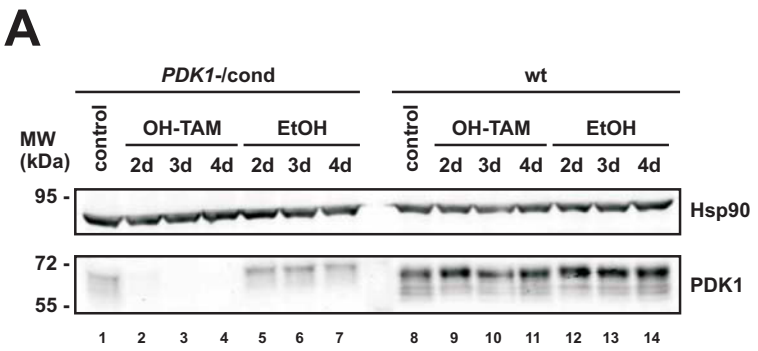
A
PDK1-/cond
wt
MW (kDa)
control
OH-TAM
EtOH
2d 3d 4d 2d 3d 4d
control
OH-TAM
EtOH
2d 3d 4d 2d 3d 4d
95 -
72 -
55 -
Hsp90
PDK1
1 2 3 4 5 6 7 8 9 10 11 12 13 14

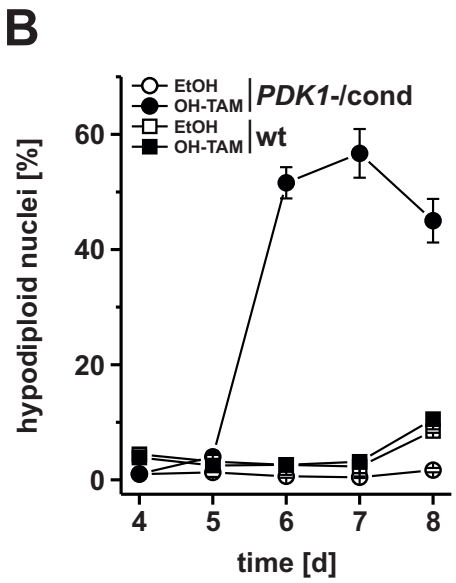
B
EtOH
OH-TAM
PDK1-/cond
EtOH
OH-TAM
wt
hypodiploid nuclei [%]
60
40
20
0
4 5 6 7 8
time [d]

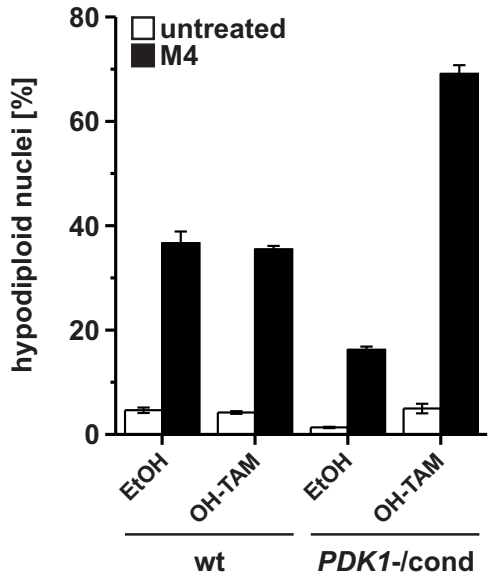
C
untreated
M4
hypodiploid nuclei [%]
80
60
40
20
0
EtOH
OH-TAM
EtOH
OH-TAM
wt
PDK1-/cond

Figure 2

A

gene title	regulation
known targets of PDK1	
TRAIL (tumor necrosis factor ligand superfamily member 10)	↑
cyclin-dependent kinase inhibitor 1B (p27, Kip1)	↑
Bcl-6 (B-cell CLL/lymphoma 6 protein)	↑
cyclin G2	↑
cyclin D1	↓
new targets of PDK1	
PI3K p110β (phosphoinositide-3-kinase, catalytic, beta polypeptide)	↑
PI3K p110δ (phosphoinositide-3-kinase, catalytic, delta polypeptide)	↑
PI3K p85α (Phosphoinositide-3-kinase, regulatory subunit 1)	↑
inositol polyphosphate-5-phosphatase (INPP5B)	↓
phosphatidylinositol-4-phosphate 5-kinase type-1 β (PIP5K1-β)	↑
Phosphoinositide-3-kinase interacting protein 1 (PIK3IP1)	↑
Lyn (v-yes-1 Yamaguchi sarcoma viral related oncogene homolog)	↑

B

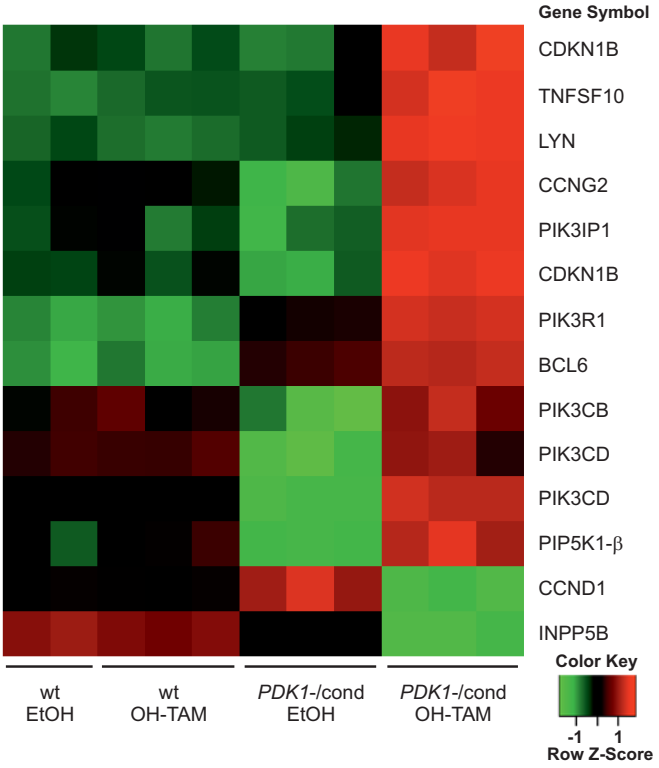

C

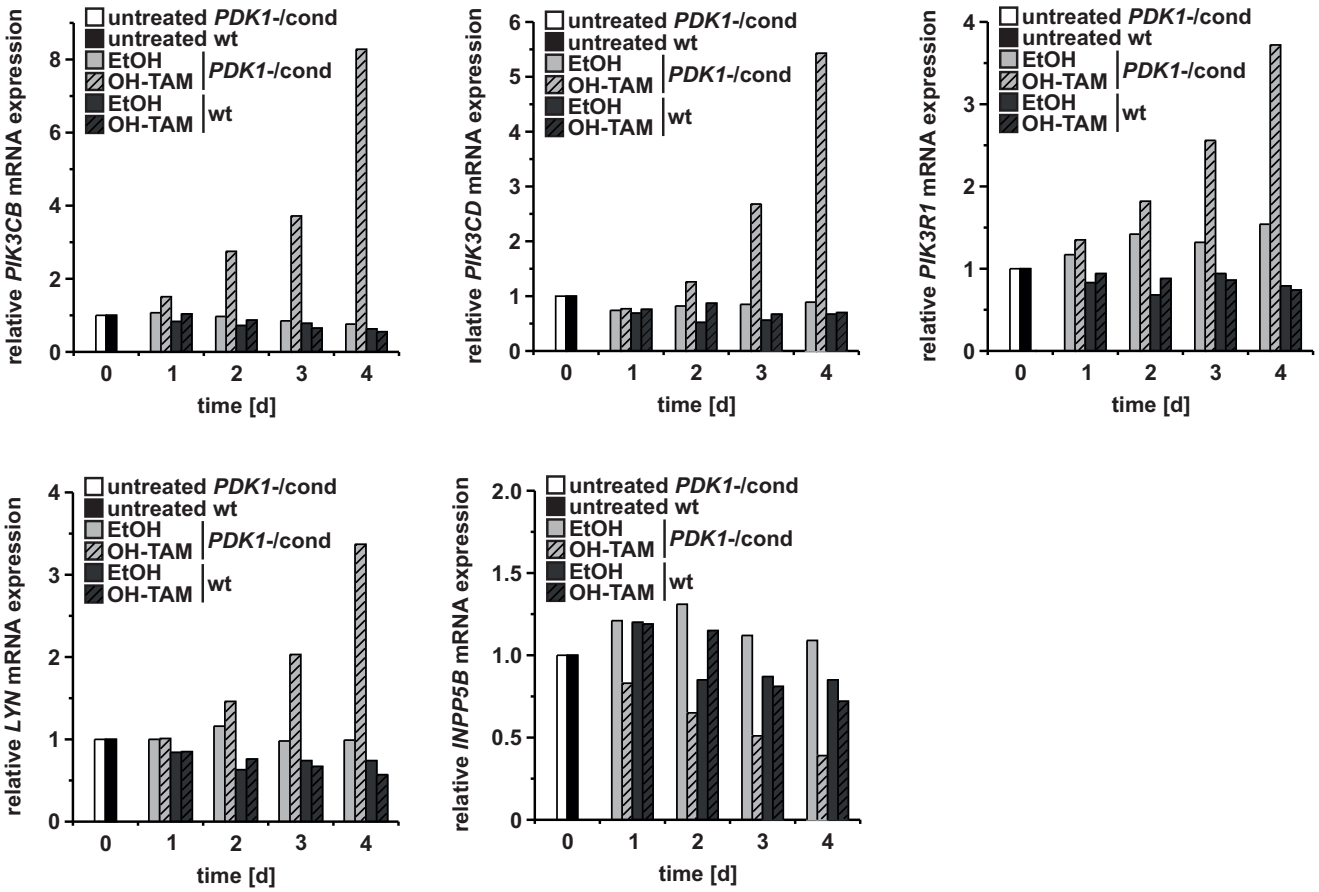

Figure 3

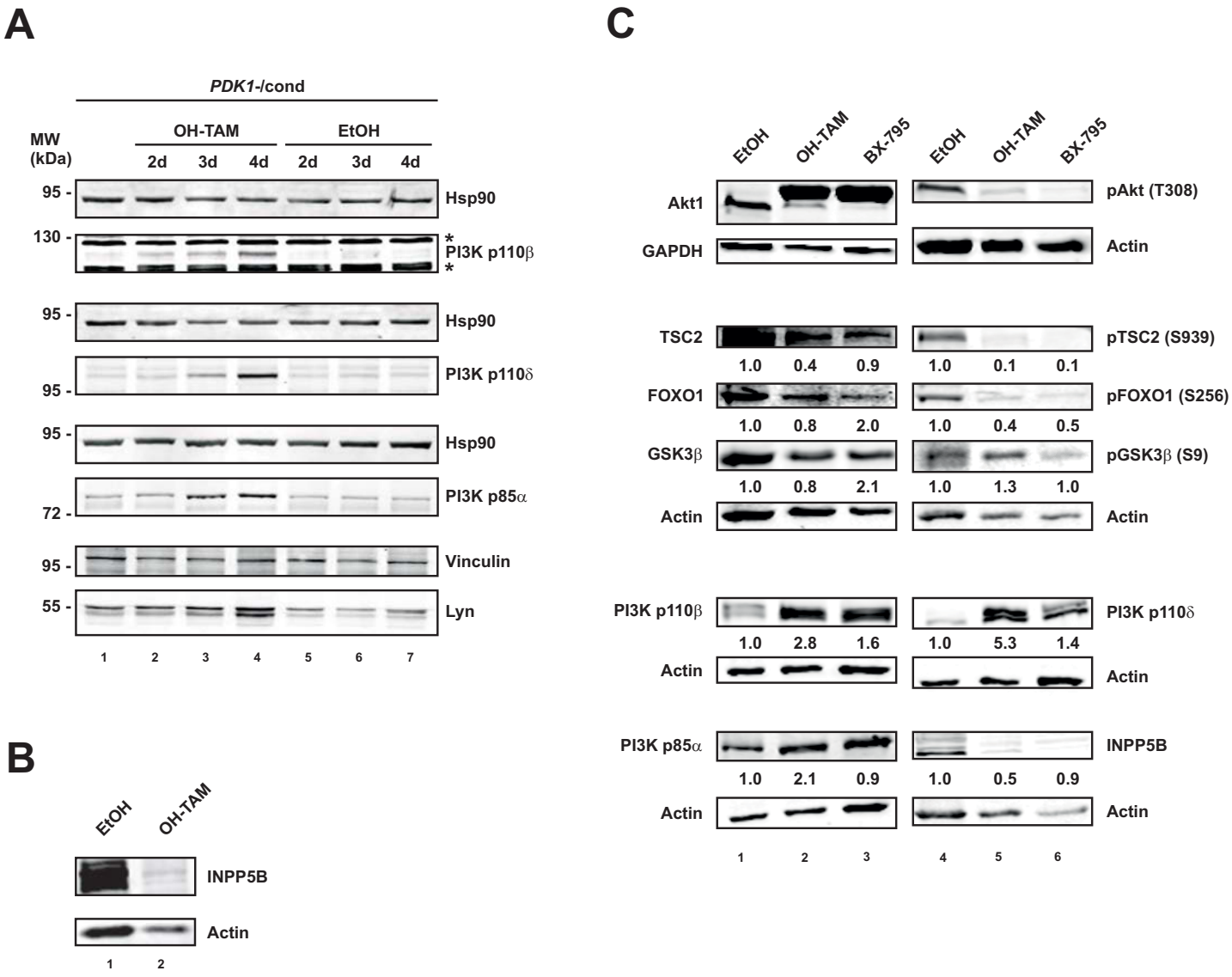
A
PDK1-/cond
MW (kDa)
OH-TAM
EtOH
2d 3d 4d 2d 3d 4d
95 -
Hsp90
130 -
*
PI3K p110β
*
95 -
Hsp90
PI3K p110δ
95 -
95 -
Hsp90
72 -
PI3K p85α
95 -
Vinculin
55 -
Lyn
1 2 3 4 5 6 7
B
EtOH
OH-TAM
INPP5B
Actin
1 2
C
EtOH
OH-TAM
BX-795
EtOH
OH-TAM
BX-795
Akt1
pAkt (T308)
GAPDH
Actin
TSC2
pTSC2 (S939)
1.0 0.4 0.9 1.0 0.1 0.1
FOXO1
pFOXO1 (S256)
1.0 0.8 2.0 1.0 0.4 0.5
GSK3β
pGSK3β (S9)
1.0 0.8 2.1 1.0 1.3 1.0
Actin
Actin
PI3K p110β
PI3K p110δ
1.0 2.8 1.6 1.0 5.3 1.4
Actin
Actin
PI3K p85α
INPP5B
1.0 2.1 0.9 1.0 0.5 0.9
Actin
Actin
1 2 3 4 5 6

Figure 4

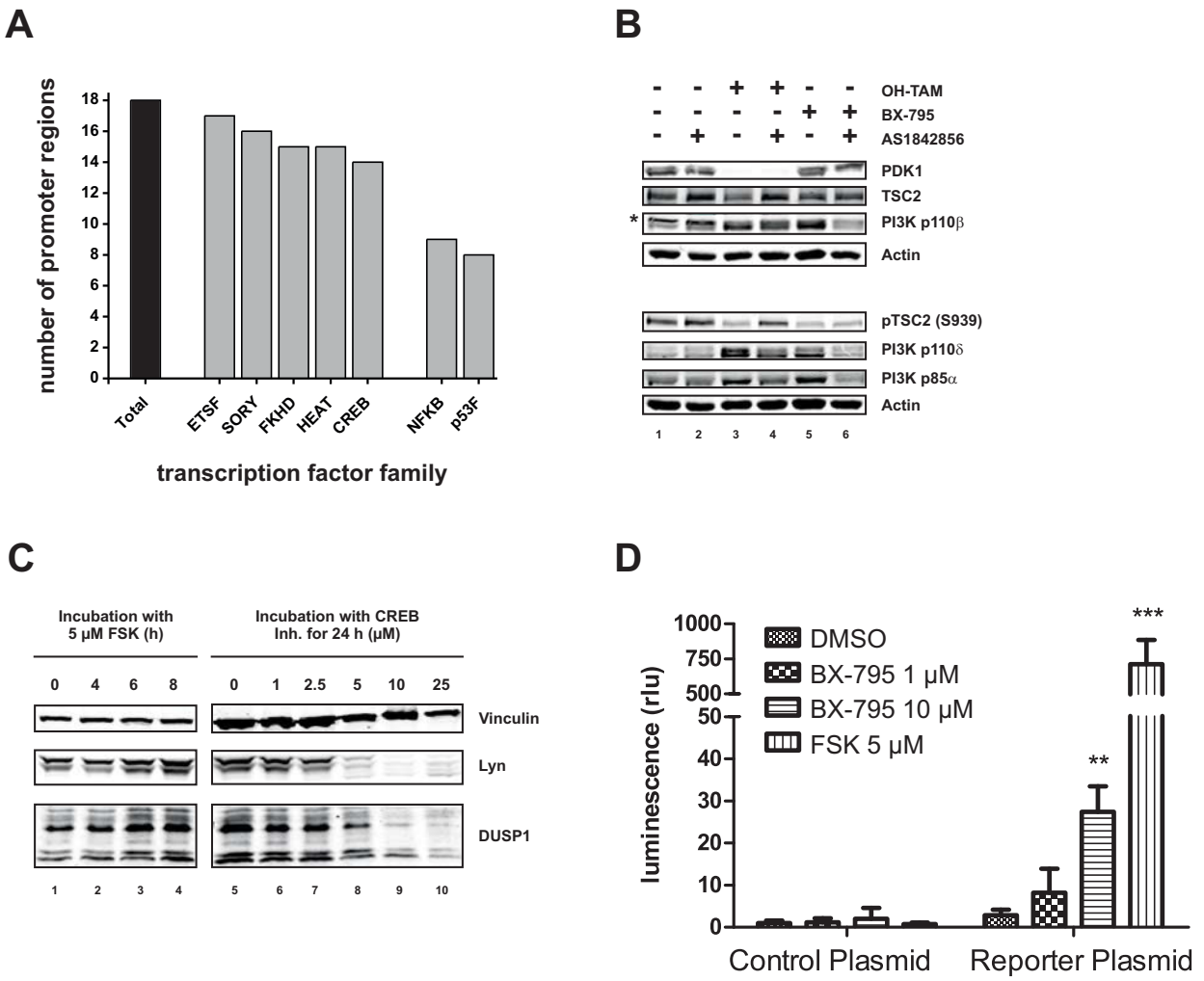
A
number of promoter regions
18
16
14
12
10
8
6
4
2
0
Total
ETSF
SORY
FKHD
HEAT
CREB
NFKB
p53F
transcription factor family
B
OH-TAM
BX-795
AS1842856
PDK1
TSC2
PI3K p110β
Actin
pTSC2 (S939)
PI3K p110δ
PI3K p85α
Actin
1 2 3 4 5 6
C
Incubation with 5 μM FSK (h)
Incubation with CREB Inh. for 24 h (μM)
0 4 6 8
0 1 2.5 5 10 25
Vinculin
Lyn
DUSP1
1 2 3 4 5 6 7 8 9 10
D
luminescence (rlu)
1000
750
500
50
40
30
20
10
0
DMSO
BX-795 1 μM
BX-795 10 μM
FSK 5 μM
***
**
Control Plasmid
Reporter Plasmid

Figure 5

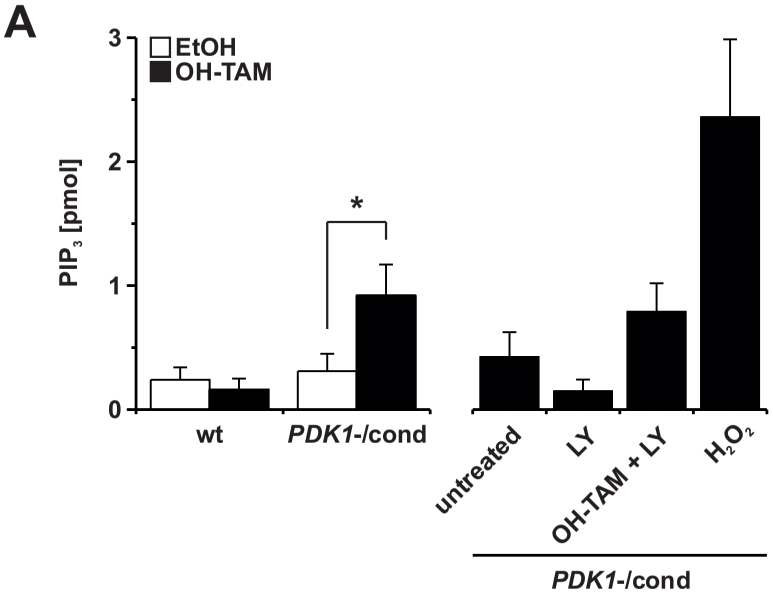
A
EtOH
OH-TAM
PIP3 [pmol]
3
2
1
0
*
wt
PDK1-/cond
untreated
LY
OH-TAM + LY
H2O2
PDK1-/cond

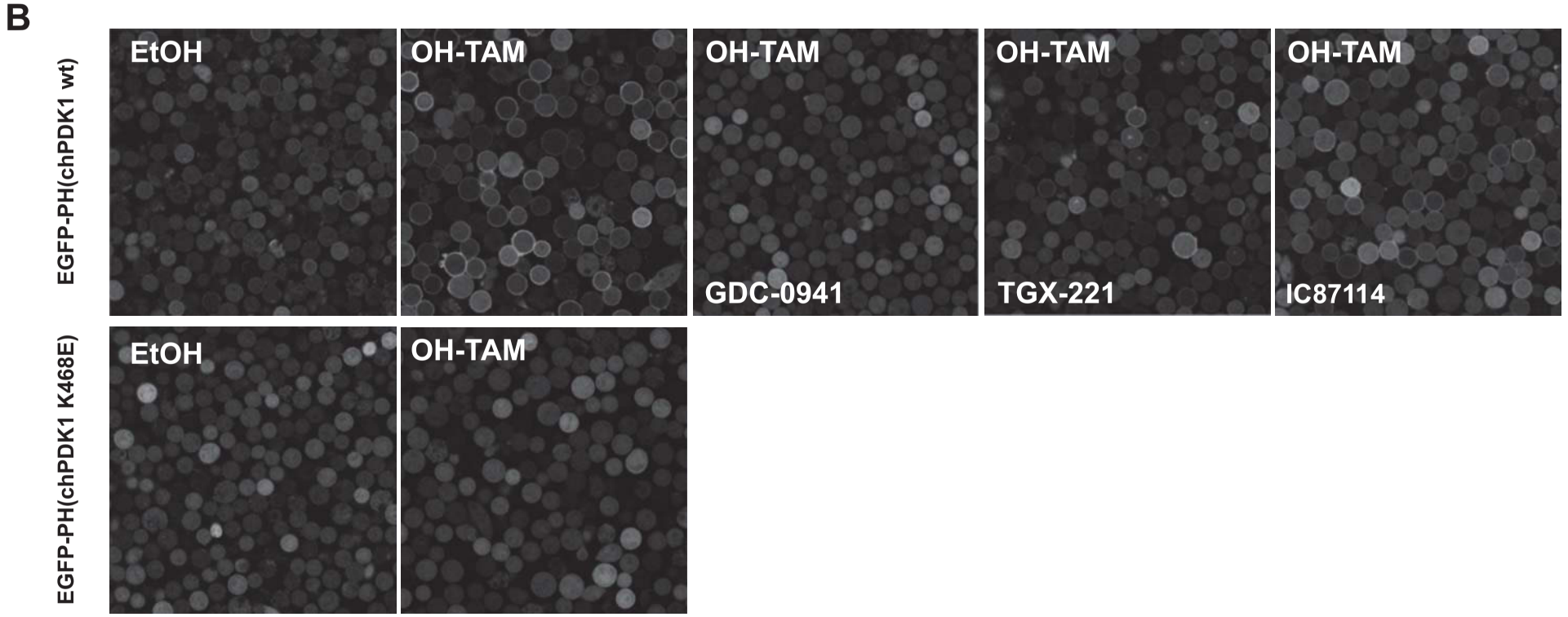
B
EGFP-PH(chPDK1 wt)
EtOH
OH-TAM
OH-TAM
GDC-0941
OH-TAM
TGX-221
OH-TAM
IC87114
EGFP-PH(chPDK1 K468E)
EtOH
OH-TAM

Figure 6

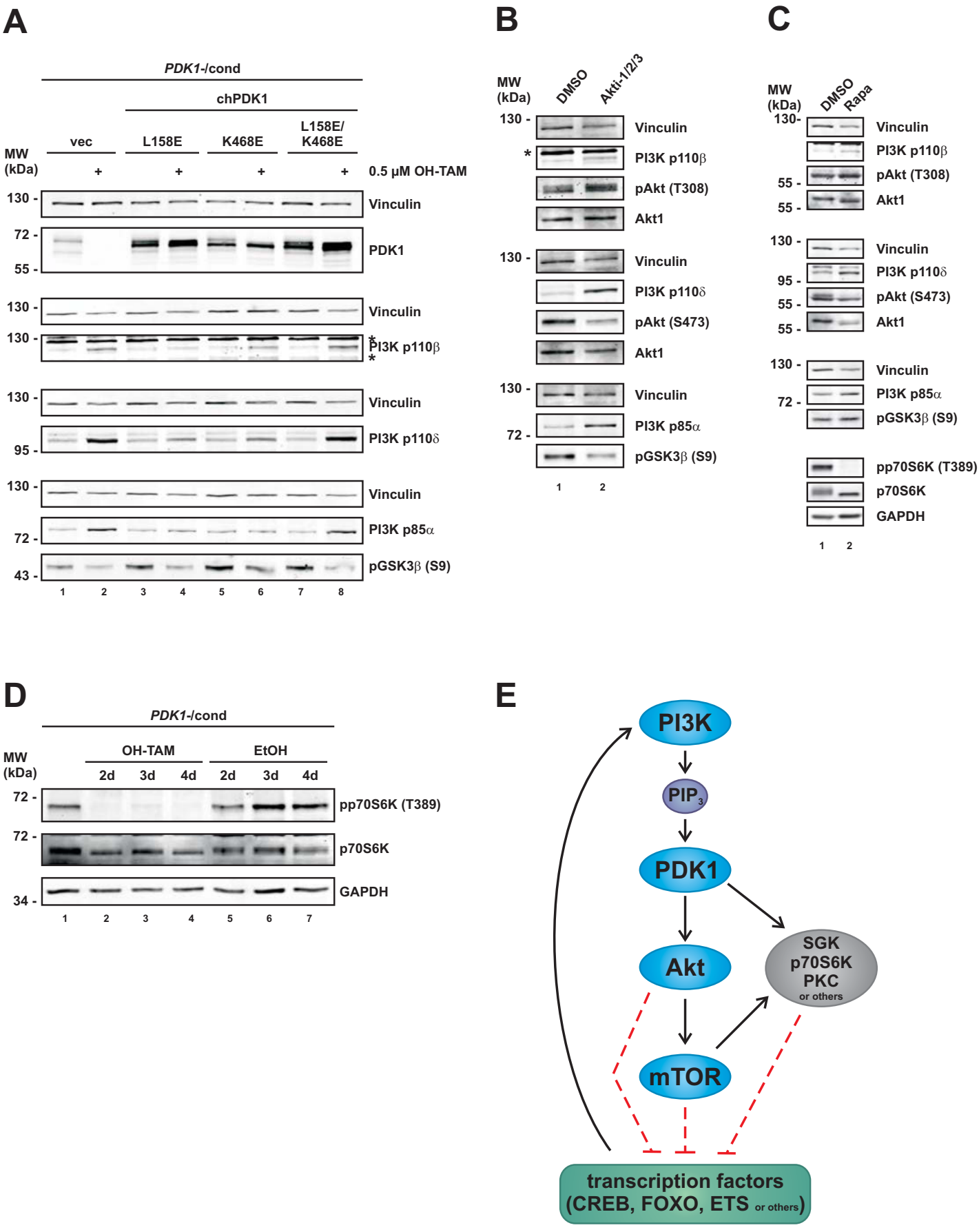
A
PDK1-/cond
chPDK1
vec
L158E
K468E
L158E/
K468E
MW
(kDa)
0.5 μM OH-TAM
Vinculin
PDK1
PI3K p110β
PI3K p110δ
PI3K p85α
pGSK3β (S9)
B
DMSO
Akti-1/2/3
Vinculin
PI3K p110β
pAkt (T308)
Akt1
PI3K p110δ
pAkt (S473)
PI3K p85α
pGSK3β (S9)
C
DMSO
Rapa
pp70S6K (T389)
p70S6K
GAPDH
D
OH-TAM
EtOH
2d
3d
4d
E
PI3K
PIP3
PDK1
Akt
mTOR
SGK
p70S6K
PKC
or others
transcription factors
(CREB, FOXO, ETS or others)

Triggering of a novel intrinsic apoptosis pathway by the kinase inhibitor staurosporine: activation of caspase-9 in the absence of Apaf-1

Joachim Manns,*[,1] Merle Daubrawa,*[,1] Stefan Driessen,*[,2] Florian Paasch,* Nadine Hoffmann,* Antje Löffler,*[,2] Kirsten Lauber,*[,3] Alexandra Dieterle,* Sebastian Alers,* Thomas Iftner,[†] Klaus Schulze-Osthoff,[‡] Björn Stork,*[,2,4] and Sebastian Wesselborg*[,2,4,5]

*Department of Internal Medicine I, [†]Division of Experimental Virology, Institute for Medical Virology and Epidemiology of Viral Diseases, and [‡]Interfaculty Institute for Biochemistry, University of Tübingen, Tübingen, Germany

ABSTRACT **The protein kinase inhibitor staurosporine is one of the most potent and frequently used proapoptotic stimuli, although its mechanism of action is poorly understood. Here, we show that staurosporine as well as its analog 7-hydroxystaurosporine (UCN-01) not only trigger the classical mitochondrial apoptosis pathway but, moreover, activate an additional novel intrinsic apoptosis pathway. Unlike conventional anticancer drugs, staurosporine and UCN-01 induced apoptosis in a variety of tumor cells overexpressing the apoptosis inhibitors Bcl-2 and Bcl-x_L. Furthermore, activation of this novel intrinsic apoptosis pathway by staurosporine did not rely on Apaf-1 and apoptosome formation, an essential requirement for the mitochondrial pathway. Nevertheless, as demonstrated in caspase-9-deficient murine embryonic fibroblasts, human lymphoma cells, and chicken DT40 cells, staurosporine-induced apoptosis was essentially mediated by caspase-9. Our results therefore suggest that, in addition to the classical cytochrome *c*/Apaf-1-dependent pathway of caspase-9 activation, staurosporine can induce caspase-9 activation and apoptosis independently of the apoptosome. Since staurosporine derivatives have proven efficacy in clinical trials, activation of this novel pathway might represent a powerful target to induce apoptosis in multidrug-resistant tumor cells.—Manns, J., Daubrawa, M., Driessen, S., Paasch, F., Hoffmann, N., Löffler, A., Lauber, K., Dieterle, A., Alers, S., Iftner, T., Schulze-Osthoff, K., Stork, B., Wesselborg, S. Triggering of a novel intrinsic apoptosis pathway by the kinase inhibitor staurosporine: activation of caspase-9 in the absence of Apaf-1. *FASEB J.* 25, 3250–3261 (2011). www.fasebj.org**

Key Words: UCN-01 · apoptosome · mitochondria · Bcl-2

A MAJOR MECHANISM OF action of DNA-damaging agents, such as conventional anticancer drugs and ionizing irradiation, is the activation of apoptosis in cancer cells. Conversely, tumor cells frequently gain resistance to chemo- and radiotherapy by inactivation of the apoptotic machinery (1). In mammalian cells, apoptosis can be activated by at least two major signaling routes, namely, the extrinsic death receptor and the intrinsic mitochondrial pathway, which both depend on the activation of intracellular cysteine proteases, termed caspases. The extrinsic pathway is activated by ligation of death receptors, such as CD95, TRAIL-R1, TRAIL-R2, and TNF-R1, by their respective ligands. Trimerization of death receptors by their ligands or agonistic antibodies recruits the adapter molecule FADD to the receptor *via* mutual interaction of their death domains. FADD, in turn, recruits procaspase-8 through interaction between the death effector domain of FADD and procaspase-8. On formation of this death-inducing signaling complex (DISC), procaspase-8 becomes activated by dimerization and autoproteolytic cleavage.

The intrinsic death pathway is initiated at the mitochondrion by the release of cytochrome *c*. The release of cytochrome *c* can be induced either through death receptor-mediated activation of the Bcl-2 protein Bid or independently of this pathway by cellular stress signals, such as DNA damage, which induce the activation of various proapoptotic Bcl-2 proteins, such as Bax, Puma, or Noxa. Conversely, antiapoptotic members of the Bcl-2 family, including Bcl-2, Bcl-x_L, Bcl-w, A1, and Mcl-1, can block the mitochondrial release of cytochrome *c* and the subsequent activation of caspases and

[1] These authors contributed equally to this work.
[2] Current address: Institute of Molecular Medicine, Heinrich-Heine-University, Düsseldorf, Germany.
[3] Current address: Department of Radiation Oncology, Ludwig-Maximilians University, Munich, Germany.
[4] These authors contributed equally to this work.
[5] Correspondence: Institute of Molecular Medicine, Heinrich-Heine-University, Universitätsstr. 1, D-40225 Düsseldorf, Germany. E-mail: sebastian.wesselborg@uni-tuebingen.de

doi: 10.1096/fj.10-177527

This article includes supplemental data. Please visit *http://www.fasebj.org* to obtain this information.

0892-6638/11/0025-3250 © FASEB

apoptosis (2). Once released in the cytosol, cytochrome *c* together with (d)ATP binds to the adapter protein Apaf-1 that subsequently oligomerizes and recruits procaspase-9 *via* a mutual interaction of their caspase recruitment domains (CARDs). In this high-molecular-weight complex, termed apoptosome, procaspase-9 is activated and, in turn, proteolytically activates downstream effector caspases, such as caspase-3 and caspase-7 (3). Thus, caspase-9 constitutes the central initiator caspase for the mitochondrial pathway, as caspase-8 does for the death receptor pathway. Activation of both pathways *via* initiator caspases triggers an amplifying cascade of effector caspases, which after cleavage of vital death substrates, leads to the final demise of the cell.

The fact that activation of the mitochondrial death pathway represents the major mechanism of most conventional anticancer drugs and radiotherapy explains why cancer cells acquire therapy resistance by inactivation of the mitochondrial pathway. Therefore, it will be of a great benefit for the successful treatment of cancers if novel intrinsic pathways could be identified that would enable the elimination of anticancer drug-resistant tumor cells.

The ATP-analog staurosporine is a broad-range protein kinase inhibitor that inhibits numerous Ser/Thr and Tyr kinases (4). Beyond that, staurosporine represents one of the most potent apoptotic stimuli and induces apoptosis with similar rapid kinetics as death receptor signaling. For this reason, staurosporine is one of the most widely used proapoptotic agents in various experimental systems. Despite its unspecific mode of action, derivatives of staurosporine, such as 7-hydroxystaurosporine (UCN-01), are successfully used in phase I and II clinical trials (5). The mechanism of apoptosis induction by staurosporine derivatives, however, remains largely elusive.

We have previously shown that staurosporine can induce apoptosis in anticancer drug-resistant tumor cells (6). Therefore, we were interested to further dissect the signaling pathways activated by staurosporine. To this end, we specifically blocked known apoptosis pathways, such as the death receptor, mitochondrial cytochrome *c*/Apaf-1, and the ER stress pathway. We show that staurosporine—similar to anticancer drugs—directly activates the mitochondrial death pathway, independent of death receptor signaling. Although the classical mitochondrial apoptotic pathway was activated by staurosporine, overexpression of Bcl-2 or Bcl-x_L only partially inhibited staurosporine-induced apoptosis. More important, we show that, in contrast to conventional anticancer drugs, staurosporine activates an additional intrinsic pathway that is not inhibited by antiapoptotic Bcl-2 proteins but mediated by an Apaf-1-independent activation of caspase-9. Drug-targeted activation of this apoptosis signaling pathway might be, therefore, exploited to eliminate anticancer drug-resistant tumor cells.

MATERIALS AND METHODS

Cells and reagents

All cell lines were maintained at 5% CO_2 and 37°C in RPMI 1640 medium supplemented with 10% heat-inactivated FCS, 100 U of penicillin/ml, 0.1 mg streptomycin/ml, and 10 mM HEPES (all from Gibco BRL, Eggenstein, Germany). The anticancer drug-resistant human Jurkat T cell clone JM319 and its parental drug-sensitive cell line JE6.1 were previously described (6) and kindly provided by Ottmar Janssen (University of Kiel, Kiel, Germany). Caspase-8 and FADD-deficient Jurkat cells and the parental cell line A3 were kindly provided by John Blenis (Harvard Medical School, Boston, MA, USA). Jurkat cells stably overexpressing Bcl-x_L were a gift from Henning Walczak (Imperial College London, London, UK). Stable transfectants of Jurkat cells with Bcl-2 expression restricted to the outer mitochondrial membrane by replacing its membrane anchor with the mitochondrial insertion sequence of ActA (Bcl-2-mito) or restricted to the ER by using the ER-specific sequence of cytochrome b5 (Bcl-2-ER) or cells expressing wild-type Bcl-2 (Bcl-2-wild type) were kindly provided by Claus Belka (Ludwig-Maximilians University, Munich, Germany) and previously described (7). Human MCF7 breast cancer cells stably transfected with Bcl-2 or Bcl-x_L cDNA and vector control cells were a kind gift of Marja Jäättelä (Danish Cancer Society, Copenhagen, Denmark). Human SH-EP neuroblastoma cells stably expressing murine Bcl-2 or a vector control were kindly provided by Simone Fulda (Goethe University, Frankfurt am Main, Germany). Caspase-9-deficient Jurkat cells stably transfected with vector control or caspase-9 were previously described (8). Alternatively, caspase-9 deficient Jurkat cells were retrovirally transduced with either empty pMSCVpuro (Clontech, Heidelberg, Germany) or pMSCVpuro containing cDNAs coding for cMyc-tagged, FLAG-tagged, or untagged human wild-type caspase-9. The Apaf-1-deficient human melanoma cell line SK-Mel-94 and Apaf-1-proficient melanoma lines SK-Mel-19 and SK-Mel-29 were kindly provided by Maria S. Soengas (University of Michigan, Ann Arbor, MI, USA; ref. 9). MEFs deficient for caspase-9 or Apaf-1 and the respective control cells were kindly provided by Andreas Strasser (Walter and Eliza Hall Institute of Medical Research, Melbourne, VIC, Australia; refs. 10, 11). The broad-range caspase inhibitors benzyloxycarbonyl-Val-Ala-Asp-fluoromethyl ketone (zVAD-fmk) and *N*-(2-quinolyl)valyl-aspartyl-(2,6-difluorophenoxy) methyl ketone (QVD-OPh) were purchased from Bachem (Heidelberg, Germany) and Calbiochem (Merck, Darmstadt, Germany), respectively. Staurosporine was purchased from Roche Molecular Biochemicals (Mannheim, Germany), and UCN-01 (7-hydroxystaurosporine) was kindly provided by Edward A. Sausville (National Cancer Institute, Rockville, MD, USA) and the Drug Synthesis and Chemistry Branch, Developmental Therapeutics Program, National Cancer Institute (Bethesda, MD, USA) or acquired from Calbiochem. The PI3K inhibitor LY294002 was obtained from Cell Signaling Technology (Frankfurt, Germany). The PKA inhibitors H89 and Ro31–8220 (Bis-IX), the PKC and GSK3 inhibitor bisindolylmaleimide (Bis-I), and the PKC inhibitor Gö6976 were obtained from Sigma (Deisenhofen, Germany). The Akt inhibitor Akti-1/2, the MEK kinase inhibitors PD98059 and UO126, the CDK1 inhibitors purvalanol A and aloisine, the DNA PK inhibitor, the ATM/ATR kinase inhibitor, the p38 MAPK inhibitor SB203580, the mTOR inhibitor rapamycin, the PKC inhibitor Gö6983, the PKCξ pseudosubstrate, and the casein kinase 1 (CK1) and CK2 inhibitor were all obtained from Calbiochem. Agonistic anti-CD95 antibody CH11 was obtained from Medical Biological Laboratories (Woburn, MA, USA) and TRAIL from R&D Systems (Wiesbaden, Germany). The anticancer drugs etoposide, mitomycin C, and daunorubicin were

obtained from Sigma and the clinical pharmacy (Medical Clinics, Tübingen, Germany), respectively.

Generation of *apaf-1*$^{-/-}$ and *caspase-9*$^{-/-}$ DT40 cell lines

Apaf-1$^{-/-}$ and *caspase-9*$^{-/-}$ DT40 cell lines were generated by targeted disruption of the corresponding two alleles. For Apaf-1, the targeting vectors pApaf-1/HisD and pApaf-1/Bsr were constructed by replacing the genomic fragment containing exons 6–11 with HisD and Bsr cassettes, respectively. The cassettes were flanked by 3.6 and 3.7 kb of genomic *apaf-1* sequence on the 5′ and 3′ sides. The replacement vector pApaf-1/HisD was transfected into DT40 cells, and the selection was done in the presence of histidinol (1 mg/ml). The pApaf-1/Bsr was then transfected into two independent HisD-targeted clones, and the clones were selected with both histidinol (0.5 mg/ml) and blasticidin S (50 μg/ml). All successful targeting events were confirmed by genomic PCR. Apaf-1 deficiency was verified by RT-PCR and immunoblot analysis (Supplemental Fig. S1*A–D*). For caspase-9, the HisD and Bsr targeting constructs were made by replacing the genomic fragment containing exons 4–6. The cassettes were flanked by 2.9 kb (5′ side) and 2.7 kb (3′ side), respectively. The sequential transfection of pCaspase-9/HisD and pCaspase-9/Bsr led to the isolation of one null mutant. Successful targeting events were confirmed by genomic PCR, and caspase-9-deficiency was verified by RT-PCR (Supplemental Fig. S1*E–G*). All DT40 cell lines were maintained at 5% CO_2 and 37°C in RPMI 1640 medium supplemented with 10% heat-inactivated FCS, 1% heat-inactivated chicken serum, 3 mM L-glutamine, 50 U/ml penicillin, 50 μg streptomycin/ml, and 50 μM β-mercaptoethanol.

Measurement of apoptosis and cell viability

For determination of apoptosis, 5×10^4 cells/well were seeded in microtiter plates and treated for the indicated time with anti-CD95, chemotherapeutic agents, staurosporine, UCN-01, or other kinase inhibitors. Where indicated, cells were preincubated for 30 min with the caspase inhibitors zVAD-fmk (50 μM) or QVD-OPh (10 μM). The leakage of fragmented DNA from apoptotic nuclei was measured by the method of Nicoletti *et al.* (12). Briefly, nuclei were prepared by lysing cells in a hypotonic lysis buffer (1% sodium citrate, 0.1% Triton X-100, 50 μg/ml propidium iodide) and subsequently analyzed by flow cytometry. Nuclei to the left of the 2N peak containing hypodiploid DNA were considered apoptotic. All flow cytometric analyses were performed on a FACSCalibur (Becton Dickinson, Heidelberg, Germany) using CellQuest analysis software.

For determination of cell viability of MCF7 cells and MEFs, 1×10^5 cells/well were plated into a microplate in a final volume of 150 μl and treated as indicated. After 24 h, 3-(4,5-dimethylthiazole-2-yl)-2,5-diphenyl-tetrazoliumbromide (MTT; Sigma) was added to a final concentration of 450 μg/ml, and cells were incubated for another 5 h at 37°C. The resulting formazan crystals were dissolved by addition of 4% SDS and another 3 h of incubation at 37°C. The assay was analyzed spectrophotometrically at 550 nm (reference wavelength 690 nm), and results were shown as mean values of duplicates.

Fluorometric assay of caspase activity

For detection of caspase-3-like DEVDase activity, cytosolic extracts of 5×10^4 cells were prepared in lysis buffer containing 0.5% Nonidet P-40, 20 mM HEPES (pH 7.4), 84 mM KCl, 10 mM $MgCl_2$, 0.2 mM EDTA, 0.2 mM EGTA, 1 mM DTT, 5 μg/ml aprotinin, 1 μg/ml leupeptin, 1 μg/ml pepstatin, and 1 mM phenylmethylsulfonyl fluoride (PMSF). Caspase activity was determined by incubation of cell lysates with 50 μM of the fluorogenic substrate Ac-DEVD-AMC (*N*-acetyl-Asp-Glu-Val-Asp-aminomethyl-coumarin; Biomol, Hamburg, Germany) in 200 μl buffer containing 50 mM HEPES (pH 7.3), 100 mM NaCl, 10% sucrose, 0.1% CHAPS, and 10 mM DTT. The release of aminomethylcoumarin was measured in a kinetic assay by spectrofluorometry using an excitation wavelength of 360 nm and an emission wavelength of 475 nm. Caspase activity was determined as the slope of the resulting linear regressions and expressed in arbitrary fluorescence units per minute, as described previously (13).

Determination of cytosolic cytochrome *c* release

For detection of cytosolic translocation of cytochrome *c*, 6×10^6 Jurkat vector control cells or cells stably transfected with Bcl-2 were treated as indicated. Cells were washed with ice-cold PBS and then resuspended in 150 μl MT buffer (70 mM Tris, 250 mM sucrose, and 1 mM EDTA, pH 7.4). An equal volume of MES/digitonin buffer was added (20 mM EDTA, 20 mM EGTA, 0.25 M D-manitol, 20 mM MES, and 163 μM digitonin, pH 7.4). After 4 min incubation, the cells were harvested (900 *g*, 2 min), and the supernatant was removed and ultracentrifuged (20,000 *g*, 5 min). The supernatant represents the cytosolic fraction. The mitochondrial fraction residing in the pellet was resuspended in 50 μl MT buffer. The release of cytochrome *c* into the cytosol was determined by immunoblotting.

Cell extracts and immunoblotting

Cleavage of caspases and caspase substrates was detected by immunoblotting. Cells (2×10^6/well) were seeded into 6-well plates and on adherence treated with the respective apoptotic stimuli. After the indicated time, cells were washed in cold PBS and lysed in 1% Triton X-100, 50 mM Tris-HCl (pH 7.6), and 150 mM NaCl containing 3 μg/ml aprotinin, 3 μg/ml leupeptin, 3 μg/ml pepstatin A, and 2 mM PMSF. Subsequently, proteins were separated under reducing conditions on an SDS-polyacrylamide gel and electroblotted to a polyvinylidene difluoride membrane (Amersham Pharmacia, Freiburg, Germany). Membranes were blocked for 1 h with 5% nonfat dry milk powder in TBS and then incubated for 1 h with murine monoclonal antibodies against poly(ADP-ribose)polymerase (PARP; Qbiogene-Alexis, Grünberg, Germany), caspase-3, cytochrome *c*, Apaf-1, or GAPDH (BD Biosciences, Heidelberg, Germany). Caspase-9 was detected with a rabbit antiserum generated against full-length caspase-9 (generated in the laboratory of S.W.). Membranes were washed 4 times with TBS/0.02% Triton X-100 and incubated with the respective peroxidase-conjugated affinity-purified secondary antibody for 1 h. Following extensive washing, the reaction was developed by enhanced chemiluminescent staining using ECL reagents (Amersham Pharmacia).

In vitro activation of the apoptosome with cytochrome *c* and dATP

For *in vitro* activation of the apoptosome, 5×10^7 Jurkat cells were collected by centrifugation, washed with ice-cold PBS, and lysed in 20 mM HEPES (pH 7.5), 50 mM NaCl, 0.3% CHAPS, 10 mM KCl, 1.5 mM $MgCl_2$, 1 mM EDTA, 1 mM EGTA, 1 mM DTT, 2 μg/ml aprotinin, 1 μg/ml leupeptin, and 250 μM PMSF. For apoptosome formation, extracts were incubated at 37°C in the presence of 8.6 μM cytochrome *c* and 2.4 mM ATP for 15 min. Subsequently, lysates were diluted in lysis buffer and precleared over protein A/G agarose beads (Santa Cruz Biotechnology,

Santa Cruz, CA, USA) at 4°C for 1.5 h. Precleared extracts were incubated with fresh protein A/G agarose beads and anti-caspase-9 antibody for 2 h at 4°C. After extensive washing in lysis buffer, proteins were separated under reducing conditions on an SDS-polyacrylamide gel, transferred to a polyvinylidene difluoride membrane, and immunoblotted for Apaf-1 or caspase-9.

RESULTS

Staurosporine induces apoptosis in anticancer drug-resistant tumor cells independently of death receptors

It is assumed that staurosporine triggers apoptosis by the mitochondrial pathway independently of death receptors. We confirmed this assumption in Jurkat cells deficient in FADD or caspase-8, which underwent apoptosis induced by staurosporine with a similar dose dependency as wild-type cells (Supplemental Fig. S2*A*). Likewise, apoptosis induced by the anticancer drug etoposide was not affected, whereas cell death triggered by agonistic anti-CD95 antibodies was completely abrogated in the absence of either FADD or caspase-8 (Supplemental Fig. S2*A*). Moreover, staurosporine, similar to DNA-damaging anticancer drugs, was able to directly activate the mitochondrial pathway, as, in contrast to death receptor triggering, caspase inhibitors did not affect the mitochondrial release of cytochrome *c* (14). However, in comparison to anticancer drugs, staurosporine induced apoptosis with a considerably faster time course. Furthermore, as shown in Supplemental Fig. S2*B*, staurosporine induced apoptosis in the Jurkat clone JM319, which is completely resistant to anticancer drugs (6). Although higher concentrations of staurosporine were required, as compared to the anticancer drug-sensitive parental Jurkat cell line JE6.1, staurosporine was able to induce substantial apoptosis in the drug-resistant JM319 cells (Supplemental Fig. S2*C*, *D*). Accordingly, processing of the caspase substrate PARP was only delayed but not inhibited in JM319 cells (Supplemental Fig. S2*E*). Inhibition of caspases by QVD-OPh completely abrogated staurosporine- and mitomycin C-induced apoptosis (Supplemental Fig. S2*F*). These results, therefore, indicate that, although anticancer drugs and staurosporine share common signaling elements, staurosporine exerts additional proapoptotic activities.

Staurosporine can induce apoptosis independently of the ER stress or the mitochondrial apoptosis pathway

Since staurosporine induced apoptosis in the absence of death receptor signaling, we focused on intrinsic apoptosis pathways. Besides the mitochondrial cytochrome *c*/Apaf-1 pathway, at least two other intrinsic organelle-specific apoptosis pathways have been described, including the endoplasmic reticulum (ER) stress and the nuclear PIDDosomal pathways. We investigated the role of the ER stress and the mitochondrial pathway using Jurkat cells stably expressing Bcl-2 either at the outer mitochondrial membrane (Bcl-2-mito) or at the ER (Bcl-2-ER) and in cells expressing wild-type Bcl-2 (Bcl-2-wt) (7). Expression of Bcl-2 did not affect TRAIL-induced apoptosis. In contrast, etoposide-induced apoptosis was strongly inhibited by both wild-type and mitochondria-targeted Bcl-2, whereas ER-targeted Bcl-2 had no effect (**Fig. 1*A***). Interestingly, staurosporine was still able to induce potent apoptosis in Jurkat cells overexpressing wild-type, ER- or mitochondria-targeted Bcl-2, albeit at higher concentrations as in control cells (Fig. 1*A*). Overexpression of wild-type Bcl-2 completely blocked the mitochondrial cytochrome *c* release on treatment with staurosporine, etoposide, and mitomycin C (Fig. 1*B*), arguing against the possibility that staurosporine induced apoptosis due to an insufficient blockage of cytochrome *c* relocation. The caspase inhibitor zVAD-fmk only slightly reduced cytochrome *c* release in vector control cells (Fig. 1*B*), indicating that the release of cytochrome *c* by staurosporine did not involve caspases as in case of death receptor signaling (14).

Staurosporine induces apoptosis in the presence of Bcl-2 and Bcl-x_L

The observation that staurosporine can induce apoptosis in Bcl-2-overexpressing cells was further confirmed by investigating the processing of the caspase substrate PARP. Again, staurosporine triggered rapid PARP processing within 3 h in vector control and Bcl-2-overexpressing cells. Interestingly, the staurosporine derivative UCN-01 (7-hydroxystaurosporine), which is already tested for its tumoricidal potential in clinical trials (5), was also capable to induce PARP processing in cells overexpressing Bcl-2 (Fig. 1*C*). However, conventional DNA-damaging anticancer drugs, such as etoposide and mitomycin C, did not induce cleavage of PARP in the presence of Bcl-2.

To corroborate these findings, we further tested the effects of Bcl-x_L. Similar to Bcl-2, overexpression of Bcl-x_L in Jurkat cells did reduce but could not block staurosporine-induced apoptosis, whereas etoposide-mediated apoptosis was almost completely abrogated (**Fig. 2*A***). In addition, we observed that staurosporine triggered cell death and PARP processing in breast carcinoma MCF7 cells overexpressing Bcl-2 or Bcl-x_L (Fig. 2*B–D*). Similarly, staurosporine induced apoptosis regardless of Bcl-2 in SH-EP neuroblastoma cells, whereas etoposide-induced cell death was completely prevented by Bcl-2 (Fig. 2*E*). Therefore, these results suggest that, unlike anticancer drugs, staurosporine-triggered cell death is at best attenuated but not abrogated by antiapoptotic Bcl-2 proteins.

Caspase-9 is indispensable for staurosporine-induced apoptosis

Since caspase-8 was not required for staurosporine-induced apoptosis, we next investigated the involvement of caspase-9, the central caspase of the cyto-

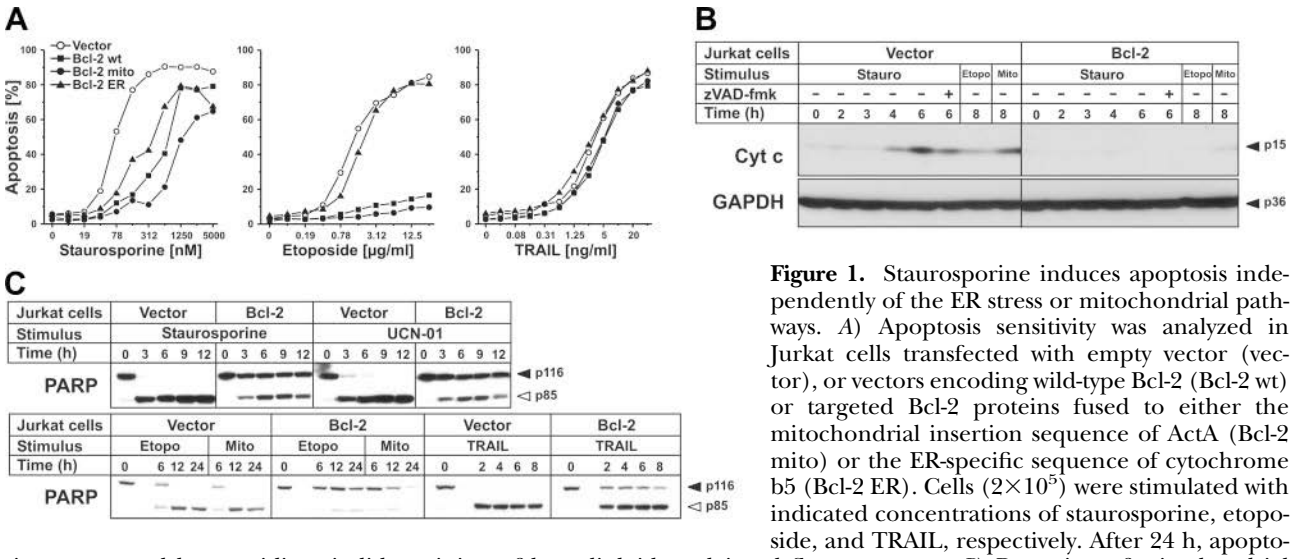

Figure 1. Staurosporine induces apoptosis independently of the ER stress or mitochondrial pathways. *A*) Apoptosis sensitivity was analyzed in Jurkat cells transfected with empty vector (vector), or vectors encoding wild-type Bcl-2 (Bcl-2 wt) or targeted Bcl-2 proteins fused to either the mitochondrial insertion sequence of ActA (Bcl-2 mito) or the ER-specific sequence of cytochrome b5 (Bcl-2 ER). Cells (2×10^5) were stimulated with indicated concentrations of staurosporine, etoposide, and TRAIL, respectively. After 24 h, apoptosis was assessed by propidium iodide staining of hypodiploid nuclei and flow cytometry. *B*) Detection of mitochondrial release of cytochrome *c*. Jurkat vector control cells or cells stably transfected with Bcl-2 (6×10^6) were preincubated for 30 min in the presence or absence of zVAD-fmk and subsequently stimulated with staurosporine (stauro; 2.5 μM), etoposide (etopo; 25 μg/ml), or mitomycin C (mito; 25 μg/ml). After the indicated time, cells were homogenized, and 150 μg of the cytosolic S10 fraction depleted of mitochondria was subjected to SDS-PAGE. Cytosolic cytochrome *c* was detected by immunoblotting. Equal protein loading was confirmed by reprobing the membrane with anti-GAPDH antibody. *C*) Jurkat cells (2×10^6) transfected with either empty vector (vector) or vector encoding Bcl-2 (Bcl-2) were treated with 2.5 μM staurosporine or 10 μM 7-hydroxystaurosporine (UCN-01; top panel). Alternatively, cells were incubated with 25 μg/ml etoposide, 25 μg/ml mitomycin C, and 40 ng/ml TRAIL, respectively (bottom panel). After treatment for the indicated time, cellular proteins were resolved by SDS-PAGE and investigated for the proteolytic processing of PARP by immunoblotting. Solid arrowheads indicate the uncleaved form of PARP; open arrowheads indicate the cleaved form.

chrome *c*/Apaf-1 pathway. Using caspase-9-deficient murine embryonic fibroblasts (MEFs), we found that caspase-9 was essentially required for staurosporine-induced cell death, since neither apoptosis nor caspase activation were observed in the absence of caspase-9 (**Fig. 3*A, B***). These data were further confirmed using caspase-9-deficient Jurkat cells (8). Apoptosis and caspase activation were completely blocked in caspase-9-deficient Jurkat cells treated with staurosporine or UCN-01, but not in cells restored with caspase-9 (Fig. 3*C, D*). Accordingly, processing of caspase-3 was only detected in caspase-9-positive but not in caspase-9-negative Jurkat cells (**Fig. 4**). Similarly, anticancer drug-induced apoptosis, caspase activation, and processing of caspase-3 were abrogated in caspase-9-deficient Jurkat cells, whereas TRAIL-induced events were not affected (Figs. 3*A, B, D* and 4). This observation was further confirmed using chicken DT40 cells, where caspase-9 had been knocked out by homologous recombination. Thus, in contrast to caspase-9-proficient DT40 cells, caspase activation and apoptosis induction by staurosporine were completely abrogated in caspase-$9^{-/-}$ cells (Fig. 3*E, F*).

Staurosporine activates caspase-9 in the absence of Apaf-1

Since staurosporine-induced apoptosis required caspase-9 but was not blocked by Bcl-2 or Bcl-x_L, we next investigated whether Apaf-1 is essential for staurosporine-mediated activation of caspase-9 by using Apaf-1-deficient MEFs. In comparison to wild-type MEFs, higher concentrations of staurosporine were required to reduce cell viability and to trigger caspase activation in Apaf-1-deficient MEFs. In contrast, mitomycin C-induced caspase activation was completely blocked in Apaf-$1^{-/-}$ cells (**Fig. 5*A, B***).

Since MEFs usually exert a higher apoptosis resistance than tumor cells, we additionally investigated the melanoma cell line SK-Mel-94, which was previously shown to be resistant to anticancer drugs due to the loss of Apaf-1 expression (9). In contrast to the melanoma lines SK-Mel-19 and SK-Mel-29, which have been shown to be Apaf-1 proficient (9), SK-Mel-94 cells expressed no Apaf-1 at protein level. Therefore, we tested these cells for their sensitivity to staurosporine and UCN-01. Accordingly, the absence of Apaf-1 rendered SK-Mel-94 cells completely resistant to etoposide-induced caspase activation, apoptosis, and reduction in viability, even at high concentrations of 200 μg/ml (Fig. 5*D–F*). On the contrary, staurosporine and UCN-01 were still able to induce apoptosis and loss of viability in SK-Mel-94 cells (Fig. 5*D–F*). Likewise, processing of caspase-9 and PARP were detected in SK-Mel-94 cells in response to staurosporine but not to etoposide treatment (Fig. 5*G*). To further corroborate that staurosporine can induce apoptosis in the absence of Apaf-1, we established a complete knockout of Apaf-1 in chicken DT40 cells by homologous recombination. In comparison to wild-type cells, staurosporine-induced apoptosis was reduced but still substantial in 5 different Apaf-1-deficient DT40 clones (Fig. 5*H*).

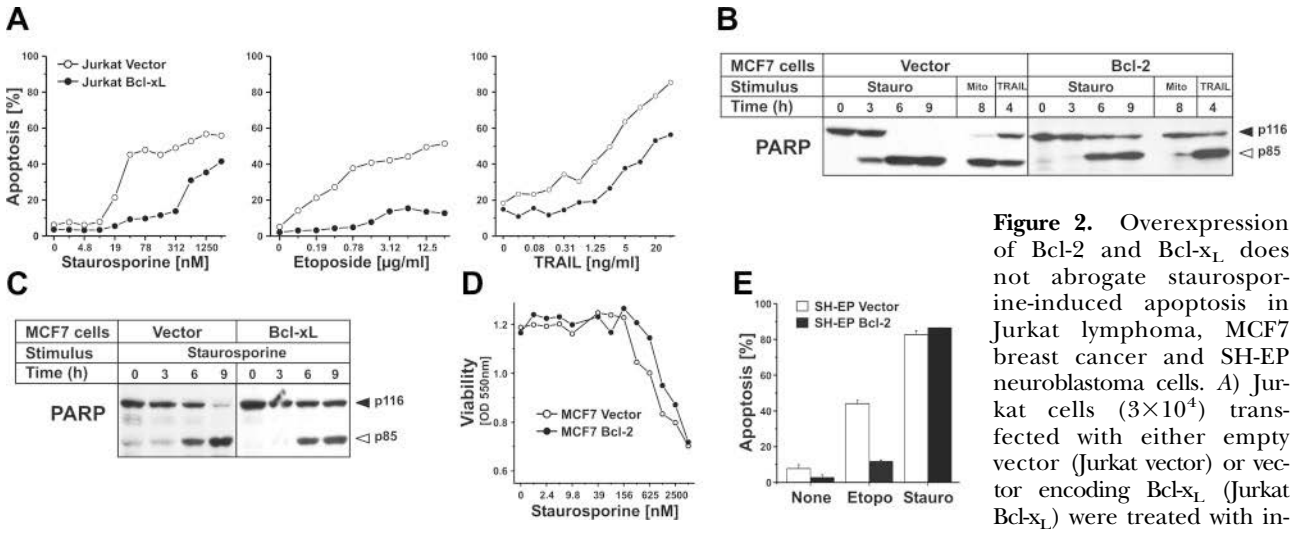

Figure 2. Overexpression of Bcl-2 and Bcl-x_L does not abrogate staurosporine-induced apoptosis in Jurkat lymphoma, MCF7 breast cancer and SH-EP neuroblastoma cells. *A*) Jurkat cells (3×10^4) transfected with either empty vector (Jurkat vector) or vector encoding Bcl-x_L (Jurkat Bcl-x_L) were treated with indicated concentrations of staurosporine, etoposide or TRAIL. After 24 h, apoptosis was assessed by propidium iodide staining of hypodiploid nuclei and flow cytometry. Mean values of duplicates are shown. *B*) MCF7 cells transfected with either empty vector (vector) or vector encoding Bcl-2 (Bcl-2) were treated for the indicated time with 2.5 μM staurosporine, 25 μg/ml mitomycin C, or 40 ng/ml TRAIL. Cellular proteins were resolved by SDS-PAGE, and the proteolytic processing of PARP was detected by immunoblotting. Solid arrowhead indicates uncleaved p116 form; open arrowhead indicates p85 fragment of PARP. *C*) MCF7 cells transfected with either empty vector (vector) or a vector encoding Bcl-x_L (Bcl-x_L) were treated with 2.5 μM staurosporine. Cellular proteins were resolved by SDS-PAGE, and the proteolytic processing of PARP was detected by immunoblotting. *D*) MCF7 cells expressing the vector control (MCF7 vector) or Bcl-2 (MCF7 Bcl-2) were incubated with indicated concentrations of staurosporine. After 24 h, cell viability was assessed in an MTT assay, as described in Materials and Methods. Mean values of duplicates are given. *E*) SH-EP neuroblastoma cells transfected with either empty vector (SH-EP vector) or vector-encoding murine Bcl-2 (SH-EP Bcl-2) were treated with 25 μg/ml etoposide or 0.625 μM staurosporine. Apoptosis was assessed after 48 h by propidium iodide staining of hypodiploid nuclei and flow cytometry. Mean ± SD values of triplicate cultures are shown.

The observation that staurosporine can activate caspase-9 in Apaf-1-deficient MEFs, SK-Mel-94 cells, and DT40 cells implies a mechanism of caspase-9 activation in the absence of apoptosome formation. To address this point, we used caspase-9-deficient Jurkat cells that were stably reconstituted with caspase-9 variants incapable of apoptosome formation. In this context, we observed that a Flag or cMyc tag linked to the N-terminal CARD region of caspase-9 completely obstructs the binding to Apaf-1, subsequent apoptosome formation and caspase-9 activation in cell lysates activated with dATP and cytochrome *c* (**Fig. 6*A***). Only when caspase-9-deficient Jurkat cells were transfected with untagged caspase-9, dATP and cytochrome *c* could induce *in vitro* interaction with Apaf-1 and processing of caspase-9 (Fig. 6*A*). Accordingly, activation of the mitochondrial pathway by mitomycin C was blocked in cells reconstituted with Flag- or cMyc-tagged caspase-9 but not with untagged caspase-9 (Fig. 6*B, C*). Interestingly, staurosporine was capable of inducing apoptosis and caspase activation in Jurkat cells reconstituted with tagged or untagged caspase-9 (Fig. 6*B, C*). However, in contrast to TRAIL (Fig. 6*B*), staurosporine-induced apoptosis was obstructed in caspase-9-deficient vector control cells (Fig. 6*B, C*). Using Western blot analysis, we further found that staurosporine was able to induce the processing of both tagged and untagged caspase-9, whereas mitomycin C only induced processing of apoptosome-proficient (*i.e.*, untagged) caspase-9. However, in caspase-9-deficient Jurkat cells staurosporine, unlike TRAIL, could not induce any processing of caspase-3 and PARP (Fig. 6*D*), supporting the concept that staurosporine-induced apoptosis requires caspase-9 (Fig. 3).

Taken together, our data show that staurosporine, like anticancer drugs, can directly activate the canonical mitochondrial pathway. Unlike conventional anticancer drugs, however, staurosporine exerts additional apoptotic activities and a dual mode of action. Staurosporine triggers a direct activation of the cytochrome *c*/Apaf-1 pathway that is blocked in the presence of Bcl-2 or the absence of Apaf-1. Beyond that, staurosporine can trigger a Bcl-2-independent pathway that does not rely on cytochrome *c*/Apaf-1, but activates caspase-9 in the absence of an apoptosome. Nevertheless, both pathways share caspase-9 as a common denominator and are completely blocked in caspase-9-deficient cells (Supplemental Fig. S3).

DISCUSSION

Because the major mechanism of anticancer drugs is the activation of the mitochondrial apoptosis pathway, it is comprehensible that cancer cells frequently gain therapy resistance by inactivating the cytochrome *c*/Apaf-1 pathway. The most efficient way to achieve this is the inactivation of p53, but cancer cells can also down-regulate the expression of proapoptotic Bcl-2 members, up-regulate antiapoptotic Bcl-2 members, or epigenetically inactivate the expression of Apaf-1 (1, 9).

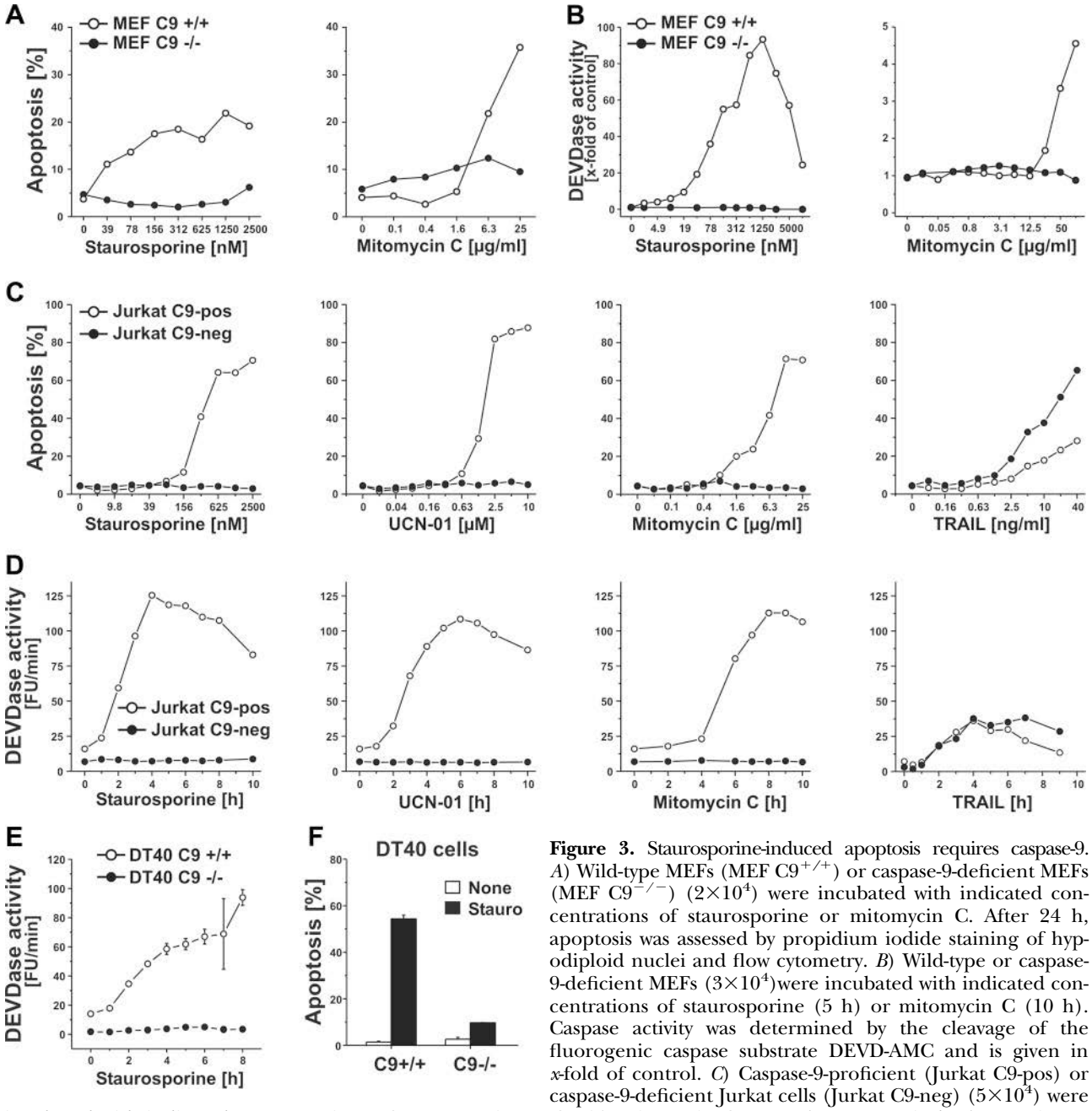

Figure 3. Staurosporine-induced apoptosis requires caspase-9. *A*) Wild-type MEFs (MEF $C9^{+/+}$) or caspase-9-deficient MEFs (MEF $C9^{-/-}$) (2×10^4) were incubated with indicated concentrations of staurosporine or mitomycin C. After 24 h, apoptosis was assessed by propidium iodide staining of hypodiploid nuclei and flow cytometry. *B*) Wild-type or caspase-9-deficient MEFs (3×10^4)were incubated with indicated concentrations of staurosporine (5 h) or mitomycin C (10 h). Caspase activity was determined by the cleavage of the fluorogenic caspase substrate DEVD-AMC and is given in *x*-fold of control. *C*) Caspase-9-proficient (Jurkat C9-pos) or caspase-9-deficient Jurkat cells (Jurkat C9-neg) (5×10^4) were incubated with indicated concentrations of staurosporine, UCN-01, mitomycin C, or TRAIL, respectively. Apoptosis was assessed after 24 h by propidium iodide staining of hypodiploid nuclei and flow cytometry. *D*) Cells described in *C* were treated with 2.5 μM staurosporine, 10 μM UCN-01, 25 μg/ml mitomycin C, or 40 ng/ml TRAIL for the indicated time points. Caspase activity was assessed by the cleavage of DEVD-AMC and is given in arbitrary fluorescent units/min. *E*) $C9^{+/+}$ or $C9^{-/-}$ chicken DT40 cells (3×10^4) were stimulated with 2.5 μM staurosporine for the indicated time points, and caspase activity was assessed by the cleavage of DEVD-AMC and given in arbitrary fluorescent units/min. *F*) $C9^{+/+}$ or $C9^{-/-}$ chicken DT40 cells (3×10^4) were incubated with 2.5 μM staurosporine (stauro), and apoptosis induction was assessed after 24 h by propidium iodide staining of hypodiploid nuclei and flow cytometry. Values are means from duplicate experiments (*A–D*) or means ± SD from triplicate experiments (*E, F*).

Therefore, the discovery of alternative intrinsic pathways that enable the elimination of anticancer drug-resistant tumors would be a great advancement for cancer therapies. Here, we demonstrate that the kinase inhibitor staurosporine and its derivative UCN-01 display such a potential by activating a novel pathway that triggers apoptosis in anticancer drug-resistant tumor cells independently of the classical mitochondrial pathway.

Staurosporine is one of the most frequently used apoptotic stimuli, but the mechanism underlying its potent apoptosis-inducing effect is largely unknown. Albeit initially isolated as an inhibitor of PKC, it became soon evident that staurosporine represents one of the most unspecific inhibitors by targeting >100 serine/threonine and tyrosine kinases (4). Its most remarkable feature is the fast kinetics of apoptosis induction.

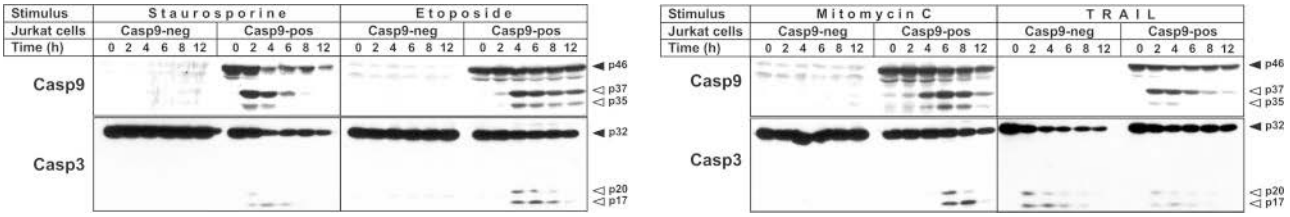

Figure 4. Staurosporine-induced processing of caspases requires caspase-9. Caspase-9-proficient or -deficient Jurkat cells (2×10^6) were incubated for the indicated time with 2.5 μM staurosporine, 50 μg/ml etoposide (left panel), 25 μg/ml mitomycin C, or 40 ng/ml TRAIL (right panel). Cellular proteins were resolved by SDS-PAGE, and the proteolytic processing of caspase-9 and caspase-3 was detected by immunoblotting. Solid arrowheads indicate uncleaved form of indicated caspases; open arrowheads indicate cleaved form.

Whereas anticancer drug-induced apoptosis usually requires at least 8–12 h, staurosporine elicits caspase activation and phosphatidylserine externalization within 1–2 h (15). Unlike most DNA-damaging drugs, staurosporine-induced apoptosis is not dependent on p53 (16). In addition to these early apoptotic events, staurosporine can induce delayed cell death in a caspase-independent manner (17) or induce autophagy on caspase inhibition (data not shown). Irrespective of these potential alternative outcomes, we focused in this study on

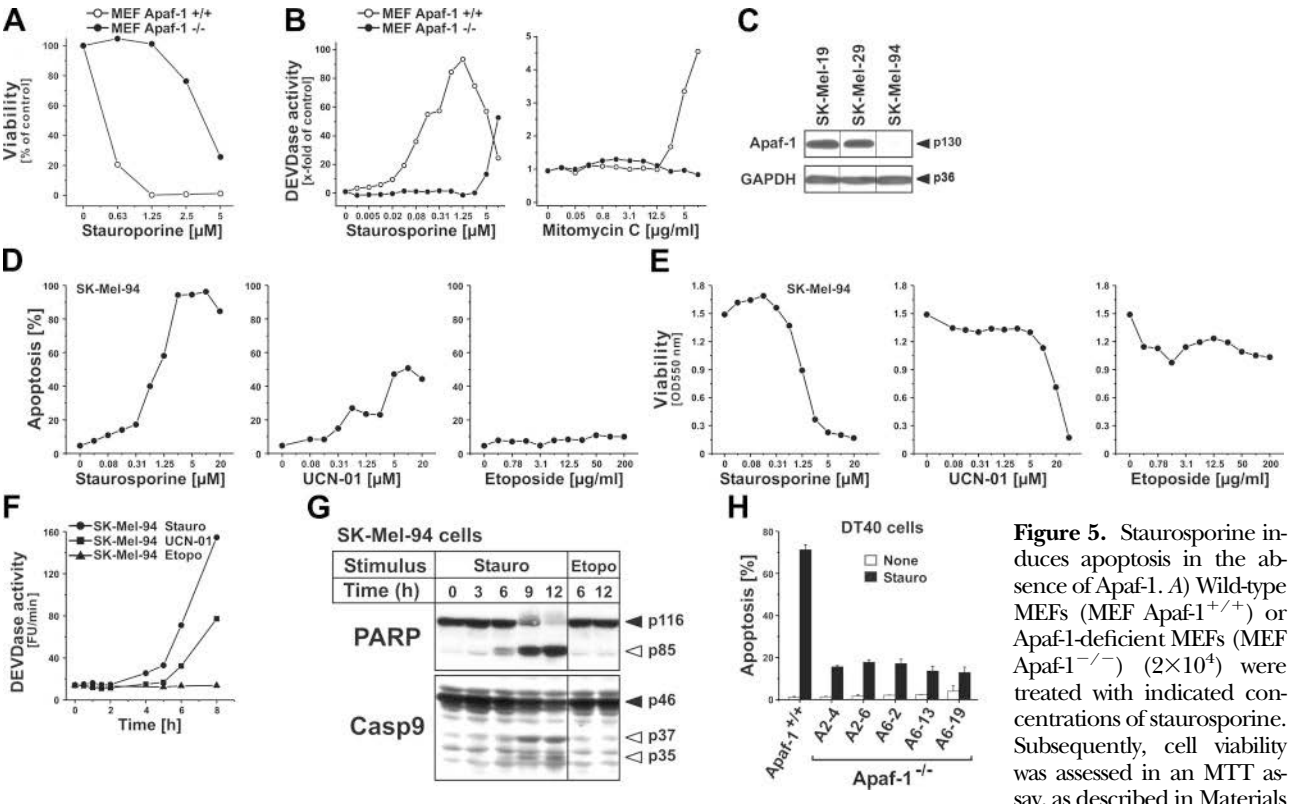

Figure 5. Staurosporine induces apoptosis in the absence of Apaf-1. *A*) Wild-type MEFs (MEF Apaf-$1^{+/+}$) or Apaf-1-deficient MEFs (MEF Apaf-$1^{-/-}$) (2×10^4) were treated with indicated concentrations of staurosporine. Subsequently, cell viability was assessed in an MTT assay, as described in Materials and Methods. *B*) Wild-type or Apaf-1-deficient MEFs (3×10^4) were incubated with indicated concentrations of staurosporine (5 h) and mitomycin C (10 h), respectively. Caspase activity was assessed by the cleavage of DEVD-AMC and is given in *x*-fold increase of control from duplicate experiments. Data from wild-type cells were gathered in parallel with data shown in Fig. 3*B*. *C*) Lysates from the melanoma cell lines SK-Mel-19, -29, and -94 were subjected to SDS-PAGE and investigated for Apaf-1 expression by immunoblotting. Equal protein loading was confirmed by reprobing the membrane with anti-GAPDH antibody. *D*, *E*) SK-Mel-94 cells were incubated with indicated concentrations of staurosporine, UCN-01, and etoposide, respectively. After 24 h, cells were analyzed for apoptosis by propidium iodide staining of hypodiploid nuclei (*D*) and cell viability by an MTT assay (*E*). *F*) SK-Mel-94 cells were incubated for indicated times with 2.5 μM staurosporine (SK-Mel-94 stauro), 10 μM UCN-01 (SK-Mel-94 UCN-01), or 25 μg/ml etoposide (SK-Mel-94 etopo). Caspase activity was assessed by cleavage of DEVD-AMC and is given in arbitrary fluorescent units per minute. *G*) SK-Mel-94 cells were incubated for the indicated time with 2.5 μM staurosporine or 25 μg/ml etoposide. Cellular proteins were resolved by SDS-PAGE and analyzed for the proteolytic processing of PARP and caspase-9 by immunoblotting. Solid arrowheads indicate uncleaved form of indicated proteins; open arrowheads indicate cleaved form. *H*) Apaf-$1^{+/+}$ or different Apaf-$1^{-/-}$ DT40 clones (A2–4, A2–6, A6–2, A6–13, and A6–19) (3×10^4 cells) were left untreated or stimulated with 2.5 μM staurosporine. After 24 h, apoptosis was assessed by propidium iodide staining of hypodiploid apoptotic nuclei and flow cytometry. Values are means from duplicate experiments (*A*, *D–F*) or means ± SD of triplicate experiments (*H*).

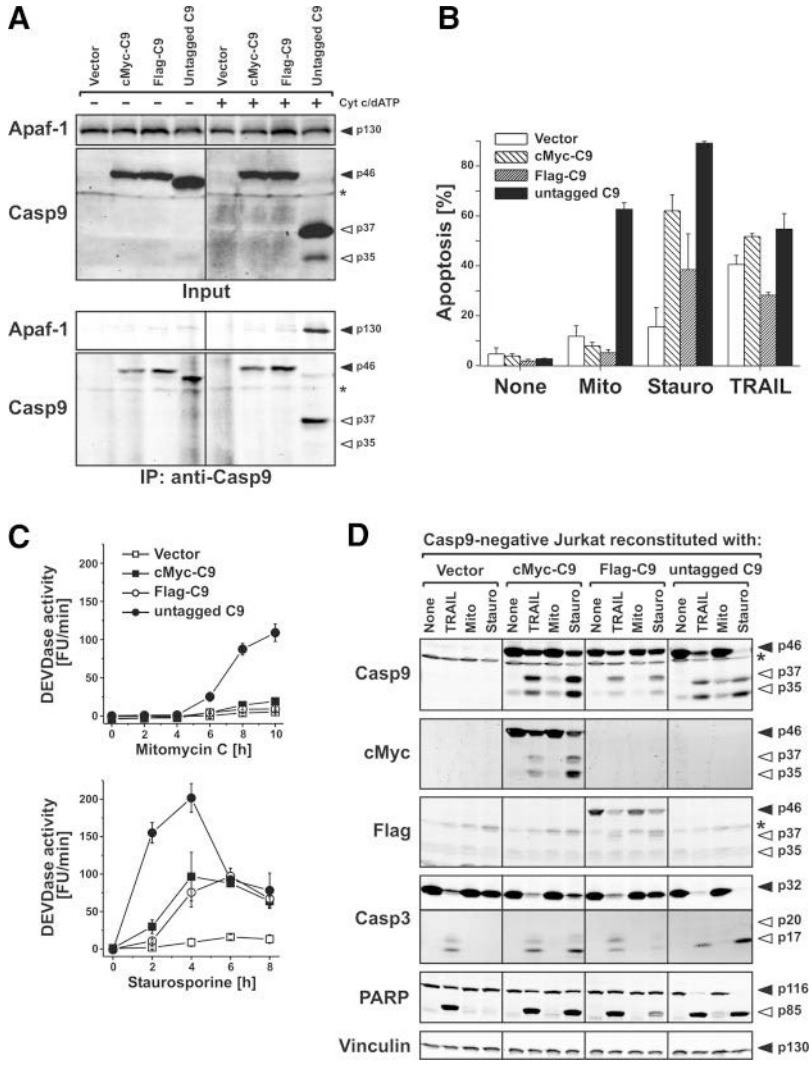

Figure 6. Staurosporine-induced processing of caspase-9 and apoptosis is independent of Apaf-1 and apoptosome formation. *A*) Lysates of 5×10^7 caspase-9-deficient Jurkat cells stably transfected with vector alone or untagged (untagged C9), N-terminal cMyc-tagged (cMyc-C9), or Flag-tagged (Flag-C9) human wild-type caspase-9 were left untreated or treated with 8.6 μM cytochrome *c* and 2.4 mM dATP (Cytc/dATP) for 15 min. Subsequently, cell lysates (input; top panel) were subjected to immunoprecipitation with anti-caspase-9 (IP: anti-casp9) and analyzed for the presence of caspase-9 and Apaf-1 by immunoblotting (bottom panel). Solid arrowheads mark uncleaved form of indicated proteins; open arrowheads indicate cleaved form. Asterisk indicates nonspecific band. *B*) In parallel, caspase-9-deficient Jurkat cells reconstituted with tagged and untagged caspase-9 (as described in *A*) were treated with 25 μg/ml mitomycin C (mito), 2.5 μM staurosporine (stauro), or 40 ng/ml TRAIL, respectively. After 24 h, cell apoptosis induction was analyzed by flow cytometric analysis of hypodiploid nuclei. *C*) Caspase-9-negative Jurkat cells stably reconstituted with caspase-9 (as described in *A*) were treated with 25 μg/ml mitomycin C or 2.5 μM staurosporine for indicated time points. Caspase activity was assessed by cleavage of DEVD-AMC and is given in arbitrary fluorescent units/min. Results in *B* and *C* are given as mean values ± SD of triplicate experiments. *D*) Caspase-9-negative Jurkat cells stably transfected with empty vector (vector) or vector containing untagged (untagged C9), N-terminal cMyc-tagged (cMyc-C9) or Flag-tagged (Flag-C9) human wild-type caspase-9 were left untreated or treated with 40 ng/ml TRAIL (4 h), 25 μg/ml mitomycin C (8 h) or 2.5 μM staurosporine (4 h). Cleared cellular lysates were prepared and analyzed by immunoblotting for caspase-9, cMyc, Flag, caspase-3, PARP, and vinculin, respectively.

the still unclear, but remarkably rapid and potent induction of classical apoptotic events triggered by staurosporine, including the proteolytic activation of caspases and formation of hypodiploid DNA.

Among different derivatives, staurosporine comprises the strongest apoptotic potential, followed by UCN-01 (7-hydroxystaurosporine) and its stereoisomer UCN-02 (18, 19). In comparison to staurosporine, UCN-01 appears to be less nonspecific (20, 21), and especially its potential to abrogate the G2/M checkpoint by targeting the kinase Chk1 renders it a promising anticancer drug (5, 22). Meanwhile, several phase I and II trials of UCN-01, either alone or in combination with other drugs, are under way (http://clinicaltrials.gov/search/intervention=ucn+01), and evidence of efficacy against certain tumor entities has been reported (5, 23, 24). So far, the clinical development of UCN-01 is impeded by its unfavorable pharmacokinetic profile and side effects (*e.g.*, hyperglycemia and hypotension; refs. 5, 23, 25).

In this study, we show that staurosporine and UCN-01, like anticancer drugs, can activate the mitochondrial apoptosis pathway in a direct way, independently of death receptor signaling. Thus, inhibition of caspases did not block the release of cytochrome *c* on staurosporine stimulation. This effect upstream of mitochondria is likely mediated by proapoptotic BH3-only proteins. For instance, staurosporine-induced apoptosis is reduced but not completely blocked in Puma-deficient MEFs (26). However, staurosporine displays at least a dual mode of action, since it can additionally induce apoptosis independently of known intrinsic apoptosis pathways, such as the mitochondrial cytochrome *c*/Apaf-1 or the ER-stress pathway. In addition, we observed that staurosporine induced apoptosis in caspase-2-deficient MEFs, thus excluding the involvement of the PIDDosomal pathway (data not shown). In general, both the ER-stress pathway and the PIDDosomal pathway are thought to converge at the activation of mitochondria (27). The mitochondrial pathway thereby seems to constitute a common denominator of different signaling pathways: the ER-stress pathway, the nuclear PIDDosomal caspase-2-pathway and an amplification loop in death receptor signaling.

So far, all known intrinsic pathways are obstructed by antiapoptotic Bcl-2 proteins. Recent findings show that Bcl-2 and Bcl-x_L can also block apoptosis independently of Apaf-1, caspase-9, and caspase-2 (10, 11, 28). Thus, the only route that is not necessarily affected by anti-

apoptotic Bcl-2 members appears to be the extrinsic death receptor pathway. It is, therefore, intriguing that overexpression of Bcl-2 or Bcl-x_L in Jurkat T lymphoma cells, MCF7 breast cancer cells, or SH-EP neuroblastoma cells did only attenuate but did not prevent staurosporine-induced apoptosis. However, caspase-9 seems to represent a crucial signaling element, since caspase-9-deficient MEFs, human Jurkat cells, and chicken DT40 cells were protected from staurosporine- and UCN-01-induced apoptosis.

Several recent reports have also observed the activation of caspase-9 in response to cytotoxic agents in the absence of Apaf-1, though in most cases apoptosis was blocked by antiapoptotic Bcl-2 proteins (11, 28–32). Staurosporine-induced apoptosis, however, was not completely blocked by Bcl-2 but required caspase-9. Conversely, staurosporine-mediated apoptosis was unaffected in caspase-8-deficient Jurkat cells, caspase-2-deficient MEFs (data not shown), and caspase-3-deficient MCF7 cells, the latter excluding a putative upstream processing of caspase-9 by caspase-3.

Caspase-9 is usually activated at the apoptosome through its interaction with Apaf-1. It is thought that, following its release from mitochondria, cytochrome *c* together with (d)ATP enables Apaf-1 oligomerization by a mutual interaction of the CED-4-like regions of Apaf-1. Oligomerized Apaf-1, in turn, recruits procaspase-9 *via* a homophilic CARD/CARD interaction (3, 33). According to the induced proximity model, aggregation of Apaf-1 enforces a locally high concentration of procaspase-9 that allows the immature proteases to self-activate because of their low intrinsic enzymatic activity (34, 35). Alternatively, Apaf-1 might act as an allosteric activator, since caspase-9 is only highly active when bound in a complex with Apaf-1 (36, 37). In contrast to effector caspases, however, proteolytic processing is not required for activation of caspase-9 (38, 39).

Interestingly, we observed that staurosporine could induce apoptosis and activation of caspase-9 in Apaf-1-deficient MEFs and SK-Mel-94 melanoma cells. Furthermore, we obtained similar results in *apaf-1*-targeted DT40 cells. The observation that staurosporine-triggered apoptosis, in contrast to anticancer drug-induced events, is not entirely obstructed in Apaf-1-deficient MEFs can be already deduced from original publications describing Apaf-$1^{-/-}$ mice, though this issue was not specifically addressed by the authors (40, 41). Similarly, Nagata's group (42) recently reported that treatment of Apaf-$1^{-/-}$ thymocytes with staurosporine, but not with etoposide, induced processing of procaspase-9 and procaspase-3. Accordingly, staurosporine-induced processing of caspase-9 appears to occur in the absence of apoptosome formation. Thus, we observed that N-terminal cMyc or Flag tags linked to the CARD region of caspase-9 obstructed Apaf-1 interaction and processing of caspase-9 *in vitro* on addition of cytochrome *c* and dATP. Consequently, activation of the cytochrome *c*/Apaf-1 pathway by mitomycin C was completely blocked in caspase-9-deficient Jurkat cells reconstituted with cMyc- or Flag-tagged caspase-9 variants, whereas staurosporine still comprised its potential to induce apoptosis in cells with disabled apoptosome formation. However, though the CARD region of caspase-9 is essential for apoptosome formation, overexpression of a CARD-deficient caspase-9 mutant (lacking aa 2–93) in caspase-9-deficient Jurkat cells not only disabled anticancer drug, but also staurosporine-induced apoptosis, whereas death receptor signaling remained functional (data not shown). Thus, this observation indicates that the CARD region of caspase-9 is not only required for apoptosome formation in the canonical cytochrome *c*/Apaf-1 pathway, but also for apoptosome-independent apoptosis induced by staurosporine.

The most intriguing question is how staurosporine activates caspase-9 in the absence of apoptosome formation. Usually, caspase-9 is thought to be active only in association with the apoptosome, and apoptosome-bound caspase-9 displays a 1000-fold higher catalytic activity than isolated caspase-9 (36). However, we previously observed that overexpression of catalytically inactive (C287A) caspase-9 did not inhibit staurosporine-mediated processing of endogenous wild-type caspase-9, whereas anticancer drug-induced caspase-9 cleavage was completely blocked (6). Although further analysis is required to understand this phenomenon, this observation indicates that the mechanism of staurosporine-induced activation of caspase-9 obviously differs substantially from conventional caspase-9 activation at the apoptosome.

Since staurosporine is a broad-range kinase inhibitor that requires caspase-9 for apoptosis induction, it is conceivable that staurosporine interferes with the phosphorylation of caspase-9. In this context, different caspase-9 kinases have been described, such as Akt, ERK1/2, PKCζ, PKA, CDK1/cyclin B1, CK2, cAbl, and DYRK (43–50). In most of these studies, the functional effects of phosphorylation on caspase-9 activity have been analyzed in cell-free systems but not in intact cells (44–46, 51). Because most of the described caspase-9 kinases are targeted by staurosporine (ref. 4; http://tools.invitrogen.com/downloads/SelectScreen_Data_193.pdf), we tested different kinase inhibitors for their potential to induce apoptosis. In addition, a database search (http://scansite.mit.edu/cgi-bin/motifscan_seq) using the different phosphorylation consensus sites of caspase-9 yielded further putative caspase-9 kinases, such as ATM; CK1; PKCα, β, δ, ε, γ, μ; GSK3; and DNA-PK. Unexpectedly, however, none of the kinase inhibitors targeting the known (Akt, ERK, PKCζ, PKA, CDK1, and CK2) or the putative caspase-9 kinases was able to induce apoptosis in Jurkat cells overexpressing Bcl-2 or vector control cells (Supplemental Fig. S4). Likewise, inhibition of mTOR, a downstream target of Akt, exhibited no apoptotic effects (Supplemental Fig. S4).

The lack of apoptosis induction by any of these kinase inhibitors could be attributed to the fact that other caspase-9-inactivating kinases are targeted by staurosporine. Alternatively, staurosporine might not target caspase-9 itself, but caspase-9 interaction part-

ners, *e.g.*, XIAP, in a similar way, as has been proposed for Apaf-1 (46). Phosphorylation of XIAP or other so far unknown interaction proteins might then disable their interaction with caspase-9 and its subsequent activation. Since staurosporine inhibits a plethora of kinases, it is also conceivable that the simultaneous inhibition of more than one kinase is required in order to activate caspase-9 in this pathway.

Taken together, our data show that staurosporine exerts at least two modes of action of apoptosis induction. Similar to anticancer drugs, staurosporine can directly activate the classical cytochrome *c*/Apaf-1 pathway, which is inhibited by Bcl-2 or the absence of Apaf-1. In addition, and unlike conventional anticancer drugs, staurosporine activates a novel intrinsic cell death pathway that is independent of Apaf-1 and not affected by Bcl-2 (Supplemental Fig. S3). It is this signaling pathway that most likely enables the elimination of anticancer drug-resistant tumor cells by staurosporine and UCN-01. Both pathways converge at the activation of caspase-9, since staurosporine- and UCN-01-induced apoptosis is completely blocked in caspase-9-deficient cells. Though various different kinases have been reported to phosphorylate caspase-9, inhibition of known and putative caspase-9 kinases did not induce apoptosis in intact cells. Therefore, future studies have to unravel the identity of the kinases that on inhibition by staurosporine are able to activate caspase-9 in the absence of apoptosome formation. Identification of the activation mechanism of caspase-9 might provide new targets for the development of cytotoxic drugs that could enable the elimination of multidrug-resistant tumor cells. Fj

The authors thank Claus Belka (Ludwig-Maximilians University, Munich, Germany), John Blenis (Harvard Medical School, Boston, MA, USA), Simone Fulda (Universitätsklinikum Ulm, Ulm, Germany), Marja Jäättelä (Danish Cancer Society, Copenhagen, Denmark), Ottmar Janssen (University of Kiel, Kiel, Germany), Maria S. Soengas (University of Michigan, Ann Arbor, MI, USA), Edward A. Sausville (National Cancer Institute, Rockville, MD, USA), Andreas Strasser (Walter and Eliza Hall Institute of Medical Research, Melbourne, VIC, Australia), Henning Walczak (Imperial College London, London, UK), and the Drug Synthesis and Chemistry Branch (Division of Cancer Treatment and Diagnosis, National Cancer Institute, Bethesda, MD, USA) for providing valuable cell lines and reagents. This work was supported by grants from the Deutsche Forschungsgemeinschaft We 1801/2-4 (S.W.), GRK 1302 (B.S., K.S.O., S.W.), SFB 685 (K.L., K.S.O., S.W.), SFB 773 (B.S., K.S.O., S.W., T.I.), the Interdisciplinary Center of Clinical Research Tübingen (IZKF; Fö. 01KS9602 to S.W.; Fö. 1866-0-0 to B.S.) and the Wilhelm Sander-Stiftung (2004.099.1; S.W.).

REFERENCES

1. Johnstone, R. W., Ruefli, A. A., and Lowe, S. W. (2002) Apoptosis: a link between cancer genetics and chemotherapy. *Cell* **108,** 153–164
2. Walensky, L. D. (2006) BCL-2 in the crosshairs: tipping the balance of life and death. *Cell Death Differ.* **13,** 1339–1350
3. Hu, Y., Benedict, M. A., Ding, L., and Nunez, G. (1999) Role of cytochrome *c* and dATP/ATP hydrolysis in Apaf-1-mediated caspase-9 activation and apoptosis. *EMBO J.* **18,** 3586–3595
4. Fabian, M. A., Biggs, W. H., 3rd, Treiber, D. K., Atteridge, C. E., Azimioara, M. D., Benedetti, M. G., Carter, T. A., Ciceri, P., Edeen, P. T., Floyd, M., Ford, J. M., Galvin, M., Gerlach, J. L., Grotzfeld, R. M., Herrgard, S., Insko, D. E., Insko, M. A., Lai, A. G., Lelias, J. M., Mehta, S. A., Milanov, Z. V., Velasco, A. M., Wodicka, L. M., Patel, H. K., Zarrinkar, P. P., and Lockhart, D. J. (2005) A small molecule-kinase interaction map for clinical kinase inhibitors. *Nat. Biotechnol.* **23,** 329–336
5. Tse, A. N., Carvajal, R., and Schwartz, G. K. (2007) Targeting checkpoint kinase 1 in cancer therapeutics. *Clin. Cancer Res.* **13,** 1955–1960
6. Stepczynska, A., Lauber, K., Engels, I. H., Janssen, O., Kabelitz, D., Wesselborg, S., and Schulze-Osthoff, K. (2001) Staurosporine and conventional anticancer drugs induce overlapping, yet distinct pathways of apoptosis and caspase activation. *Oncogene* **20,** 1193–1202
7. Rudner, J., Lepple-Wienhues, A., Budach, W., Berschauer, J., Friedrich, B., Wesselborg, S., Schulze-Osthoff, K., and Belka, C. (2001) Wild-type, mitochondrial and ER-restricted Bcl-2 inhibit DNA damage-induced apoptosis but do not affect death receptor-induced apoptosis. *J. Cell Sci.* **114,** 4161–4172
8. Samraj, A. K., Sohn, D., Schulze-Osthoff, K., and Schmitz, I. (2007) Loss of caspase-9 reveals its essential role for caspase-2 activation and mitochondrial membrane depolarization. *Mol. Biol. Cell* **18,** 84–93
9. Soengas, M. S., Capodieci, P., Polsky, D., Mora, J., Esteller, M., Opitz-Araya, X., McComble, R., Herman, J. G., Gerald, W. L., Lazebnik, Y. A., Cordon-Cardo, C., and Lowe, S. W. (2001) Inactivation of the apoptosis effector Apaf-1 in malignant melanoma. *Nature* **409,** 207–211
10. Marsden, V. S., Ekert, P. G., Van Delft, M., Vaux, D. L., Adams, J. M., and Strasser, A. (2004) Bcl-2-regulated apoptosis and cytochrome *c* release can occur independently of both caspase-2 and caspase-9. *J. Cell Biol.* **165,** 775–780
11. Marsden, V. S., O'Connor, L., O'Reilly, L. A., Silke, J., Metcalf, D., Ekert, P. G., Huang, D. C., Cecconi, F., Kuida, K., Tomaselli, K. J., Roy, S., Nicholson, D. W., Vaux, D. L., Bouillet, P., Adams, J. M., and Strasser, A. (2002) Apoptosis initiated by Bcl-2-regulated caspase activation independently of the cytochrome c/Apaf-1/caspase-9 apoptosome. *Nature* **419,** 634–637
12. Nicoletti, I., Migliorati, G., Pagliacci, M. C., Grignani, F., and Riccardi, C. (1991) A rapid and simple method for measuring thymocyte apotosis by propidium iodide staining and flow cytometry. *J. Immunol. Methods* **139,** 271–279
13. Lauber, K., Appel, H. A., Schlosser, S. F., Gregor, M., Schulze Osthoff, K., and Wesselborg, S. (2001) The adapter protein Apaf-1 is proteolytically processed during apoptosis. *J. Biol. Chem.* **276,** 29772–29781
14. Engels, I. H., Stepczynska, A., Stroh, C., Lauber, K., Berg, C., Schwenzer, R., Wajant, H., Janicke, R. U., Porter, A. G., Belka, C., Gregor, M., Schulze Osthoff, K., and Wesselborg, S. (2000) Caspase-8/FLICE functions as an executioner caspase in anticancer drug-induced apoptosis. *Oncogene* **19,** 4563–4573
15. Waibel, M., Kramer, S., Lauber, K., Lupescu, A., Manns, J., Schulze-Osthoff, K., Lang, F., and Wesselborg, S. (2007) Mitochondria are not required for death receptor-mediated cytosolic acidification during apoptosis. *Apoptosis* **12,** 623–630
16. Shao, R. G., Shimizu, T., and Pommier, Y. (1997) 7-Hydroxystaurosporine (UCN-01) induces apoptosis in human colon carcinoma and leukemia cells independently of p53. *Exp. Cell Res.* **234,** 388–397
17. Zhang, X. D., Gillespie, S. K., and Hersey, P. (2004) Staurosporine induces apoptosis of melanoma by both caspase-dependent and -independent apoptotic pathways. *Mol. Cancer Ther.* **3,** 187–197
18. Harkin, S. T., Cohen, G. M., and Gescher, A. (1998) Modulation of apoptosis in rat thymocytes by analogs of staurosporine: lack of direct association with inhibition of protein kinase C. *Mol. Pharmacol.* **54,** 663–670
19. Gescher, A. (2000) Staurosporine analogues-pharmacological toys or useful antitumour agents? *Crit. Rev. Oncol. Hematol.* **34,** 127–135
20. Bain, J., Plater, L., Elliott, M., Shpiro, N., Hastie, C. J., McLauchlan, H., Klevernic, I., Arthur, J. S., Alessi, D. R., and

Cohen, P. (2007) The selectivity of protein kinase inhibitors: a further update. *Biochem. J.* **408,** 297–315
21. Davies, S. P., Reddy, H., Caivano, M., and Cohen, P. (2000) Specificity and mechanism of action of some commonly used protein kinase inhibitors. *Biochem. J.* **351,** 95–105
22. Kawabe, T. (2004) G2 checkpoint abrogators as anticancer drugs. *Mol. Cancer Ther.* **3,** 513–519
23. Sausville, E. A., Arbuck, S. G., Messmann, R., Headlee, D., Bauer, K. S., Lush, R. M., Murgo, A., Figg, W. D., Lahusen, T., Jaken, S., Jing, X., Roberge, M., Fuse, E., Kuwabara, T., and Senderowicz, A. M. (2001) Phase I trial of 72-hour continuous infusion UCN-01 in patients with refractory neoplasms. *J. Clin. Oncol.* **19,** 2319–2333
24. Wilson, W. H., Sorbara, L., Figg, W. D., Mont, E. K., Sausville, E., Warren, K. E., Balis, F. M., Bauer, K., Raffeld, M., Senderowicz, A. M., and Monks, A. (2000) Modulation of clinical drug resistance in a B cell lymphoma patient by the protein kinase inhibitor 7-hydroxystaurosporine: presentation of a novel therapeutic paradigm. *Clin. Cancer Res.* **6,** 415–421
25. Dees, E. C., Baker, S. D., O'Reilly, S., Rudek, M. A., Davidson, S. B., Aylesworth, C., Elza-Brown, K., Carducci, M. A., and Donehower, R. C. (2005) A phase I and pharmacokinetic study of short infusions of UCN-01 in patients with refractory solid tumors. *Clin. Cancer Res.* **11,** 664–671
26. Villunger, A., Michalak, E. M., Coultas, L., Mullauer, F., Bock, G., Ausserlechner, M. J., Adams, J. M., and Strasser, A. (2003) p53- and drug-induced apoptotic responses mediated by BH3-only proteins Puma and Noxa. *Science* **302,** 1036–1038
27. Danial, N. N., and Korsmeyer, S. J. (2004) Cell death: critical control points. *Cell* **116,** 205–219
28. Haraguchi, M., Torii, S., Matsuzawa, S., Xie, Z., Kitada, S., Krajewski, S., Yoshida, H., Mak, T. W., and Reed, J. C. (2000) Apoptotic protease activating factor 1 (Apaf-1)-independent cell death suppression by Bcl-2. *J. Exp. Med.* **191,** 1709–1720
29. Aleo, E., Henderson, C. J., Fontanini, A., Solazzo, B., and Brancolini, C. (2006) Identification of new compounds that trigger apoptosome-independent caspase activation and apoptosis. *Cancer Res.* **66,** 9235–9244
30. Milleron, R. S., and Bratton, S. B. (2006) Heat shock induces apoptosis independently of any known initiator caspase-activating complex. *J. Biol. Chem.* **281,** 16991–17000
31. Katoh, I., Tomimori, Y., Ikawa, Y., and Kurata, S. (2004) Dimerization and processing of procaspase-9 by redox stress in mitochondria. *J. Biol. Chem.* **279,** 15515–15523
32. Zanon, M., Piris, A., Bersani, I., Vegetti, C., Molla, A., Scarito, A., and Anichini, A. (2004) Apoptosis protease activator protein-1 expression is dispensable for response of human melanoma cells to distinct proapoptotic agents. *Cancer Res.* **64,** 7386–7394
33. Srinivasula, S. M., Ahmad, M., Fernandes-Alnemri, T., and Alnemri, E. S. (1998) Autoactivation of procaspase-9 by Apaf-1-mediated oligomerization. *Mol. Cell* **1,** 949–957
34. Salvesen, G. S., and Dixit, V. M. (1999) Caspase activation: the induced-proximity model. *Proc. Natl. Acad. Sci. U. S. A.* **96,** 10964–10967
35. Bao, Q., and Shi, Y. (2007) Apoptosome: a platform for the activation of initiator caspases. *Cell Death Differ.* **14,** 56–65
36. Rodriguez, J., and Lazebnik, Y. (1999) Caspase-9 and APAF-1 form an active holoenzyme. *Genes Dev.* **13,** 3179–3184
37. Schafer, Z. T., and Kornbluth, S. (2006) The apoptosome: physiological, developmental, and pathological modes of regulation. *Dev. Cell* **10,** 549–561
38. Stennicke, H. R., Deveraux, Q., Humke, E. W., Reed, J. C., Dixit, V. M., and Salvesen, G. S. (1999) Caspase-9 can be activated without proteolytic processing. *J. Biol. Chem.* **274,** 8359–8362
39. Srinivasula, S. M., Hegde, R., Saleh, A., Datta, P., Shiozaki, E., Chai, J., Lee, R. A., Robbins, P. D., Fernandes Alnemri, T., Shi, Y., and Alnemri, E. S. (2001) A conserved XIAP-interaction motif in caspase-9 and Smac/DIABLO regulates caspase activity and apoptosis. *Nature* **410,** 112–116
40. Yoshida, H., Kong, Y. Y., Yoshida, R., Elia, A. J., Hakem, A., Hakem, R., Penninger, J. M., and Mak, T. W. (1998) Apaf1 is required for mitochondrial pathways of apoptosis and brain development. *Cell* **94,** 739–750
41. Cecconi, F., Alvarez-Bolado, G., Meyer, B. I., Roth, K. A., and Gruss, P. (1998) Apaf1 (CED-4 homolog) regulates programmed cell death in mammalian development. *Cell* **94,** 727–737
42. Nagasaka, A., Kawane, K., Yoshida, H., and Nagata, S. (2009) Apaf-1-independent programmed cell death in mouse development. *Cell Death Differ.* **17,** 931–941
43. Cardone, M. H., Roy, N., Stennicke, H. R., Salvesen, G. S., Franke, T. F., Stanbridge, E., Frisch, S., and Reed, J. C. (1998) Regulation of cell death protease caspase-9 by phosphorylation. *Science* **282,** 1318–1321
44. Allan, L. A., Morrice, N., Brady, S., Magee, G., Pathak, S., and Clarke, P. R. (2003) Inhibition of caspase-9 through phosphorylation at Thr 125 by ERK MAPK. *Nat. Cell Biol.* **5,** 647–654
45. Brady, S. C., Allan, L. A., and Clarke, P. R. (2005) Regulation of caspase 9 through phosphorylation by protein kinase C zeta in response to hyperosmotic stress. *Mol. Cell. Biol.* **25,** 10543–10555
46. Martin, M. C., Allan, L. A., Lickrish, M., Sampson, C., Morrice, N., and Clarke, P. R. (2005) Protein kinase A regulates caspase-9 activation by Apaf-1 downstream of cytochrome *c*. *J. Biol. Chem.* **280,** 15449–15455
47. Allan, L. A., and Clarke, P. R. (2007) Phosphorylation of caspase-9 by CDK1/cyclin B1 protects mitotic cells against apoptosis. *Mol. Cell* **26,** 301–310
48. McDonnell, M. A., Abedin, M. J., Melendez, M., Platikanova, T. N., Ecklund, J. R., Ahmed, K., and Kelekar, A. (2008) Phosphorylation of murine caspase-9 by the protein kinase casein kinase 2 regulates its cleavage by caspase-8. *J. Biol. Chem.* **283,** 20149–20158
49. Seifert, A., Allan, L. A., and Clarke, P. R. (2008) DYRK1A phosphorylates caspase 9 at an inhibitory site and is potently inhibited in human cells by harmine. *FEBS J.* **275,** 6268–6280
50. Raina, D., Pandey, P., Ahmad, R., Bharti, A., Ren, J., Kharbanda, S., Weichselbaum, R., and Kufe, D. (2005) c-Abl tyrosine kinase regulates caspase-9 autocleavage in the apoptotic response to DNA damage. *J. Biol. Chem.* **280,** 11147–11151
51. Tashker, J. S., Olson, M., and Kornbluth, S. (2002) Post-cytochrome *c* protection from apoptosis conferred by a MAPK pathway in *Xenopus* egg extracts. *Mol. Biol. Cell* **13,** 393–401

Received for publication January 11, 2011.
Accepted for publication May 19, 2011.

Cellular Signalling 22 (2010) 914–925

Contents lists available at ScienceDirect

Cellular Signalling

journal homepage: www.elsevier.com/locate/cellsig

AMPK-independent induction of autophagy by cytosolic Ca^{2+} increase

Antje Grotemeier [a,1], Sebastian Alers [a,1], Simon G. Pfisterer [b,1], Florian Paasch [a], Merle Daubrawa [a], Alexandra Dieterle [a], Benoit Viollet [c,d], Sebastian Wesselborg [a], Tassula Proikas-Cezanne [b,*,2], Björn Stork [a,*,2]

[a] Department of Internal Medicine I, University Clinic of Tübingen, Germany
[b] Autophagy Laboratory, Department of Molecular Biology, Institute for Cell Biology, University of Tübingen, Germany
[c] Department of Endocrinology, Metabolism and Cancer, Institut Cochin Université Paris Descartes, Paris, France
[d] INSERM U567, Paris, France

ARTICLE INFO

Article history:
Received 18 September 2009
Received in revised form 10 January 2010
Accepted 19 January 2010
Available online 28 January 2010

Keywords:
Autophagy
LC3
Mammalian target of rapamycin
Phosphoinositide-3 phosphate
Thapsigargin
WIPI-1

ABSTRACT

Autophagy is a eukaryotic lysosomal bulk degradation system initiated by cytosolic cargo sequestration in autophagosomes. The Ser/Thr kinase mTOR has been shown to constitute a central role in controlling the initiation of autophagy by integrating multiple nutrient-dependent signaling pathways that crucially involves the activity of PI3K class III to generate the phosphoinositide PI(3)P. Recent reports demonstrate that the increase in cytosolic Ca^{2+} can induce autophagy by inhibition of mTOR via the CaMKK-α/β-mediated activation of AMPK. Here we demonstrate that Ca^{2+} signaling can additionally induce autophagy independently of the Ca^{2+}-mediated activation of AMPK. First, by LC3-II protein monitoring in the absence or presence of lysosomal inhibitors we confirm that the elevation of cytosolic Ca^{2+} induces autophagosome generation and does not merely block autophagosome degradation. Further, we demonstrate that Ca^{2+}-chelation strongly inhibits autophagy in human, mouse and chicken cells. Strikingly, we found that the PI(3)P-binding protein WIPI-1 (Atg18) responds to the increase of cytosolic Ca^{2+} by localizing to autophagosomal membranes (WIPI-1 puncta) and that Ca^{2+}-chelation inhibits WIPI-1 puncta formation, although PI(3)P-generation is not generally affected by these Ca^{2+} flux modifications. Importantly, using AMPK-$\alpha1^{-/-}\alpha2^{-/-}$ MEFs we show that thapsigargin application triggers autophagy in the absence of AMPK and does not involve complete mTOR inhibition, as detected by p70S6K phosphorylation. In addition, STO-609-mediated CaMKK-α/β inhibition decreased the level of thapsigargin-induced autophagy only in AMPK-positive cells. We suggest that apart from reported AMPK-dependent regulation of autophagic degradation, an AMPK-independent pathway triggers Ca^{2+}-mediated autophagy, involving the PI(3)P-effector protein WIPI-1 and LC3.

1. Introduction

Macroautophagy (hereafter referred to as autophagy) is an essential process of cellular self-digestion that allows cell survival under certain stress conditions and represents an evolutionary highly conserved and critical starvation response pathway [1,2]. Central to the process of autophagy is the formation of autophagosomes, unique multi-membrane vesicles that sequester cytoplasmic material, including long-lived proteins and organelles and that fuse with lysosomes in order to acquire acidic hydrolases for degradation. Autophagy is constitutively active on a basal level [3]. As a consequence, the constant turnover of cytoplasmic material maintains cellular homeostasis. Above this basal level, autophagy is further induced upon activation of the hVps34/beclin 1 complex, that generates PI(3)P [4]. The generation of PI(3)P is considered to be required for canonical induction of autophagy. In addition, release of mTOR inhibition on autophagy-related proteins (Atgs) also induces autophagy [5]. Hence activation of pathways that stimulate mTOR activity is considered to inhibit autophagy. However, molecular details of signaling pathways that modulate the autophagic activity are poorly understood, mainly due to the lack of sufficient assay systems that monitor autophagic degradation at different stages.

Changes in cytosolic Ca^{2+} levels have been implicated to regulate the induction of autophagy by signaling through CaMKK, AMPK and mTOR, and AMPK has been proposed to be a universal regulator of the autophagic response [6,7]. However, conflicting results have been achieved in studies that focussed on the role of cytosolic Ca^{2+} in the regulation of autophagy. Recent studies demonstrated that cytosolic Ca^{2+} triggers the activation of AMPK and permits a release of mTOR-mediated inhibition of autophagy [6,7]. In contrast, other studies provided evidence that the increase in cytosolic calcium should inhibit autophagy [8].

* Corresponding authors. Proikas-Cezanne is to be contacted at Auf der Morgenstelle 15, 72076 Tübingen, Germany. Fax: +49 7071 29 5359. Stork, Otfried-Müller-Str. 12, 72076 Tübingen, Germany. Fax: +49 7071 29 4680.
E-mail addresses: tassula.proikas-cezanne@uni-tuebingen.de (T. Proikas-Cezanne), bjoern.stork@med.uni-tuebingen.de (B. Stork).
[1] Equal first authorship.
[2] Equal senior authorship.

0898-6568/$ – see front matter © 2010 Elsevier Inc. All rights reserved.
doi:10.1016/j.cellsig.2010.01.015

However, systems used to monitor autophagy were mainly limited to LC3 read-out analyses. LC3 (microtubule-associated protein 1 light chain 3), distributed throughout the cytoplasm and nucleus (LC3-I), becomes conjugated to phosphatidylethanolamine (LC3-II) by an Atg12-Atg5 E3-like activity upon autophagic stimulation (LC3 lipidation) [9]. LC3-II localizes at autophagosomal membranes [10], hence monitoring the increase of LC3-II protein abundance has been widely used to monitor the induction of autophagy [11]. In addition, lysosomal inhibition during autophagic assays permits to conclude whether the increase of LC3-II protein abundance reflects the induction or inhibition of autophagy [12]. In a standard autophagy assay the abundance of LC3-I and LC3-II reflects basal autophagy levels. Modulating basal autophagy levels by compound administration that either induces or inhibits autophagy leads to an increase in LC3-II protein abundance. In order to distinguish between induction and inhibition of autophagy, the same compound is administered in the presence of a lysosomal inhibitor, such as bafilomycin A1. Here, a further increase in LC3-II protein abundance in comparison to compound administration alone reflects the induction of autophagy because the interference with the lysosomal compartment blocks autophagic degradation and LC3-II-bound autophagosomes accumulate. In the absence of a further increase in LC3-II protein levels a compound should itself block lysosomal degradation and is considered to inhibit autophagy. Likewise, the increase in LC3-II/LC3-I ratio reflects either the induction or inhibition of autophagy [12].

Human WIPI-1 (WD-repeat protein interacting with phosphoinositides 1) specifically binds PI(3)P and localizes at autophagosomal membranes upon PI(3)P-mediated induction of autophagy [13,14]. At autophagosomal membranes, WIPI-1 and LC3 colocalize [13,14], and the increase of fluorescent puncta for both of these markers reflects the increase of autophagosomal membranes upon the induction of autophagy [13,15]. In specific, the WIPI-1 puncta formation analysis provides a novel quantitative analysis system to assess mammalian autophagy. Upon the induction of autophagy WIPI-1 localizes at autophagosomal membranes. This specific localization can be visualized by indirect immunofluorescence or by using GFP-WIPI-1. Autophagosomal membrane localization of WIPI-1 is recognized by the appearance of fluorescent WIPI-1 dots (WIPI-1 puncta) in the cytoplasm. In the absence of autophagosomal membrane localization WIPI-1 is distributed throughout the cytoplasm indicated by the absence of fluorescent WIPI-1 puncta in the cytoplasm. Using quantitative fluorescent microcopy measures the induction of autophagy is reflected by an increase, and the inhibition of autophagy is reflected by a decrease in the amount of cells that display WIPI-1 puncta. Thereby, the amount of WIPI-1 puncta-positive cells in control settings reflects cells that undergo basal autophagy [13–15].

Here, we employed LC3-II protein monitoring and automated quantitative WIPI-1 puncta formation analyses as well as live cell imaging of GFP-WIPI-1 to monitor the influence of cytosolic Ca^{2+} increase or decrease on the autophagic activity in human, mouse and chicken cells.

We provide evidence, that the increase of cytosolic Ca^{2+} leads to the induction of autophagy independent of AMPK and we suggest that both, AMPK-dependent and independent pathways provide an opportunity to alter the autophagic activity in response to changes in cytosolic Ca^{2+} levels. In addition, our data further indicate that Ca^{2+}-mediated autophagy might not need complete mTOR inhibition. These facts should be taken into consideration when designing screening approaches for the identification of substances that modulate autophagy in response to Ca^{2+}-mobilization.

2. Materials and methods

2.1. Cells

Human J16 (RPMI-1640, 10% FCS, 10 mM HEPES, 50 U/ml penicillin, 50 µg/ml streptomycin), avian DT40 (RPMI-1640, 10% FCS, 1% chicken serum, 3 mM L-glutamine, 50 µM β-mercaptoethanol, 50 U/ml penicillin, 50 µg/ml streptomycin), stable human U2OS-GFP-WIPI-1 (Jacob and Proikas-Cezanne, unpublished) and U2OS-GFP-2xFYVE (GE Healthcare) (DMEM Glutamax, 10% FCS, 100 U/ml penicillin, 100 µg/ml streptomycin, 0.6 mg/ml G418, 5 µg/ml Plasmocin), AMPK-$\alpha1^{-/-}\alpha2^{-/-}$ MEFs and wild-type controls [16] (DMEM 4.5 g/l D-Glucose, 10% FCS, 50 U/ml penicillin, 50 µg/ml streptomycin), Flp-In™ T-REx™ 293 cells (Invitrogen) (DMEM 4.5 g/l D-Glucose, 10% FCS, 50 U/ml penicillin, 50 µg/ml streptomycin).

2.2. Antibodies

Anti-AMPK-α, anti-phospho-AMPK-α (p-Thr172), anti-phospho-p70S6K (p-Thr389), anti-LC3 from Cell Signaling Technology; anti-LC3 (5F10) from nanoTools, anti-GAPDH (6C5) from Abcam; anti-phosphoAcetyl-CoA-Carboxylase (p-Ser79) from upstate; anti-GFP from Boehringer, anti-Vinculin (hVIN-1) and anti-FLAG from Sigma; IRDye800 and IRDye680 conjugated secondary antibodies from LI-COR Biosciences.

2.3. Compounds

TG, rapamycin, Compound C from Calbiochem; BAPTA-AM from Molecular Probes; bafilomycin A1, STO-609 from Sigma; pepstatin A, Ponceau S from Fluka; Ku-0063794 from AstraZeneca.

2.4. Expression constructs and transfections

Full-length chicken LC3B cDNA (NM_001031461) was amplified from DT40 cells and cloned into pMSCV-mCitrine to generate a retroviral mCitrine-chLC3B expression construct. For the production of retroviral supernatants, the packaging cell line Plat-E (provided by Dr. Toshio Kitamura, Tokyo, Japan [17]) was transfected using Fugene transfection reagent (Roche). The MMLV was pseudotyped with VSV-G. For transduction, 1×10^6 cells were incubated with retroviral supernatant containing 3 µg/ml Polybrene (Sigma) and selected with 1 µg/ml puromycin (Sigma). Full-length human Ulk1 was amplified from J16 cells and cloned into pcDNA5/FRT/TO-FLAG (kindly provided by D. Alessi). This expression construct was co-transfected with pOG44 into Flp-In™ T-REx™ 293 cells (Invitrogen). Stable transfectants were selected with 200 µg/ml hygromycin B (Invitrogen) and 5 µg/ml blasticidin (Invitrogen). FLAG-Ulk1 expression was induced using 1 µg/ml tetracycline (Sigma).

2.5. Cell extracts and immunoblotting

J16 cells, DT40 cells, Flp-In™ T-REx™ 293 cells or MEFs were stimulated with TG (1 µM), Ku-0063794 (1 µM) or rapamycin (100 nM) for the indicated time, or treated with solvent as control. Alternatively, cells were preincubated 30 min with Compound C (10 µM), BAPTA-AM (30 µM), STO-609 (10 µg/ml) or bafilomycin A1 (1 or 10 nM) and pepstatin A (10 µg/ml). Cells were lysed in 20 mM Tris–HCl (pH 7.5), 150 mM NaCl, 0.5 mM EDTA, 1% Triton X-100, 10 mM NaF, 2.5 mM NaPP, 10 µM Na_2MoO_4, 1 mM Na_3VO_4, and protease inhibitors (P2714 Sigma). Equal total protein amounts (Bradford) were separated on an 8–15% gradient SDS-polyacrylamide gel followed by standard western blot analyses. Results were quantified over GAPDH or vinculin levels using ImageJ 1.41 (http://www.rsb.info.nih.gov/ij/).

2.6. Confocal laser scanning microscopy

DT40 cells were resuspended in Krebs Ringer solution [10 mM HEPES (pH 7.0), 140 mM NaCl, 4 mM KCl, 1 mM $MgCl_2$, 1 mM $CaCl_2$ and 10 mM glucose] and seeded onto chambered coverglasses (Nunc). After 20 min, cells were examined on a Leica TCS SP II

confocal laser scanning microscope. mCitrine was excited at 514 nm wavelength, and emission was detected at 530 nm.

2.7. Autophagy assays

Autophagy assays were performed as described previously [13–15]. For automation, cells were cultured in 96 well plates for 24 h in DMEM/10% FCS followed by autophagy assays for 1 h using EBSS, wortmannin (233 nM), TG (100 nM), BAPTA-AM (30 μM), Compound C (10 μM), STO-609 (10 μg/ml). For BAPTA-AM, Compound C and STO-609, the cells were pre-treated for 30 min. Cells were fixed with 3.7% paraformaldehyde for 15 min and stained with DAPI (5 μg/ml in PBS) for 15 min.

2.8. Live cell video microscopy

Live cell video microscopy was performed as described previously [15].

2.9. Automated image acquisition and analysis using the IN Cell Analyzer 1000 (GE Healthcare)

Using a Nikon Plan Fluor ELWD 40 × 0.6 objective, three wells were imaged (20–30 images/well) for every treatment. GFP-WIPI-1 puncta formation [15] was automatically analyzed using the dual area object assay (IN Cell Analyzer Workstation 3.4). Nuclei were detected with a top hat segmentation algorithm (minimum size of 100 μm^2) and used as input. GFP images were used to detect the cell area (multiscale top hat algorithm, 1500 μm^2 per cell) and inclusions (GFP-WIPI-1 puncta or GFP-2xFYVE inclusions) from 0.5 μm to 5 μm. A decision tree was applied to classify the cells as puncta or non-puncta cells based on the analysis parameters inclusion intensity and inclusion intensity/cell intensity.

3. Results

3.1. Thapsigargin treatment leads to an increased autophagosome number by the direct activation of the autophagic machinery

Previously, it has been shown that treatment with the SERCA inhibitor thapsigargin (TG) mediates an increase in LC3-II protein abundance and GFP-LC3 puncta formation [6,18,19], both of which may either be caused by an increased autophagosome formation or by reduced autophagosome degradation but this question has not been sufficiently answered yet. Here, we treated human J16 Jurkat T lymphocytes or chicken DT40 B lymphocytes with TG for 3 or 6 h in the absence or presence of bafilomycin A1, which blocks the fusion of autophagosomes and lysosomes, and pepstatin A, which inhibits the activity of lysosomal aspartyl proteases (Fig. 1A, B). Under these conditions, TG led to an increase in LC3-II abundance.

Importantly, in further experiments we employed a stable GFP-WIPI-1 U2-OS cell line and provide strong evidence that TG significantly induces autophagy and that the autophagic flux is unaffected by TG administration (Fig. 1C). Compared to control cells, Baf A1 administration alone led to an increase in LC3-II protein abundance and provides evidence that this cell line properly undergoes basal autophagy. TG administration led to an increase in LC3-II protein abundance when compared to control cells. Coadministration of TG and Baf A1 led to a further significant increase in LC3-II protein abundance compared to TG alone and also to Baf A1 alone (Fig. 1C).

3.2. WIPI puncta formation is Ca^{2+}-dependent

The WIPI-1 puncta formation assay has been established as a novel marker system for assessing autophagy [11,13,15]. Here, we analyzed the effect of TG and BAPTA-AM on WIPI-1 puncta formation. First, we performed live cell video microscopy using U2-OS cells stably expressing GFP-WIPI-1. Control cells (mock) either lacked WIPI-1 puncta or displayed small motile WIPI-1 puncta (Fig. 2A, Supp. Movie 1), reflecting basal autophagy [13,15]. TG administration led to a substantial increase of WIPI-1 puncta positive cells and accumulation of WIPI-1 at autophagosomal membranes (large WIPI-1 puncta) (Fig. 2B, Supp. Movie 2), reflecting the induction of autophagy. Pretreatment with BAPTA-AM for 30 min followed by co-administration of TG and BAPTA-AM for 1 h nullified the formation of WIPI-1 puncta (Fig. 2C, Supp. Movie 3).

To quantify the effects of TG and BAPTA-AM on WIPI-1 puncta formation we used an automated high content system to image and analyze cells displaying WIPI-1 puncta (Fig. 3A). U2-OS cells stably expressing GFP-WIPI-1 were cultured in 96 well plates and were treated with EBSS, TG or TG plus BAPTA-AM for 1 h. Indicating basal autophagy, 20% of control cells (mock) displayed GFP-WIPI-1 puncta (Fig. 3B). Amino acid deprivation (EBSS) or TG treatment significantly increased the number of GFP-WIPI-1 puncta positive cells to 77% or 65%, respectively. Co-administration of TG/BAPTA-AM decreased the number of GFP-WIPI-1 puncta positive cells to 16%, comparable with the PI3 kinase inhibitor wortmannin (14% puncta positive cells) (Fig. 3B). From this quantification the ratio of GFP-WIPI-1 puncta/non-puncta cells was deduced (Fig. 3C) and *p*-values presented in Fig. 3B also apply for Fig. 3C. Further, a representative dynamic heat map displaying puncta-positive (red) or puncta-negative (yellow) counting events for every well within a single experiment are shown (Fig. 3D). In total, more than 3800 cells from 3 independent experiments were analyzed per treatment (Supp. Fig. 1), no effects on cell death were observed (Supp. Fig. 1). We conclude that TG-mediated autophagy reflects the increase in cytosolic Ca^{2+}, as co-administration of the cell permeable Ca^{2+}-chelator BAPTA-AM nullified GFP-WIPI-1 puncta formation in the presence of TG.

3.3. Ca^{2+}-chelation abolishes LC3 puncta formation and LC3 lipidation

Next, we investigated whether Ca^{2+}-chelation also affects LC3 lipidation. We incubated DT40 cells with BAPTA-AM prior to TG administration (Fig. 4A). Non-transfected DT40 cells or cells transfected with either vector or mCitrine-chLC3B cDNA were left untreated, or were treated with TG and/or BAPTA-AM as indicated. In all cell lines, BAPTA-AM-treatment completely abolished TG-induced LC3-II increase (Fig. 4A). These results were confirmed by laser scanning microscopy. DT40 cells transfected with mCitrine-chLC3B cDNA were treated with TG and/or BAPTA-AM as indicated. Verifying the results described above, TG-induced formation of mCitrine-chLC3B puncta was inhibited by BAPTA-AM (Fig. 4B, panels in column 3). The complete abrogation of Ca^{2+}-fluxes was confirmed for DT40 and J16 cells by Ca^{2+} measurements (Supp. Fig. 2).

3.4. Thapsigargin and BAPTA-AM leave PI(3)P levels unaffected

Depletion of cytosolic Ca^{2+} by BAPTA-AM showed drastic effects on TG-induced WIPI-1 puncta formation (Figs. 2 and 3). Therefore, we investigated whether TG and BAPTA-AM influence the availability of PI(3)P in human cells. A stable U2-OS cell line expressing GFP-2xFYVE was used and GFP fluorescence was quantified by high content analysis (Fig. 5). We found that 97% of the cells were positive for distinct GFP-2xFYVE signals (Fig. 5B) and that inhibitors of PI3 kinases, LY294002 and wortmannin, significantly decreased positive cells to 25% and 53%, respectively (Fig. 5B). In contrast, cells treated with EBSS, TG or TG plus BAPTA-AM showed no differences in GFP-2xFYVE signal compared with control (mock) cells (Fig. 5B). Also, different parameters such as the total GFP-2xFYVE inclusion area per cell (Fig. 5C, D), the amount of GFP-2xFYVE inclusions per cell or the GFP-2xFYVE inclusion intensity versus cell intensity showed no drastic differences between control, EBSS, TG and TG plus BAPTA-

AM treated cells (Supp. Fig. 3A, B). Again, administration of wortmannin or LY294002 led to a significant decrease of the GFP-2xFYVE inclusion area per cell, the amount of GFP-2xFYVE inclusions per cell and the GFP-2xFYVE inclusion intensity versus cell intensity (Supp. Fig 3A, B). In total more than 6200 cells were analyzed per treatment (Supp. Fig. 3C) and a representative dynamic heat map displaying the total inclusion area per cell for every well within a single experiment is shown (Fig. 5D, negative (yellow) and positive (red) GFP-2xFYVE signals). As expected, wortmannin and LY294002 lead to an inhibition of PI(3)P formation, resulting in a decrease of intracellular PI(3)P. EBSS, TG or BAPTA-AM did not affect the availability of PI(3)P.

3.5. Thapsigargin-induced autophagy might not require complete mTOR repression

It has been reported that AMPK-mediated inhibition of mTOR activity is a prerequisite for TG-induced autophagy [6]. Here, we analyzed the phosphorylation status of p70S6K, a direct downstream target of mTOR (Fig. 6). Interestingly, in our cellular model systems TG did not entirely abrogate p70S6K phosphorylation (Fig. 6A, B), whereas rapamycin abolishes p70S6K phosphorylation already after 30 min (Fig. 6A). Although TG slightly reduced p70S6K phosphorylation in human J16 cells, this reduction was less strong as seen with rapamycin (Fig. 6A). Using DT40 chicken cells we found that p70S6K phosphorylation was not significantly reduced (Fig. 6B). This indicates that autophagy induction by TG does not necessarily rely on total mTOR inhibition. This argument was further strengthened by the analysis of Atg1/Ulk1 phosphorylation in HEK293 cells (Fig. 6C). It has been recently reported that mTOR (mTORC1) associates with the Ulk1-Atg13-FIP200 complex in a nutrient-dependent manner and that mTOR phosphorylates Atg1/Ulk1 and Atg13 in mammalian cells [20–22]. In our study, treatment with rapamycin or Ku-0063794, which is a specific inhibitor of both mTORC1 and mTORC2 [23], led to an increased migration of Flag-Ulk1 protein in SDS-PAGE, reflecting a decrease in mTOR-mediated phosphorylation. In contrast, TG

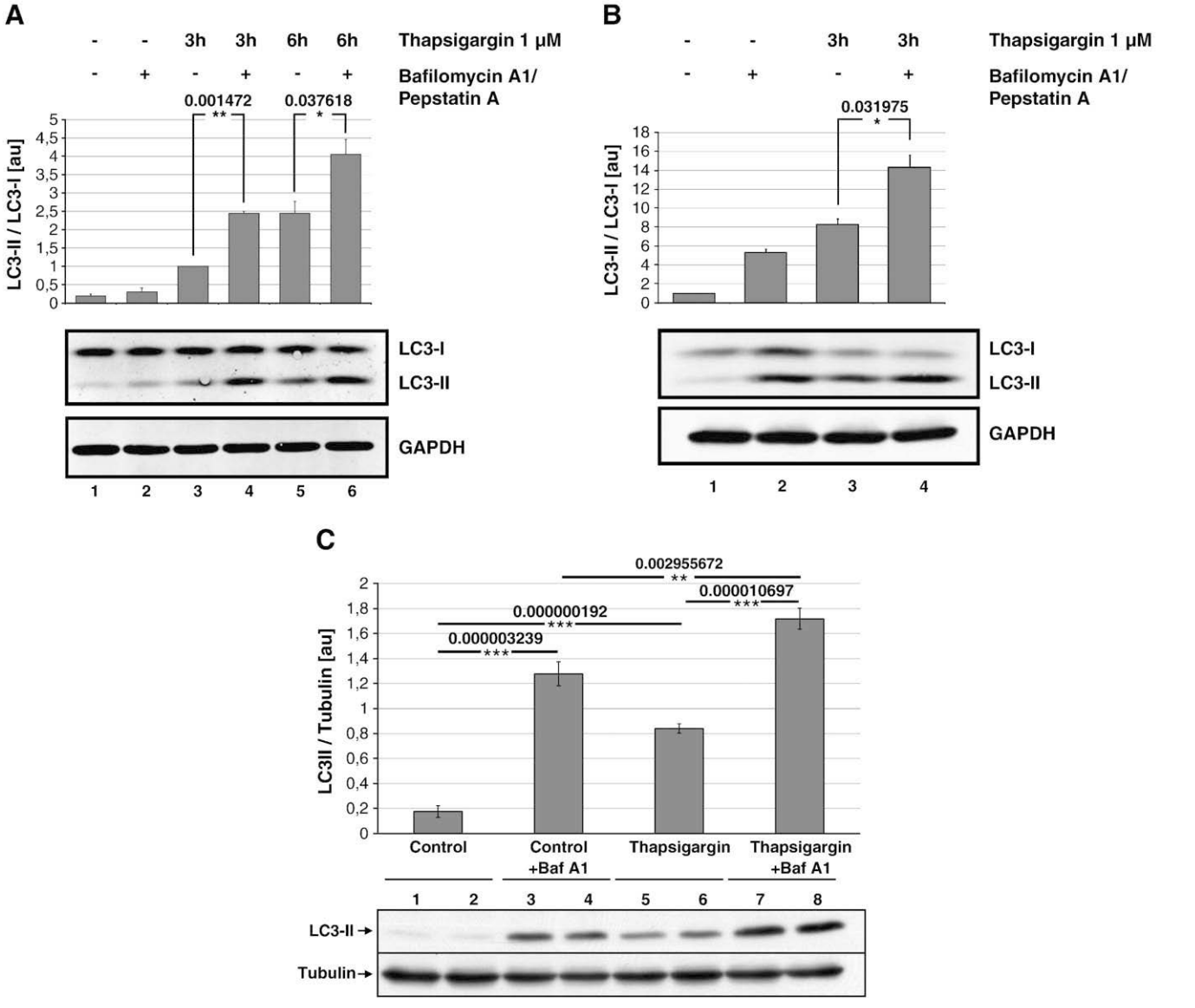

Fig. 1. The endoplasmic reticulum Ca^{2+}-ATPase inhibitor thapsigargin (TG) induces autophagic degradation. (A) Human Jurkat T cells (J16) were treated with TG (1 µM) for 3 and 6 h, either in the presence or absence of bafilomycin A1 (1 nM) and pepstatin A (10 µg/ml). Equal amounts of total protein were subjected to anti-LC3 and anti-GAPDH immunoblotting and quantified using ImageJ. LC3-II/LC3-I ratios were expressed in arbitrary units. Each bar represents mean values of 3 independent experiments ± SEM. (B) Chicken B cells (DT40) were treated with TG (1 µM) for 3 h in the absence or presence of bafilomycin A1 (10 nM) and pepstatin A (10 µg/ml). Each bar represents mean values of 3 independent experiments ± SEM. (C) U2-OS cells stably expressing GFP-WIPI-1 were mock treated (M) or treated with 100 nM TG. Each bar represents mean values of 7 independent experiments ± SEM. Calculated *p*-values from heteroscedastic *t*-tests are presented.

treatment did not result in an increased migration of FLAG-Ulk1, indicating that the phosphorylation status differs. These results strongly indicate that TG might induce autophagy independently of mTOR. However, under certain circumstances a partial mTOR inhibition might be sufficient to release the inhibitory function of mTOR on autophagy.

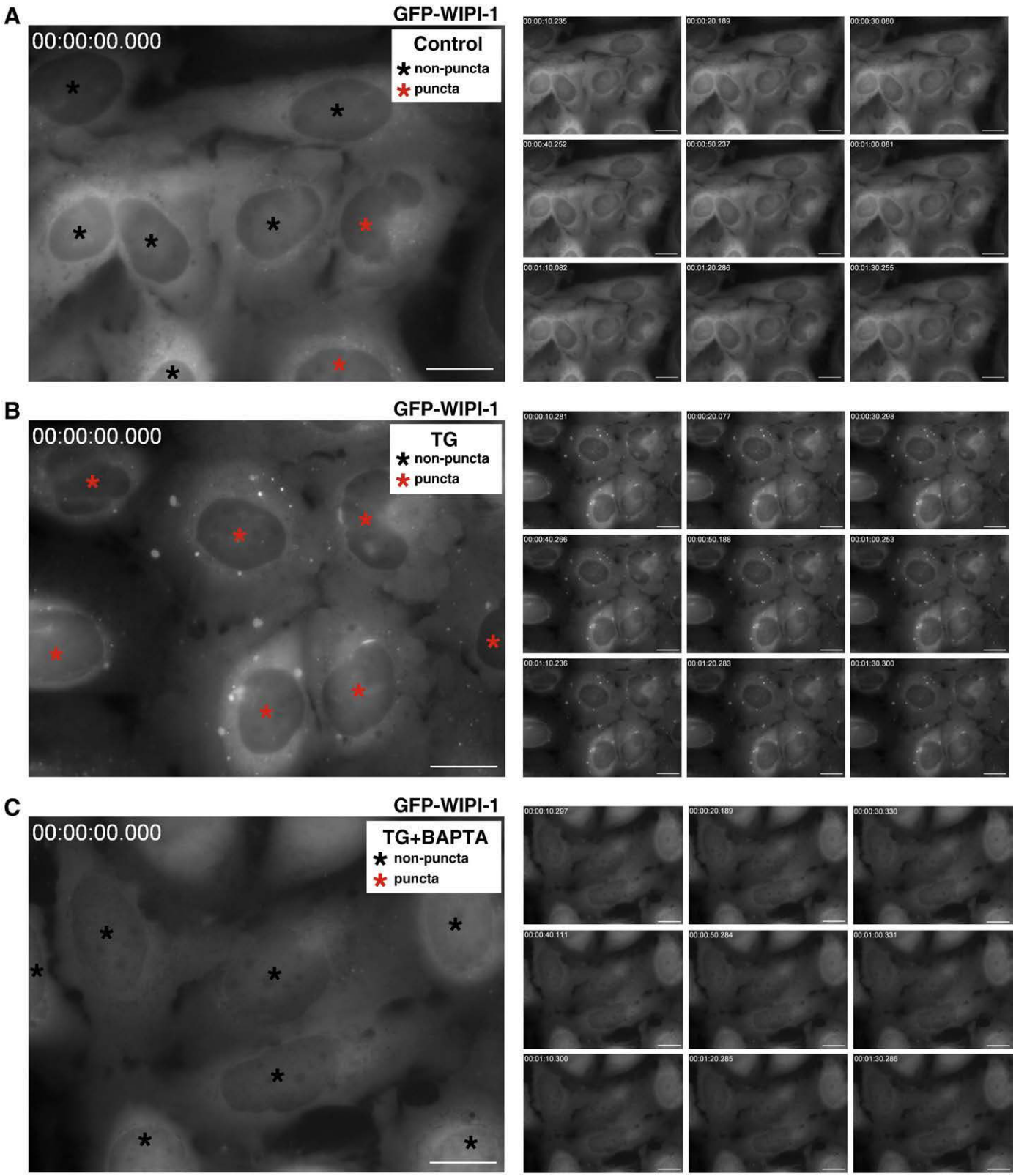

Fig. 2. WIPI-1 puncta formation is Ca^{2+}-dependent. (A, B and C) Live cell microscopy of U2-OS cells stably expressing GFP-WIPI-1. (A) Live images from control cells (mock treatment) are shown. (B) Cells were treated with thapsigargin (TG) (100 nM) for 1 h and live images were acquired hereafter. (C) Alternatively, cells were treated with thapsigargin (100 nM) combined with BAPTA-AM (30 μM) (TG + BAPTA) (C) for 1 h. All images were acquired every 10 s over a period of 90 s (see image galleries on the left panels). Black asterisks indicate GFP-WIPI-1 non-puncta and red asterisks indicate GFP-WIPI-1 puncta cells. (bars: 20 μm).

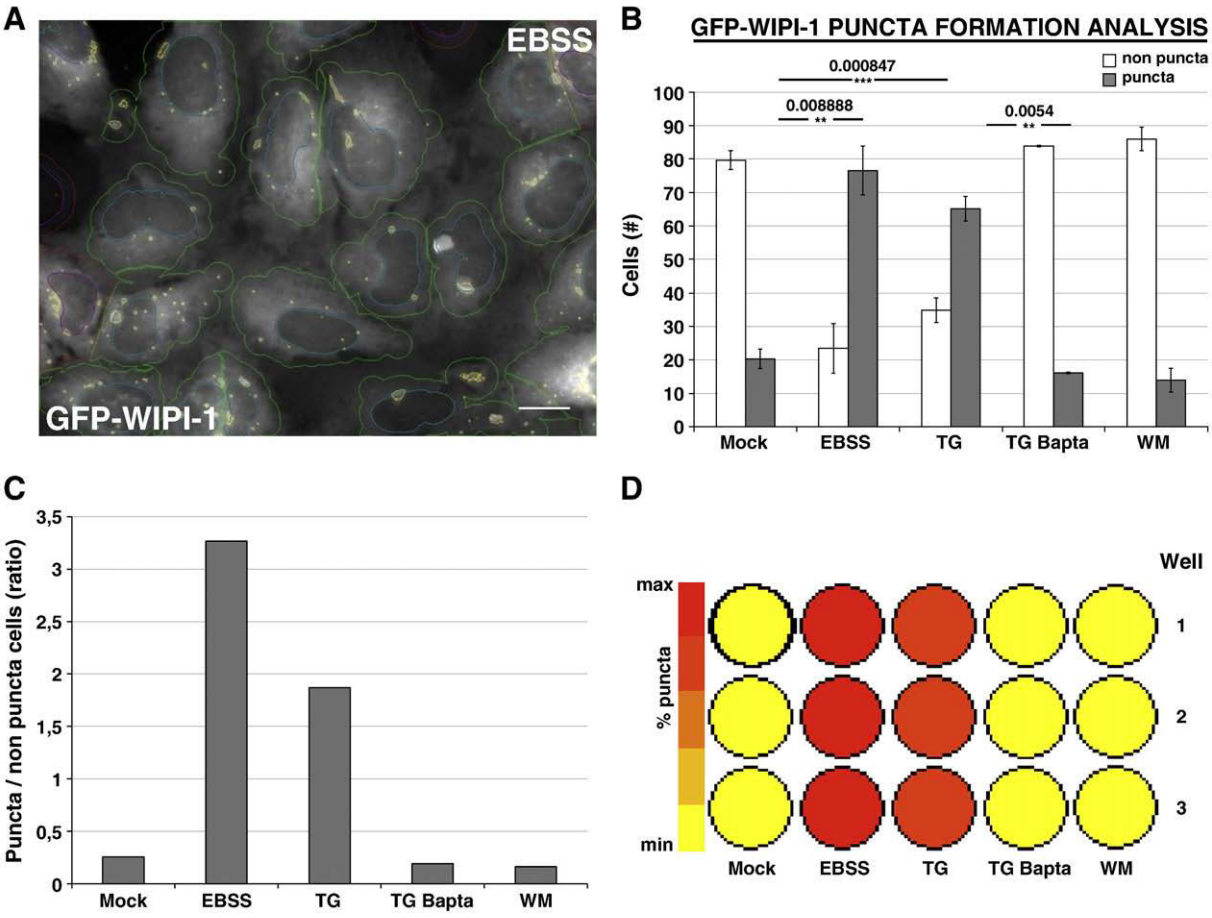

Fig. 3. Automated WIPI-1 puncta formation assay. (A) Automated quantification of GFP-WIPI-1 puncta and non-puncta cells upon EBSS treatment. Detected inclusions and nuclei surrounded by yellow (inclusions) and blue (nuclei) lines. Cells classified as GFP-WIPI-1 puncta positive are delineated in green, non-puncta cells in red. Results of at least 3800 cells per treatment were quantified (B). Values represent mean ± SEM values from three independent triplicate experiments (at least 3800 cells per treatment in total). Calculated *p*-values from heteroscedastic *t*-tests are presented. From this quantification, ratios of GFP-WIPI-1 puncta/non-puncta cells were deduced (C); hence calculated *p*-values apply for both result representations in B and C. (D) Dynamic heat map displaying puncta positive or puncta negative (non-puncta) counting per well during image analysis of a single experiment (3 independent wells per treatment). (bars: 20 μm).

3.6. Elevated Ca^{2+} levels induce LC3-II generation independently of AMPK

Increased cytosolic Ca^{2+} concentrations were connected to AMPK activation by CaMKK-β [6]. Here, we treated AMPK-$\alpha1^{-/-}\alpha2^{-/-}$ MEFs [16], which are devoid of the AMPK catalytic subunits, with TG (Fig. 7A). In these cells, TG was still capable to induce LC3 lipidation (Fig. 7A). Furthermore, we show that the pharmacological AMPK-inhibitor Compound C, which has been used in previous studies to analyze the role of AMPK during autophagic processes [6], unexpectedly induces autophagy in our model systems (Fig. 7B). Compound C exhibited inhibitory potential towards AMPK in wt MEFs, as shown by a reduced phosphorylation of both ACC and AMPK (Fig. 7B). However, significant autophagy induction occurred in AMPK-$\alpha1^{-/-}\alpha2^{-/-}$ MEFs (Fig. 7B). Thus, it seems that Compound C on its own has pro-autophagic activities which are independent of AMPK. Using these MEFs, we confirmed that TG-induced autophagy is blocked by BAPTA-AM (Fig. 7C). Furthermore, p70S6K phosphorylation remained essentially unaltered upon treatment with TG, supporting the above finding that autophagy occurred independently of mTOR (Fig. 7D).

3.7. CaMKK-α/β contributes to the AMPK-dependent branch of autophagy induction

Since autophagy initiation did not rely on AMPK activation and subsequent mTOR inhibition in our study, we next wanted to validate the role of CaMKKs during TG-induced autophagy. Therefore, we treated stable GFP-WIPI-1 U2-OS cells with TG and/or the CaMKK-α/β-inhibitor STO-609 and quantified the level of GFP-WIPI-1 puncta formation by high content analysis. Coadministration of STO-609 and TG resulted in a decrease of WIPI-1 puncta formation induced by TG from 68% to 46% (Fig. 8A, B). Therefore, STO-609 addition resulted in a partial block of TG-induced WIPI-1 puncta formation (Fig. 8A). Compound C significantly increased WIPI-1 puncta formation (Fig. 8A). Coadministration of Compound C and TG led to a further increase in WIPI-1 puncta formation compared to TG or Compound C alone (Fig. 8A). These results are also represented as WIPI-1 puncta/non-puncta ratio (Fig. 8B). A representative dynamic heat map displaying the WIPI-1 puncta formation in every well within a single experiment is shown (Fig. 8B). In total, more than 5100 cells were analyzed per treatment (Supp. Fig. 4).

Further, we treated J16 Jurkat T lymphocytes with TG and/or the CaMKK-α/β-inhibitor STO-609 (Fig. 8C). The inhibitory potential of STO-609 could be confirmed by a prominently reduced phosphorylation of AMPK at Thr172 (Fig. 8C). Furthermore, inhibition of CaMKK-α/β by STO-609 significantly reduced LC3-II abundance induced by TG (Fig. 8C).

Next, we analyzed the role of CaMKK-α/β in the AMPK-deficient background. Following TG treatment, STO-609 reduced LC3 lipidation significantly in wild-type MEFs (Fig. 8D). In contrast, STO-609 treatment had no significant effect on LC3 lipidation in AMPK-$\alpha1^{-/-}\alpha2^{-/-}$ MEFs (Fig. 8D). Hence, STO-609 blunted AMPK phosphorylation whereas LC3

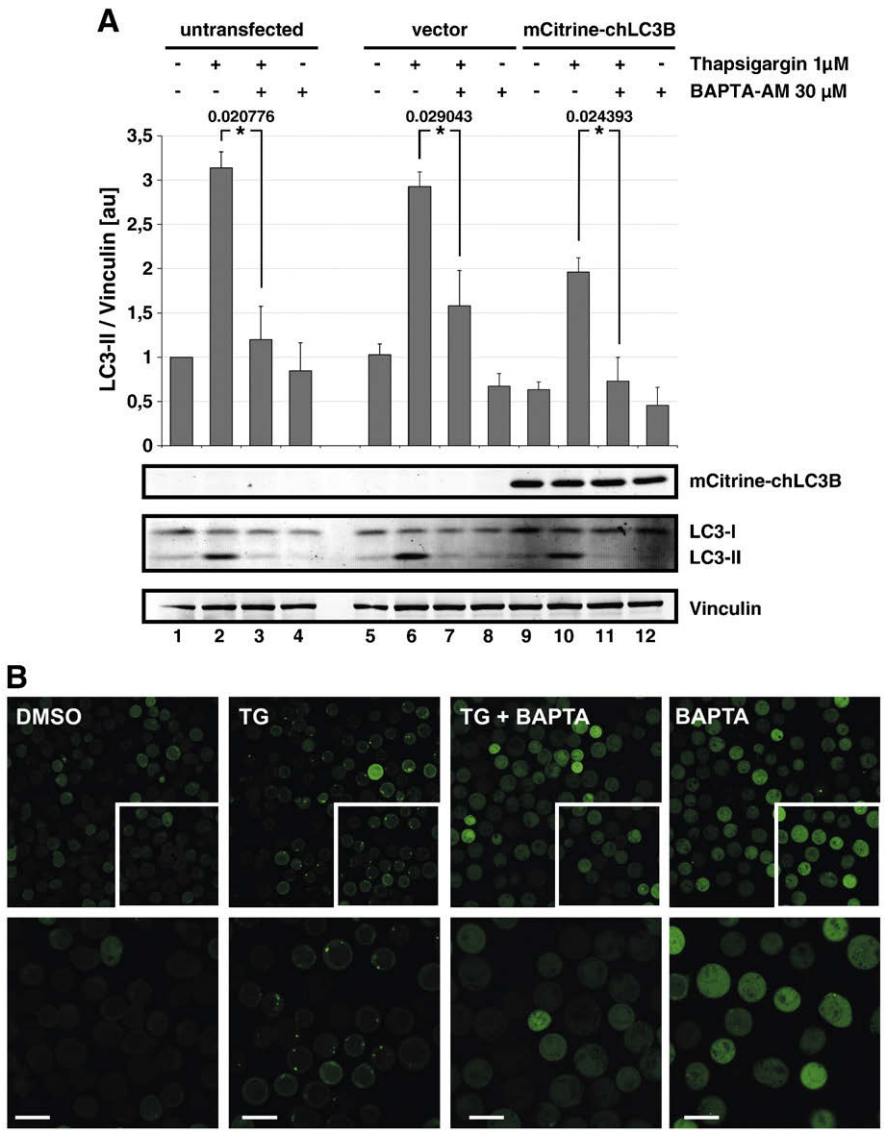

Fig. 4. Ca^{2+}-chelation abolishes mCitrine-LC3 puncta formation and LC3 lipidation. (A) DT40 cells, transduced with mCitrine-chLC3B or empty vector, were treated with TG (1 μM) for 6 h either alone or after preincubation with BAPTA-AM (30 μM) for 30 min. As control, cells were incubated with BAPTA-AM or solvent alone. Each bar represents mean values of 3 independent experiments ± SEM. Heteroscedastic *t*-tests were carried out and the calculated *p*-values are presented. (B) DT40 cells stably expressing mCitrine-chLC3B were treated as indicated, resuspended in Krebs-Ringer solution and visualized by confocal laser scanning microscopy (bars: 10 μm).

lipidation was partly reduced indicating AMPK-dependent and independent effects.

4. Discussion

Functional autophagy allows eukaryotic cells to compensate for a variety of environmental challenges, including inadequate supply of nutrients and oxygen [2]. This cytoprotective function of autophagy is critical to secure cell survival. However, the induction of autophagy by certain signaling cascades, including the DNA damage response, has also been found to trigger cell death pathways, either programmed cell death type I (apoptosis) or type II (autophagosomal cell death) [4]. Dysfunctional autophagy has been implicated in a variety of pathophysiological conditions in human, including cancer, neurodegeneration, myopathies, reduced immunity and infectious diseases [2]. This notion acquired tremendous interest in the recent past, resulting in attempts to identify molecular modulators, either physiological factors or synthetic molecules that could specifically alter the autophagic activity *in vivo*. However, few assay systems exist that reliably monitor the process of autophagy in higher eukaryotic cells, leading to a variety of conflicting experimental outcomes in different studies, such as the involvement of cytosolic Ca^{2+} in modulating autophagy.

Landmark work by the Seglen laboratory suggested that autophagy depends on the presence of Ca^{2+} in intracellular compartments, providing the first concept by which cellular Ca^{2+} changes regulate autophagy [24]. Using different cellular systems, including *S. cerevisiae* and human hepatocytes, conflicting results about the role of Ca^{2+} have been reported subsequently [25]. However, it became evident that also the increase in cytosolic Ca^{2+} concentration leads to autophagy, providing a concept that integrated previous conflicting results. In this model, the activation of AMPK via CaMKK results in the inactivation of mTOR, thereby releasing the inhibitory function of mTOR on autophagy [6,26].

We have reinvestigated the role of cytosolic Ca^{2+} levels by automated high through put microscopy and live cell imaging using human WIPI-1 puncta formation analyses. Using this assay, we not only monitored the induction of autophagy, but also the involvement of PI(3)P, a crucial phospholipid found to be enriched at the inner

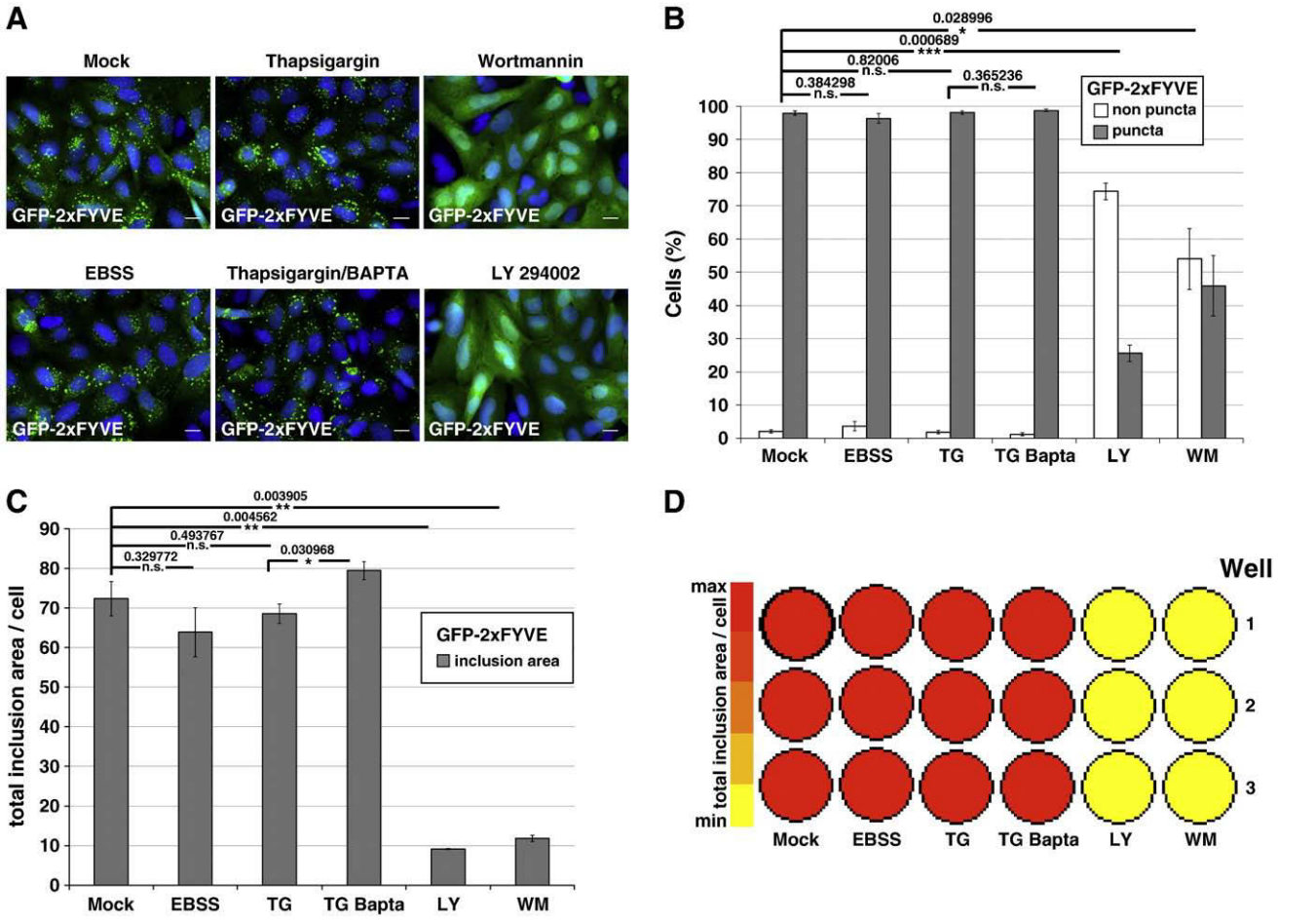

Fig. 5. Thapsigargin and BAPTA-AM do not alter PI(3)P levels. (A) Representative U2-OS-GFP-2xFYVE images acquired during automated fluorescent analysis. Cells were left untreated or treated with EBSS, TG (100 nM), WM (233 nM), TG (100 nM)/BAPTA-AM (30 μM) for 1 h. Results of at least 6200 cells per treatment were quantified, (B) GFP-WIPI-1 puncta formation analyses program applied for GFP-2xFYVE signals, (C) size of the total inclusion area per cell. (D) Dynamic heat map displaying positive (red) or negative (yellow) inclusion area obtained during image analysis of a single experiment with 3 independent wells per treatment. Values represent mean ± standard error for 3 independent triplicate experiments (at least 6200 cells per treatment in total). Calculated *p*-values from heteroscedastic *t*-tests are presented. (bars: 20 μm).

autophagosomal membrane [27]. WIPI-1 (Atg18) is the only human Atg protein that specifically binds PI(3)P, resulting in the localization of PI(3)P-bound WIPI-1 at autophagosomal membranes [13–15]. In addition, we extended the analyses regarding LC3 lipidation and GFP-LC3 puncta formation to a variety of different cells of human, mouse and chicken origin. Using the above systems, we demonstrate that the pharmacological increase of cytosolic Ca^{2+} profoundly induces autophagy and that this induction can be readily blocked by Ca^{2+}-chelation. Strikingly, it appears that neither Ca^{2+}-mobilization by TG nor its inhibition by BAPTA-AM affects the overall availability of PI(3)P, a product of hVps34/PI3K class III activity, shown by automated high through put analyses of endosomal GFP-2xFYVE. However, WIPI-1 puncta formation was completely blocked by Ca^{2+}-chelation, and the increase in WIPI-1 puncta upon cytosolic Ca^{2+} increase occurred rapidly. This finding might suggest that, apart from PI(3)P generation, an instant binding of PI(3)P by WIPI-1 from the available cellular PI(3)P pool is triggered by cytosolic Ca^{2+} increase, leading to the recruitment of WIPI-1/PI(3)P at autophagosomal membranes and the induction of autophagy.

Rapamycin-mediated mTOR inhibition also triggers WIPI-1 accumulation [13]. However, co-administration of rapamycin and wortmannin at concentrations that predominantly inhibit hVps34 overrides the effect mediated by rapamycin. This indicates that blocking PI(3)P availability abrogates the effect of releasing the mTOR inhibition on Atg proteins, including WIPI-1. Strikingly, here we found that TG administration does not lead to complete inhibition of mTOR, as measured by p70S6K phosphorylation, a *bona fide* read-out for mTOR activity. Interestingly, similar observations have been made by other groups who analyzed the effect of Ca^{2+} during autophagic degradation [8,19,28–30]. In this regard IP3 and its receptors seem to be central for the independence from mTOR repression. It could be shown that both reduced IP3 levels and the blockage of IP3R lead to an increase of the autophagic flux [18,30]. However, reduced IP3 levels and/or the blockage of IP3Rs usually result in decreased cytosolic Ca^{2+} concentrations. This obvious discrepancy between those reports and our results might be explained by the observation that the anti-autophagic potential of IP3Rs is mediated by its ligand-binding domain, which by itself lacks Ca^{2+} channel properties [31]. It could be shown that the IP3R-LBD can suppress autophagy irrespective of its subcellular localization, supporting the notion that modified Ca^{2+}-fluxes do not mediate the anti-autophagic effects of IP3Rs [31]. The Ca^{2+}-independence of this pathway was further confirmed by the fact that beclin 1 knockdown did not have any effect on cytosolic or luminal ER Ca^{2+} levels [31].

Further, we observed that mTOR-dependent Atg1/Ulk1 phosphorylation is less sensitive to TG treatment when compared to treatment with rapamycin or the mTORC1- and mTORC2-specific inhibitor Ku-0063794 [23]. This led us to question about the involvement of

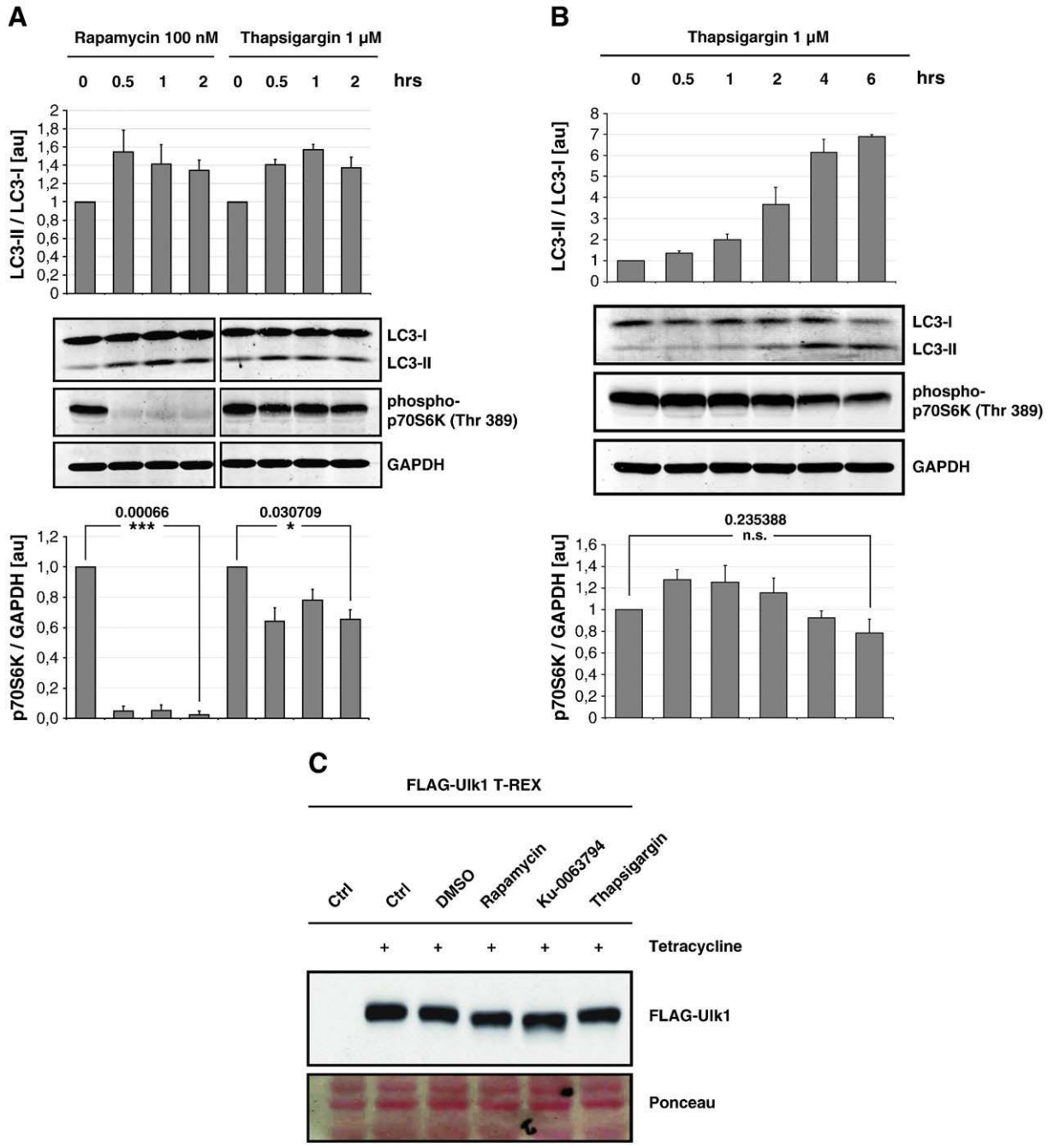

Fig. 6. Thapsigargin-mediated induction of autophagy does not necessarily parallel mTOR inhibition. (A) J16 T cells were treated with TG (1 μM) or rapamycin (100 nM) (0–2 h). (B) DT40 B cells were treated with TG (1 μM) (0–6 h). Equal amounts of total protein were subjected to immunoblot analysis for LC3, phospho-p70S6K (Thr389) and GAPDH. LC3-II/LC3-I and phospho-p70S6K/GAPDH ratios were quantified. A representative experiment is shown. Each bar represents mean values of 3 independent experiments ± SEM. Heteroscedastic *t*-tests were carried out and the calculated *p*-values are presented. (C) Flp-In™ T-REx™ 293 cells stably transfected with cDNA encoding inducible FLAG-tagged human Ulk1 were left untreated or incubated with tetracycline for 24 h. Then cells were left untreated or stimulated with DMSO (0.1%), rapamycin (100 nM), Ku-0063794 (1 μM) or TG (1 μM) for 6 h. Cleared cellular lysates were subjected to immunoblot analysis for FLAG. Uniform protein migration was confirmed by Ponceau S staining.

upstream regulators of mTOR implicated in Ca^{2+} signaling that control autophagy, such as AMPK and CaMKKα/β [6]. Strikingly, using AMPK-$\alpha1^{-/-}\alpha2^{-/-}$ MEFs, we demonstrate that Ca^{2+}-mobilization permits LC3 lipidation in the absence of AMPK. Also, the level of LC3 lipidation appeared to be slightly reduced in AMPK double-deficient cells suggesting that both, AMPK-dependent and AMPK-independent pathways control Ca^{2+} signaling to switch on autophagy. Of note, the AMPK-inhibitor Compound C, frequently applied in a variety of studies, seems to function pro-autophagic in the AMPK-deficient background. Therefore, results using Compound C for the inhibition of AMPK should be interpreted with caution, as already discussed by others [32].

5. Conclusion

We suggest that both, AMPK-dependent and AMPK-independent signaling cascades control the modulation of autophagy by sensoring cytosolic Ca^{2+} concentration alterations (Supp. Fig. 5). We further suggest that both AMPK-dependent and independent entries to

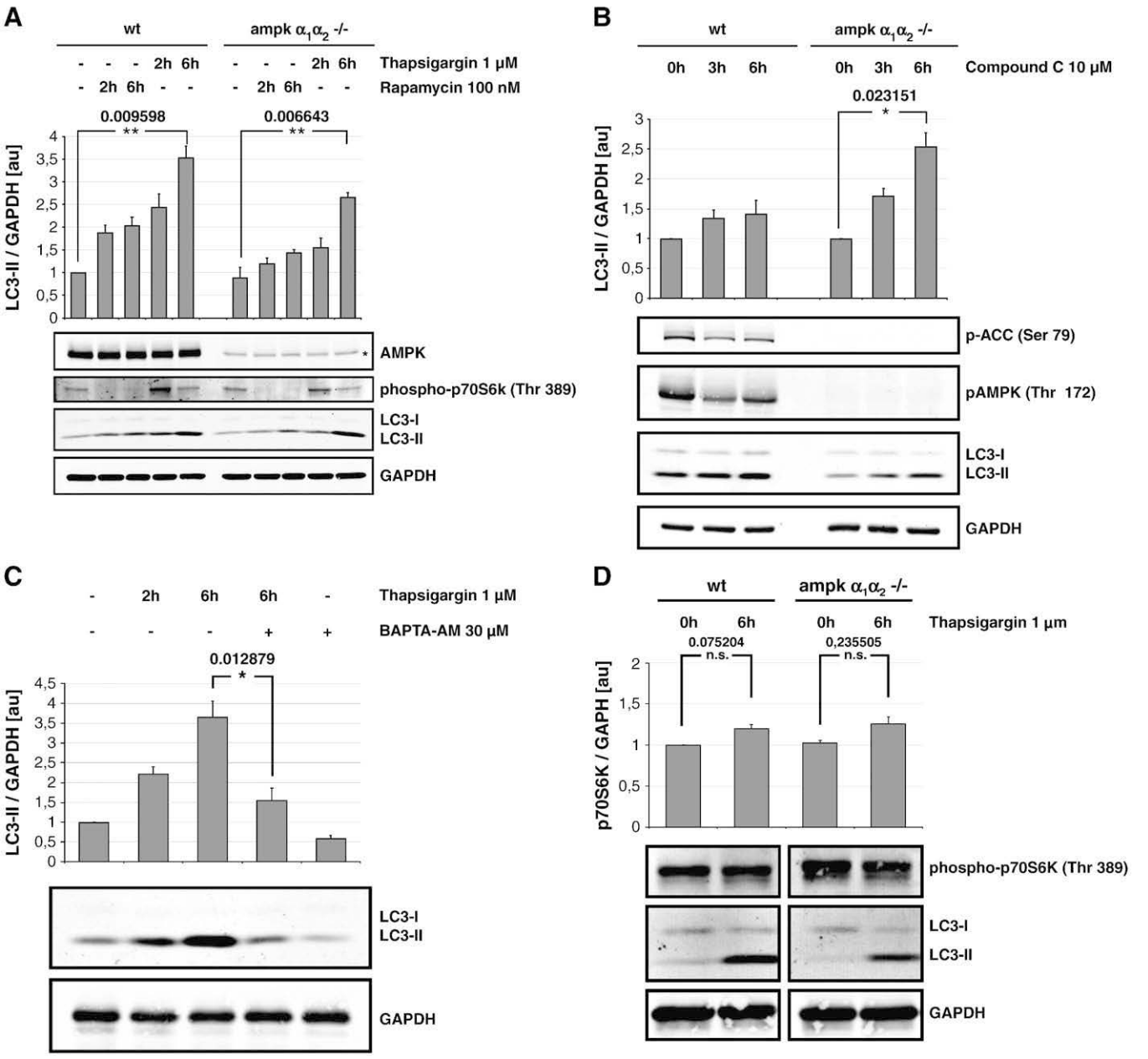

Fig. 7. Elevated Ca^{2+} levels induce LC3-II generation independently of AMPK. (A) Wild-type (wt) and AMPK-$\alpha1^{-/-}\alpha2^{-/-}$ MEFs were treated with TG (1 μM) or rapamycin (100 nM) for 2 and 6 h. Equal amounts of protein were subjected to immunoblot analysis for LC3, phospho-p70S6K (Thr389), AMPK and GAPDH. The asterisk indicates an unspecific background band. (B) MEFs were treated with Compound C (10 μM) for 3 and 6 h. Cell lysates were analyzed by immunoblotting with antibodies against LC3, phospho-AMPK (Thr172), phospho-ACC (Ser79) and GAPDH. (C) Wt MEFs were treated with TG (1 μM) for 2 and 6 h alone or for 6 h after 30 min preincubation with BAPTA-AM (30 μM). As control, cells were incubated with BAPTA-AM or solvent alone. LC3-II relative to GAPDH levels, expressed in arbitrary units, is quantified. Representatives of three independent experiments are shown. (D) WT and AMPK-$\alpha1^{-/-}\alpha2^{-/-}$ MEFs were treated with TG (1 μM) for 6 h. Equal amounts of protein were subjected to immunoblot analysis for LC3, phospho-p70S6K (Thr389) and GAPDH. Each bar represents mean values of 3 independent experiments ± SEM. Heteroscedastic *t*-tests were carried out and the calculated *p*-values are presented.

autophagic degradation might partially proceed independently of mTOR inhibition, since both p70S6K and Ulk1 phosphorylation are largely unaffected by TG treatment.

Acknowledgements

We are grateful to Dario Alessi for providing laboratory support in obtaining inducible FLAG-Ulk1 Flp-In™ T-REx™ 293 cells, and we acknowledge AstraZeneca for providing Ku-0063794. This work was supported by grants from the Deutsche Forschungsgemeinschaft SFB 773 (A03 to TP-C; C01 to SW and BS), GK1302 (to SW and BS); Federal Ministry for Education and Science (BMBF BioProfile, to TP-C); Ministry of Science, Research and Arts, Baden-Württemberg 1423-98101 (TP-C; SW); Interdisciplinary Center of Clinical Research, Faculty of Medicine, Tübingen (*f*ortüne 1805-0-0, to BS), and Landesgraduierten Stiftung Baden-Württemberg (pre-doctoral fellowship to SP).

Appendix A. Supplementary data

Supplementary data associated with this article can be found, in the online version, at doi:10.1016/j.cellsig.2010.01.015.

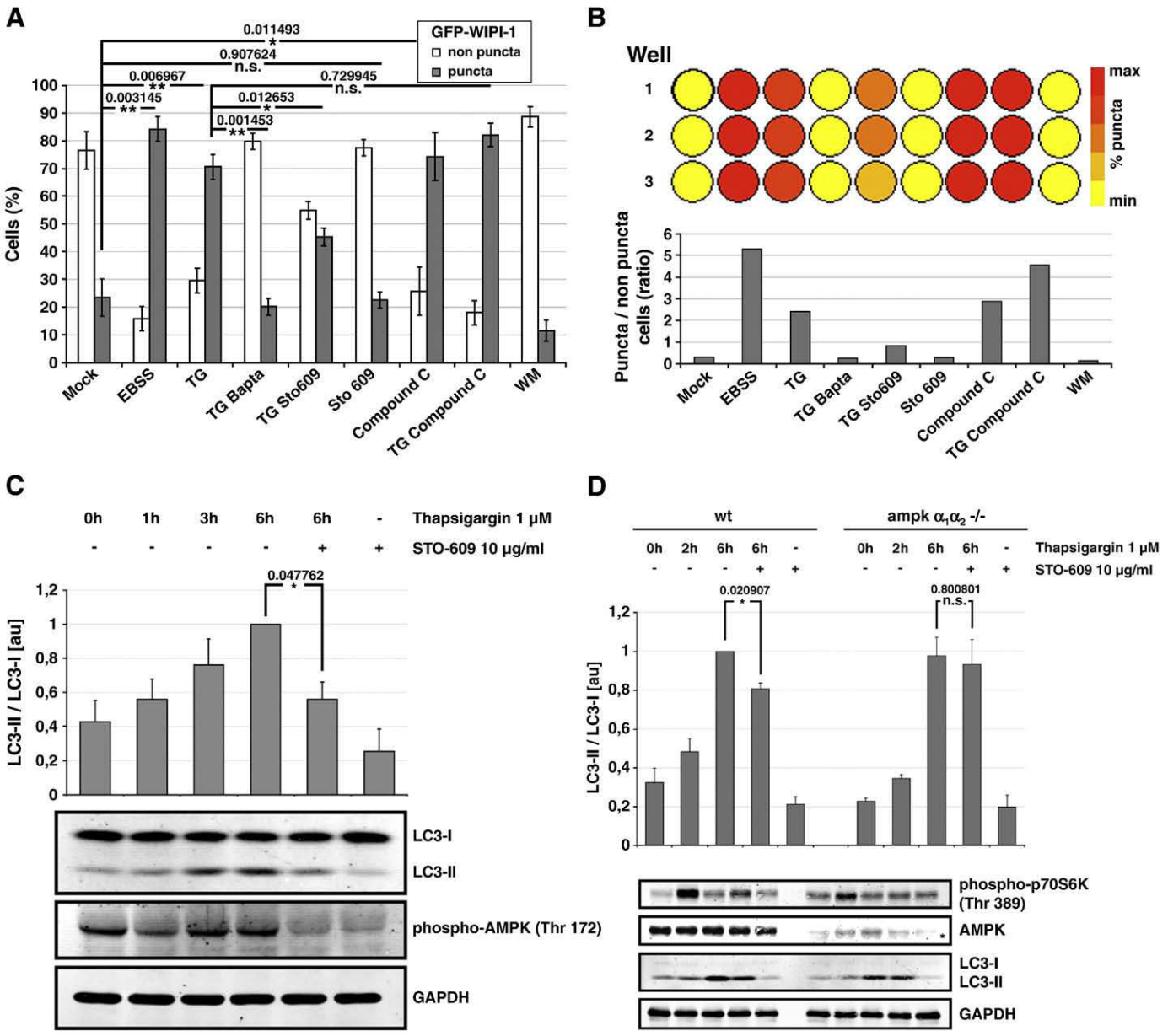

Fig. 8. Thapsigargin-mediated induction of autophagy partially depends on CaMKK-α/β. (A) U2-OS-GFP-WIPI-1 cells were treated for 1 h with EBSS, TG (100 nM), TG (100 nM)/BAPTA-AM (30 µM), TG (100 nM)/STO-609 (10 µg/ml), Compound C (10 µM), TG (100 nM)/Compound C (10 µM), WM (233 nM), or mock treated (control). Values (GFP-WIPI-1 puncta-positive or puncta-negative cells) represent mean ± SEM for 3 independent triplicate experiments (at least 5100 cells per treatment in total). Heteroscedastic *t*-tests were carried out and the calculated *p*-values are presented. (B) GFP-WIPI-1 puncta/non-puncta ratios were determined and a dynamic heat map displays puncta positive (red) and puncta-negative (yellow) cells per well during image analysis of a single experiment, 3 independent wells per treatment. (C) J16 cells were left untreated or treated with 1 µM TG for 1 h, 3 h and 6 h. 10 µg/ml STO-609 were added to inhibit CaMKK-α/β. (D) Wt and AMPK-$\alpha1^{-/-}\alpha2^{-/-}$ MEFs were treated with TG (1 µM) for 2 and 6 h and for 6 h after 30 min preincubation with STO-609 (10 µg/ml). Equal amounts of total protein were analyzed by immunoblotting for LC3, phospho-p70S6K (Thr389), AMPK and GAPDH. The asterisk indicates an unspecific background band. LC3-II levels relative to GAPDH levels were quantified. A representative experiment is shown. Each bar represents mean values of 3 independent experiments ± SEM. Calculated *p*-values from heteroscedastic *t*-tests are presented.

References

[1] T. Shintani, D.J. Klionsky, Science 306 (5698) (2004) 990.
[2] N. Mizushima, B. Levine, A.M. Cuervo, D.J. Klionsky, Nature 451 (7182) (2008) 1069.
[3] B. Levine, D.J. Klionsky, Dev. Cell 6 (4) (2004) 463.
[4] M.C. Maiuri, E. Zalckvar, A. Kimchi, G. Kroemer, Nat. Rev. Mol. Cell Biol. 8 (9) (2007) 741.
[5] S. Pattingre, L. Espert, M. Biard-Piechaczyk, P. Codogno, Biochimie 90 (2) (2008) 313.
[6] M. Hoyer-Hansen, L. Bastholm, P. Szyniarowski, M. Campanella, G. Szabadkai, T. Farkas, K. Bianchi, N. Fehrenbacher, F. Elling, R. Rizzuto, I.S. Mathiasen, M. Jaattela, Mol. Cell 25 (2) (2007) 193.
[7] G. Herrero-Martin, M. Hoyer-Hansen, C. Garcia-Garcia, C. Fumarola, T. Farkas, A. Lopez-Rivas, M. Jaattela, EMBO J. 28 (6) (2009) 677.
[8] A. Williams, S. Sarkar, P. Cuddon, E.K. Ttofi, S. Saiki, F.H. Siddiqi, L. Jahreiss, A. Fleming, D. Pask, P. Goldsmith, C.J. O'Kane, R.A. Floto, D.C. Rubinsztein, Nat. Chem. Biol. 4 (5) (2008) 295.
[9] T. Hanada, N.N. Noda, Y. Satomi, Y. Ichimura, Y. Fujioka, T. Takao, F. Inagaki, Y. Ohsumi, J. Biol. Chem. 282 (52) (2007) 37298.
[10] Y. Kabeya, N. Mizushima, T. Ueno, A. Yamamoto, T. Kirisako, T. Noda, E. Kominami, Y. Ohsumi, T. Yoshimori, EMBO J. 19 (21) (2000) 5720.
[11] D.J. Klionsky, H. Abeliovich, P. Agostinis, D.K. Agrawal, G. Aliev, D.S. Askew, M. Baba, E.H. Baehrecke, B.A. Bahr, A. Ballabio, B.A. Bamber, D.C. Bassham, E. Bergamini, X. Bi, M. Biard-Piechaczyk, J.S. Blum, D.E. Bredesen, J.L. Brodsky, J.H. Brumell, U.T. Brunk, W. Bursch, N. Camougrand, E. Cebollero, F. Cecconi, Y. Chen, L.S. Chin, A. Choi, C.T. Chu, J. Chung, P.G. Clarke, R.S. Clark, S.G. Clarke, C. Clave, J.L. Cleveland, P. Codogno, M.I. Colombo, A. Coto-Montes, J.M. Cregg, A.M. Cuervo, J. Debnath, F. Demarchi, P.B. Dennis, P.A. Dennis, V. Deretic, R.J. Devenish, F. Di Sano, J.F. Dice, M. Difiglia, S. Dinesh-Kumar, C.W. Distelhorst, M. Djavaheri-Mergny, F.C.

Dorsey, W. Droge, M. Dron, W.A. Dunn Jr., M. Duszenko, N.T. Eissa, Z. Elazar, A. Esclatine, E.L. Eskelinen, L. Fesus, K.D. Finley, J.M. Fuentes, J. Fueyo, K. Fujisaki, B. Galliot, F.B. Gao, D.A. Gewirtz, S.B. Gibson, A. Gohla, A.L. Goldberg, R. Gonzalez, C. Gonzalez-Estevez, S. Gorski, R.A. Gottlieb, D. Haussinger, Y.W. He, K. Heidenreich, J.A. Hill, M. Hoyer-Hansen, X. Hu, W.P. Huang, A. Iwasaki, M. Jaattela, W.T. Jackson, X. Jiang, S. Jin, T. Johansen, J.U. Jung, M. Kadowaki, C. Kang, A. Kelekar, D.H. Kessel, J.A. Kiel, H.P. Kim, A. Kimchi, T.J. Kinsella, K. Kiselyov, K. Kitamoto, E. Knecht, M. Komatsu, E. Kominami, S. Kondo, A.L. Kovacs, G. Kroemer, C.Y. Kuan, R. Kumar, M. Kundu, J. Landry, M. Laporte, W. Le, H.Y. Lei, M.J. Lenardo, B. Levine, A. Lieberman, K.L. Lim, F.C. Lin, W. Liou, L.F. Liu, G. Lopez-Berestein, C. Lopez-Otin, B. Lu, K.F. Macleod, W. Malorni, W. Martinet, K. Matsuoka, J. Mautner, A.J. Meijer, A. Melendez, P. Michels, G. Miotto, W.P. Mistiaen, N. Mizushima, B. Mograbi, I. Monastyrska, M.N. Moore, P.I. Moreira, Y. Moriyasu, T. Motyl, C. Munz, L.O. Murphy, N.I. Naqvi, T.P. Neufeld, I. Nishino, R.A. Nixon, T. Noda, B. Nurnberg, M. Ogawa, N.L. Oleinick, L.J. Olsen, B. Ozpolat, S. Paglin, G.E. Palmer, I. Papassideri, M. Parkes, D.H. Perlmutter, G. Perry, M. Piacentini, R. Pinkas-Kramarski, M. Prescott, T. Proikas-Cezanne, N. Raben, A. Rami, F. Reggiori, B. Rohrer, D.C. Rubinsztein, K.M. Ryan, J. Sadoshima, H. Sakagami, Y. Sakai, M. Sandri, C. Sasakawa, M. Sass, C. Schneider, P.O. Seglen, O. Seleverstov, J. Settleman, J.J. Shacka, I.M. Shapiro, A. Sibirny, E.C. Silva-Zacarin, H.U. Simon, C. Simone, A. Simonsen, M.A. Smith, K. Spanel-Borowski, V. Srinivas, M. Steeves, H. Stenmark, P.E. Stromhaug, C.S. Subauste, S. Sugimoto, D. Sulzer, T. Suzuki, M.S. Swanson, I. Tabas, F. Takeshita, N.J. Talbot, Z. Talloczy, K. Tanaka, I. Tanida, G.S. Taylor, J.P. Taylor, A. Terman, G. Tettamanti, C.B. Thompson, M. Thumm, A.M. Tolkovsky, S.A. Tooze, R. Truant, L.V. Tumanovska, Y. Uchiyama, T. Ueno, N.L. Uzcategui, I. van der Klei, E.C. Vaquero, T. Vellai, M.W. Vogel, H.G. Wang, P. Webster, J.W. Wiley, Z. Xi, G. Xiao, J. Yahalom, J.M. Yang, G. Yap, X.M. Yin, T. Yoshimori, L. Yu, Z. Yue, M. Yuzaki, O. Zabirnyk, X. Zheng, X. Zhu, R.L. Deter, Autophagy 4 (2) (2008) 151.

[12] N. Mizushima, T. Yoshimori, Autophagy 3 (6) (2007) 542.

[13] T. Proikas-Cezanne, S. Ruckerbauer, Y.D. Stierhof, C. Berg, A. Nordheim, FEBS Lett. 581 (18) (2007) 3396.

[14] T. Proikas-Cezanne, S. Waddell, A. Gaugel, T. Frickey, A. Lupas, A. Nordheim, Oncogene 23 (58) (2004) 9314.

[15] T. Proikas-Cezanne, Pfisterer SG, Methods Enzymol. 452 (2009) 247.

[16] K.R. Laderoute, K. Amin, J.M. Calaoagan, M. Knapp, T. Le, J. Orduna, M. Foretz, B. Viollet, Mol. Cell. Biol. 26 (14) (2006) 5336.

[17] S. Morita, T. Kojima, T. Kitamura, Gene Ther. 7 (12) (2000) 1063.

[18] A. Criollo, M.C. Maiuri, E. Tasdemir, I. Vitale, A.A. Fiebig, D. Andrews, J. Molgo, J. Diaz, S. Lavandero, F. Harper, G. Pierron, D. di Stefano, R. Rizzuto, G. Szabadkai, G. Kroemer, Cell Death Differ. 14 (5) (2007) 1029.

[19] K. Sakaki, J. Wu, R.J. Kaufman, J. Biol. Chem. 283 (22) (2008) 15370.

[20] T. Hara, A. Takamura, C. Kishi, S. Iemura, T. Natsume, J.L. Guan, N. Mizushima, J. Cell Biol. 181 (3) (2008) 497.

[21] E.Y. Chan, A. Longatti, N.C. McKnight, S.A. Tooze, Mol. Cell. Biol. 29 (1) (2009) 157.

[22] N. Hosokawa, T. Hara, T. Kaizuka, C. Kishi, A. Takamura, Y. Miura, S. Iemura, T. Natsume, K. Takehana, N. Yamada, J.L. Guan, N. Oshiro, N. Mizushima, Mol. Biol. Cell 20 (7) (2009) 1981.

[23] J.M. Garcia-Martinez, J. Moran, R.G. Clarke, A. Gray, S.C. Cosulich, C.M. Chresta, D.R. Alessi, Biochem. J. (2009).

[24] P.B. Gordon, I. Holen, M. Fosse, J.S. Rotnes, P.O. Seglen, J. Biol. Chem. 35 (1993) 26107.

[25] A.J. Meijer, P. Codogno, Autophagy 3 (3) (2007) 238.

[26] W. Gao, W.X. Ding, D.B. Stolz, X.M. Yin, Autophagy 4 (6) (2008) 754.

[27] K. Obara, Y. Ohsumi, Autophagy 4 (7) (2008) 952.

[28] S. Sarkar, V. Korolchuk, M. Renna, A. Winslow, D.C. Rubinsztein, Autophagy 5 (3) (2009) 307.

[29] S. Sarkar, E.O. Perlstein, S. Imarisio, S. Pineau, A. Cordenier, R.L. Maglathlin, J.A. Webster, T.A. Lewis, C.J. O'Kane, S.L. Schreiber, D.C. Rubinsztein, Nat. Chem. Biol. 3 (6) (2007) 331.

[30] S. Sarkar, D.C. Rubinsztein, Autophagy 2 (2) (2006) 132.

[31] J.M. Vicencio, C. Ortiz, A. Criollo, A.W. Jones, O. Kepp, L. Galluzzi, N. Joza, I. Vitale, E. Morselli, M. Tailler, M. Castedo, M.C. Maiuri, J. Molgo, G. Szabadkai, S. Lavandero, G. Kroemer, Cell Death Differ (2009).

[32] J. Bain, L. Plater, M. Elliott, N. Shpiro, C.J. Hastie, H. McLauchlan, I. Klevernic, J.S. Arthur, D.R. Alessi, P. Cohen, Biochem. J. 408 (3) (2007) 297.

Autophagy 7:7, 696-706; July 2011; © 2011 Landes Bioscience

Ulk1-mediated phosphorylation of AMPK constitutes a negative regulatory feedback loop

Antje S. Löffler,[1,†] Sebastian Alers,[1] Alexandra M. Dieterle,[1] Hildegard Keppeler,[1] Mirita Franz-Wachtel,[2] Mondira Kundu,[3] David G. Campbell,[4] Sebastian Wesselborg,[1,†] Dario R. Alessi[4,‡] and Björn Stork[1,†,‡,*]

[1]Department of Internal Medicine I; and [2]Proteome Center Tübingen; University of Tübingen; Tübingen, Germany; [3]Department of Pathology; St. Jude Children's Hospital; Memphis, TN USA; [4]MRC Protein Phosphorylation Unit; College of Life Sciences; University of Dundee; Dundee, Scotland UK

[†]Current Address: Institute of Molecular Medicine; Heinrich-Heine-University; Düsseldorf, Germany

[‡]These authors contributed equally to this work.

Key words: Ulk1, Ulk2, AMPK, mTOR, negative feedback, phosphorylation

Abbreviations: ACC, acetyl-CoA carboxylase; AMPK, AMP-activated protein kinase; *Atg*, autophagy-related gene; CTD, C-terminal domain; FAK ,focal adhesion kinase; FIP200, family interacting protein of 200 kDa; mTORC1, mammalian target of rapamycin complex 1; Ulk1, Unc-51-like kinase 1

Unc-51-like kinase 1 (Ulk1) plays a central role in autophagy induction. It forms a stable complex with Atg13 and focal adhesion kinase (FAK) family interacting protein of 200 kDa (FIP200). This complex is negatively regulated by the mammalian target of rapamycin complex 1 (mTORC1) in a nutrient-dependent way. AMP-activated protein kinase (AMPK), which is activated by LKB1/Strad/Mo25 upon high AMP levels, stimulates autophagy by inhibiting mTORC1. Recently, it has been described that AMPK and Ulk1 interact and that the latter is phosphorylated by AMPK. This phosphorylation leads to the direct activation of Ulk1 by AMPK bypassing mTOR-inhibition. Here we report that Ulk1/2 in turn phosphorylates all three subunits of AMPK and thereby negatively regulates its activity. Thus, we propose that Ulk1 is not only involved in the induction of autophagy, but also in terminating signaling events that trigger autophagy. In our model, phosphorylation of AMPK by Ulk1 represents a negative feedback circuit.

Introduction

Macroautophagy (hereafter referred to as autophagy) is an evolutionarily conserved catabolic process by which proteins and organelles are engulfed by double-membraned vesicles, the so-called autophagosomes, which then fuse with lysosomes for degradation.[1-5] Even though 33 autophagy-related (*Atg*) genes have been identified in the last 13 years, the signaling that leads to the induction and termination of autophagy is still not fully understood.

One of the critical components during the induction of autophagy in yeast is the serine/threonine protein kinase Atg1.[6] In mammals Atg1 has five orthologs: the Unc-51-like kinases (Ulk) 1, 2, 3, 4 and fused (STK36). Ulk1 and Ulk2 share considerable homology whereas Ulk3, 4 and fused are only conserved within the kinase domain.[7,8] Although Ulk1, 2 and 3 seem to contribute to autophagic processes, only Ulk1 and Ulk2 appear to be relevant in starvation-induced autophagy[9] and can complement each other—at least partially. Thus, Ulk1 knockout mice do undergo autophagy in response to glucose deprivation.[10] However, in a different study it could be shown that rapamycin-induced autophagy was significantly reduced in Ulk1-deficient mouse embryonic fibroblasts (MEFs) and in Ulk1-silenced HEK293T cells.[11] Hence, the different roles of Ulk1 and Ulk2 in autophagy and their redundancy are still controversial.

Ulk1 forms a stable complex with Atg13 and the focal adhesion kinase family-interacting protein of 200 kDa (FIP200), and binding of both proteins is required for maximal kinase activity of Ulk1. The C-terminal domain (CTD) of Ulk1 is essential for the formation of the Ulk1-Atg13-FIP200 complex and has been reported to be required for binding of additional proteins.[12,13] Conversely, the regulatory associated protein of mTOR (Raptor), which is a component of the mammalian target of rapamycin complex 1 (mTORC1), binds Ulk1 in a CTD-independent manner.[14] This implies the existence of two different types of Ulk1 complexes: one type containing proteins in addition to Atg13 and FIP200 that interact with Ulk1 in a CTD-dependent manner and another type of complex formed by proteins that do not require the CTD of Ulk1 for interaction such as Raptor.[13] Further proteins that bind Ulk1 independent of its CTD have yet to be discovered.

*Correspondence to: Björn Stork; Email: bjoern.stork@med.uni-tuebingen.de
Submitted: 11/18/10; Revised: 03/04/11; Accepted: 03/14/11
DOI: 10.4161/auto.7.7.15451

Upstream regulation of autophagy occurs via different signaling pathways, one of which includes the AMP-activated protein kinase (AMPK), which is a heterotrimeric complex consisting of a catalytic α-subunit and regulatory β- and γ-subunits.[15] The role of AMPK during autophagy has previously been discussed.[16-21] AMPK is activated upon various stress conditions that are known to induce autophagy. At high AMP levels for example, the LKB1/STRAD/Mo25-complex phosphorylates AMPKα at Thr172 and thus activates AMPK.[22,23] AMPK in turn inactivates mTORC1 directly by phosphorylating Raptor and indirectly by phosphorylating TSC2,[24] ultimately resulting in the induction of autophagy.

mTORC1, which is often referred to as the gatekeeper to autophagy, is a key regulator of the Ulk1-Atg13-FIP200 kinase complex.[11,14,25] Under nutrient-rich conditions, active mTORC1 associates with and inactivates the Ulk1-Atg13-FIP200 complex by phosphorylating Ulk1 and Atg13. Under starvation conditions inactive mTORC1 dissociates from the multiprotein-complex and mTOR phosphorylation sites in Ulk1 and Atg13 become dephosphorylated. Thereafter, Ulk1 autophosphorylates and phosphorylates Atg13 and FIP200, leading to an active Ulk1-Atg13-FIP200 complex that functions at the autophagosome nucleation step. Recently it could be shown that AMPK and Ulk1 interact,[26,27] and in two additional studies it was demonstrated that Ulk1 is phosphorylated by AMPK and thereby directly activated without prior inhibition of mTOR.[28,29] However, the two groups identified different phospo-acceptor sites in Ulk1. Thus, it appears that the mechanism of Ulk1 activation is rather complex and requires further investigation.[30] Even though many studies addressed upstream regulation of the Ulk1-Atg13-FIP200 complex, downstream signaling cascades of this complex have not been resolved so far. Thus, no additional autophagy-related substrates of this kinase-complex, besides their components themselves and the activating molecule in Beclin 1-regulated autophagy (AMBRA1),[31] have been discovered to date.

Another intriguing question is how termination of autophagy is regulated. Recently it has been shown that prolonged starvation leads to reactivation of mTOR and subsequently to attenuated autophagy.[32] In an alternative study, the death-associated protein 1 (DAP1) has been proposed as a suppressor of autophagy. DAP1 is phosphorylated at inhibitory sites by mTOR under nutrient-rich conditions. During starvation, the phosphorylation of DAP1 is reduced and autophagy is suppressed.[33] Whether these mechanisms are solely responsible for negative feedback has yet to be investigated.

In order to identify novel interacting proteins and substrates of Ulk1 we performed co-immunopurification analyses from Flp-In™ T-REx™ 293 cells that express inducible GFP-Ulk1. We identified AMPK among various co-immunopurified proteins. Here, we report that all three subunits of AMPK could be co-immunopurified with Ulk1 and that this interaction was independent of the CTD of Ulk1. Furthermore, all AMPK subunits were phosphorylated by Ulk1/Ulk2. By making use of Flp-In™ T-REx™ 293 cells inducibly expressing Ulk1, *ulk1*$^{-/-}$ MEFs and RNAi in HEK293 cells we could show that the phosphorylation of AMPK by Ulk1 exerted a negative impact on both AMPK activation (as detected by phosphorylation of AMPKα Thr172) and activity (as detected by phosphorylation of AMPK substrates). Accordingly, AMPK as a major upstream activator of autophagy in general and of Ulk1 in particular is in turn negatively regulated by Ulk1 kinase activity. Thus, Ulk1 is not only involved in the induction of autophagy but also in the termination of signaling events that trigger autophagy.

Results

Ulk1 interacts with AMPK. In order to identify new interaction partners or particular substrates of mammalian Ulk1, we generated Flp-In™ T-REx™ 293 cells stably expressing GFP-Ulk1 variants. Following tetracycline-induction, GFP (to exclude unspecific interaction partners), wild-type GFP-Ulk1 (GFP-Ulk1wt) or a mutant lacking the C-terminal domain (GFP-Ulk1/ΔCTD) (aa1-829) were purified from these cells. Co-immunopurified proteins were separated by SDS-PAGE, and gel pieces were digested with trypsin and analyzed by mass spectrometry (**Fig. 1A**).

These analyses confirmed the presence of previously reported interacting proteins such as Raptor, Atg13, Atg101 and FIP200. Furthermore, all three subunits of AMP-activated kinase (AMPKα, β and γ) were identified and different isoforms of all three subunits could be co-immunopurified with GFP-Ulk1 (**Sup. S1**).

To verify these results we performed immunoblot analyses with Ulk1- and FLAG-immunopurifications from HEK293 cells and Flp-In™ T-REx™ 293 cells stably expressing FLAG or FLAG-Ulk1wt, respectively. AMPKα was detected in immunopurifications of FLAG-Ulk1wt and vice versa (**Fig. 1B and C**). Furthermore, endogenous Ulk1 was co-immunopurified with AMPKα (**Fig. 1D**).

It has previously been demonstrated that the C-terminal domain of Ulk1 is important for the interaction with Atg13 and FIP200. To evaluate the requirement of the C-terminal residues of Ulk1 for its interaction with AMPK, we investigated if AMPK is binding to GFP-Ulk1/ΔCTD. All three subunits AMPKα, β and γ were co-immunopurified with GFP-tagged Ulk1 lacking the C-terminal domain, as shown by mass spectrometry (AMPKα, β and γ) and immunoblotting (AMPKα, β) (**Sup. S1, Fig. 1E**).

Taken together, these data confirm that Ulk1 associates with its upstream regulator AMPK and that the C-terminal domain of Ulk1 is dispensable for this interaction.

All three subunits of AMPK are phosphorylated by Ulk1/Ulk2. Though the kinase activity of Ulk1 was not required for its interaction with AMPK the question remained whether AMPK serves as a substrate for Ulk1. Therefore, we made use of Flp-In™ T-REx™ 293 cells which express GFP only, GFP-Ulk1wt, GFP-Ulk1/ΔCTD, or a kinase-dead mutant of Ulk1 (GFP-Ulk1kd) upon tetracycline treatment. With the induction of GFP-Ulk1wt and GFP-Ulk1/ΔCTD expression the apparent molecular weights of AMPKα and AMPKβ increased in immunoblot analyses indicating a putative phosphorylation. These

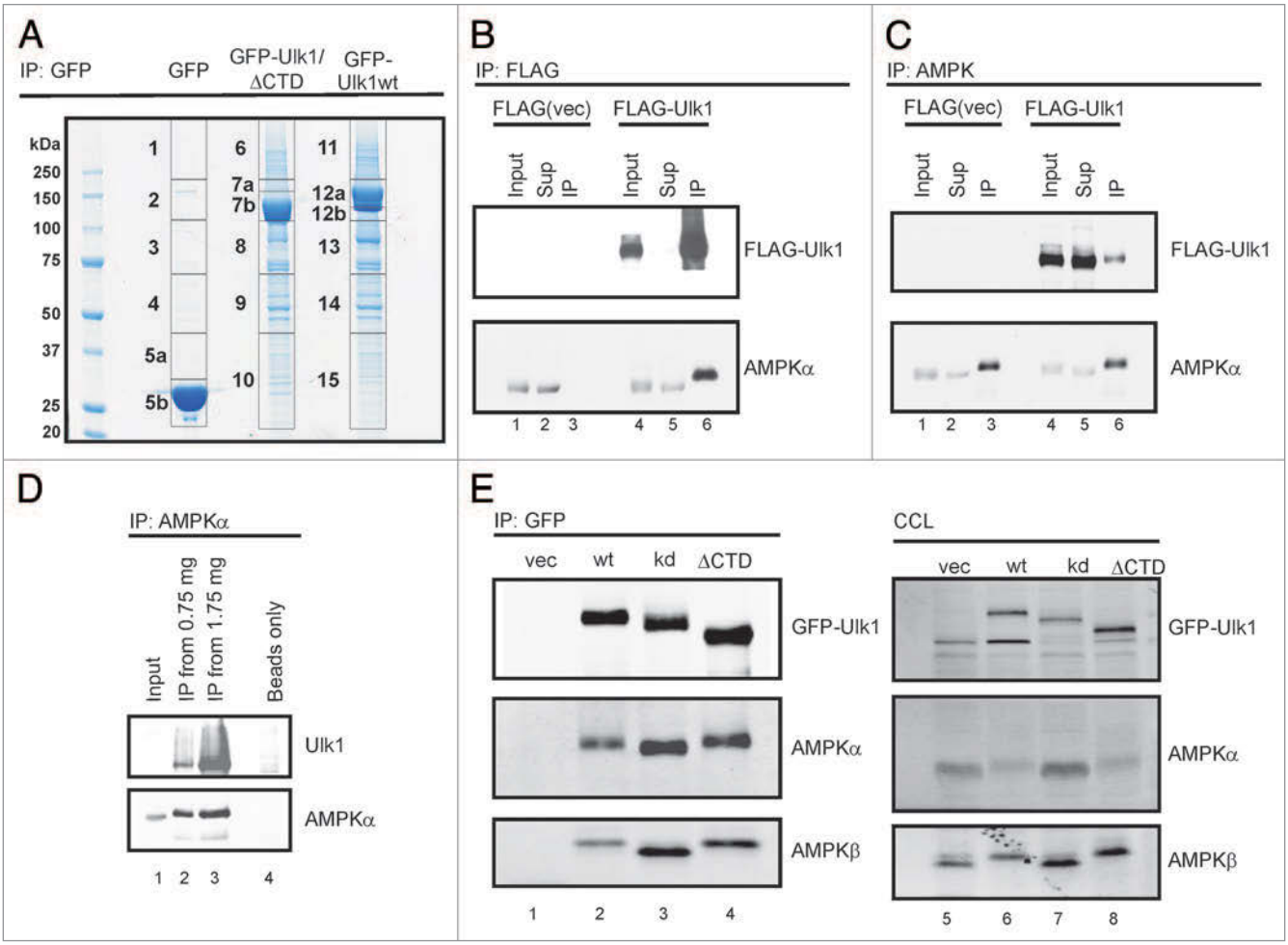

Figure 1. Ulk1 interacts with AMPK. (A) Following tetracycline-treatment, GFP, GFP-Ulk1wt or GFP-Ulk1/ΔCTD expression was induced in Flp-In™ T-REx™ 293 cells. After 24 h cells were lysed and GFP-immunopurifications were performed. GFP, GFP-Ulk1wt, GFP-Ulk1/ΔCTD and co-immunopurified proteins were separated by SDS-PAGE. Following Coomassie staining the different lanes were cut in pieces, washed, and subjected to trypsin digest. Eluted peptides were analyzed by mass spectrometry. (B and C) Following tetracycline-treatment, FLAG or FLAG-Ulk1wt expression was induced in Flp-In™ T-REx™ 293. After 24 h cells were lysed and either FLAG-(B) or AMPK-(C) immunopurifications were performed. Purified proteins, cleared cellular lysates (input) and supernatants (sup) were subjected to SDS-PAGE and analyzed by immunoblotting using antibodies against FLAG and AMPKα. (D) HEK293 cells were lysed and an AMPK-immunopurification was performed. The immunopurification and cleared cellular lysates were separated by SDS-PAGE and analyzed by immunoblotting using antibodies against AMPKα and Ulk1. (E) Following tetracycline-treatment, GFP, GFP-Ulk1wt, GFP-Ulk1kd or GFP-Ulk1/ΔCTD expression was induced in Flp-In™ T-REx™ 293 cells. After 24 h cells were lysed and GFP-immunopurifications were performed. Purified proteins (left part) and cleared cellular lysates (CCL; right part) were separated by SDS-PAGE and analyzed by immunoblotting using antibodies against GFP, AMPKα and AMPKβ.

shifts appeared in a time- and kinase activity-dependent manner (**Fig. 2A**). Accordingly, this could not be observed in cells expressing either GFP-Ulk1kd or GFP alone. These results indicate that GFP-Ulk1wt and GFP-Ulk1/ΔCTD expression led to phosphorylation of AMPK subunits α and β (**Fig. 2A**). To verify that the shift in molecular weight of AMPK was actually due to direct phosphorylation of AMPK by Ulk1, we performed an in vitro kinase assay with either FLAG- or GST-tagged Ulk1 variants. The trimeric-complex of rat His_6-AMPKα1, human AMPKβ2 and rat AMPKγ1 was bacterially expressed, and GST-Atg13 was used as a positive control. The substrates were incubated with either FLAG-Ulk1wt or FLAG-Ulk1kd immunopurified from corresponding Flp-In™ T-REx™ 293 cells. All three subunits of AMPK showed strong ^{32}P incorporation when incubated with FLAG-Ulk1wt (**Fig. 2B**, lane 9). In particular, the AMPKβ subunit revealed a significantly reduced migration in SDS-PAGE after incubation with FLAG-Ulk1wt, indicating a strong phosphorylation (**Fig. 2B**, lane 3). FLAG-Ulk2 also phosphorylated all three subunits of AMPK in vitro (**Sup. S2**). GST-Ulk1/ΔCTD purified from transiently transfected HEK293 cells phosphorylated all three subunits of AMPK in vitro (**Fig. 2C**, lane 6), suggesting that the C-terminal domain of Ulk1 is dispensable for the phosphorylation of AMPK. Furthermore, endogenous Ulk1 immunopurified from HEK293 cells phosphorylated AMPKα and AMPKβ (**Fig. 2D**). Apparently, the phosphorylation of AMPK was increased when Ulk1 was immunopurified from serum-starved or PBS treated cells compared to Ulk1 from cells incubated with complete media. Collectively, these data prove

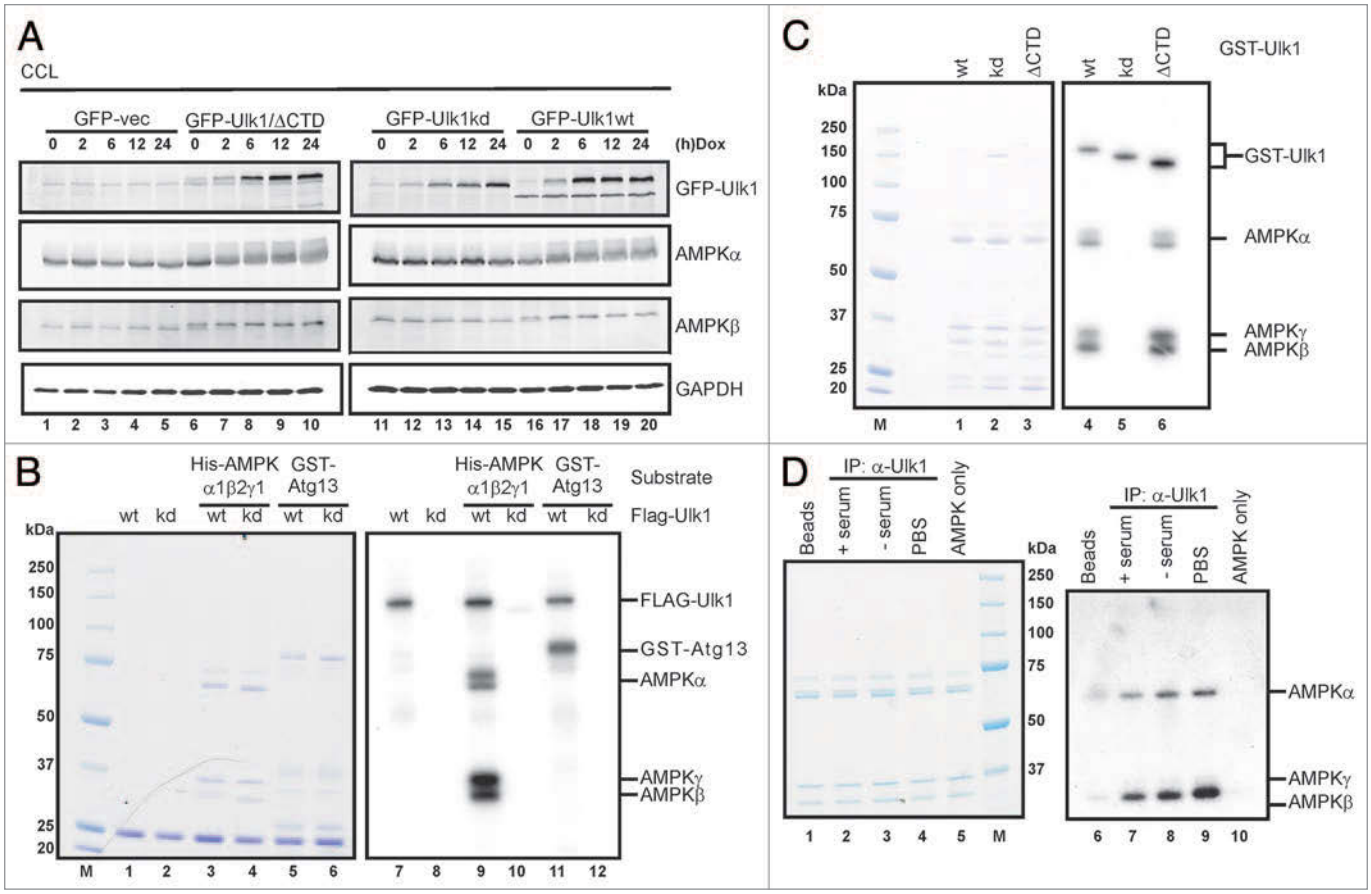

Figure 2. Ulk1 phosphorylates all three subunits of the AMPK complex. (A) Following doxycycline(Dox)-treatment, GFP, GFP-Ulk1/ΔCTD, GFP-Ulk1kd or GFP-Ulk1wt, expression was induced in Flp-In™ T-REx™ 293 cells. After indicated times, cells were lysed. Cleared cellular lysates (CCL) were separated by SDS-PAGE and analyzed by immunoblotting using antibodies against GFP, AMPKα, AMPKβ and GAPDH. (B and C) Following tetracycline-treatment, FLAG-Ulk1wt and FLAG-Ulk1kd expression was induced in Flp-In™ T-REx™ 293 cells (B). For GST-Ulk1wt and GST-Ulk1kd expression, HEK293 cells were transiently transfected (C). After 24 h cells were lysed and FLAG-immuno-/GST-affinitypurifications were performed. Purified kinases were employed for in vitro phosphorylation of GST-Atg13 and His-AMPK$\alpha_1\beta_2\gamma_1$ with [^{32}P] ATP. (D) For the kinase assay with endogenous Ulk1, HEK293 cells were starved in PBS, serum starved or treated with full media. Subsequently, cells were lysed and Ulk1-immunopurifications were performed. As a control experiment, lysate from HEK293 cells treated with full media was incubated with protein G sepharose beads without antibodies against Ulk1. (B–D) The reactions were subjected to SDS-PAGE. After coomassie staining of the gels, autoradiography was performed. See also Supplemental S2 for phosphorylation of AMPK by FLAG-Ulk2.

that all three AMPK subunits are direct substrates of Ulk1/2, and that the C-terminal domain of Ulk1 is not necessary for this phosphorylation.

Mapping of Ulk1 phosphorylation sites in AMPK. To map the Ulk1 phosphorylation sites in AMPKα, β and γ, we repeated the kinase assay and analyzed tryptic peptides from phosphorylated AMPK by mass spectrometry. The major phosphorylation sites are listed in **Supplemental S3**. The sites within the catalytic α-subunit are all located in a region that is C-terminal to the kinase domain. This region consists of an autoinhibitory and the AMPKβ-binding domain.[34] The sites within the β-subunit are located at the N-terminus of the glycogen-binding domain and in the linker region between the glycogen-binding domain and the C-terminal domain that interacts with the α- and γ-subunits, respectively. Phosphorylation sites in the γ-subunit are located in the linker region between the cystathionine β-synthase motifs 3 and 4. They act in pair to form one of two AMP/ATP-binding Bateman domains.[34] In summary, we could confirm that Ulk1 is capable of in vitro phosphorylation of all three AMPK subunits.

Ulk1-mediated phosphorylation decreases starvation-induced activation and activity of AMPK. Next we wanted to investigate the effect of Ulk1-mediated phosphorylation of AMPK on both the activation and activity of AMPK. Therefore we analyzed the phosphorylation status of the catalytic subunit AMPKα at Thr172. This is a conserved residue within the activation loop of the kinase domain, which must be phosphorylated for activation. At high AMP levels, the LKB1/STRAD/Mo25-complex phosphorylates AMPKα at Thr172 and thus activates AMPK.[22,23] We investigated whether activation of AMPK is impaired in cells expressing wild-type Ulk1. For that purpose, we either starved Flp-In™ T-REx™ 293 cells expressing GFP-Ulk1wt or GFP-Ulk1kd in EBSS for two hours, or treated them with full medium or full medium supplemented with rapamycin. Subsequently, phosphorylation of AMPKα at Thr172 was

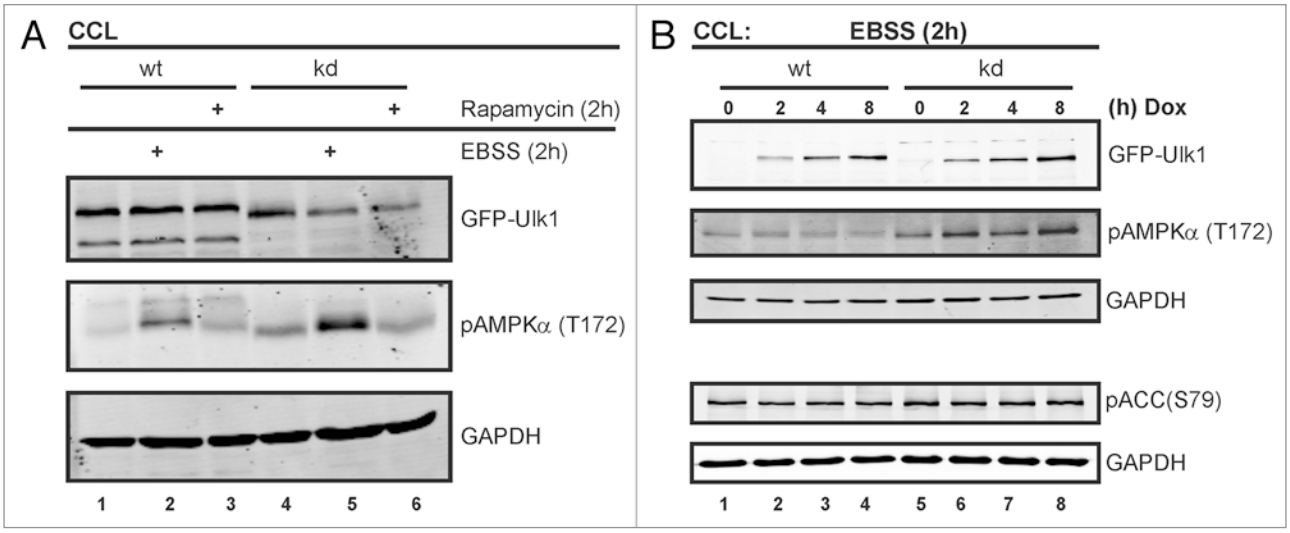

Figure 3. GFP-Ulk1-mediated phosphorylation decreases starvation-induced activation and activity of AMPK. (A) Following doxycycline-treatment, GFP-Ulk1wt or GFP-Ulk1kd expression was induced in Flp-In™ T-REx™ 293 cells. After 12 h cells were treated with full media, starved in EBSS for 2 h or treated with full media supplemented with rapamycin (100 nM). Subsequently cells were lysed and cleared cellular lysates (CCL) were separated by SDS-PAGE and analyzed by immunoblotting using antibodies against GFP, phosphoAMPKα (phospho-Thr172) and GAPDH. (B) GFP-Ulk1wt or GFP-Ulk1kd expression was induced in Flp-In™ T-REx™ 293 cells following doxycycline(Dox)-treatment. After indicated times, cells were starved in EBSS for 2 h. Subsequently cells were lysed and cleared cellular lysates were separated by SDS-PAGE and analyzed by immunoblotting using antibodies against GFP, phosphoAMPKα (phospho-Thr172), GAPDH and phosphoACC (phospho-Ser79).

analyzed. In cells expressing GFP-Ulk1kd, phosphorylation of AMPKα at Thr172 was increased upon starvation. This effect was impaired in cells expressing GFP-Ulk1wt (**Fig. 3A**), indicating that Ulk1 activity has a negative impact on AMPK activation by stimuli such as starvation. Treatment with rapamycin had no effect on AMPK activation in either cell line. Since expression of GFP-Ulk1 was induced for 12 hours, we wanted to investigate next if shorter induction times and therefore smaller amounts of GFP-Ulk1wt are sufficient to decrease AMPK activation upon starvation. As can be seen in **Figure 3B**, already two hours of GFP-Ulk1wt expression led to a decreased AMPK activation compared to expression of the kinase-dead version. Additionally, reduced AMPK activity upon GFP-Ulk1wt expression could be observed by analyzing phosphorylation of the AMPK substrate acetyl-CoA carboxylase (ACC) in this set-up (**Fig. 3B**).

To further assess AMPK activity following phosphorylation by Ulk1, we analyzed ACC phosphorylation in cells expressing either GFP-Ulk1wt or GFP-Ulk1kd under full nutrient conditions. By immunoblot analysis we detected a decrease in phosphorylation of ACC following prolonged expression of GFP-Ulk1wt, but not with induction of GFP-Ulk1kd (**Sup. S4a**). Furthermore, we analyzed AMPKα co-immunopurified with either GFP-Ulk1wt or GFP-Ulk1kd following different durations of induction. We could show that Thr172 phosphorylation of co-immunopurified AMPKα is diminished following GFP-Ulk1wt expression for 24 hours compared to AMPKα co-immunopurified following GFP-Ulk1kd expression (**Sup. S4b**). To summarize, Ulk1-activity showed a negative impact on both AMPK activation and activity upon starvation. Under full-nutrient culture conditions this negative impact was less pronounced and could only be achieved after long-term overexpression of GFP-Ulk1wt.

Starvation-induced activation and activity of AMPK is higher in *ulk1*$^{-/-}$ MEFs than in wt MEFs. Since Ulk1 is overexpressed in the Flp-In™ T-REx™ 293 cell system, we next wanted to investigate the effect of endogenous Ulk1 on AMPK activation and activity. For that, we made use of mouse embryonic fibroblasts that were either wild-type (wt) or deficient for Ulk1 (*ulk1*$^{-/-}$). We observed that activation of AMPK, reflected by phosphorylation of AMPKα at Thr172, upon EBSS starvation was higher in MEFs deficient for Ulk1 (**Fig. 4A**, lanes 2 and 6) compared to wt MEFs. Additional knockdown of Ulk2 led to a further increase in AMPK activation and activity upon EBSS starvation (**Fig. 4A**, lanes 6 and 8; **Fig. 4B**). Investigating AMPKβ, we found that AMPKβ2 from wt MEFs revealed a reduced migration in SDS-PAGE upon starvation, but not from *ulk1*$^{-/-}$ MEFs (**Fig. 4A**, lanes 2 and 4). This indicates a starvation-induced phosphorylation of AMPKβ by Ulk1. In summary, we could confirm the data obtained with Flp-In™ T-REx™ 293 cells with MEFs expressing Ulk1 at endogenous levels. Ulk1-mediated phosphorylation of AMPK had a negative effect on its starvation-induced activation and activity. Accordingly, the absence of both Ulk1 and Ulk2 resulted in increased levels of AMPKα Thr172 and Raptor phosphorylation, respectively.

Knockdown of Ulk1 in HEK293 cells increases starvation-induced AMPK activation and activity. Next we wanted to analyze the impact of Ulk1 knockdown on AMPK activity and activation in HEK293 cells. In this cell system, it has previously been shown that only Ulk1 displays a regulatory function in autophagy, whereas Ulk2 appears to be dispensable.[9] We performed RNAi experiments and analyzed the cells under full-nutrient and starvation conditions. By analyzing phosphorylation of AMPKα

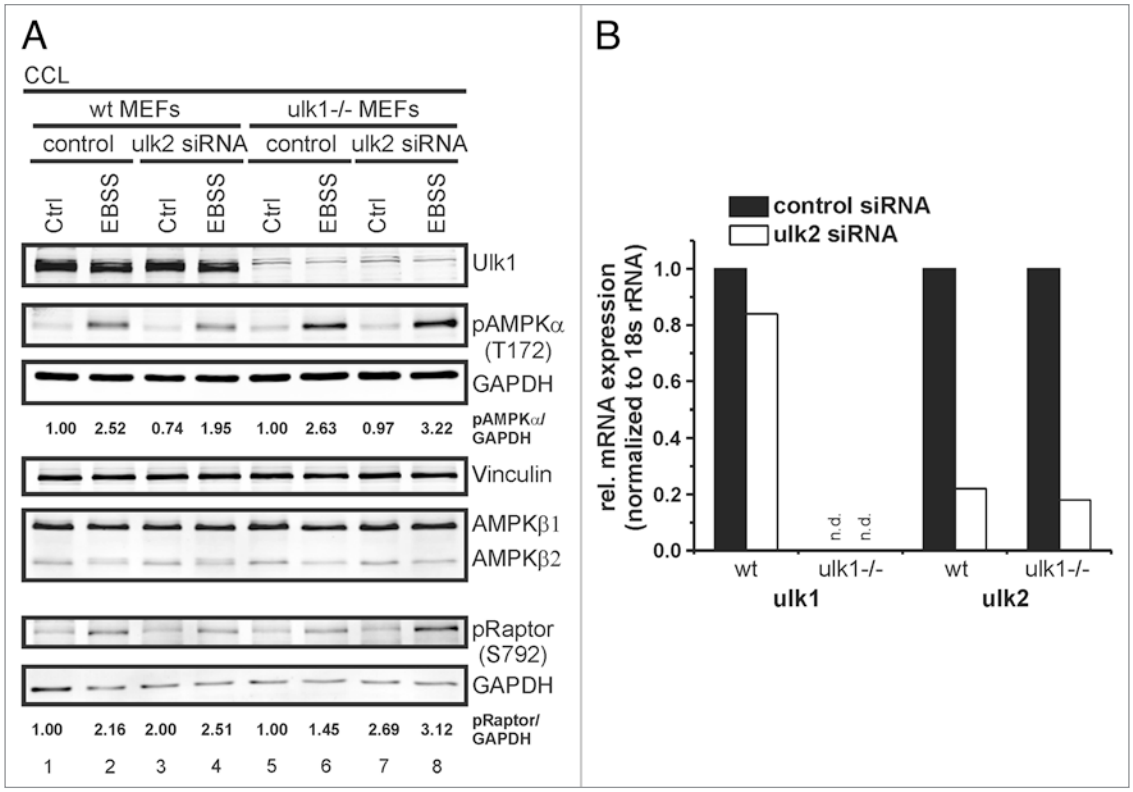

Figure 4. Starvation-induced activation and activity of AMPK is higher in *ulk1*$^{-/-}$ MEFs than in wt MEFs. Wild-type and *ulk1*$^{-/-}$ mouse embryonic fibroblasts were transfected with control siRNA or siRNA targeted against mouse *ulk2*. (A) After 48 h, cells were placed in DMEM with 10% FCS or EBSS for 2 h and subsequently lysed. Cleared cellular lysates were separated by SDS-PAGE and analyzed by immunoblotting using antibodies against mouse Ulk1, phosphoAMPKα (phospho-Thr172), GAPDH, Vinculin, AMPKβ and phosphoRaptor (phospho-Ser792). Ratios of phosphoAMPKα/GAPDH and phosphoRaptor/GAPDH were calculated and are depicted in arbitrary units. (B) Successful knockdown of *ulk2* after 48 h was confirmed by quantitative real-time PCR. n.d., not detectable.

at Thr172 we found that activation of AMPK upon EBSS starvation was increased in *ulk1*-silenced cells compared to wt cells (**Fig. 5A**, lanes 4, 8 and 12). The increased AMPK activation was paralleled by an enhanced AMPK activity as detected by higher phosphorylation of ACC and Raptor in EBSS-starved *ulk1*-silenced cells compared to non-silenced cells (**Fig. 5A**, lanes 4, 8 and 12; **Fig. 5B**). Similar to the MEFs, AMPKβ derived from cells expressing Ulk1 at normal levels showed a reduced migration in SDS-PAGE. Notably, this shift could also be observed in nonstarved cells (**Fig. 5A**, lanes 1, 2, 5, 6, 9 and 10).

As an additional readout for AMPK activity we performed an in vitro AMPK activity assay. To this end we immunopurified AMPK from EBSS-starved HEK293 cells that were transfected with either nontargeting control siRNA or *ulk1* siRNA, respectively. AMPK that was immunopurified from *ulk1*-silenced cells showed a significantly increased activity compared to AMPK from nonsilenced cells (**Fig. 5C and D**). Collectively, in HEK293 cells Ulk1 decreased AMPK activation and activity upon EBSS starvation. This effect was analyzed by knockdown of Ulk1 in HEK293 cells and subsequent immunoblot analyses as well as an AMPK activity assay.

Taken together, in this report we identified a negative regulatory signaling circuit involving Ulk1/2 and AMPK. We could show that the autophagy-relevant kinase Ulk1 regulates AMPK activation and activity by direct phosphorylation of all three AMPK subunits.

Discussion

Recent studies investigating the role of the Atg1/Ulk1 complex have revealed its essential role for the execution of autophagy.[8] Atg1/Ulk1 is the sole protein kinase of the autophagy-related genes, and it is the central signaling node governing the recruitment of downstream Atgs and autophagosome formation. Additionally, recent reports have demonstrated how Ulk1 links signals from mTORC1 and AMPK to the regulation of autophagy. However, to date only a few substrates of Ulk1 have been identified in mammals, e.g., the interacting proteins Atg13 and FIP200. Therefore, current studies aim at the identification of additional Ulk1 substrates. This will be essential for a comprehensive understanding of Ulk1 function in autophagy and other pathways. In this study, using immunopurifications and subsequent mass spectrometric analyses, we showed that Ulk1 interacts with and phosphorylates the heterotrimeric AMPK complex. Furthermore, we demonstrate that the C-terminal domain of Ulk1 is dispensable for both interaction and phosphorylation. Ultimately, we could prove that Ulk1-mediated phosphorylation of AMPK reduced its level of phosphorylation at T172 of the

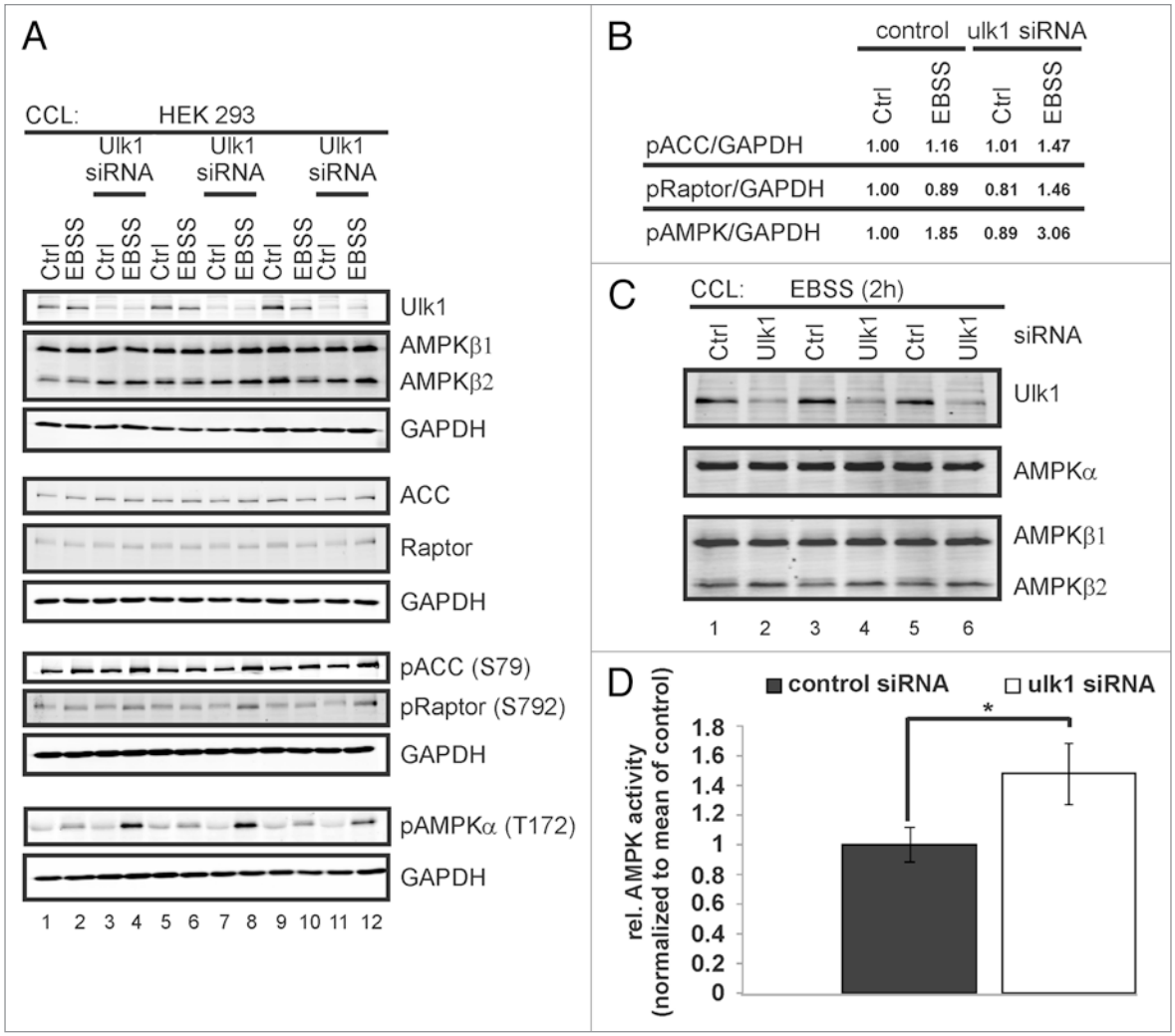

Figure 5. Starvation-induced activation and activity of AMPK is higher in *ulk1* silenced HEK293 cells than in wt HEK293 cells. HEK293 cells were transfected with control siRNA or siRNA targeted against human *ulk1* in triplicates. (A) After 48 h, cells were placed in DMEM with 10% FCS or EBSS for 2 h and subsequently lysed. Cleared cellular lysates were separated by SDS-PAGE and analyzed by immunoblotting using antibodies against Ulk1, AMPKβ, GAPDH, ACC, Raptor, phosphoACC (phospho-Ser79), phosphoRaptor (phospho-Ser792) and phosphoAMPKα (phospho-Thr172). (B) Ratios of phospho-ACC/GAPDH, phosphoRaptor/GAPDH and phosphoAMPKα/GAPDH were calculated and are depicted in arbitrary units. (C and D) For the AMPK-activity assay, cells were placed in EBSS 48 h after transfection for 2 h and subsequently lysed. (C) To validate the knockdown of Ulk1, cleared cellular lysates were separated by SDS-PAGE and analyzed by immunoblotting using antibodies against Ulk1, AMPKα and AMPKβ. (D) To measure AMPK activity, AMPK was purified from cleared cellular lysates and subjected to a non-radioisotopic activity assay (see Materials & Methods for details). Data shown are mean of triplicates ± SEM; *p < 0.05.

α-subunit and hence interferes with its catalytic activity. In summary, the Ulk1-mediated phosphorylation of AMPK establishes a negative feedback loop targeting the AMPK-mTOR signaling axis.

During the preparation of this manuscript, the physical interaction of Ulk1/2 and AMPK has been reported.[26,27] AMPK is required for autophagy in yeast and drosophila. Regarding mammalian autophagy, activated AMPK has been described as a central inhibitor of mTOR and thus as an upstream activator of autophagy. Furthermore, it could be recently demonstrated by two independent groups that AMPK phosphorylates and thereby activates Ulk1.[28,29] This presents a more direct regulation of the Ulk1 complex bypassing mTORC1. Surprisingly, our results show the reverse effect: Ulk1 regulates AMPK activity.

In our experiments, AMPK was co-immunopurified with GFP-Ulk1kd. This observation indicates that neither autophosphorylation of Ulk1 nor phosphorylation of AMPK is required for the interaction of the two kinases. Furthermore, our results reveal that the truncated GFP-Ulk1/ΔCTD can readily phosphorylate AMPK. This indicates that Ulk1 does not have to be in complex with Atg13 and FIP200 to phosphorylate AMPK which is surprising, since other reports show that maximum kinase activity of Ulk1 is achieved when the latter associates with Atg13 and FIP200. Apparently, binding of Atg13 and FIP200 to accomplish maximum kinase activity is not required for phosphorylation of all substrates of Ulk1. Furthermore, one can conclude that the binding sites of Atg13/FIP200 and AMPK are physically separated in Ulk1. Thus, the interaction

of Ulk1 and AMPK does not necessarily prevent binding to Atg13-FIP200.

We demonstrated that starvation-induced activation of AMPK and its activity are decreased in cells expressing GFP-Ulk1wt compared to cells expressing GFP-Ulk1kd (**Fig. 3**). Since the decrease in AMPK activity upon expression of GFP-Ulk1wt under full-nutrient conditions is rather moderate (**Sup. S4**), we hypothesize that Ulk1-mediated phosphorylation of AMPK rather affects AMPK activation and thus only indirectly its activity. This hypothesis is supported by the fact that EBSS-induced activation of AMPK and the resulting phosphorylation of its substrates ACC and Raptor are increased in *ulk1*$^{-/-}$ MEFs and in *ulk1*-silenced HEK293 cells compared to the corresponding wild-type cells. Additionally, the AMPK subunit β2 from wild-type cells shows a reduced migration in SDS-PAGE compared to that derived from cells with reduced or absent Ulk1 expression, suggesting phosphorylation of AMPKβ by endogenous Ulk1.

Regarding a possible mechanism for the reduced AMPK activation following Ulk1-mediated phosphorylation, one might speculate that AMPKα Thr172 phosphorylation by upstream kinases such as LKB1/STRAD/Mo25 or CaMKKβ is impeded by Ulk1 phosphorylation. Since we have mapped the Ulk1-phosphorylation sites in AMPK, future mutational analyses will reveal if and how these phosphorylation events alter the conformation of AMPK subunits, ultimately leading to a decreased Thr172 phosphorylation. Furthermore, they might help to clarify the chronological order and importance of AMPK-mediated Ulk1 phosphorylation and Ulk1-mediated AMPK phosphorylation.

In summary, our results provide an interesting novel catalytic link between the autophagy-regulating Ulk1 and the energy-sensing AMPK. We could show that Ulk1 regulates AMPK activity by direct phosphorylation of all three AMPK subunits. Interestingly, the Atg13/FIP200-binding C-terminal domain of Ulk1 appears to be dispensable for this regulatory function. We propose that phosphorylation of AMPK by Ulk1 decreases AMPK activation, thus establishing a direct negative feedback loop on the AMPK-mTOR and AMPK-Ulk1 signaling axes (**Sup. S5**).

Materials and Methods

Cells. HEK293 cells and Flp-In™ T-REx™ 293 cells (Invitrogen, R780-07) were cultured in DMEM (4.5 g/l D-Glucose), supplemented with 10% FCS, 50 U/ml penicillin and 50 μg/ml streptomycin. Expression of the respective fusion protein was induced with 0.1 μg/ml tetracycline or doxycycline, respectively. For transfection, typically 10-cm-diameter dishes of HEK293 cells were cultured, and each dish was transfected with 5 μg of DNA using polyethylenimine. SV40-immortalized wild-type and *ulk1*$^{-/-}$ MEFs were described previously,[10] and cultured in DMEM (4.5 g/l D-Glucose), supplemented with 10% FCS, 50 U/ml penicillin and 50 μg/ml streptomycin.

Antibodies and proteins. Anti-AMPKα (for immunoblotting and immunopurification, 2603), anti-AMPKβ (4150), anti-phosphoAMPKα (p-Thr172, 2531), anti-Acetyl-CoA-Carboxylase (3662), anti-phosphoAcetyl-CoA-Carboxylase (p-Ser79, 3661), anti-Raptor (2280), anti-phosphoRaptor (p-Ser792, 2083) were obtained from Cell Signaling Technology; anti-GAPDH (clone 6C5, ab8245) was obtained from Abcam; anti-AMPKα (for immunopurification) was provided by the Division of Signal Transduction Therapy (DSTT), University of Dundee; anti-GFP was provided by the Division of Signal Transduction Therapy (DSTT), University of Dundee and Boehringer; anti-FLAG (clone M2) was purchased from Sigma (F3165); anti-Ulk1 was obtained from the DSTT. For the generation of the anti-Ulk1 antibodies, the cDNA coding for the C-terminal domain of Ulk1 (coding for aa 828–1050) was amplified from Jurkat J16 cells and cloned into pGEX-3X (Amersham, 27-4803-01). Expression of the protein and generation of the antibodies was performed by the DSTT. Alternatively, anti-Ulk1 antibodies from Santa Cruz Biotechnology (clone H-240, sc-33182) or Sigma-Aldrich (A7481) were used. IRDye800 and IRDye680 conjugated secondary antibodies were purchased from LI-COR Biosciences (926-32210/11 and 926-68020/21). Secondary antibodies coupled to horseradish peroxidase (used for immunoblotting using enhanced chemiluminescence) were obtained from Thermo Scientific. *Atg13* (Isoform 2) was amplified from human cells. Purification of the protein was performed by the DSTT. The heterotrimeric complex of rat His_6-AMPKα1, human AMPKβ2 and rat AMPKγ1 was purified by the DSTT following the protocol from Neumann et al.[35]

Expression constructs. Full-length and truncated (coding for aa 1–827) human *Ulk1* cDNAs were amplified from Jurkat J16 cells and cloned into the corresponding vectors pcDNA5/FRT/TO-FLAG or pcDNA5/FRT/TO-GFP, respectively. Using the QuikChange® site-directed mutagenesis protocol (Stratagene, 200518), the Mg^{2+}-binding DFG motif of the kinase domain was substituted for AFG (D165A) to generate an Ulk1 kinase-dead (Ulk1kd) mutant construct. The respective expression constructs were co-transfected with pOG44 into Flp-In™ T-REx™ 293 cells (Invitrogen, R780-07). Stable transfectants were selected with 200 μg/ml hygromycin B (Invitrogen, 10687-010) and 5 μg/ml blasticidin (Invitrogen, A11139-02).

RNAi experiments. For siRNA-mediated knockdown of Ulk1 expression in HEK293 cells, 1.3 x 10^5 cells/ml were transfected with ON-TARGETplus siRNA J-005049-06 and J-005049-07 (Dharmacon) against human *Ulk1* at a final concentration of 100 nM (50 nM each siRNA) using DharmaFECT 1 (Dharmacon, T-2001) according to the manufacturer's instructions. After 48 h, cells were placed in DMEM with 10% FCS or EBSS for the indicated times and subsequently lysed for immunoblot analyses or in vitro AMPK activity assays, respectively. For siRNA-mediated knockdown of Ulk2 expression in wild-type and *ulk1*$^{-/-}$ mouse embryonic fibroblasts,[10] 1 x 10^5 cells were transfected with ON-TARGETplus set of four siRNA (Dharmacon, LQ-040619-00-0010) against murine *Ulk2* at a final concentration of 100 nM (25 nM each siRNA) using Lipofectamine RNAiMAX (Invitrogen, 13778075) according to the manufacturer's instructions. After 48 h, cells were either analyzed by quantitative real-time PCR, or placed in DMEM with 10% FCS or EBSS for the indicated times and subsequently lysed for immunoblot analysis. For all RNAi experiments, cells were transfected with

ON-TARGETplus nontargeting pool (Dharmacon, D-001810-10) at equal final concentrations as control.

Quantitative real-time PCR. Quantitative real-time RT-PCR analysis was performed using the ABI Prism 7000 Sequence Detection System (Applied Biosystems) and qPCR Mastermix Plus (Fermentas). The following probes and primers (Sigma-Aldrich) were used: mUlk1 forward, 5'-CAT CGT GGC GCT GTA TGA CT-3'; mUlk1 reverse, 5'-TTA CAA TAC TCC ATG ACC AGG TAG ACA-3'; mUlk2 forward, 5'-GGA ATT GCC CAA CTC TGT CTT T-3'; mUlk2 reverse, 5'-CCC TGT GGA TTA TCC CTT TGC-3'; 18S rRNA forward, 5'-CGG CTA CCA CAT CCA AGG AA-3'; 18S rRNA reverse, 5'-GCT GGA ATT ACC GCG GCT-3'; 18S rRNA probe JOE-5'-TGC TGG CAC CAG ACT TGC CCT C-3'-TAMRA. Total RNA from approximately 2 x 10^6 cells was extracted with the NucleoSpin™ RNA II-Kit (Macherey & Nagel). cDNA was generated from 1 μg of total RNA with 200 units RevertAid H Minus™ reverse transcriptase (Fermentas), 50 μM random hexamers (Fermentas), 400 μM dNTPs (Fermentas) and 1.6 u/μl RiboLock™ RNase inhibitor (Fermentas) in a volume of 25 μl according to the manufacturer's recommendations. Fifty ng of the resulting cDNA were applied to qRT-PCR analyses (20 μl final volume) and amplified in the presence of 200 nM primers and 100 nM probe or 300 nM primers in the case of SYBR Green detection with the standard temperature profile (2 min 50°C, 10 min 95°C, 40 cycles 15 s 95°C, 1 min 60°C). Relative quantification was performed employing the standard curve method. The results were normalized on the reference gene 18S rRNA. The cell population transfected with the control oligonucleotide was used as calibrator.

Kinase assay. Ulk1 was purified from Flp-In™ T-REx™ 293 cells expressing FLAG-Ulk1wt or FLAG-Ulk1kd, respectively. Alternatively, GST-Ulk1 was purified from transiently transfected HEK293 cells. For kinase assays with endogenous Ulk1, this was immunopurified from HEK293 cells. Following three washes with lysis buffer, immunopurifications were additionally washed with Buffer A (see below). Then 1–2 μg of substrate were incubated with the purified kinases in 50 mM Tris/HCl (pH 7.5), 0.1 mM EGTA, 0.1% (v/v) DTT, 5 mM $Mg(CH_3COO)_2$ and 0.1 mM [^{32}P]ATP (PerkinElmer, NEG002X001MC). The reaction was stopped by the addition of SDS sample buffer after 40 min at 30°C. The reaction was subjected to SDS-PAGE. After coomassie staining of the gel, autoradiography was performed. For mapping of the phosphorylation sites nonradioactive ATP was used.

AMPK activity assay. HEK293 cells were transfected with either nontargeting siRNA or siRNA against human *Ulk1*. After 48 h, cells were placed in EBSS for 2 h and subsequently lysed. Then AMPK was immunopurified from 500 μg of cleared cellular lysate and subjected to a nonradioisotopic activity assay using the CycLex AMPK Kinase Assay Kit (CY-1182) according to the manufacturer's instructions.

Buffers. The following buffers were used: Tris lysis buffer [50 mM Tris/HCl, pH 7.5, 1 mM EDTA, 1% (v/v) Triton X-100, 1 mM Na_3VO_4, 50 mM NaF, 5 mM $Na_4P_2O_7$, 0.15 M NaCl, Protease Inhibitor Cocktail (Sigma, P2714)], IP-Tris lysis buffer [50 mM Tris/HCl, pH 7.5, 1 mM EGTA, 1 mM EDTA, 0.3% (w/v) CHAPS or 1% (v/v) Triton X-100, 1 mM Na_3VO_4, 10 mM sodium β-glycerophosphate, 50 mM NaF, 5 mM $Na_4P_2O_7$, 0.27 M sucrose, 0.15 M NaCl, 0.1% (v/v) DTT, 1 mM benzamidine and 0.1 mM PMSF] and Buffer A [50 mM Tris/HCl, pH 7.5, 0.1 mM EGTA and 0.1% (v/v) DTT].

Immuno-/affinity-purifications and immunoblotting. For immunoblotting cells were lysed in Tris lysis buffer. The lysates were clarified by centrifugation at 16,000 g for 15 min at 4°C. Equal total protein amounts (as determined by Bradford) were separated on a SDS-PAGE followed by standard immunoblot analysis. For co-immunopurifications cells were lysed in IP-Tris lysis buffer containing 0.3% CHAPS. Clarified lysates were incubated with either GFP-Trap® Beads (Chromotek, gta-400), Glutathione Sepharose 4B (Amersham, 17-0756-05), Anti-FLAG M2 agarose beads (Sigma, A2220), or the respective antibody in combination with Protein A/G PLUS-Agarose (Santa Cruz Biotechnology, sc-2003) or Protein G Sepharose (Amersham, 17-0618-02) at 4°C for 3 h or o/n with rotation. Purified immunocomplexes were washed three times with IP-Tris lysis buffer.

Mass spectrometry. For the identification of co-immunopurified proteins, GFP-immunopurifications were separated by SDS-PAGE. This was performed using precast BisTris 4–12% gradient polyacrylamide gels in the Mops buffer system (Invitrogen, NP0323) followed by staining with colloidal Coomassie Blue (Invitrogen, LC6025). Gel bands were excised, washed and digested with trypsin. Peptides were extracted with 2.5% (v/v) formic acid/50% (v/v) MeOH and the combined extracts were dried under vacuum.

Mass spectrometric analysis was performed by LC-MS-MS using a linear ion trap-orbitrap hybrid mass spectrometer (LTQ-Orbitrap Classic, Thermo Fisher Scientific) equipped with a nanoelectrospray ion source (Thermo) and coupled to a Proxeon EASY-nLC system. Peptides were typically injected into a PepMap 100 reverse phase C_{18} 3 μm column with a flow of 300 nl/min and eluted with a 30 min linear gradient of 95% solvent A (2% Acetonitrile, 0.1% formic acid in H_2O) to 50% solvent B (90% acetonitrile, 0.08% formic acid in H_2O). The instrument was operated with the "lock mass" option to improve the mass accuracy of precursor ions and data were acquired in the data-dependent mode, automatically switching between MS and MS-MS acquisition. Full scan spectra (m/z 300–1,800) were acquired in the orbitrap with resolution R = 60,000 at m/z 400 (after accumulation to a target value of 500,000). The five most intense ions, above a specified minimum signal threshold, based upon a low resolution (R = 15,000) preview of the survey scan, were fragmented by collision induced dissociation and recorded in the linear ion trap (target value of 10,000). Data was searched against the IPI-Human database using the Mascot search algorithm (www.matrixscience.com).

For the identification of phospho-acceptor sites, kinase assay reactions were first separated by SDS-PAGE and tryptic peptides then prepared both as above for protein identification. Digests were reconstituted and analyzed by LC-MS on a Dionex Ultimate 3000 HPLC system interfaced to an Applied Biosystems 4000 Q TRAP system.

Eluted peptides were typically injected onto a PepMap 100 reverse phase C_{18} 3 μm column with a flow of 300 nl/min and eluted with a 40 min linear gradient of 95% solvent A (2% acetonitrile, 0.1% formic acid in H_2O) to 50% solvent B (90% acetonitrile, 0.08% formic acid in H_2O). A Harvard syringe pump was used to deliver isopropanol at a flow of 100 nl/min with mixing occurring at a T-junction after the LC and prior to the MS. Phosphopeptides were identified and analyzed by the use of a precursor ion scan of m/z-79 in negative ion mode followed by an ion trap high resolution scan (an enhanced resolution scan) and a high sensitivity MS/MS scan (enhanced product ion scan) in positive mode.[36] MS/MS spectra were searched against local databases using Mascot and sites of phosphorylation were manually assigned from individual MS/MS spectra viewed using a combination of the Mascot data and Analyst software (MDS-Sciex).

Alternatively, phospho-acceptor sites were identified by the following protocol. Elution of proteins was performed by boiling the beads in LDS loading buffer at 95°C for 5 min and the eluates were subjected to a NuPAGE Bis-Tris 4%–12% gradient gel (Invitrogen, Germany). Coomassie stained AMPK bands were digested in gel using trypsin as described elsewhere.[37] Resulting peptide mixtures were desalted using C_{18} StageTips.[38] Peptide separation and analysis was done on a Proxeon Easy-LC system (Proxeon Biosystems, Denmark) coupled to a LTQ-Orbitrap-XL (Thermo Fisher Scientific, Germany) equipped with a nano-electrospray LC-MS interface (Proxeon Biosystems, Denmark). Chromatographic separations of the peptides were performed in a 15 cm fused silica emitter of 75 μm inner diameter in-house packed[39] with reversed-phase ReproSil-Pur C_{18}-AQ 3 μm resin (Dr. Maisch GmbH, Ammerbuch-Entringen, Germany). Peptides were subsequently eluted using a segmented gradient of 5–80% solvent B (80% ACN, 0.5% acetic acid) over 128 min. Full scan MS spectra were acquired in a mass range from *m/z* 300 to 2,000 at a resolution of 60,000 using the lock-mass option for internal calibration.[40] The five most intense ions were sequentially isolated for fragmentation in the linear ion trap using collisionally induced dissociation with normalized collision energy of 35% at a target value of 5,000 charges. Multistage activation of ions at -98, -49 and -32.6 Th relative to the precursor ion was enabled. Mass spectra were analyzed using the software suite MaxQuant, version 1.0.14.3.[41] The data were searched using Mascot search engine (Matrix Science, UK) against a decoy human database (ipi.HUMAN.v3.64), containing protein sequences of AMPKα1, AMPKβ2, AMPKγ1, GFP-ULK1wt and GFP-ULK1kd. The database contained 179428 forward and reversed protein entries. The following database search criteria were applied: mass tolerance 7 ppm (precursor ions) and 0.5 Da (fragment ions); full trypsin specificity was required and two missed cleavages were allowed. Localization of the phosphate groups was determined as described previously,[42] AMPK spectra were further manually validated.

Acknowledgements

We thank M. Deak, MRC Protein Phosphorylation University of Dundee, for cloning GST-Atg13 and FLAG-Ulk2 and the antibody and protein purification teams of the Division of Signal Transduction Therapy (DSTT), University of Dundee, for providing antibodies, GST-Atg13 and His-AMPK$\alpha_1\beta_2\gamma_1$. We are grateful to G. Hardie, K. Sakamoto and N. Morrice for helpful discussions. This work was supported by grants from the Deutsche Forschungsgemeinschaft SFB 773 (to S.W. and B.S.), GRK 1302 (to S.W. and B.S.), from the Interdisciplinary Center of Clinical Research, Faculty of Medicine, Tübingen (Nachwuchsgruppe 1866-0-0, to B.S.) and the UK Medical Research Council (to D.R.A. and D.G.C.). The DSTT Unit (D.R.A. and D.G.C.) is supported by the following pharmaceutical companies: AstraZeneca, Boehringer-Ingelheim, GlaxoSmithKline, Merck-Serono and Pfizer. The authors declare that there are no competing financial interests in relation to this work.

Note

Supplemental materials can be found at:
www.landesbioscience.com/journals/autophagy/article/15451

References

1. Klionsky DJ. Autophagy: from phenomenology to molecular understanding in less than a decade. Nat Rev Mol Cell Biol 2007; 8:931-7.
2. Mizushima N. Autophagy: process and function. Genes Dev 2007; 21:2861-73.
3. Levine B, Kroemer G. Autophagy in the pathogenesis of disease. Cell 2008; 132:27-42.
4. Mizushima N, Levine B, Cuervo AM, Klionsky DJ. Autophagy fights disease through cellular self-digestion. Nature 2008; 451:1069-75.
5. Yang Z, Klionsky DJ. Eaten alive: a history of macroautophagy. Nat Cell Biol 2010; 12:814-22.
6. Matsuura A, Tsukada M, Wada Y, Ohsumi Y. Apg1p, a novel protein kinase required for the autophagic process in *Saccharomyces cerevisiae*. Gene 1997; 192:245-50.
7. Chan EY, Tooze SA. Evolution of Atg1 function and regulation. Autophagy 2009; 5:758-65.
8. Mizushima N. The role of the Atg1/ULK1 complex in autophagy regulation. Curr Opin Cell Biol 2010; 22:132-9.
9. Chan EY, Kir S, Tooze SA. siRNA screening of the kinome identifies ULK1 as a multidomain modulator of autophagy. J Biol Chem 2007; 282:25464-74.
10. Kundu M, Lindsten T, Yang CY, Wu J, Zhao F, Zhang J, et al. Ulk1 plays a critical role in the autophagic clearance of mitochondria and ribosomes during reticulocyte maturation. Blood 2008; 112:1493-502.
11. Jung CH, Jun CB, Ro SH, Kim YM, Otto NM, Cao J, et al. ULK-Atg13-FIP200 complexes mediate mTOR signaling to the autophagy machinery. Mol Biol Cell 2009; 20:1992-2003.
12. Tomoda T, Kim JH, Zhan C, Hatten ME. Role of Unc51.1 and its binding partners in CNS axon outgrowth. Genes Dev 2004; 18:541-58.
13. Chan EY, Longatti A, McKnight NC, Tooze SA. Kinase-inactivated ULK proteins inhibit autophagy via their conserved C-terminal domains using an Atg13-independent mechanism. Mol Cell Biol 2009; 29:157-71.
14. Hosokawa N, Hara T, Kaizuka T, Kishi C, Takamura A, Miura Y, et al. Nutrient-dependent mTORC1 association with the ULK1-Atg13-FIP200 complex required for autophagy. Mol Biol Cell 2009; 20:1981-91.
15. Hardie DG, Carling D. The AMP-activated protein kinase—fuel gauge of the mammalian cell? Eur J Biochem 1997; 246:259-73.
16. Meley D, Bauvy C, Houben-Weerts JH, Dubbelhuis PF, Helmond MT, Codogno P, et al. AMP-activated protein kinase and the regulation of autophagic proteolysis. J Biol Chem 2006; 281:34870-9.
17. Meijer AJ, Codogno P. AMP-activated protein kinase and autophagy. Autophagy 2007; 3:238-40.
18. Høyer-Hansen M, Jäättelä M. AMP-activated protein kinase: a universal regulator of autophagy? Autophagy 2007; 3:381-3.
19. Grotemeier A, Alers S, Pfisterer SG, Paasch F, Daubrawa M, Dieterle A, et al. AMPK-independent induction of autophagy by cytosolic Ca^{2+} increase. Cell Signal 2010; 22:914-25.
20. Vingtdeux V, Giliberto L, Zhao H, Chandakkar P, Wu Q, Simon JE, et al. AMP-activated protein kinase signaling activation by resveratrol modulates amyloid-beta peptide metabolism. J Biol Chem 2010; 285:9100-13.
21. Papandreou I, Lim AL, Laderoute K, Denko NC. Hypoxia signals autophagy in tumor cells via AMPK activity, independent of HIF-1, BNIP3 and BNIP3L. Cell Death Differ 2008; 15:1572-81.
22. Hawley SA, Boudeau J, Reid JL, Mustard KJ, Udd L, Makela TP, et al. Complexes between the LKB1 tumor suppressor, STRAD alpha/beta and MO25 alpha/beta are upstream kinases in the AMP-activated protein kinase cascade. J Biol 2003; 2:28.

23. Zeqiraj E, Filippi BM, Deak M, Alessi DR, van Aalten DM. Structure of the LKB1-STRAD-MO25 complex reveals an allosteric mechanism of kinase activation. Science 2009; 326:1707-11.
24. Hardie DG. AMPK and Raptor: matching cell growth to energy supply. Mol Cell 2008; 30:263-5.
25. Ganley IG, Lam du H, Wang J, Ding X, Chen S, Jiang X. ULK1.ATG13.FIP200 complex mediates mTOR signaling and is essential for autophagy. J Biol Chem 2009; 284:12297-305.
26. Behrends C, Sowa ME, Gygi SP, Harper JW. Network organization of the human autophagy system. Nature 2010; 466:68-76.
27. Lee JW, Park S, Takahashi Y, Wang HG. The association of AMPK with ULK1 regulates autophagy. PLoS One 2010; 5:15394.
28. Egan DF, Shackelford DB, Mihaylova MM, Gelino S, Kohnz RA, Mair W, et al. Phosphorylation of ULK1 (hATG1) by AMP-activated protein kinase connects energy sensing to mitophagy. Science 2011; 331:456-61.
29. Kim J, Kundu M, Viollet B, Guan KL. AMPK and mTOR regulate autophagy through direct phosphorylation of Ulk1. Nat Cell Biol 2011; 13:132-41.
30. Hardie DG. AMPK and autophagy get connected. EMBO J 2011; 30:634-5.
31. Di Bartolomeo S, Corazzari M, Nazio F, Oliverio S, Lisi G, Antonioli M, et al. The dynamic interaction of AMBRA1 with the dynein motor complex regulates mammalian autophagy. J Cell Biol 2010; 191:155-68.
32. Yu L, McPhee CK, Zheng L, Mardones GA, Rong Y, Peng J, et al. Termination of autophagy and reformation of lysosomes regulated by mTOR. Nature 2010; 465:942-6.
33. Koren I, Reem E, Kimchi A. DAP1, a novel substrate of mTOR, negatively regulates autophagy. Curr Biol 2010; 20:1093-8.
34. Hardie DG. AMP-activated/SNF1 protein kinases: conserved guardians of cellular energy. Nat Rev Mol Cell Biol 2007; 8:774-85.
35. Neumann D, Woods A, Carling D, Wallimann T, Schlattner U. Mammalian AMP-activated protein kinase: functional, heterotrimeric complexes by co-expression of subunits in *Escherichia coli*. Protein Expr Purif 2003; 30:230-7.
36. Williamson BL, Marchese J, Morrice NA. Automated identification and quantification of protein phosphorylation sites by LC/MS on a hybrid triple quadrupole linear ion trap mass spectrometer. Mol Cell Proteomics 2006; 5:337-46.
37. Borchert N, Dieterich C, Krug K, Schutz W, Jung S, Nordheim A, et al. Proteogenomics of *Pristionchus pacificus* reveals distinct proteome structure of nematode models. Genome Res 2010; 20:837-46.
38. Rappsilber J, Mann M, Ishihama Y. Protocol for micro-purification, enrichment, pre-fractionation and storage of peptides for proteomics using StageTips. Nat Protoc 2007; 2:1896-906.
39. Ishihama Y, Rappsilber J, Andersen JS, Mann M. Microcolumns with self-assembled particle frits for proteomics. J Chromatogr A 2002; 979:233-9.
40. Olsen JV, de Godoy LM, Li G, Macek B, Mortensen P, Pesch R, et al. Parts per million mass accuracy on an Orbitrap mass spectrometer via lock mass injection into a C-trap. Mol Cell Proteomics 2005; 4:2010-21.
41. Cox J, Matic I, Hilger M, Nagaraj N, Selbach M, Olsen JV, et al. A practical guide to the MaxQuant computational platform for SILAC-based quantitative proteomics. Nat Protoc 2009; 4:698-705.
42. Olsen JV, Blagoev B, Gnad F, Macek B, Kumar C, Mortensen P, et al. Global, in vivo and site-specific phosphorylation dynamics in signaling networks. Cell 2006; 127:635-48.

Autophagy 7:12, 1424–1433; December 2011; © 2011 Landes Bioscience

Atg13 and FIP200 act independently of Ulk1 and Ulk2 in autophagy induction

Sebastian Alers,[1] Antje S. Löffler,[1,†] Florian Paasch,[1,‡] Alexandra M. Dieterle,[1] Hildegard Keppeler,[1] Kirsten Lauber,[2] David G. Campbell,[3] Birgit Fehrenbacher,[4] Martin Schaller,[4] Sebastian Wesselborg[1,†] and Björn Stork[1,†,*]

[1]Department of Internal Medicine I; University Clinic of Tübingen; Tübingen, Germany; [2]Molecular Oncology; Department of Radiation Oncology; Ludwig-Maximilians-University; Munich, Germany; [3]MRC Protein Phosphorylation Unit; College of Life Sciences; University of Dundee; Dundee Scotland, UK; [4]Department of Dermatology; University of Tübingen; Tübingen, Germany

Current Affiliation: [†]Institute of Molecular Medicine; Heinrich-Heine-University; Düsseldorf, Germany; [‡]Department of Molecular Cell Biology; Max Planck Institute of Biochemistry; Martinsried, Germany

Keywords: Atg13, autophagy, FIP200, Ulk1, Ulk2

Under normal growth conditions the mammalian target of rapamycin complex 1 (mTORC1) negatively regulates the central autophagy regulator complex consisting of Unc-51-like kinases 1/2 (Ulk1/2), focal adhesion kinase family-interacting protein of 200 kDa (FIP200) and Atg13. Upon starvation, mTORC1-mediated repression of this complex is released, which then leads to Ulk1/2 activation. In this scenario, Atg13 has been proposed as an adaptor mediating the interaction between Ulk1/2 and FIP200 and enhancing Ulk1/2 kinase activity. Using Atg13-deficient cells, we demonstrate that Atg13 is indispensable for autophagy induction. We further show that Atg13 function strictly depends on FIP200 binding. In contrast, the simultaneous knockout of Ulk1 and Ulk2 did not have a similar effect on autophagy induction. Accordingly, the Ulk1-dependent phosphorylation sites we identified in Atg13 are expendable for this process. This suggests that Atg13 has an additional function independent of Ulk1/2 and that Atg13 and FIP200 act in concert during autophagy induction.

Introduction

Macroautophagy (hereafter referred to as autophagy) is an essential and highly conserved lysosomal degradation process, helping to maintain cellular homeostasis by constitutive turnover of cytoplasmic material. Cellular components, such as long-lived proteins and entire organelles, are sequestered by a double membrane known as the isolation membrane or phagophore. After closure, the resulting autophagosome subsequently fuses with lysosomes, leading to the degradation of its content. The provided amino acids can be reused for protein synthesis as well as an energy source for ATP production. By this means, autophagy represents a cellular adaptation mechanism to starvation, and is hence strongly enhanced after nutrient deprivation. Despite its essential role for cell growth, survival and development, the molecular details of autophagy induction and its underlying signaling cascade are still poorly understood.

In yeast, two serine/threonine protein kinases could be identified as essential prerequisites for the regulation of autophagy induction. The nutrient-sensing kinase target of rapamycin (TOR) inhibits autophagy induction under nutrient-rich conditions through negative regulation of another serine/threonine kinase, Atg1. In yeast, Atg1 differentially interacts with the regulatory proteins Atg13 and Atg17, which are both important for Atg1 kinase activity.[1,2] Under normal growth conditions Atg13 is hyperphosphorylated in a TOR-dependent manner. Upon starvation or rapamycin treatment, it is immediately dephosphorylated, leading to Atg1-Atg13-Atg17 complex formation and autophagy induction.

Vertebrates have at least two Atg1 homologs, Unc-51-like kinase 1 (Ulk1) and Ulk2,[3-6] that seem to fulfill partially redundant functions.[7-9] Although there is no Atg17 homolog, the focal adhesion kinase family-interacting protein of 200 kDa (FIP200) has been proposed as the functional counterpart of Atg17.[8] Furthermore, a vertebrate homolog of Atg13 has been predicted by sequence homology[10] and has already been proven to be relevant for autophagy induction.[7] Ulk1/2, Atg13 and FIP200 form a large, stable complex of >3 MDa that, in contrast to the yeast Atg1-Atg13-Atg17 complex, is insensitive to the cellular nutrient status. Recently, several groups have simultaneously characterized the molecular details of this Ulk-Atg13-FIP200 complex and even more important, its direct regulation by mTOR complex 1 (mTORC1).[11-15] Under nutrient-rich conditions mTORC1 joins the Ulk-Atg13-FIP200 complex, via interaction between Raptor and Ulk1/2,[14] and mTOR directly phosphorylates Atg13 and Ulk1/2[13-15] presumably at inhibitory sites, to suppress the kinase activity of Ulk1/2. Under starvation conditions or when mTORC1 activity is repressed, Ulk1/2

*Correspondence to: Björn Stork; Email: bjoern.stork@uni-duesseldorf.de
Submitted: 03/28/11; Revised: 08/28/11; Accepted: 09/08/11
http://dx.doi.org/10.4161/auto.7.12.18027

phosphorylates FIP200 and Atg13 at yet unknown sites, and the entire complex translocates to phagophore assembly sites.[11,14,15] Thus, it is reasonable to assume that the phosphorylation of either FIP200 or Atg13 by Ulk1/2 is a prerequisite for this translocation and in turn for autophagy induction.

Using a newly generated Atg13-deficient cell line, we show that Atg13 is indispensable for starvation-induced autophagy as well as basal autophagy under normal growth conditions and that direct interaction with FIP200 is essential for this function. Interestingly, double knockout of Ulk1 and Ulk2 had no significant effect on LC3 lipidation and autophagosome formation. Accordingly, the Ulk1-dependent phosphorylation sites we identified in human Atg13 are not essential for Atg13 function. Since mTOR inhibition does not fully resemble autophagy induction by starvation, we conclude that Atg13 and FIP200 act in concert during induction of autophagy, but this function does not necessarily depend on the mTOR-mediated regulation of Ulk1 or Ulk2 kinase activity.

Results

Generation of Atg13 knockout cell line. The essential role of Atg13 for TOR-mediated autophagy induction has initially been shown in a genetic screening of *Saccharomyces cerevisiae* for autophagy defective mutants.[2,16] The necessity of Atg13 seems to be conserved in higher metazoans, due to the complete autophagy-defective phenotype of the respective *Drosophila melanogaster* knockout mutant.[12] Until now, the importance of Atg13 for autophagy in higher vertebrates has been confirmed by siRNA-mediated knockdown. However, the observed effects vary depending on the respective cell line, the Atg13 knockdown efficiency and the readout used.[11,13-15]

To analyze the role of Atg13 and its regulation by Ulk1 and Ulk2 in a genetically defined background, we first generated Atg13-deficient DT40 knockout cells by disrupting exon 1 of the *atg13* gene (**Fig. S1A and S1B**). The DT40 cell system has already successfully been used to analyze autophagic processes.[17-19] Notably, the primary structure of Atg13 is highly conserved between *Homo sapiens* and *Gallus gallus*, showing 92% amino acid identity (**Fig. S1C**). Four independent homozygous *atg13*$^{-/-}$ clones could be identified by genomic PCR, which have lost both wild-type alleles (**Fig. S1B**). The complete lack of protein expression was confirmed by immunoblotting for endogenous Atg13 protein (**Fig. 1A**).

Atg13 deficiency blocks autophagy induction. In order to analyze their autophagic capacity, we first studied LC3 lipidation and autophagosome formation using fluorescently labeled chicken LC3B (mCitrine-LC3B) in wild-type and *atg13*$^{-/-}$ cells in the presence and absence of bafilomycin A_1. LC3 is a cytosolic protein that is lipidated by the autophagic machinery during autophagosome formation (LC3-II) and is thus recruited to autophagosomes.[20] The vacuolar H^+-ATPase inhibitor bafilomycin A_1 prevents the lysosomal degradation of autophagosomes[21] and therefore is frequently used to analyze the autophagic flux.

Strikingly, while bafilomycin A_1 significantly increased the number and size of autophagosomes in wild-type DT40 cells, no dot formation could be observed in *atg13*$^{-/-}$ cells (**Fig. 1B**). Next, we investigated the effect of Atg13 knockout on LC3 lipidation by immunoblotting. In wild-type cells, incubation with bafilomycin A_1 led to a prominent accumulation of endogenous and fluorescently labeled LC3-II under normal growth conditions (**Fig. 1C**, lanes 1 and 2), while *atg13*$^{-/-}$ cells showed almost no detectable accumulation of lipidated LC3 (**Fig. 1C**, lanes 3 and 4). Strikingly, in wild-type cells endogenous LC3 lipidation could be further enhanced by starvation in EBSS (**Fig. 1D**, lanes 1–4). In contrast, *atg13*$^{-/-}$ cells did not show any prominent accumulation of lipidated LC3 after starvation (**Fig. 1D**, lanes 5–8). Notably, the reconstitution of *atg13*$^{-/-}$ cells with HA-tagged full-length chicken Atg13 was partially able to rescue the autophagy-defective phenotype (**Fig. 1D**, lanes 9–12). In order to verify that LC3 lipidation correlates with autophagosome formation, we further investigated the presence of autophagosomes by transmission electron microscopy. While wild-type DT40 cells displayed numerous double-membrane autophagosomes per cell after starvation (**Fig. 2A**), almost no autophagosomes could be detected in *atg13*$^{-/-}$ cells (**Fig. 2B**). Noteworthy, Atg13-deficient cells in contrast displayed enlarged and swollen mitochondria under starvation conditions (**Fig. 2B**). In addition, we investigated the formation of autolysosomes using a tandem mRFP-EGFP-rLC3 construct.[22] Again, while wild-type DT40 cells showed numerous autophagosomes and autolysosomes after 2 h starvation in EBSS (**Fig. 2C**), mRFP-EGFP-rLC3 was mainly distributed throughout the cytoplasm in *atg13*$^{-/-}$ cells and almost no autolysosomes could be detected in these cells (**Fig. 2D**).

Collectively, these results indicate that in DT40 cells Atg13 is essential for autophagy induction and autophagosome generation under starvation conditions as well as for basal autophagy.

Deficiency for Ulk1 and Ulk2 does not resemble the phenotype of Atg13 knockout. Based on previous observations,[12-15] the following attractive working model has been proposed for starvation-induced autophagy:[11] Under nutrient-rich growth conditions, mTORC1 associates with the Ulk-Atg13-FIP200 complex, phosphorylates Ulk1 and Atg13, and is thereby suppressing Ulk1 kinase activity. Following starvation, Ulk1 phosphorylates both Atg13 and FIP200, finally leading to autophagy induction.[11]

Since Ulk2 was reported to compensate for the lack of Ulk1,[9,23] we generated DT40 cells deficient for both Ulk1 and Ulk2 (for targeting strategies see **Fig. S2A and S2B**). Starting from *ulk1*$^{-/-}$ cells (clone 16–10), two homozygous *ulk1*$^{-/-}$*ulk2*$^{-/-}$ cell lines (2–6 and 17–16) could be identified by genomic PCR (**Fig. S2C**). The complete absence of transcripts was verified by RT-PCR (**Fig. 3A**) and quantitative real-time PCR (**Fig. S6B**).

Interestingly, neither the single-deficient *ulk1*$^{-/-}$ and *ulk2*$^{-/-}$ cells (**Fig. S3A**) nor both double-deficient *ulk1*$^{-/-}$*ulk2*$^{-/-}$ cell lines resembled the phenotype of *atg13*$^{-/-}$ cells since the absence of Ulk1 and Ulk2 had obviously no effect on starvation-induced autophagy. Autophagy induction was assessed by endogenous LC3 lipidation in the presence and absence of bafilomycin A_1 (**Fig. 3B**), autophagosome generation using electron microscopy (**Fig. 3C, S3B and S3C**) and autolysosome formation using the mRFP-EGFP-rLC3 tandem construct (**Fig. 3D**).

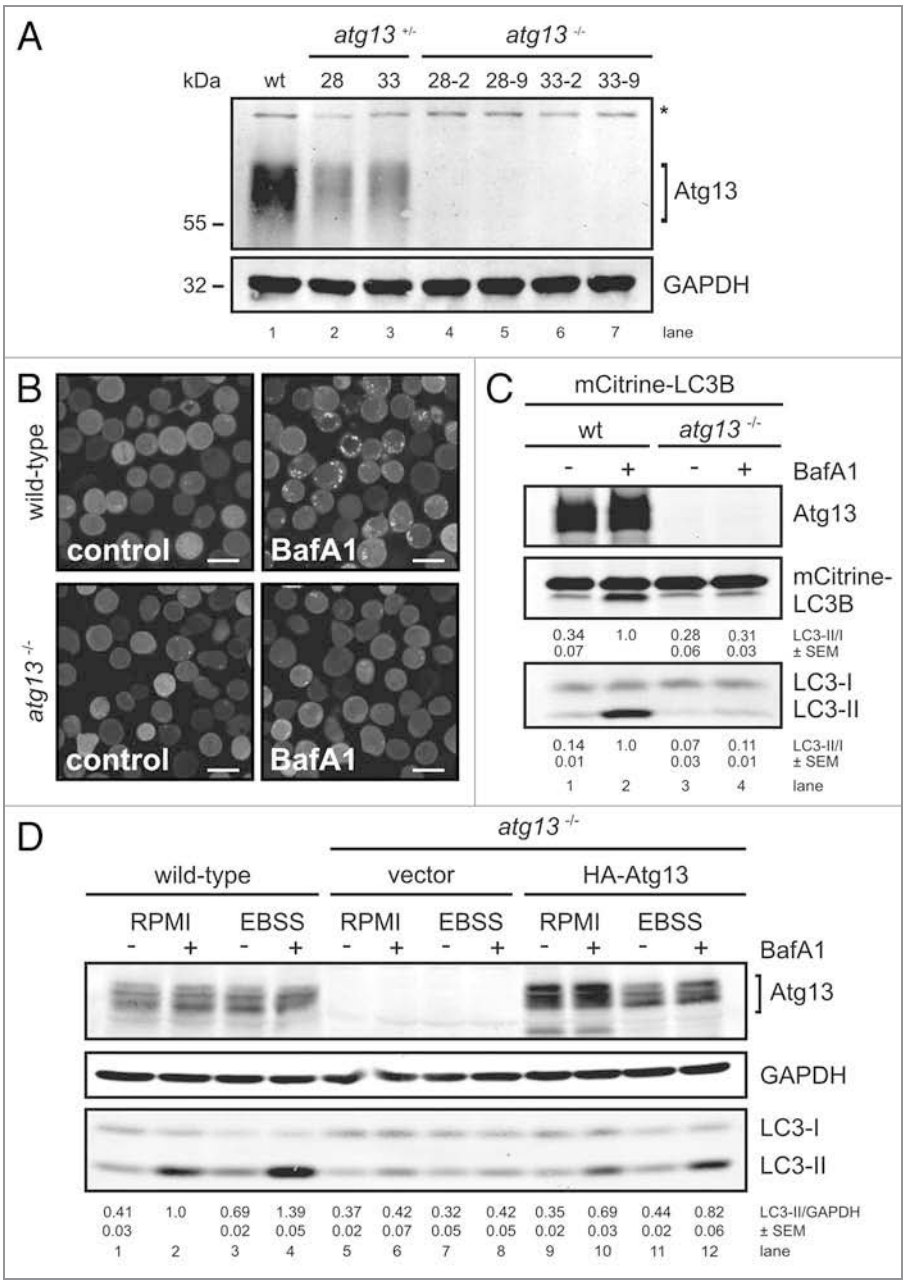

Figure 1. Generation of Atg13-deficient DT40 cells. (A) Atg13-deficient DT40 B cell lines (*atg13*$^{-/-}$) were generated by targeted disruption of both *atg13* alleles. Successful targeting was confirmed by genomic PCR using primers specific for wild-type, hisD- or bsr-targeted alleles (see **Fig. S1** for details). Equal amounts of protein from cleared cellular lysates of either wild-type (wt) cells (lane 1), *atg13*$^{+/-}$ clones (lanes 2–3) and *atg13*$^{-/-}$ clones (lanes 4–7) were analyzed for Atg13 and GAPDH by immunoblotting. The asterisk indicates an unspecific background band. (B) Wild-type and *atg13*$^{-/-}$ DT40 cells, retrovirally transfected with cDNA encoding mCitrine-LC3B, were treated with 10 nM bafilomycin A_1 (BafA1) or DMSO (control) for 6 h and directly visualized by confocal laser scanning microscopy (bars: 10 μm). (C) Cleared cellular lysates of cells described in (B) were subjected to anti-Atg13 and anti-LC3 immunoblotting. LC3-II/LC3-I ratios are represented as mean values of three independent experiments ± SEM (D) *atg13*$^{-/-}$ cells reconstituted with HA-tagged full-length chicken Atg13 isoform A (lanes 9–12) were incubated in normal growth medium (RPMI) or starvation medium (EBSS) for 1 h in the presence or absence of 10 nM (BafA1). Equal protein amounts from cleared cellular lysates were analyzed for Atg13, GAPDH and LC3 by immunoblotting. As control, wild-type cells (lanes 1–4) and *atg13*$^{-/-}$ cells reconstituted with empty vector (lanes 5–8) were analyzed in parallel. LC3-II/GAPDH ratios are represented as mean values of three independent experiments ± SEM.

We additionally found that the five Ulk1-dependent in vitro phosphorylation sites we could identify in human Atg13 were dispensable for Atg13 function in DT40 cells (**Fig. S4 and S5**). Although it is commonly accepted that only the highly related Ulk1 and Ulk2 have the capability to interact with Atg13 via their unique C-terminal domain (**Fig. S6A**) and thus can complement each other, it is nevertheless conceivable that one of the other Ulk homologs (Ulk3, Ulk4 and STK36/Fused) may regulate

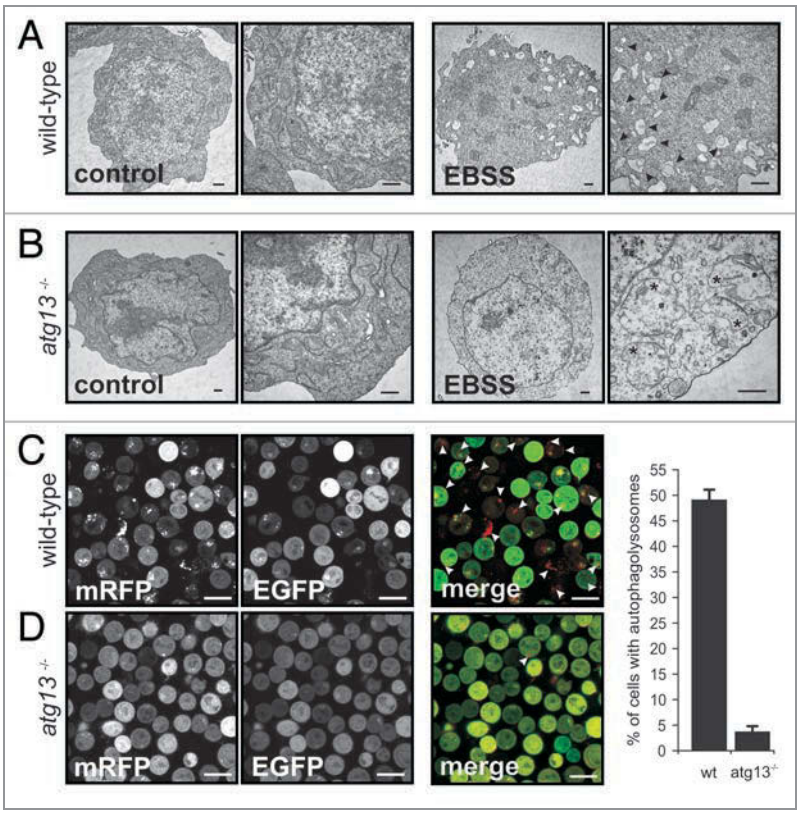

Figure 2. Atg13 is essential for autophagosome generation (A) DT40 wild-type and (B) *atg13*$^{-/-}$ cells were incubated in normal growth medium (control) or EBSS for 2 h. Cells were fixed and analyzed by transmission electron microscopy. A representative cell from each condition is shown in two different magnifications. Autophagosomes are indicated by black arrow heads in the image with higher magnification, swollen mitochondria are indicated by asterisks (bars: 500 nm). (C) Wild-type and (D) *atg13*$^{-/-}$ cells, retrovirally transfected with cDNA encoding mRFP-EGFP-rLC3 were incubated in EBSS for 2 h and analyzed by confocal laser scanning microscopy. The mRFP signal is shown in red and the EGFP signal in green in the merged image. Autolysosomes are indicated by white arrow heads (bars: 10 μm). The percentage of autolysosome containing cells (>200 cells/experiment) is represented as mean ± range of two independent experiments.

starvation-induced autophagy in the absence of Ulk1 and Ulk2. To address this question, we analyzed the abundance of all known Ulk homologs (Ulk1, Ulk2, Ulk3, Ulk4 and STK36/Fused) by quantitative real-time PCR in wild-type DT40 cells, *ulk1*$^{-/-}$, *ulk2*$^{-/-}$ and both double-deficient *ulk1*$^{-/-}$*ulk2*$^{-/-}$ cell lines (**Fig. S6B**). Ulk2 seems to be the most highly abundant Ulk homolog in wild-type DT40 cells. Notably, none of the other Ulk homologs is significantly upregulated in the *ulk1*$^{-/-}$*ulk2*$^{-/-}$ cells. Since Ulk3 has been implicated in autophagy induction after overexpression[24] and *ulk3* mRNA is found at moderate levels in DT40 cells (**Fig. S6B**), we analyzed autophagy induction after transient siRNA mediated knockdown of Ulk3 in the *ulk1*$^{-/-}$*ulk2*$^{-/-}$ cells. However, starvation-induced autophagy was not affected by additional Ulk3 downregulation (**Fig. S6C**).

These results strongly suggest that in DT40 cells, the crucial function of Atg13 in autophagy induction is autonomous from Ulk1 and Ulk2. This surprising finding might be further explained by the fact that in our cells mTOR appears to play a minor role in autophagy induction. While starvation in EBSS leads to a prominent LC3-II accumulation already after 1 h, direct mTOR inhibition by rapamycin or Torin1 does not show a similar effect, although mTOR activity is repressed almost immediately (**Fig. S7A–C**). Interestingly, Atg13 did not display an altered migrational behavior in SDS-PAGE after starvation or mTOR inhibition (**Fig. S7D**). Thus, we conclude that Atg13 has an additional function in starvation-induced autophagy independent of mTORC1-regulated Ulk1/2 kinase activity.

Atg13 function depends on FIP200 binding. Since Ulk1 and Ulk2 seem to be dispensable for autophagy induction in this cell line, we investigated next whether FIP200 binding is essential for Atg13 function, or if Atg13 has additional functions completely independent of the Ulk1/2-Atg13-FIP200 complex.

Interestingly, during cloning of chicken Atg13 we found that *atg13* mRNA is alternatively spliced in DT40 cells (**Fig. 4A**), which is consistent with previous findings in other species.[15] We determined the absolute abundance of these isoforms (named A-G) by quantitative real-time PCR using splice variant-specific primer combinations (**Fig. S8A**) and found that the full-length splice variant A, corresponding to human isoform 2[15], is most highly expressed (**Fig. 4B**). Although the additional exon found in human isoform 1 is present on genomic level, it is not part of mature mRNA in DT40 cells (data not shown). Notably, this high variety of splice variants implicates a rather complex regulatory mechanism and hence might explain the incomplete reconstitution of *atg13*$^{-/-}$ cells with a single isoform (**Fig. 1D**).

In order to analyze their capacity to interact with FIP200 we transfected *atg13*$^{-/-}$ cells and *ulk1*$^{-/-}$*ulk2*$^{-/-}$ cells with cDNAs encoding HA-tagged versions of these splice variants and immunopurified Atg13 using anti-HA agarose. The cDNA of isoform C was generated by molecular cloning and is not expressed at detectable level (**Fig. 4B**). Interestingly, FIP200 could be successfully co-immunopurified only with isoforms containing exon 12 both in the presence (**Fig. 4C**) and absence of Ulk1 and Ulk2 (**Fig. S8B**). This suggests that the FIP200 binding site within Atg13, previously narrowed down to the C-terminal region by Jung et al.,[15] is exclusively encoded by exon 12 and that the interaction between Atg13 and FIP200 does not depend on Ulk1 and Ulk2. Accordingly, only isoforms capable of FIP200 interaction (B and E) were able to reconstitute the autophagy-defective phenotype in *atg13*$^{-/-}$ cells to the same extent as full-length isoform A (**Fig. 5A**). Furthermore, only the full-length isoform A but not isoform C (Δexon12) was able to efficiently restore autophagolysosome generation in *atg13*$^{-/-}$ cells (**Fig. 5B**). These results clearly demonstrate that in DT40 cells, Atg13 has an essential function for basal as well as starvation-induced autophagy. It appears that this function necessarily requires the FIP200 binding capacity of

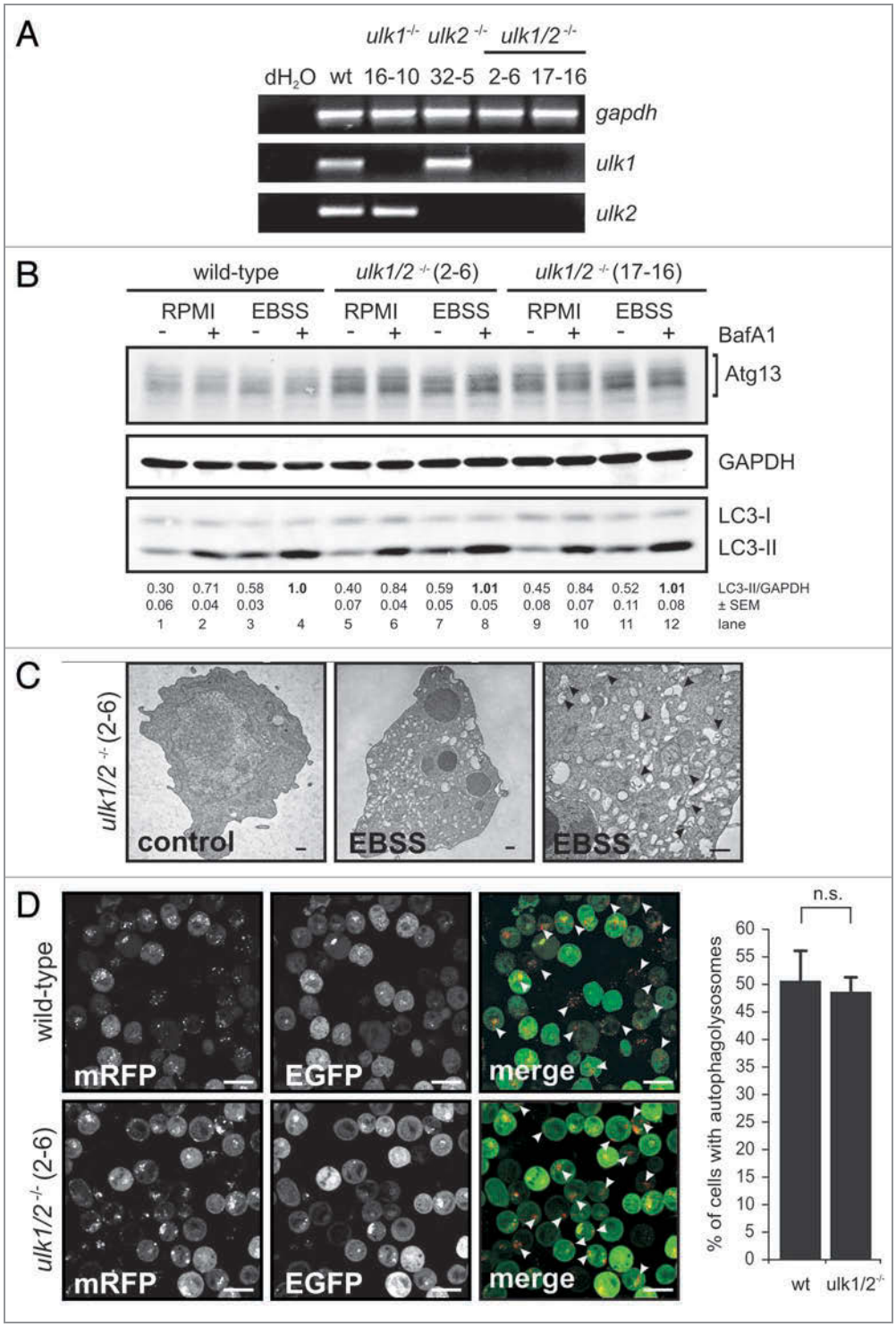

Figure 3. Ulk1 and Ulk2 are dispensable for autophagy induction in DT40 cells. (A) DT40 cells deficient for Ulk1 (*ulk1*$^{-/-}$), Ulk2 (*ulk2*$^{-/-}$) or Ulk1 and Ulk2 (*ulk1/2*$^{-/-}$) were generated by gene targeting and loss of wild-type alleles was confirmed by genomic PCR (for details see **Figure S2**). The absence of *ulk1* and *ulk2* transcripts was verified by RT-PCR. (B) Wild-type cells and two independent double deficient *ulk1/2*$^{-/-}$ clones (2–6 and 17–16) were incubated in full medium (RPMI) or EBSS in the presence or absence of 10 nM BafA1 for 1 h. Equal amounts of protein from cleared cellular lysates were analyzed for Atg13, GAPDH and LC3 by immunoblotting. LC3-II/GAPDH ratios are represented as mean values of three independent experiments ± SEM (C) *ulk1/2*$^{-/-}$ cells (clone 2–6) were incubated in normal growth medium (control) or EBSS for 2 h, cells were fixed and analyzed by transmission electron microscopy. For starvation condition, a representative cell is shown in two different magnifications. Autophagosomes are indicated by black arrow heads in the image with higher magnification (bars: 500 nm). (D) *ulk1/2*$^{-/-}$ cells (clone 2–6) retrovirally transfected with cDNA encoding mRFP-EGFP-rLC3 were incubated in EBSS for 2 h and analyzed by confocal laser scanning microscopy. The mRFP signal is shown in red and the EGFP signal in green in the merged image. Autolysosomes are indicated by white arrow heads (bars: 10 μm). The percentage of cells with autolysosomes (> 100 cells/experiment) is represented as mean value ± SD from three independent experiments. n.s. indicates a non-significant difference between wild-type and *ulk1/2*$^{-/-}$ cells (Student's t-test).

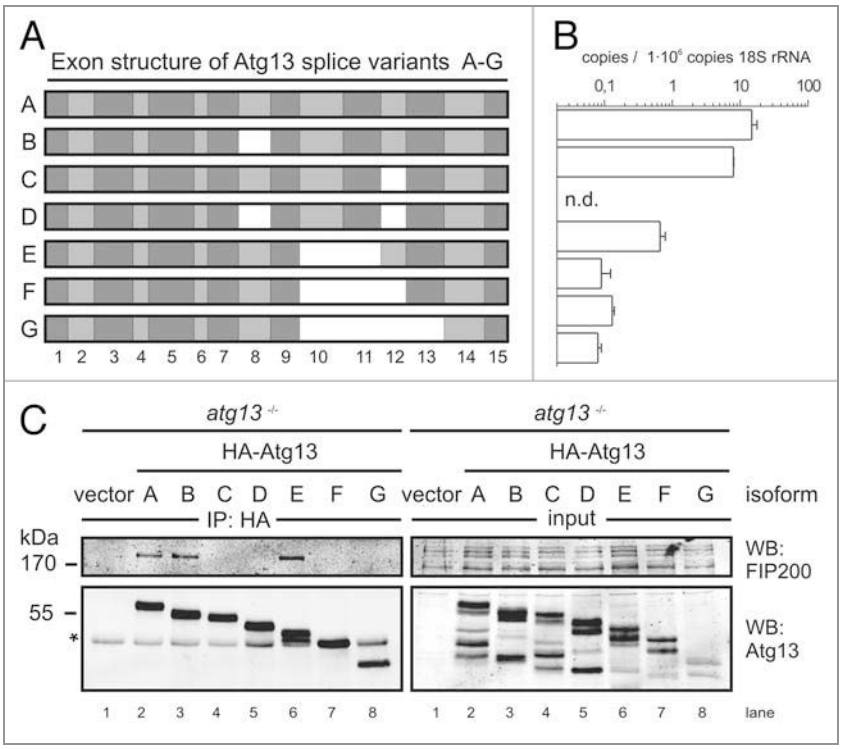

Figure 4. FIP200 binding site in Atg13 is encoded by exon 12. (A) Schematic representation of Atg13 splice variants (named A-G) amplified from DT40 cells. (B) The relative abundance of these splice variants was analyzed by qRT-PCR using splice variant-specific primer combinations (see **Supplementary Material and Methods and Fig. S8A**). (C) *atg13*$^{-/-}$ cells were reconstituted with HA-tagged versions of splice variants A-G and lysates were subjected to anti-HA immunoprecipitation and analyzed for Atg13 and FIP200 by immunoblotting. Asterisk indicates an unspecific background band.

Atg13 but seems to be completely independent of Ulk1 and Ulk2 and its regulation by mTOR.

Discussion

The mTORC1-regulated Ulk-Atg13-FIP200 complex plays a crucial role in autophagy induction. In particular, the mTORC1 substrates Ulk1 and Ulk2 have been suggested as major players in the initiation of autophagosome formation. In this report we investigated the role of the Ulk-Atg13-FIP200 complex in higher vertebrates by targeted disruption of the *atg13, ulk1* and *ulk2* loci in the same cellular system. Using this approach, we would like to propose the existence of an additional function of Atg13 that is completely independent of Ulk1/2 for the following reasons: First, the knockout of Atg13 clearly confirms its necessity for autophagy induction and hence the suitability of our system. Second, the function of Atg13 strongly depends on its interaction with FIP200, underlining their mutual dependence in autophagy regulation. Third, the simultaneous knockout of Ulk1 and Ulk2 does not resemble the phenotype of Atg13 knockout cells. Thus, we conclude that the joint action of Atg13 and FIP200 is a prerequisite for autophagy induction, whereas the mTOR-dependent regulation of Ulk1 and Ulk2 kinase activity seems to be expendable for starvation-induced autophagy in this model system.

The identification of autophagy-related genes in yeast and the direct regulation of their products by TOR once ushered in the molecular era of autophagy research. Meanwhile orthologs of most of these genes have been identified in higher eukaryotes.[25] However, it becomes more and more apparent that the regulation of the molecular machinery is more heterogenous than initially thought. While yeast, *C. elegans* and Drosophila possess only one Atg1 gene, higher vertebrates have at least five different kinases highly related to Atg1 (Ulk1-Ulk4 and STK36). Ulk1 and Ulk2 were the first identified homologs of *C. elegans* uncoordinated-51 (Unc-51). Although the knockdown of Ulk1 is sufficient to inhibit autophagy in some cell lines[3,26] the respective knockout mouse has only a mild phenotype,[9] indicating that the most closely related Ulk1 and Ulk2 have at least partially redundant functions and can compensate for each other. This is further supported by the observation that Ulk1 and Ulk2 both can interact with Atg13 and FIP200, though with different affinities.[15] Notably, the C-terminal domain in Ulk1 and Ulk2 mediating this interaction is not conserved in Ulk3, Ulk4 and STK36.[27] Accordingly, only Ulk1 and Ulk2 have been found in a complex with Atg13, FIP200 and Atg101.[28]

Based on previous findings it has been proposed that Atg13 primarily serves as an adaptor molecule mediating the interaction between Ulk1/2 and its substrate FIP200 as well as enhancing Ulk1/2 kinase activity.[29] Surprisingly, Ulk1 and Ulk2 appear to be dispensable for autophagy induction in DT40 cells. In contrast, *atg13*$^{-/-}$ cells do resemble the phenotype of *FIP200*$^{-/-}$ MEFs[8] and show a complete blockage of the autophagic flux. Furthermore, Atg13 function necessarily depends on FIP200 binding, since only those isoforms interacting with FIP200 were able to reconstitute the autophagy-defective phenotype of *atg13*$^{-/-}$ cells. The FIP200 binding site in Atg13 was found to be exclusively encoded by exon 12. Thus, it seems that Atg13 has an additional role, besides the mediation of Ulk1/2-dependent FIP200 phosphorylation.

Nutrient deprivation is one of the most potent and rapid inducers of autophagy. In yeast, the dephosphorylation of TOR-dependent phosphorylation sites in Atg13 is the initial step and sufficient for autophagy induction under starvation conditions.[30] In this regard, mTOR has been proposed as the major junction for nutrient status dependent signaling in higher vertebrates. Indeed, mTOR activity is immediately and dramatically reduced after nutrient deprivation (**Fig. S7D**). However, the mTOR inhibitors rapamycin and Torin1 fail to induce autophagy to a similar extent as starvation, although mTOR activity is repressed immediately after treatment with inhibitors (**Fig. S7A–C**). Furthermore, Atg13 protein did not display any prominent downshift in SDS-PAGE upon starvation or mTOR inhibition

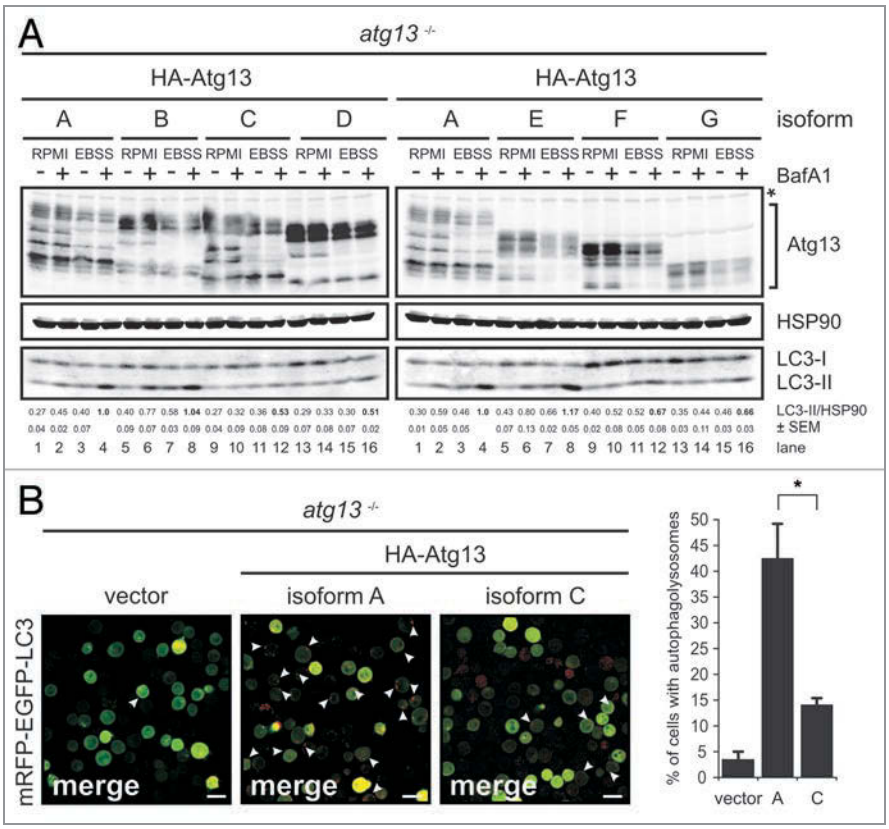

Figure 5. FIP200 binding site is essential for Atg13 function. (A) *atg13*$^{-/-}$ cells were reconstituted with HA-tagged versions of splice variants A-G and incubated in full medium (RPMI) or EBSS for 1 h in the presence or absence of 10 nM BafA1. Equal protein amounts from cleared cellular lysates were analyzed for Atg13, HSP90 and LC3 by immunoblotting. LC3-II/HSP90 ratios from three independent experiments are represented as mean values ± SEM (B) *atg13*$^{-/-}$ retrovirally transfected with cDNAs encoding either HA-Atg13 isoform A (full-length) or HA-Atg13 isoform C (Δexon12) or the empty vector were stably transfected with pmRFP-EGFP-rLC3. Cells were incubated in EBSS for 2 h and analyzed by confocal laser scanning microscopy. The mRFP signal is displayed in red and the EGFP signal in green in the merged image. The percentage of autolysosome containing cells (>100 cells/experiment) from three independent experiments is represented as mean value ± SD *p < 0.05, Student's t-test.

(**Fig. S7D**). If the release of mTOR-mediated repression on the Ulk-Atg13-FIP200 complex would fully account for the immediate autophagic response after starvation, one would expect the same kinetic response of autophagy induction following mTOR inhibition by rapamycin or Torin1. However, the recently identified direct regulation of Ulk1 kinase activity by AMPK might provide an explanation for this discrepancy.[31,32]

The dissimilar phenotypes of *atg13*$^{-/-}$ and *ulk1/2*$^{-/-}$ DT40 cells let us assume that Atg13 has a more basal function in these cells that is closely related to FIP200, but not necessarily regulated by Ulk1 or Ulk2. Interestingly, since *FIP200*$^{-/-}$ MEFs are resistant to autophagy induction by LiCl[8] it has been suggested that FIP200 is additionally involved in mTOR-independent pathways. Although DT40 wild-type cells failed to respond to LiCl (data not shown), this might provide an explanation for the observed independence of autophagy induction from mTOR, Ulk1 and Ulk2 in DT40 cells. Furthermore, during revision of this manuscript Cheong et al. provided further evidence for an Ulk1/2-independent autophagy induction pathway in mammalian cells.[33] Though *ulk1/2*$^{-/-}$ MEFs were resistant to amino acid starvation, they did respond to bioenergetic stress from glucose withdrawal.[33] Thus, although we cannot exclude a cell type-specific feature, it is conceivable that DT40 cells preferentially use such an unconventional autophagy induction pathway upon starvation (for schematic model see **Fig. 6**).

Since Atg13-FIP200 can obviously be triggered by upstream signaling events other than the already known major mTOR-Ulk1/2 axis, it is conceivable that Atg13 constitutes a central signaling node that integrates different upstream pathways. In yeast, PKA is known to regulate autophagy induction, in addition to TOR, by direct phosphorylation of Atg13.[34] However, none of these PKA phosphorylation sites is conserved in Atg13 orthologs of higher vertebrates. Hence, it would be reasonable to assume an additional regulation of Atg13 and FIP200 by other kinases in response to starvation. However, in a recent publication the authors failed to identify nutrient-regulated phosphorylation sites in Atg13.[35] Thus, future studies have to reveal the relevance of those alternative induction pathways in more detail.

Supplementary information is available at *Autophagy*'s website.

Material and Methods

Cell culture. Chicken DT40 cells were cultured in RPMI 1640 (BE12-702F, Lonza) supplemented with 10% FCS, 1% chicken

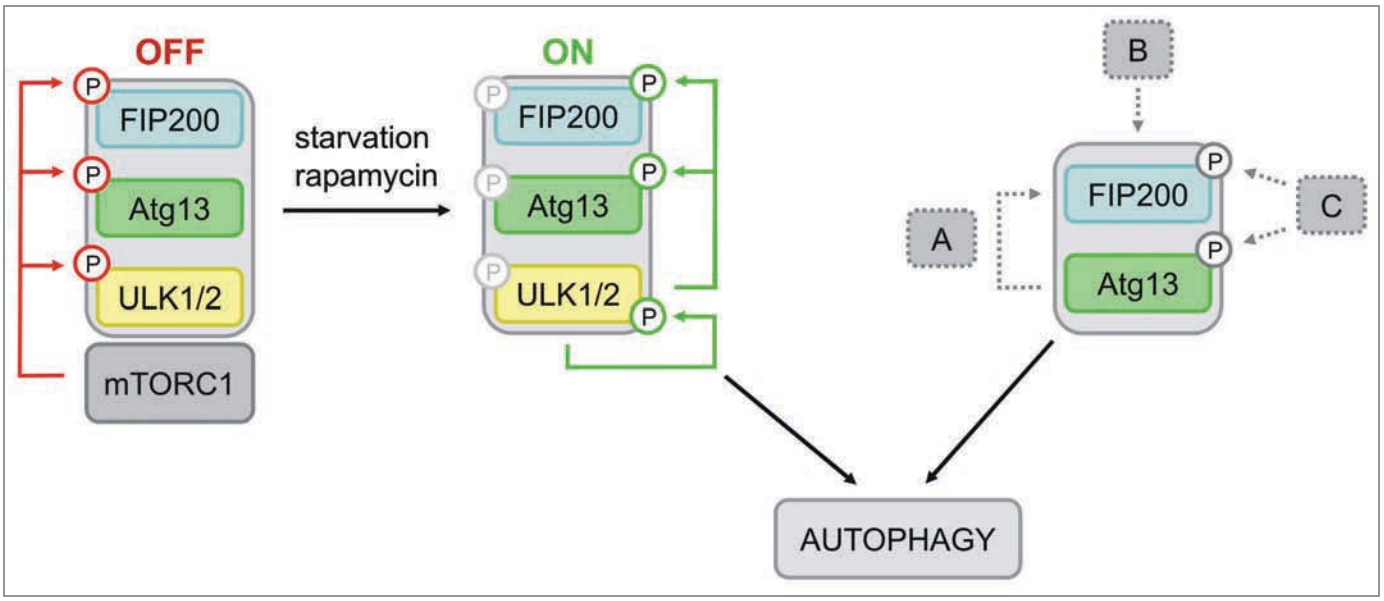

Figure 6. Model of differential Atg13-dependent autophagy induction pathways. Based on previous findings it has been proposed that mTORC1 associates with the Ulk-Atg13-FIP200 complex under nutrient-rich conditions, phosphorylates Ulk1/2 and Atg13 at inhibitory sites and suppresses Ulk1/2 kinase activity. Following starvation or direct mTORC1 inhibition, this negative regulation is released, Ulk1/2 autophosphorylates itself at activating sites and subsequently phosphorylates both Atg13 and FIP200. This in turn leads to autophagy induction (mTORC1-Ulk1/2-axis). In cells that do respond to mTORC1 inhibition by autophagy induction and do depend on Ulk1 and Ulk2, this pathway is most likely favored. However, the incomparable phenotypes of *atg13*$^{-/-}$ and *ulk1/2*$^{-/-}$ DT40 cells let us assume that Atg13 has a more basal function that is not necessarily regulated by Ulk1 or Ulk2, but necessarily requires FIP200 binding capacity. Thus, Atg13 surprisingly has an additional role, besides its proposed function as an adaptor molecule that bridges Ulk1/2 and its substrate FIP200. Several modes of action are conceivable: (A) Atg13 acts in a kinase-independent way, e.g. by stabilizing or recruiting FIP200, (B) the Atg13-FIP200 complex is regulated in a kinase-independent manner, or (C) Atg13-FIP200 is regulated by other kinases than Ulk1/2.

serum, 3 mM L-glutamine, 50 μM β-mercaptoethanol, 50 U/ml penicillin and 50 μg/ml streptomycin (full medium). For starvation, DT40 cells were washed twice and incubated in EBSS (14155-048, Gibco) for the indicated time. Flp-In™ T-REx™ 293 cells (R780–07, Invitrogen) stably expressing FLAG-Ulk1 wt or FLAG-Ulk1 kinase dead (D165A) and Plat-E cells (kindly provided by Toshio Kitamura, Tokyo, Japan)[36] were cultured in DMEM (4.5 g/l D-Glucose, E15-810, PAA) supplemented with 10% FCS, 50 U/ml penicillin and 50 μg/ml streptomycin. All cell lines were maintained at 37°C in a 5% CO_2 incubator.

Antibodies and reagents. Anti-p70S6K (9202), anti-phospho-p70S6K (p-Thr389) (9206) and anti-LC3B antibodies (2775) were purchased from Cell Signaling Technology, anti-GAPDH (6C5, ab8245) from Abcam, anti-HSP90 from BD Transduction laboratories (610418) and anti-GFP from Boehringer Mannheim (1814460). Monoclonal anti-HA agarose (A2095) was purchased from Sigma. Anti-Atg13 antibodies were kindly provided by Do-Hyung Kim (Department of Biochemistry and Biophysics, University of Minnesota, Minneapolis, USA).[15] Anti-FIP200 antibodies were kindly provided by Noboru Mizushima (Department of Physiology and Cell Biology, Tokyo Medical and Dental University, Japan).[8] IRDye®800 and IRDye®680 conjugated secondary antibodies were purchased from LI-COR Biosciences (926-32210/11 and 926-68020/21). Torin1 was kindly provided by Nathanael Gray (Dana-Farber Cancer Institute, Harvard Medical School, Boston, Massachusetts, USA) and David Sabatini (Whitehead Institute for Biomedical Research, Cambridge, Massachusetts, USA),[37] rapamycin (553210) and Bleocin® (203408) were purchased from Calbiochem; G418 from Biochrom (A2912), bafilomycin A_1 (B1793), histidinol (H6647) and mycophenolic acid (M3536) from Sigma. Blasticidin (ant-bl-1) and puromycin (ant-pr-1) were purchased from InvivoGen.

Expression constructs and retroviral infection. Chicken *atg13* cDNAs for isoforms A, B, D, E, F and G were amplified by RT-PCR from DT40 RNA and cloned into pCR®-II TOPO® vector (Invitrogen, 10351-021). Coding sequence for HA tag was introduced at the 5'-end by PCR. Isoform C was generated from isoforms A and D by molecular cloning, using a unique *Bbs*I site in exon 9. Amino acid substitutions in Atg13 were generated by site-directed mutagenesis of *atg13* cDNA and verified by sequencing. For transfection, Atg13 cDNA was subcloned into retroviral expression vector pMSCVpuro (Clontech, PT3303-5) via *Eco*RI. pMSCV-mRFP-EGFP-rLC3 expression vector was generated by cloning of mRFP-EGFP-rLC3 cDNA from pmRFP-EGFP-rLC3 (kindly provided by Tamotsu Yoshimori, Department of Genetics, Osaka, Japan) via *Nhe*I/*Eco*RI into the *Hpa*I site of pMSCVpuro. Alternatively, cells were transfected with *Dra*III linearized pmRFP-EGFP-rLC3 by electroporation and selected in medium containing 2 mg/ml G418. The pMSCV-mCitrine-chLC3B expression vector has been previously described.[17] For the production of recombinant retroviruses, Plat-E cells were transfected with pMSCV-based vector using FuGENE transfection reagent (Roche, 11988387001). The MMLV was pseudotyped with VSV-G. 1 × 10^6 DT40 cells were incubated

with retroviral supernatant containing 3 μg/ml Polybrene (Sigma, H9268) and selected in medium containing 0.5 μg/ml puromycin.

Generation of DT40 knockout cell lines. For Atg13 targeting vectors, a 6 kb fragment was amplified from DT40 genomic DNA and cloned into pBluescript II SK(-) vector. The start codon in exon 1 was mutated and a histidinol (hisD) or blasticidin (bsr) resistance cassette was inserted into this newly generated *Bam*HI site, respectively. DT40 cells were transfected with linearized targeting vectors by electroporation at 250 V and 975 μF and selected in 1 mg/ml histidinol and 50 μg/ml blasticidin. *Atg13*-deficient clones were screened by genomic PCR and immunoblotting. For further details and generation of *Ulk1* and *Ulk2* targeting vectors see Supplementary Material and Methods.

Immunoblotting and immunopurification. DT40 cells were incubated in full medium or EBSS, containing 10 nM bafilomycin A_1 or DMSO as control, at a density of 1×10^6 cells/ml for the indicated time. Cells were lysed in lysis buffer [10 mM TRIS-HCl pH 7.5, 150 mM NaCl, 0.5 mM EDTA, 1% Triton X-100, 10 mM NaF, 2.5 mM NaPP, 10 μM Na_2MoO_4, 1 mM Na_3VO_4, and protease inhibitors (P2714, Sigma)] and clarified by centrifugation at 16,000 g for 20 min. Equal total protein amounts, as determined by Bradford, were separated on an 8–15% gradient SDS-polyacrylamide gel and transferred to PVDF membrane (Millipore). Immunoblot analysis was performed using the indicated primary antibodies and appropriate IRDye®800 or IRDye®680 conjugated secondary antibodies (LI-COR Biosciences). Signals were detected with an Odyssey® Infrared Imaging system (LI-COR Biosciences) and quantified using ImageJ 1.41 (http://rsb.info.nih.gov/ij/). For immuno-purifications, cells were lysed in IP buffer [40 mM HEPES pH 7.5, 2 mM EGTA, 0.3% CHAPS, 10 mM NaPP, 1 mM Na_3VO_4 and protease inhibitors (P2714, Sigma)] and equal total protein amounts were incubated with monoclonal anti-HA-agarose (A2095, Sigma) over night. Beads were washed four times with lysis buffer (without protease inhibitors), boiled in sample buffer and supernatant was subjected to SDS-PAGE.

Quantitative real-time PCR. Quantitative real-time RT-PCR analysis was performed using the ABI Prism 7000 Sequence Detection System (Applied Biosystems) and SYBR Green-containing qPCR Mastermix Plus (Fermentas, K0222). Total RNA from 1×10^6 cells was isolated using the NucleoSpin™ RNA II-Kit (Macherey & Nagel, 740955.50). cDNA was generated from 1 μg of total RNA with 200 U RevertAid H Minus™ reverse transcriptase (Fermentas, EP0452), 50 μM random hexamers (Fermentas, SO142), 400 μM dNTPs (Fermentas, R0192), and 1.6 U/μl RiboLock™ RNase inhibitor (Fermentas, EO0381) according to manufacturer's recommendations. 80/8/0.8 ng of the resulting cDNA (in duplicates) were applied to qRT-PCR analyses and amplified in the presence of 300 nM primers (for sequences see **Supplementary Materials**) with the standard temperature profile (2 min 50°C, 10 min 95°C, 40 cycles 15 sec 95°C, 1 min 60°C). For absolute quantification of splice variants, cDNA standards for each variant were generated by *Eco*RI digestion of the corresponding plasmid, isolated from agarose gels and quantified by spectrophotometry. The copy number of standard DNA molecules was calculated using the following formula: X (g/μl) DNA / [DNA fragment length (bp) × 660 (g/mole)] × 6.022×10^{23} = Y (copies/μl). Standard curves (plot of C_T value/crossing point against log of copy number) were generated from serial 10-fold dilutions, ranging from 1×10^{10} to 1×10^0 copies per point. The detection limits were 10 copies per reaction for Ulk1, Ulk2, Ulk3, Ulk4 and 100 copies per reaction for STK36 and 18S rRNA. Results of absolute copy numbers detected in the samples were normalized to the absolute copy numbers of 18S rRNA to account for RT-PCR efficiency and are displayed as copies per 1×10^9 copies 18S rRNA. Mean values ± SD over three dilutions (80/8/0.8 ng cDNA per reaction) are given.

Confocal laser scanning microscopy. For starvation conditions, cells were washed once with EBSS, resuspended in EBSS and seeded onto chambered coverglasses (Nunc). After 2 h cells were analyzed on a Leica TCS SP II confocal laser scanning microscope. As control, cells were resuspended in Krebs Ringer solution [10 mM HEPES (pH 7.0), 140 mM NaCl, 4 mM KCl, 1 mM $MgCl_2$, 1 mM $CaCl_2$ and 10 mM glucose] directly prior to analysis. EGFP and mCitrine were excited at 488 nm, and mRFP at 543 nm wavelength.

Transmission electron microscopy. Transmission electron microscopy was performed as previously decribed.[38,39] Briefly, DT40 cells were incubated in normal growth medium or EBSS at a density of 1×10^6 cells/ml for 2 h at 37°C. Cells were harvested, washed with prewarmed PBS, fixed with warm Karnovsky's solution for 10 min at 37°C and stored at 4°C. For electron microscopic analysis, cells were embedded in 3.5% agarose at 37°C, coagulated at room temperature and fixed again in Karnovsky's solution. Post-fixation was based on 1.0% osmium tetroxide containing 1.5% K-ferrocyanide in 0.1 M cacodylate buffer for 2 h. After following standard methods, blocks were embedded in glycide ether and cut using an ultra microtome (Ultracut). Ultra-thin sections (30 nm) were mounted on copper grids and analyzed using a Zeiss LIBRA 120 transmission electron microscope (Carl Zeiss) operating at 120 kV.

Disclosure of Potential Conflicts of Interest

No potential conflicts of interest were disclosed.

Acknowledgment

We thank Toshio Kitamura for providing Plat-E cells, Do-Hyung Kim for Atg13 antibodies, Nathanael Gray and David Sabatini for Torin1, Tamotsu Yoshimori for the pmRFP-EGFP-rLC3 construct, and Noboru Mizushima for FIP200 antibodies and helpful discussions. We thank Maria Deak (MRC Protein and Phosphorylation Unit, University of Dundee, UK) and protein purification teams of the Division of Signal Transduction Therapy (University of Dundee) for GST-Atg13. We are grateful to Dario Alessi for carefully reading the manuscript and for helpful suggestions. We also thank Tassula Proikas-Cezanne for helpful discussions. This work was supported by grants from the Deutsche Forschungsgemeinschaft SFB 773 (to S.W., B.S. and M.S.), GRK 1302 (to S.W. and B.S.), from the Interdisciplinary Center of Clinical Research, Faculty of Medicine, Tübingen (Nachwuchsgruppe 1866-0-0, to B.S.) and the UK Medical Research Council (to D.G.C.). The Division of Signal Transduction Therapy

(University of Dundee) is supported by the following pharmaceutical companies: AstraZeneca, Boehringer-Ingelheim, GlaxoSmithKline, Merck-Serono and Pfizer.

Note

Supplemental materials can be found at:
www.landesbioscience.com/journals/autophagy/article/18027

References

1. Kabeya Y, Kamada Y, Baba M, Takikawa H, Sasaki M, Ohsumi Y. Atg17 functions in cooperation with Atg1 and Atg13 in yeast autophagy. Mol Biol Cell 2005; 16:2544-53; PMID:15743910; http://dx.doi.org/10.1091/mbc.E04-08-0669
2. Kamada Y, Funakoshi T, Shintani T, Nagano K, Ohsumi M, Ohsumi Y. Tor-mediated induction of autophagy via an Apg1 protein kinase complex. J Cell Biol 2000; 150:1507-13; PMID:10995454; http://dx.doi.org/10.1083/jcb.150.6.1507
3. Chan EY, Kir S, Tooze SA. siRNA screening of the kinome identifies ULK1 as a multidomain modulator of autophagy. J Biol Chem 2007; 282:25464-74; PMID:17595159; http://dx.doi.org/10.1074/jbc.M703663200
4. Kuroyanagi H, Yan J, Seki N, Yamanouchi Y, Suzuki Y, Takano T, et al. Human ULK1, a novel serine/threonine kinase related to UNC-51 kinase of Caenorhabditis elegans: cDNA cloning, expression, and chromosomal assignment. Genomics 1998; 51:76-85; PMID:9693035; http://dx.doi.org/10.1006/geno.1998.5340
5. Tomoda T, Bhatt RS, Kuroyanagi H, Shirasawa T, Hatten ME. A mouse serine/threonine kinase homologous to C. elegans UNC51 functions in parallel fiber formation of cerebellar granule neurons. Neuron 1999; 24:833-46; PMID:10624947; http://dx.doi.org/10.1016/S0896-6273(00)81031-4
6. Yan J, Kuroyanagi H, Tomemori T, Okazaki N, Asato K, Matsuda Y, et al. Mouse ULK2, a novel member of the UNC-51-like protein kinases: unique features of functional domains. Oncogene 1999; 18:5850-9; PMID:10557072; http://dx.doi.org/10.1038/sj.onc.1202988
7. Chan EY, Longatti A, McKnight NC, Tooze SA. Kinase-inactivated ULK proteins inhibit autophagy via their conserved C-terminal domains using an Atg13-independent mechanism. Mol Cell Biol 2009; 29:157-71; PMID:18936157; http://dx.doi.org/10.1128/MCB.01082-08
8. Hara T, Takamura A, Kishi C, Iemura S, Natsume T, Guan JL, et al. FIP200, a ULK-interacting protein, is required for autophagosome formation in mammalian cells. J Cell Biol 2008; 181:497-510; PMID:18443221; http://dx.doi.org/10.1083/jcb.200712064
9. Kundu M, Lindsten T, Yang CY, Wu J, Zhao F, Zhang J, et al. Ulk1 plays a critical role in the autophagic clearance of mitochondria and ribosomes during reticulocyte maturation. Blood 2008; 112:1493-502; PMID:18539900; http://dx.doi.org/10.1182/blood-2008-02-137398
10. Meijer WH, van der Klei IJ, Veenhuis M, Kiel JA. ATG genes involved in non-selective autophagy are conserved from yeast to man, but the selective Cvt and pexophagy pathways also require organism-specific genes. Autophagy 2007; 3:106-16; PMID:17204848
11. Chan EY. mTORC1 phosphorylates the ULK1-mAtg13-FIP200 autophagy regulatory complex. Sci Signal 2009; 2:pe51; PMID:19690328; http://dx.doi.org/10.1126/scisignal.284pe51
12. Chang YY, Neufeld TP. An Atg1/Atg13 complex with multiple roles in TOR-mediated autophagy regulation. Mol Biol Cell 2009; 20:2004-14; PMID:19225150; http://dx.doi.org/10.1091/mbc.E08-12-1250
13. Ganley IG. Lam du H, Wang J, Ding X, Chen S, Jiang X. ULK1.ATG13.FIP200 complex mediates mTOR signaling and is essential for autophagy. J Biol Chem 2009; 284:12297-305; PMID:19258318; http://dx.doi.org/10.1074/jbc.M900573200
14. Hosokawa N, Hara T, Kaizuka T, Kishi C, Takamura A, Miura Y, et al. Nutrient-dependent mTORC1 association with the ULK1-Atg13-FIP200 complex required for autophagy. Mol Biol Cell 2009; 20:1981-91; PMID:19211835; http://dx.doi.org/10.1091/mbc.E08-12-1248
15. Jung CH, Jun CB, Ro SH, Kim YM, Otto NM, Cao J, et al. ULK-Atg13-FIP200 complexes mediate mTOR signaling to the autophagy machinery. Mol Biol Cell 2009; 20:1992-2003; PMID:19225151; http://dx.doi.org/10.1091/mbc.E08-12-1249
16. Funakoshi T, Matsuura A, Noda T, Ohsumi Y. Analyses of APG13 gene involved in autophagy in yeast, Saccharomyces cerevisiae. Gene 1997; 192:207-13; PMID:9224892; http://dx.doi.org/10.1016/S0378-1119(97)00031-0
17. Grotemeier A, Alers S, Pfisterer SG, Paasch F, Daubrawa M, Dieterle A, et al. AMPK-independent induction of autophagy by cytosolic Ca2+ increase. Cell Signal 2010; 22:914-25; PMID:20114074; http://dx.doi.org/10.1016/j.cellsig.2010.01.015
18. Khan MT, Joseph SK. Role of inositol trisphosphate receptors in autophagy in DT40 cells. J Biol Chem 2010; 285:16912-20; PMID:20308071; http://dx.doi.org/10.1074/jbc.M110.114207
19. Vicencio JM, Ortiz C, Criollo A, Jones AW, Kepp O, Galluzzi L, et al. The inositol 1,4,5-trisphosphate receptor regulates autophagy through its interaction with Beclin 1. Cell Death Differ 2009; 16:1006-17; PMID:19325567; http://dx.doi.org/10.1038/cdd.2009.34
20. Kabeya Y, Mizushima N, Ueno T, Yamamoto A, Kirisako T, Noda T, et al. LC3, a mammalian homologue of yeast Apg8p, is localized in autophagosome membranes after processing. EMBO J 2000; 19:5720-8; PMID:11060023; http://dx.doi.org/10.1093/emboj/19.21.5720
21. Fass E, Shvets E, Degani I, Hirschberg K, Elazar Z. Microtubules support production of starvation-induced autophagosomes but not their targeting and fusion with lysosomes. J Biol Chem 2006; 281:36303-16; PMID:16963441; http://dx.doi.org/10.1074/jbc.M607031200
22. Kimura S, Noda T, Yoshimori T. Dissection of the autophagosome maturation process by a novel reporter protein, tandem fluorescent-tagged LC3. Autophagy 2007; 3:452-60; PMID:17534139
23. Lee EJ, Tournier C. The requirement of uncoordinated 51-like kinase 1 (ULK1) and ULK2 in the regulation of autophagy. Autophagy 2011; 7:689-95; PMID:21460635; http://dx.doi.org/10.4161/auto.7.7.15450
24. Young AR, Narita M, Ferreira M, Kirschner K, Sadaie M, Darot JF, et al. Autophagy mediates the mitotic senescence transition. Genes Dev 2009; 23:798-803; PMID:19279323; http://dx.doi.org/10.1101/gad.519709
25. Meléndez A, Neufeld TP. The cell biology of autophagy in metazoans: a developing story. Development 2008; 135:2347-60; PMID:18567846; http://dx.doi.org/10.1242/dev.016105
26. Young AR, Chan EY, Hu XW, Kochl R, Crawshaw SG, High S, et al. Starvation and ULK1-dependent cycling of mammalian Atg9 between the TGN and endosomes. J Cell Sci 2006; 119:3888-900; PMID:16940348; http://dx.doi.org/10.1242/jcs.03172
27. Mizushima N. The role of the Atg1/ULK1 complex in autophagy regulation. Curr Opin Cell Biol 2010; 22:132-9; PMID:20056399; http://dx.doi.org/10.1016/j.ceb.2009.12.004
28. Behrends C, Sowa ME, Gygi SP, Harper JW. Network organization of the human autophagy system. Nature 2010; 466:68-76; PMID:20562859; http://dx.doi.org/10.1038/nature09204
29. Jung CH, Ro SH, Cao J, Otto NM, Kim DH. mTOR regulation of autophagy. FEBS Lett 2010; 584:1287-95; PMID:20083114; http://dx.doi.org/10.1016/j.febslet.2010.01.017
30. Kamada Y, Yoshino K, Kondo C, Kawamata T, Oshiro N, Yonezawa K, et al. Tor directly controls the Atg1 kinase complex to regulate autophagy. Mol Cell Biol 2010; 30:1049-58; PMID:19995911; http://dx.doi.org/10.1128/MCB.01344-09
31. Egan DF, Shackelford DB, Mihaylova MM, Gelino S, Kohnz RA, Mair W, et al. Phosphorylation of ULK1 (hATG1) by AMP-activated protein kinase connects energy sensing to mitophagy. Science 2011; 331:456-61; PMID:21205641; http://dx.doi.org/10.1126/science.1196371
32. Kim J, Kundu M, Viollet B, Guan KL. AMPK and mTOR regulate autophagy through direct phosphorylation of Ulk1. Nat Cell Biol 2011; 13:132-41; PMID:21258367; http://dx.doi.org/10.1038/ncb2152
33. Cheong H, Lindsten T, Wu J, Lu C, Thompson CB. Ammonia-induced autophagy is independent of ULK1/ULK2 kinases. Proc Natl Acad Sci USA 2011; 108:11121-6; PMID:21690395; http://dx.doi.org/10.1073/pnas.1107969108
34. Stephan JS, Yeh YY, Ramachandran V, Deminoff SJ, Herman PK. The Tor and PKA signaling pathways independently target the Atg1/Atg13 protein kinase complex to control autophagy. Proc Natl Acad Sci USA 2009; 106:17049-54; PMID:19805182; http://dx.doi.org/10.1073/pnas.0903316106
35. Shang L, Chen S, Du F, Li S, Zhao L, Wang X. Nutrient starvation elicits an acute autophagic response mediated by Ulk1 dephosphorylation and its subsequent dissociation from AMPK. Proc Natl Acad Sci USA 2011; 108:4788-93; PMID:21383122; http://dx.doi.org/10.1073/pnas.1100844108
36. Morita S, Kojima T, Kitamura T. Plat-E: an efficient and stable system for transient packaging of retroviruses. Gene Ther 2000; 7:1063-6; PMID:10871756; http://dx.doi.org/10.1038/sj.gt.3301206
37. Thoreen CC, Kang SA, Chang JW, Liu Q, Zhang J, Gao Y, et al. An ATP-competitive mammalian target of rapamycin inhibitor reveals rapamycin-resistant functions of mTORC1. J Biol Chem 2009; 284:8023-32; PMID:19150980; http://dx.doi.org/10.1074/jbc.M900301200
38. Gröbner S, Fritz E, Schoch F, Schaller M, Berger AC, Bitzer M, et al. Lysozyme activates Enterococcus faecium to induce necrotic cell death in macrophages. Cell Mol Life Sci 2010; 67:3331-44; PMID:20458518; http://dx.doi.org/10.1007/s00018-010-0384-9
39. Schroeder BO, Wu Z, Nuding S, Groscurth S, Marcinowski M, Beisner J, et al. Reduction of disulphide bonds unmasks potent antimicrobial activity of human beta-defensin 1. Nature 2011; 469:419-23; PMID:21248850; http://dx.doi.org/10.1038/nature09674